

# UC Santa Barbara

## UC Santa Barbara Electronic Theses and Dissertations

### Title

New Approaches to Sustainable Organic Synthesis: From Aqueous Micellar Catalysis to Solvent-Free Techniques

### Permalink

<https://escholarship.org/uc/item/9q1421nx>

### Author

Li, Xiaohan

### Publication Date

2023

Peer reviewed|Thesis/dissertation

UNIVERSITY OF CALIFORNIA

Santa Barbara

New Approaches to Sustainable Organic Synthesis: From Aqueous Micellar Catalysis to  
Solvent-Free Techniques

A dissertation submitted in partial satisfaction of the  
requirements for the degree Doctor of Philosophy  
in Chemistry

by

Xiaohan Li

Committee in charge:

Professor Bruce H. Lipshutz, Chair

Professor Liming Zhang

Professor Mahdi Abu-Omar

Professor Yang Yang

March 2024

The dissertation of Xiaohan Li is approved.

---

Liming Zhang

---

Mahdi Abu-Omar

---

Yang Yang

---

Bruce H. Lipshutz

December 2023

New Approaches to Sustainable Organic Synthesis: From Aqueous Micellar Catalysis to  
Solvent-Free Techniques

Copyright © 2023

by

Xiaohan Li

## ACKNOWLEDGEMENTS

As time swiftly passes, the day I've long anticipated has finally arrived. I am profoundly honored to receive my PhD. The journey here demanded immense dedication and hard work. Here, I extend my deepest gratitude to everyone who has supported me along this path, thank you for shaping my path and being part of my story.

First and foremost, my deepest gratitude goes to my advisor, Bruce Lipshutz. I still remember our initial Skype conversation, where his passion and pride in his research left a lasting impression on me. His academic guidance over four and a half years has been invaluable, complemented by his kindness, open-mindedness, and humor, making my PhD journey less stressful. Joining the Lipshutz group was, undoubtedly, the best decision of my academic career.

I'm grateful to my first-year mentors, Ruchita and Balaram. Their guidance in familiarizing me with our department and involving me in significant projects like Stille coupling and nitro reduction was pivotal. They not only introduced me to chemistry in water but also helped me grow as a researcher.

Thanks to my colleagues in the Lipshutz group: Julie, for her collaboration on the CF2 project and initiating the IRED project; Alex, an experienced and reliable collaborator on the allylation project; and Karthik, for his talent and enthusiasm shown in our reductive amination project. I must mention Haobo, for his advice in my early days and during job hunting, and Rahul, for his expertise in chemistry and partnership in our job searches, offering mutual support and confidence. And, to all past and present members of the Lipshutz lab: Bo, Nicholas, Vani, Joseph, Haley, Melvin, Maddy, Katie, Juan, Rohan, Erfan, Chandler, Yuki,

Yuzo, Simone, Erika, Denny, John, Komal, Max, Kylee, Trevor, Scott, Robert, and others. Your presence enriched my PhD experience, making this journey complete and beautiful.

My sincere thanks to my committee members, Prof. Liming Zhang, Prof. Mahdi Abu-Omar, and Prof. Yang Yang, for their insightful questions and advice during my candidacy exams and final defense.

Thanks to the staff in the Chemistry Department: Hongjun, Dmitriy, Felix (UCI), Dezmond, Richard, Cabe, Adrian, Trevor, Chris, Iris, Rosemary, and others for your dedication in organizing the facilities in department, providing a solid foundation for my research.

Appreciation to my TAs Supervisors, Morgan and Petra, for teaching me how to effectively impart knowledge and connect with students, enhancing my teaching experience. A thank you to all my students for their trust, tolerance, and for adding vibrant colors to my PhD journey.

Acknowledging my previous advisors and mentors at NKU and Scripps: Huabin Li, Keary Engle, and Zhen Liu, for laying my research foundation and teaching invaluable techniques still in use today.

Thanks to my friends at UCSB: Lingyu Zhao, Yuyang Wu, Tianyou Li, Yang Li, Zhishuai Geng, Cheng Zhang, Ke Zhao, Xuan Wu, Rui Guo, and to my longstanding friends: Weixingyue Li, Xuefei Li, Ruye Li, Ziyang Qin, Xudong Lv, Jingda Zhang.

Gratitude to my friends and coaches at Ice in Paradise: Frank, Breanne, Nadia, Sabina, Ashley, Summer, Jinelle, Cheyenne, Gregoire, Karla, Coleen, Katie, Rose, Kestrel, Mirka, Ildi, Lindsay, Sam, Tongxi, Shirley, and many others for creating a welcoming community and enhancing my joy in skating.

To my hero, Yuzuru Hanyu, whose spirit of constantly challenging the unknown and conquer difficulties has always inspired me. In many difficult days, he is my guiding light.

My beloved kitten, Jetta, for the comfort and joy she brings into my life.

Finally, the most profound gratitude to my family, whose love and selfless support have been my constant foundation. And my significant other, Yuting Hu, our shared academic endeavors and personal bond have been a source of immense strength and love.

VITA OF XIAOHAN LI  
Dec 2023

EDUCATION

Bachelor of Science in Chemistry, Nankai University, June 2019

Doctor of Philosophy in Chemistry, University of California, Santa Barbara, Dec 2023

PROFESSIONAL EMPLOYMENT

2019-2023: Teaching Assistant, Department of Chemistry and Biochemistry, University of California, Santa Barbara.

PUBLICATIONS

- 1) Yu, J.<sup>‡</sup>; **Li, X.**<sup>‡</sup>; Wong, M. J.; Oftadeh, E.; Cao, Y.; Lipshutz, B. H. "Reactions of *in situ*-generated difluorocarbene (:CF<sub>2</sub>) with aromatic/heteroaromatic alcohols, thiols, olefins, and alkynes under environmentally responsible conditions" *Manuscript in preparation*.  
<sup>‡</sup>These authors contributed equally.
- 2) Li, X.; Hu, Y.; Lipshutz, B. H. "Surfactant-Mediated Efficiency Boost in IRED Reactions: Exploration and Applications in One-Pot Bio-Chemo Sequences" *Org. Lett.* **2023**, acs.orglett.3c02790.
- 3) Hu, Y.; **Li, X.**; Jin, G.; Lipshutz, B. H. "A New Preparation of ppm Pd-Containing Nanoparticles as Catalysts for Chemistry in Water" *ACS Catal.* **2022**, *13*, 3179-3186.
- 4) **Li, X.**; Wood, A.; Lee, N.; Gallou, F.; Lipshutz, B. H. "Allylations of Aryl/Heteroaryl Ketones: Neat, Clean, and Green. Applications to Targets in the Pharma- and Nutraceuical Industries." *Green Chem.*, **2022**, *24*, 4909-4914.
- 5) **Li, X.**; Thakore, R. R.; Takale, B. S.; Gallou, F.; Lipshutz, B. H. "High Turnover Pd/C Catalyst for Nitro Group Reductions in Water. One-Pot Sequences and Syntheses of Pharmaceutical Intermediates." *Org. Lett.* **2021**, *23*, 8114-8118.
- 6) **Li, X.**; Iyer, K.S.; Thakore, R. R.; Bailey, J. D.; Leahy, D. K.; Lipshutz, B. H. "Bisulfite addition compounds as educts for reductive aminations in water." *Org. Lett.* **2021**, *23*, 7205-7208.
- 7) Gu, J.<sup>‡</sup>; **Li, X.**<sup>‡</sup>; Wang, Z.; Chen, Y.; Chen, X.; Li, H. "Synthesis and herbicidal activities of 4*H*-pyrazolo[3,4-*d*] [1,2,3]triazine-4-one with bulky substituents." *Chin. J. Pestic. Sci.* **2021**, *23*, 680-687. <sup>‡</sup>These authors contributed equally.
- 8) Takale, B. S.; Thakore, R. R.; Casotti, G., **Li, X.**; Gallou, F.; Lipshutz, B. H. "Mild and robust Stille reactions in water using ppm levels of a new triphenylphosphine-based palladacycle" *Angew. Chem., Int. Ed.* **2021**, *60*, 4158-4163.



- 9) Liu, Z.; Chen, J.; Lu, Hou-X.; **Li, X.**; Gao, Y.; Coombs, J. R.; Goldfogel, M, J.; Engle, K. M. “Palladium(0)-Catalyzed Directed *syn*-1,2-Carboboration and -Silylation: Alkene Scope, Applications in Dearomatization, and Stereocontrol by a Chiral Auxiliary.” *Angew. Chem., Int. Ed.* **2019**, *58*, 17068-17073.
- 10) Liu, Z.; **Li, X.**; Zeng, T.; Engle, K. M. “Palladium-Catalyzed Enantioselective Carboboration of Alkenyl Carbonyl Compounds.” *ACS Catal.* **2019**, *9*, 3260–3265.
- 11) Li, H; Li, L; Guo, L; **Li, X**; Kuang, X; Gu, J. Process for Preparation of Pyrazolo[3,4-*d*]pyrimidine-4(5*H*)-ketone Derivative and Its Application, Patent CN108484614.

## ABSTRACT

### New Approaches to Sustainable Organic Synthesis: From Aqueous Micellar Catalysis to Solvent-Free Techniques

by

Xiaohan Li

I. A sustainable method for reductive aminations using shelf-stable bisulfite addition compounds of aldehydes under aqueous micellar catalysis is presented. Using  $\alpha$ -picolineborane as a readily available stoichiometric hydride source, we successfully synthesized highly valued compounds, inclusive of those pertinent to the pharmaceutical domain. Moreover, this method allows for straightforward recycling of the aqueous reaction medium, emphasizing its environmental benefits.

II. Under micellar catalysis conditions, an eco-friendly nitro group reduction has been developed using readily accessible Pd/C as a catalyst with a minimal Pd loading of 0.4 mol %. This methodology efficiently facilitates the transformation of a diverse range of nitro compounds into their corresponding amines, yielding notable results. The robustness of this process is further showcased through the one-pot synthesis of specific pharmaceutical intermediates. Notably, both the catalyst and the surfactant have demonstrated consistent recyclability without any decrease in effectiveness.

III. The introduction of nonionic surfactant to aqueous reaction systems with varied IREDs significantly enhances both the reaction rate and the yield of the target amines, with improvements reaching more than 40% in comparison to buffer only. Moreover, these findings underscore the potential of combining chemocatalysis and biocatalysis into a 1-pot sequence under aqueous micellar environments. Multiple 1-pot procedures integrating the use of IREDs with diverse chemo-catalytic methods were shown.

IV. Ketones, both aromatic and heteroaromatic, possessing an  $\alpha$ -methine proton, have been demonstrated to undergo deprotonation and subsequent mono-allylation rapidly and exclusively in the absence of any solvent. This process consistently delivers the targeted products with excellent isolated yields. The versatility and applicability of this novel method are further highlighted through its successful application to the synthesis of notable compounds such as MK-7, MK-9, and coenzyme Q<sub>9</sub> (CoQ<sub>9</sub>).

## TABLE OF CONTENTS

I.	Bisulfite addition compounds as substrates for reductive aminations in water .....	1
1.1.	Background and introduction.....	2
1.2.	Result and Discussion.....	5
1.2.1.	Substrate scope.....	5
1.2.2.	Application: API synthesis and 1-pot sequence.....	9
1.2.3.	Recycling and E Factor calculations.....	12
1.3.	Summary.....	13
1.4.	References.....	13
1.5.	Experimental section.....	17
1.5.1.	General information.....	17
1.5.2.	General procedure for the preparation of a bisulfite adduct.....	18
1.5.3.	General procedure for reductive amination.....	18
1.5.4.	1-pot sequence.....	21
1.5.5.	Recycle and E Factor study.....	23
1.5.6.	Analytical data.....	25
1.5.7.	References.....	40
1.5.8.	NMR spectra.....	42
II.	High turnover Pd/C catalyst for nitro group reductions in water enabling 1-pot sequences and syntheses of pharmaceutical intermediates .....	86
2.1.	Background and introduction.....	87
2.2.	Results and Discussion.....	90
2.2.1.	screening of conditions.....	90
2.2.2.	Application: 1-pot synthesis of pharmaceutical intermediates.....	93
2.2.3.	Substrate scope.....	95
2.2.4.	Recycle study.....	98
2.3.	Summary.....	98
2.4.	References.....	99

2.5. Experimental section.....	104
2.5.1. General information .....	104
2.5.2. General procedure for nitro group reductions.....	105
2.5.3. Optimization details .....	105
2.5.4. Experimental procedures for 1-pot synthesis of pharmaceutical intermediates.....	106
2.5.5. Recycling studies .....	110
2.5.6. Analytical Data .....	111
2.5.7. References .....	118
2.5.8. NMR spectra .....	120
III. Impact of Nonionic Surfactants on Reactions of IREDs. Applications to Tandem Chemoenzymatic Sequences in Water.....	140
3.1. Background and introduction.....	141
3.1.1. Project background .....	141
3.1.2. Reaction mechanism of IRED.....	144
3.2. Result and Discussion.....	145
3.2.1. Surfactant screening.....	145
3.2.2. Kinetic studies.....	147
3.2.3. Substrate scope.....	150
3.2.4 Tandem Chemoenzymatic Sequences.....	153
3.3. Summary.....	157
3.4. References.....	158
3.5. Experimental section.....	162
3.5.1. General information .....	162
3.5.2. Optimization detail for imine formation .....	163
3.5.3. Procedure for preparation of tris-HCl buffer, and surfactant/buffer solutions.....	164
3.5.4. General procedure for IRED screening.....	165
3.5.5. General procedure for surfactant screening .....	166
3.5.6. General procedure for obtaining kinetic data.....	167

3.5.7. General procedure for the synthesis of secondary amines by IRED.....	168
3.5.8. General procedure for the synthesis of standard racemic secondary amines.....	169
3.5.9. 1-Pot sequence .....	171
3.5.10. Analytical data .....	176
3.5.11. References .....	186
3.5.12. NMR Spectra.....	187
3.5.13. HPLC traces .....	207
<b>IV. Allylations of Aryl/Heteroaryl Ketones: Neat, Clean, and Green. Applications to Targets in the Pharma- and Nutraceuical Industries .....</b>	<b>214</b>
4.1. Background and introduction.....	215
4.1.1. $\alpha$ -allylation of ketones.....	215
4.1.2. Solvent-free reactions .....	217
4.2. Result and Discussion.....	220
4.2.1. Condition screening .....	220
4.2.2. Substrate scope.....	224
4.2.3. Calorimetry study and gram-scale reaction .....	227
4.2.4. Application: synthesis of MK-7, MK-9, CoQ <sub>9</sub> .....	229
4.2.5. One-pot sequence.....	233
4.3. Summary.....	234
4.4. References.....	235
4.5. Experimental section.....	243
4.5.1. General information .....	243
4.5.2. Optimization details .....	244
4.5.3. Synthesis and characterization of substrates .....	245
4.5.4. General procedure for solvent-free $\alpha$ -allylation reactions .....	247
4.5.5. Large-scale reaction .....	248
4.5.6. Procedures for gram scale syntheses of MK-7, MK-9, and CoQ <sub>9</sub> .....	249
4.5.7. 1-Pot sequence .....	252

4.5.8. E Factor calculation .....	253
4.5.9. Calorimetry data.....	254
4.5.10. Analytical data .....	257
4.5.11. References .....	273
4.5.12. NMR spectra .....	274

# **I. Bisulfite addition compounds as substrates for reductive aminations in water**

Reproduced with permission from:

Li, X.; Iyer, K.S.; Thakore, R. R.; Bailey, J. D.; Leahy, D. K.; Lipshutz, B. H. “Bisulfite addition compounds as educts for reductive aminations in water.” *Org. Lett.* **2021**, *23*, 7205-7208.

Copyright © 2022 The Authors. Published by American Chemical Society. This publication is licensed under CC-BY-NC-ND 4.0.



## ***1.1. Background and introduction***

Reductive amination stands as a fundamental and pivotal strategy in the direct synthesis of secondary and tertiary amines via C-N bond formation, serving as a robust and strategic pathway that has found profound application, particularly within the realms of pharmaceutical and medicinal chemistry.<sup>1</sup> According to Roughley's analysis of pharmaceutical synthesis, a quarter of C-N bond-forming reactions involves reductive amination.<sup>2</sup>

Since its discovery in early 20<sup>th</sup> century, the field of reductive amination has witnessed remarkable advancements; from initial approaches utilizing stoichiometric amounts of metal hydrides such as NaBH<sub>4</sub>, NaBH<sub>3</sub>CN, and NaBH(OAc)<sub>3</sub>,<sup>3</sup> to later catalytic methods involving transition metals<sup>4-6</sup>, organocatalysts<sup>7</sup>, and enzymes.<sup>8-12</sup> Concurrently, the emergence of enantioselective reductive amination protocols has provided a powerful toolset for accessing chiral amines, which are prevalent in bioactive molecules and chiral catalysts.<sup>5,6,13</sup> Despite the numerous successes achieved in reductive amination chemistry, challenges persist, particularly pertaining to substrate scope, chemoselectivity, and regioselectivity, especially in the context of complex molecules. Moreover, developing methodologies that embrace the principles of green chemistry, which involve not only the use of nontoxic solvents but also the implementation of milder reaction conditions represents an ongoing and future direction in the field.

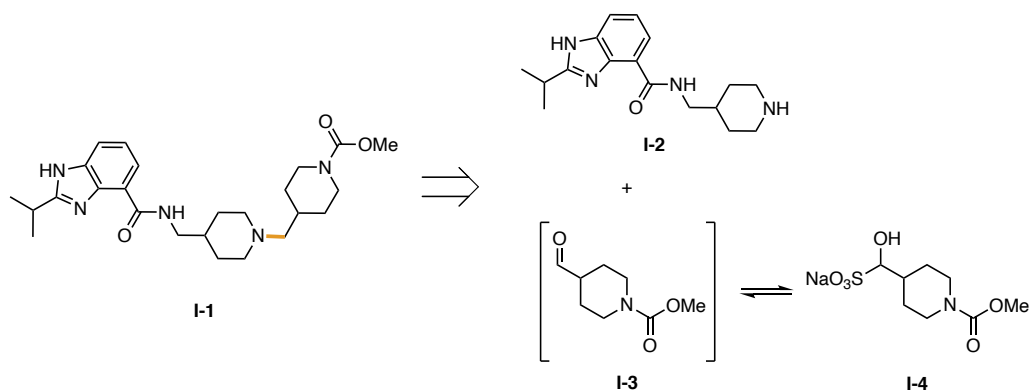
Aldehyde bisulfite addition compounds are generated *via* nucleophilic addition of bisulfite ion to the carbonyl group of an aldehyde. Historically, these adducts were primarily employed for the purification and characterization of aldehydes. In recent times, bisulfite adducts have gained prominence as substitutes for free aldehydes in reductive amination reactions. In 2003, Pfizer developed the first laboratory-scale method for bisulfite adduct utilization in reductive amination reactions, necessitated by the failure of traditional methods to convert the adduct

into its free aldehyde form.<sup>14</sup> The process was capable of being scaled up to 3 kilograms. However, it required harsh conditions, including the use of hazardous organic solvents (*i.e.* DMP and cyclohexane), as well as the requirement of azeotropic distillation to facilitate imine formation. Subsequent to this innovation, alternative methodologies have been developed, advocating for milder conditions and more streamlined operational procedures.<sup>15,16</sup> These newer methods enable *in situ* imine formation and reduced reaction temperatures. Nevertheless, they still depend on the utilization of organic solvents, such as methanol.

In 2021, Takeda reported a multistep synthesis of their 5-HT receptor agonist TAK-954, with each step prominently featuring water as the sole reaction medium.<sup>17</sup> This environmentally friendly method remarkably decreased material input by 77%, utilized 94% less organic solvent, and even reduced water usage by 48%, while simultaneously increasing the overall yield from 35% to 56%. A significant highlight of this method was the utilization of a reductive amination in the last step (*i.e.*, **I-2** + **I-3**; Scheme I-1). In this reductive amination process, the aldehyde bisulfite addition compound **I-4**, in equilibrium with its aldehyde equivalent **I-3**, was efficiently converted to the corresponding tertiary amine in aqueous micellar media using  $\alpha$ -picolineborane (1.5 equiv) as reducing agent. Interestingly, no external base was needed to convert the bisulfite addition compound **I-4** to its aldehydic state; the aqueous medium itself was adequate.

These existing reports indicate that when used in reductive amination reactions, bisulfite adduct offers several advantages:

1. Physical Form: Aldehyde bisulfite addition compounds, owing to their crystalline nature, present several handling and processing benefits. Unlike some aldehydes, which can be volatile or oily, the crystalline form of these adducts allows for straightforward weighing, transferring, and incorporation into reactions.



**Scheme I-1.** Key reductive amination involving bisulfite addition compound **I-4**; reducing agent =  $\alpha$ -picolineborane.

2. Stability: Bisulfite adducts of aldehydes offer enhanced stability compared to free aldehydes, which can undergo autooxidation or other side reactions. This protection of the reactive carbonyl group in the adduct form minimizes risks associated with degradation, ensuring a longer shelf-life and reducing the need for specialized storage conditions often required for sensitive aldehydes.

3. Enhanced Solubility: Aldehyde bisulfite adducts often exhibit enhanced solubility in aqueous media compared to their parent aldehydes. This can be especially advantageous in reductive amination reactions performed in aqueous systems.

4. Tunable Equilibrium: The balance between the free aldehyde and its bisulfite adduct can be modulated by altering parameters such as pH. This offers chemists a means to adjust the rate and extent of imine formation in reductive amination, potentially optimizing chemo-selectivity and overall yields.

5. Purification Opportunities: The transformation of an aldehyde to its bisulfite adduct results in well-defined crystalline solids. This inherent property provides an opportunity to employ recrystallization as a purification technique. Such a purification step is invaluable,

especially for aldehydes that may be tainted with oxidized impurities or contaminants acquired during synthesis or storage.

Owing to the considerable benefits presented by bisulfite addition compounds, coupled with the mild conditions and the aqueous-centric methodology demonstrated in the synthesis of TAK-954, this approach exhibits promise for wider applications. In this context, we undertook a detailed exploration of this process under green chemistry conditions, aiming to establish a sustainable, standardized protocol and assess its viability for the synthesis of a diverse array of pharmaceutical entities.

## ***1.2. Result and Discussion***

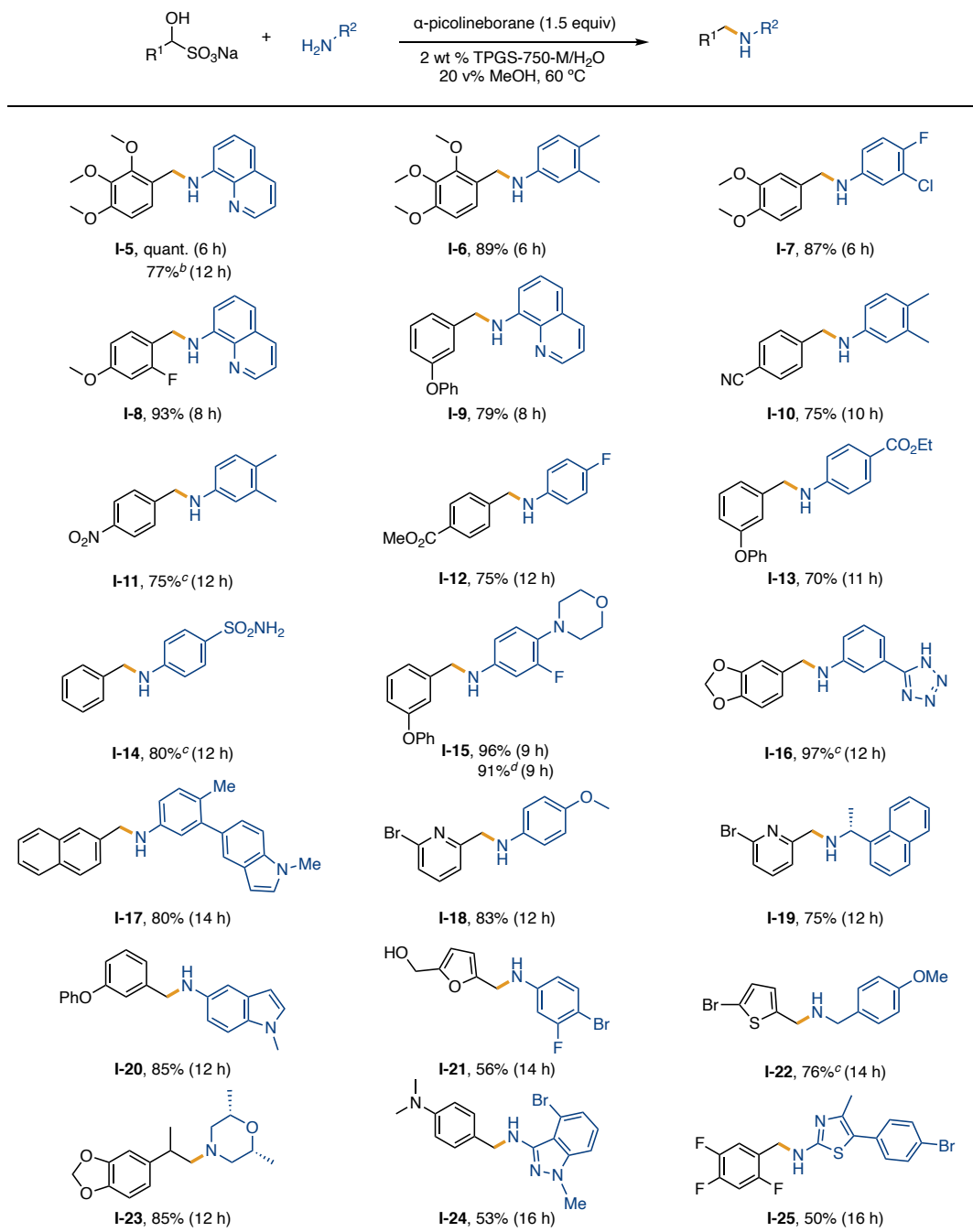
### ***1.2.1. Substrate scope***

Using the conditions previously optimized for TAK-954,<sup>14</sup> a series of reductive amination reactions starting with various functionalized bisulfite addition compounds and primary amines was investigated in order to establish the scope of these reductive aminations. The conditions involved encompassed use of an aqueous medium containing 2 wt % TPGS-750-M,<sup>18</sup> augmented by 20% v/v MeOH as co-solvent,<sup>19</sup> and  $\alpha$ -picolineborane (1.5 equiv)<sup>20,21</sup> as the hydride donor. As shown in Table I-1, most combinations afforded the desired products, isolated in typically  $\geq 70\%$  to quantitative yields. Several reducible groups are well-tolerated under standard conditions, including nitriles (**I-10**), nitro compounds (**I-11**), and esters (**I-12**, **I-13**), delivering the corresponding amine products in moderate yields. Notably, the method showcased adaptability with an expansive array of nitrogenous substrates like quinolines (**I-5**, **I-8**, **I-9**), morpholines (**I-15**, **I-23**), tetrazoles (**I-16**), indoles (**I-17**, **I-20**), pyridines (**I-19**), indazoles (**I-24**), and thiazoles (**I-25**). This broad substrate scope, especially with nitrogenous

moieties, underscores the potential utility of this methodology for synthesizing pharmaceutical-like targets.

Control experiments were conducted to gain deeper insights into the reaction conditions. Initially, utilizing free aldehyde in lieu of its bisulfite adduct yielded product **I-5** with a diminished yield (*i.e.*, quantitative to 77%). Additionally, the reaction necessitated an extended duration to reach completion. This reduced efficiency can be attributed to competitive reduction processes of aldehyde leading to the formation of the corresponding alcohol. Such findings highlight the superior chemoselectivity offered by bisulfite adducts. Further investigation was carried out to test the necessity of a co-solvent in the synthesis, particularly with a complex product like **I-15**. Remarkably, the complete omission of MeOH from the reaction system had minimal impact on overall efficiency. The product was obtained in comparable yields within the same nine-hour duration, implying that the incorporation of the co-solvent might be dispensable in certain scenarios.

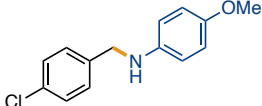
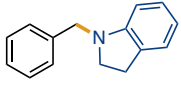
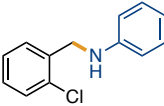
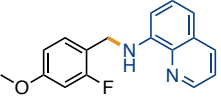
**Table I-1.** Representative products from reductive aminations in aqueous nanoreactors<sup>a</sup>



<sup>a</sup>Reaction conditions unless otherwise noted: 0.20 mmol of amine, 0.30 mmol of bisulfite adduct, 0.30 mmol  $\alpha$ -picolineborane, stirred in 2 wt % TPGS-750-M/H<sub>2</sub>O and 20 v % MeOH, 60 °C. Yields are for isolated purified products. <sup>b</sup>Free aldehyde instead of bisulfite adduct. <sup>c</sup>Run with 20 mol % HOAc present. <sup>d</sup>Without 20 v % MeOH as co-solvent.

In evaluating the efficiency of our approach, it was important to compare it with existing methodologies, even though many of these recent strategies predominantly engage simpler amines. As listed in Table I-2, the initial three cases document a consistent trend associated with these recent strategies that lead to low-to-modest yields,<sup>22-24</sup> regardless of the choice of metal catalyst or the reaction environment. In the last case, our preceding methodology could only realize a maximum yield of 75% for secondary amines.<sup>25</sup> When compared to outcomes from our aqueous micellar approach with conventional methods, which frequently employ organic solvents, elevated thermal conditions, and occasionally specialized equipment to manage the inherent pressures, the merits of our strategy become evident. It not only offers more benign reaction conditions but also demonstrates heightened precision and superior efficiency.

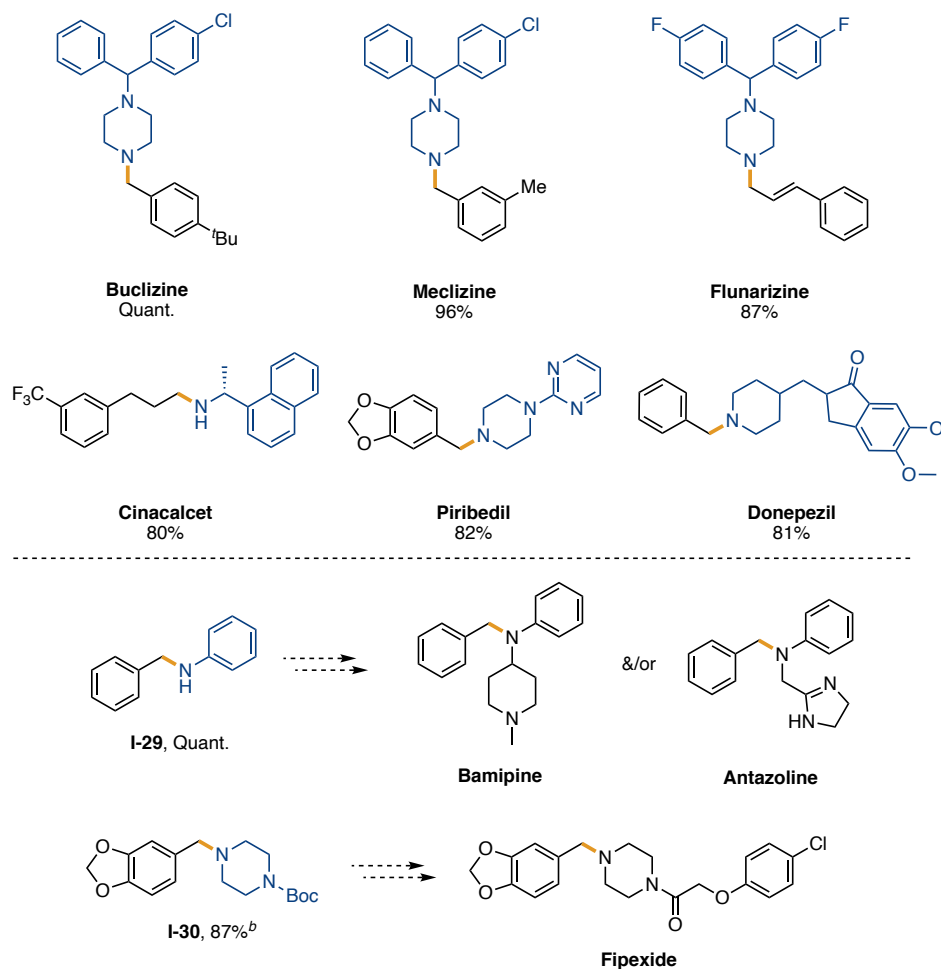
**Table I-2.** Comparison cases: representative literature methods vs. this work.

2° amines from reductive aminations	Literature condition:	our condition (yield, %)
 <p>I-26</p>	4 mol% Fe <sub>3</sub> (CO) <sub>12</sub> 50 bar H <sub>2</sub> toluene, 65 °C <b>73% yield<sup>22</sup></b>	Quant.
 <p>I-27</p>	5 mol% nanoporous Au 8 atm H <sub>2</sub> EtOH, 90 °C <b>53% yield<sup>23</sup></b>	88%
 <p>I-28</p>	Pd/ImS3-14 (540 ppm Pd) 5 equiv HCOOH 5 equiv NaCOOH iPrOH/H <sub>2</sub> O, 70 °C <b>35% yield<sup>24</sup></b>	Quant.
 <p>I-8</p>	8000 ppm 1 wt% Pd/C 1.5 equiv Et <sub>3</sub> SiH 2 wt% TPGS-750-M, 45°C <b>75% yield<sup>25</sup></b>	93%

### 1.2.2. Application: API synthesis and 1-pot sequence

In an effort to showcase the practical utility of reductive amination conducted under aqueous conditions, a series of recognized pharmaceuticals and drug intermediates were synthesized. The resultant secondary and tertiary amines echo key structural motifs characteristic of established active pharmaceutical ingredients (APIs).

**Figure I-1.** Reductive aminations used to prepare known targets in the pharma space<sup>a</sup>



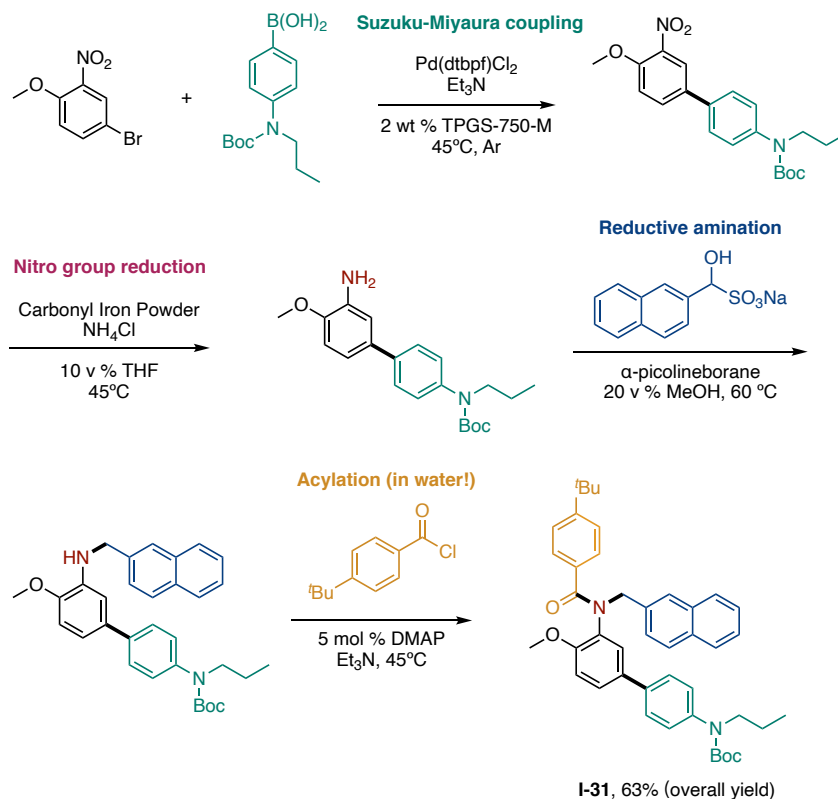
As shown in Figure I-1, several pharmaceuticals that have been prepared by leveraging the principles of reductive amination include: (a) Buclizine: an antihistamine and antiemetic compound;<sup>26</sup> (b) Meclizine: administered primarily to mitigate or prevent symptoms such as nausea, vomiting, and dizziness stemming from motion sickness;<sup>27</sup> (c) Flunarizine: Functions



as a selective calcium entry blocker;<sup>28</sup> (d) Cinacalcet: acts as a calcium-sensing receptor agonist;<sup>29</sup> (e) Piribedil: employed in addressing Parkinson's disease;<sup>30</sup> (f) Donepezil: prescribed for alleviating behavioral and cognitive manifestations observed in Alzheimer's Disease and other forms of dementia;<sup>31</sup> intermediate **I-29** which plays a pivotal role in the synthesis of both Bamipine: an antipruritic ointment,<sup>32</sup> and Antazoline: an antihistamine;<sup>33</sup> Furthermore, compound **I-30** has been established as a precursor integral to the synthesis of Fipexide, a nootropic pharmaceutical primarily prescribed for treating senile dementia.<sup>34</sup> The success of these applications highlights that the aqueous-based reductive amination approach serves as a robust methodology for synthesizing key pharmaceutical entities. Furthermore, it accentuates the method's versatility and potential as an instrumental tool in contemporary drug synthesis and development.

As aqueous chemistry technologies have evolved, the spectrum of reactions amenable to continuous, one-pot sequences has seen a marked expansion.<sup>35</sup> Notably, our reductive amination protocols have demonstrated compatibility with various other reaction types when conducted under micellar conditions, thereby facilitating the construction of complex molecular structures. As illustrated in the example shown Scheme I-2, the synthetic pathway initiates with a Suzuki-Miyaura coupling,<sup>36</sup> producing a biaryl compound containing a nitro group. Bypassing the need for isolation, this structure directly undergoes reduction via carbonyl iron powder (CIP)<sup>37</sup> leading to the generation of an aniline derivative. This primary amine subsequently engages in a reductive amination with the bisulfite adduct derived from 2-naphthaldehyde. The resulting secondary amine, in the following step, is subjected to acylation using an acid chloride, leading to formation of the final amide, compound **I-31**. Remarkably, this 4-step sequence is all done in a singular vessel utilizing the same aqueous medium, while the process achieves a commendable overall yield of 63%.

The adoption of such telescoped methodologies provides several noteworthy advantages. Foremost among these is a significant reduction in waste generation, mainly attributed to the omission of intermediate product separation and purification processes. This strategy also improves time efficiency, enhancing rates from reactants to final products.<sup>38</sup> Additionally, the nature of one-pot synthesis fits seamlessly with pot economy principles; the single-vial approach throughout the synthesis increases planetary resource conservation and process simplification.<sup>39</sup> Collectively, these advantages highlight the alignment of this method with the goals of sustainable and efficient chemical synthesis, heralding it as a foundational approach for future work in the discipline.

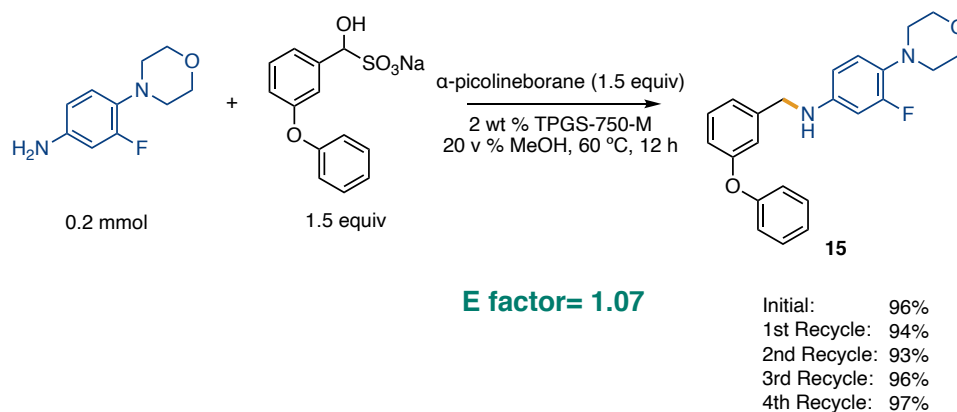


**Scheme I-2.** 4-Step, 1-pot sequence run in water without isolation of intermediates

### 1.2.3. Recycling and E Factor calculations

Aqueous chemistry usually presents opportunities for recycling the reaction media,<sup>40</sup> and the potential for reusing the aqueous medium in these reductive amination reactions was also explored. Following the initial conversion which resulted in a 96% yield of the secondary amine **I-15**, as detailed in Scheme I-2, the product was efficiently isolated by simple decantation. Thereafter, the same aqueous reaction mixture could be reused for an additional four cycles. Impressively, the yields across these subsequent runs remained consistent, oscillating between 93% and 97%. Such results point to the environmental benefits of this approach: substantial reduction in waste generation by recycling the medium while maintaining reaction efficiency.

The E Factor was utilized to evaluate the environmental impact of this methodology,<sup>41</sup> focusing primarily on the solvent contributions (methanol and water). The resulting E Factor of 1.07 is indicative of the environmentally respectful nature of this approach. It's worth noting that over time the water used might become “polluted” with surfactants, salts, etc., leading to downstream wastewater concerns. However, a recent disclosure by Novartis delineates one effective strategy for mitigating this specific challenge.<sup>42</sup>



**Scheme I-3.** Recycling study and E Factor evaluation

### 1.3. Summary

In summary, the method of reductive amination using shelf-stable bisulfite addition compounds has been validated as a versatile technology, well-suited for micellar conditions in recyclable water. Our methodology showcases a broad substrate range, and its efficacy is highlighted by successful syntheses of multiple pharmaceutical targets, underscoring its pivotal role in modern pharmaceutical synthesis. Comparative analyses illustrate the competitiveness of our approach *versus* traditional methods, emphasizing the greener and more efficient reaction conditions involved. Furthermore, the feasibility of integrating reductive amination into a multi-step aqueous sequence without the need for isolating intermediates was convincingly demonstrated. The potential for recycling the aqueous reaction medium while maintaining consistent yields over multiple runs further bolsters the environmental merits of this technology. With an encouraging E Factor signaling our process's eco-responsibility, this research sets a benchmark for sustainable, efficient, and versatile chemical synthesis in the domain of pharmaceuticals.

### 1.4. References

1. Afanasyev, O. I.; Kuchuk, E.; Usanov, D. L.; Chusov, D. Reductive Amination in the Synthesis of Pharmaceuticals. *Chem. Rev.* **2019**, *119*, 11857–11911.
2. Roughley, S. D.; Jordan, A. M. The Medicinal Chemist's Toolbox: An Analysis of Reactions Used in the Pursuit of Drug Candidates. *J. Med. Chem.* **2011**, *54*, 3451–3479.
3. Abdel-Magid, A. F.; Mehrman, S. J. A Review on the Use of Sodium Triacetoxyborohydride in the Reductive Amination of Ketones and Aldehydes. *Org. Process Res. Dev.* **2006**, *10*, 971–1031.
4. Irrgang, T.; Kempe, R. Transition-Metal-Catalyzed Reductive Amination Employing Hydrogen. *Chem. Rev.* **2020**, *120*, 9583–9674.
5. Tian, Y.; Hu, L.; Wang, Y.-Z.; Zhang, X.; Yin, Q. Recent Advances on Transition-Metal-Catalysed Asymmetric Reductive Amination. *Org. Chem. Front.* **2021**, *8*, 2328–2342.

6. Reshi, N. U. D.; Saptal, V. B.; Beller, M.; Bera, J. K. Recent Progress in Transition-Metal-Catalyzed Asymmetric Reductive Amination. *ACS Catal.* **2021**, *11*, 13809–13837.
7. Tripathi, R.; Verma, S.; Pandey, J.; Tiwari, V. Recent Development on Catalytic Reductive Amination and Applications. *Curr. Org. Chem.* **2008**, *12*, 1093–1115.
8. Schrittwieser, J. H.; Velikogne, S.; Kroutil, W. Biocatalytic Imine Reduction and Reductive Amination of Ketones. *Adv. Synth. Catal.* **2015**, *357*, 1655–1685.
9. Grogan, G.; Turner, N. J. InspiRED by Nature: NADPH-Dependent Imine Reductases (IREDs) as Catalysts for the Preparation of Chiral Amines. *Chemistry – A European Journal* **2016**, *22*, 1900–1907.
10. Lenz, M.; Borlinghaus, N.; Weinmann, L.; Nestl, B. M. Recent Advances in Imine Reductase-Catalyzed Reactions. *World J Microbiol Biotechnol* **2017**, *33*, 199.
11. Mangas-Sanchez, J.; France, S. P.; Montgomery, S. L.; Aleku, G. A.; Man, H.; Sharma, M.; Ramsden, J. I.; Grogan, G.; Turner, N. J. Imine Reductases (IREDs). *Curr. Opin. Chem. Biol.* **2017**, *37*, 19–25.
12. Gilio, A. K.; Thorpe, T. W.; Turner, N.; Grogan, G. Reductive Aminations by Imine Reductases: From Milligrams to Tons. *Chem. Sci.* **2022**, *13*, 4697–4713.
13. Wang, C.; Xiao, J. Asymmetric Reductive Amination. In *Stereoselective Formation of Amines*; Li, W., Zhang, X., Eds.; Topics in Current Chemistry; Springer: Berlin, Heidelberg, 2014; pp 261–282.
14. Ragan, J. A.; Am Ende, D. J.; Brenek, S. J.; Eisenbeis, S. A.; Singer, R. A.; Tickner, D. L.; Teixeira, J. J.; Vanderplas, B. C.; Weston, N. Safe Execution of a Large-Scale Ozonolysis: Preparation of the Bisulfite Adduct of 2-Hydroxyindan-2-Carboxaldehyde and Its Utility in a Reductive Amination. *Org. Process Res. Dev.* **2003**, *7*, 155–160.
15. Barniol-Xicota, M.; Turcu, A. L.; Codony, S.; Escolano, C.; Vázquez, S. Direct Reductive Alkylation of Amine Hydrochlorides with Aldehyde Bisulfite Adducts. *Tetrahedron Lett.* **2014**, *55*, 2548–2550.
16. Faul, M.; Larsen, R.; Levinson, A.; Tedrow, J.; Vounatsos, F. Direct Reductive Amination of Aldehyde Bisulfite Adducts Induced by 2-Picoline Borane: Application to the Synthesis of a DPP-IV Inhibitor. *J. Org. Chem.* **2013**, *78*, 1655–1659.
17. Bailey, J. D.; Helbling, E.; Mankar, A.; Stirling, M.; Hicks, F.; Leahy, D. K. Beyond Organic Solvents: Synthesis of a 5-HT<sub>4</sub> Receptor Agonist in Water. *Green Chem.* **2021**, *23*, 788–795.
18. Lipshutz, B. H.; Ghorai, S.; Abela, A. R.; Moser, R.; Nishikata, T.; Duplais, C.; Krasovskiy, A.; Gaston, R. D.; Gadwood, R. C. TPGS-750-M: A Second-Generation Amphiphile for Metal-Catalyzed Cross-Couplings in Water at Room Temperature. *J. Org. Chem.* **2011**, *76*, 4379–4391.

19. Gabriel, C. M.; Lee, N. R.; Bigorne, F.; Klumphu, P.; Parmentier, M.; Gallou, F.; Lipshutz, B. H. Effects of Co-Solvents on Reactions Run under Micellar Catalysis Conditions. *Org. Lett.* **2017**, *19*, 194–197.
20. Cosenza, V. A.; Navarro, D. A.; Stortz, C. A. Usage of  $\alpha$ -Picoline Borane for the Reductive Amination of Carbohydrates. *Arkivoc* **2011**, *7*, 182–194.
21. Sato, S.; Sakamoto, T.; Miyazawa, E.; Kikugawa, Y. One-Pot Reductive Amination of Aldehydes and Ketones with  $\alpha$ -Picoline-Borane in Methanol, in Water, and in Neat Conditions. *Tetrahedron* **2004**, *60*, 7899–7906.
22. Fleischer, S.; Zhou, S.; Junge, K.; Beller, M. An Easy and General Iron-Catalyzed Reductive Amination of Aldehydes and Ketones with Anilines. *Chem. Asian J.* **2011**, *6*, 2240–2245.
23. Takale, B. S.; Feng, X.; Lu, Y.; Bao, M.; Jin, T.; Minato, T.; Yamamoto, Y. Unsupported Nanoporous Gold Catalyst for Chemoselective Hydrogenation Reactions under Low Pressure: Effect of Residual Silver on the Reaction. *J. Am. Chem. Soc.* **2016**, *138*, 10356–10364.
24. Drinkel, E. E.; Campedelli, R. R.; Manfredi, A. M.; Fiedler, H. D.; Nome, F. Zwitterionic-Surfactant-Stabilized Palladium Nanoparticles as Catalysts in the Hydrogen Transfer Reductive Amination of Benzaldehydes. *J. Org. Chem.* **2014**, *79*, 2574–2579.
25. Thakore, R. R.; Takale, B. S.; Casotti, G.; Gao, E. S.; Jin, H. S.; Lipshutz, B. H. Chemoselective Reductive Aminations in Aqueous Nanoreactors Using Parts per Million Level Pd/C Catalysis. *Org. Lett.* **2020**, *22*, 6324–6329.
26. Mostafa, G. A. E.; Al-Badr, A. A. Chapter 1 - Buclizine. In *Profiles of Drug Substances, Excipients and Related Methodology*; Brittain, H. G., Ed.; Academic Press, 2011; Vol. 36, pp 1–33.
27. Cohen, B.; deJong, J. M. B. V. Meclizine and Placebo in Treating Vertigo of Vestibular Origin: Relative Efficacy in a Double-Blind Study. *Arch. Neurol.* **1972**, *27*, 129–135.
28. Amery, W. K. Flunarizine, a Calcium Channel Blocker: A New Prophylactic Drug in Migraine. *Headache J. Head Face Pain* **1983**, *23*, 70–74.
29. Iqbal, J.; Zaidi, M.; Schneider, A. E. Cinacalcet Hydrochloride (Amgen). *IDrugs: Investig. Drugs J.* **2003**, *6*, 587-592.
30. Perez-Lloret, S.; Rascol, O. Piribedil for the Treatment of Motor and Non-Motor Symptoms of Parkinson Disease. *CNS Drugs* **2016**, *30*, 703–717.
31. Dooley, M.; Lamb, H. M. Donepezil: A Review of Its Use in Alzheimer's Disease. *Drugs Aging* **2000**, *16*, 199–226.

32. Birknes, B. An Antihistaminic Agent: Soventol Hydrochloride Monohydrate Ethanol Solvate. *Acta Crystallogr. Sect. B* **1977**, *33*, 2301–2303.
33. Bertolasi, V.; Borea, P. A.; Gilli, G. Antazoline Hydrochloride. *Acta Crystallogr. Sect. B* **1982**, *38*, 2522–2525.
34. Bompani, R.; Scali, G. Fipexide, an Effective Cognition Activator in the Elderly: A Placebo-Controlled, Double-Blind Clinical Trial. *Curr. Med. Res. Opin.* **1986**, *10*, 99–106.
35. Cortes-Clerget, M.; Yu, J.; Kincaid, J. R. A.; Walde, P.; Gallou, F.; Lipshutz, B. H. Water as the Reaction Medium in Organic Chemistry: From Our Worst Enemy to Our Best Friend. *Chem. Sci.* **2021**, *12*, 4237–4266.
36. Lipshutz, B. H.; Abela, A. R. Micellar Catalysis of Suzuki–Miyaura Cross-Couplings with Heteroaromatics in Water. *Org. Lett.* **2008**, *10*, 5329–5332.
37. Lee, N. R.; Bikovtseva, A. A.; Cortes-Clerget, M.; Gallou, F.; Lipshutz, B. H. Carbonyl Iron Powder: A Reagent for Nitro Group Reductions under Aqueous Micellar Catalysis Conditions. *Org. Lett.* **2017**, *19*, 6518–6521.
38. Hayashi, Y. Time Economy in Total Synthesis. *J. Org. Chem.* **2021**, *86*, 1–23.
39. Hayashi, Y. Pot Economy and One-Pot Synthesis. *Chem. Sci.* **2016**, *7*, 866–880.
40. Lipshutz, B. H.; Isley, N. A.; Fennewald, J. C.; Slack, E. D. Cover Picture: On the Way Towards Greener Transition-Metal-Catalyzed Processes as Quantified by E Factors. *Angew. Chem., Int. Ed.* **2013**, *52*, 10911–10911.
41. Sheldon, R. A. E Factors, Green Chemistry and Catalysis: An Odyssey. *Chem. Commun.* **2008**, 3352.
42. Krell, C.; Schreiber, R.; Hueber, L.; Sciascera, L.; Zheng, X.; Clarke, A.; Haenggi, R.; Parmentier, M.; Baguia, H.; Rodde, S.; Gallou, F. Strategies to Tackle the Waste Water from  $\alpha$ -Tocopherol-Derived Surfactant Chemistry. *Org. Process Res. Dev.* **2021**, *25*, 900–915.

## ***1.5. Experimental section***

### ***1.5.1. General information***

Reagents and chemicals were purchased from Sigma-Aldrich, Combi-Blocks, Alfa Aesar, or Acros Organics and used without further purification.  $\alpha$ -Picolineborane was purchased from Sigma-Aldrich. Deuterated solvents were purchased from Cambridge Isotopes Laboratories. TPGS-750-M is either prepared or supplied by PHT International (also available from Sigma-Aldrich catalog #733857). The desired 2 wt % of surfactant solution in HPLC water was prepared by dissolving 2 g of surfactant to 98 g of HPLC water (which was degassed with argon prior to use) and stored under argon.

Thin-layer chromatography (TLC) was performed using Silica Gel 60 F254 plates (Merck, 0.25 mm thick). Flash chromatography is either performed in an automated Biotage system using Silica Gel 60 (Silicycle, 40-63 nm).

$^1\text{H}$  and  $^{13}\text{C}$  NMR spectra were recorded on either a Bruker Avance III HD 400 MHz (400 MHz for  $^1\text{H}$ , 100 MHz for  $^{13}\text{C}$ ), a Bruker Avance NEO 500 MHz (500 MHz for  $^1\text{H}$ , 125 MHz for  $^{13}\text{C}$ ) or on a Varian Unity Inova 500 MHz (500 MHz for  $^1\text{H}$ , 125 MHz for  $^{13}\text{C}$ );  $\text{D}_2\text{O}$ ,  $\text{CDCl}_3$  and  $\text{CD}_3\text{OD}$  were used as solvent. Residual peaks for  $\text{H}_2\text{O}$  in  $\text{D}_2\text{O}$  ( $^1\text{H} = 4.76$  ppm),  $\text{CHCl}_3$  in  $\text{CDCl}_3$  ( $^1\text{H} = 7.26$  ppm,  $^{13}\text{C} = 77.20$  ppm),  $\text{CD}_3\text{OD}$  in  $\text{CH}_3\text{OH}$  ( $^1\text{H} = 3.31$  ppm,  $^{13}\text{C} = 49.00$  ppm) have been assigned. The chemical shifts are reported in part per million (ppm), the coupling constants  $J$  values are given in hertz (Hz). The peak patterns are indicated as follows: bs, broad singlet; s, singlet; d, doublet; t, triplet; q, quartet; p, pentet; m, multiplet.

HRMS were recorded on a Waters Micromass LCT TOF ES+ Premier mass spectrometer using ESI ionization.



### ***1.5.2. General procedure for the preparation of a bisulfite adduct***

To a stirred solution of the aldehyde (5 mmol) in ethanol (0.5 M, 10 mL) at rt was added dropwise a solution of sodium metabisulfite ( $\text{Na}_2\text{S}_2\text{O}_5$ , 0.7 equiv, 3.5 mmol, 665.4 mg) in water (5 M with respect to aldehyde; 1 mL). The resulting suspension was stirred at 60 °C in oil bath overnight. Stirring was then stopped and the reaction vial was transferred to a refrigerator at -20 °C for 1 h. The product was then filtered with a Büchner funnel, with the minimum amount of methanol being used to help transfer the product. The filter cake was washed with hexane and dried *in vacuo* to afford the bisulfite adducts as white powders.

### ***1.5.3. General procedure for reductive amination***

#### ***(a) General procedure for reductive amination using a bisulfite adduct.***

$\alpha$ -Picolineborane (1.5 equiv, 0.3 mmol, 32.1 mg) was added to a 1-dram vial along with a Teflon-coated magnetic stir bar. Bisulfite adducts (1.5 equiv, 0.3 mmol) and any solid amine (1 equiv, 0.2 mmol, 1.0 equiv) were then added to this vial. The vial was capped with a rubber septum and then evacuated and backfilled with argon for three times. Next, 20 v% MeOH (0.08 mL) and 2 wt % TPGS-750-M solution in water (0.32 mL) was added via syringes through the septum. If the starting material amine is a liquid, then it was added *via* micro-syringe before the addition of solvent. The vial was then heated at 60 °C and stirred vigorously in an aluminum block placed over IKA hot plate overnight. After the reaction, the septum was removed. Minimal EtOAc (~1 mL) was added, and the mixture was stirred gently for 1 min. Stirring was stopped and the organic layer was then allowed to separate, after which it was removed *via* pipette. The same extraction procedure was repeated, after which silica was added to the combined organic extracts without further drying. Volatiles were evaporated under reduced pressure and semi-pure product was purified by flash chromatography over silica gel using EtOAc and hexanes as eluent.

*(b) General procedure reductive amination with the addition of acetic acid*

To a 1-dram vial charged with a Teflon-coated magnetic stir bar, bisulfite adducts (1.5 equiv, 0.3 mmol), and any solid amine (1 equiv, 0.2 mmol, 1.0 equiv) were added. The vial was capped with a rubber septum and then evacuated and backfilled with argon for three times. Next, 2 wt % TPGS-750-M / water solution (0.32 mL) and acetic acid (20 mol %, 0.04 mmol, 2.3  $\mu$ L) was added via syringes through the septum. If the starting material amine is a liquid, then it was added via micro-syringe before the addition of solvent. The vial was then heated at 60 °C and stirred vigorously for 2-3 h until the imine is observed to be formed by TLC. A sample of a  $\alpha$ -picolineborane/MeOH stock solution\* (20 v %, 0.08 mL) was added *via* syringe through the septum in one portion. Then, the reaction was heated in an aluminum block placed over IKA hot plate overnight. After the reaction, the septum was removed. Minimal EtOAc (~1 mL) was added, and the mixture was stirred gently for 1 min. Stirring was stopped and the organic layer was then allowed to separate, after which it was removed *via* pipette. The same extraction procedure was repeated, silica was added to the combined organic extracts without further drying. Volatiles were evaporated under reduced pressure and semi-pure product was purified by flash chromatography over silica gel using EtOAc and hexanes or methanol and DCM as eluent.

\* The  $\alpha$ -picolineborane/MeOH stock solution was prepared by dissolving 80.2 mg of  $\alpha$ -picolineborane into 0.2 mL MeOH.

*(c) General procedure reductive amination without co-solvent*

$\alpha$ -Picolineborane (1.5 equiv, 0.3 mmol, 32.1 mg) was added to a 1-dram vial along with a Teflon-coated magnetic stir bar. Bisulfite adducts (1.5 equiv, 0.3 mmol) and any solid amine (1.0 equiv, 0.2 mmol) were then added to this vial. The vial was capped with a rubber septum and then evacuated and backfilled with argon for three times. Next, 2 wt % TPGS-750-M

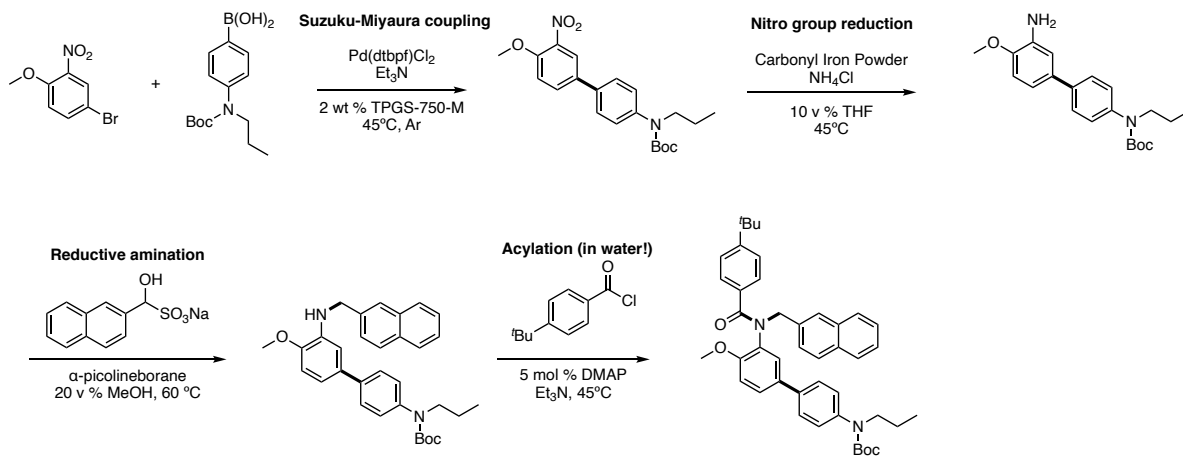
solution in water (0.4 mL, 0.5 M) was added via syringes through the septum. If the starting material amine is a liquid, then it was added *via* micro-syringe before the addition of solvent. The vial was then heated at 60 °C and stirred vigorously in an aluminum block placed over IKA hot plate overnight. After the reaction, the septum was removed. Minimal EtOAc (~1 mL) was added, and the mixture was stirred gently for 1 min. Stirring was stopped and the organic layer was then allowed to separate, after which it was removed *via* pipette. The same extraction procedure was repeated, after which silica was added to the combined organic extracts without further drying. Volatiles were evaporated under reduced pressure and semi-pure product was purified by flash chromatography over silica gel using EtOAc and hexanes as eluent.

*(d) General procedure reductive amination using free aldehyde*

$\alpha$ -Picolineborane (1.5 equiv, 0.3 mmol, 32.1 mg) was added to a 1-dram vial along with a Teflon-coated magnetic stir bar. Free aldehyde (1.5 equiv, 0.3 mmol) and any solid amine (1.0 equiv, 0.2 mmol) were then added to this vial. The vial was capped with a rubber septum and then evacuated and backfilled with argon for three times. Next, 20 v% MeOH (0.08 mL) and 2 wt % TPGS-750-M solution in water (0.32 mL) was added via syringes through the septum. If the starting material amine is a liquid, then it was added *via* micro-syringe before the addition of solvent. The vial was then heated at 60 °C and stirred vigorously in an aluminum block placed over IKA hot plate overnight. After the reaction, the septum was removed. Minimal EtOAc (~1 mL) was added, and the mixture was stirred gently for 1 min. Stirring was stopped and the organic layer was then allowed to separate, after which it was removed *via* pipette. The same extraction procedure was repeated, after which silica was added to the combined organic extracts without further drying. Volatiles were evaporated under reduced

pressure and semi-pure product was purified by flash chromatography over silica gel using EtOAc and hexanes as eluent.

#### 1.5.4. 1-pot sequence



##### 1<sup>st</sup> step: Suzuki–Miyaura coupling:

Pd(dtbpf)Cl<sub>2</sub> (1 mol %, 0.005 mmol, 3.3 mg) was weighed and then added to a 2-dram vial in the glovebox. The vial was then capped and removed from the glovebox. 4-Bromo-1-methoxy-2-nitrobenzene (1 equiv, 0.5 mmol, 116 mg) and (4-((t-butoxycarbonyl)propylamino)phenyl)boronic acid (1.5 equiv, 0.75 mmol, 207 mg) was then added sequentially to the vial. The vial was capped with a rubber septum and then evacuated and backfilled with argon for three times. Next, Et<sub>3</sub>N (3 equiv, 1.5 mmol, 0.21 mL), then 2 wt % TPGS-750-M aqueous solution (1 mL) was added via syringe through the septum. The vial was stirred vigorously at 45 °C in an aluminum block placed over IKA hot plate for 12 h.

##### 2<sup>nd</sup> step: Nitro group reduction:

After cooling to rt, the septum was removed and NH<sub>4</sub>Cl (3 equiv, 1.5 mmol, 80.2 mg) and carbonyl iron powder (5 equiv, 2.5 mmol, 140 mg), and THF (10 v %, 0.1 mL) were added. The vial was capped again and stirred vigorously at 45 °C in an aluminum block placed over IKA hot plate for 12 h.

*3<sup>rd</sup> step: Reductive amination:*

After cooling to rt, the cap was removed and sodium hydroxy(naphthalen-2-yl)methanesulfonate (1.5 equiv, 0.75 mmol, 195.18 mg) was added. The vial was then sealed with a new rubber septum and the headspace was purged using argon and a vent needle for 5 min. A sample of  $\alpha$ -picolineborane/MeOH stock solution\* (0.2 mL) was added via syringe through the septum in one portion. The mixture was stirred vigorously at 60 °C in an aluminum block placed over IKA hot plate for 12 h.

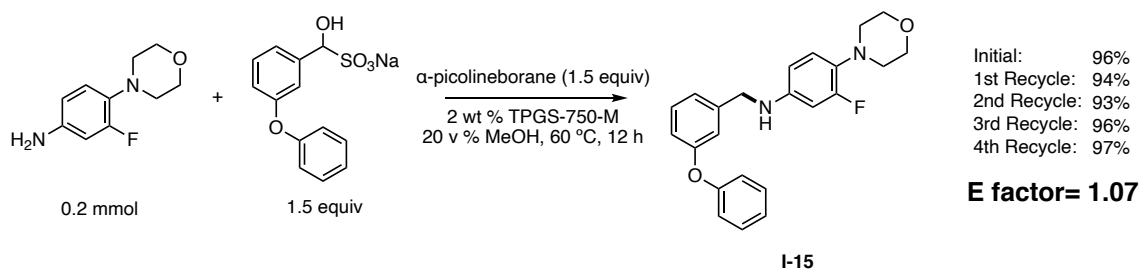
\* The  $\alpha$ -picolineborane/MeOH stock solution was prepared by dissolving 120.3 mg of  $\alpha$ -picolineborane into 0.3 mL MeOH.

*4<sup>th</sup> step: acylation:*

Subsequently, Et<sub>3</sub>N (3.0 equiv, 1.5 mmol, 0.21 mL), 4-(*t*-butyl)benzoyl chloride (1.5 equiv, 0.75 mmol 97.4  $\mu$ L) and DMAP (5 mol %, 0.025 mmol, 3.1 mg) were added. The mixture was stirred under 45 °C in an aluminum block placed over IKA hot plate for 6 h. Then a second portion of 4-(*t*-butyl)benzoyl chloride (1.5 equiv, 0.75 mmol 97.4  $\mu$ L) was added and the reaction mixture was allowed to stirred under 45 °C in an aluminum block placed over IKA hot plate for another 6 h.

Upon completion, the mixture was diluted with EtOAc and then combined directly with silica gel. The volatiles were evaporated under reduced pressure and semi-pure product was purified by flash chromatography over silica gel using 20% EtOAc in hexanes to afford **31** as a light-yellow oil (206.9 mg, 63% overall yield).

### 1.5.5. Recycle and E Factor study



*Recycle procedure:*

*Initial reaction:*

$\alpha$ -Picolineborane (1.5 equiv, 0.3 mmol, 32.1 mg) was added to a 1-dram vial along with a Teflon-coated magnetic stir bar. Sodium hydroxy(3-phenoxyphenyl)methane-sulfonate (1.5 equiv, 0.3 mmol, 97.7 mg) and 3-fluoro-4-morpholinoaniline (1 equiv, 0.2 mmol, 39.2 mg) were then added to this vial. The vial was capped with a rubber septum and then evacuated and backfilled with argon for three times. Next, 20 v% MeOH (0.08 mL) and 2 wt% TPGS-750-M aqueous solution (0.32 mL) was added via syringe through the septum. The vial was then heated at 60 °C and stirred vigorously in an aluminum block placed over IKA hot plate overnight. After the reaction, the product formed a brown oil layer on top of the aqueous TPGS-750-M solution. The TPGS-750-M solution was removed via syringe through the septum and then used for the 2nd recycle. The leftover mixture was purified directly by flash chromatography over silica gel using 15% EtOAc in hexanes as eluent to give 3-fluoro-4-morpholino-N-(3-phenoxybenzyl)aniline as a nearly colorless oil in 96% yield (72.6 mg).

*The 1st recycle:*

$\alpha$ -Picolineborane (1.5 equiv, 0.3 mmol, 32.1 mg) was added to a new 1-dram vial along with a Teflon-coated magnetic stir bar. Sodium hydroxy(3-phenoxyphenyl)methane-sulfonate (1.5 equiv, 0.5 mmol, 97.7 mg) and 3-fluoro-4-morpholinoaniline (1 equiv, 0.2 mmol, 39.2 mg) were then added to this vial. The vial was capped with a rubber septum and then evacuated

and backfilled with argon for three times. Next, the TPGS-750-M aqueous solution from the initial reaction was added via syringe through the septum. Additional MeOH was not added. The vial was then heated at 60 °C and stirred vigorously in an aluminum block placed over IKA hot plate overnight. After the reaction, the product again formed a brown oil layer on top of the aqueous TPGS-750-M solution. The TPGS-750-M solution was then removed via syringe through the septum and used for the 3rd recycle. The leftover mixture was purified directly by flash chromatography over silica gel using 15% EtOAc in hexanes as eluent to give 3-fluoro-4-morpholino-N-(3-phenoxybenzyl)aniline as a nearly colorless oil in 94% yield (71.1 mg).

*The 2nd recycle and 3rd recycle:*

The same procedure from the 1st recycle was repeated for the 2nd recycle (70.3 mg, 93% yield), and the 3rd recycle (72.6 mg, 96% yield).

*The 4th recycle:*

$\alpha$ -Picolineborane (1.5 equiv, 0.3 mmol, 32.1 mg) was added to a fresh 1-dram vial along with a Teflon-coated magnetic stir bar. Sodium hydroxy(3-phenoxy-phenyl)methanesulfonate (1.5 equiv, 0.3 mmol, 97.7 mg) and 3-fluoro-4-morpholino-aniline (1 equiv, 0.2 mmol, 39.2 mg) were then added to this vial. The vial was capped with a rubber septum and then evacuated and backfilled with argon for three times. Next, an aqueous TPGS-750-M solution from the initial reaction was added via syringe through the septum. The vial was then heated at 60 °C and stirred vigorously in an aluminum block placed over IKA hot plate overnight. After the reaction, the septum was removed. Minimal EtOAc (~1 mL) was added, and the mixture was stirred gently for 1 min. Stirring was stopped and the organic layer was then allowed to separate, after which it was removed via pipette. The same extraction procedure was repeated, silica was added to the combined organic extracts without further drying. The volatiles were

evaporated under reduced pressure and the mixture was purified directly by flash chromatography over silica gel using 15% EtOAc in hexanes as eluent give 3-fluoro-4-morpholino-N-(3-phenoxy-benzyl)aniline as a nearly colorless oil in 97% yield (72.6 mg).

*E Factor calculation:*

Mass of product:  $378 \text{ mg/mmol} \times 0.2 \text{ mmol} \times (96\% + 94\% + 93\% + 96\% + 97\%) = 359.9 \text{ mg}$

Mass if waste (consider both water and MeOH as waste):

MeOH:  $0.08 \text{ mL} \times 0.792 \text{ g/mL} = 63.4 \text{ mg}$

water:  $0.32 \text{ mL} \times 1 \text{ g/mL} = 320 \text{ mg}$

E Factor = mass of waste/mass of product =  $(63.4 \text{ mg MeOH} + 320 \text{ mg water})/359.9 \text{ mg product} = 1.07$

**1.5.6. Analytical data**

*Analytical data for bisulfite adducts*

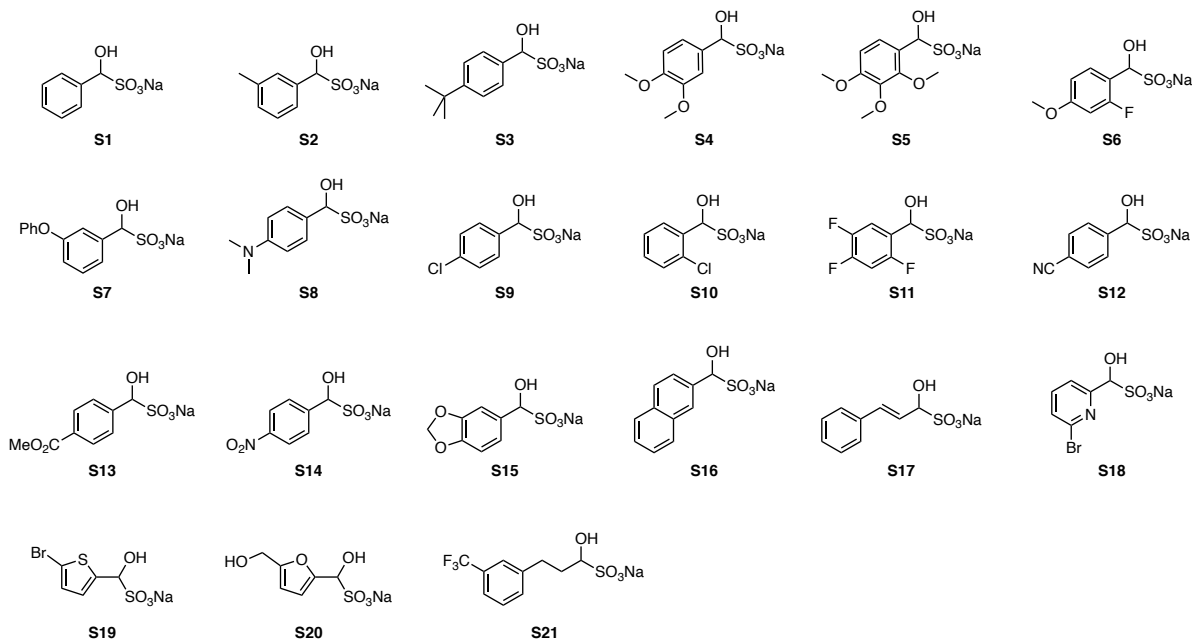
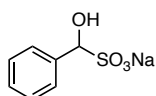


**Table I-3** Bisulfite adducts



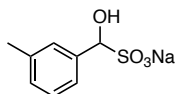


**Sodium hydroxy(phenyl)methanesulfonate (S1):**

White crystalline solid. 2.04 g, 97% yield (run on 10 mmol scale).

$^1\text{H NMR}$  (500 MHz,  $\text{D}_2\text{O}$ )  $\delta$  7.50 (dq,  $J = 6.5, 1.9$  Hz, 2H), 7.44 – 7.35 (m, 3H), 5.46 (d,  $J = 1.7$  Hz, 1H).

$^{13}\text{C NMR}$  (126 MHz,  $\text{D}_2\text{O}$ )  $\delta$  135.4, 129.2, 128.4, 127.6, 85.6.

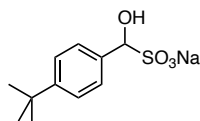


**Sodium hydroxy(*m*-tolyl)methanesulfonate (S2):**

White crystalline solid. 439.1 mg, 98% yield (run on 2 mmol scale).

$^1\text{H NMR}$  (500 MHz,  $\text{D}_2\text{O}$ )  $\delta$  7.36 – 7.16 (m, 4H), 5.42 (s, 1H), 2.30 (s, 3H).

$^{13}\text{C NMR}$  (126 MHz,  $\text{D}_2\text{O}$ )  $\delta$  138.5, 135.4, 129.8, 128.3, 128.2, 124.6, 85.6, 20.5.

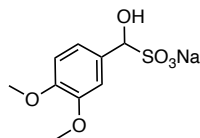


**Sodium (4-(*t*-butyl)phenyl)(hydroxy)methanesulfonate (S3):**

White crystalline solid. 1.26 g, 95% yield (run on 5 mmol scale).

$^1\text{H NMR}$  (500 MHz,  $\text{D}_2\text{O}$ )  $\delta$  7.49 – 7.41 (m, 4H), 5.42 (d,  $J = 1.8$  Hz, 1H), 1.24 (s, 9H).

$^{13}\text{C NMR}$  (126 MHz,  $\text{D}_2\text{O}$ )  $\delta$  152.8, 132.5, 127.5, 125.3, 85.4, 34.0, 30.5.

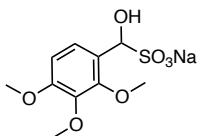


**Sodium (3,4-dimethoxyphenyl)(hydroxy)methanesulfonate (S4):**

White solid. 1.34 mg, 99% yield (run on 5 mmol scale).

**<sup>1</sup>H NMR** (500 MHz, D<sub>2</sub>O) δ 7.14 (d, *J* = 2.1 Hz, 1H), 7.05 (dd, *J* = 8.3, 2.1 Hz, 1H), 6.95 (d, *J* = 8.4 Hz, 1H), 5.38 (s, 1H), 3.80 (s, 3H), 3.78 (s, 3H).

**<sup>13</sup>C NMR** (126 MHz, D<sub>2</sub>O) δ 148.6, 147.7, 128.4, 121.0, 111.3, 110.8, 85.3, 55.6, 55.6.

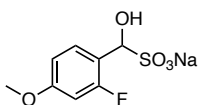


**Sodium hydroxy(2,3,4-trimethoxyphenyl)methanesulfonate (S5):**

White solid. 1.47 g, 98% yield (run on 5 mmol scale).

**<sup>1</sup>H NMR** (500 MHz, D<sub>2</sub>O) δ 7.33 (dd, *J* = 8.9, 1.1 Hz, 1H), 6.87 (dd, *J* = 8.9, 1.2 Hz, 1H), 5.73 (d, *J* = 1.2 Hz, 1H), 3.84 (d, *J* = 1.2 Hz, 3H), 3.81 (d, *J* = 1.2 Hz, 3H), 3.79 (d, *J* = 1.2 Hz, 3H).

**<sup>13</sup>C NMR** (126 MHz, D<sub>2</sub>O) δ 153.6, 151.1, 140.8, 123.2, 122.0, 108.6, 78.9, 61.7, 60.9, 56.0.

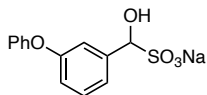


**Sodium (2-fluoro-4-methoxyphenyl)(hydroxy)methanesulfonate (S6):**

White solid. 735.3 mg, 95% yield (run on 3 mmol scale).

**<sup>1</sup>H NMR** (500 MHz, D<sub>2</sub>O) δ 7.50 (td, *J* = 8.7, 3.1 Hz, 1H), 6.80 (dt, *J* = 8.8, 3.0 Hz, 1H), 6.72 (dt, *J* = 12.2, 2.9 Hz, 1H), 5.70 (d, *J* = 3.1 Hz, 1H), 3.76 (d, *J* = 3.2 Hz, 3H).

**<sup>13</sup>C NMR** (126 MHz, D<sub>2</sub>O) δ 161.7, 160.9, 160.8, 159.7, 129.1, 129.0, 115.2, 115.0, 110.5, 110.5, 101.4, 101.2, 78.6, 78.6, 55.7.

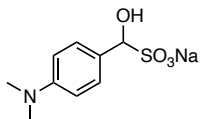


**Sodium hydroxy(3-phenoxyphenyl)methanesulfonate (S7):**

White crystalline solid. 1.46 g, 97% yield (run on 5 mmol scale).

$^1\text{H NMR}$  (500 MHz,  $\text{D}_2\text{O}$ )  $\delta$  7.40 – 7.32 (m, 3H), 7.27 (dt,  $J = 7.8, 1.5$  Hz, 1H), 7.15 (dd,  $J = 2.7, 1.5$  Hz, 2H), 7.01 (dddd,  $J = 9.2, 8.1, 2.4, 1.2$  Hz, 3H), 5.40 (s, 1H)

$^{13}\text{C NMR}$  (126 MHz,  $\text{D}_2\text{O}$ )  $\delta$  156.6, 156.5, 137.5, 130.1, 129.9, 123.9, 122.8, 119.3, 119.0, 117.9, 85.1.

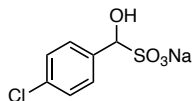


**Sodium (4-(dimethylamino)phenyl)(hydroxy)methanesulfonate (S8):**

Pale yellow solid. 1.1 g, 88% yield (run on 5 mmol scale).

$^1\text{H NMR}$  (400 MHz,  $\text{D}_2\text{O}$ )  $\delta$  7.42 (d,  $J = 8.3$  Hz, 2H), 7.02 (d,  $J = 8.4$  Hz, 2H), 5.37 (s, 1H), 2.86 (s, 6H).

$^{13}\text{C NMR}$  (101 MHz,  $\text{D}_2\text{O}$ )  $\delta$  128.8, 115.9, 85.2, 42.0.

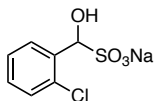


**Sodium (4-chlorophenyl)(hydroxy)methanesulfonate (S9):**

White solid. 478.4 mg, 98% yield (run on 2 mmol scale).

$^1\text{H NMR}$  (500 MHz,  $\text{D}_2\text{O}$ )  $\delta$  7.49 – 7.43 (m, 2H), 7.41 – 7.36 (m, 2H), 5.45 (s, 1H).

$^{13}\text{C NMR}$  (126 MHz,  $\text{D}_2\text{O}$ )  $\delta$  134.3, 134.1, 129.1, 128.4, 84.9.

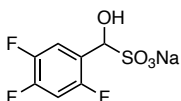


**Sodium (2-chlorophenyl)(hydroxy)methanesulfonate (S10):**

White solid. 473.4 mg, 97% yield (run on 2 mmol scale).

$^1\text{H NMR}$  (500 MHz,  $\text{D}_2\text{O}$ )  $\delta$  7.68 – 7.65 (m, 1H), 7.43 – 7.40 (m, 1H), 7.36 – 7.32 (m, 2H), 5.98 (d,  $J = 1.9$  Hz, 1H).

$^{13}\text{C NMR}$  (126 MHz,  $\text{D}_2\text{O}$ )  $\delta$  133.3, 133.3, 130.5, 129.4, 128.6, 127.2, 81.3.

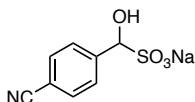


**Sodium hydroxy(2,4,5-trifluorophenyl)methanesulfonate (S11):**

White solid. 776.2 mg, 98% yield (run on 3 mmol scale).

$^1\text{H NMR}$  (400 MHz,  $\text{D}_2\text{O}$ )  $\delta$  9.99 (ddd,  $J = 10.6, 8.9, 6.4$  Hz, 1H), 9.67 – 9.56 (m, 1H), 8.24 (s, 1H).

$^{13}\text{C NMR}$  (126 MHz,  $\text{D}_2\text{O}$ )  $\delta$  156.3, 156.3, 156.2, 156.2, 154.3, 154.3, 154.2, 151.3, 151.2, 151.1, 149.3, 149.2, 147.8, 147.7, 145.8, 145.8, 145.7, 145.7, 119.9, 119.9, 119.9, 119.8, 119.8, 119.7, 116.3, 116.3, 116.2, 116.1, 105.8, 105.6, 105.5, 105.4, 78.0.

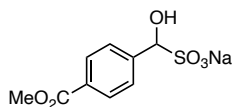


**Sodium (4-cyanophenyl)(hydroxy)methanesulfonate (S12):**

White solid. 676.8 mg, 96% yield (run on 3 mmol scale).

$^1\text{H NMR}$  (500 MHz,  $\text{D}_2\text{O}$ )  $\delta$  7.72 (d,  $J = 8.3$  Hz, 2H), 7.64 (d,  $J = 8.2$  Hz, 2H), 5.55 (s, 1H).

$^{13}\text{C}$  NMR (126 MHz,  $\text{D}_2\text{O}$ )  $\delta$  141.1, 132.3, 128.2, 119.5, 111.4, 84.9.

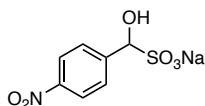


**Sodium hydroxy(4-(methoxycarbonyl)phenyl)methanesulfonate (S13):**

White solid. 1.3 g, 96% yield (run on 5 mmol scale).

$^1\text{H}$  NMR (500 MHz,  $\text{D}_2\text{O}$ )  $\delta$  7.95 (d,  $J = 8.2$  Hz, 2H), 7.59 (d,  $J = 8.3$  Hz, 2H), 5.53 (s, 1H), 3.85 (s, 3H).

$^{13}\text{C}$  NMR (126 MHz,  $\text{D}_2\text{O}$ )  $\delta$  169.1, 140.9, 129.9, 129.3, 127.8, 85.1, 52.7.

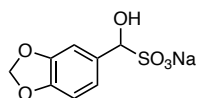


**Sodium hydroxy(4-nitrophenyl)methanesulfonate (S14):**

White solid. 711.5 mg, 93% yield (run on 3 mmol scale).

$^1\text{H}$  NMR (500 MHz,  $\text{D}_2\text{O}$ )  $\delta$  8.23 – 8.15 (m, 2H), 7.70 (dd,  $J = 9.0, 2.4$  Hz, 2H), 5.60 (d,  $J = 3.2$  Hz, 1H).

$^{13}\text{C}$  NMR (126 MHz,  $\text{D}_2\text{O}$ )  $\delta$  147.8, 143.0, 128.6, 123.4, 84.7.

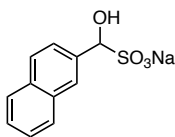


**Sodium benzo[d][1,3]dioxol-5-yl(hydroxy)methanesulfonate (S15):**

White solid. 1.17 g, 92% yield (run on 5 mmol scale).

$^1\text{H}$  NMR (500 MHz,  $\text{D}_2\text{O}$ )  $\delta$  7.01 (d,  $J = 2.0$  Hz, 1H), 6.97 (dt,  $J = 8.0, 2.2$  Hz, 1H), 6.84 (dd,  $J = 8.1, 2.2$  Hz, 1H), 5.92 (d,  $J = 2.2$  Hz, 2H), 5.36 (d,  $J = 2.2$  Hz, 1H).

$^{13}\text{C}$  NMR (126 MHz,  $\text{D}_2\text{O}$ )  $\delta$  147.7, 147.0, 129.3, 121.9, 108.2, 107.8, 101.3, 85.3.

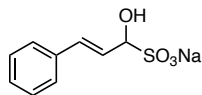


**Sodium hydroxy(naphthalen-2-yl)methanesulfonate (S16):**

White solid. 1.27 g, 98% yield (run on 5 mmol scale).

$^1\text{H}$  NMR (500 MHz,  $\text{D}_2\text{O}$ )  $\delta$  7.98 (d,  $J = 1.7$  Hz, 1H), 7.94 – 7.85 (m, 3H), 7.66 – 7.60 (m, 1H), 7.57 – 7.48 (m, 2H), 5.62 (d,  $J = 2.5$  Hz, 1H).

$^{13}\text{C}$  NMR (126 MHz,  $\text{D}_2\text{O}$ )  $\delta$  133.2, 133.1, 132.6, 128.2, 127.9, 127.7, 127.2, 126.8, 126.6, 125.0, 85.7.

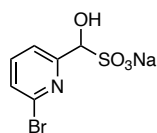


**Sodium (*E*)-1-hydroxy-3-phenylprop-2-ene-1-sulfonate (S17):**

White solid. 1.1 g, 90% yield (run on 5 mmol scale).

$^1\text{H}$  NMR (500 MHz,  $\text{D}_2\text{O}$ )  $\delta$  7.50 – 7.44 (m, 2H), 7.39 – 7.27 (m, 3H), 6.82 (d,  $J = 16.0$  Hz, 1H), 6.32 (dd,  $J = 16.0, 7.0$  Hz, 1H), 5.04 (dd,  $J = 7.0, 1.3$  Hz, 1H).

$^{13}\text{C}$  NMR (126 MHz,  $\text{D}_2\text{O}$ )  $\delta$  135.8, 135.1, 128.9, 128.6, 126.8, 122.7, 84.8.

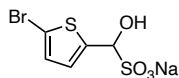


**Sodium (6-bromopyridin-2-yl)(hydroxy)methanesulfonate (S18):**

Pale yellow solid. 1.39 g, 96% yield (run on 5 mmol scale).

$^1\text{H NMR}$  (500 MHz,  $\text{D}_2\text{O}$ )  $\delta$  7.70 (dtt,  $J = 8.1, 6.0, 2.9$  Hz, 1H), 7.61 – 7.53 (m, 2H), 5.49 – 5.40 (m, 1H).

$^{13}\text{C NMR}$  (126 MHz,  $\text{D}_2\text{O}$ )  $\delta$  155.8, 140.3, 140.2, 128.7, 121.9, 85.1.

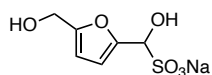


**Sodium (5-bromothiophen-2-yl)(hydroxy)methanesulfonate (S19):**

Pale yellow solid. 1.38 g, 94% yield (run on 5 mmol scale).

$^1\text{H NMR}$  (500 MHz,  $\text{D}_2\text{O}$ )  $\delta$  7.02 (dd,  $J = 3.8, 0.9$  Hz, 1H), 6.99 (dt,  $J = 3.8, 0.9$  Hz, 1H), 5.63 (t,  $J = 0.8$  Hz, 1H).

$^{13}\text{C NMR}$  (126 MHz,  $\text{D}_2\text{O}$ )  $\delta$  139.6, 129.8, 128.5, 113.1, 81.7.

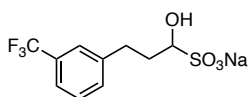


**Sodium hydroxy(5-(hydroxymethyl)furan-2-yl)methanesulfonate (S20):**

Yellow solid. 1.1 g, 96% yield (run on 5 mmol scale).

$^1\text{H NMR}$  (500 MHz,  $\text{D}_2\text{O}$ )  $\delta$  6.51 (d,  $J = 3.2$  Hz, 1H), 6.37 (q,  $J = 3.8, 3.0$  Hz, 1H), 5.52 – 5.43 (m, 1H), 4.53 – 4.51 (m, 2H).

$^{13}\text{C NMR}$  (126 MHz,  $\text{D}_2\text{O}$ )  $\delta$  154.4, 148.6, 111.0, 109.3, 79.6, 55.8.



**Sodium 1-hydroxy-3-(3-(trifluoromethyl)phenyl)propane-1-sulfonate (S21):**

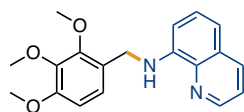
White solid. 281.5 mg, 92% yield (run on 1 mmol scale).

**<sup>1</sup>H NMR** (500 MHz, D<sub>2</sub>O) δ 7.56 (d, *J* = 1.8 Hz, 1H), 7.52 – 7.40 (m, 3H), 4.23 (ddd, *J* = 10.2, 3.0, 1.6 Hz, 1H), 2.91 (ddd, *J* = 14.0, 9.1, 5.0 Hz, 1H), 2.76 (dt, *J* = 13.9, 8.4 Hz, 1H), 2.24 – 2.13 (m, 1H), 1.95 (dddd, *J* = 13.9, 10.1, 8.8, 5.1, 1.2 Hz, 1H).

**<sup>13</sup>C NMR** (126 MHz, D<sub>2</sub>O) δ 142.1, 132.4, 130.1, 129.9, 129.1, 125.4, 125.3, 125.2, 125.2, 125.2, 123.2, 123.0, 123.0, 122.9, 82.9, 32.3, 30.6.

*Analytical data for products of reductive amination:*

Compounds **I-7<sup>1</sup>**, **I-8<sup>1</sup>**, **I-10<sup>1</sup>**, **I-11<sup>2</sup>**, **I-12<sup>3</sup>**, **I-13<sup>4</sup>**, **I-14<sup>5</sup>**, **I-18<sup>1</sup>**, **I-22<sup>1</sup>**, **I-23<sup>1</sup>**, **I-26<sup>6</sup>**, **I-27<sup>7</sup>**, **I-28<sup>8</sup>**, **I-29<sup>9</sup>**, **I-30<sup>10</sup>**, **Bucizine<sup>11</sup>**, **Meclizine<sup>12</sup>**, **Flunarizine<sup>13</sup>**, **Cinacalcet<sup>14</sup>**, **Piribedil<sup>15</sup>**, and **Donepezil<sup>16</sup>** were identified by comparisons with literature NMR data, the <sup>1</sup>H NMR spectra for these known compounds were also attached at the end of the NMR spectra section. All other new compounds were characterized by <sup>1</sup>H and <sup>13</sup>C NMR, and HRMS.



***N*-(2,3,4-Trimethoxybenzyl)quinolin-8-amine (I-5)**

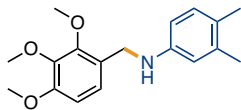
yellow oil, flash chromatography using 25% EtOAc/ hexanes (*R<sub>f</sub>* = 0.31). 64.8 mg, quantitative yield.

**<sup>1</sup>H NMR** (400 MHz, CDCl<sub>3</sub>) δ 8.71 (dd, *J* = 4.2, 1.7 Hz, 1H), 8.07 (d, *J* = 8.3 Hz, 1H), 7.40 – 7.34 (m, 2H), 7.10 – 7.03 (m, 2H), 6.72 (d, *J* = 7.6 Hz, 1H), 6.62 (d, *J* = 8.5 Hz, 1H), 4.51 (s, 2H), 3.95 (s, 3H), 3.90 (s, 3H), 3.84 (s, 3H).

**<sup>13</sup>C NMR** (101 MHz, CDCl<sub>3</sub>) δ 153.1, 152.0, 146.8, 144.6, 142.3, 136.1, 128.7, 127.9, 124.9, 123.2, 121.3, 113.9, 107.2, 105.1, 61.2, 60.8, 56.0, 42.3.

**HRMS** (ESI-TOF) *m/z*: [M+Na]<sup>+</sup> calcd for C<sub>19</sub>H<sub>20</sub>N<sub>2</sub>O<sub>3</sub>Na: 347.1372; found 347.1364.





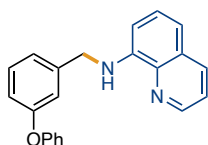
### 3,4-Dimethyl-N-(2,3,4-trimethoxybenzyl)aniline (I-6)

colorless oil, flash chromatography using 10% EtOAc/hexanes ( $R_f = 0.31$ ). 53.6 mg, 89% yield.

$^1\text{H NMR}$  (400 MHz,  $\text{CDCl}_3$ )  $\delta$  7.02 (d,  $J = 8.5$  Hz, 1H), 6.94 (d,  $J = 8.0$  Hz, 1H), 6.61 (d,  $J = 8.5$  Hz, 1H), 6.56 (d,  $J = 2.5$  Hz, 1H), 6.49 (dd,  $J = 8.1, 2.6$  Hz, 1H), 4.25 (s, 2H), 3.90 (s, 3H), 3.87 (s, 3H), 3.84 (s, 3H), 2.19 (s, 3H), 2.15 (s, 3H).

$^{13}\text{C NMR}$  (101 MHz,  $\text{CDCl}_3$ )  $\delta$  153.1, 151.9, 146.4, 142.2, 137.3, 130.2, 125.5, 125.4, 123.5, 115.0, 110.6, 107.2, 61.1, 60.8, 56.0, 43.7, 20.1, 18.7.

**HRMS** (ESI-TOF)  $m/z$ :  $[2\text{M}+\text{Na}]^+$  calcd for  $\text{C}_{36}\text{H}_{46}\text{N}_2\text{O}_6\text{Na}$ : 625.3254; found 625.3226.



### N-(3-Phenoxybenzyl)quinolin-8-amine (I-9)

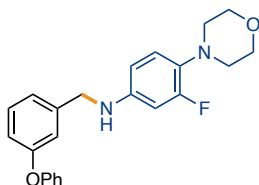
yellow oil, flash chromatography using 10% EtOAc/hexanes ( $R_f = 0.31$ ). 51.5 mg, 79% yield.

$^1\text{H NMR}$  (400 MHz,  $\text{CDCl}_3$ )  $\delta$  8.72 (dd,  $J = 4.2, 1.7$  Hz, 1H), 8.09 (d,  $J = 8.3$  Hz, 1H), 7.39 (dd,  $J = 8.2, 4.2$  Hz, 1H), 7.37 – 7.23 (m, 5H), 7.19 (ddd,  $J = 7.6, 1.7, 0.9$  Hz, 1H), 7.12 – 7.03 (m, 3H), 7.02 – 6.93 (m, 2H), 6.90 (ddd,  $J = 8.1, 2.6, 1.0$  Hz, 1H), 6.63 (dd,  $J = 7.6, 1.2$  Hz, 1H), 4.55 (d,  $J = 2.9$  Hz, 2H).

$^{13}\text{C NMR}$  (101 MHz,  $\text{CDCl}_3$ )  $\delta$  157.58, 157.13, 146.88, 144.38, 141.49, 136.15, 129.93, 129.72, 128.67, 127.76, 123.22, 122.13, 121.43, 119.52, 118.90, 117.84, 117.45, 114.32, 105.34, 47.48.

$^{13}\text{C}$  NMR (101 MHz,  $\text{CDCl}_3$ )  $\delta$  157.6, 157.1, 146.9, 144.4, 141.5, 136.2, 129.9, 129.7, 128.7, 127.8, 123.2, 122.1, 121.4, 118.9, 117.8, 117.4, 114.3, 105.3, 47.5.

HRMS (ESI-TOF)  $m/z$ :  $[\text{M}+\text{Na}]^+$  calcd for  $\text{C}_{22}\text{H}_{18}\text{N}_2\text{ONa}$ : 349.1317; found 349.1314.



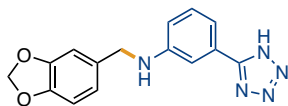
### 3-Fluoro-4-morpholino-*N*-(3-phenoxybenzyl)aniline (I-15)

Colorless oil, flash chromatography using 15% EtOAc/hexanes ( $R_f = 0.35$ ). 72.6 mg, 96% yield.

$^1\text{H}$  NMR (400 MHz,  $\text{CDCl}_3$ )  $\delta$  7.35 – 7.25 (m, 3H), 7.13 – 7.07 (m, 2H), 7.03 – 6.98 (m, 3H), 6.91 (dd,  $J = 8.1, 2.5$  Hz, 1H), 6.82 (t,  $J = 9.2$  Hz, 1H), 6.36 (d,  $J = 14.6$  Hz, 2H), 4.25 (s, 2H), 3.85 (t,  $J = 4.6$  Hz, 4H), 2.96 (s, 4H).

$^{13}\text{C}$  NMR (101 MHz,  $\text{CDCl}_3$ )  $\delta$  158.3, 157.7, 157.0, 155.8, 130.0, 129.8, 123.4, 122.1, 119.1, 119.0, 117.7, 117.6, 101.7, 101.5.

HRMS (ESI-TOF)  $m/z$ :  $[\text{M}+\text{H}]^+$  calcd for  $\text{C}_{23}\text{H}_{24}\text{FN}_2\text{O}_2$ : 379.1822; found 379.1825.



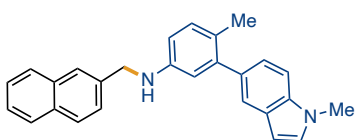
### *N*-(Benzo[*d*][1,3]dioxol-5-ylmethyl)-3-(1*H*-tetrazol-5-yl)aniline (I-16)

White solid, flash chromatography using 5% MeOH/DCM ( $R_f = 0.25$ ). 57.2 mg, 97% yield.

**<sup>1</sup>H NMR** (400 MHz, MeOD-*d*<sub>4</sub>) δ 7.29 – 7.21 (m, 2H), 7.20 – 7.13 (m, 1H), 6.85 (d, *J* = 7.6 Hz, 2H), 6.80 (dd, *J* = 8.0, 2.4 Hz, 1H), 6.77 – 6.68 (m, 1H), 5.88 (d, *J* = 1.4 Hz, 2H), 4.27 (s, 2H).

**<sup>13</sup>C NMR** (101 MHz, MeOD-*d*<sub>4</sub>) δ 156.2, 149.5, 147.9, 146.6, 133.4, 129.7, 124.1, 120.2, 115.7, 114.7, 110.3, 107.7, 107.4, 100.8, 70.1.

**HRMS** (ESI-TOF) *m/z*: [M+Na]<sup>+</sup> calcd for C<sub>15</sub>H<sub>13</sub>N<sub>5</sub>O<sub>2</sub>Na: 318.0967; found 318.0952.



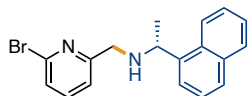
**4-Methyl-3-(1-methyl-1*H*-indol-5-yl)-*N*-(naphthalen-2-ylmethyl)aniline (I-17):**

Light yellow solid, flash chromatography using 20% EtOAc/hexanes (*R*<sub>f</sub> = 0.28). 60.2 mg, 80% yield.

**<sup>1</sup>H NMR** (500 MHz, CDCl<sub>3</sub>) δ 7.89 – 7.81 (m, 4H), 7.60 (d, *J* = 1.8 Hz, 1H), 7.56 – 7.46 (m, 3H), 7.37 (dd, *J* = 8.5, 2.1 Hz, 1H), 7.25 (dd, *J* = 8.4, 1.9 Hz, 1H), 7.16 – 7.07 (m, 2H), 6.75 (d, *J* = 2.5 Hz, 1H), 6.65 (dt, *J* = 8.3, 2.4 Hz, 1H), 6.54 (t, *J* = 2.7 Hz, 1H), 4.54 (d, *J* = 2.1 Hz, 2H), 3.85 (d, *J* = 2.0 Hz, 3H), 2.24 (d, *J* = 2.0 Hz, 3H).

**<sup>13</sup>C NMR** (126 MHz, CDCl<sub>3</sub>) δ 146.1, 143.9, 137.2, 135.7, 133.7, 133.5, 131.0, 129.2, 128.3, 128.3, 127.8, 127.7, 126.1, 126.1, 126.0, 125.7, 125.0, 123.3, 121.2, 115.5, 111.6, 108.6, 101.1, 48.9, 32.9, 19.7.

**HRMS** (ESI-TOF) *m/z*: [M+H]<sup>+</sup> calcd for C<sub>27</sub>H<sub>25</sub>N<sub>2</sub>: 377.2018; found 377.2010.



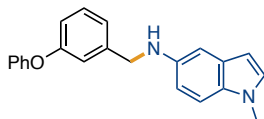
**(*R*)-*N*-((6-Bromopyridin-2-yl)methyl)-1-(naphthalen-1-yl)ethan-1-amine (I-19)**

Off white solid, flash chromatography using 25% EtOAc/hexanes ( $R_f = 0.30$ ). 51.5 mg, 75% yield.

$^1\text{H NMR}$  (400 MHz,  $\text{CDCl}_3$ )  $\delta$  8.19 – 8.14 (m, 1H), 7.90 – 7.86 (m, 1H), 7.75 (t,  $J = 7.8$  Hz, 2H), 7.53 – 7.42 (m, 4H), 7.34 (d,  $J = 7.8$  Hz, 1H), 7.17 (d,  $J = 7.5$  Hz, 1H), 4.70 (q,  $J = 6.6$  Hz, 1H), 3.83 (d,  $J = 5.2$  Hz, 2H), 1.56 (d,  $J = 6.5$  Hz, 3H).

$^{13}\text{C NMR}$  (101 MHz,  $\text{CDCl}_3$ )  $\delta$  161.6, 141.8, 140.4, 138.7, 134.0, 131.3, 129.0, 127.4, 126.3, 125.8, 125.8, 125.4, 123.1, 123.0, 121.3, 53.3, 52.6, 23.6.

**HRMS** (ESI-TOF)  $m/z$ :  $[\text{M}+\text{H}]^+$  calcd for  $\text{C}_{18}\text{H}_{18}\text{BrN}_2$ : 343.0635; found 343.0639.



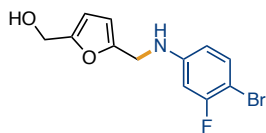
**1-Methyl-N-(3-phenoxybenzyl)-1H-indol-5-amine (I-20)**

Brown solid, flash chromatography using 25% EtOAc/hexanes ( $R_f = 0.30$ ). 55.8 mg, 85% yield.

$^1\text{H NMR}$  (400 MHz,  $\text{CDCl}_3$ )  $\delta$  7.31 (dt,  $J = 9.1, 7.5$  Hz, 3H), 7.20 – 7.07 (m, 4H), 7.04 – 6.98 (m, 2H), 6.96 (d,  $J = 3.1$  Hz, 1H), 6.91 (ddd,  $J = 8.1, 2.6, 1.0$  Hz, 1H), 6.84 (d,  $J = 2.2$  Hz, 1H), 6.68 (dd,  $J = 8.7, 2.3$  Hz, 1H), 6.31 (dd,  $J = 3.0, 0.8$  Hz, 1H), 4.36 (s, 2H), 3.73 (s, 3H).

$^{13}\text{C NMR}$  (126 MHz,  $\text{CDCl}_3$ )  $\delta$  157.5, 157.2, 142.3, 141.7, 131.5, 129.9, 129.7, 129.3, 128.9, 123.2, 122.4, 118.9, 118.1, 117.4, 111.7, 109.9, 102.8, 99.8, 49.6, 32.9.

**HRMS** (ESI-TOF)  $m/z$ :  $[\text{M}+\text{Na}]^+$  calcd for  $\text{C}_{22}\text{H}_{20}\text{N}_2\text{ONa}$ : 351.1473; found 351.1468.



**(5-(((4-Bromo-3-fluorophenyl)amino)methyl)furan-2-yl)methanol (I-21)**

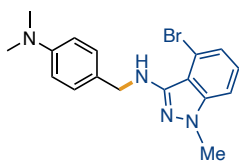
Yellow oil, flash chromatography using 33% EtOAc/hexanes ( $R_f = 0.31$ ). 50.4 mg, 56% yield.

$^1\text{H NMR}$  (400 MHz,  $\text{CDCl}_3$ )  $\delta$  7.29 – 7.26 (m, 1H, overlap with  $\text{CHCl}_3$ ), 6.44 (dd,  $J = 10.9, 2.7$  Hz, 1H), 6.36 – 6.33 (m, 1H), 6.24 – 6.18 (m, 2H), 4.58 (s, 2H), 4.27 (d,  $J = 0.7$  Hz, 2H).

$^{13}\text{C NMR}$  (101 MHz,  $\text{CDCl}_3$ )  $\delta$  160.99, 158.56, 153.70, 151.75, 148.51, 148.42, 133.39, 133.37, 110.36, 110.33, 108.74, 108.23, 101.03, 100.77, 95.58, 95.36, 77.36, 77.05, 76.73, 57.48, 41.29.

$^{13}\text{C NMR}$  (101 MHz,  $\text{CDCl}_3$ )  $\delta$  161.0, 153.7, 151.7, 148.5, 148.4, 133.4, 133.4, 110.4, 110.3, 108.7, 108.2, 101.0, 100.8, 95.6, 95.4, 57.5, 41.3.

**HRMS** (ESI-TOF)  $m/z$ :  $[\text{M}+\text{Na}]^+$  calcd for  $\text{C}_{12}\text{H}_{11}\text{BrFNO}_2\text{Na}$ : 622.9794; found 622.9769.



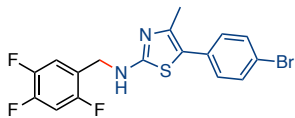
**4-Bromo-N-(4-(dimethylamino)benzyl)-1-methyl-1H-indazol-3-amine (I-24)**

Pale yellow solid, flash chromatography using 30% EtOAc/hexanes ( $R_f = 0.31$ ). 38.1 mg, 53% yield.

$^1\text{H NMR}$  (400 MHz,  $\text{CDCl}_3$ )  $\delta$  7.68 – 7.55 (m, 1H), 7.37 (dd,  $J = 8.9, 1.8$  Hz, 1H), 7.34 – 7.25 (m, 2H), 7.06 (d,  $J = 8.9$  Hz, 1H), 6.76 (d,  $J = 8.4$  Hz, 2H), 4.46 (s, 2H), 3.85 (s, 3H), 2.94 (d,  $J = 8.5$  Hz, 6H).

$^{13}\text{C NMR}$  (101 MHz,  $\text{CDCl}_3$ )  $\delta$  150.2, 148.5, 140.3, 129.8, 129.2, 127.2, 122.1, 115.8, 112.8, 110.5, 109.9, 48.2, 40.8, 35.1.

**HRMS** (ESI-TOF)  $m/z$ :  $[\text{M}+\text{Na}]^+$  calcd for  $\text{C}_{17}\text{H}_{19}\text{BrN}_4\text{Na}$ : 381.0691; found 381.0697.



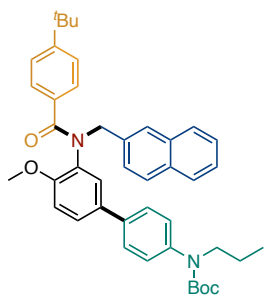
**5-(4-Bromophenyl)-4-methyl-N-(2,4,5-trifluorobenzyl)thiazol-2-amine (I-25)**

Off White solid, flash chromatography using 30% EtOAc/hexanes ( $R_f = 0.31$ ). 41.3 mg, 50% yield.

$^1\text{H NMR}$  (400 MHz,  $\text{CDCl}_3$ )  $\delta$  7.51 – 7.45 (m, 2H), 7.45 – 7.39 (m, 2H), 7.29 – 7.20 (m, 1H), 6.93 (td,  $J = 9.7, 6.4$  Hz, 1H), 4.40 (s, 2H), 2.35 (s, 3H).

$^{13}\text{C NMR}$  (126 MHz,  $\text{CDCl}_3$ )  $\delta$  165.3, 156.7, 156.6, 154.8, 154.3, 157.7, 150.5, 150.4, 150.3, 148.5, 148.4, 148.3, 147.9, 147.7, 145.9, 145.8, 145.9, 134.2, 131.4, 129.9, 121.8, 121.7, 121.7, 121.7, 121.3, 117.4, 117.4, 117.3, 117.2, 116.9, 105.8, 105.6, 105.6, 105.4, 42.5, 42.4, 12.4.

**HRMS** (ESI-TOF)  $m/z$ :  $[\text{M}+\text{H}]^+$  calcd for  $\text{C}_{17}\text{H}_{13}\text{BrF}_3\text{N}_2\text{S}$ : 412.9935; found 412.9930.



***t*-Butyl (3'-(4-(*t*-butyl)-*N*-(naphthalen-2-ylmethyl)benzamido)-4'-methoxy-[1,1'-biphenyl]-4-yl)(propyl)carbamate (I-31)**

Pale yellow oil, flash chromatography using 33% EtOAc/hexanes ( $R_f = 0.28$ ). 206.9 mg, 63% overall yield.

**<sup>1</sup>H NMR** (400 MHz, CDCl<sub>3</sub>) δ 7.81 – 7.71 (m, 4H), 7.54 (d, *J* = 8.5 Hz, 1H), 7.43 (d, *J* = 9.4 Hz, 2H), 7.33 (d, *J* = 8.1 Hz, 2H), 7.29 – 7.24 (m, 1H), 7.16 (d, *J* = 8.1 Hz, 2H), 7.06 (t, *J* = 7.0 Hz, 4H), 6.90 (s, 1H), 6.77 (d, *J* = 8.6 Hz, 1H), 5.71 (d, *J* = 14.4 Hz, 1H), 4.78 (d, *J* = 14.5 Hz, 1H), 3.67 (s, 3H), 3.55 (t, *J* = 7.4 Hz, 2H), 1.53 (q, *J* = 7.4 Hz, 2H), 1.44 (s, 9H), 1.21 (s, 9H), 0.87 (t, *J* = 7.4 Hz, 3H).

**<sup>13</sup>C NMR** (126 MHz, CDCl<sub>3</sub>) δ 171.6, 154.8, 153.9, 152.8, 141.5, 137.3, 135.5, 133.0, 132.8, 132.1, 128.8, 128.0, 128.0, 127.9, 127.6, 127.3, 127.1, 126.9, 126.8, 125.9, 125.7, 124.4, 112.0, 55.5, 52.5, 51.6, 34.7, 31.1, 21.7, 11.2.

**HRMS** (ESI-TOF) *m/z*: [M+Na]<sup>+</sup> calcd for C<sub>43</sub>H<sub>48</sub>N<sub>2</sub>O<sub>4</sub>Na: 679.3512; found 679.3511.

### 1.5.7. References

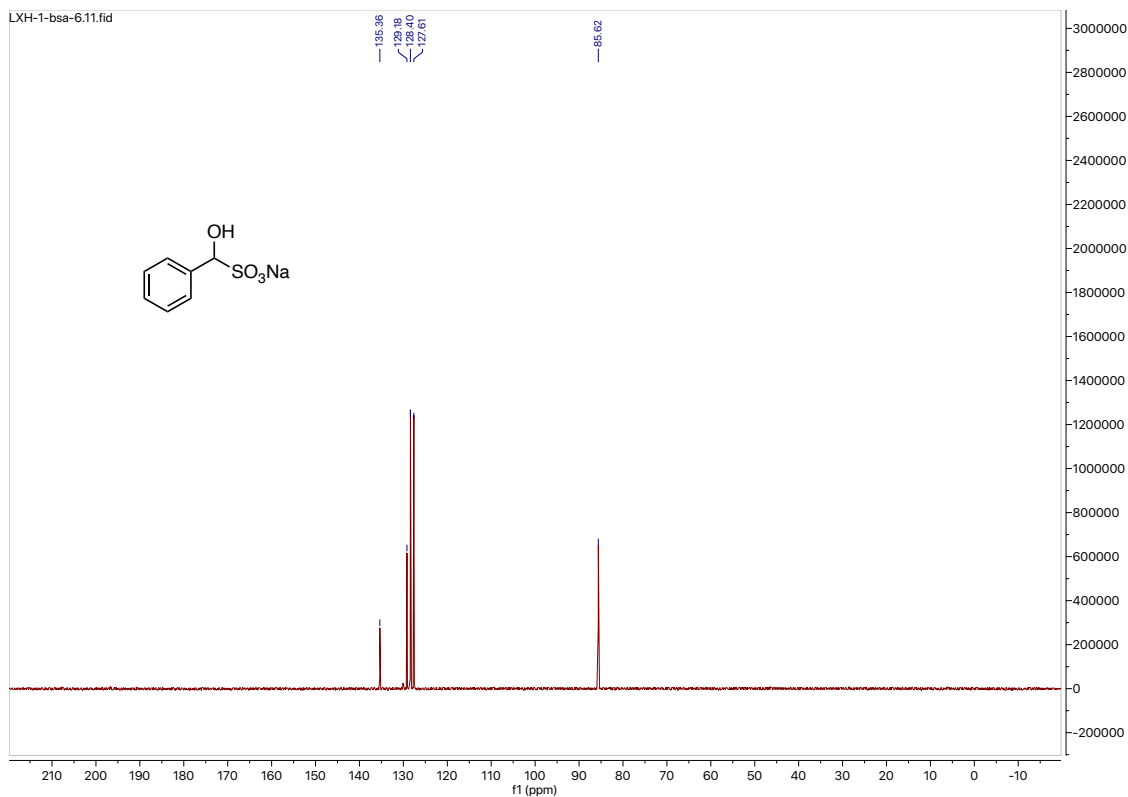
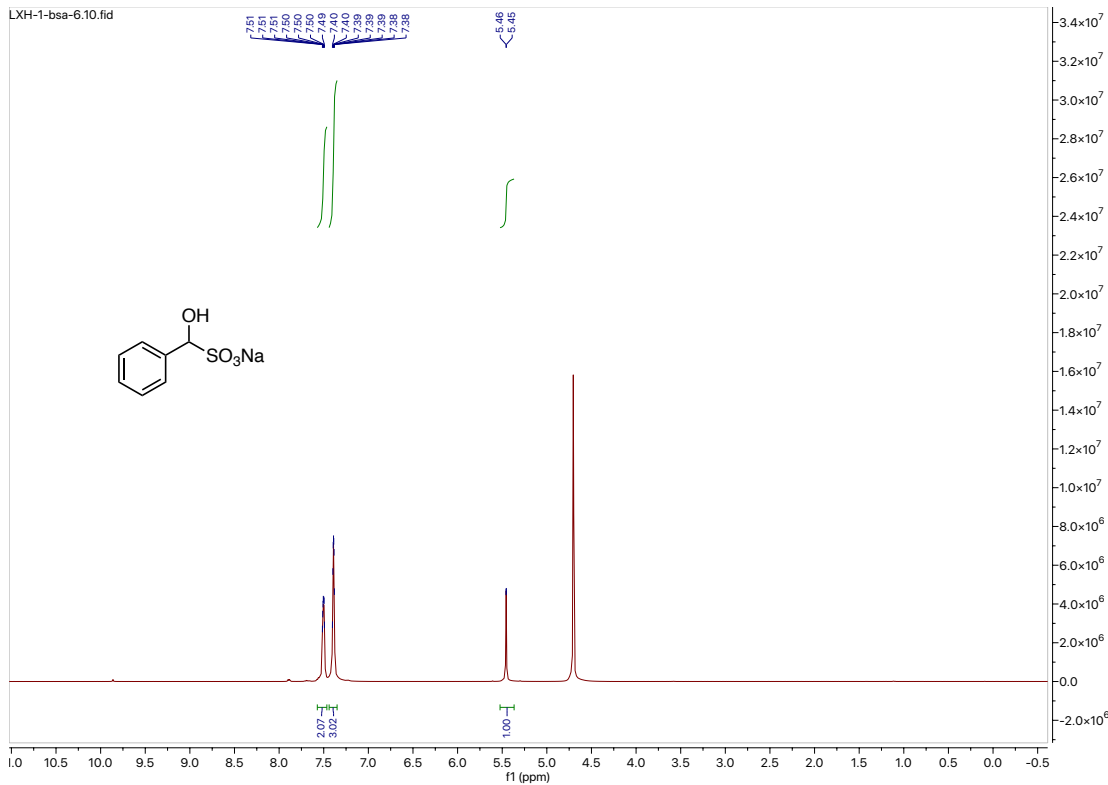
1. Thakore, R. R.; Takale, B. S.; Casotti, G.; Gao, E. S.; Jin, H. S.; Lipshutz, B. H. Chemoselective Reductive Aminations in Aqueous Nanoreactors Using Parts per Million Level Pd/C Catalysis. *Org. Lett.* **2020**, *22*, 6324–6329.
2. Verma, A. K.; Malhotra, S.; Ghorpade, S. M.; Dawange, M. B.; Ray, A.; Gupta, S.; Srivastava, P.; Dastidar, S. G. 5-Lipoxygenase Inhibitors, February 2, 2012.
3. Amari, G.; Armani, E.; Riccaboni, M.; Baker-Glenn, C. Phenylethylpyridine Derivatives as Pde4-Inhibitors. WO2014086855A1, June 12, 2014.
4. Cheung, S.-Y.; Werner, M.; Esposito, L.; Troisi, F.; Cantone, V.; Liening, S.; König, S.; Gerstmeier, J.; Koeberle, A.; Bilancia, R.; Rizza, R.; Rossi, A.; Roviezzo, F.; Temml, V.; Schuster, D.; Stuppner, H.; Schubert-Zsilavecz, M.; Werz, O.; Hanke, T.; Pace, S. Discovery of a Benzenesulfonamide-Based Dual Inhibitor of Microsomal Prostaglandin E<sub>2</sub> Synthase-1 and 5-Lipoxygenase That Favorably Modulates Lipid Mediator Biosynthesis in Inflammation. *Eur. J. Med. Chem.* **2018**, *156*, 815–830.
5. Hoshimoto, Y.; Kinoshita, T.; Hazra, S.; Ohashi, M.; Ogoshi, S. Main-Group-Catalyzed Reductive Alkylation of Multiply Substituted Amines with Aldehydes Using H<sub>2</sub>. *J. Am. Chem. Soc.* **2018**, *140*, 7292–7300.
6. Fleischer, S.; Zhou, S.; Junge, K.; Beller, M. An Easy and General Iron-Catalyzed Reductive Amination of Aldehydes and Ketones with Anilines. *Chem. Asian J.* **2011**, *6*, 2240–2245.
7. Takale, B. S.; Feng, X.; Lu, Y.; Bao, M.; Jin, T.; Minato, T.; Yamamoto, Y. Unsupported Nanoporous Gold Catalyst for Chemoselective Hydrogenation Reactions under Low

- Pressure: Effect of Residual Silver on the Reaction. *J. Am. Chem. Soc.* **2016**, *138*, 10356–10364.
8. Drinkel, E. E.; Campedelli, R. R.; Manfredi, A. M.; Fiedler, H. D.; Nome, F. Zwitterionic-Surfactant-Stabilized Palladium Nanoparticles as Catalysts in the Hydrogen Transfer Reductive Amination of Benzaldehydes. *J. Org. Chem.* **2014**, *79*, 2574–2579.
  9. Li, J.; Huang, C.; Wen, D.; Zheng, Q.; Tu, B.; Tu, T. Nickel-Catalyzed Amination of Aryl Chlorides with Amides. *Org. Lett.* **2021**, *23*, 687–691.
  10. Burkhard, J. A.; Wagner, B.; Fischer, H.; Schuler, F.; Müller, K.; Carreira, E. M. Synthesis of Azaspirocycles and Their Evaluation in Drug Discovery. *Angew. Chem., Int. Ed.* **2010**, *49*, 3524–3527.
  11. Lal, B.; Lahiri, S.; Bapat, C. P.; Kulkarni, R. S.; Mulla, D. K.; Hawaldar, A. Y. Novel Water Based Process for the Preparation of Substituted Diphenylmethyl Piperazines. US2011172425 (A1), July 14, 2011.
  12. Roy, D.; Panda, G. Benzhydryl Amines: Synthesis and Their Biological Perspective. *ACS Omega* **2020**, *5*, 19–30.
  13. Younes, S.; Baziard-Mouysset, G.; de Saqui-Sannes, G.; Stigliani, J.; Payard, M.; Bonnafous, R.; Tisne-Versailles, J. Synthesis and Pharmacological Study of New Calcium Antagonists, Analogues of Cinnarizine and Flunarizine. *Eur. J. Med. Chem.* **1993**, *28*, 943–948.
  14. Thiel, O. R.; Bernard, C.; Tormos, W.; Brewin, A.; Hirotsu, S.; Murakami, K.; Saito, K.; Larsen, R. D.; Martinelli, M. J.; Reider, P. J. Practical Synthesis of the Calcimimetic Agent, Cinacalcet. *Tetrahedron Lett.* **2008**, *49*, 13–15.
  15. Hamid, M. H. S. A.; Williams, J. M. J. Ruthenium-Catalysed Synthesis of Tertiary Amines from Alcohols. *Tetrahedron Lett.* **2007**, *48*, 8263–8265.
  16. Elati, C. R.; Kolla, N.; Chalamala, S. R.; Vankawala, P. J.; Sundaram, V.; Vurimidi, H.; Mathad, V. T. New Synthesis of Donepezil Through Palladium-Catalyzed Hydrogenation Approach. *Synth. Commun.* **2006**, *36*, 169–174.

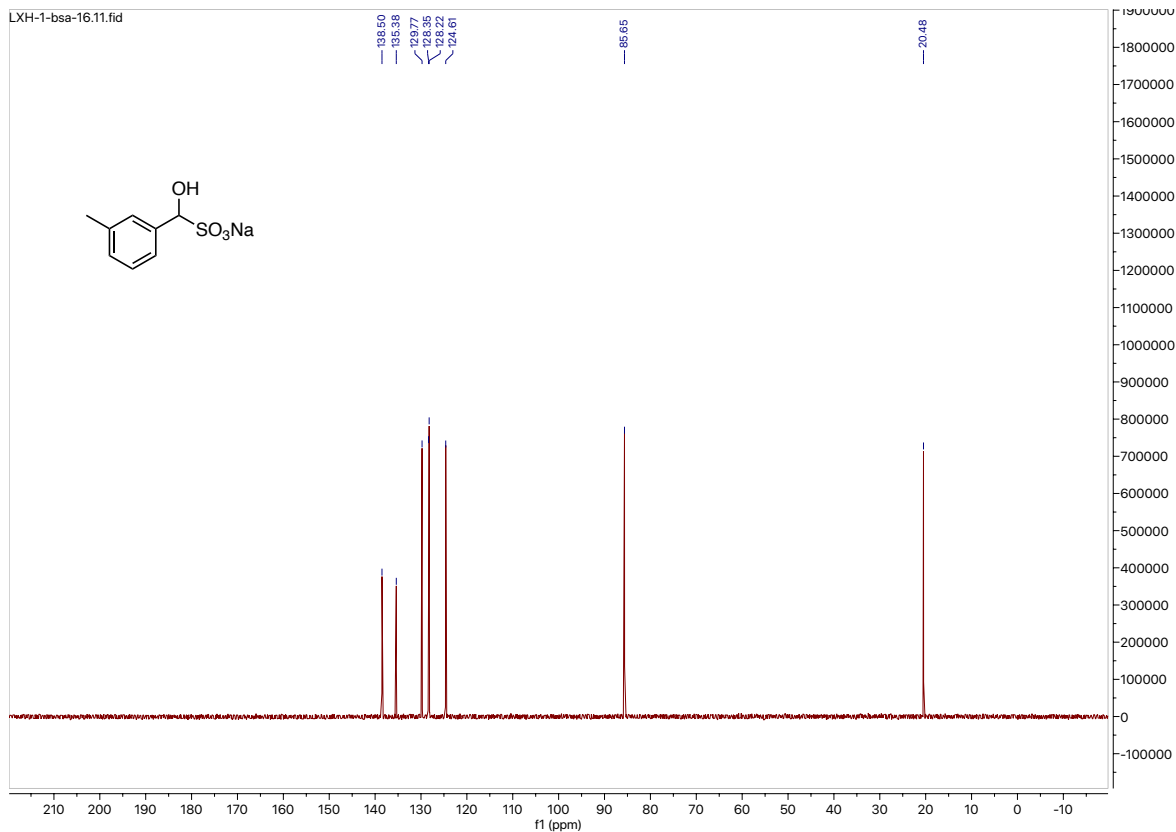
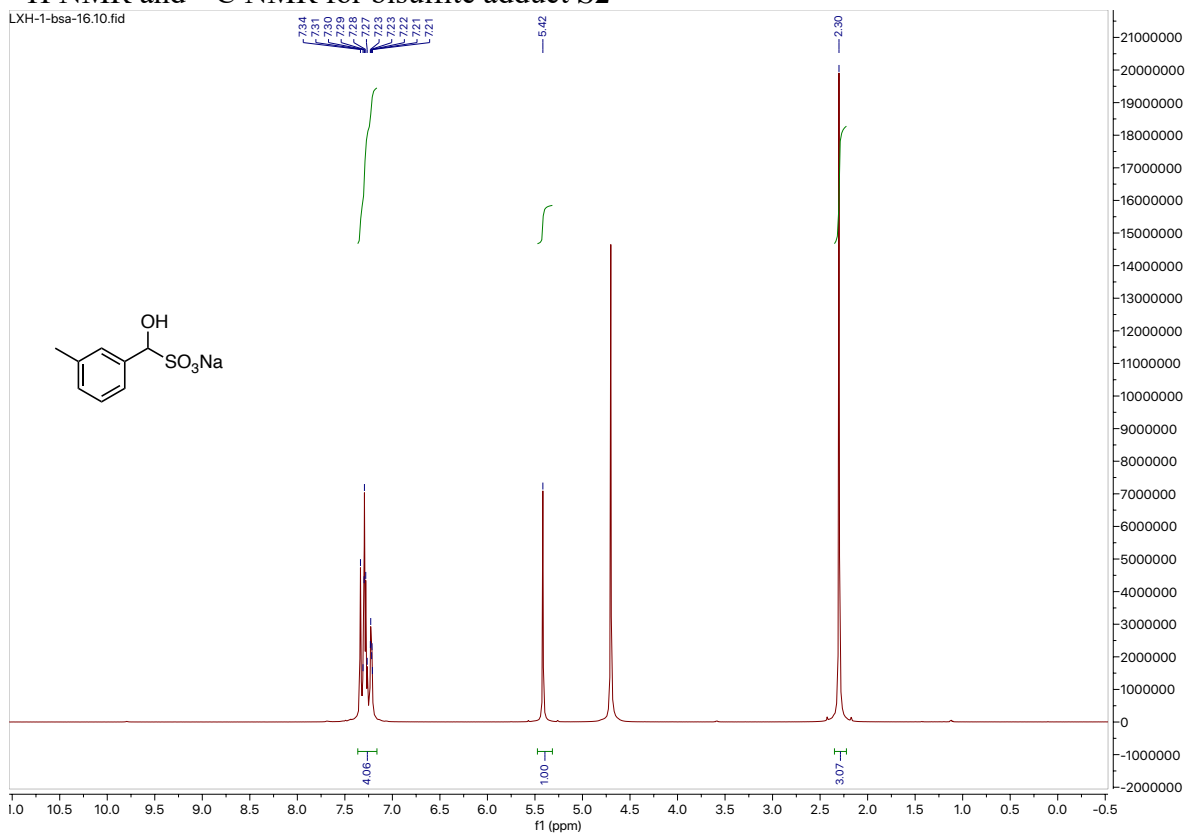


### 1.5.8 NMR spectra

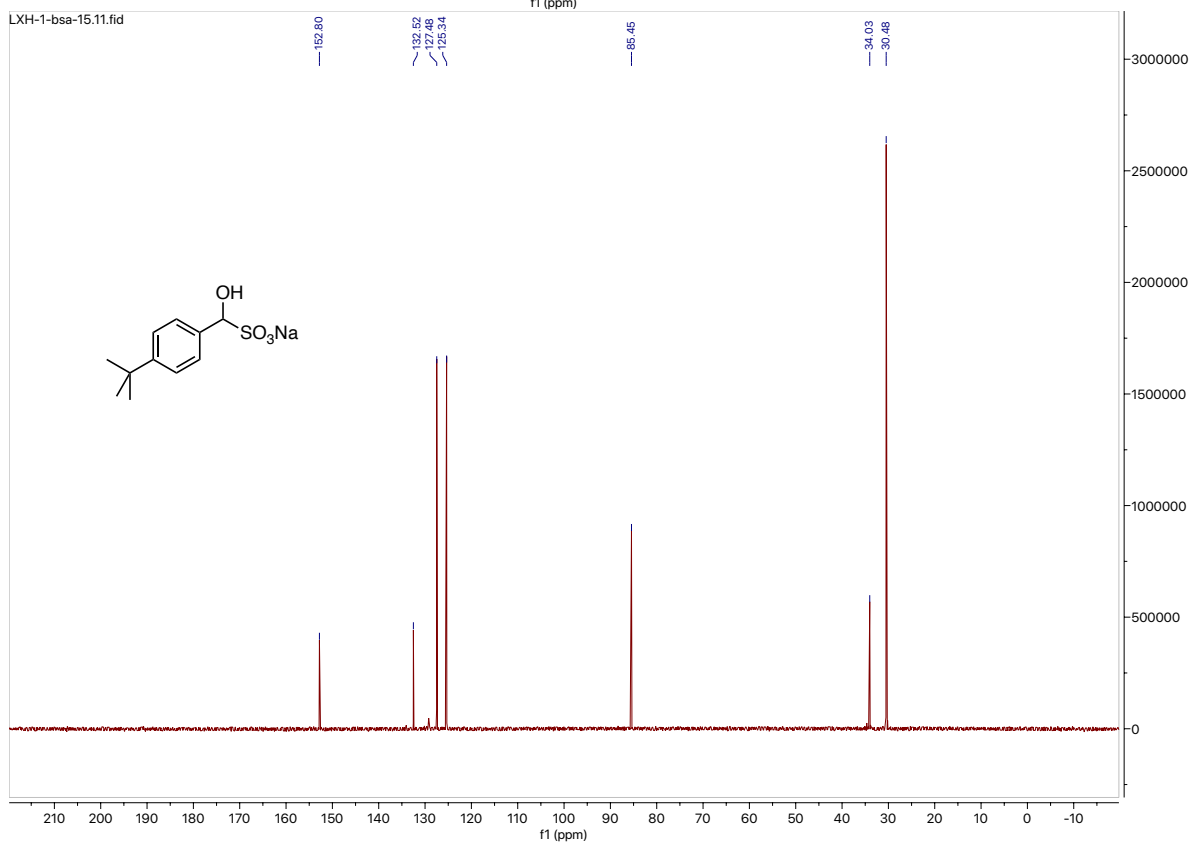
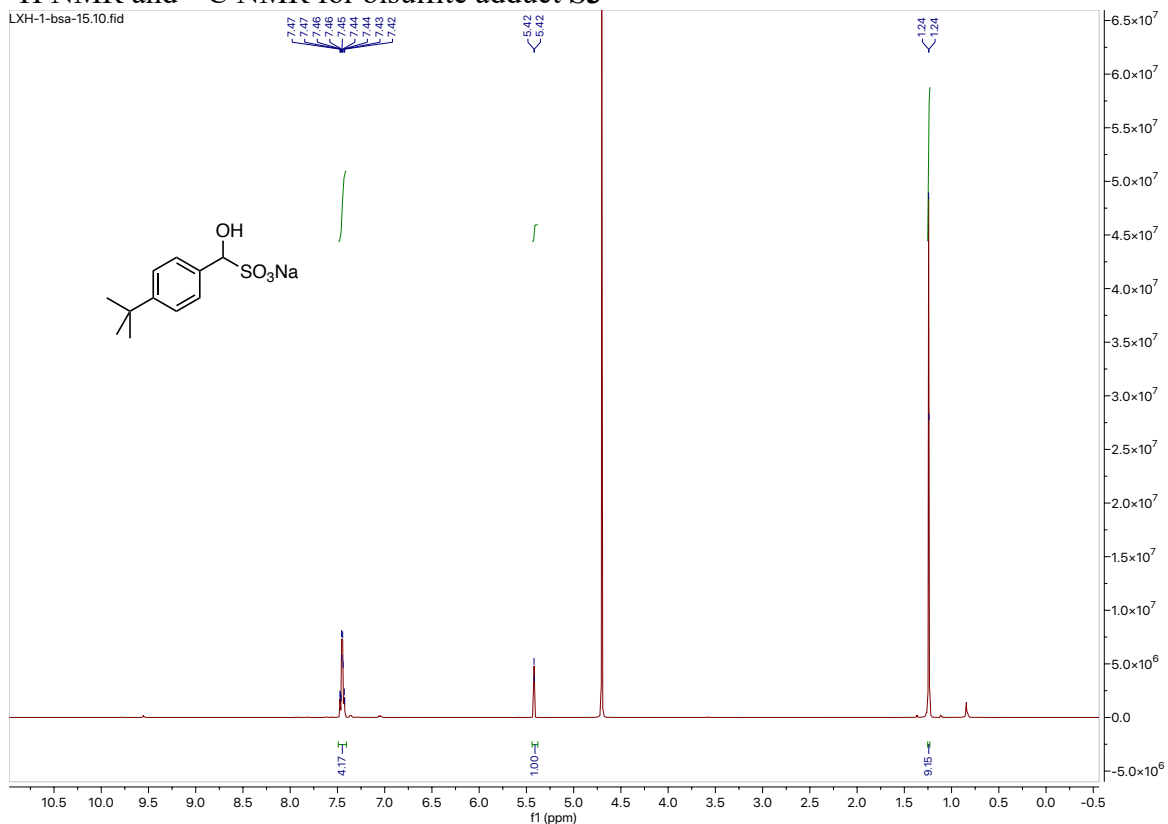
#### $^1\text{H}$ NMR and $^{13}\text{C}$ NMR for bisulfite adduct S1



# $^1\text{H}$ NMR and $^{13}\text{C}$ NMR for bisulfite adduct S2

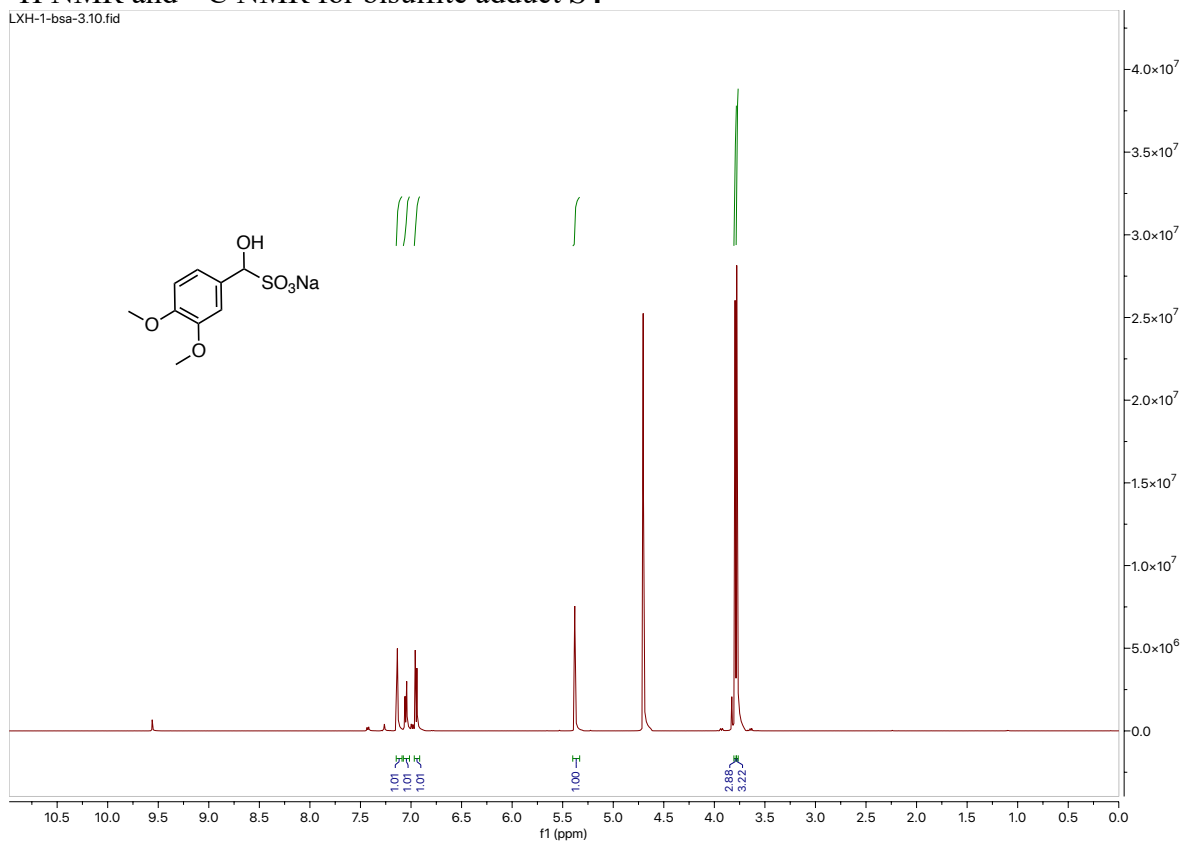


# $^1\text{H}$ NMR and $^{13}\text{C}$ NMR for bisulfite adduct S3

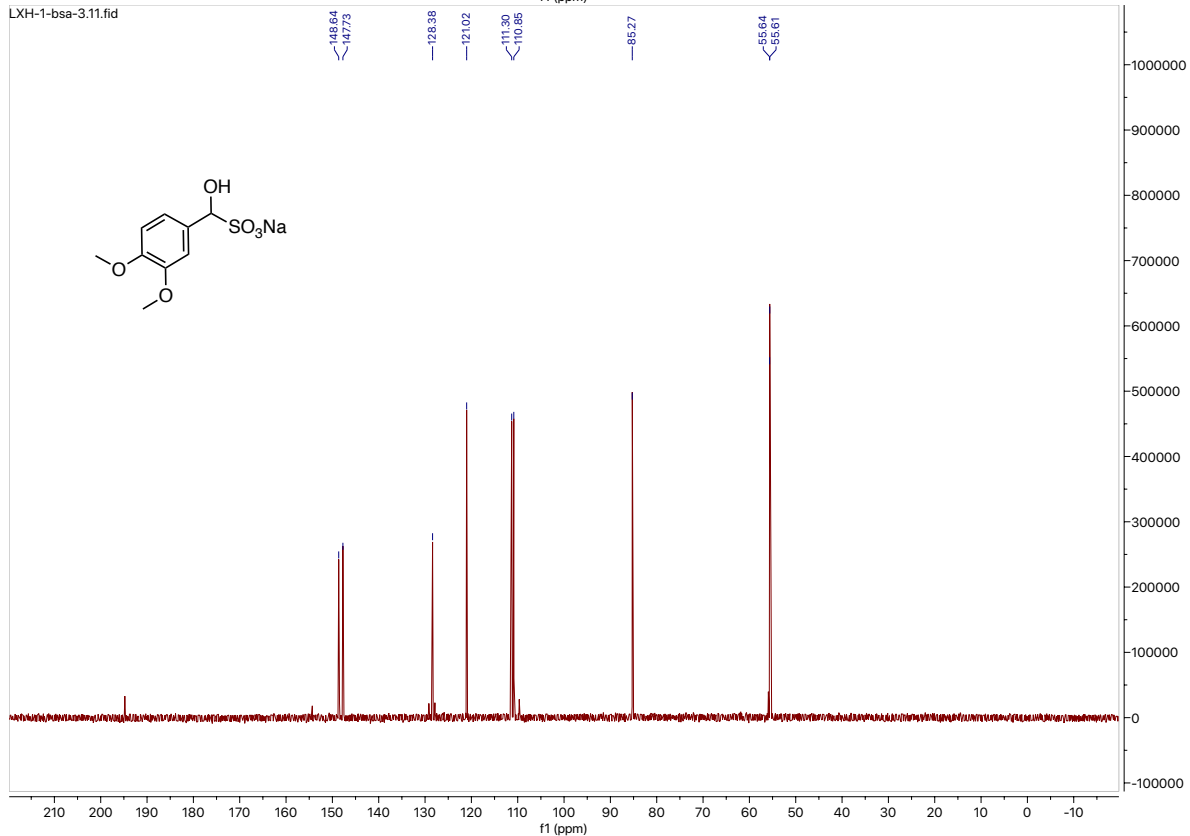


# <sup>1</sup>H NMR and <sup>13</sup>C NMR for bisulfite adduct S4

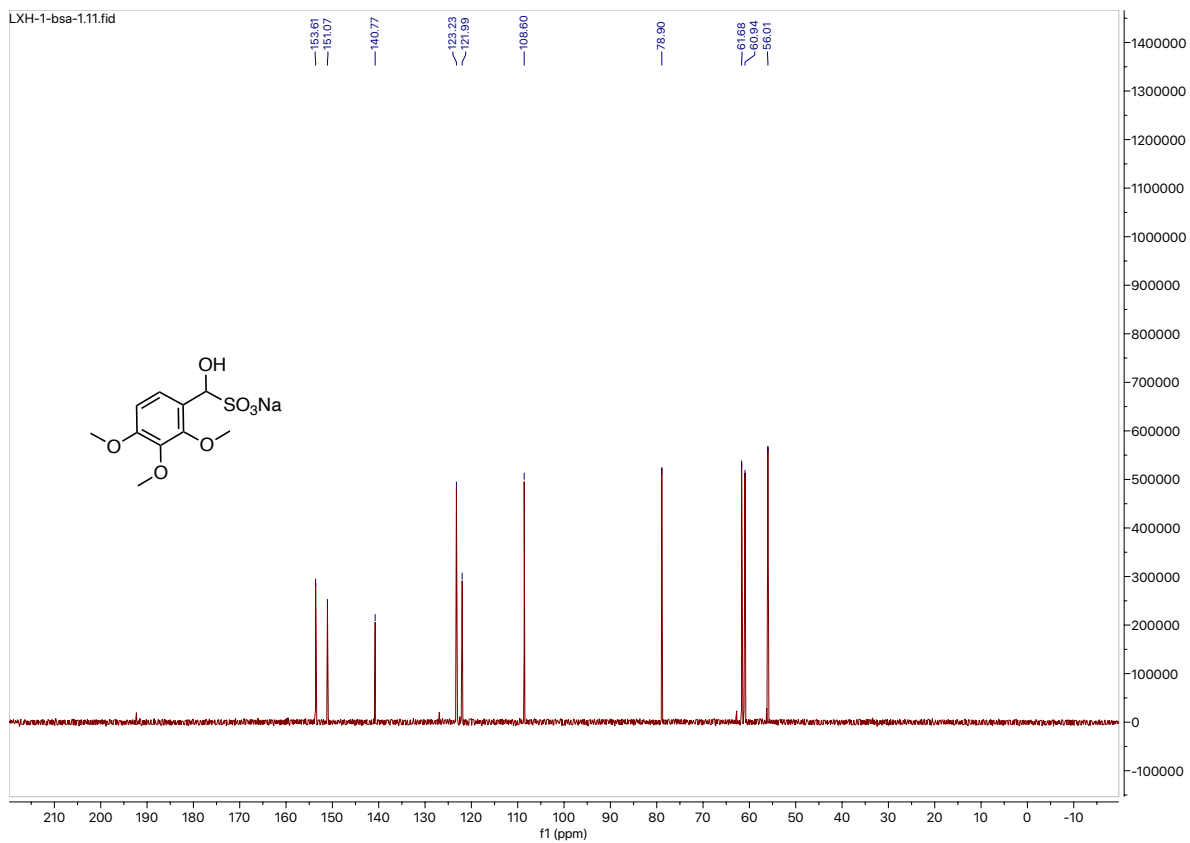
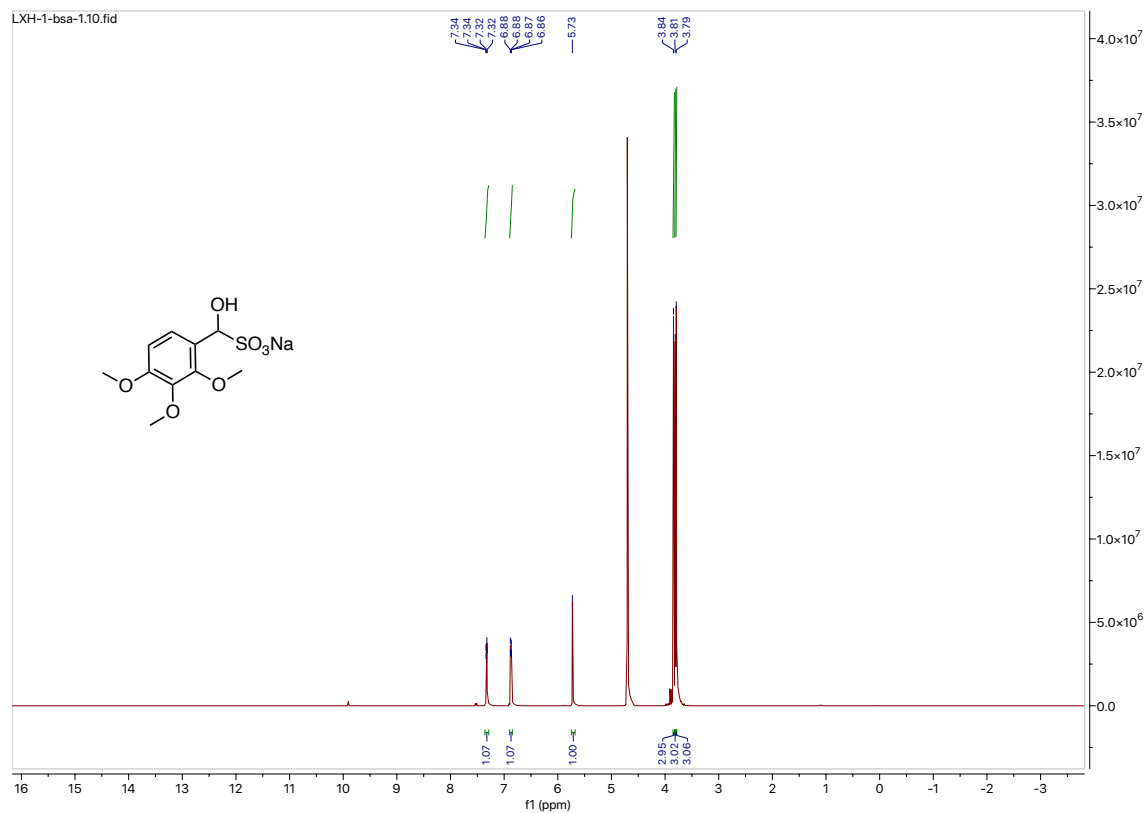
LXH-1-bsa-3.10.fid



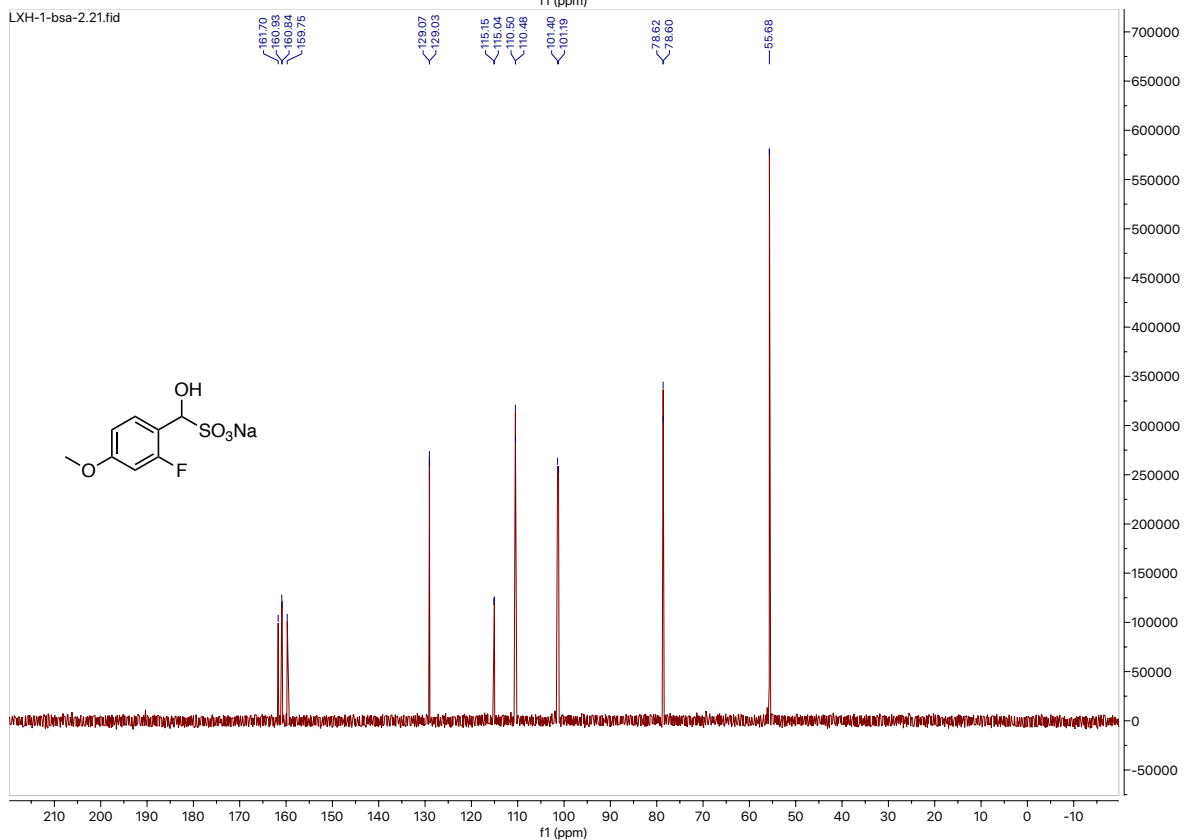
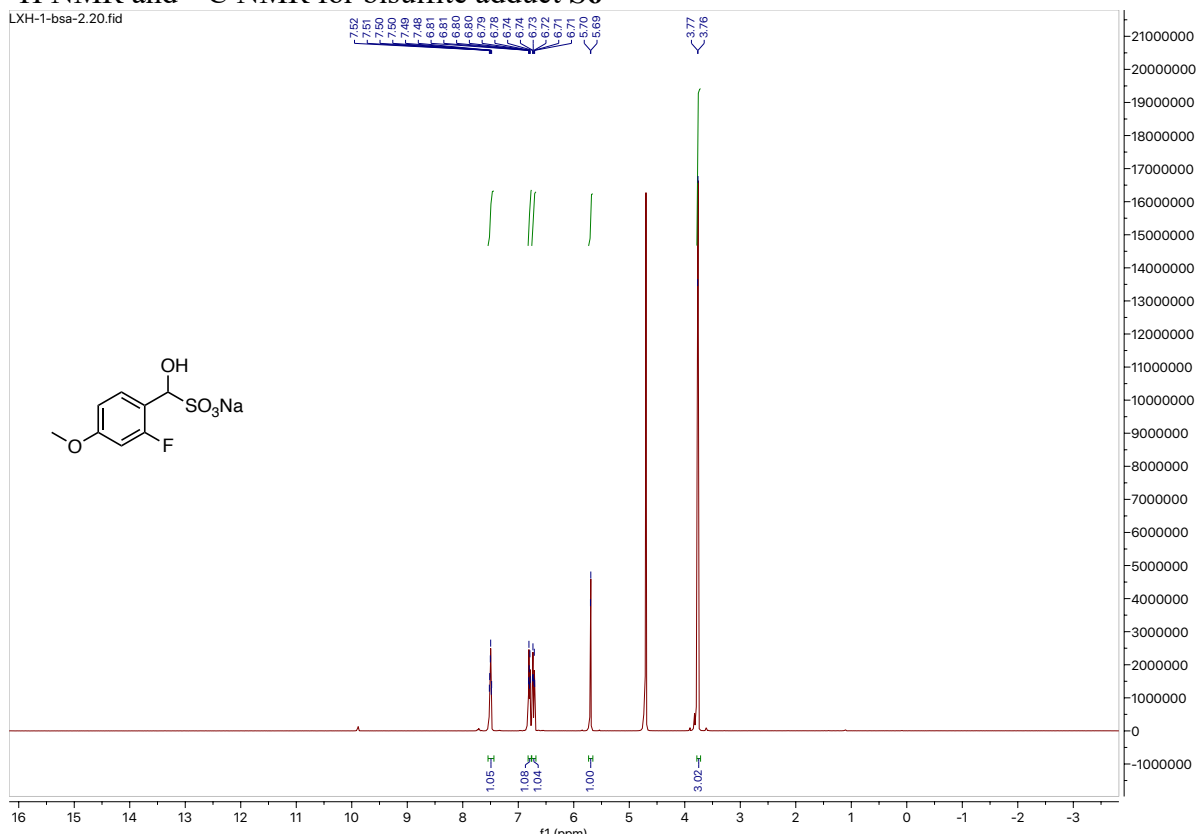
LXH-1-bsa-3.11.fid



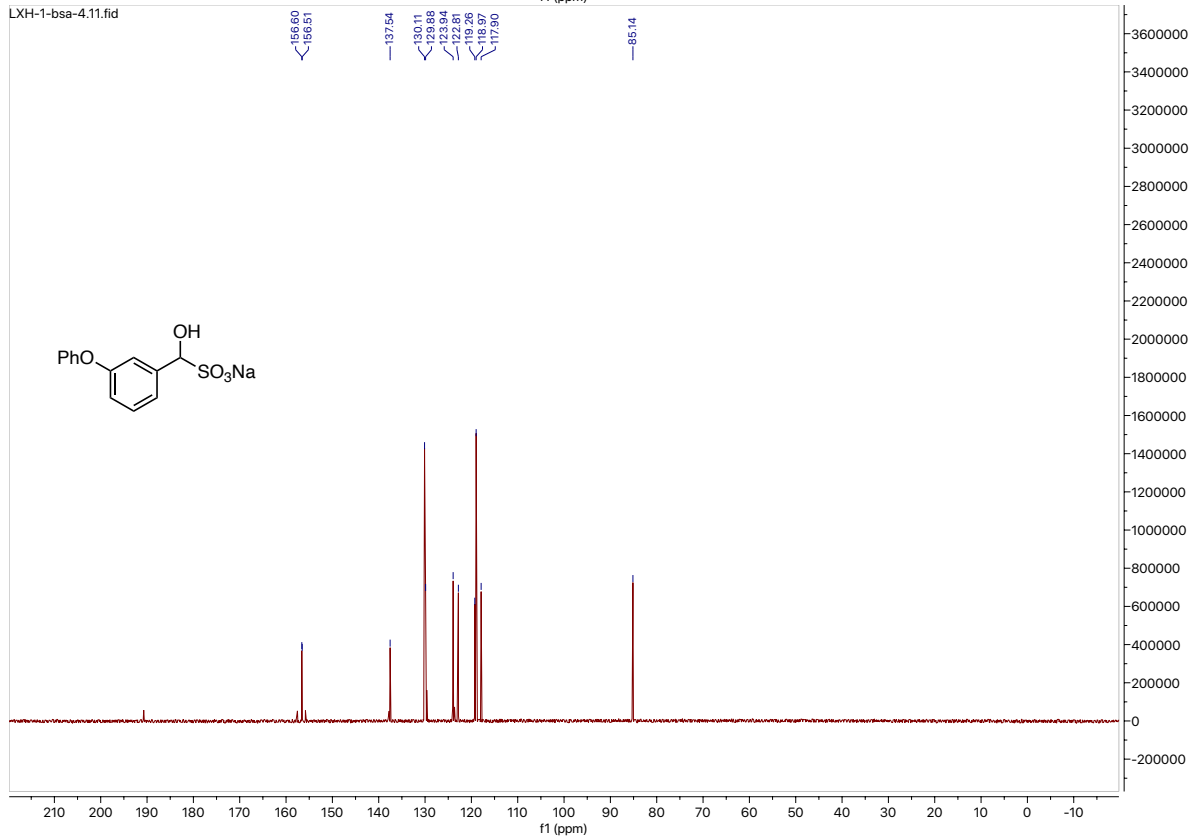
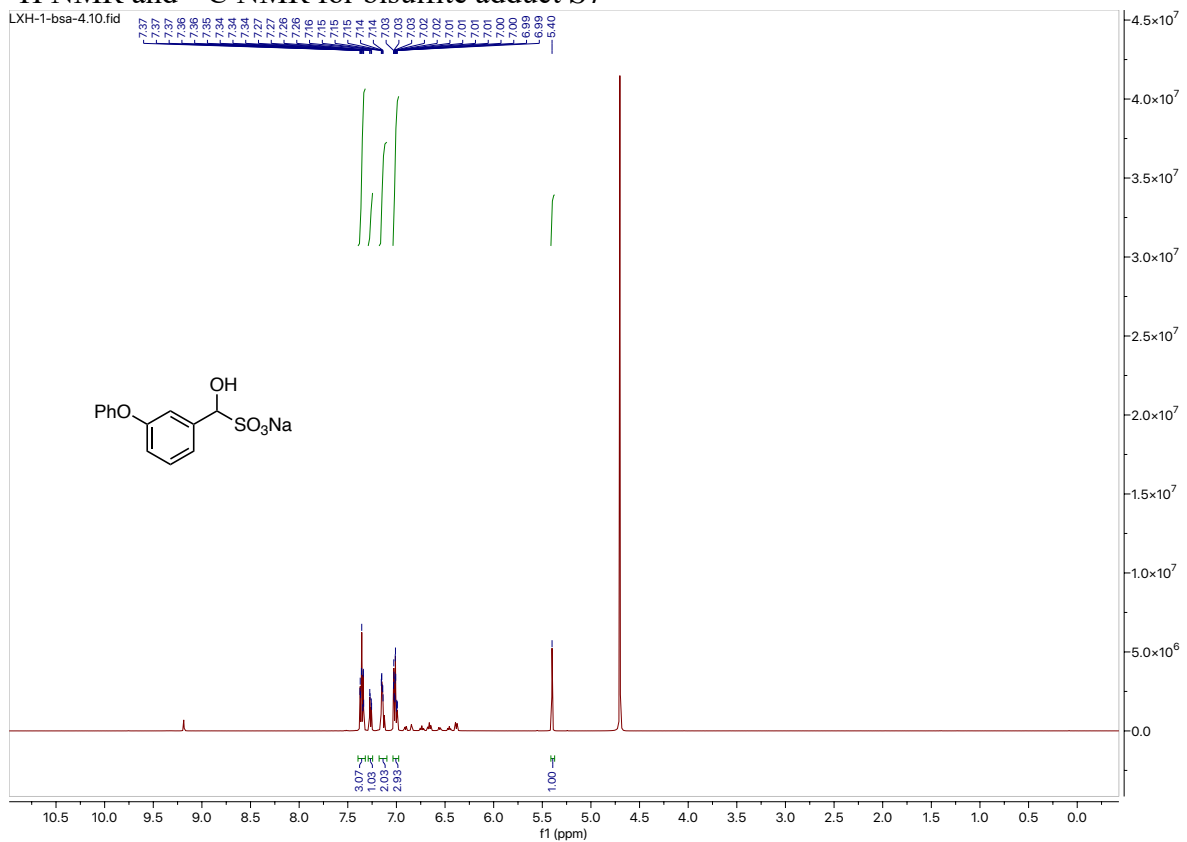
# $^1\text{H}$ NMR and $^{13}\text{C}$ NMR for bisulfite adduct S5



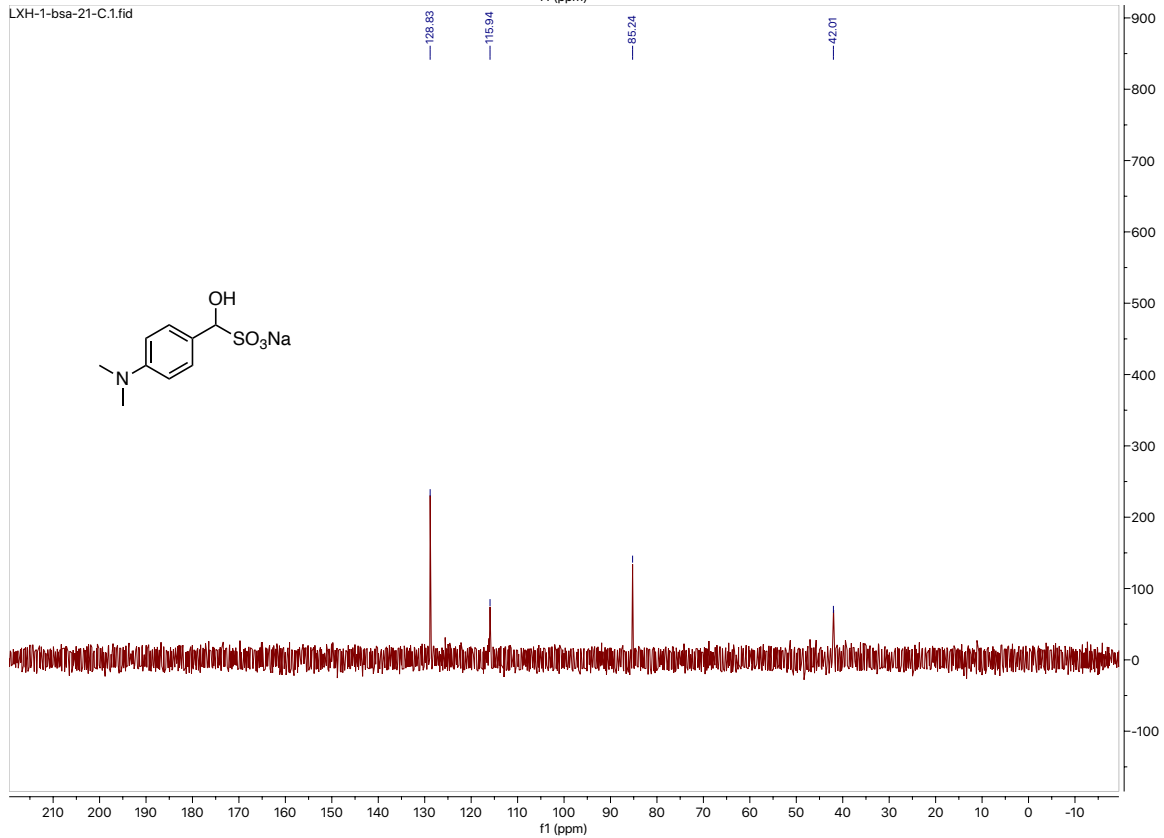
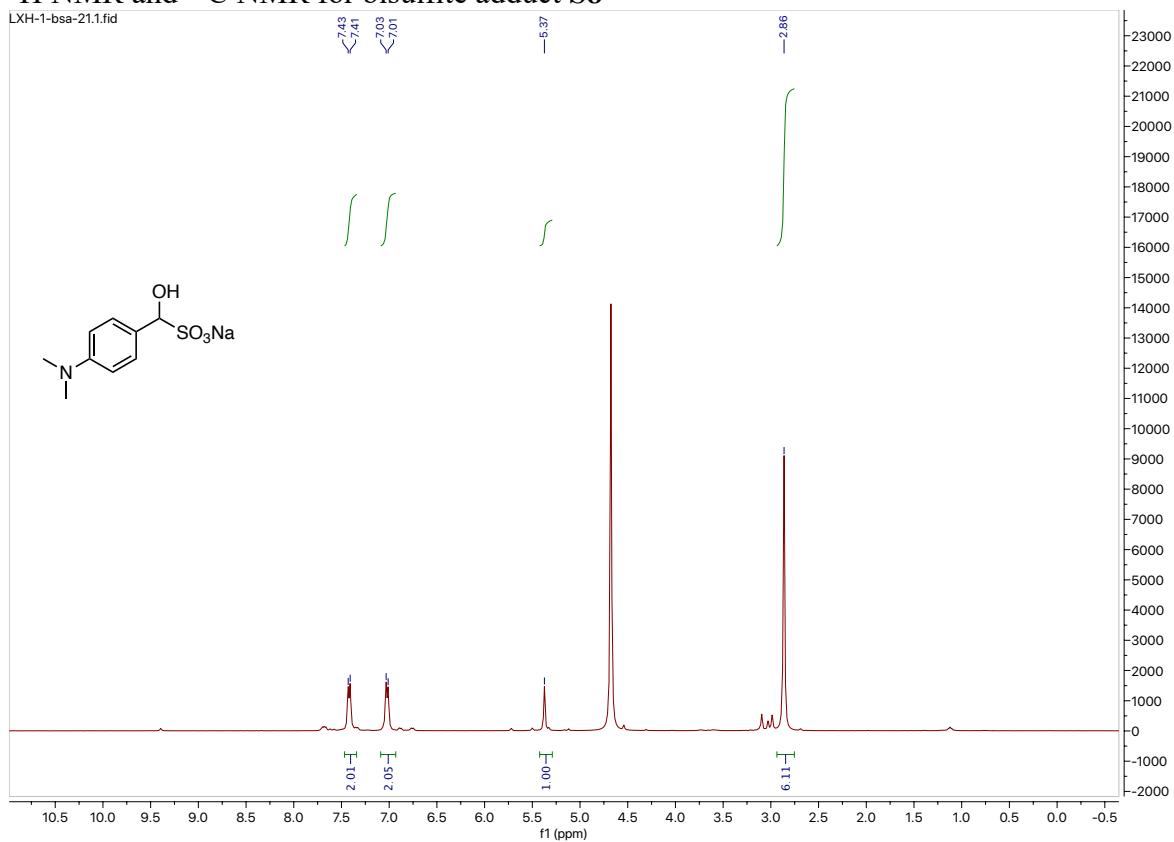
# <sup>1</sup>H NMR and <sup>13</sup>C NMR for bisulfite adduct S6



# <sup>1</sup>H NMR and <sup>13</sup>C NMR for bisulfite adduct S7

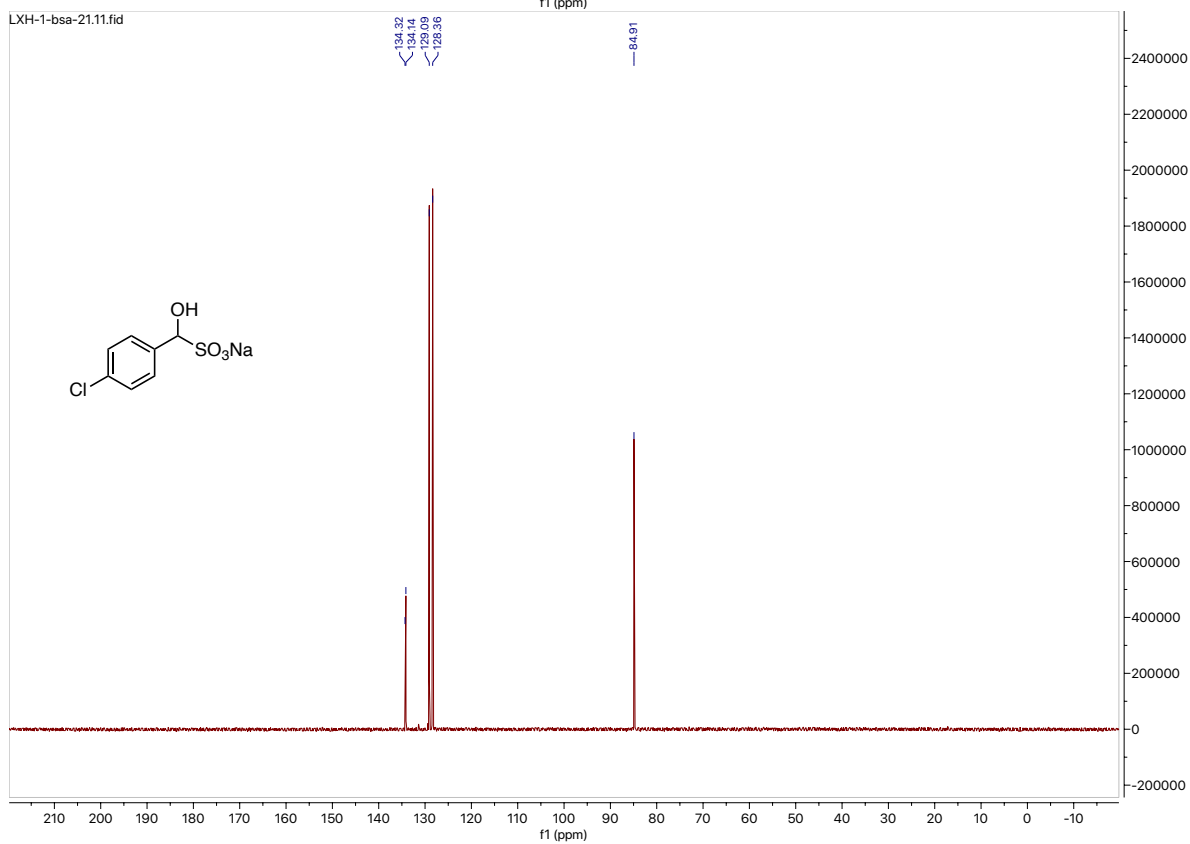
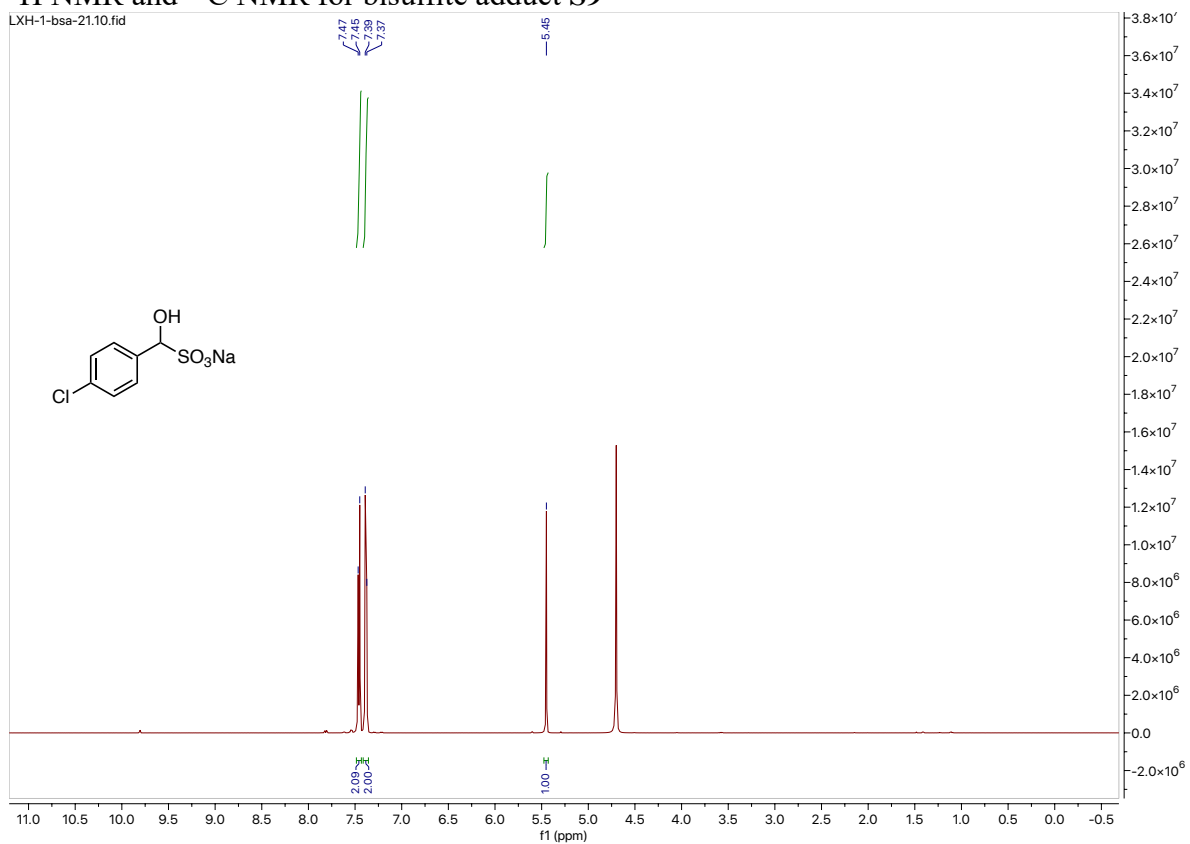


# $^1\text{H}$ NMR and $^{13}\text{C}$ NMR for bisulfite adduct **S8**

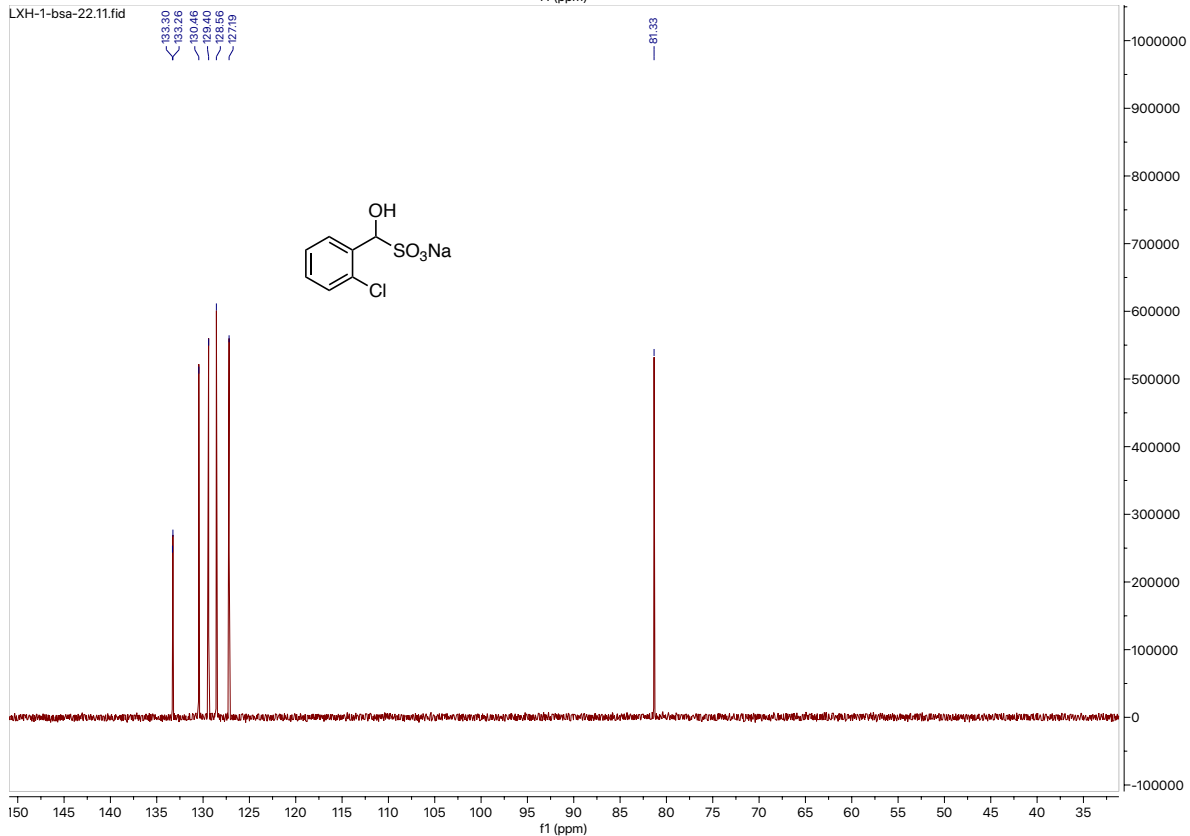
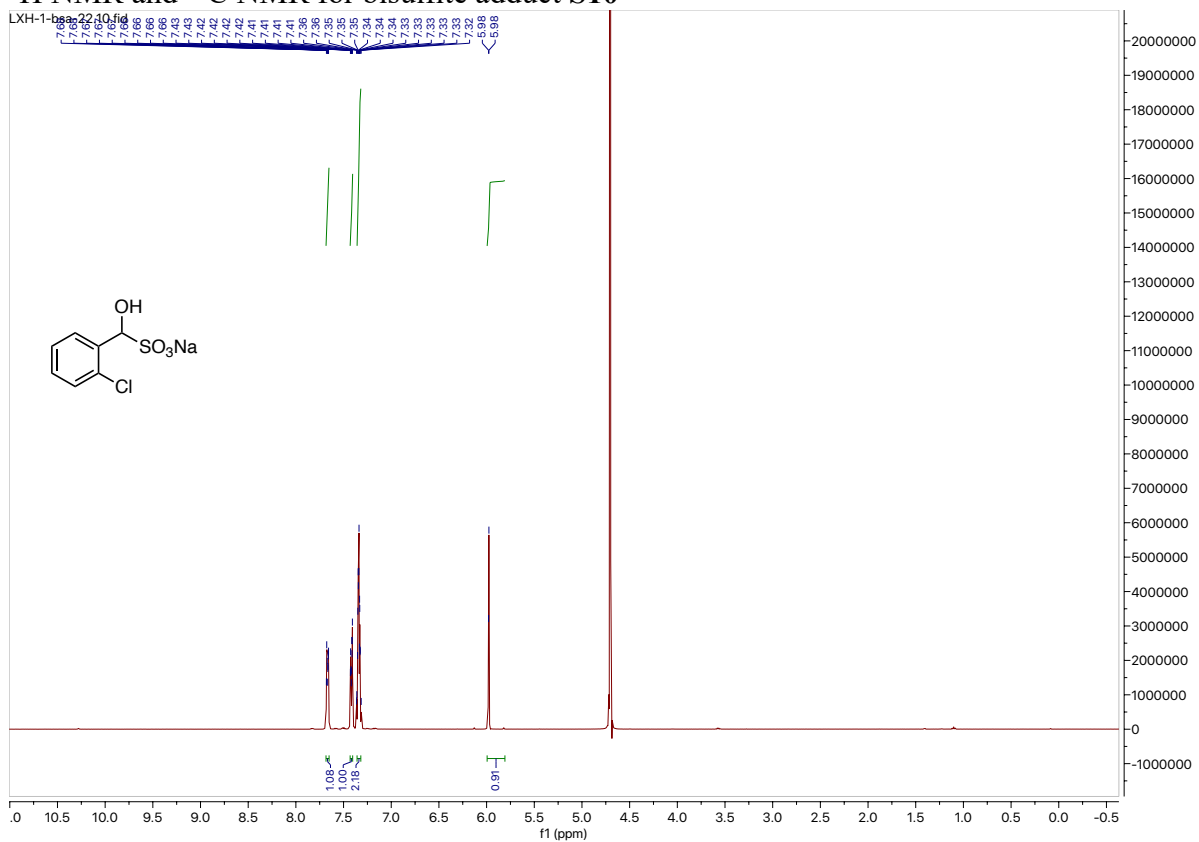




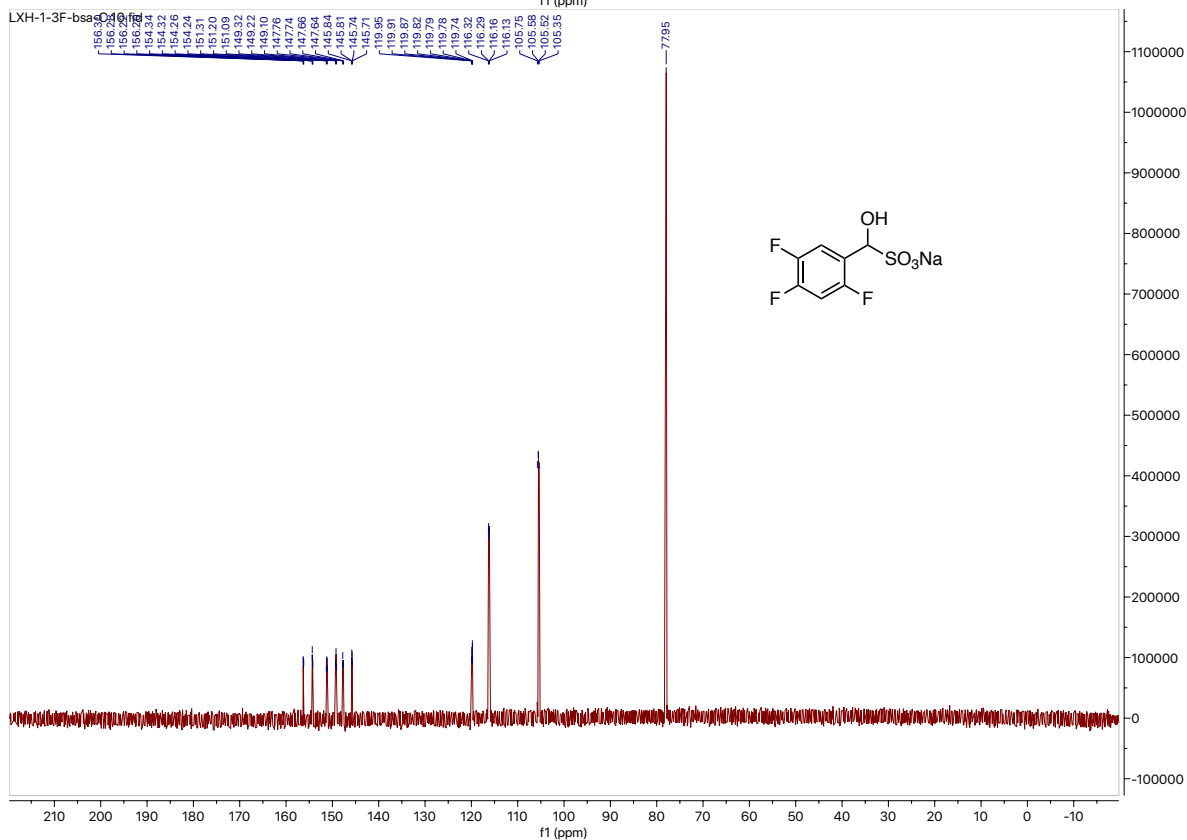
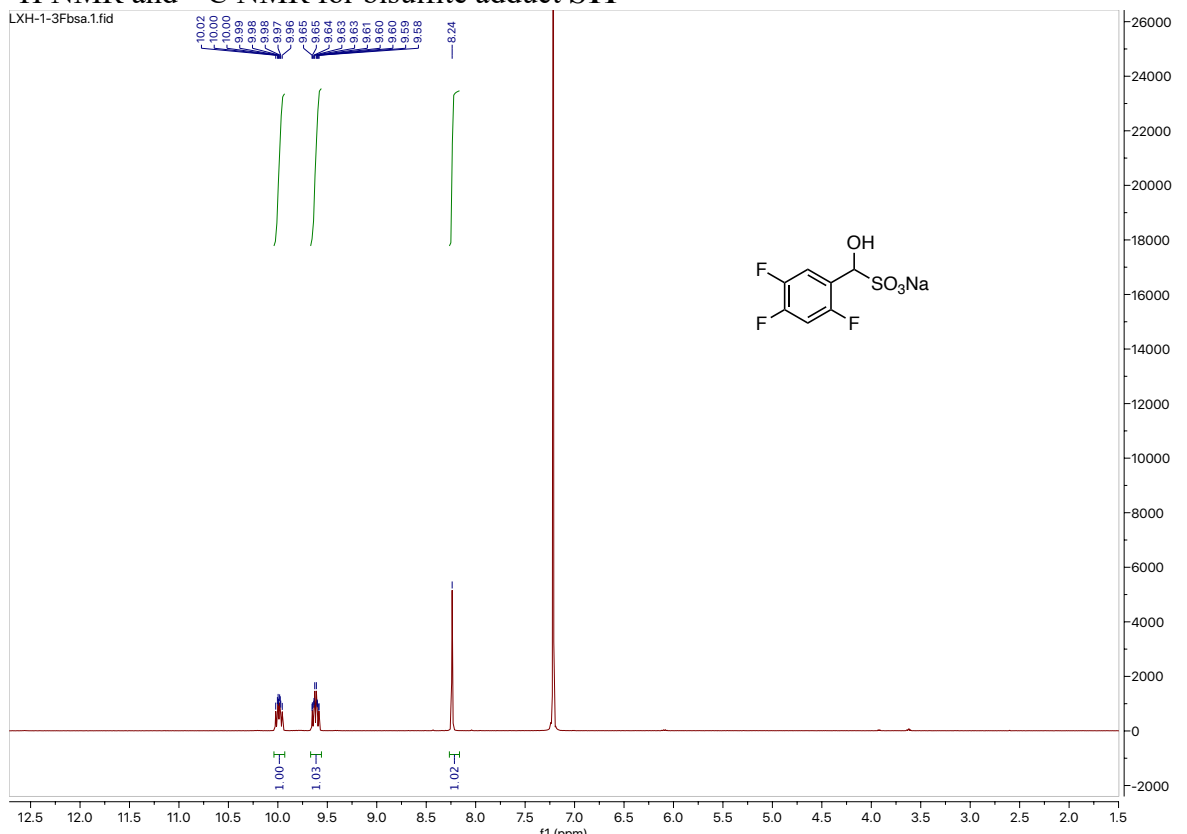
# $^1\text{H}$ NMR and $^{13}\text{C}$ NMR for bisulfite adduct S9



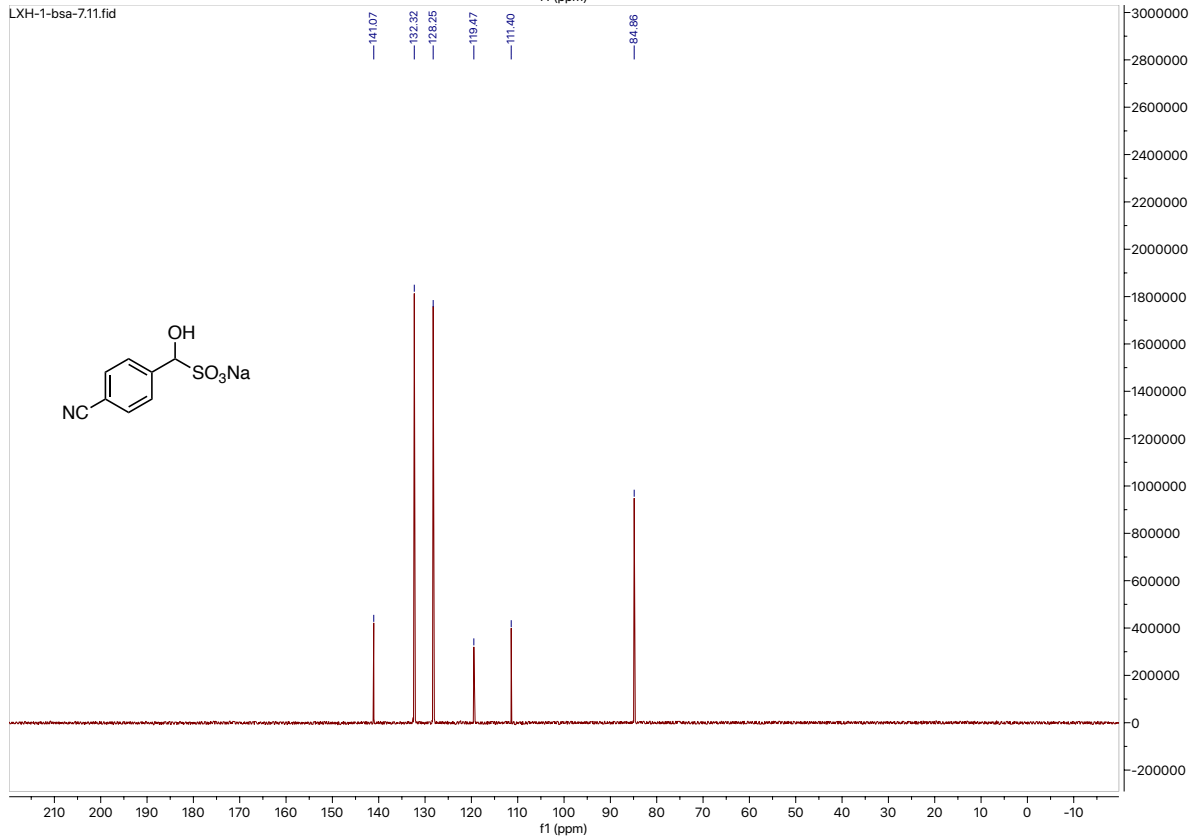
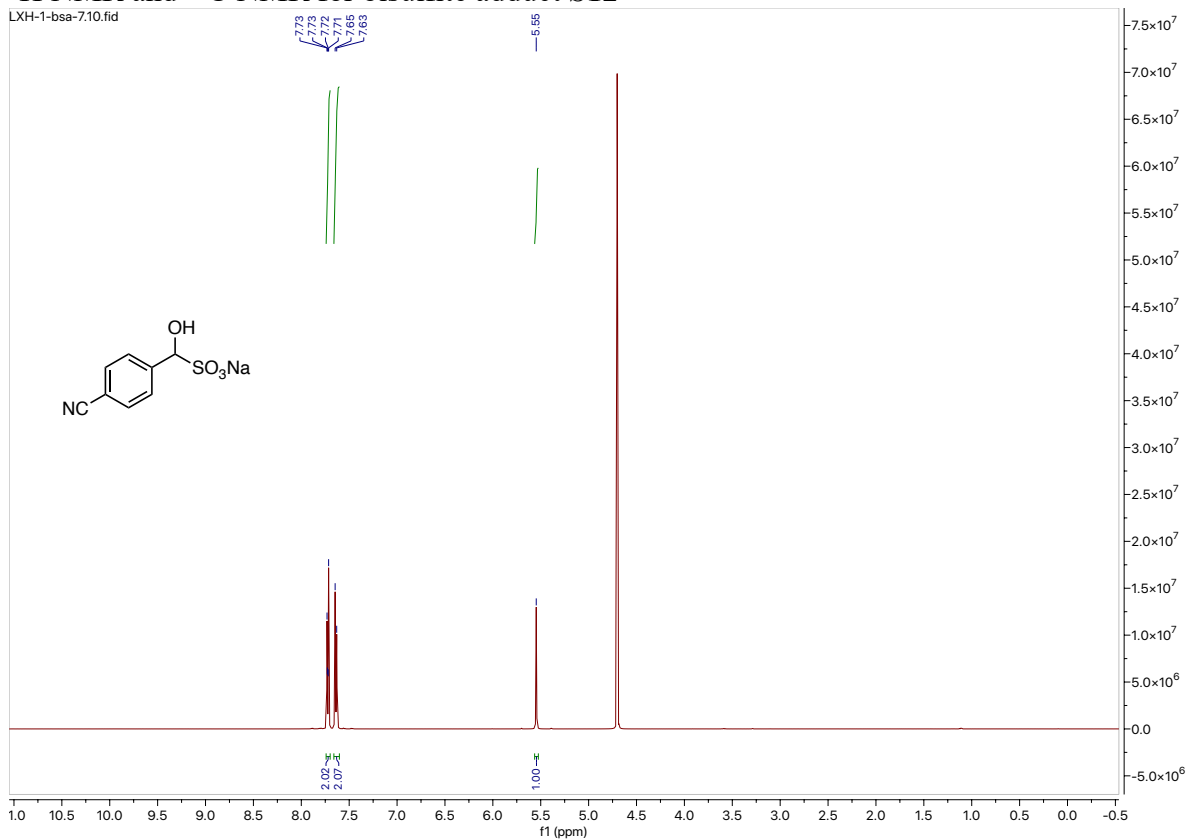
# <sup>1</sup>H NMR and <sup>13</sup>C NMR for bisulfite adduct S10



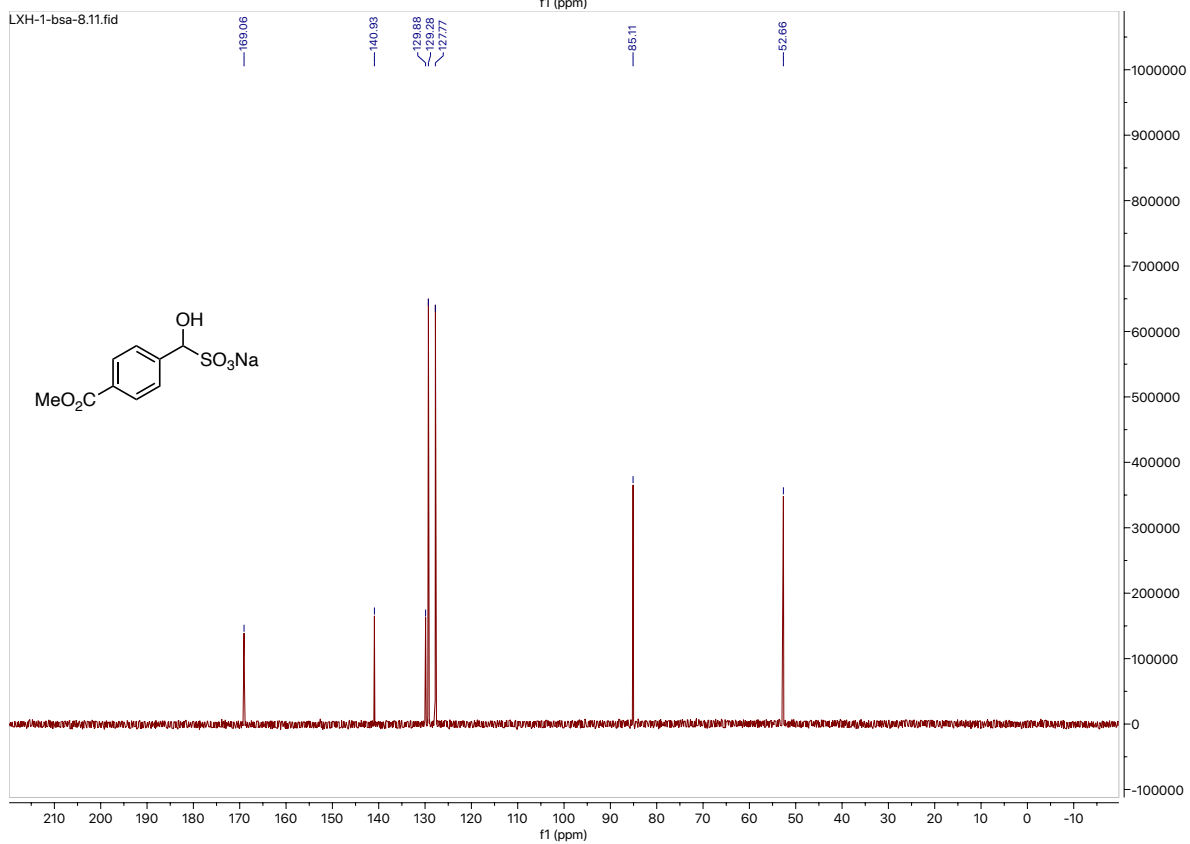
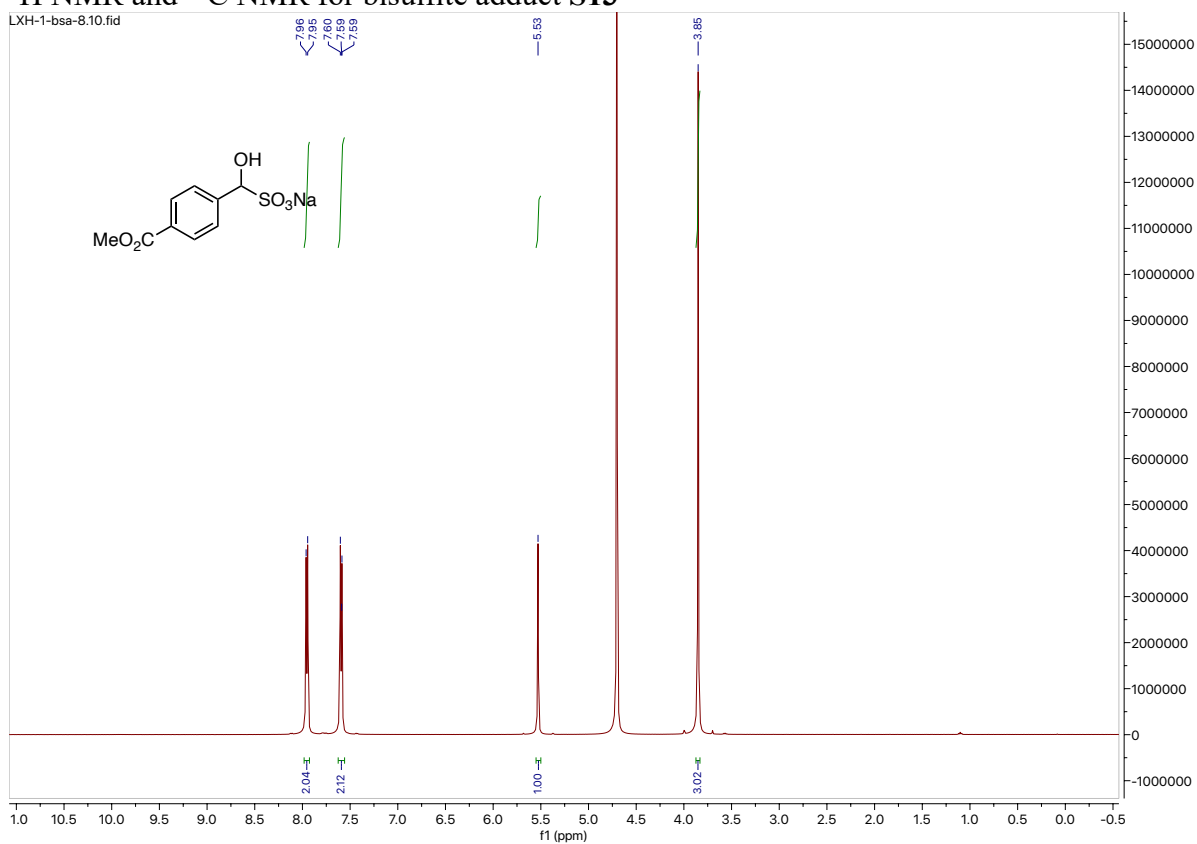
# <sup>1</sup>H NMR and <sup>13</sup>C NMR for bisulfite adduct S11



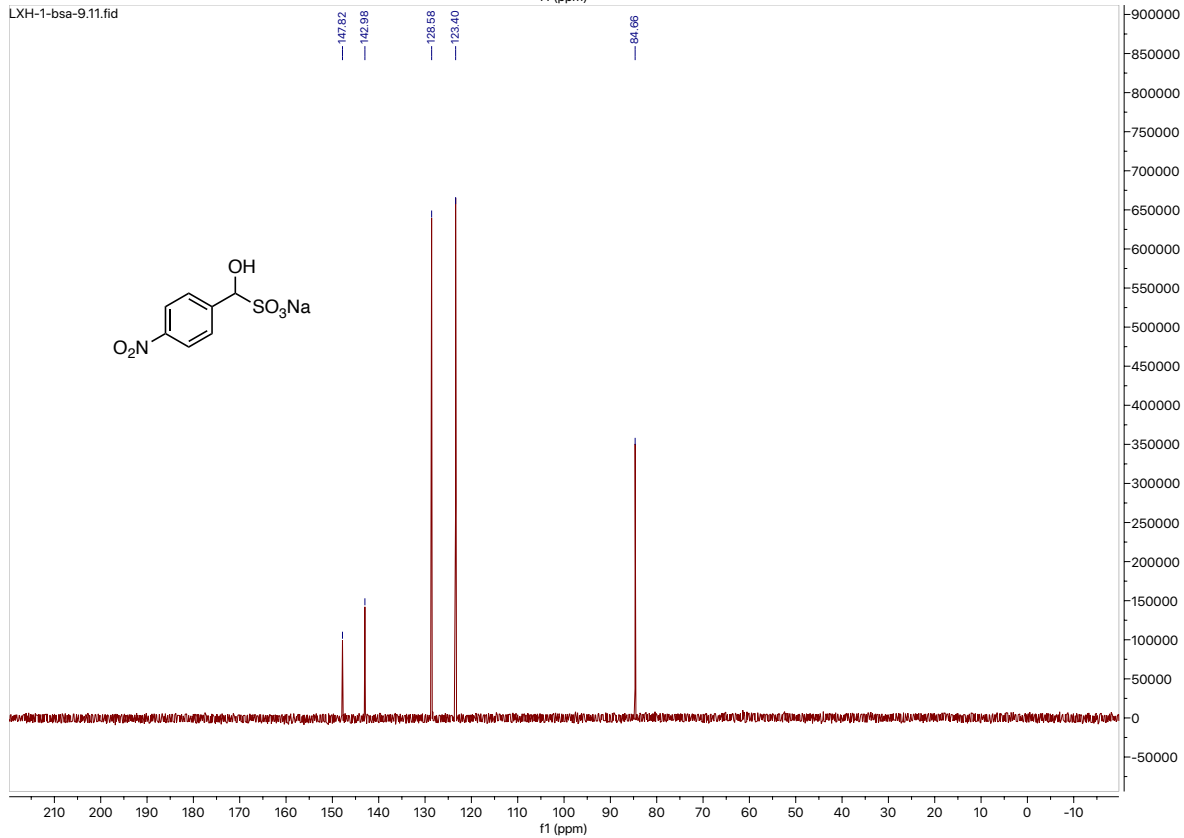
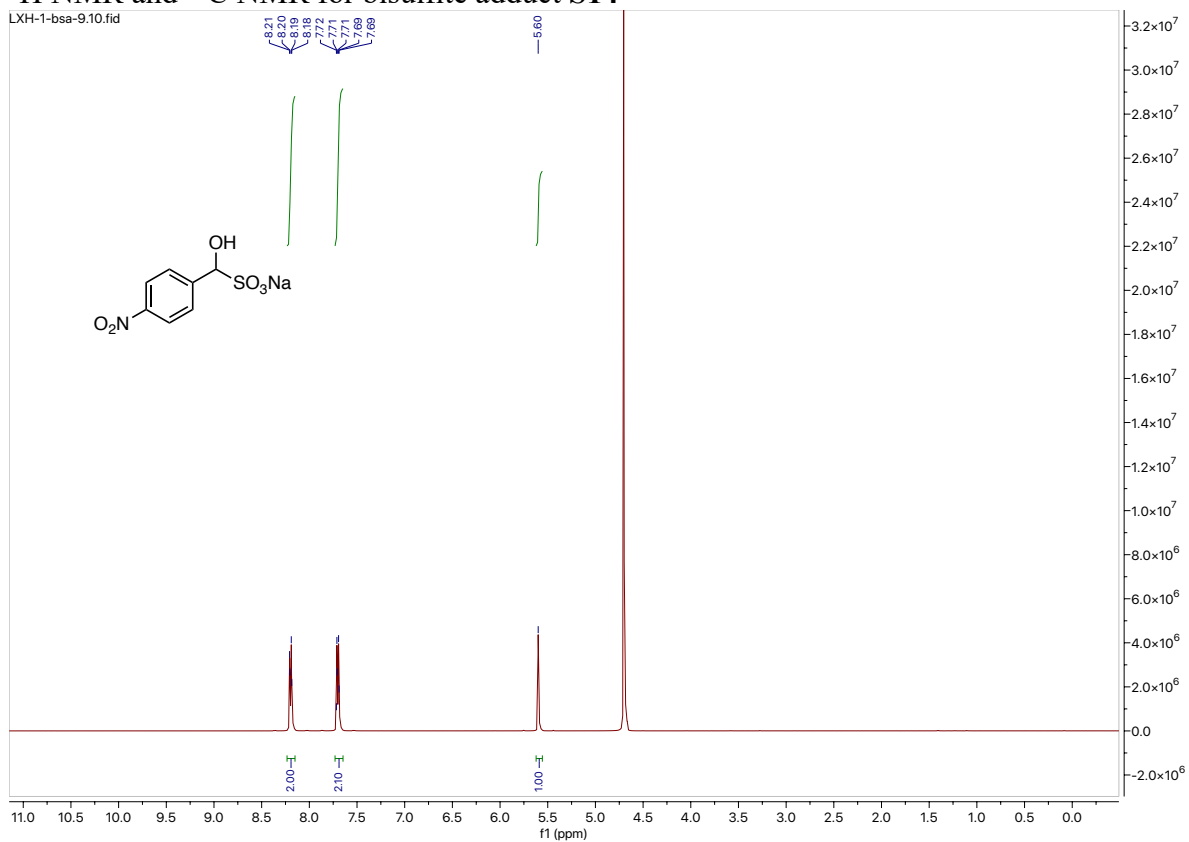
# $^1\text{H}$ NMR and $^{13}\text{C}$ NMR for bisulfite adduct S12



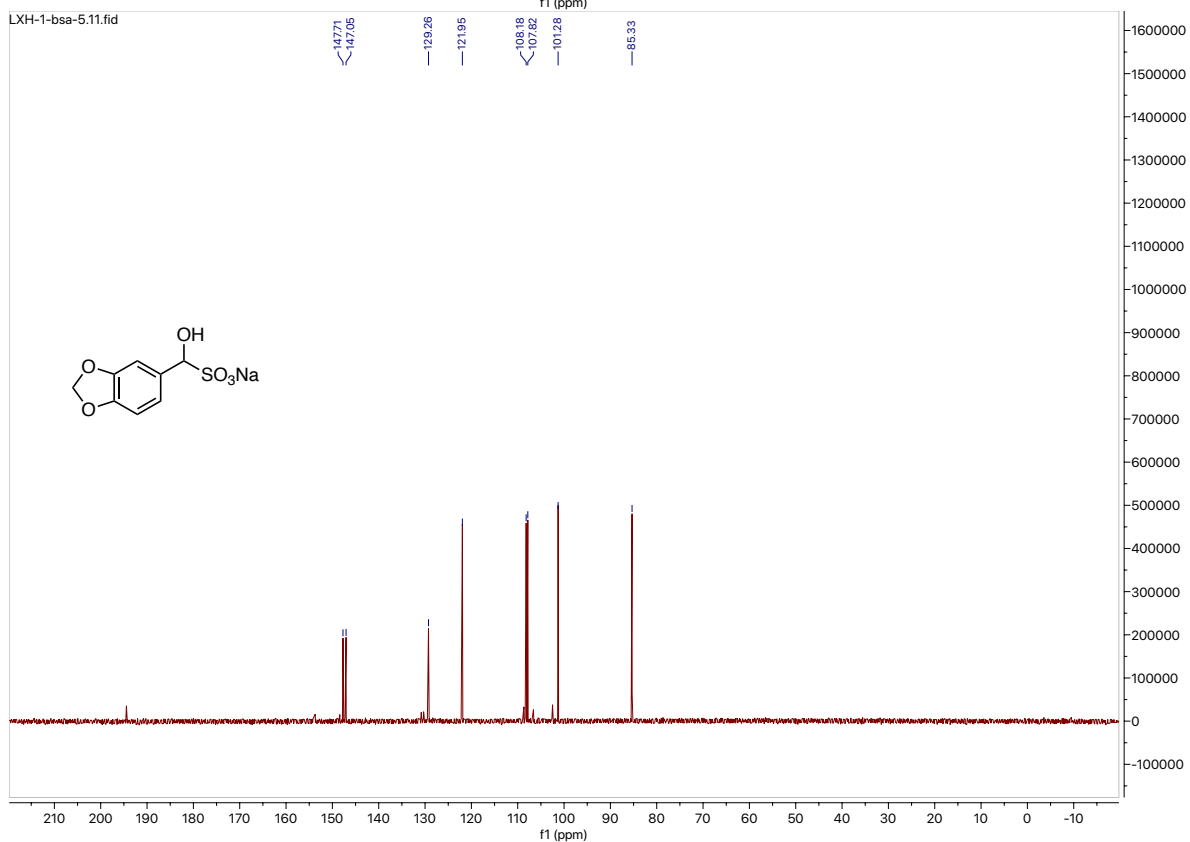
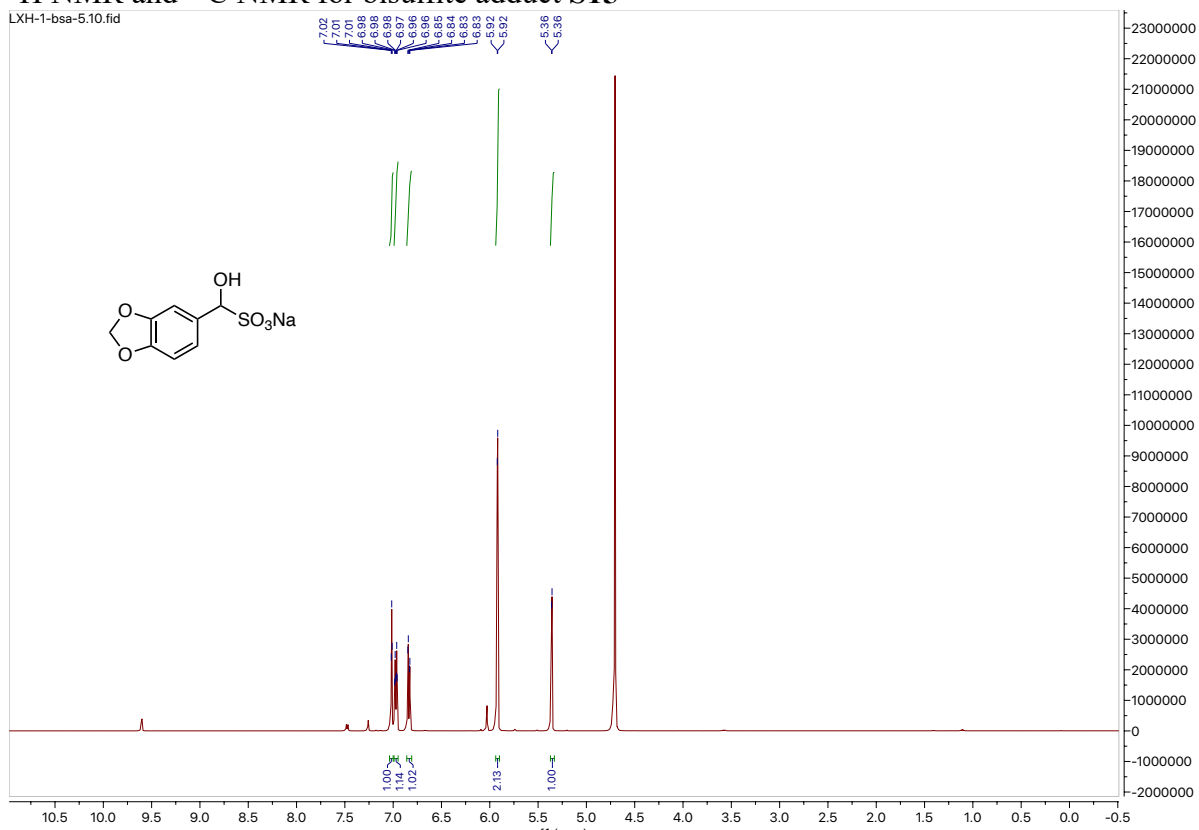
# $^1\text{H}$ NMR and $^{13}\text{C}$ NMR for bisulfite adduct S13



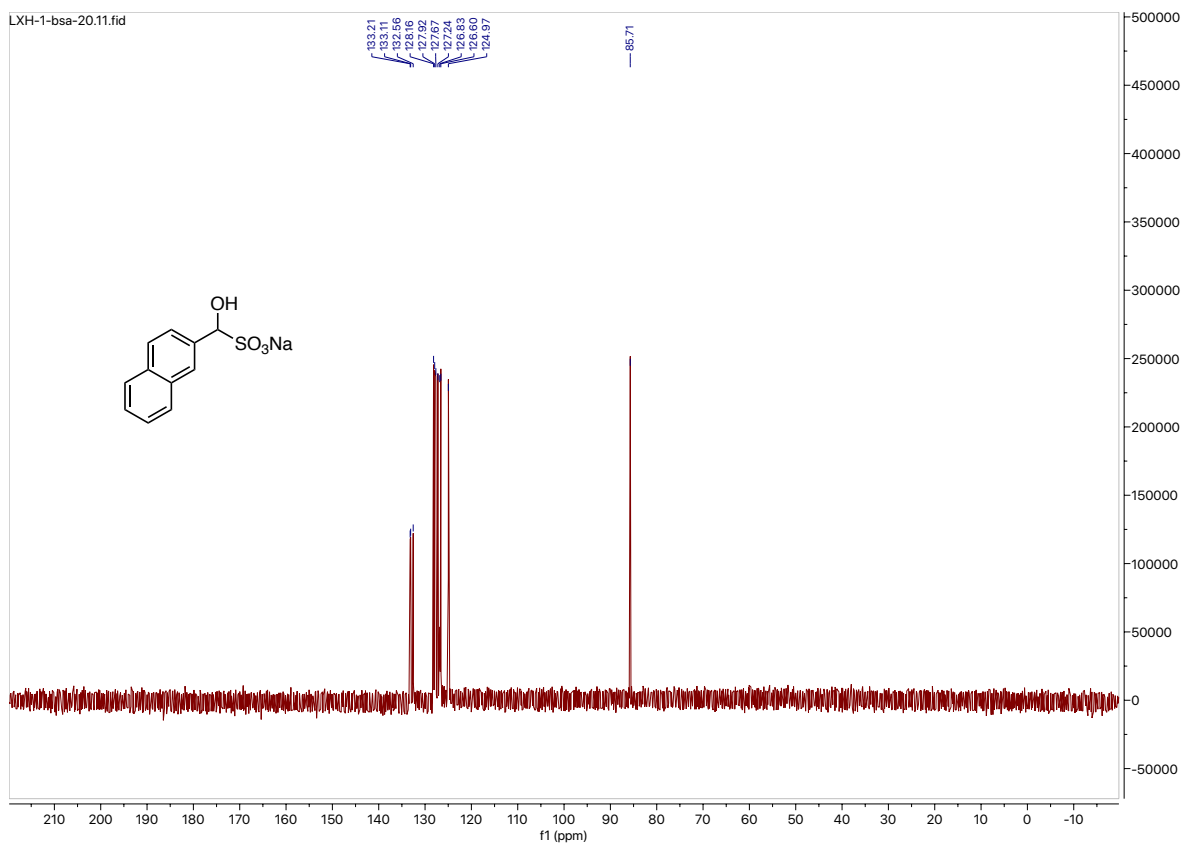
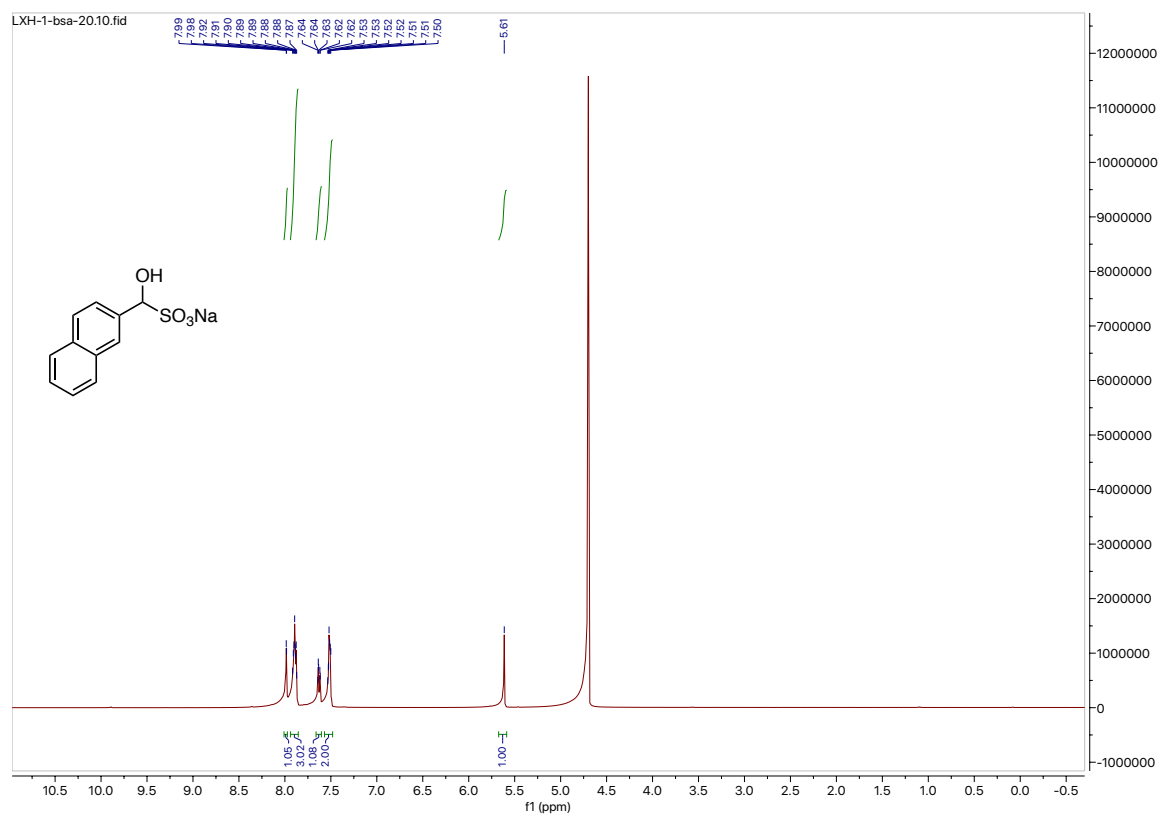
# $^1\text{H}$ NMR and $^{13}\text{C}$ NMR for bisulfite adduct S14



# <sup>1</sup>H NMR and <sup>13</sup>C NMR for bisulfite adduct S15

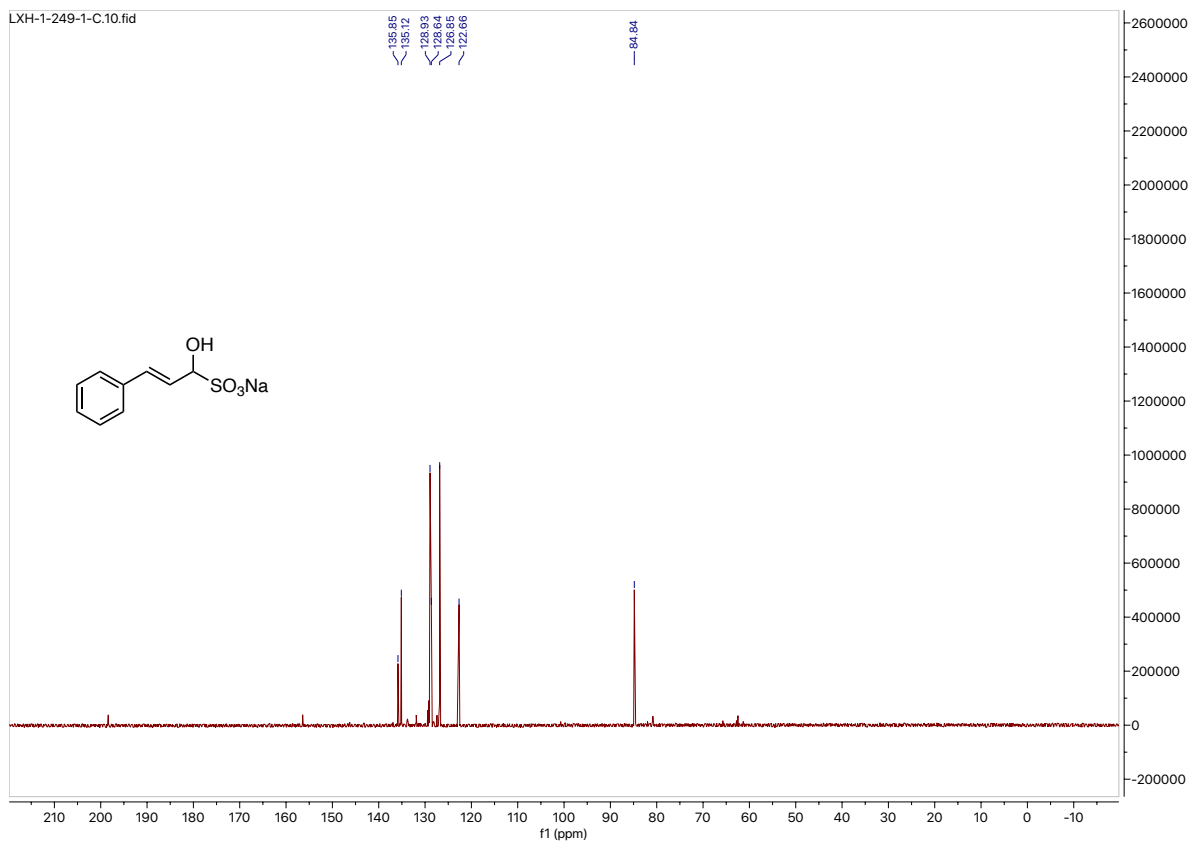
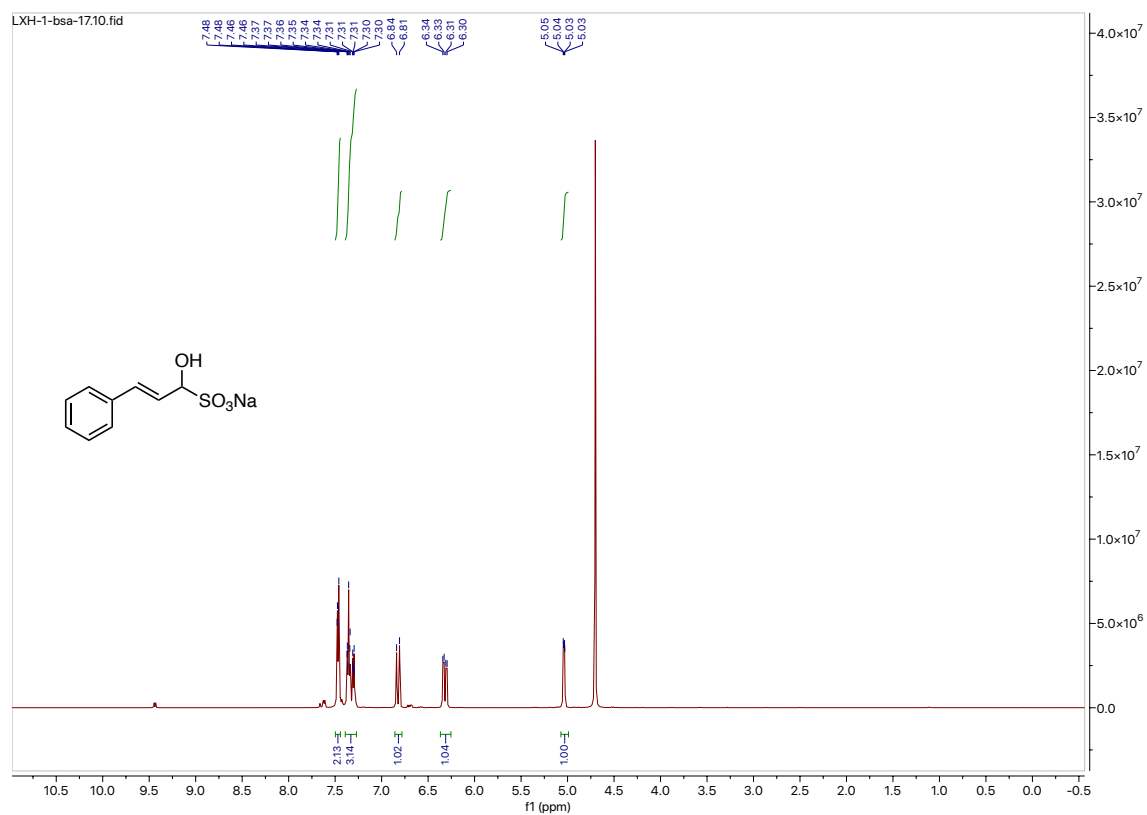


# $^1\text{H}$ NMR and $^{13}\text{C}$ NMR for bisulfite adduct S16

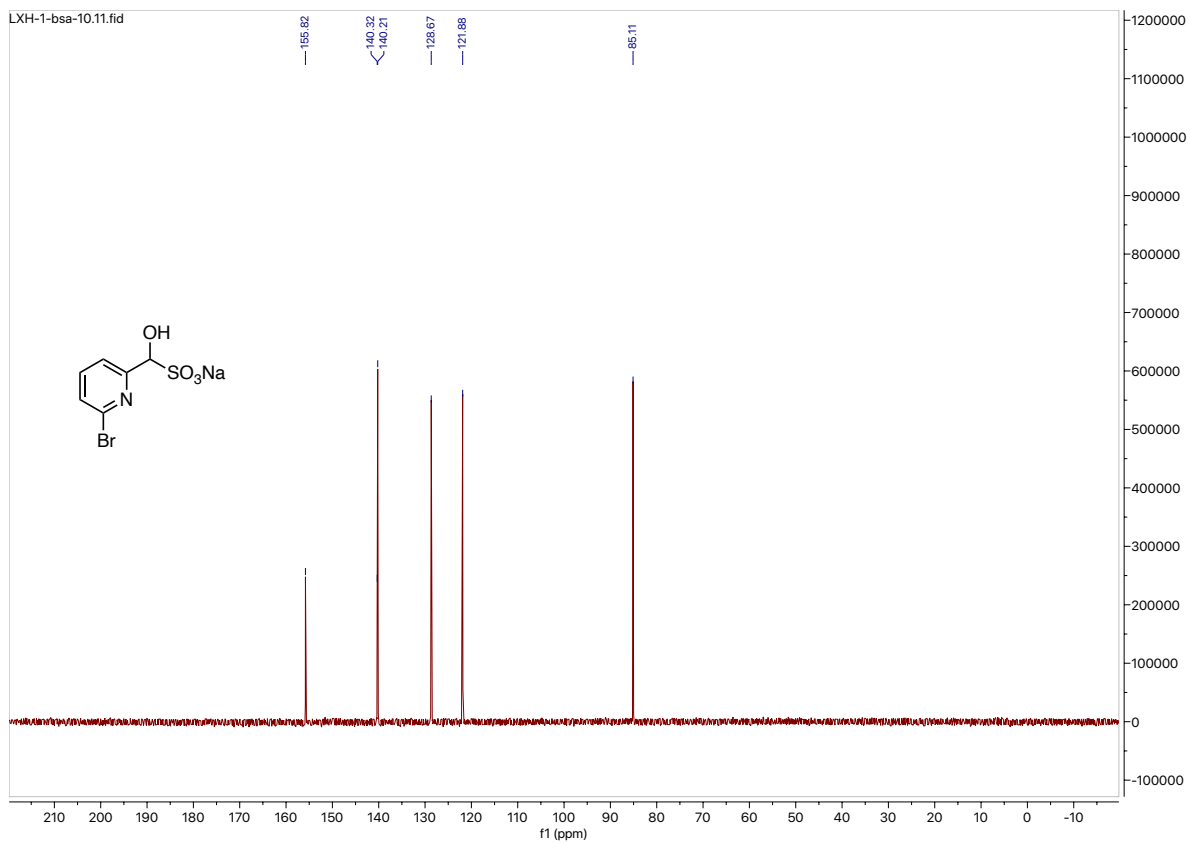
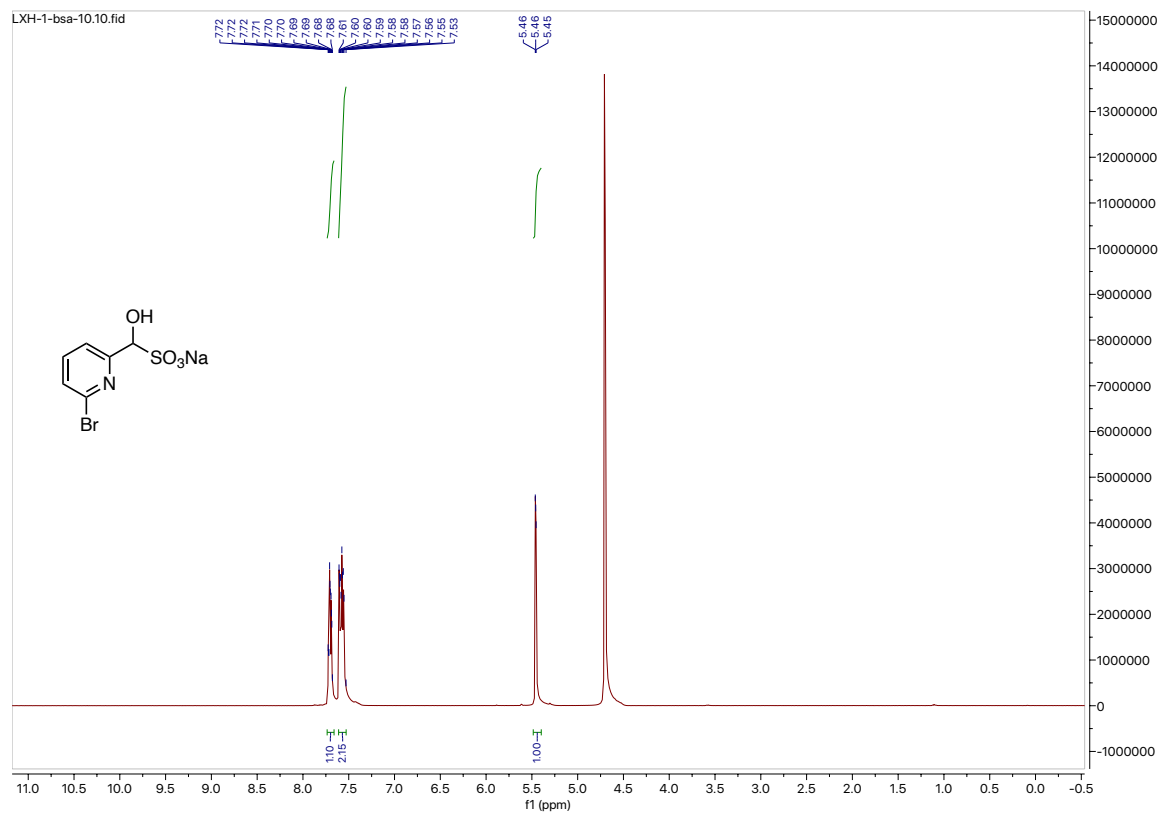




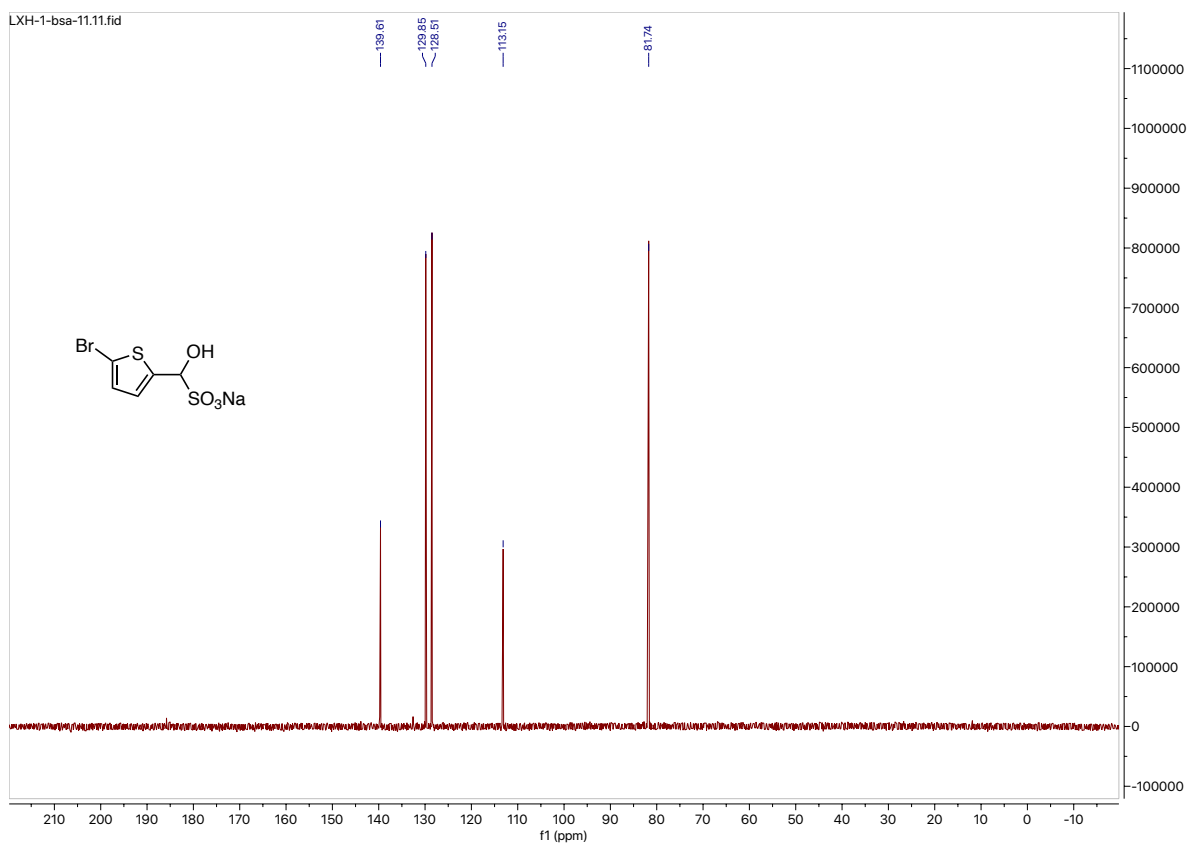
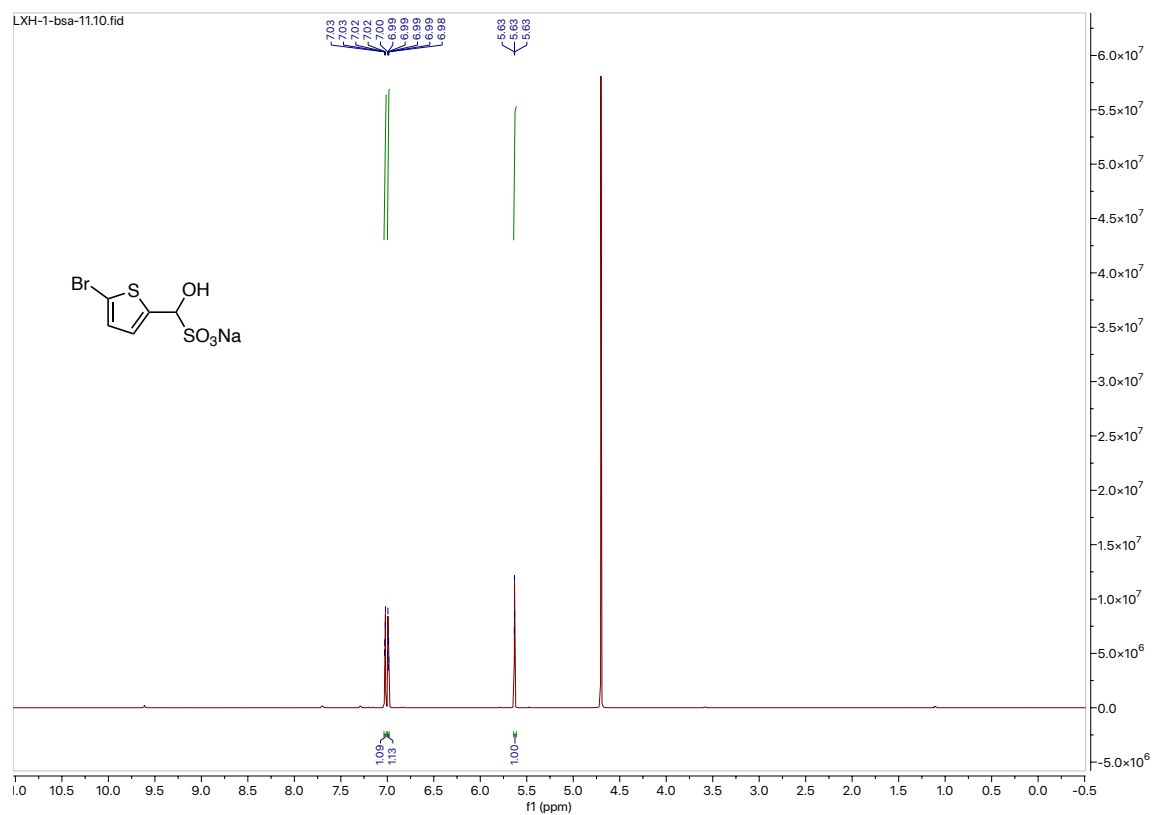
# $^1\text{H}$ NMR and $^{13}\text{C}$ NMR for bisulfite adduct S17



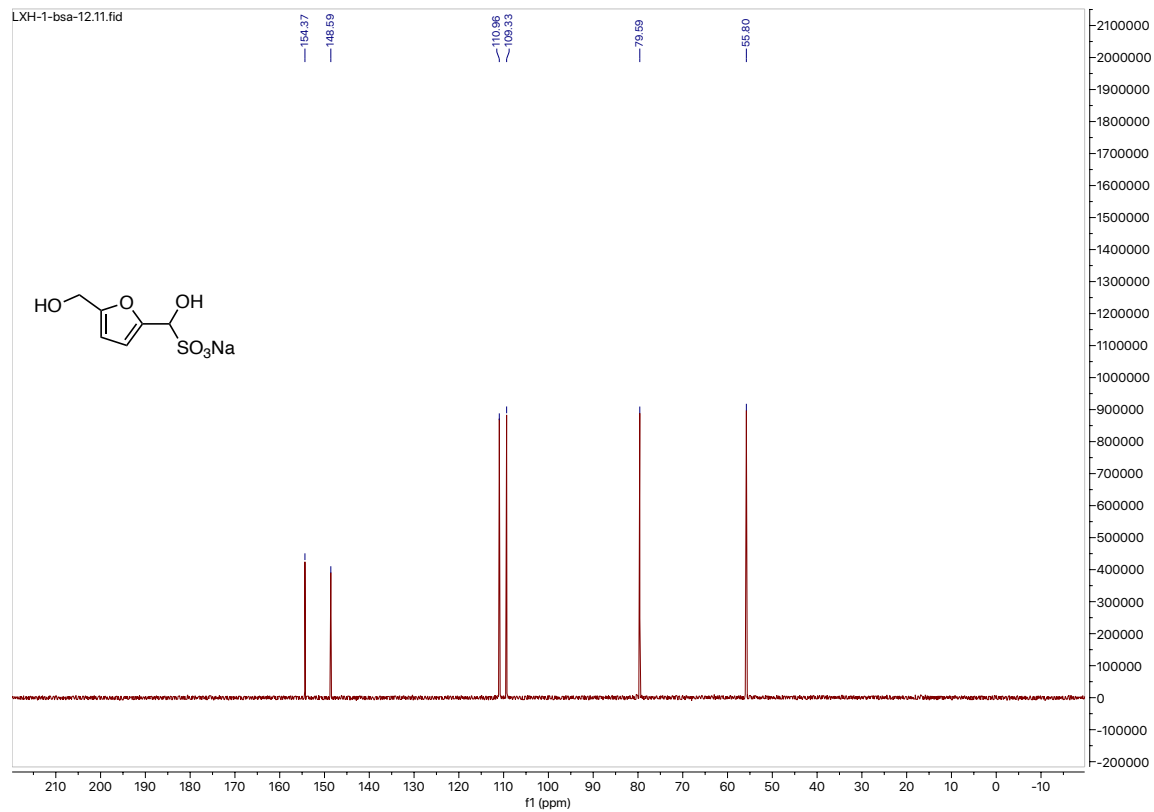
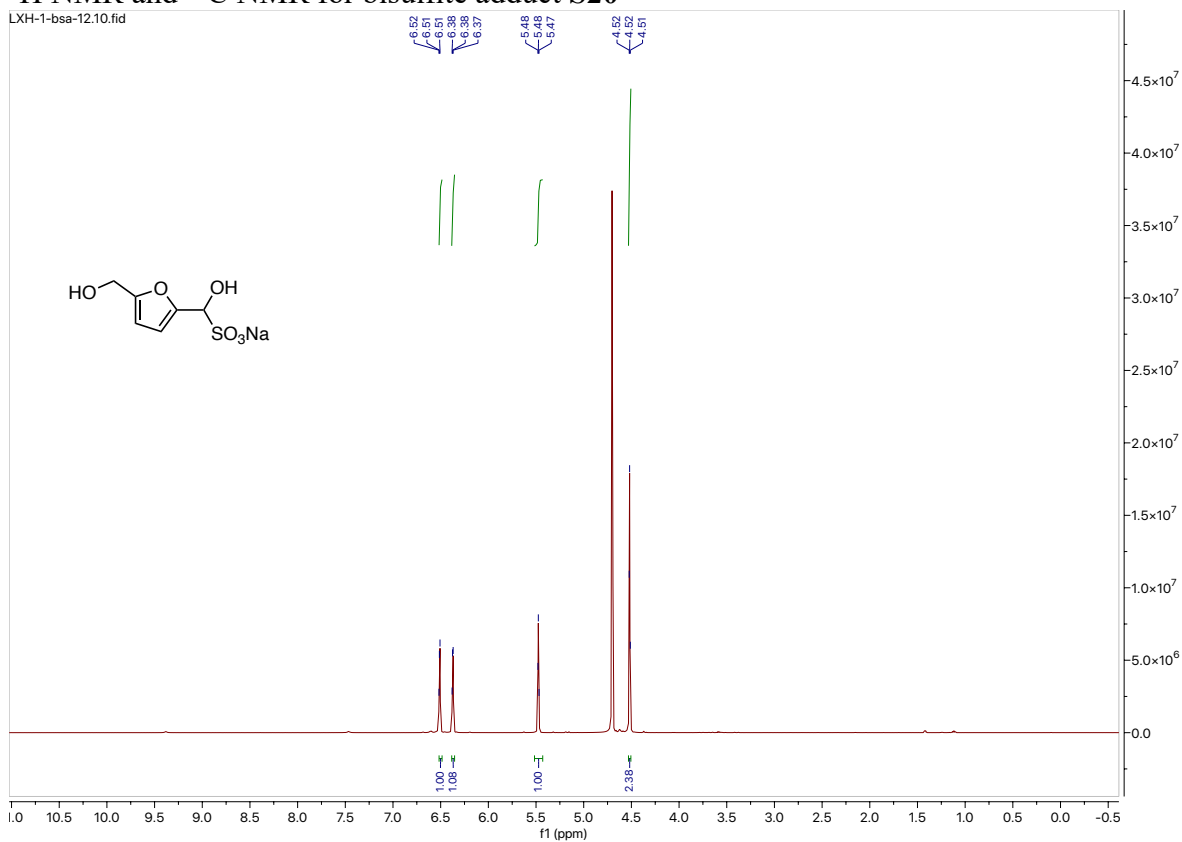
# $^1\text{H}$ NMR and $^{13}\text{C}$ NMR for bisulfite adduct **S18**



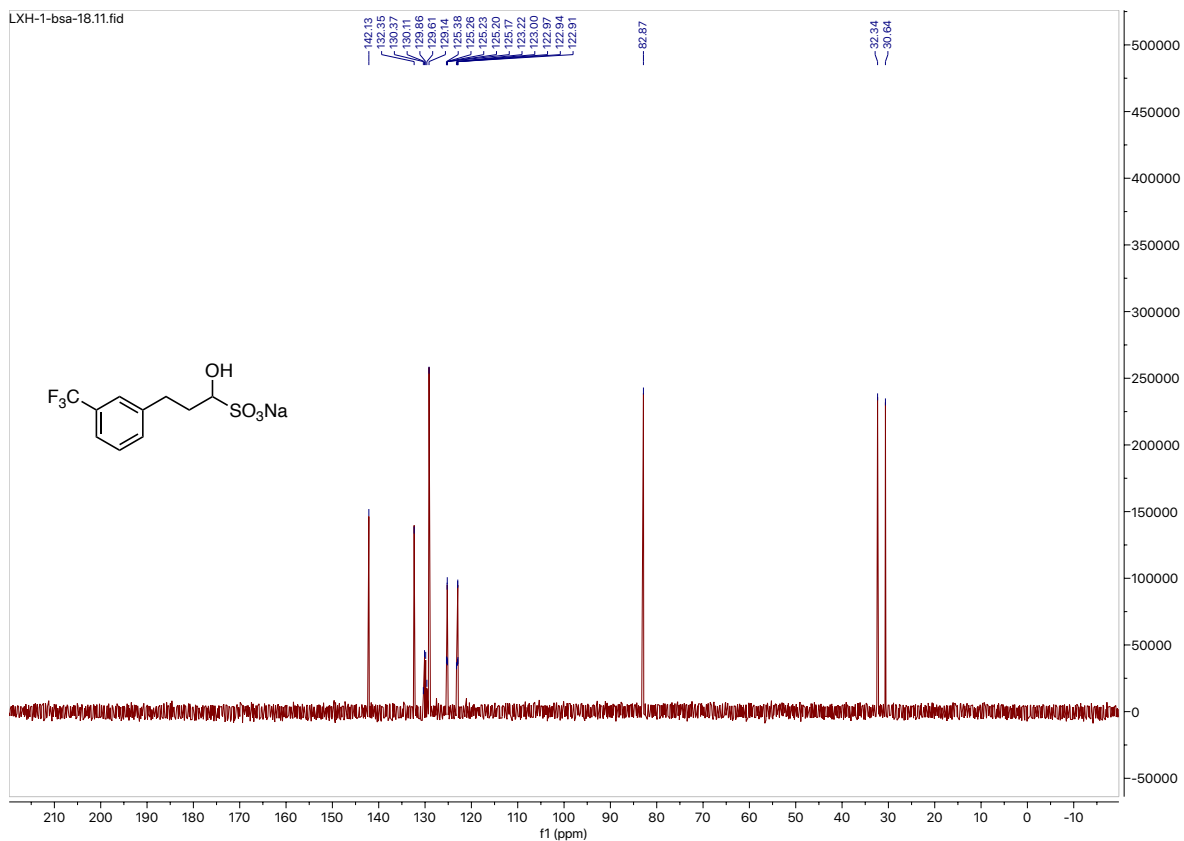
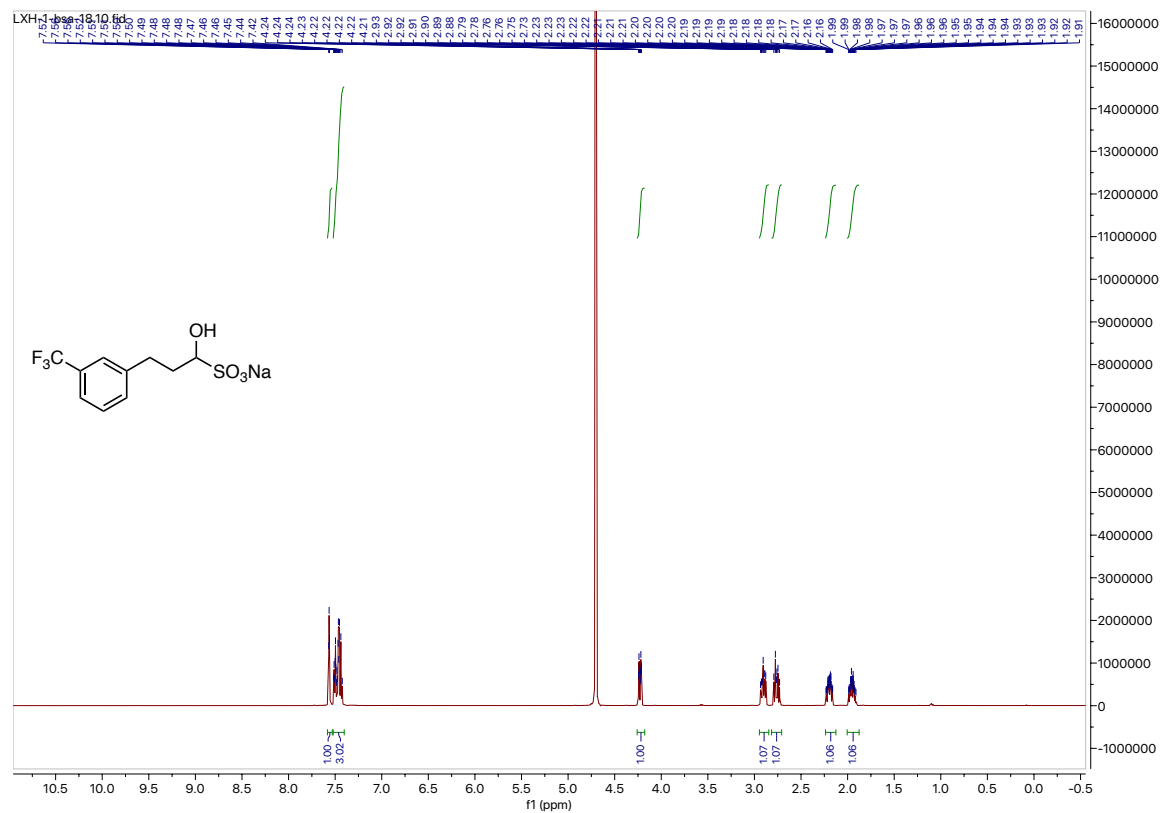
# $^1\text{H}$ NMR and $^{13}\text{C}$ NMR for bisulfite adduct S19



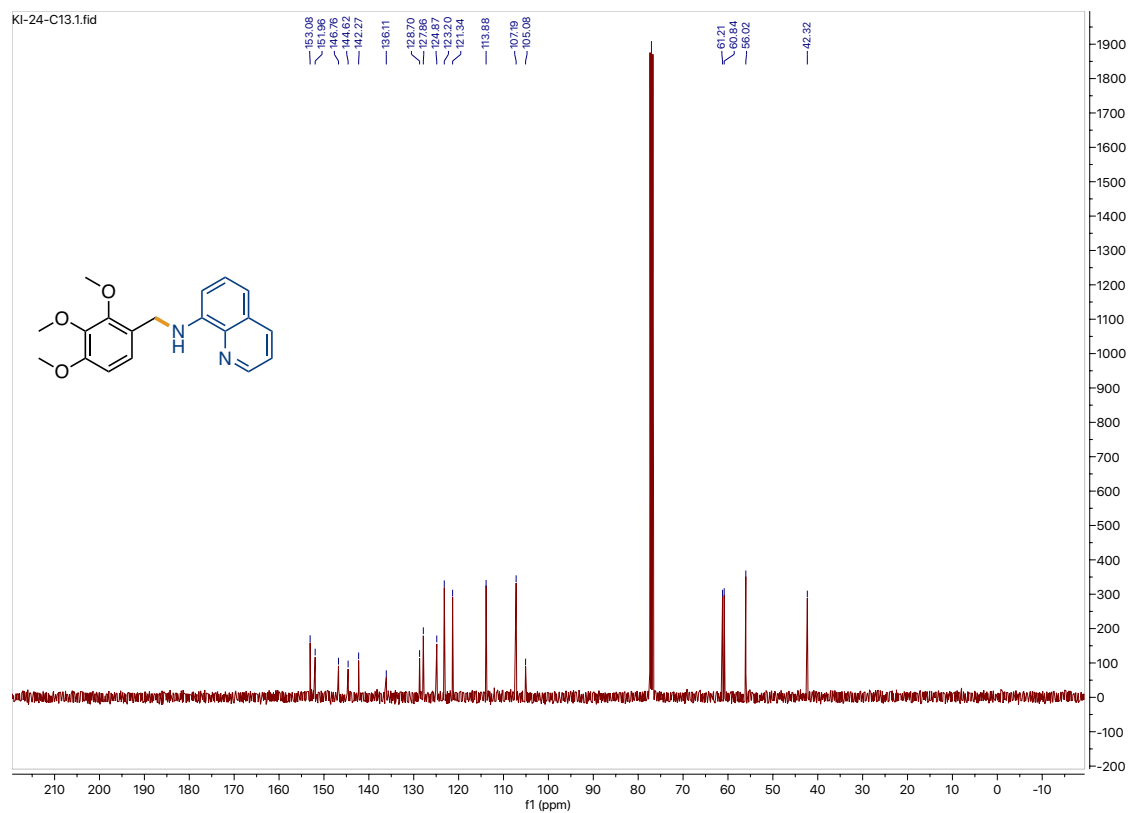
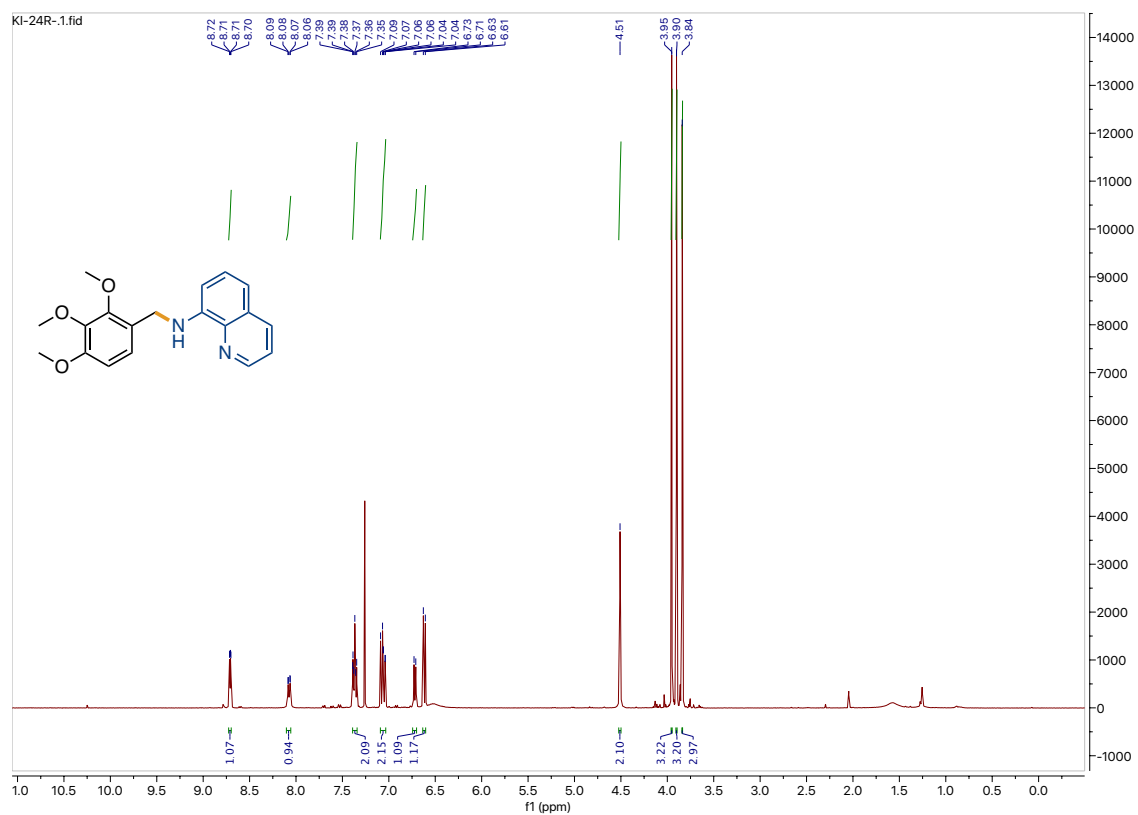
# $^1\text{H}$ NMR and $^{13}\text{C}$ NMR for bisulfite adduct S20



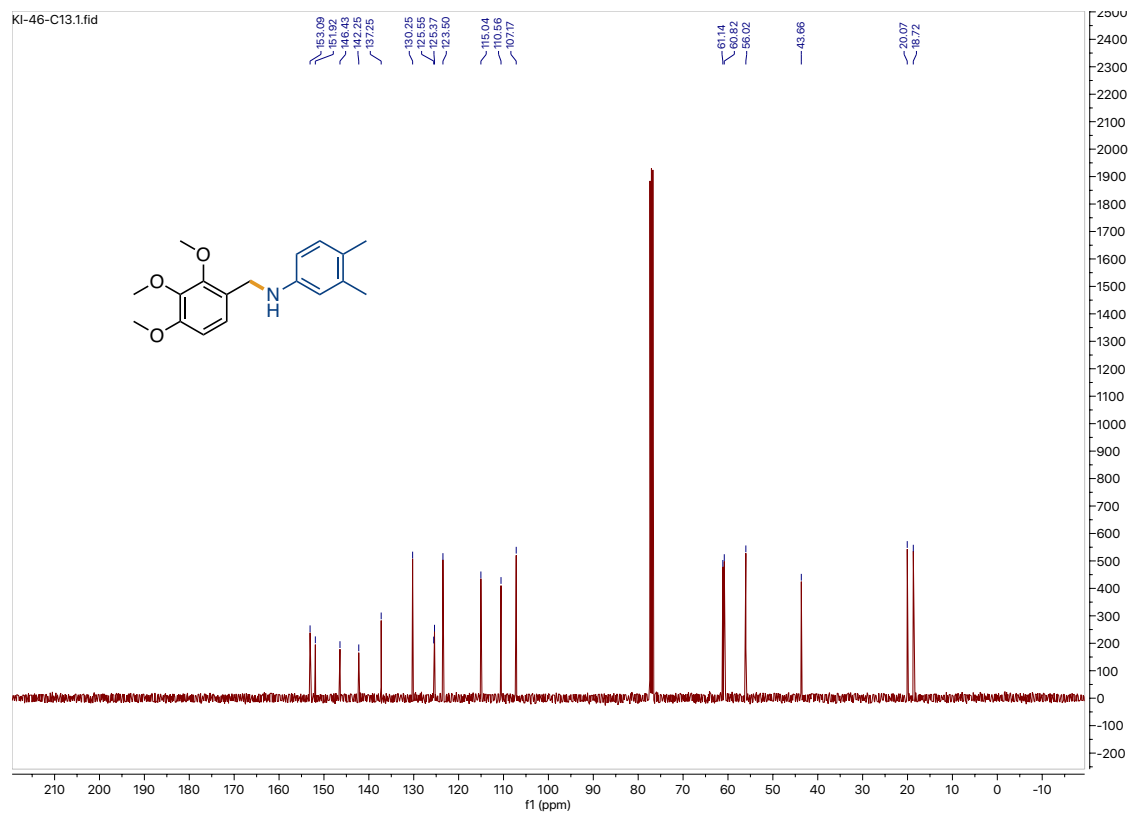
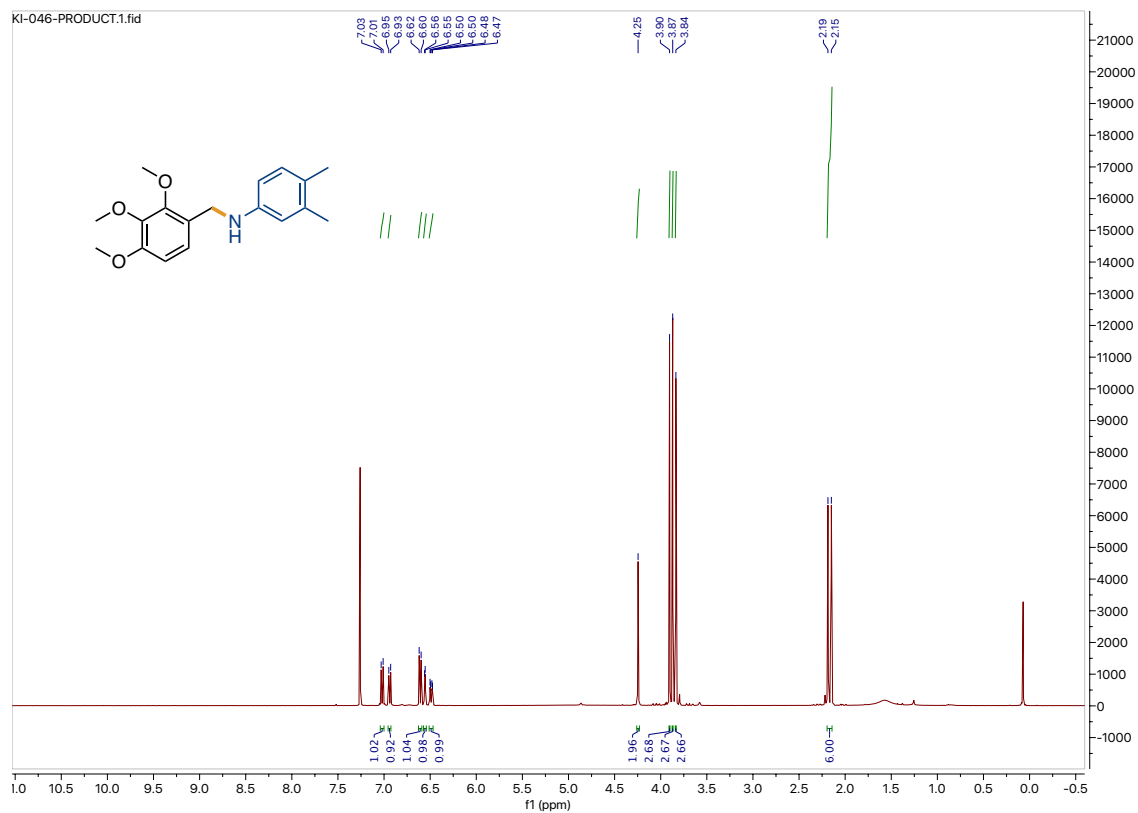
<sup>1</sup>H NMR and <sup>13</sup>C NMR for bisulfite adduct S21



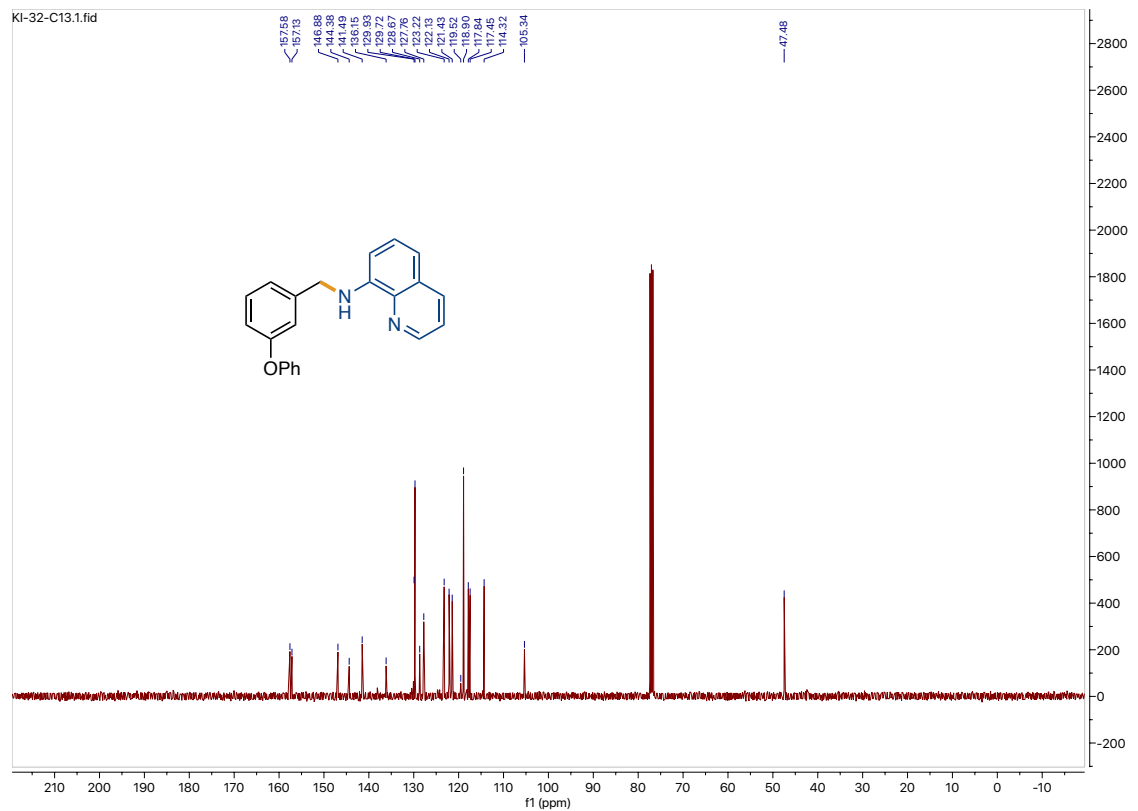
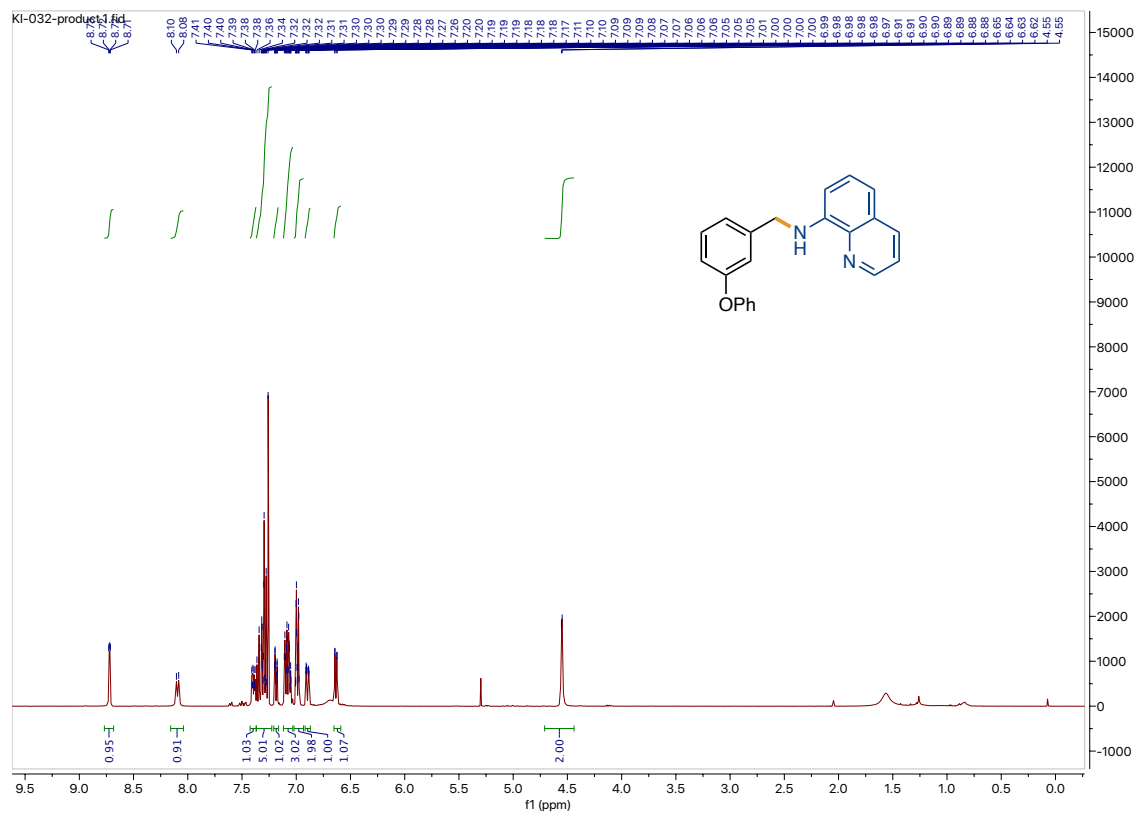
# $^1\text{H}$ NMR and $^{13}\text{C}$ NMR for compound I-5



# $^1\text{H}$ NMR and $^{13}\text{C}$ NMR for compound I-6



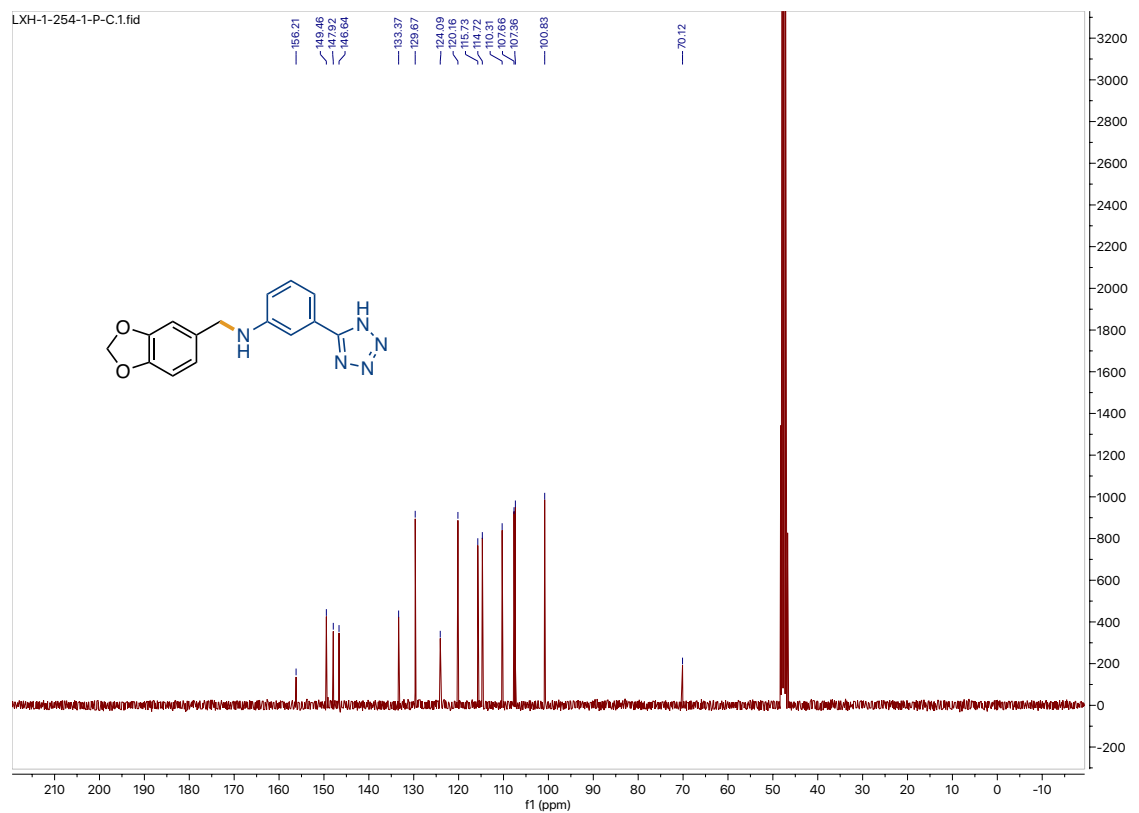
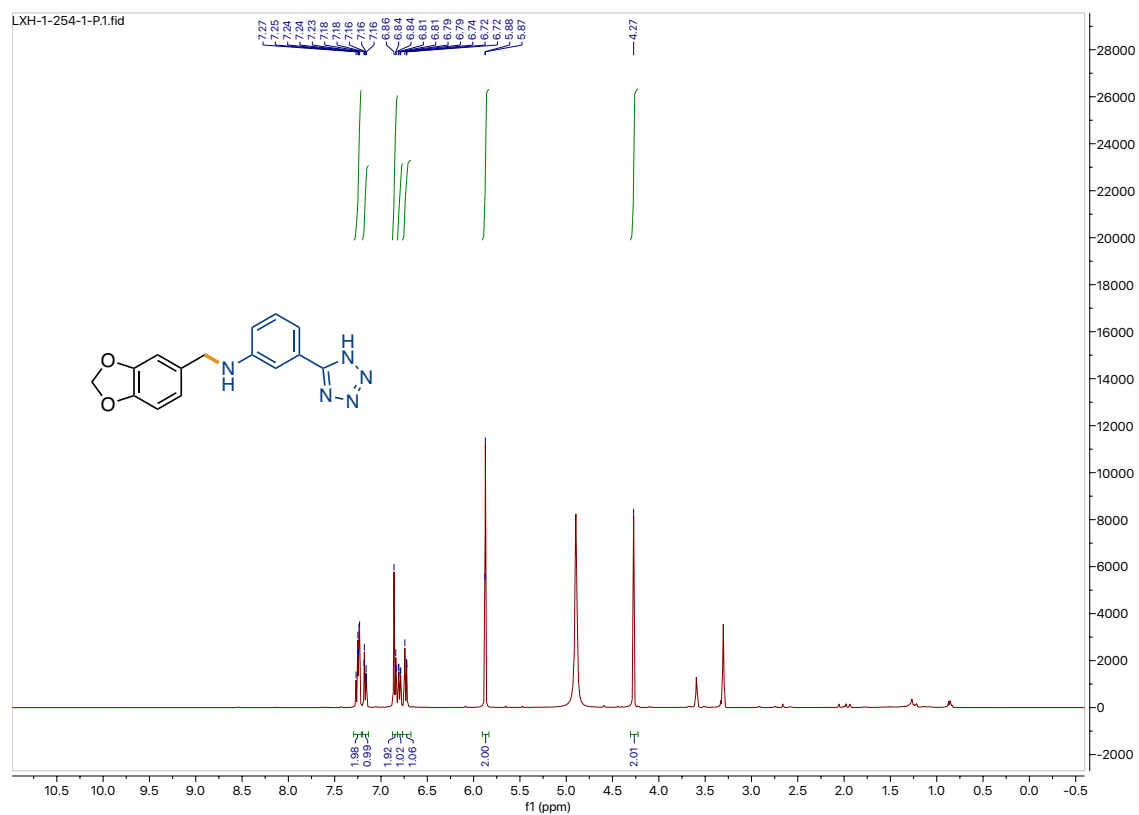
# $^1\text{H}$ NMR and $^{13}\text{C}$ NMR for compound I-9



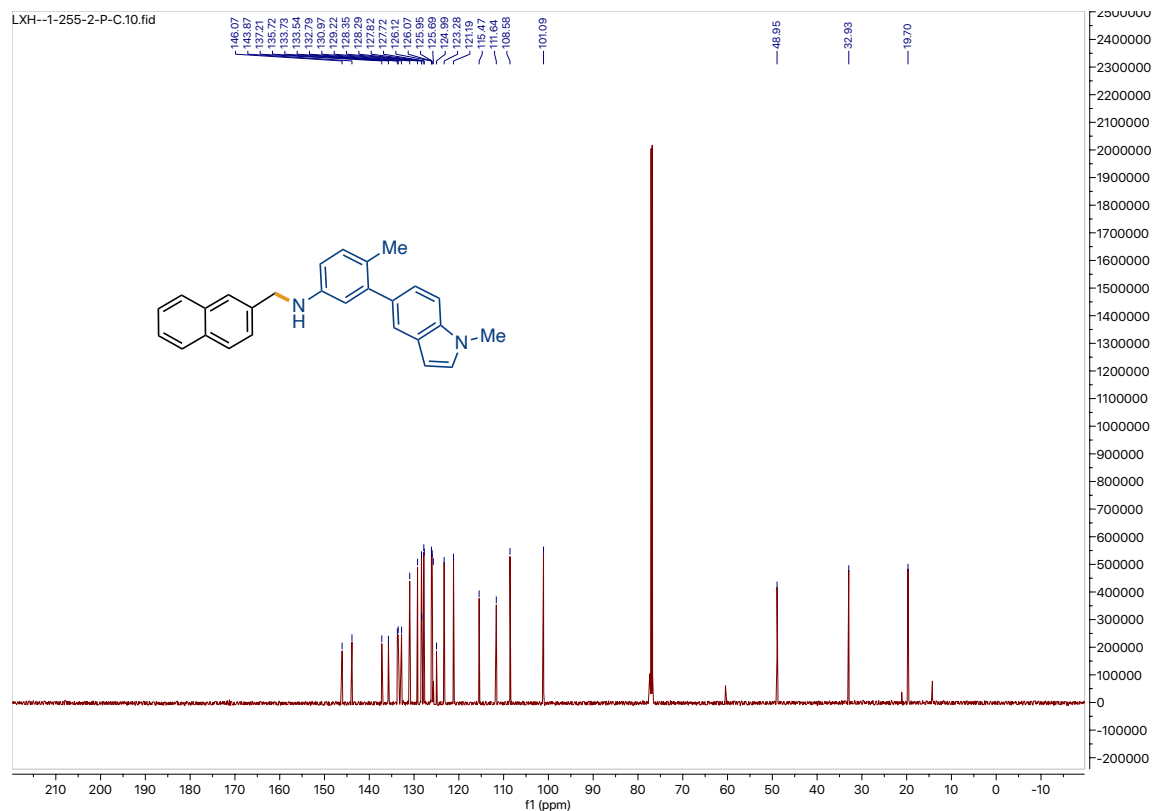
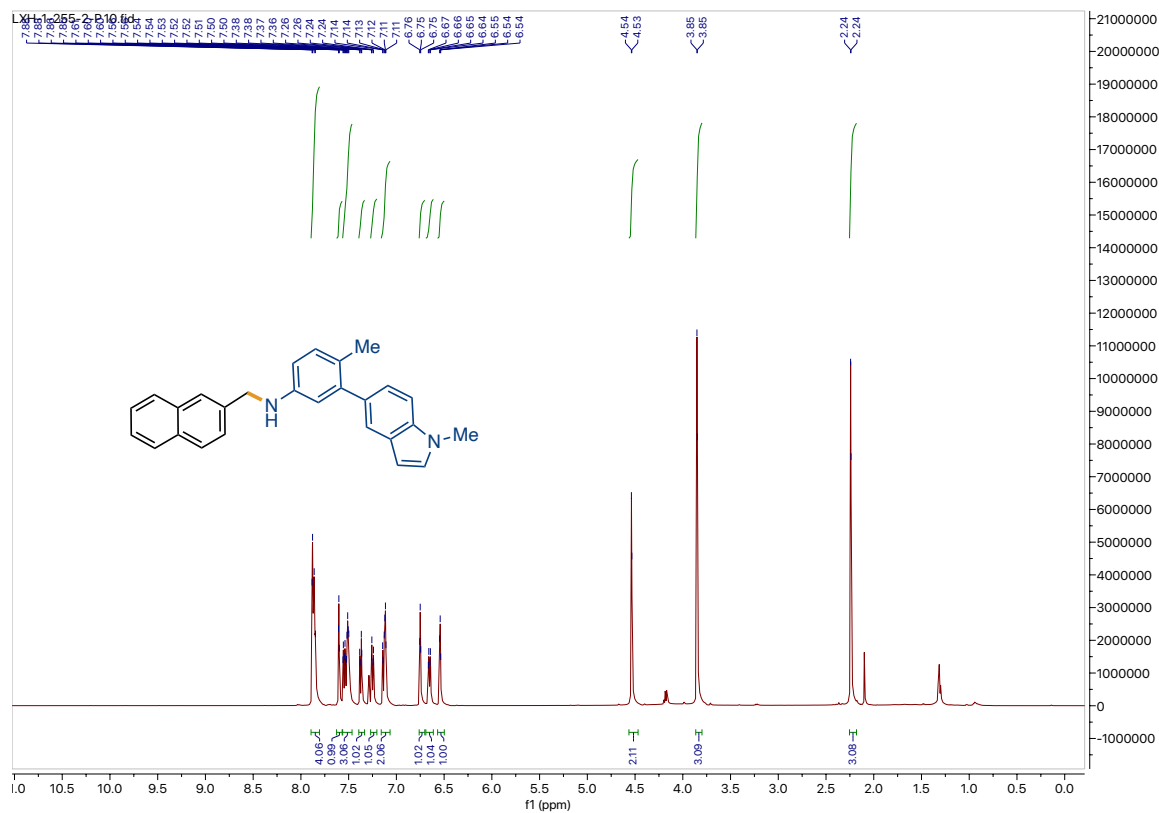




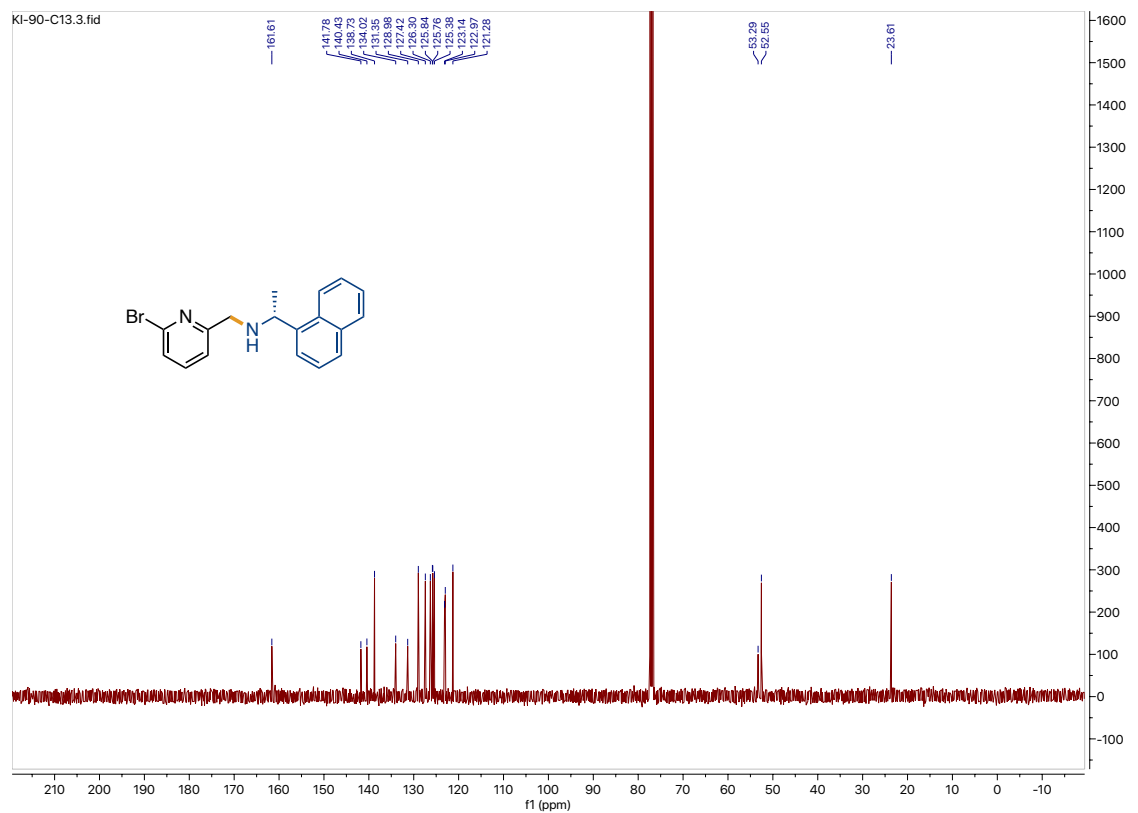
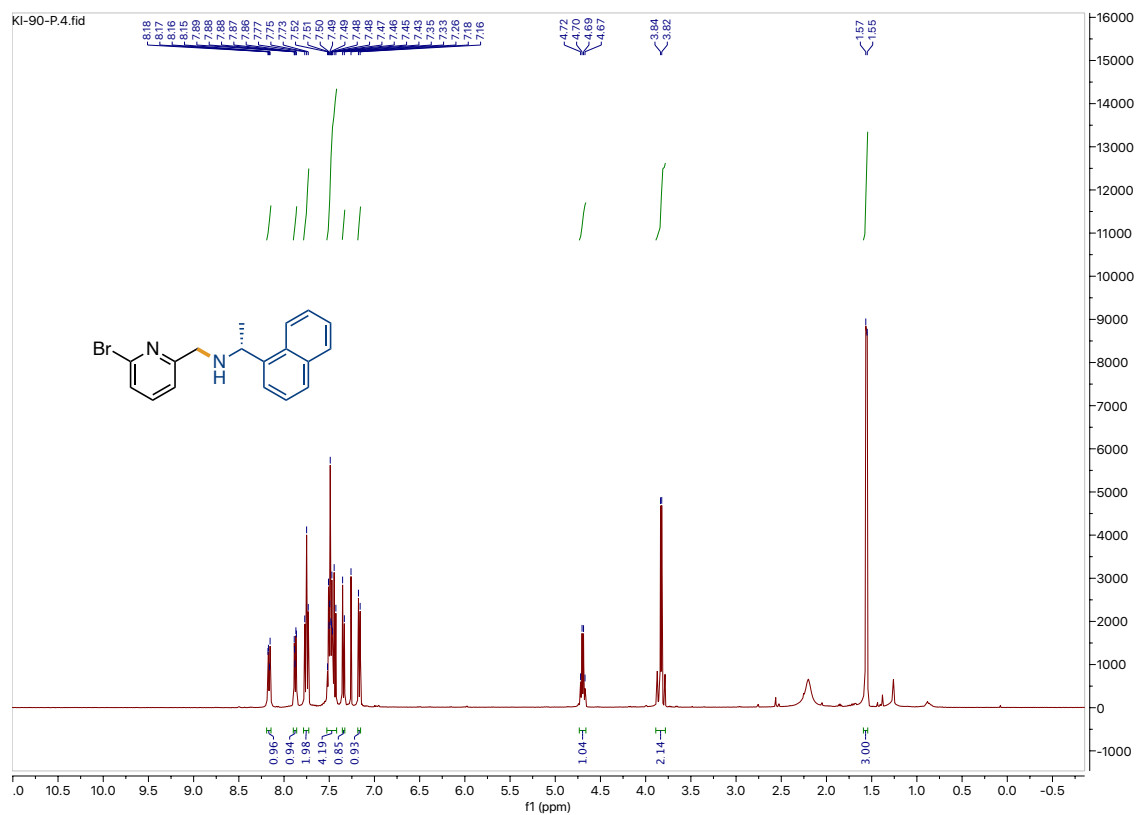
# $^1\text{H}$ NMR and $^{13}\text{C}$ NMR for compound I-16



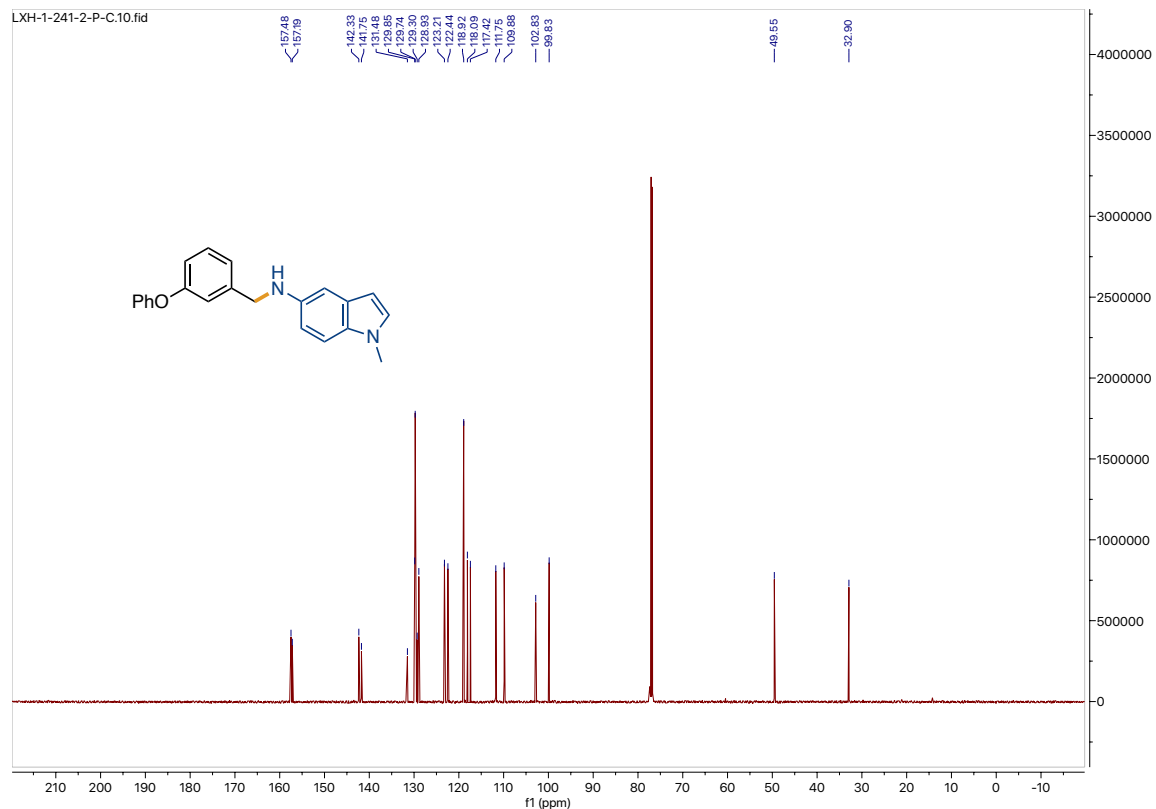
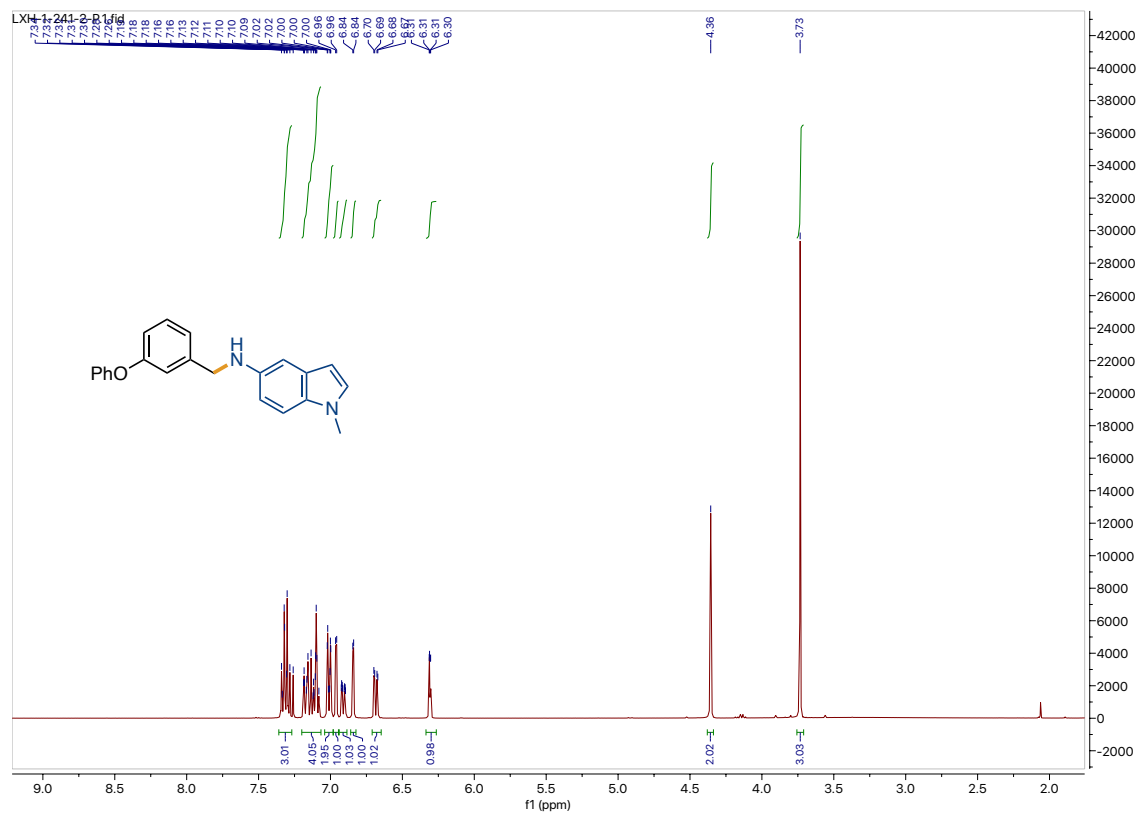
# $^1\text{H}$ NMR and $^{13}\text{C}$ NMR for compound I-17



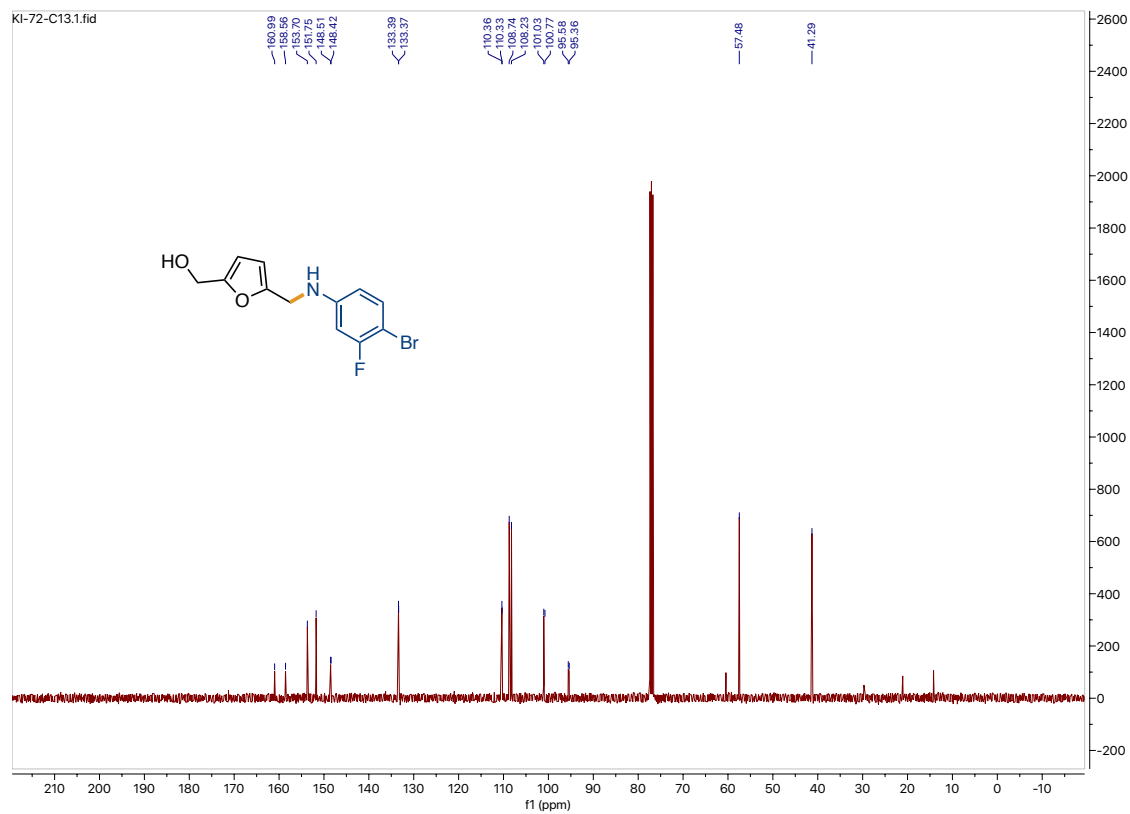
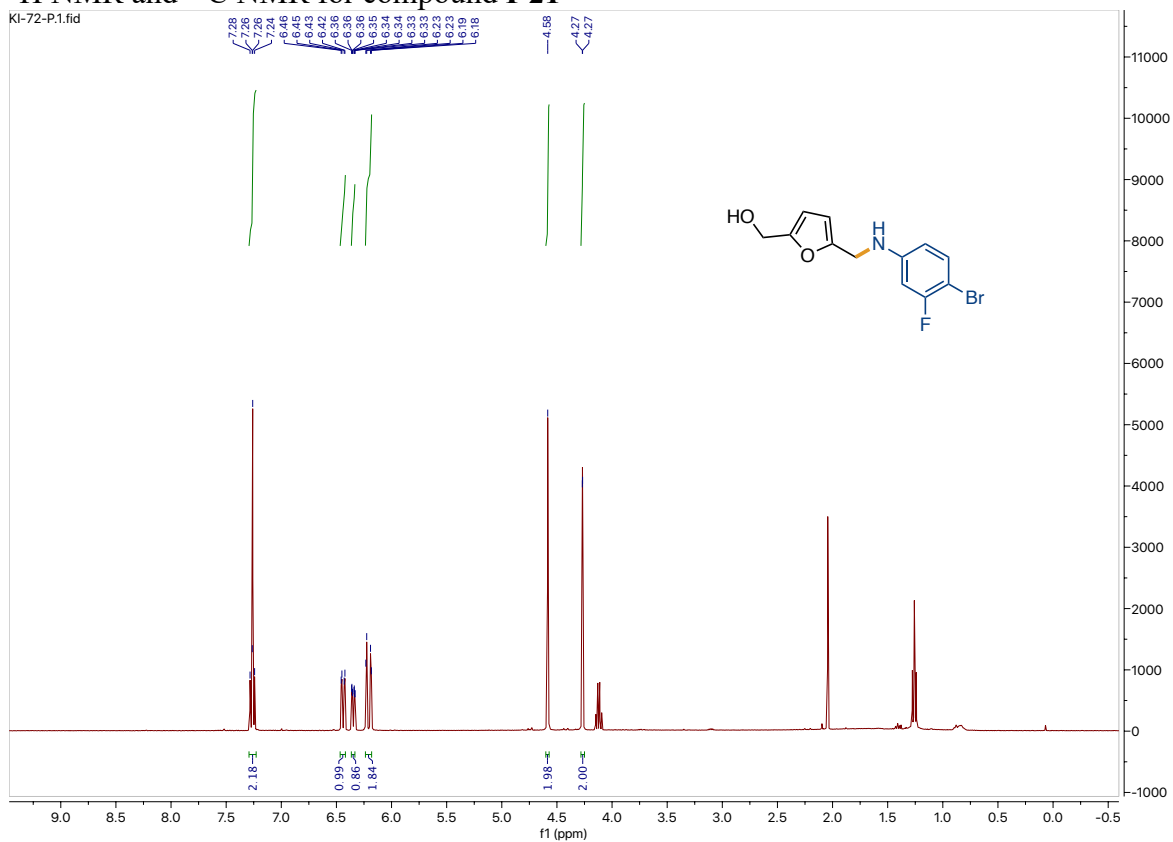
# $^1\text{H}$ NMR and $^{13}\text{C}$ NMR for compound **I-19**



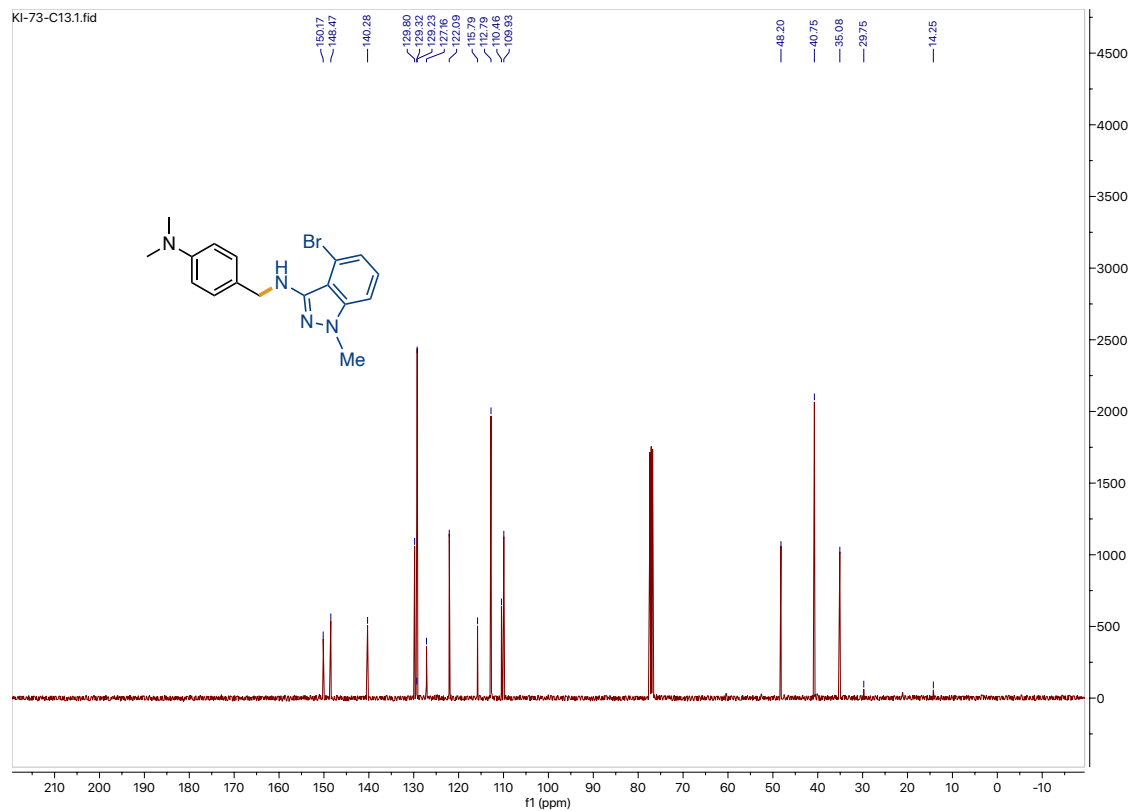
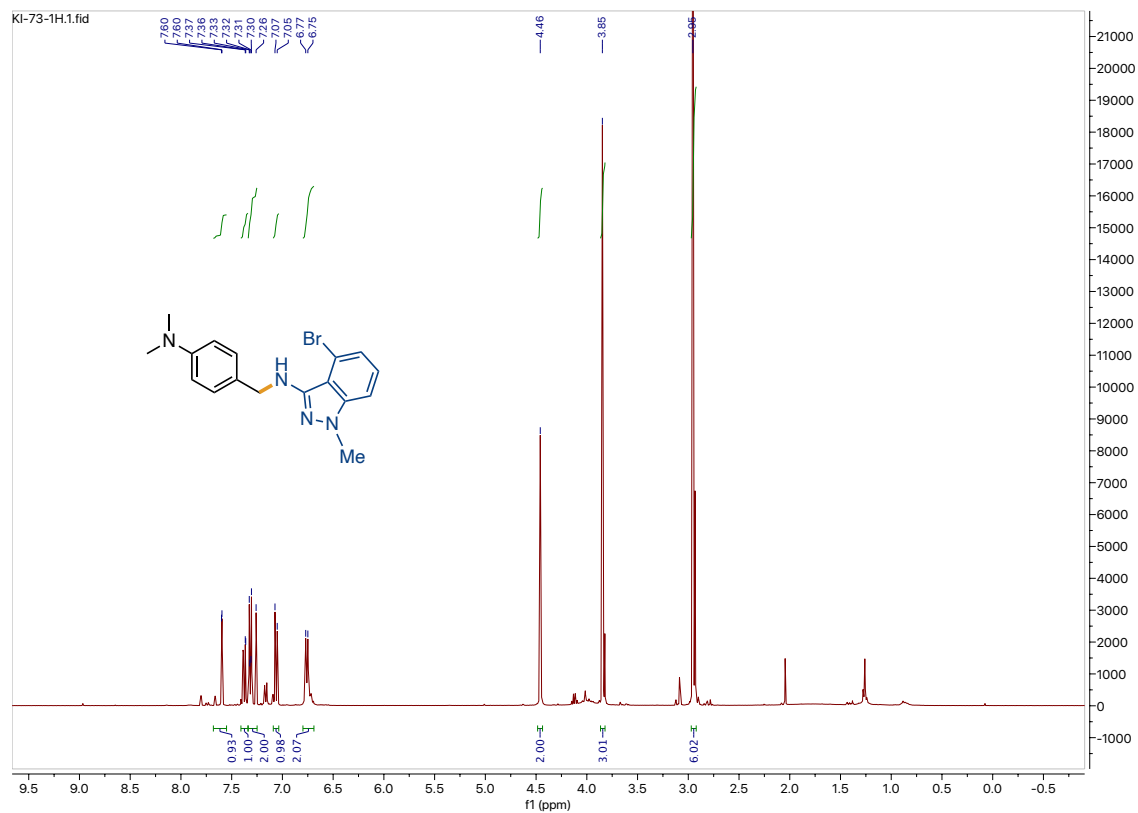
# $^1\text{H}$ NMR and $^{13}\text{C}$ NMR for compound **I-20**



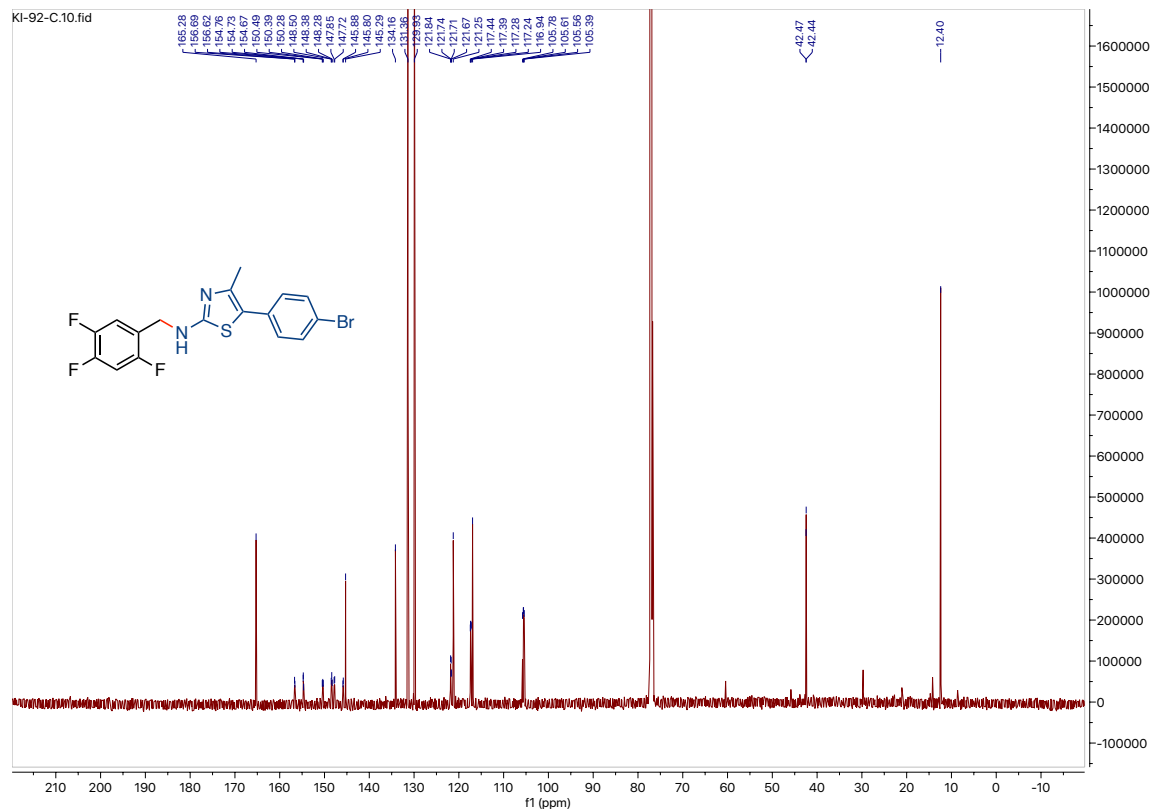
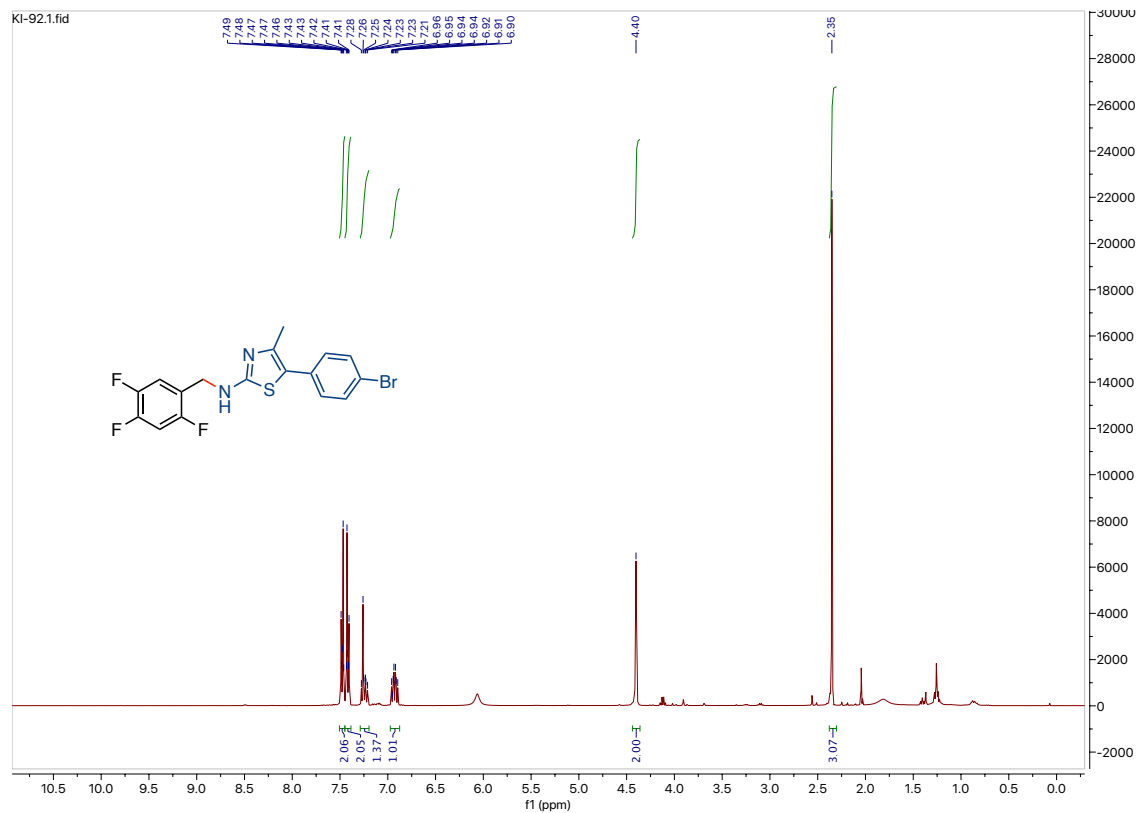
# $^1\text{H}$ NMR and $^{13}\text{C}$ NMR for compound I-21



# $^1\text{H}$ NMR and $^{13}\text{C}$ NMR for compound **I-24**

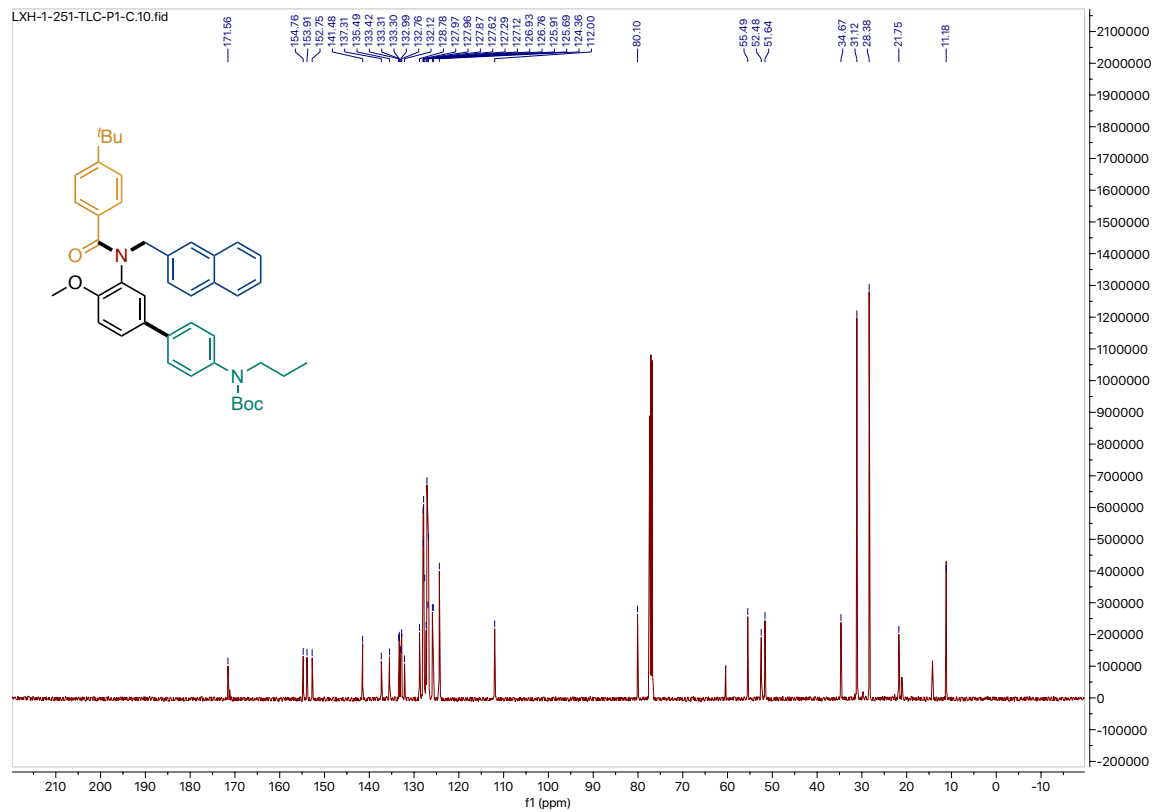
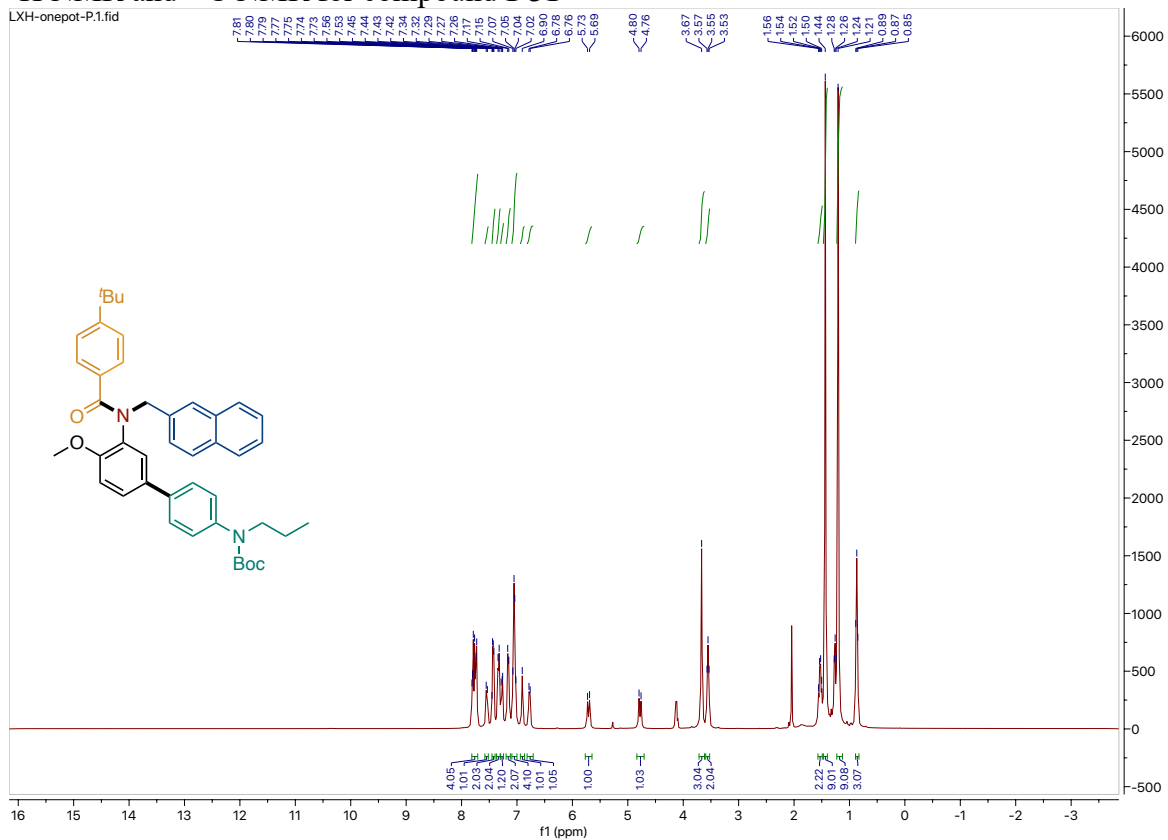


$^1\text{H}$  NMR and  $^{13}\text{C}$  NMR for compound **I-25**

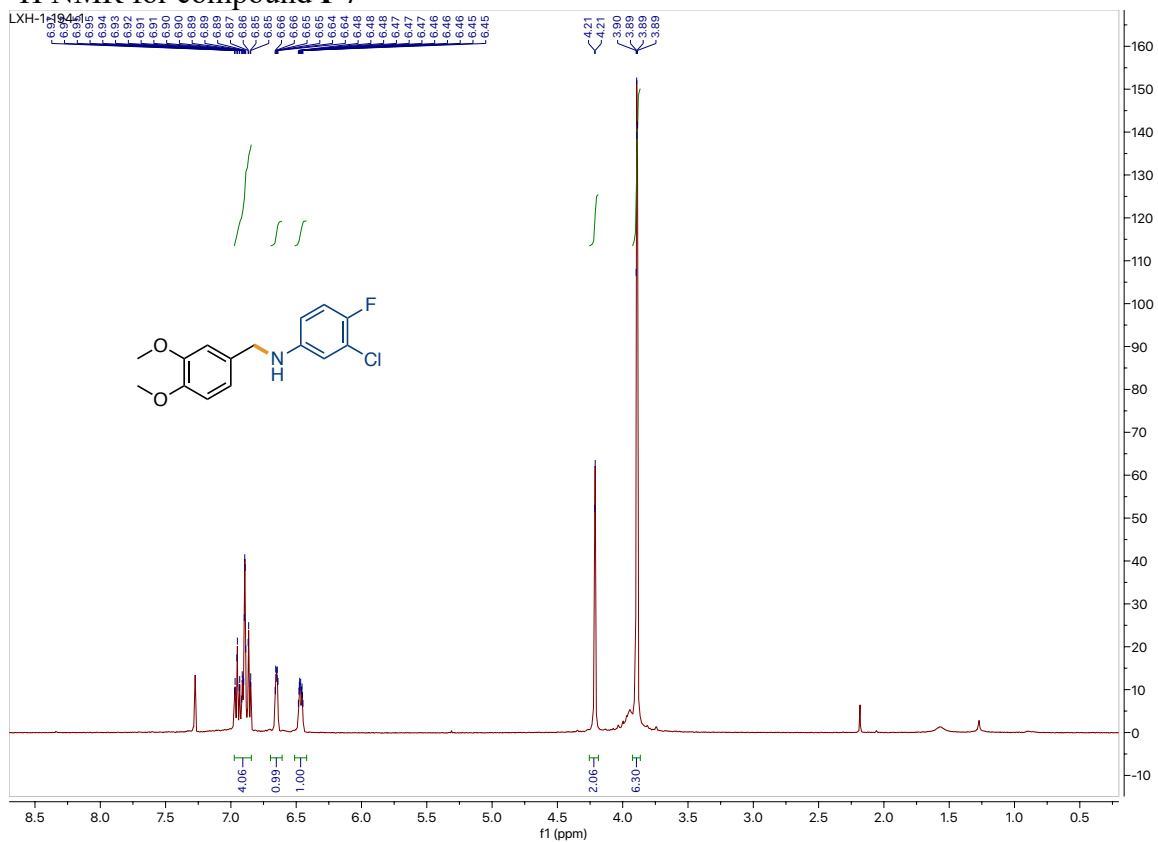




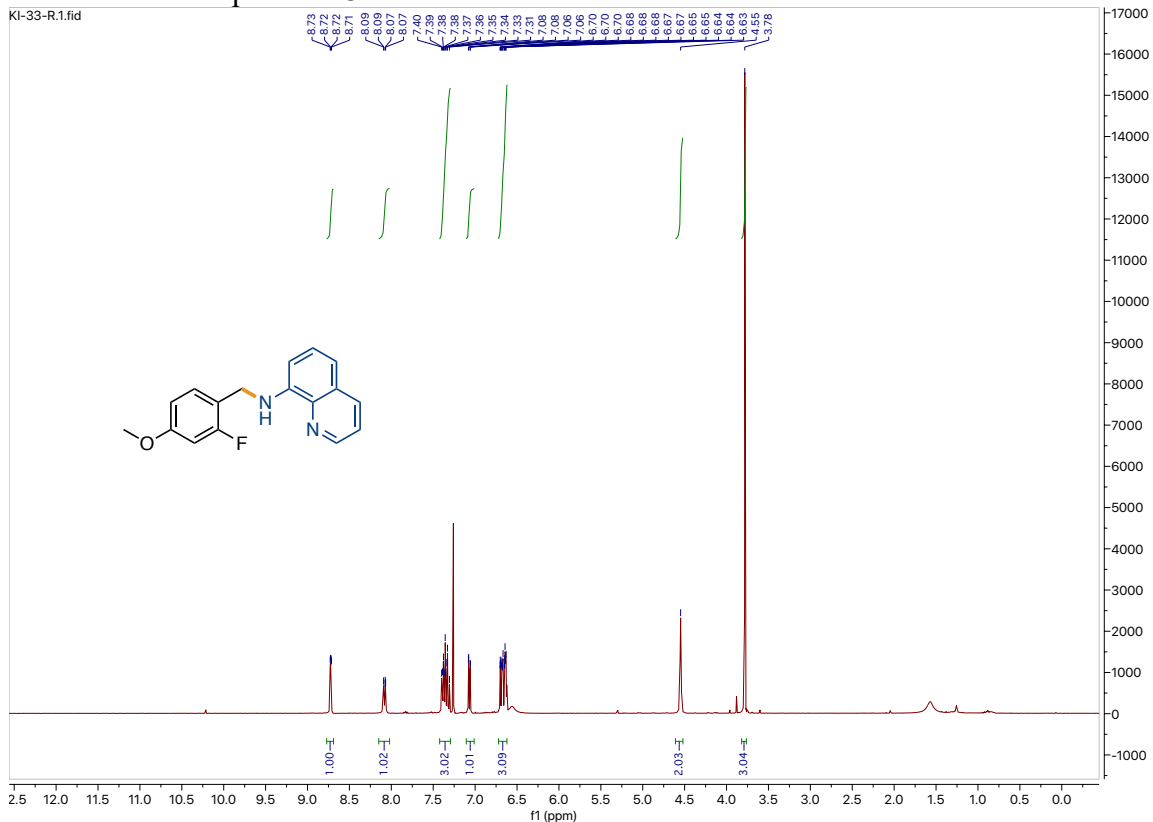
# <sup>1</sup>H NMR and <sup>13</sup>C NMR for compound I-31



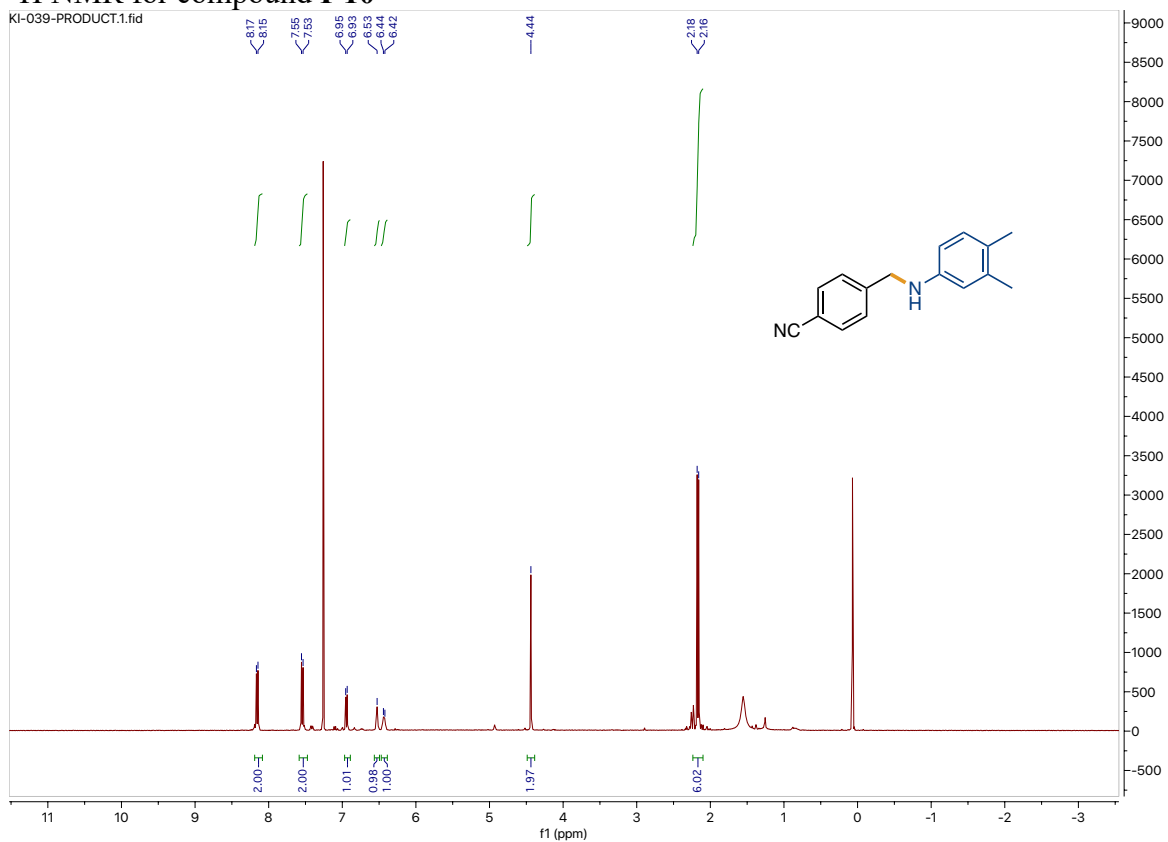
### <sup>1</sup>H NMR for compound I-7



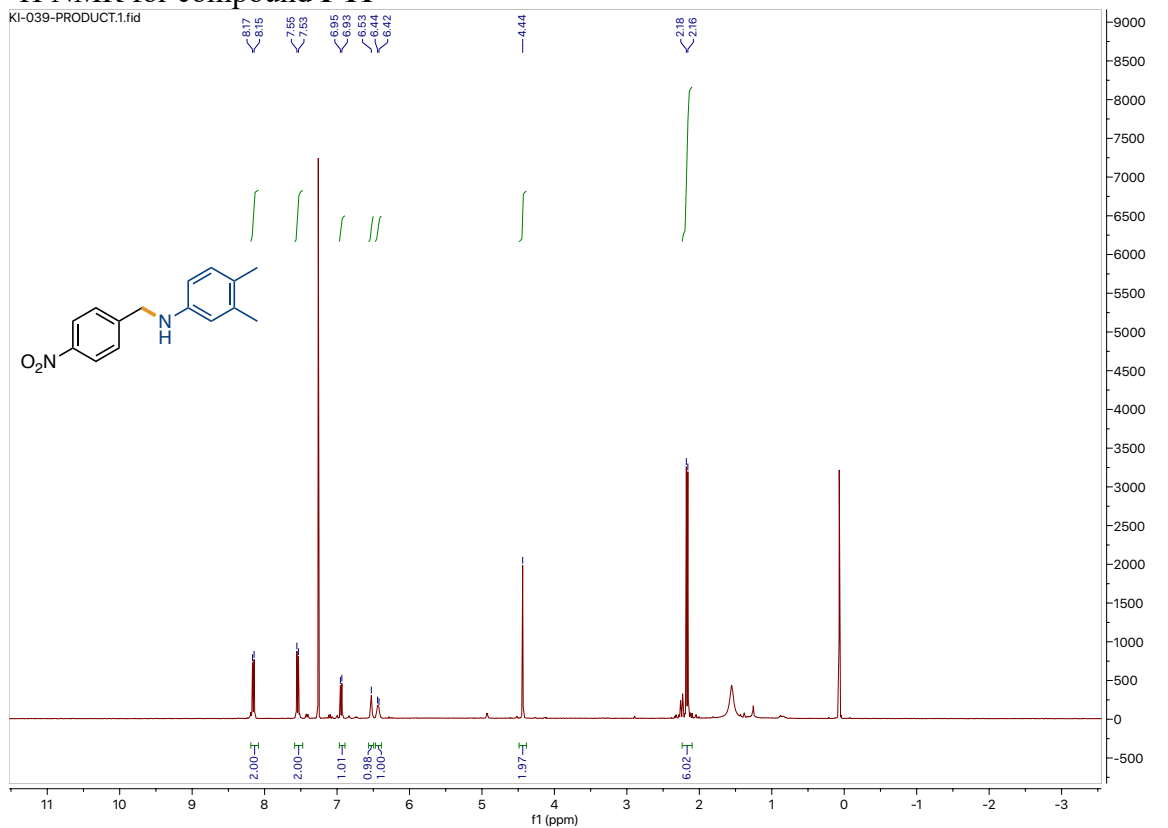
### <sup>1</sup>H NMR for compound I-8



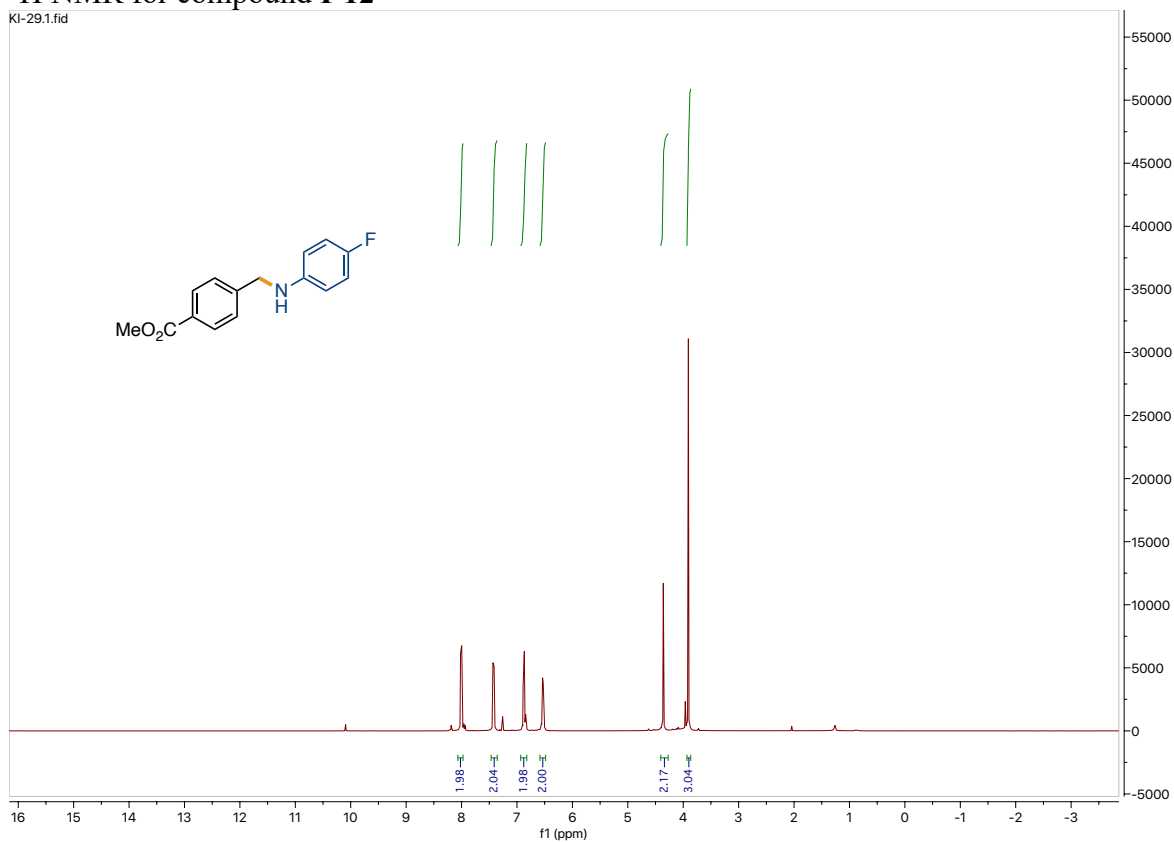
### <sup>1</sup>H NMR for compound I-10



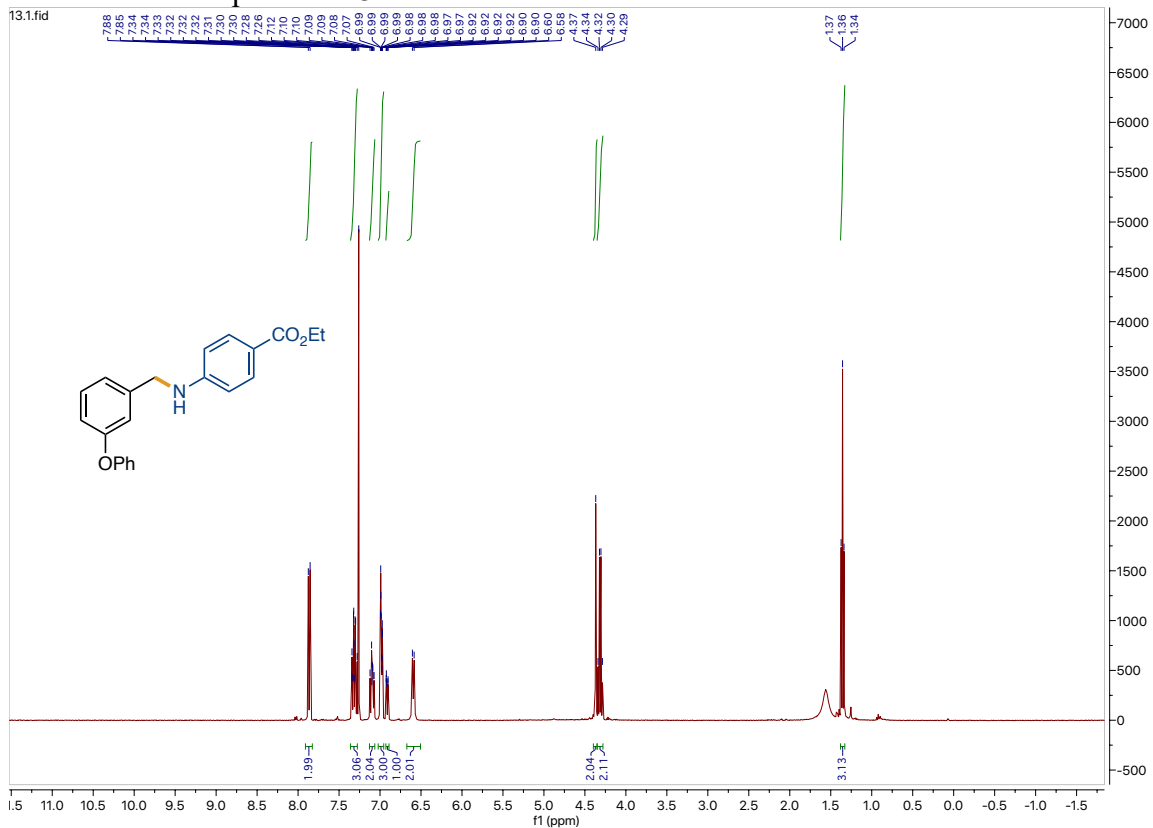
### <sup>1</sup>H NMR for compound I-11



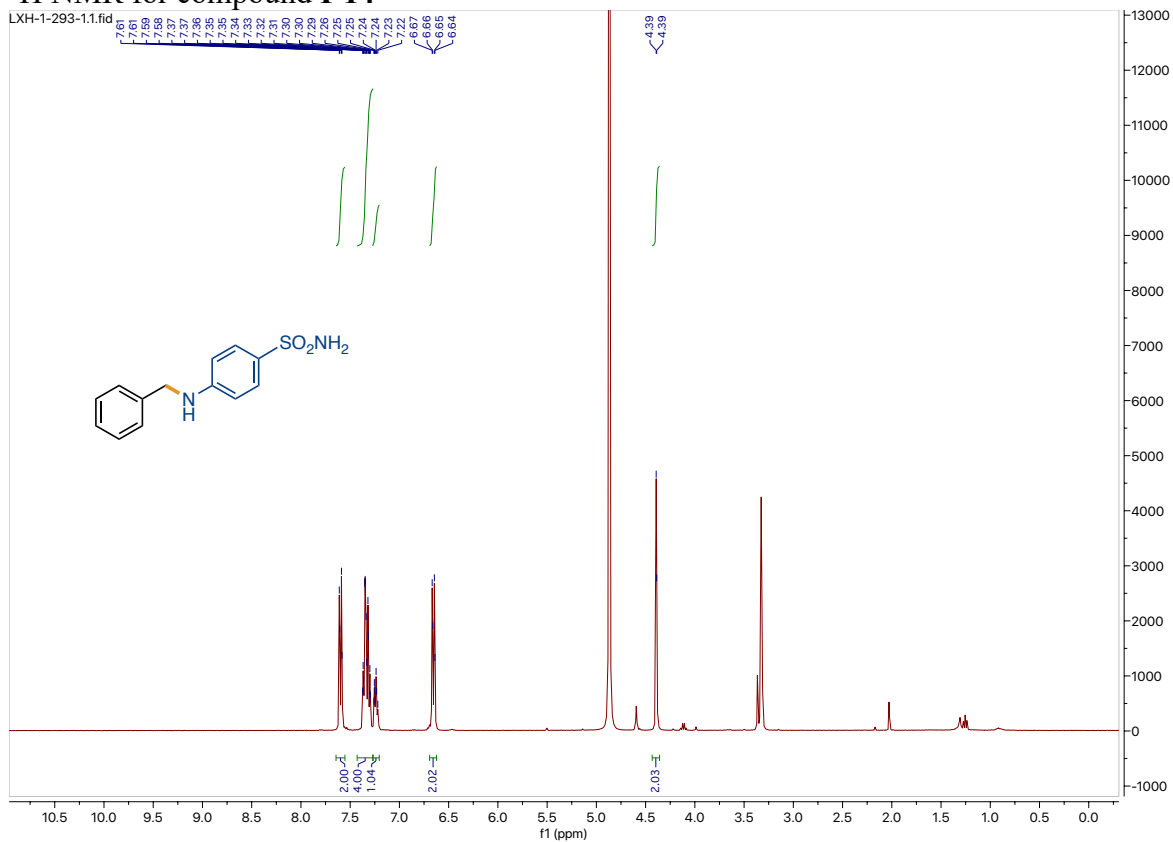
# <sup>1</sup>H NMR for compound I-12



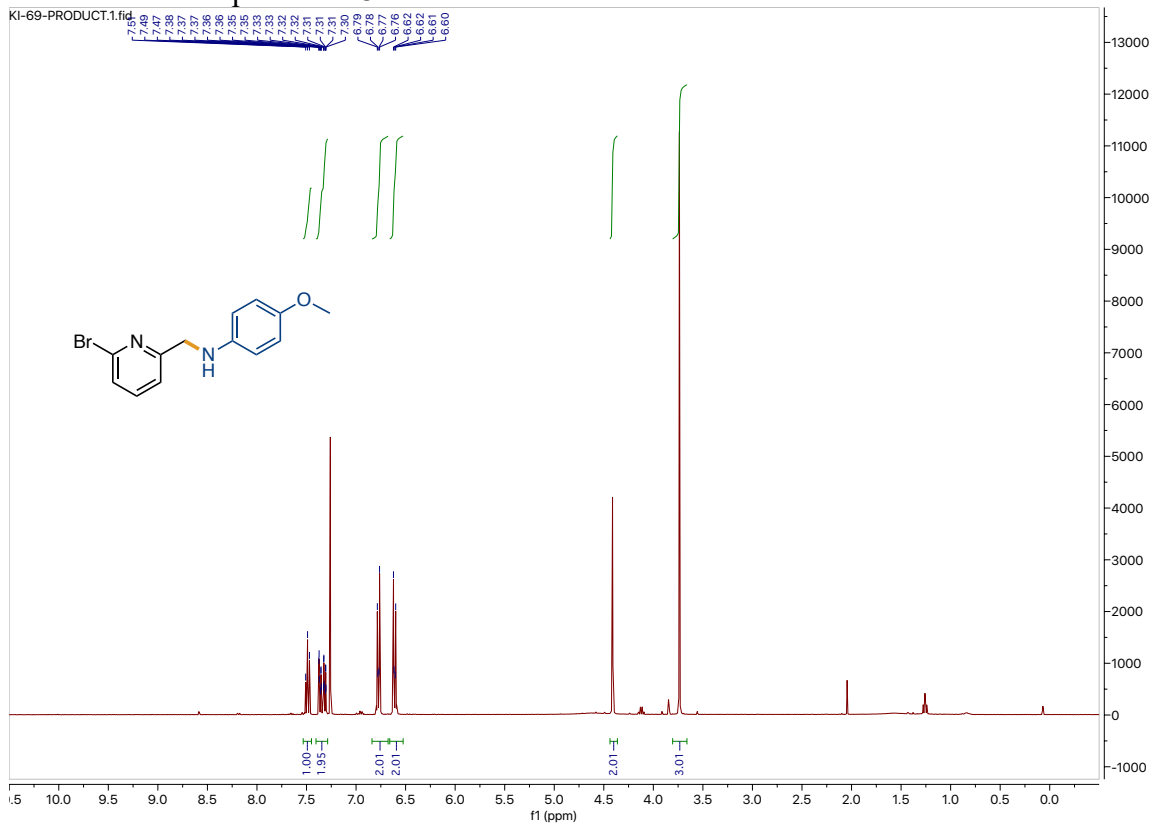
# <sup>1</sup>H NMR for compound I-13



### <sup>1</sup>H NMR for compound I-14

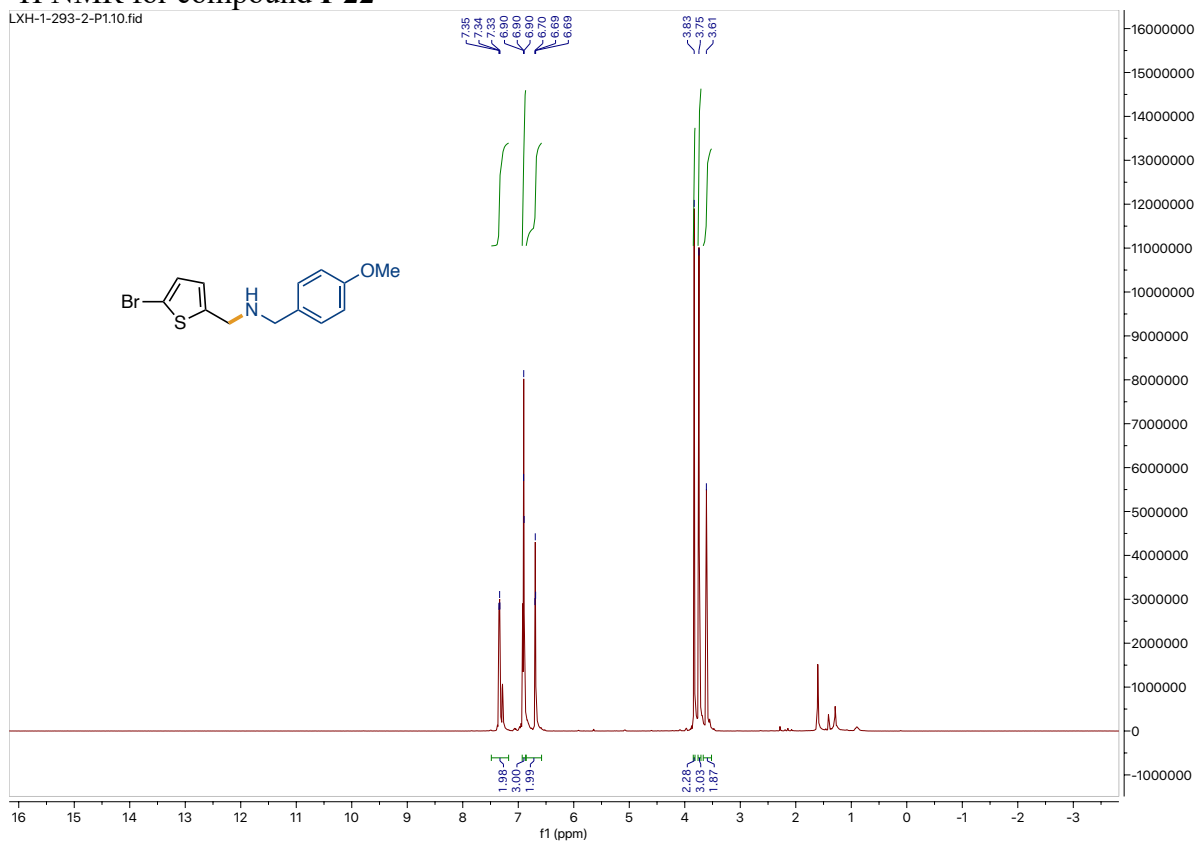


### <sup>1</sup>H NMR for compound I-18

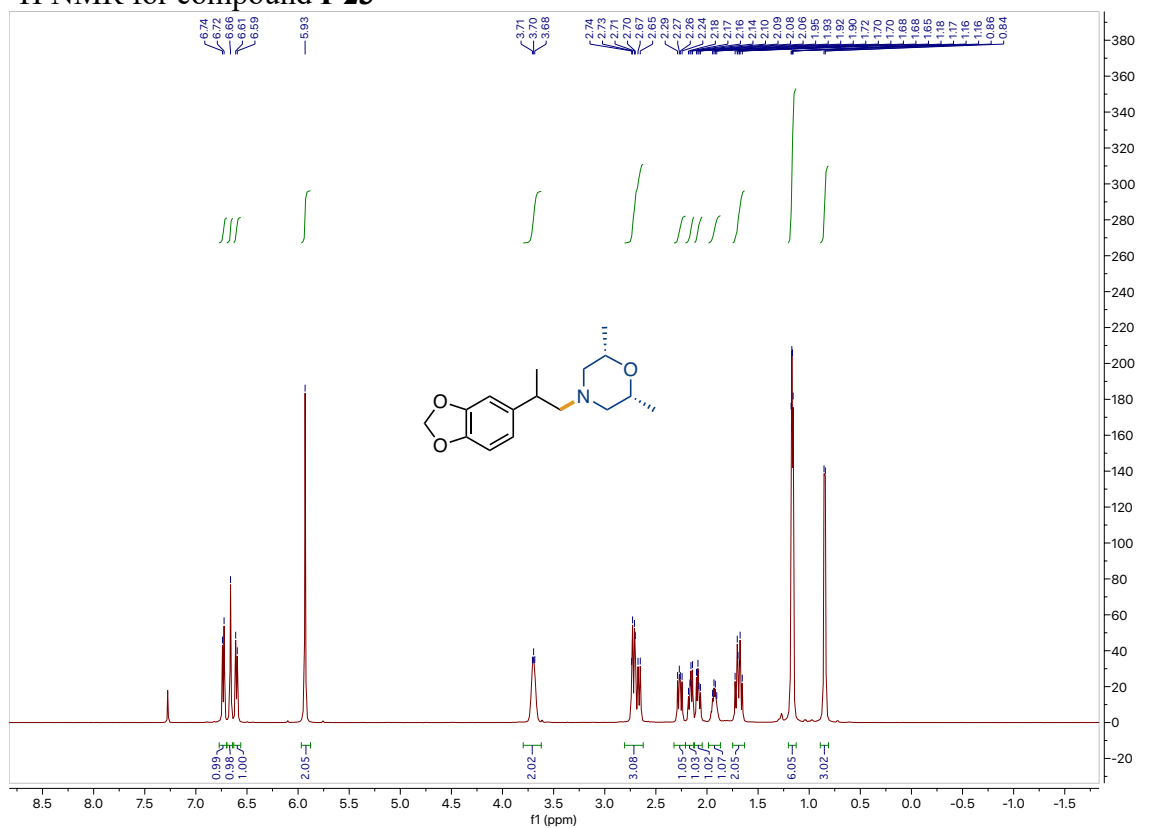


# <sup>1</sup>H NMR for compound I-22

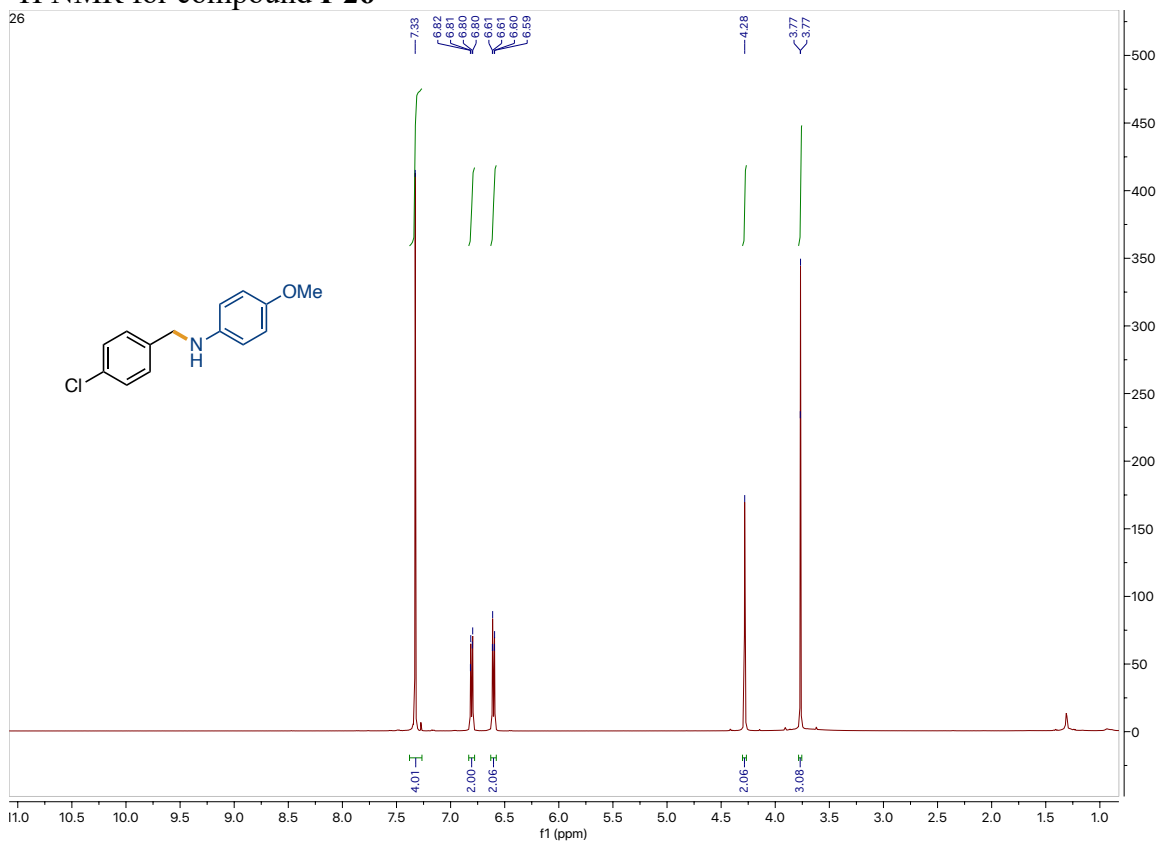
LXH-1-293-2-P1.10.fid



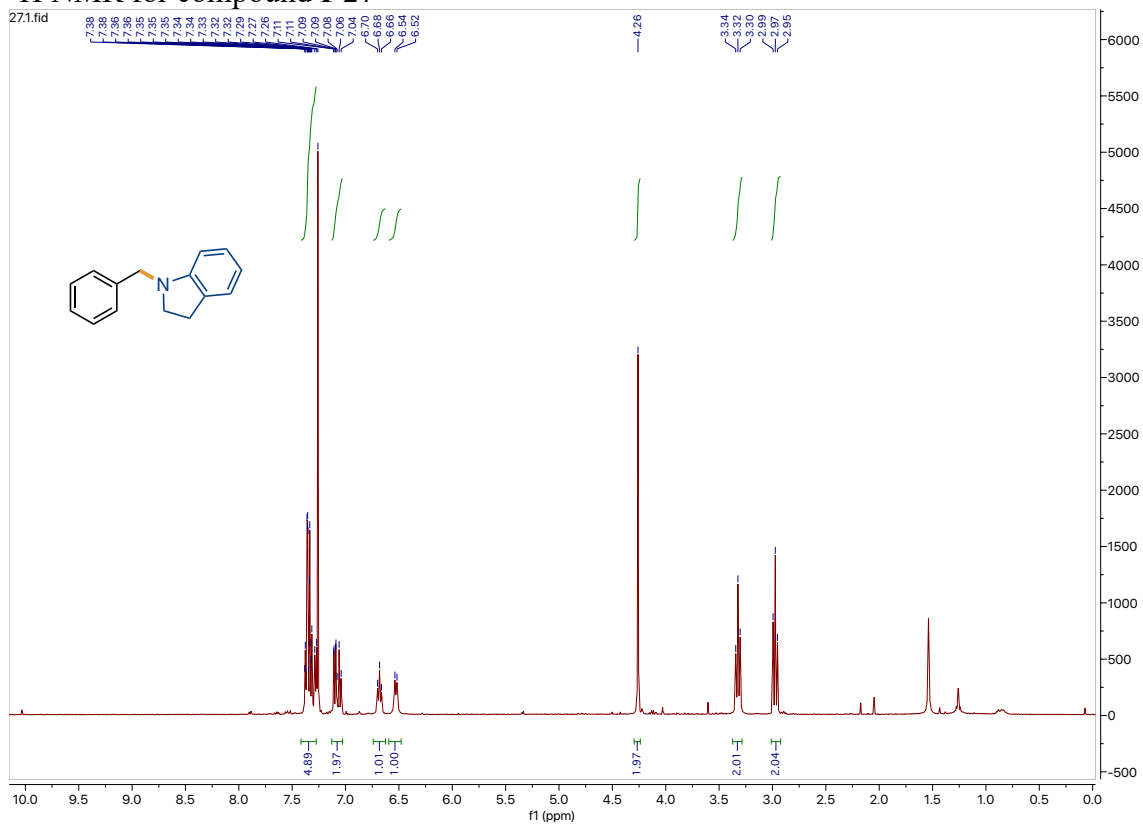
# <sup>1</sup>H NMR for compound I-23



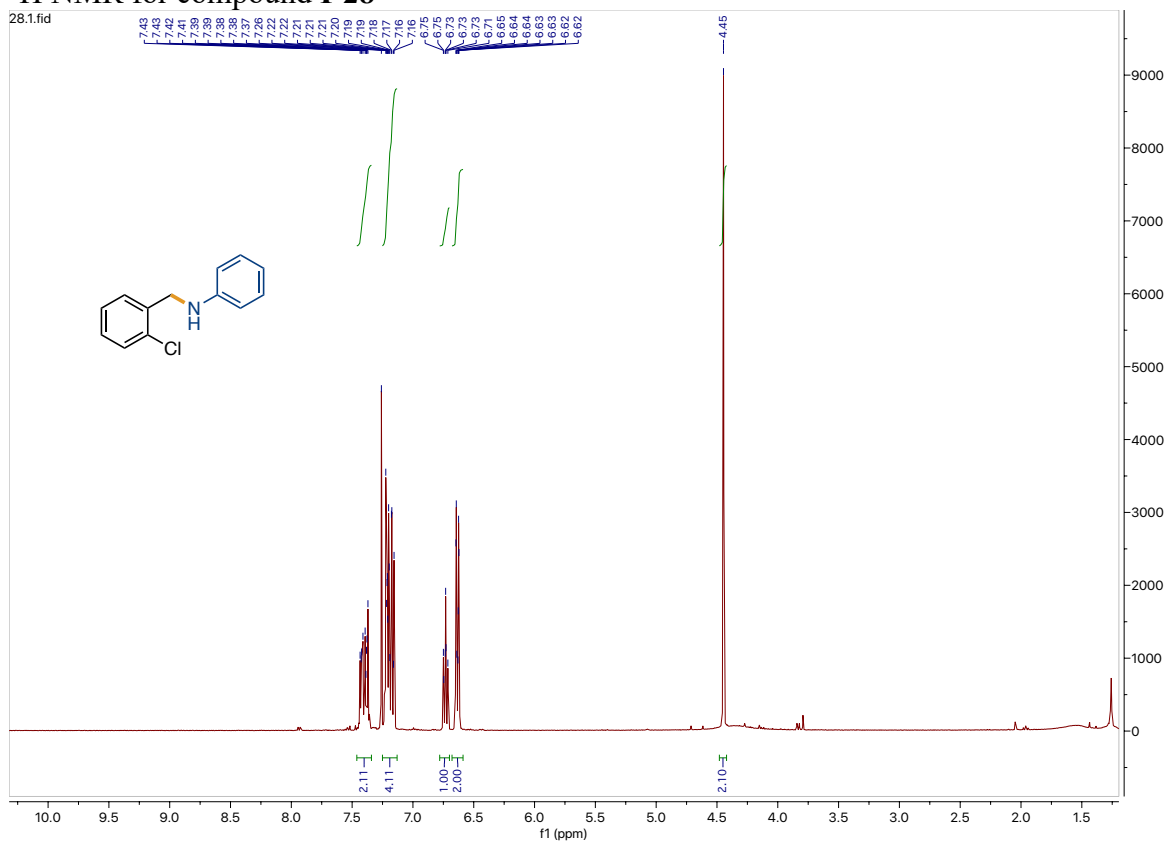
### <sup>1</sup>H NMR for compound I-26



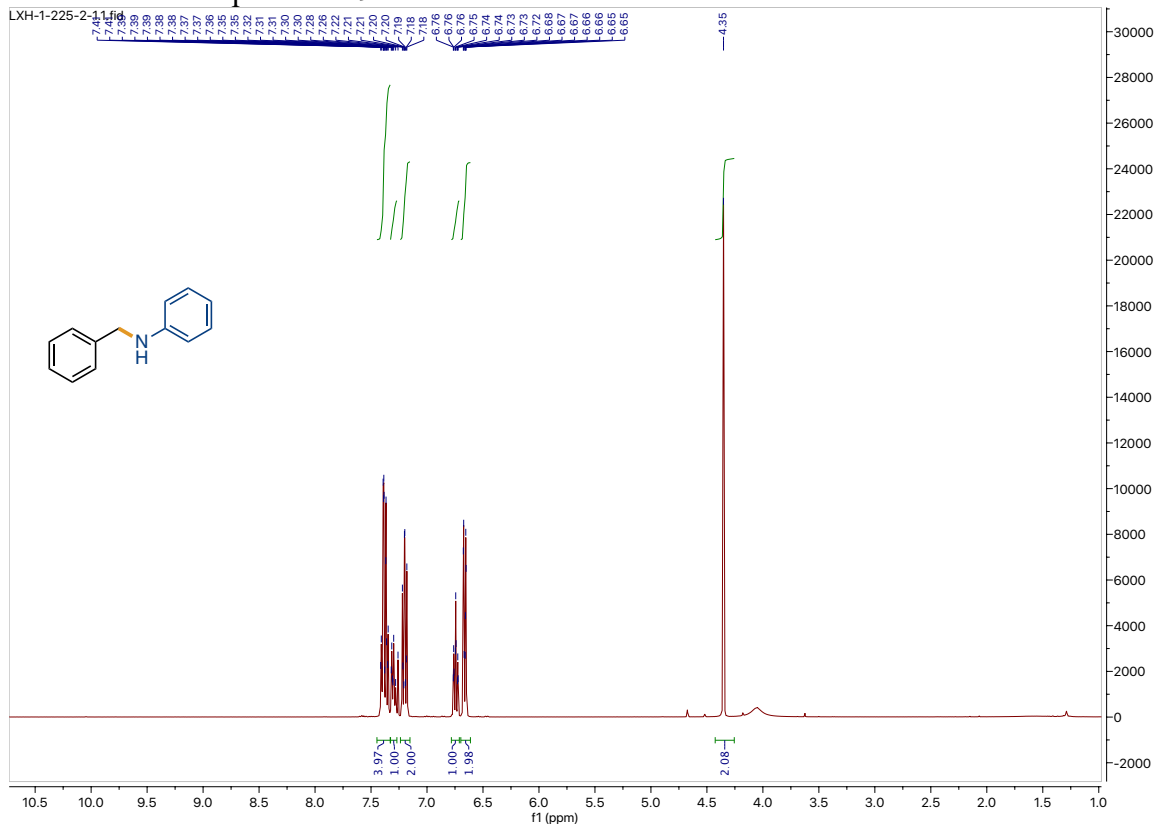
### <sup>1</sup>H NMR for compound I-27



### <sup>1</sup>H NMR for compound I-28

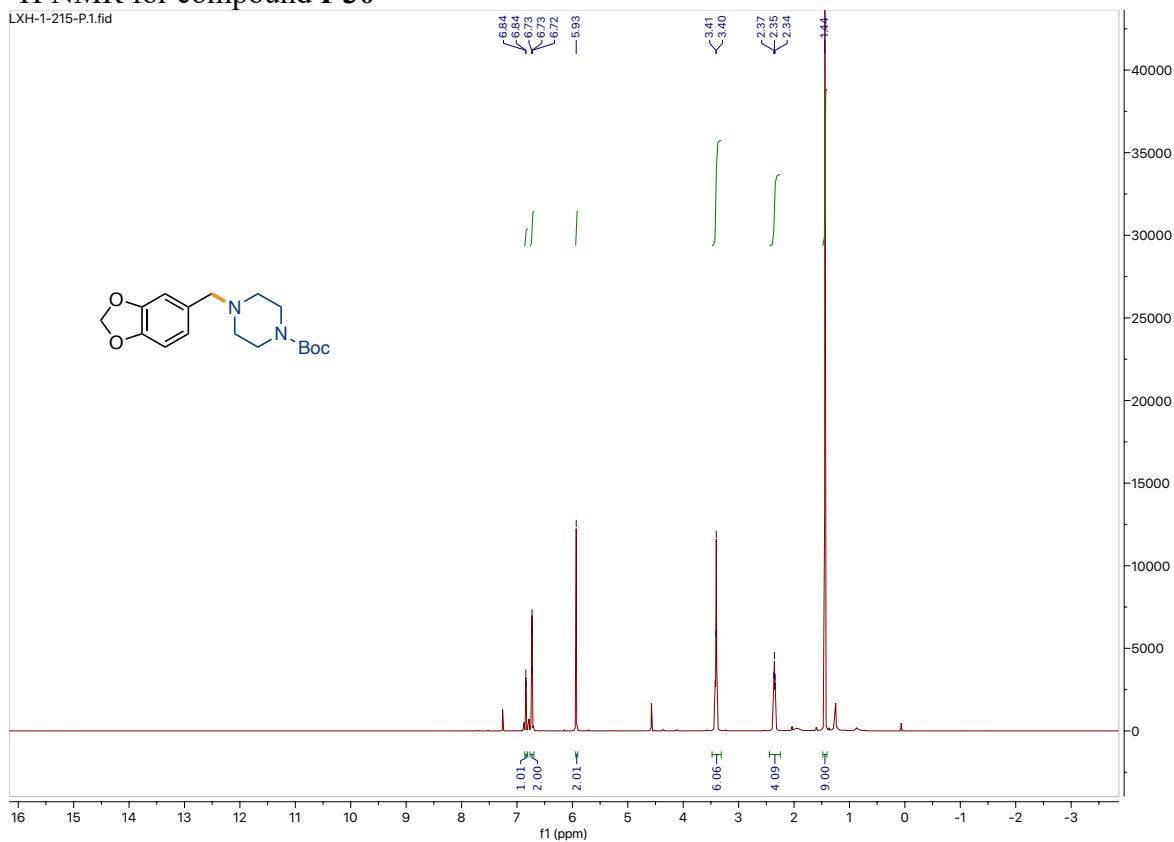


### <sup>1</sup>H NMR for compound I-29

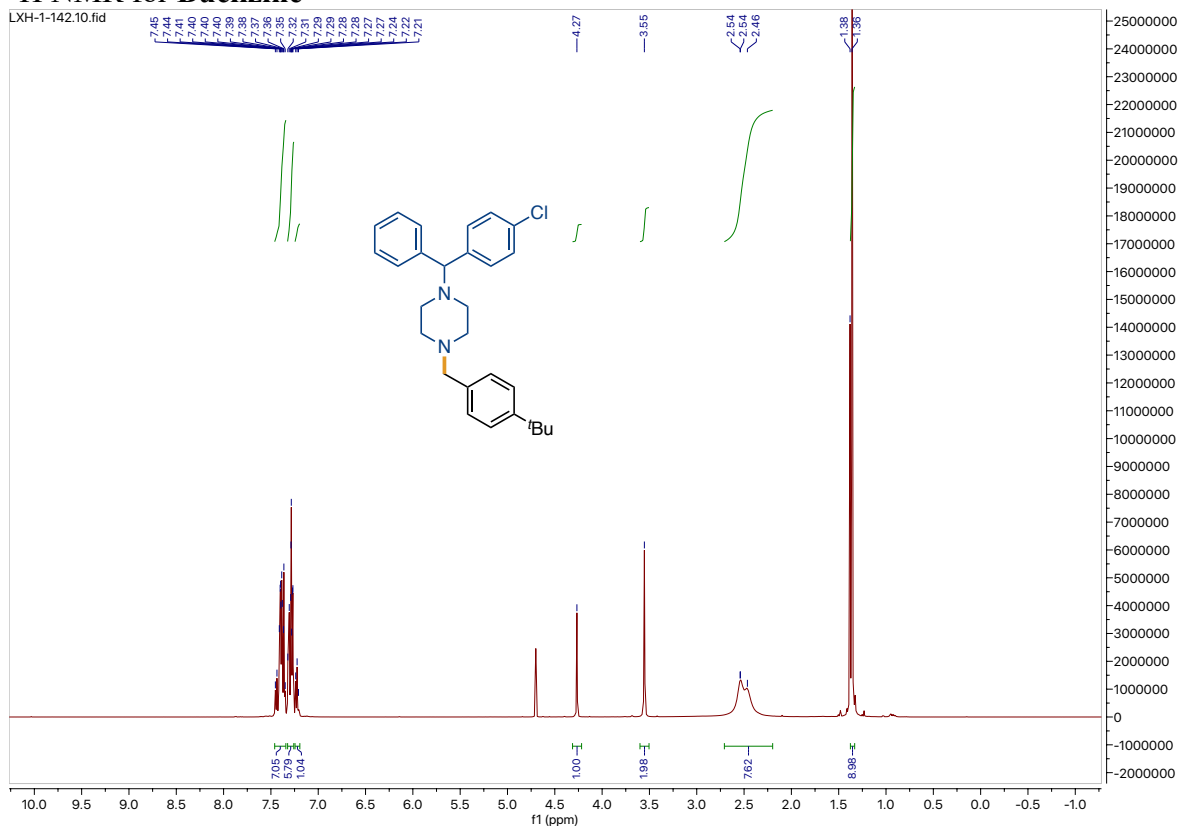




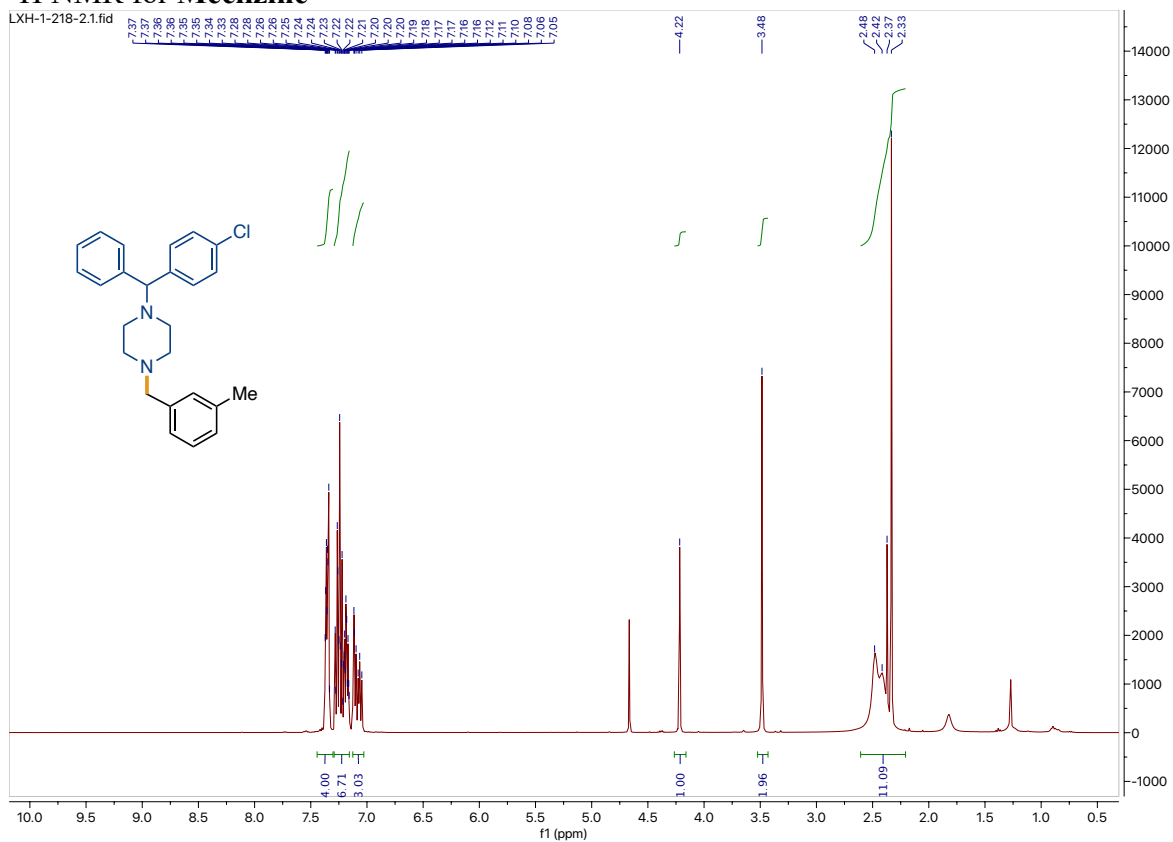
# <sup>1</sup>H NMR for compound I-30



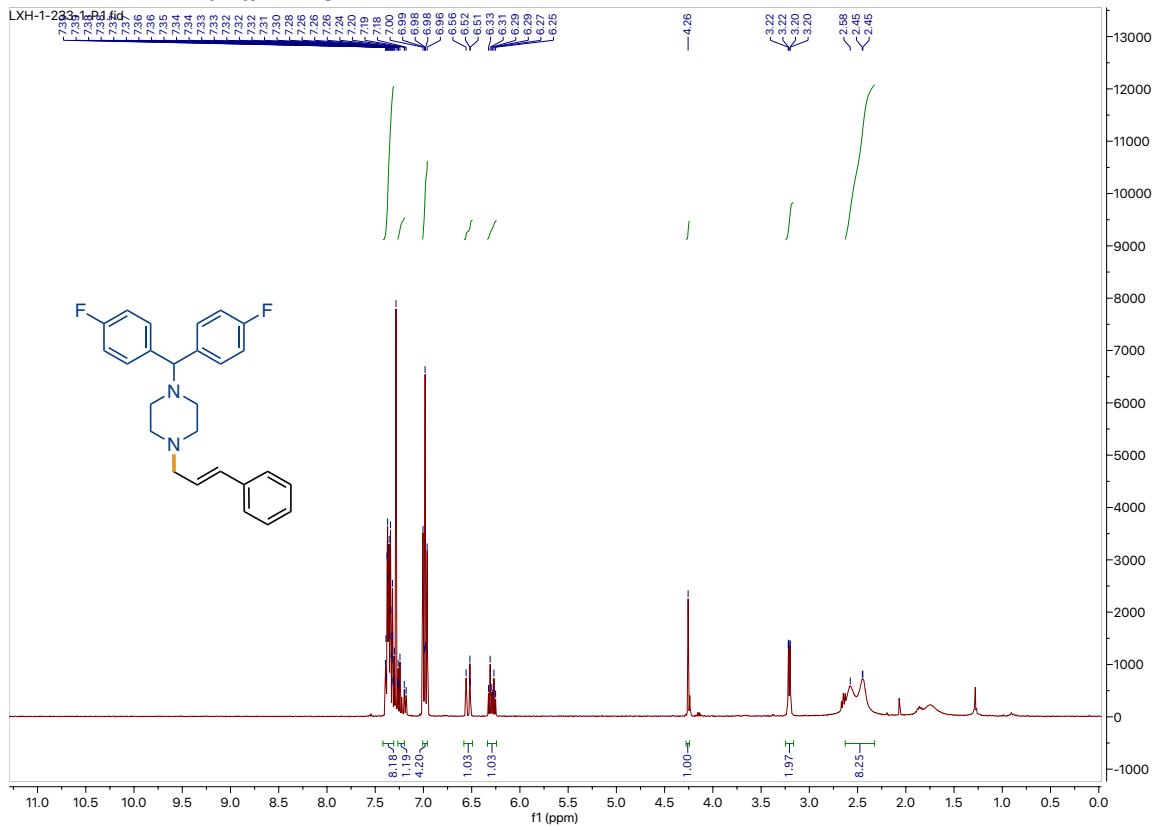
# <sup>1</sup>H NMR for Buclizine



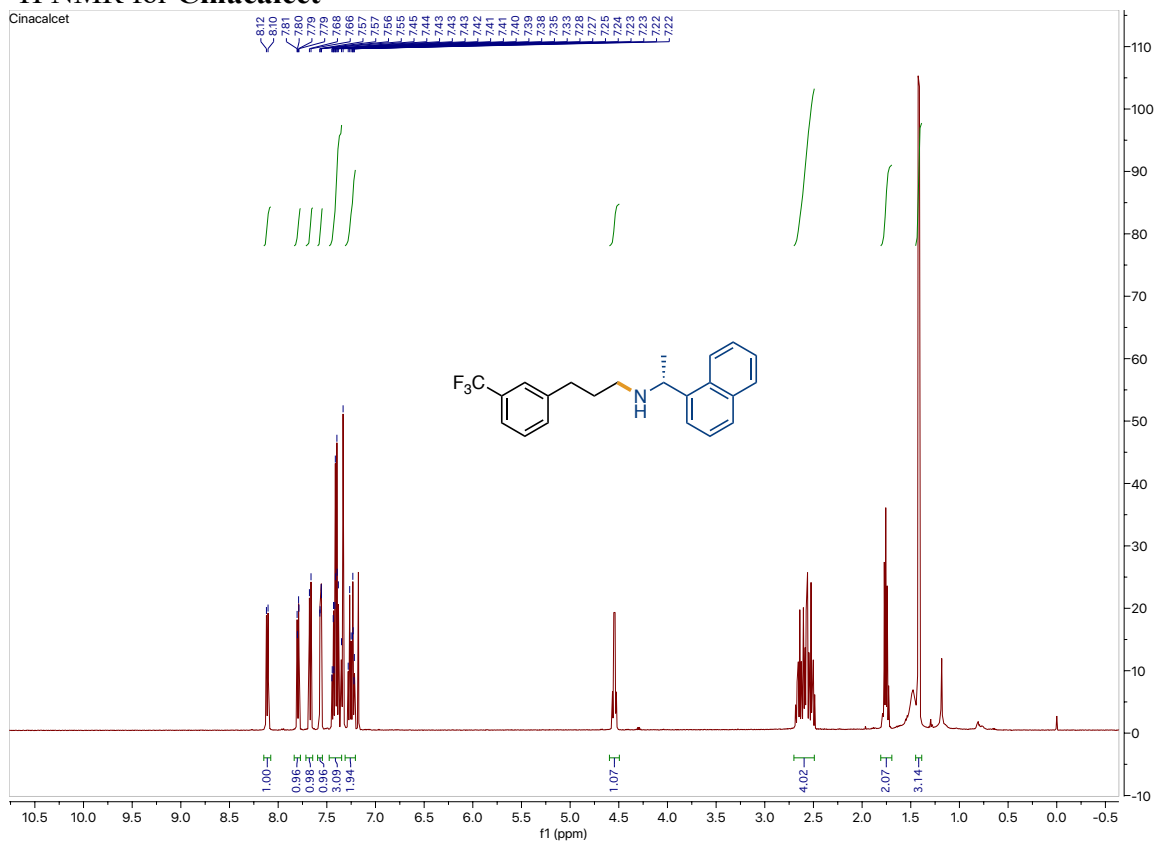
# <sup>1</sup>H NMR for Meclizine



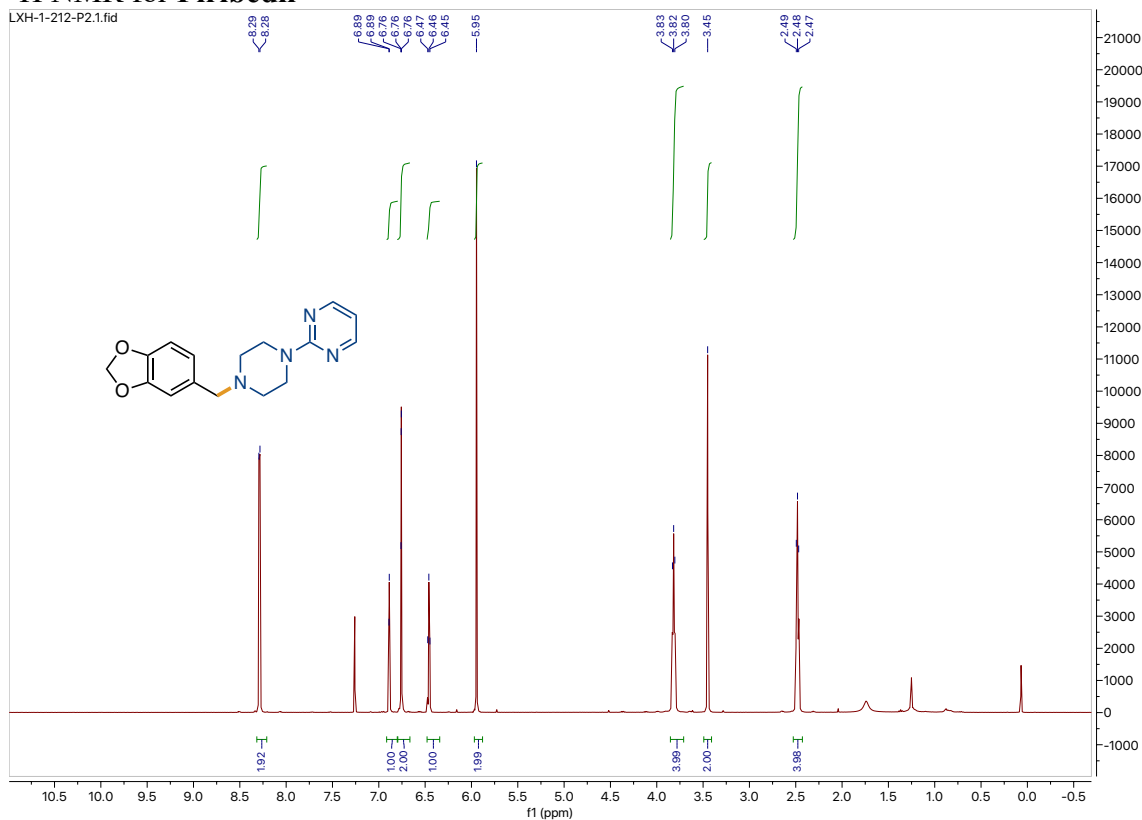
# <sup>1</sup>H NMR for Flunarizine



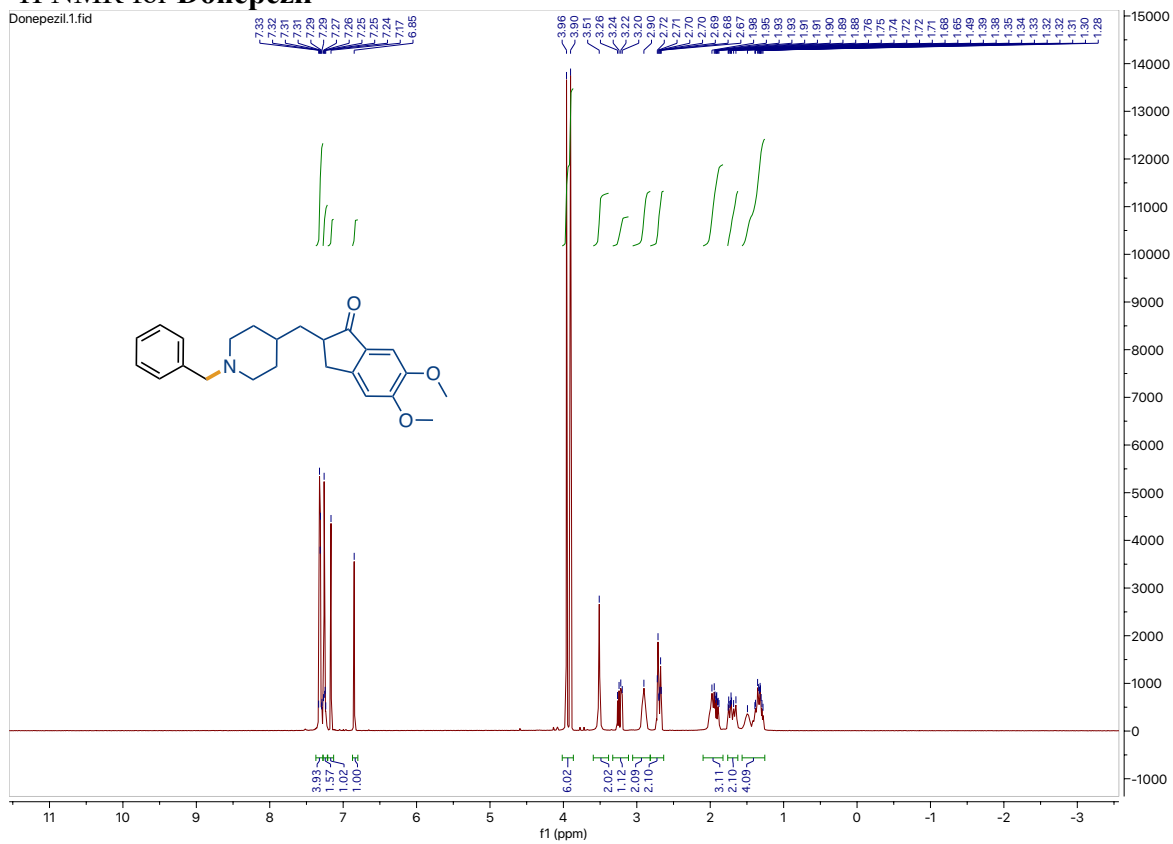
# <sup>1</sup>H NMR for Cinacalcet



# <sup>1</sup>H NMR for Piribedil



# <sup>1</sup>H NMR for Donepezil



## **II. High turnover Pd/C catalyst for nitro group reductions in water enabling 1-pot sequences and syntheses of pharmaceutical intermediates**

Reproduced with permission from:

Li, X.; Thakore, R. R.; Takale, B. S.; Gallou, F.; Lipshutz, B. H. “High Turnover Pd/C Catalyst for Nitro Group Reductions in Water. One-Pot Sequences and Syntheses of Pharmaceutical Intermediates.” *Org. Lett.* **2021**, 23, 8114–8118.

Copyright © 2022 American Chemical Society.

## ***2.1. Background and introduction***

The reduction of the nitro group is a pivotal transformation in organic chemistry that leads to introduction of an amino group into a molecule.<sup>1-3</sup> The significance of this transformation is highlighted by the widespread nature of amine derivatives in various fields, including pharmaceuticals, agrochemicals, dye intermediates, pigments, and a myriad of other fine chemicals.<sup>4-5</sup> Beyond this, the nitro group serves a dual purpose in synthetic strategies. The inherent electron-withdrawing character of the nitro group increases the reactivity of substrates towards specific reactions, such as Pd-catalyzed couplings<sup>6</sup> and nucleophilic aromatic substitution ( $S_NAr$ )<sup>7</sup> reactions, thereby further broadening its utility as an indispensable residue in modern organic synthesis.

The history of nitro compound reduction extends to the 19th century. Initial methodologies prominently featured the use of stoichiometric metals under acidic conditions, exemplified by the Bechamp reduction employing iron in the presence of hydrochloric acid.<sup>8</sup> While these protocols are effective, their broader applicability is curtailed by certain limitations, notably the substantial generation of metallic waste and a frequent lack of chemoselectivity in the presence of other reducible and/or acid-sensitive functionalities.

Subsequent to initial discoveries, synthetic chemists have dedicated significant efforts towards the discovery of novel and efficient catalysts, aiming to establish both streamlined and environmentally benign methodologies for this transformation. Catalytic hydrogenation with transition metals has emerged as a central strategy in this domain. Precious metals like Pd,<sup>9-11</sup> Au,<sup>12</sup> Rh,<sup>13-14</sup> and Pt<sup>15,16</sup> have frequently been employed, owing to their remarkable catalytic reactivity. Meanwhile, more economical alternatives such as Cu,<sup>17-19</sup> Co,<sup>20-21</sup> Ni,<sup>22-24</sup> Fe,<sup>25-27</sup> Mo,<sup>28</sup> and Ti<sup>29</sup> have also gained attention, offering both cost-effective and efficient pathways for nitro group reduction.

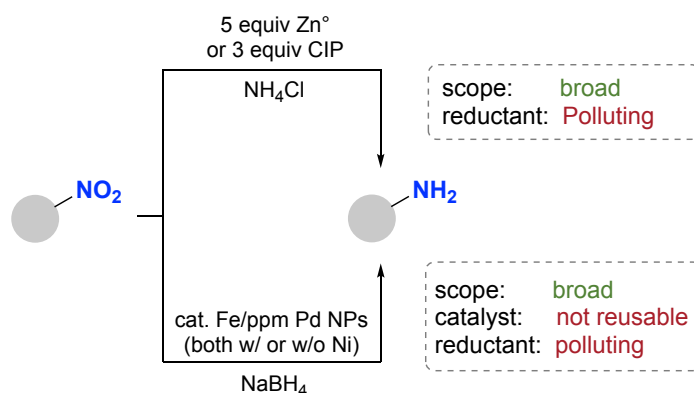
In addition to these catalytic strategies, several alternative methodologies have been designed, each presenting distinct advantages. For instance, electrochemical reduction has gained prominence due to its utilization of simple electrolytes which effectively circumvents the requirement for metal reagents, thus minimizing waste generation.<sup>29</sup> Enzymatic reduction represents another approach and is especially praised for its operation under benign conditions while delivering exceptional selectivity.<sup>30-32</sup> Furthermore, metal-free reduction, typically employing silanes or borohydrides, emerges as a noteworthy counterpart, presenting viable alternatives to conventional metal-centric reduction methods.<sup>33-35</sup>

Thus, despite considerable advancements in the realm of nitro group reductions, many existing methods still exhibit suboptimal properties, such as high loading of precious or toxic metals, expensive ligands, elevated pressures and/or temperatures, dangerous reagents, toxic solvents, long reaction times, commercially unavailable materials, lack of selectivity, and inconsistent yields, particularly with complex molecules, etc. It is critical to develop efficient methodologies that not only achieve the same desired outcomes but also to prevent environmental damage and avoid issues related to flammability or potential explosiveness.

In alignment with the trends towards sustainable methodologies, our group has pioneered an array of nitro group reduction techniques employing recyclable aqueous media facilitated by micellar catalysis<sup>36-39</sup> (Scheme II-1). Historically, in 2013, we developed a robust, eco-friendly protocol for the reduction of functionalized nitroarenes, using inexpensive zinc dust in aqueous TPGS-750-M solution (2 wt %).<sup>36</sup> This procedure was characterized by its mild reaction parameters and exhibited commendable selectivity towards variety of protecting groups. Advancing this approach, in 2017, we transitioned to carbonyl iron powder (CIP) as a substitute for zinc dust, a shift motivated by the greater earth-abundance of iron, marking an enhancement in sustainability.<sup>37</sup> Notwithstanding the merits of these approaches, they were

not without drawbacks, primarily the generation of waste owing to the stoichiometric utilization of metals.

Parallel to these endeavors, we also explored catalytic hydrogenation strategies. In 2015, we introduced a novel nanoparticle (NP)-containing iron with ppm levels of palladium.<sup>38</sup> This NP catalyst facilitated reduction of nitro groups in aqueous micellar media using stoichiometric  $\text{NaBH}_4$ , yielding arylamines with impressive efficiency. Further optimization in 2018 achieved an enhancement in the reactivity of these NPs by incorporating ppm levels of nickel, which served to modulate the palladium surface content and mitigate formation of less-reactive Pd-Pd aggregates.<sup>39</sup> Consequently, this modified system ensured enhanced yields within decreased reaction durations. While these methodologies demonstrated remarkable functional group tolerance and notably diminished the metal input into the reaction system, the mandatory use of stoichiometric  $\text{NaBH}_4$  posed sustainability challenges due to consequential waste generation.



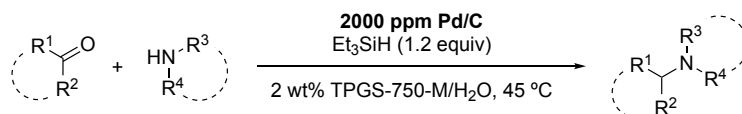
**Scheme II-1.** Previous approaches to nitro group reductions in aqueous micellar media.

In more recent investigations, we documented that commercially available Pd/C can facilitate reductive aminations<sup>40</sup> and hydrogenation of olefins<sup>41</sup> under aqueous micellar conditions with an impressively low Pd loading at ppm levels. Such conditions, benefiting from the "nano-to-nano" effect,<sup>42</sup> enable utilization of mild conditions, notably,

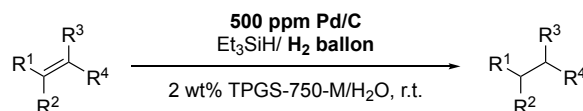


environmentally benign reductants like dihydrogen, while avoiding potentially polluting reagents such as boranes or silanes. Given this backdrop, we were intrigued by the potential adaptability of these conditions to more challenging nitro group reductions. In this work, we illustrate that a mere 0.4 mol % of commercially available Pd/C, under atmospheric hydrogen within nanomicelle-containing water, can readily reduce nitro groups, including those associated with the preparation of pharmaceutical intermediates.

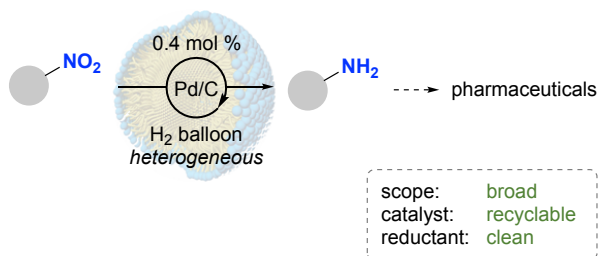
**Reductive amination:**



**hydrogenation of olefins:**



**Scheme II-2.** Recent report on reductions using ppm Pd/C



**Scheme II-3.** This work: nitro reductions in water with Pd/C and H<sub>2</sub>

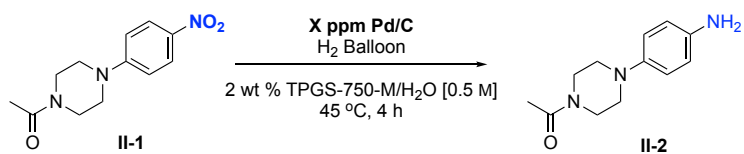
## 2.2. Results and Discussion

### 2.2.1. screening of conditions

Our preliminary assessment was conducted using model substrate **II-1** (Table II-1). Inspired by our prior research on the Pd/C reduction system,<sup>40-41</sup> we employed the same 1 wt % Pd/C purchased from Sigma-Aldrich as catalyst. Dihydrogen (H<sub>2</sub>) was selected as the reductant due to its environmentally benign nature, where water is the sole by-product. Using

a 2 wt % TPGS-750-M/H<sub>2</sub>O solution as reaction medium, the system was purged with an H<sub>2</sub> balloon and subsequently heated to 45 °C.

**Table II-1.** Screening palladium loading for nitro group reductions.<sup>a</sup>

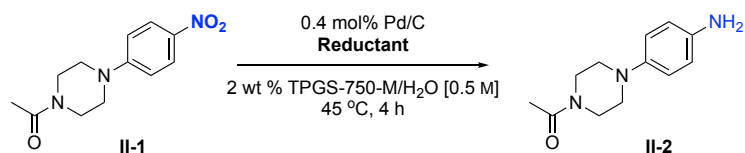


Entry	Pd/C Loading (ppm)	Conversion (%) <sup>b</sup>
1	500	trace
2	1000	31
3	2000	52
4	4000	98

<sup>a</sup> Reaction conditions unless otherwise noted: 0.5 mmol of **II-1**, 1 wt % Pd/C, H<sub>2</sub> balloon, stirred in 1 mL 2 wt % TPGS-750-M/H<sub>2</sub>O at 45 °C. <sup>b</sup> Conversion determined by GC-MS.

Our initial screening emphasized optimization of palladium loading (Table II-1). Notably, remarkably, with only 4000 ppm (0.4 mol %) Pd, the desired nitro group reduction occurred smoothly, yielding the desired product with near-complete conversion (entry 4). Attempts to decrease the Pd loading further, however, failed to maintain the same degree of catalyst reactivity. Hence, when reduced to 2000 ppm, the extent of conversion fell to a mere 52%, and a further decrease to 500 ppm resulted in no observable reaction. Consequently, 4000 ppm of 1 wt % Pd/C was deemed optimal and selected for subsequent experiments.

**Table II-2.** Screening reductants for nitro group reductions.<sup>a</sup>



Entry	Reductant	Yield (%) <sup>b</sup>
1	NaBH <sub>4</sub>	<1
2	PhSiH <sub>3</sub>	40
3	PhMeSiH <sub>2</sub>	27
4	(EtO) <sub>3</sub> SiH	<1
5	PMHS	<1
6	Et <sub>3</sub> SiH	90
7 <sup>c</sup>	Et <sub>3</sub> SiH	62
8	H <sub>2</sub> Balloon	95
9 <sup>c</sup>	H <sub>2</sub> Balloon	81

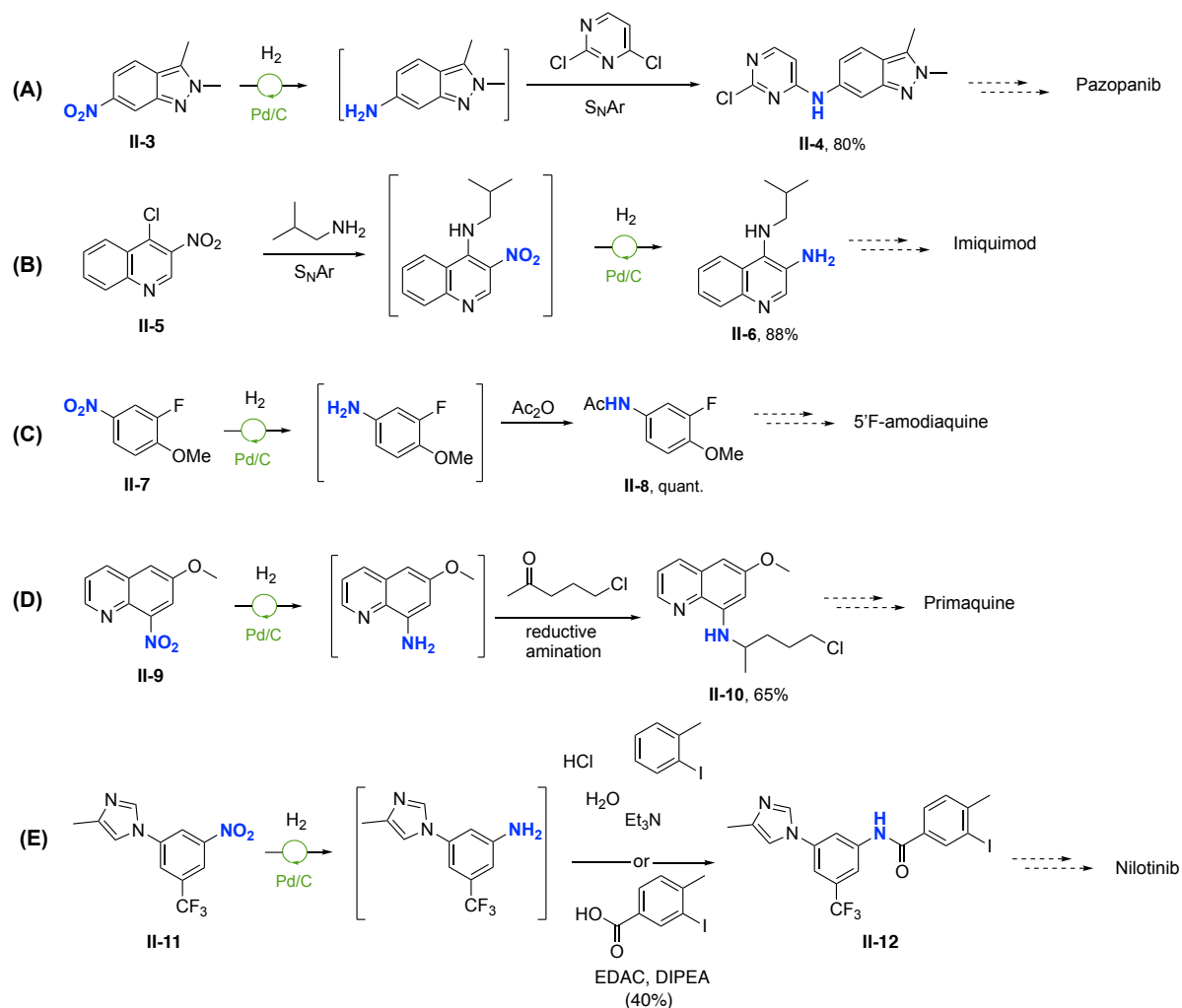
<sup>a</sup> Reaction conditions unless otherwise noted: 0.5 mmol of **II-1**, 0.4 mol % of 1 wt % Pd/C, reductant (1.5 equiv), stirred in 1 mL 2 wt % TPGS-750-M/H<sub>2</sub>O at 45 °C. <sup>b</sup> Isolated yield. <sup>c</sup> Reaction was run "on water."

While dihydrogen (H<sub>2</sub>) emerges as an ideal reductant from an environmental perspective, its gaseous nature could potentially necessitate specialized equipment, posing practical challenges. Consequently, we broadened our scope to explore both liquid and solid phase reductants as viable alternatives (Table II-2). Through a detailed screening of various reductants, H<sub>2</sub> gas was reaffirmed as the best choice, giving the desired target product with 95% isolated yield (entry 8). Notably, triethylsilane (Et<sub>3</sub>SiH) also demonstrated commendable efficacy, yielding a nearly comparable 90% of the product (entry 6). These results highlight the adaptability and robustness of our methodology. However, it is also worth noting that in the absence of surfactant (TPGS-750-M), the reactions (entries 7, 9) conducted "on water" gave aniline **II-2** but with diminished yields of 62% and 81%, respectively, underscoring the indispensable role of the surfactant in achieving optimal results.

### 2.2.2. Application: 1-pot synthesis of pharmaceutical intermediates

Utilizing the newly optimized conditions, several one-pot syntheses of pharmaceutical intermediates were undertaken. As shown in Scheme II-4, this ppm-level Pd/C nitro reduction method is versatile, integrating seamlessly at diverse stages within synthetic sequences and accommodating assorted reaction types within these one-pot processes.

For example, the intermediate for pazopanib<sup>43</sup>, an anticancer agent, was efficiently synthesized via a combination of nitro group reduction and S<sub>N</sub>Ar reaction, yielding 80% of the desired product **II-4** (A). Nitro group reduction was also feasible after an S<sub>N</sub>Ar reaction. As shown in pathway B, Initial S<sub>N</sub>Ar reaction between substrate **II-5** and isobutylamine was followed by nitro group reduction to afford **II-6** in 88% overall yield, an intermediate *en route* to imiquimod.<sup>44</sup> Another substrate, 2-fluoro-4-nitrobenzene (**7**) was smoothly hydrogenated and subsequently acylated (C) to deliver compound **II-8**, an intermediate to 5'F-adiquine,<sup>45</sup> in quantitative yield. Significantly, the resultant acetamide **II-8** could be simply isolated via filtration. Furthermore, the antimalarial primaquine<sup>46</sup> precursor **II-10** was synthesized *via* nitro group reduction of compound **II-9**, followed by reductive amination (D). In parallel, the precursor for the anticancer agent nilotinib<sup>47</sup>, a therapeutic for chronic myelogenous leukemia, can be synthesized via two aqueous-based pathways (E). The first encompasses reduction of the nitro group in compound **II-11**, followed by efficient acylation with the corresponding acid chloride resulting in compound **II-12** with an impressive overall yield of 95%. The alternative route involves reduction of the nitro group and subsequent coupling utilizing EDAC and DIPEA with the corresponding acids, yielding an identical product, albeit with lesser efficiency. From these multi-steps, one-pot sequences, it can be concluded that this novel approach for reducing aromatic and heteroaromatic nitro groups exhibits considerable robustness.



**Scheme II-4.** Nitro group reductions for one-pot synthesis of pharmaceutical intermediates.

Reaction conditions; nitro reduction: 0.4 mol % of Pd/C (w/r/t, nitro compound), H<sub>2</sub> balloon, 2 wt % TPGS-750-M/H<sub>2</sub>O [0.5 M], 55 °C. S<sub>N</sub>Ar reaction: base (1.5-2.0 equiv), aryl chloride (1.0 equiv), 45-50 °C. Acylation with acetic anhydride: 1.2 equiv of Ac<sub>2</sub>O, rt. Reductive amination: 1.5 equiv of Na(CN)BH<sub>3</sub>, rt-35 °C. Acylation with aroyl chloride: Et<sub>3</sub>N (2.0 equiv), aroyl chloride (2.0 equiv), rt. Amide coupling: acid (1.0 equiv), EDAC (1.3 equiv), DIPEA (2.0 equiv), 60 °C, 18 h. Isolated yields are shown.

### 2.2.3. Substrate scope

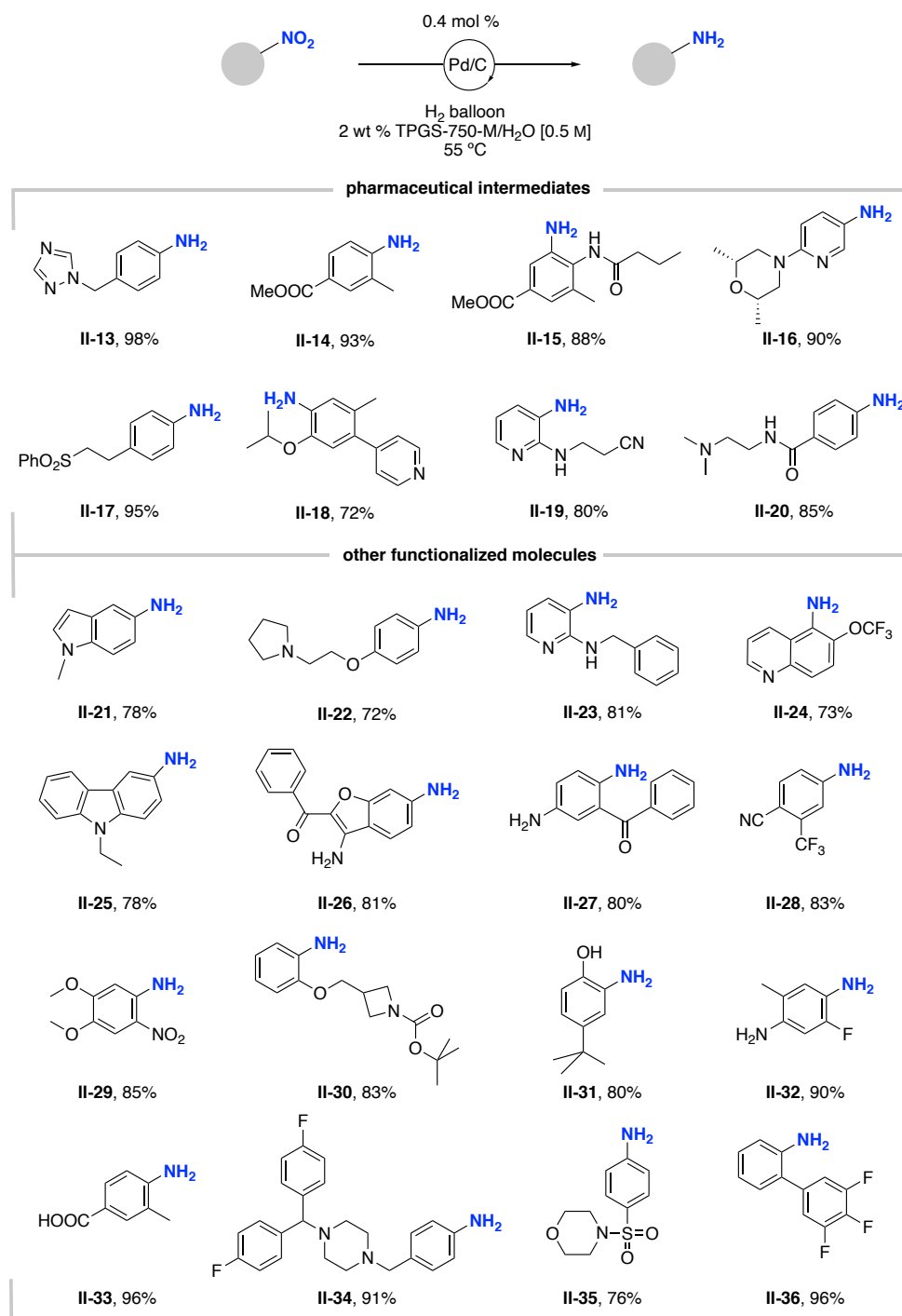
The same optimized conditions were extended to a wide variety of nitro group-containing compounds, including pharmaceutical precursors and other highly complex molecules. (Scheme II-3). First, we synthesized an array of compounds associated with recognized active pharmaceutical ingredients (APIs). Compound **II-13** serves as a pivotal intermediate leading to rizatriptan, a therapeutic agent for the amelioration of migraine headaches.<sup>48</sup> Both compounds **II-14** and **II-15** are foundational precursors for constructing the benzoimidazole core of telmisartan, an esteemed antihypertensive medication.<sup>49</sup> Compound **II-16** is involved in the synthetic pathway towards sonidegib, a targeted oncology therapeutic.<sup>50</sup> Compound **II-17**, meanwhile, is relevant to the synthesis of eletriptan, which is employed in the management of headache disorders.<sup>51</sup> Compound **II-18** plays a crucial role in the synthesis of ceritinib, a novel agent for lung cancer treatment.<sup>52</sup> Compound **II-19** is tied to the development of potential therapeutics targeting central nervous system disorders.<sup>53</sup> Finally, compound **II-20** stands as an analogue to procainamide in its structural features and potential therapeutic utilities.<sup>54</sup>

Furthermore, we broadened the substrate scope to encompass an array of functionalized molecules, facilitating a more comprehensive understanding of the system's versatility. Among our observations, a significant facet was the observed tolerance of certain reducible functionalities under the employed conditions. Specifically, esters (**II-14**, **II-15**), pyridines (**II-23**), ketones (**II-26**, **II-27**), and nitriles (**II-28**) remained largely unaffected, pointing to the chemoselectivity inherent to this reduction method. Of particular intrigue was the selective mono-reduction of dinitroveratrole to **II-29**, which was achieved in high chemical yield. This selective behavior could be attributed to a shift in the molecule's electronic character following initial reduction, making subsequent reductions less favorable. The conditions also

demonstrated an impressive compatibility with various protecting groups, typically of paramount importance in complex molecule synthesis. These includes acetyl (**II-15**), benzyl (**II-23**), and Boc (**II-30**) moieties, testifying to the method's amenability to a wide range of synthetic plans. Another compelling aspect of our study was the observation that molecules with high polarity, such as amines (**II-26**), carbamates (**II-30**), phenols (**II-31**), and acids (**II-33**) are also amenable to the conditions and underwent reduction giving the desired outcomes. Lastly, our investigation into heterocyclic structures revealed the method's applicability to a broad spectrum of such materials. Triazoles (**II-13**), indoles (**II-21**), pyridines (**II-23**), quinolines (**II-24**), benzofurans (**II-26**), and carbazoles (**II-25**) all proved to be compatible, further underscoring the generality of this nitro reduction methodology.

In light of these findings, it's evident that this nitro reduction methodology holds significant promise for a wide spectrum of applications, especially in complex molecule synthesis. Its versatility and robust nature, as showcased through compatibility with a plethora of functional groups and heterocyclic structures, highlight its potential as a cornerstone technique in modern organic synthesis.

**Table II-3.** Nitro group reductions of substrates of varying complexity.<sup>a</sup>



<sup>a</sup> Reaction conditions unless otherwise noted: 0.5 mmol of nitroarene, 0.4 mol % of 1 wt % Pd/C, H<sub>2</sub> balloon, stirred in 2 wt % TPGS-750-M/H<sub>2</sub>O [0.5 M] at 55 °C. Isolated yields are shown.

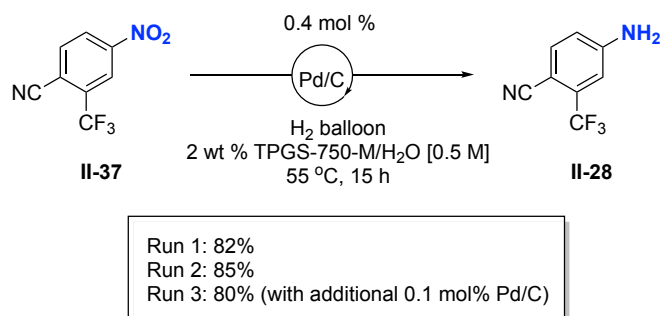


#### 2.2.4. Recycle study

As is typical of reactions run under aqueous micellar conditions, recycling of the reaction medium is readily achieved once reductions are complete (Scheme II-5). Thus, the reaction mixture is extracted “in flask” and the aqueous medium was saved and reused for two additional runs, without losing catalyst reactivity.

The Pd/C catalyst exhibits a remarkable capacity for reuse, which effectively lower the average palladium requirement per reaction. Notably, the second run proceeded without the addition of fresh palladium and achieved a yield comparable to the initial run. Although a marginal decrease in reactivity was observed in the third cycle—likely attributable to the incremental loss of catalyst during extraction—a minor supplement of 0.1 mol% fresh Pd/C was sufficient to restore reactivity to the desired level. This aspect of the methodology underscores its alignment with principles of sustainability and efficiency, reducing both waste and operational costs.

**Scheme II-5.** Recycling of the aqueous medium and catalyst.



#### 2.3. Summary

In summary, we have developed a highly efficient and eco-friendly methodology for the palladium-catalyzed reduction of nitro group-containing compounds utilizing minimal amounts of palladium on carbon (4000 ppm Pd/C) to achieve notable yields. The demonstrated versatility of this system is marked by its successful application in the one-pot synthesis of a

diverse array of pharmaceutical intermediates, as well as its compatibility with a broad spectrum of functional groups and heterocyclic compounds. The protocol further supports the principles of green chemistry through the recyclability of both the reaction medium and the Pd/C catalyst, contributing to the overall sustainability of the process. The advancements presented herein not only enhance existing reduction methods but also promote the potential integration of sustainable practices into chemical manufacturing, positioning them as a pivotal influence on future industrial protocols.

#### 2.4. References

1. Downing, R. S.; Kunkeler, P. J.; van Bekkum, H. Catalytic Syntheses of Aromatic Amines. *Catal. Today*, **1997**, *37*, 121–136.
2. Kadam, H. K.; Tilve, S. G. Advancement in Methodologies for Reduction of Nitroarenes. *RSC Adv.* **2015**, *5*, 83391–83407.
3. Blaser, H.-U.; Steiner, H.; Studer, M. Selective Catalytic Hydrogenation of Functionalized Nitroarenes: An Update. *ChemCatChem* **2009**, *1*, 210–221.
4. Roughley, S. D.; Jordan, A. M. The Medicinal Chemist's Toolbox: An Analysis of Reactions Used in the Pursuit of Drug Candidates. *J. Med. Chem.* **2011**, *54*, 3451–3479.
5. Tasler, S.; Mies, J.; Lang, M. Applicability Aspects of Transition Metal-Catalyzed Aromatic Amination Protocols in Medicinal Chemistry. *Adv. Synth. Catal.* **2007**, *349*, 2286–2300.
6. Hoi, K. H.; Çalimsiz, S.; Froese, R. D. J.; Hopkinson, A. C.; Organ, M. G. Amination with Pd–NHC Complexes: Rate and Computational Studies on the Effects of the Oxidative Addition Partner. *Chemistry – A European Journal* **2011**, *17*, 3086–3090.
7. Isley, N. A.; Linstadt, R. T. H.; Kelly, S. M.; Gallou, F.; Lipshutz, B. H. Nucleophilic Aromatic Substitution Reactions in Water Enabled by Micellar Catalysis. *Org. Lett.* **2015**, *17*, 4734–4737.
8. Bechamp reduction: Béchamp, A. De l'action des protoxides de fer sur la nitronaphtaline et la nitrobenzine. nouvelle méthode de formation des bases organiques artificielles de Zinin. *Annales de chimie et de physique.* **1854**, *42*, 186–196.
9. Verho, O.; Gustafson, K. P. J.; Nagendiran, A.; Tai, C.-W.; Bäckvall, J.-E. Mild and Selective Hydrogenation of Nitro Compounds Using Palladium Nanoparticles Supported on Amino-Functionalized Mesocellular Foam. *ChemCatChem* **2014**, *6*, 3153–3159.

10. Rahaim, R. J.; Maleczka, R. E. Pd-Catalyzed Silicon Hydride Reductions of Aromatic and Aliphatic Nitro Groups. *Org. Lett.* **2005**, *7*, 5087–5090.
11. Dell’Anna, M. M.; Intini, S.; Romanazzi, G.; Rizzuti, A.; Leonelli, C.; Piccinni, F.; Mastroilli, P. Polymer Supported Palladium Nanocrystals as Efficient and Recyclable Catalyst for the Reduction of Nitroarenes to Anilines under Mild Conditions in Water. *J. Mol. Catal. Chem.* **2014**, *395*, 307–314.
12. He, L.; Wang, L.-C.; Sun, H.; Ni, J.; Cao, Y.; He, H.-Y.; Fan, K.-N. Efficient and Selective Room-Temperature Gold-Catalyzed Reduction of Nitro Compounds with CO and H<sub>2</sub>O as the Hydrogen Source. *Angew. Chem., Int. Ed.* **2009**, *48*, 9538–9541.
13. Maeno, Z.; Mitsudome, T.; Mizugaki, T.; Jitsukawa, K.; Kaneda, K. Selective Synthesis of Rh<sub>5</sub> Carbonyl Clusters within a Polyamine Dendrimer for Chemoselective Reduction of Nitro Aromatics. *Chem. Commun.* **2014**, *50*, 6526–6529.
14. Jang, Y.; Kim, S.; Jun, S. W.; Kim, B. H.; Hwang, S.; Song, I. K.; Kim, B. M.; Hyeon, T. Simple One-Pot Synthesis of Rh–Fe<sub>3</sub>O<sub>4</sub> Heterodimer Nanocrystals and Their Applications to a Magnetically Recyclable Catalyst for Efficient and Selective Reduction of Nitroarenes and Alkenes. *Chem. Commun.* **2011**, *47*, 3601–3603.
15. Wei, H.; Liu, X.; Wang, A.; Zhang, L.; Qiao, B.; Yang, X.; Huang, Y.; Miao, S.; Liu, J.; Zhang, T. FeO<sub>x</sub>-Supported Platinum Single-Atom and Pseudo-Single-Atom Catalysts for Chemoselective Hydrogenation of Functionalized Nitroarenes. *Nat. Commun.* **2014**, *5*, 5634–5641.
16. Zhang, B.; Asakura, H.; Zhang, J.; Zhang, J.; De, S.; Yan, N. Stabilizing a Platinum<sub>1</sub> Single-Atom Catalyst on Supported Phosphomolybdic Acid without Compromising Hydrogenation Activity. *Angew. Chem. Int. Ed.* **2016**, *55*, 8319–8323. *Angew. Chem.* **2016**, *128*, 8459–8463.
17. Karahan, Ö.; Biçer, E.; Taşdemir, A.; Yürüm, A.; Gürsel, S. A. Development of Efficient Copper-Based MOF-Derived Catalysts for the Reduction of Aromatic Nitro Compounds. *Eur. J. Inorg. Chem.* **2018**, *2018*, 1073–1079.
18. Kadam, H. K.; Tilve, S. G. Copper(II) Bromide as a Precatalyst for in Situ Preparation of Active Cu Nanoparticles for Reduction of Nitroarenes. *RSC Adv.* **2012**, *2*, 6057–6060.
19. Kaur, R.; Pal, B. Cu Nanostructures of Various Shapes and Sizes as Superior Catalysts for Nitro-Aromatic Reduction and Co-Catalyst for Cu/TiO<sub>2</sub> Photocatalysis. *Appl. Catal. Gen.* **2015**, *491*, 28–36.
20. Westerhaus, F. A.; Jagadeesh, R. V.; Wienhöfer, G.; Pohl, M.-M.; Radnik, J.; Surkus, A.-E.; Rabeah, J.; Junge, K.; Junge, H.; Nielsen, M.; Brückner, A.; Beller, M. Heterogenized Cobalt Oxide Catalysts for Nitroarene Reduction by Pyrolysis of Molecularly Defined Complexes. *Nat. Chem.* **2013**, *5*, 537–543.

21. Jagadeesh, R. V.; Banerjee, D.; Arockiam, P. B.; Junge, H.; Junge, K.; Pohl, M.-M.; Radnik, J.; Brückner, A.; Beller, M. Highly Selective Transfer Hydrogenation of Functionalised Nitroarenes Using Cobalt-Based Nanocatalysts. *Green Chem.* **2015**, *17*, 898–902.
22. Chinnappan, A.; Kim, H. Transition Metal Based Ionic Liquid (Bulk and Nanofiber Composites) Used as Catalyst for Reduction of Aromatic Nitro Compounds under Mild Conditions. *RSC Adv.* **2013**, *3*, 3399-3406.
23. Mazaheri, O.; Kalbasi, R. J. Preparation and Characterization of Ni/MZSM-5 Zeolite with a Hierarchical Pore Structure by Using KIT-6 as Silica Template: An Efficient Bi-Functional Catalyst for the Reduction of Nitro Aromatic Compounds. *RSC Adv.* **2015**, *5*, 34398–34414.
24. Qu, Y.; Xu, G.; Yang, J.; Zhang, Z. Reduction of Aromatic Nitro Compounds over Ni Nanoparticles Confined in CNTs. *Appl. Catal. Gen.* **2020**, *590*, 117311-117316.
25. Junge, K.; Wendt, B.; Shaikh, N.; Beller, M. Iron-Catalyzed Selective Reduction of Nitroarenes to Anilines Using Organosilanes. *Chem. Commun.* **2010**, *46*, 1769.
26. Jagadeesh, R. V.; Wienhöfer, G.; Westerhaus, F. A.; Surkus, A.-E.; Pohl, M.-M.; Junge, H.; Junge, K.; Beller, M. Efficient and Highly Selective Iron-Catalyzed Reduction of Nitroarenes. *Chem. Commun.* **2011**, *47*, 10972.
27. MacNair, A. J.; Tran, M.-M.; Nelson, J. E.; Sloan, G. U.; Ironmonger, A.; Thomas, S. P. Iron-Catalysed, General and Operationally Simple Formal Hydrogenation Using Fe(OTf)<sub>3</sub> and NaBH<sub>4</sub>. *Org. Biomol. Chem.* **2014**, *12*, 5082–5088.
28. Pedrajas, E.; Sorribes, I.; Gushchin, A. L.; Laricheva, Y. A.; Junge, K.; Beller, M.; Llusar, R. Chemoselective Hydrogenation of Nitroarenes Catalyzed by Molybdenum Sulphide Clusters. *ChemCatChem* **2017**, *9*, 1128–1134.
29. Di Gioia, M. L.; Leggio, A.; Guarino, I. F.; Leotta, V.; Romio, E.; Liguori, A. A Simple Synthesis of Anilines by LiAlH<sub>4</sub>/TiCl<sub>4</sub> Reduction of Aromatic Nitro Compounds. *Tetrahedron Lett.* **2015**, *56*, 5341–5344.
30. Durchschein, K.; Hall, M.; Faber, K. Unusual Reactions Mediated by FMN-Dependent Ene- and Nitro-Reductases. *Green Chem.* **2013**, *15*, 1764.
31. Yamashina, I. Enzymatic Reduction of Aromatic Nitro Compounds. *BCSJ* **1954**, *27*, 85–89.
32. Viodé, C.; Bettache, N.; Cenas, N.; Krauth-Siegel, R. L.; Chauvière, G.; Bakalara, N.; Périé, J. Enzymatic Reduction Studies of Nitroheterocycles. *Biochem. Pharmacol.* **1999**, *57*, 549–557.

33. Orlandi, M.; Tosi, F.; Bonsignore, M.; Benaglia, M. Metal-Free Reduction of Aromatic and Aliphatic Nitro Compounds to Amines: A HSiCl<sub>3</sub>-Mediated Reaction of Wide General Applicability. *Org. Lett.* **2015**, *17*, 3941–3943.
34. Orlandi, M.; Tosi, F.; Bonsignore, M.; Benaglia, M. Metal-Free Reduction of Aromatic and Aliphatic Nitro Compounds to Amines: A HSiCl<sub>3</sub>-Mediated Reaction of Wide General Applicability. *Org. Lett.* **2015**, *17*, 3941–3943.
35. Jang, M.; Lim, T.; Park, B. Y.; Han, M. S. Metal-Free, Rapid, and Highly Chemoselective Reduction of Aromatic Nitro Compounds at Room Temperature. *J. Org. Chem.* **2022**, *87*, 910–919.
36. Kelly, S. M.; Lipshutz, B. H. Chemoselective Reductions of Nitroaromatics in Water at Room Temperature. *Org. Lett.* **2014**, *16*, 98–101.
37. Lee, N. R.; Bikovtseva, A. A.; Cortes-Clerget, M.; Gallou, F.; Lipshutz, B. H. Carbonyl Iron Powder: A Reagent for Nitro Group Reductions under Aqueous Micellar Catalysis Conditions. *Org. Lett.* **2017**, *19*, 6518–6521.
38. Feng, J.; Handa, S.; Gallou, F.; Lipshutz, B. H. Safe and Selective Nitro Group Reductions Catalyzed by Sustainable and Recyclable Fe/Ppm Pd Nanoparticles in Water at Room Temperature. *Angew. Chem., Int. Ed.* **2016**, *55*, 8979–8983.
39. Pang, H.; Gallou, F.; Sohn, H.; Camacho-Bunquin, J.; Delferro, M.; Lipshutz, B. H. Synergistic Effects in Fe Nanoparticles Doped with Ppm Levels of (Pd + Ni). A New Catalyst for Sustainable Nitro Group Reductions. *Green Chem.* **2018**, *20*, 130–135.
40. Thakore, R. R.; Takale, B. S.; Casotti, G.; Gao, E. S.; Jin, H. S.; Lipshutz, B. H. Chemoselective Reductive Aminations in Aqueous Nanoreactors Using Parts per Million Level Pd/C Catalysis. *Org. Lett.* **2020**, *22*, 6324–6329.
41. Takale, B. S.; Thakore, R. R.; Gao, E. S.; Gallou, F.; Lipshutz, B. H. Environmentally Responsible, Safe, and Chemoselective Catalytic Hydrogenation of Olefins: Ppm Level Pd Catalysis in Recyclable Water at Room Temperature. *Green Chem.* **2020**, *22*, 6055–6061.
42. Lipshutz, B. H. The ‘Nano-to-Nano’ Effect Applied to Organic Synthesis in Water. *Johnson Matthey Technology Review* **2017**, *61*, 196–202.
43. Keisner, S. V.; Shah, S. R. Pazopanib: The Newest Tyrosine Kinase Inhibitor for the Treatment of Advanced or Metastatic Renal Cell Carcinoma. *Drugs* **2011**, *71*, 443–454.
44. Skinner, R. B. Imiquimod. *Dermatol. Clin.* **2003**, *21*, 291–300.
45. O’Neill, P. M.; Harrison, A. C.; Storr, R. C.; Hawley, S. R.; Ward, S. A.; Park, B. K. The Effect of Fluorine Substitution on the Metabolism and Antimalarial Activity of Amodiaquine. *J. Med. Chem.* **1994**, *37*, 1362–1370.

46. Hill, D. R.; Ryan, E. T.; Parise, M. E.; Magill, A. J.; Lewis, L. S.; Baird, J. K. Primaquine: Report from CDC Expert Meeting on Malaria Chemoprophylaxis I. *Am. J. Trop. Med. Hyg.* **2006**, *75*, 402–415.
47. Deininger, M. W. Nilotinib. *Clin. Cancer Res.* **2008**, *14*, 4027–4031.
48. Dooley, M.; Faulds, D. Rizatriptan: A Review of Its Efficacy in the Management of Migraine. *Drugs* **1999**, *58*, 699–723.
49. Battershill, A. J.; Scott, L. J. Telmisartan: A Review of Its Use in the Management of Hypertension. *Drugs* **2006**, *66*, 51–83.
50. Burness, C. B. Sonidegib: First Global Approval. *Drugs* **2015**, *75*, 1559–1566.
51. McCormack, P. L.; Keating, G. M. Eletriptan: A Review of Its Use in the Acute Treatment of Migraine. *Drugs* **2006**, *66*, 1129–1149.
52. Kaminska, K. Process for the preparation of ceritinib using 'in situ' prepared 5-methyl-2-(1-methylethoxy)-4-(4-piperidinyl)-benzenamine monohydrochloride (1:1) as an intermediate. International Patent No. WO 2017041771 A1.
53. Grove, F.; McComsey, D.; McNally, J. Heterocyclic Derivatives Useful in Treating Central Nervous System Disorders. U.S. Patent No. 5968946.
54. Zicca, A.; Cafaggi, S.; Marigliò, M. A.; Vannozzi, M. O.; Ottone, M.; Bocchini, V.; Caviglioli, G.; Viale, M. Reduction of Cisplatin Hepatotoxicity by Procainamide Hydrochloride in Rats. *Eur. J. Pharmacol.* **2002**, *442*, 265–272.

## 2.5. Experimental section

### 2.5.1. General information

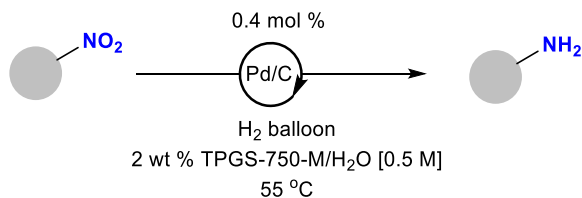
All reagents and chemicals required for the experiments that follow were procured from Combi-Blocks and Sigma-Aldrich, and used without further purification. 1 wt % Pd/C was purchased from Sigma-Aldrich (catalog #205672). Deuterated solvents were purchased from Cambridge Isotopes Laboratories. TPGS-750-M is either prepared or supplied by PHT International (also available from Sigma-Aldrich catalog #733857). The desired 2 wt % of surfactant solution in HPLC water was prepared by dissolving 2 g of surfactant to 98 g of HPLC water (which had been degassed with argon prior to use) and stored under argon.

Thin layer chromatography (TLC) was performed using Silica Gel 60 F254 plates (Merck, 0.25 mm thick). Flash chromatography was performed in glass columns using Silica Gel 60 (EMD, 40-63  $\mu\text{m}$ ).

$^1\text{H}$  and  $^{13}\text{C}$  NMR spectra were recorded on a Varian Unity Inova 500 MHz (500 MHz for  $^1\text{H}$ , 125 MHz for  $^{13}\text{C}$ ), Bruker 500 MHz (500 MHz for  $^1\text{H}$ , 125 MHz for  $^{13}\text{C}$ ) or Bruker 400 MHz (400 MHz for  $^1\text{H}$ , 100 MHz for  $^{13}\text{C}$ );  $\text{CD}_3\text{OD}$ ,  $\text{DMSO-}d_6$  and  $\text{CDCl}_3$  were used as solvent. Residual peaks for  $\text{CHCl}_3$  in  $\text{CDCl}_3$  ( $^1\text{H} = 7.26$  ppm,  $^{13}\text{C} = 77.20$  ppm),  $\text{DMSO}$  in  $\text{DMSO-}d_6$  ( $^1\text{H} = 2.50$  ppm,  $^{13}\text{C} = 39.52$  ppm) or  $\text{MeOH}$  in  $\text{MeOD}$  ( $^1\text{H} = 4.78$  ppm,  $^{13}\text{C} = 49.00$  ppm) have been assigned. The chemical shifts are reported in part per million (ppm), the coupling constants  $J$  values are given in Hertz (Hz). The peak patterns are indicated as follows: bs, broad singlet; s, singlet; d, doublet; t, triplet; q, quartet; p, pentet; m, multiplet.

HRMS were recorded on a Waters Micromass LCT TOF ES+ Premier mass spectrometer using ESI ionization. GCMS data were recorded on a 5975C Mass Selective Detector, coupled with a 7890A Gas Chromatograph (Agilent Technologies).

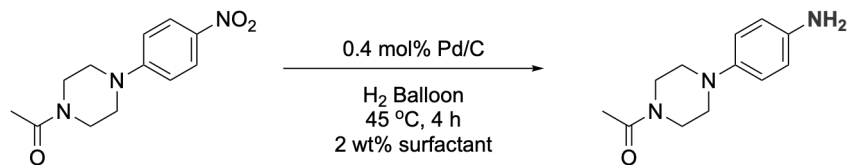
### 2.5.2. General procedure for nitro group reductions.



Pd/C (10.6 mg 1 wt %, 4000 ppm; 0.4 mol %) was added along with a Teflon-coated magnetic stir bar to a 1-dram screw cap vial. The nitro compound (0.25 mmol) was added to this vial. TPGS-750-M/H<sub>2</sub>O solution (2 wt %, 0.5 mL) was then added and the vial was covered with a hydrogen balloon and stirred at 55 °C in an aluminum block placed over an IKA hot plate until complete conversion of starting material was observed (as monitored by TLC or GC-MS). The reaction mixture was adsorbed on silica and purified using flash column chromatography to afford the desired compound.

### 2.5.3. Optimization details

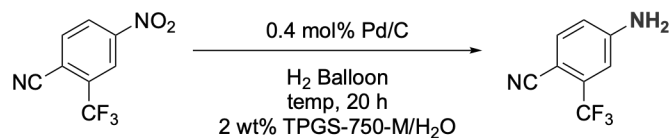
#### Surfactant screening



entry	surfactant solution	% conversion (by GC-MS)
1	TPGS-750-M	98
2	Brij-30	79



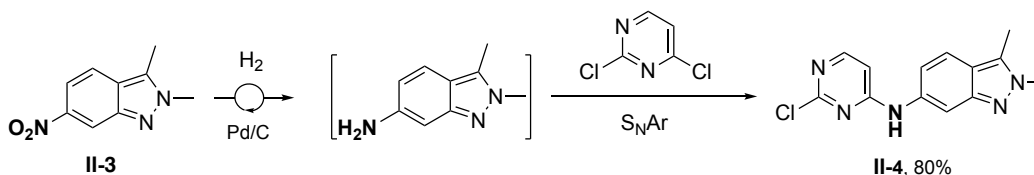
### Optimization of temperature



entry	temp °C	% conversion (by GC-MS)
1	45	51
2	55	82

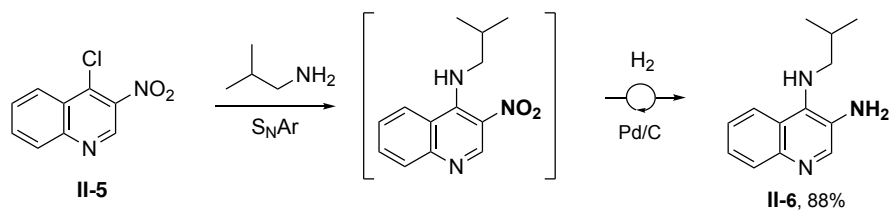
### 2.5.4. Experimental procedures for 1-pot synthesis of pharmaceutical intermediates

Sequence A:



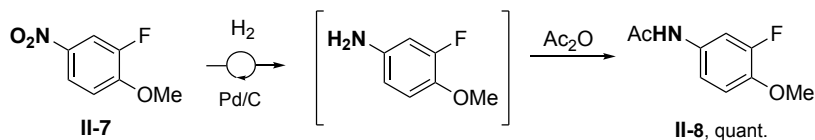
Pd/C (10.6 mg of 1 wt %; 4000 ppm; 0.4 mol %) was added along with a Teflon-coated magnetic stir bar, to a 1-dram screw cap vial. 2,3-Dimethyl-6-nitro-2H-indazole (**II-3**, 47.8 mg, 0.25 mmol) was added to this vial. TPGS-750-M/H<sub>2</sub>O solution (2 wt %, 0.5 mL) was then added and the vial was covered with a hydrogen balloon and stirred at 55 °C in an aluminum block placed over an IKA hot plate until complete conversion of starting material (as monitored by TLC or GC-MS). To the same reaction, 2,4-dichloropyrimidine (37.3 mg, 0.25 mmol, 1 equiv) and K<sub>3</sub>PO<sub>4</sub>•H<sub>2</sub>O (115.2 mg, 0.5 mmol, 2 equiv) were added. The reaction was stirred at 45 °C in an aluminum block placed over an IKA hot plate overnight. The reaction mixture was adsorbed on silica and purified using flash column chromatography to afford the desired compound **II-4** in 80% yield (54.7 mg).

*Sequence B:*



4-Chloro-3-nitroquinoline (**II-5**, 52 mg, 0.25 mmol) and  $K_3PO_4 \cdot H_2O$  (115.2 mg, 0.5 mmol, 2 equiv) were added along with a Teflon-coated magnetic stir bar to a 1-dram screw cap vial. To this vial, 2 wt % TPGS-750-M/ $H_2O$  solution (0.5 mL) and isobutylamine (19.5  $\mu$ L, 0.25 mmol, 1 equiv) were then added and, the vial was stirred at 45 °C in an aluminum block placed over an IKA hot plate for 15 h. To this vial 10.6 mg of 1 wt % Pd/C (4000 ppm; 0.4 mol %) was added and the vial was covered with a hydrogen balloon and stirred at 55 °C in an aluminum block placed over an IKA hot plate until complete conversion of starting material (as monitored by TLC or GC-MS). The reaction mixture was adsorbed on silica and purified using flash column chromatography to afford the desired compound **II-6** in 88% yield (47.4 mg).

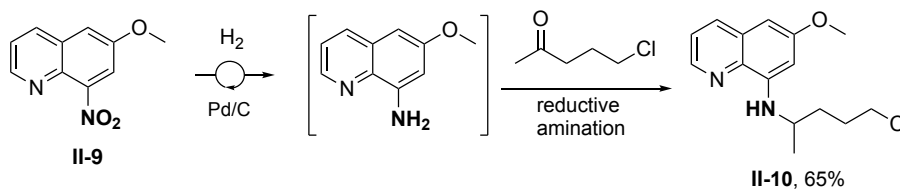
*Sequence C:*



Pd/C (10.6 mg of 1 wt %; 4000 ppm; 0.4 mol %) was added along with a Teflon-coated magnetic stir bar, to a 1-dram screw cap vial. 2-fluoro-1-methoxy-4-nitrobenzene (**II-7**, 42.8 mg, 0.25 mmol) was added to this vial. 2 wt % TPGS-750-M/ $H_2O$  solution (0.5 mL) was then added and, the vial was covered with a hydrogen balloon and stirred at 55 °C in an aluminum block placed over an IKA hot plate until complete conversion of starting material (as

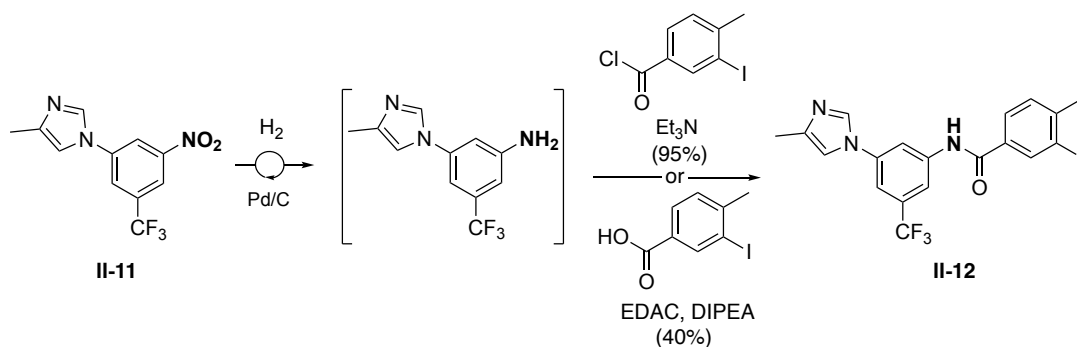
monitored by TLC or GC-MS). To the same reaction, Ac<sub>2</sub>O (28.4  $\mu$ L, 0.3 mmol, 1.2 equiv) was added. The reaction was stirred at rt in an aluminum block placed over an IKA hot plate for 5 h. The reaction mixture was adsorbed on silica and purified using flash column chromatography to afford the desired compound **II-8** in quantitative yield (45.7 mg).

*Sequence D:*



Pd/C (10.6 mg of 1 wt %; 4000 ppm; 0.4 mol %) was added along with a Teflon-coated magnetic stir bar, to a 1-dram screw cap vial. 6-methoxy-8-nitroquinoline (**II-9**, 51.0 mg, 0.25 mmol) was added to this vial. 2 wt % TPGS-750-M/H<sub>2</sub>O solution (0.5 mL) was then added and, the vial was covered with a hydrogen balloon and stirred at 55 °C in an aluminum block placed over an IKA hot plate until complete conversion of starting material (as monitored by TLC or GC-MS). To the same reaction, 5-chloropentan-2-one (45.2 mg, 0.375 mmol, 1.5 equiv) and Na(CN)BH<sub>3</sub> (31.4 mg, 2.0 equiv) was added at rt. The reaction was stirred at 35 °C in an aluminum block placed over an IKA hot plate overnight. The reaction mixture was adsorbed on silica and purified using flash column chromatography to afford the desired compound **II-10** in 65% yield (45.3 mg).

Sequence E:

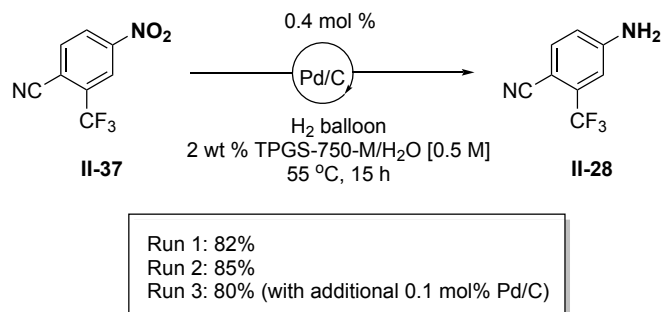


Pd/C (10.6 mg of 1 wt %; 4000 ppm; 0.4 mol %) was added along with a Teflon-coated magnetic stir bar, to a 1-dram screw cap vial. 4-methyl-1-(3-nitro-5-(trifluoromethyl)-phenyl)-1H-imidazole (**II-11**, 67.8 mg, 0.25 mmol) was added to this vial. 2 wt % TPGS-750-M/H<sub>2</sub>O solution (0.5 mL) was then added and the vial was covered with a hydrogen balloon and stirred at 55 °C in an aluminum block placed over an IKA hot plate until complete conversion of starting material (as monitored by TLC or GC-MS).

*Acylation:* To the same reaction, Et<sub>3</sub>N (69.7 μL, 0.5 mmol, 2.0 equiv) and 3-iodo-4-methylbenzoyl chloride (140.3 mg, 0.5 mmol, 2.0 equiv) were added at rt and the reaction was stirred in an aluminum block placed over an IKA hot plate overnight. The reaction mixture was then adsorbed on silica and purified using flash column chromatography to afford the desired compound **II-12** in 95% yield (115.2 mg).

*Amide coupling:* To the same reaction, 3-iodo-4-methylbenzoic acid (65.5 mg, 0.25 mmol, 1 equiv), EDAC (50.5 mg, 0.325 mmol, 1.3 equiv) and DIPEA (87.1 μL, 0.5 mmol, 2.0 equiv) were added at rt. The reaction was then heated to 60 °C in an aluminum block placed over an IKA hot plate and stirred overnight. The reaction mixture was then adsorbed on silica and purified using flash column chromatography to afford the desired compound **II-12** in 40% yield (48.5 mg).

### 2.5.5. Recycling studies



*Initial reaction:* Pd/C (10.6 mg 1 wt %; 4000 ppm; 0.4 mol %) was added along with a Teflon-coated magnetic stir bar, to a 1-dram screw cap vial. The nitro compound **II-37** was added to this vial. 2 wt % TPGS-750-M/H<sub>2</sub>O solution (0.5 mL) was then added and, the vial was covered with a cap containing hydrogen balloon and stirred at 55 °C in an aluminum block placed over an IKA hot plate until complete conversion of starting material (as monitored by TLC or GC-MS). The product **II-28** was then separated by extraction using EtOAc (0.2 mL) to give 38.13 mg (82% yield) of the corresponding amine.

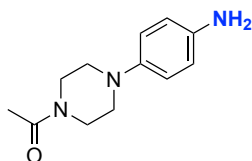
*1st recycle:* The aqueous layer from the above reaction was saved for the 2nd batch. Compound **II-37** was added into the same reaction vial and, the vial was covered with a cap containing a hydrogen balloon and stirred at 55 °C in an aluminum block placed over an IKA hot plate until complete conversion of starting material (as monitored by TLC or GC-MS). The product **II-28** was then separated by extraction using EtOAc (0.2 mL) to give 39.5 mg (85% yield) of the corresponding amine.

*2nd recycle:* The aqueous layer from the above reaction was saved for the 3rd batch. Additional Pd/C (1 wt %; 1000 ppm; 0.1 mol %) was added in the same reaction vial along with compound **II-37** and 0.2 ml 2 wt % TPGS-750-M/H<sub>2</sub>O solution. The vial was covered with a cap containing a hydrogen balloon and stirred at 55 °C in an aluminum block placed over an IKA hot plate until complete conversion of starting material (as monitored by TLC or

GC-MS). The product **II-28** was then separated by extraction process using EtOAc (0.2 mL) to give 37.2 mg (80% yield) of the corresponding amine.

### 2.5.6. Analytical Data

Compounds **II-8**<sup>1</sup>, **II-12**<sup>2</sup>, **II-13**<sup>3</sup>, **II-14**<sup>4</sup>, **II-16**<sup>5</sup>, **II-18**<sup>6</sup>, **II-20**<sup>7</sup>, **II-21**<sup>8</sup>, **II-22**<sup>9</sup>, **II-28**<sup>10</sup>, **II-29**<sup>11</sup>, **II-31**<sup>12</sup>, **II-33**<sup>13</sup>, **II-35**<sup>14</sup>, **II-36**<sup>14</sup> were confirmed by comparisons with literature NMR data. HRMS for compounds **II-2**<sup>16</sup>, **II-15**<sup>17</sup>, **II-25**<sup>18</sup> have been reported. All other new compounds were characterized by <sup>1</sup>H and <sup>13</sup>C NMR, and HRMS.

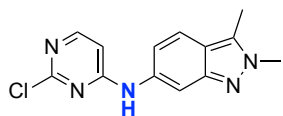


#### 1-(4-(4-aminophenyl)piperazin-1-yl)ethan-1-one (**II-2**)

Pale yellow solid. Yield 52.0 mg (95%), eluent 5:95 (MeOH : DCM)<sup>16</sup>

<sup>1</sup>H NMR (500 MHz, CD<sub>3</sub>OD)  $\delta$  6.85 (d,  $J$  = 8.4 Hz, 2H), 6.72 (d,  $J$  = 8.4 Hz, 2H), 3.71 (t,  $J$  = 5.2 Hz, 2H), 3.66 – 3.64 (m, 2H), 3.01 (t,  $J$  = 5.1 Hz, 2H), 2.95 (t,  $J$  = 5.2 Hz, 2H), 2.13 (s, 3H).

<sup>13</sup>C NMR (126 MHz, CD<sub>3</sub>OD)  $\delta$  170.2, 143.9, 141.5, 119.1, 116.4, 51.5, 51.0, 46.2, 41.4, 19.7.



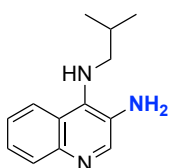
#### N-(2-chloropyrimidin-4-yl)-2,3-dimethyl-2H-indazol-6-amine (**II-4**)

Pale yellow solid. Yield 54.7 mg (80%), eluent 1:9 (MeOH : EtOAc)

**<sup>1</sup>H NMR** (500 MHz, DMSO-*d*<sub>6</sub>) δ 9.98 (d, *J* = 2.2 Hz, 1H), 8.15 (dd, *J* = 5.9, 2.2 Hz, 1H), 7.94 (s, 1H), 7.62 (dd, *J* = 8.9, 2.2 Hz, 1H), 6.06 – 6.99 (m, 1H), 6.77 (dd, *J* = 6.0, 2.2 Hz, 1H), 4.00 (s, 3H), 3.32 (s, 3H).

**<sup>13</sup>C NMR** (126 MHz, DMSO-*d*<sub>6</sub>) δ 162.1, 159.9, 157.4, 147.4, 136.4, 132.2, 121.1, 118.3, 116.4, 106.0, 37.6, 9.8.

**HRMS** (ESI-TOF) *m/z*: [M+Na]<sup>+</sup> calcd for C<sub>13</sub>H<sub>12</sub>ClN<sub>5</sub>Na: 296.0679; found 296.0684.



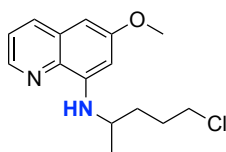
***N*<sup>4</sup>-isobutylquinoline-3,4-diamine (II-6)**

White solid. Yield 47.4 mg (88%), eluent 1:1 (hexanes : EtOAc)

**<sup>1</sup>H NMR** (500 MHz, CDCl<sub>3</sub>) δ 8.48 (s, 1H), 7.98 (d, *J* = 7.4 Hz, 1H), 7.83 (d, *J* = 7.3 Hz, 1H), 7.47 (td, *J* = 4.8, 2.1 Hz, 2H), 3.72 (s, 2H), 3.08 (dd, *J* = 6.7, 2.8 Hz, 2H), 1.90 (dtd, *J* = 13.3, 6.6, 2.7 Hz, 1H), 1.06 (d, *J* = 6.8 Hz, 6H).

**<sup>13</sup>C NMR** (126 MHz, CDCl<sub>3</sub>) δ 143.7, 130.5, 130.0, 125.8, 125.7, 120.0, 54.6, 29.9, 20.4.

**HRMS** (ESI-TOF) *m/z*: [M+H]<sup>+</sup> calcd for C<sub>13</sub>H<sub>18</sub>N<sub>3</sub> 216.1501; found 216.1504.



***N*-(5-chloropentan-2-yl)-6-methoxyquinolin-8-amine (II-10)**

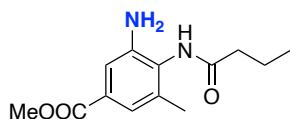
Yellow solid. Yield (65%, 45.3 mg), eluent 7:3 (hexanes : EtOAc)

**<sup>1</sup>H NMR** (500 MHz, CDCl<sub>3</sub>) δ 8.67 (dd, *J* = 4.1, 1.8 Hz, 1H), 7.96 (d, *J* = 8.4 Hz, 1H), 7.29 (q, *J* = 3.9 Hz, 1H), 6.56 (s, 2H), 4.64 (h, *J* = 6.4 Hz, 1H), 4.09 – 4.04 (m, 1H), 3.93 (s,

3H), 3.41 – 3.37 (m, 1H), 2.29 (dq,  $J = 12.1, 3.3$  Hz, 1H), 2.06 – 1.73 (m, 4H), 1.12 (d,  $J = 6.1$  Hz, 3H).

$^{13}\text{C}$  NMR (126 MHz,  $\text{CDCl}_3$ )  $\delta$  158.2, 147.9, 144.2, 139.1, 134.8, 130.6, 121.0, 105.2, 95.6, 55.4, 55.3, 52.7, 33.8, 23.8, 19.1.

HRMS (ESI-TOF)  $m/z$ :  $[\text{M}+\text{H}]^+$  calcd for  $\text{C}_{15}\text{H}_{20}\text{N}_2\text{O}$  279.1264; found 279.1259.

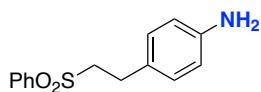


**methyl 3-amino-4-butylamido-5-methylbenzoate (II-15)**

White solid. Yield 55.0mg (88%), eluent 8:2 (hexanes : EtOAc)<sup>17</sup>

$^1\text{H}$  NMR (500 MHz,  $\text{DMSO}-d_6$ )  $\delta$  9.16 (s, 1H), 8.99 (s, 1H), 8.80 (s, 1H), 7.62 (d,  $J = 15.2$  Hz, 2H), 3.77 (s, 3H), 2.36 (d,  $J = 7.5$  Hz, 2H), 2.14 (s, 3H), 1.62 (q,  $J = 7.5$  Hz, 2H), 0.93 (t,  $J = 6.4$  Hz, 3H).

$^{13}\text{C}$  NMR (126 MHz,  $\text{DMSO}-d_6$ )  $\delta$  171.8, 167.2, 152.8, 142.8, 132.3, 120.1, 109.0, 107.2, 52.1, 38.4, 19.1, 17.4, 14.1.



**4-(2-(phenylsulfonyl)ethyl)aniline (II-17)**

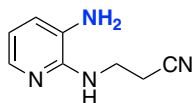
Yellow solid. Yield 61.9 mg (95%), eluent 1:1 hexanes : EtOAc.

$^1\text{H}$  NMR (500 MHz,  $\text{CDCl}_3$ )  $\delta$  7.96 – 7.91 (m, 2H), 7.70 – 7.64 (m, 1H), 7.58 (dd,  $J = 8.4, 7.1$  Hz, 2H), 6.92 – 6.86 (m, 2H), 6.61 – 6.55 (m, 2H), 3.63 (s, 2H), 3.36 – 3.27 (m, 2H), 2.95 – 2.90 (m, 2H).



$^{13}\text{C}$  NMR (126 MHz,  $\text{CDCl}_3$ )  $\delta$  145.3, 139.1, 133.7, 129.3, 129.1, 128.1, 127.1, 115.4, 57.9, 27.9.

**HRMS** (ESI-TOF)  $m/z$ :  $[\text{M}+\text{Na}]^+$  calcd for  $\text{C}_{14}\text{H}_{15}\text{NO}_2\text{SNa}$  284.0716; found 284.0721.



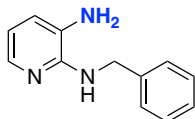
### 3-((3-aminopyridin-2-yl)amino)propanenitrile (II-19)

Dark magenta solid. Yield 61.4 mg (80%), eluent 3:2 hexanes : EtOAc.

$^1\text{H}$  NMR (500 MHz,  $\text{CDCl}_3$ )  $\delta$  7.73 (dd,  $J = 5.0, 1.5$  Hz, 1H), 6.90 (dd,  $J = 7.5, 1.5$  Hz, 1H), 6.59 (dd,  $J = 7.4, 5.0$  Hz, 1H), 4.63 (s, 1H), 3.76 (q,  $J = 6.0$  Hz, 2H), 2.81 (t,  $J = 6.3$  Hz, 2H).

$^{13}\text{C}$  NMR (126 MHz,  $\text{CDCl}_3$ )  $\delta$  148.9, 139.0, 128.6, 122.6, 119.2, 114.4, 37.8, 18.6.

**HRMS** (ESI-TOF)  $m/z$ :  $[\text{M}+\text{Na}]^+$  calcd for  $\text{C}_8\text{H}_{10}\text{N}_4\text{Na}$  185.0803; found 185.0799.



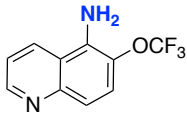
### $N^2$ -benzylpyridine-2,3-diamine (II-23)

Black oil. Yield 40.3 mg (81%), eluent 8.5:1.5 hexanes : EtOAc.

$^1\text{H}$  NMR (500 MHz,  $\text{CDCl}_3$ )  $\delta$  7.79 (dt,  $J = 4.4, 2.2$  Hz, 1H), 7.44 – 7.39 (m, 2H), 7.38 – 7.32 (m, 2H), 7.31 – 7.27 (m, 1H), 6.89 (dd,  $J = 7.5, 1.6$  Hz, 1H), 6.57 (dd,  $J = 7.4, 5.1$  Hz, 1H), 4.64 (d,  $J = 3.0$  Hz, 2H).

$^{13}\text{C}$  NMR (126 MHz,  $\text{CDCl}_3$ )  $\delta$  150.2, 139.8, 139.1, 128.6, 128.4, 128.1, 127.2, 122.1, 113.7, 46.1.

**HRMS** (ESI-TOF)  $m/z$ :  $[\text{M}+\text{H}]^+$  calcd for  $\text{C}_{12}\text{H}_{14}\text{N}_3$  200.1182; found 200.1188.



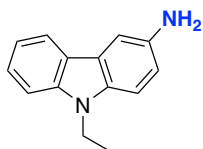
**6-(trifluoromethoxy)quinolin-5-amine (II-24)**

Pale yellow solid. Yield 41.6 mg (73%), eluent 8.5:1.5 hexanes : EtOAc.

$^1\text{H NMR}$  (500 MHz,  $\text{CDCl}_3$ )  $\delta$  8.93 (dd,  $J = 4.2, 1.7$  Hz, 1H), 8.23 (dd,  $J = 8.6, 1.6$  Hz, 1H), 7.61 – 7.52 (m, 2H), 7.42 (dd,  $J = 8.6, 4.2$  Hz, 1H), 4.46 (s, 2H).

$^{13}\text{C NMR}$  (126 MHz,  $\text{CDCl}_3$ )  $\delta$  150.4, 147.0, 134.5, 131.5, 130.0, 124.2, 124.1, 122.2, 120.1, 119.8, 119.2, 118.1.

**HRMS** (ESI-TOF)  $m/z$ :  $[\text{M}+\text{H}]^+$  calcd for  $\text{C}_{10}\text{H}_7\text{F}_3\text{N}_2\text{OH}$  229.0589; found 229.0592.

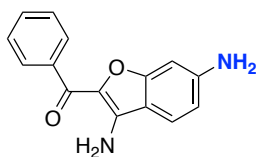


**9-ethyl-9H-carbazol-3-amine (II-25)**

White solid. Yield 41.0 mg (78%), eluent 7:3 hexanes : EtOAc.<sup>18</sup>

$^1\text{H NMR}$  (500 MHz,  $\text{CD}_3\text{OD}$ )  $\delta$  7.96 (d,  $J = 7.8$  Hz, 1H), 7.50 (d,  $J = 2.2$  Hz, 1H), 7.39 – 7.35 (m, 2H), 7.27 (d,  $J = 8.5$  Hz, 1H), 7.10 (ddd,  $J = 7.9, 5.6, 2.4$  Hz, 1H), 6.99 (dd,  $J = 8.5, 2.2$  Hz, 1H), 4.32 (q,  $J = 7.2$  Hz, 2H), 1.34 (t,  $J = 7.2$  Hz, 3H).

$^{13}\text{C NMR}$  (126 MHz,  $\text{CD}_3\text{OD}$ )  $\delta$  140.3, 138.7, 134.7, 125.0, 123.4, 122.4, 119.7, 117.6, 116.0, 108.6, 108.1, 106.7, 36.8, 12.6.



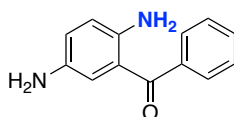
**(3,6-diaminobenzofuran-2-yl)(phenyl)methanone (II-26)**

Yellow solid. Yield 51.0 mg (81%), eluent 1.5:8.5 MeOH : EtOAc.

$^1\text{H NMR}$  (500 MHz,  $\text{CD}_3\text{OD}$ )  $\delta$  8.11 – 8.01 (m, 2H), 7.58 – 7.44 (m, 4H), 6.63 (dd,  $J = 8.6, 1.9$  Hz, 1H), 6.55 (d,  $J = 1.9$  Hz, 1H).

$^{13}\text{C NMR}$  (126 MHz,  $\text{CD}_3\text{OD}$ )  $\delta$  179.5, 158.5, 152.8, 147.2, 138.4, 133.9, 130.7, 128.4, 127.7, 122.0, 111.9, 110.2, 94.4.

**HRMS** (ESI-TOF)  $m/z$ :  $[\text{M}+\text{Na}]^+$  calcd for  $\text{C}_{15}\text{H}_{12}\text{N}_2\text{O}_2\text{Na}$  275.0797; found 275.0803.



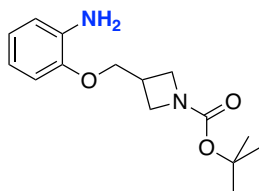
**(2,5-diaminophenyl)(phenyl)methanone (II-27)**

Yellow oil. Yield 42.4 mg (80%), eluent 3:1 hexanes : EtOAc.

$^1\text{H NMR}$  (500 MHz,  $\text{CDCl}_3$ )  $\delta$  7.67 – 7.62 (m, 2H), 7.56 – 7.49 (m, 1H), 7.45 (t,  $J = 7.5$  Hz, 2H), 6.84 – 6.76 (m, 2H), 6.65 (d,  $J = 8.3$  Hz, 1H).

$^{13}\text{C NMR}$  (126 MHz,  $\text{CDCl}_3$ )  $\delta$  144.2, 140.1, 135.6, 131.1, 129.2, 128.1, 123.8, 119.6, 118.4.

**HRMS** (ESI-TOF)  $m/z$ :  $[\text{M}+\text{Na}]^+$  calcd for  $\text{C}_{13}\text{H}_{12}\text{N}_2\text{ONa}$  235.0842; found 235.0847.



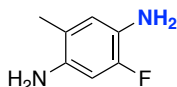
**tert-butyl 3-((2-aminophenoxy)methyl)azetidine-1-carboxylate (II-30)**

Pale yellow solid. Yield 57.7 mg (83%), eluent 8:2 hexanes : EtOAc.

**<sup>1</sup>H NMR** (500 MHz, CDCl<sub>3</sub>) δ 6.87 – 6.75 (m, 2H), 6.75 – 6.65 (m, 2H), 4.16 – 4.03 (m, 4H), 3.83 (dd, *J* = 8.8, 5.2 Hz, 2H), 3.04 – 2.89 (m, 1H), 1.45 (s, 9H).

**<sup>13</sup>C NMR** (126 MHz, CDCl<sub>3</sub>) δ 156.4, 146.2, 136.4, 121.7, 121.7, 118.4, 115.3, 111.8, 79.5, 69.7, 28.4.

**HRMS** (ESI-TOF) *m/z*: [M+Na]<sup>+</sup> calcd for C<sub>15</sub>H<sub>22</sub>N<sub>2</sub>O<sub>3</sub>Na 301.1523; found 301.1528.



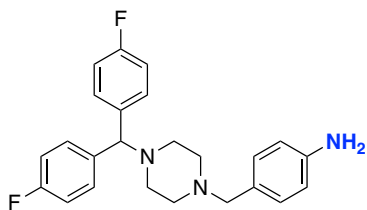
**2-fluoro-5-methylbenzene-1,4-diamine (II-32)**

Pale brown solid. Yield 31.5 mg (90%), eluent 3:2 hexanes : EtOAc.

**<sup>1</sup>H NMR** (500 MHz, CDCl<sub>3</sub>) δ 6.54 (d, *J* = 9.6 Hz, 1H), 6.41 (d, *J* = 12.0 Hz, 1H), 3.30 (s, 4H), 2.08 (s, 3H).

**<sup>13</sup>C NMR** (126 MHz, CDCl<sub>3</sub>) δ 151.9, 150.0, 137.0, 137.0, 125.6, 125.5, 119.8, 119.8, 118.7, 118.7, 103.2, 103.0, 16.8.

**HRMS** (ESI-TOF) *m/z*: [M+H]<sup>+</sup> calcd for C<sub>10</sub>H<sub>10</sub>FN 141.0828; found 141.0823.



**4-((4-(bis(4-fluorophenyl)methyl)piperazin-1-yl)methyl)aniline (II-34)**

Pale yellow solid. Yield 89.5 mg (91%), eluent 1:9 MeOH : EtOAc.

**<sup>1</sup>H NMR** (500 MHz, CDCl<sub>3</sub>) δ 7.34 (ddd, *J* = 8.8, 5.6, 2.9 Hz, 4H), 7.08 (dd, *J* = 8.3, 3.1 Hz, 2H), 6.97 (td, *J* = 8.7, 3.1 Hz, 4H), 6.63 (dd, *J* = 8.3, 3.2 Hz, 2H), 4.22 (s, 1H), 3.64 (s, 2H), 3.44 (d, *J* = 3.2 Hz, 2H), 2.69 – 2.24 (m, 8H).

$^{13}\text{C}$  NMR (126 MHz,  $\text{CDCl}_3$ )  $\delta$  162.7, 160.8, 145.5, 138.3, 130.6, 129.3, 129.2, 127.4, 115.4, 115.3, 114.9, 62.5, 53.0, 51.6.

HRMS (ESI-TOF)  $m/z$ :  $[\text{M}+\text{H}]^+$  calcd for  $\text{C}_{24}\text{H}_{26}\text{F}_2\text{N}_3$  394.2095; found 394.2093.

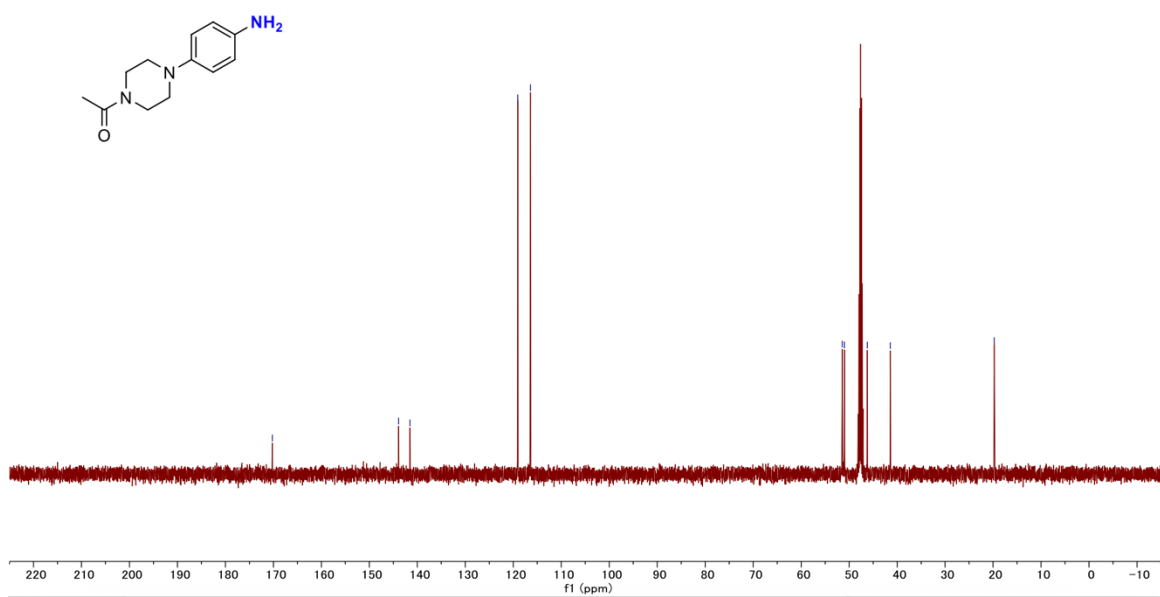
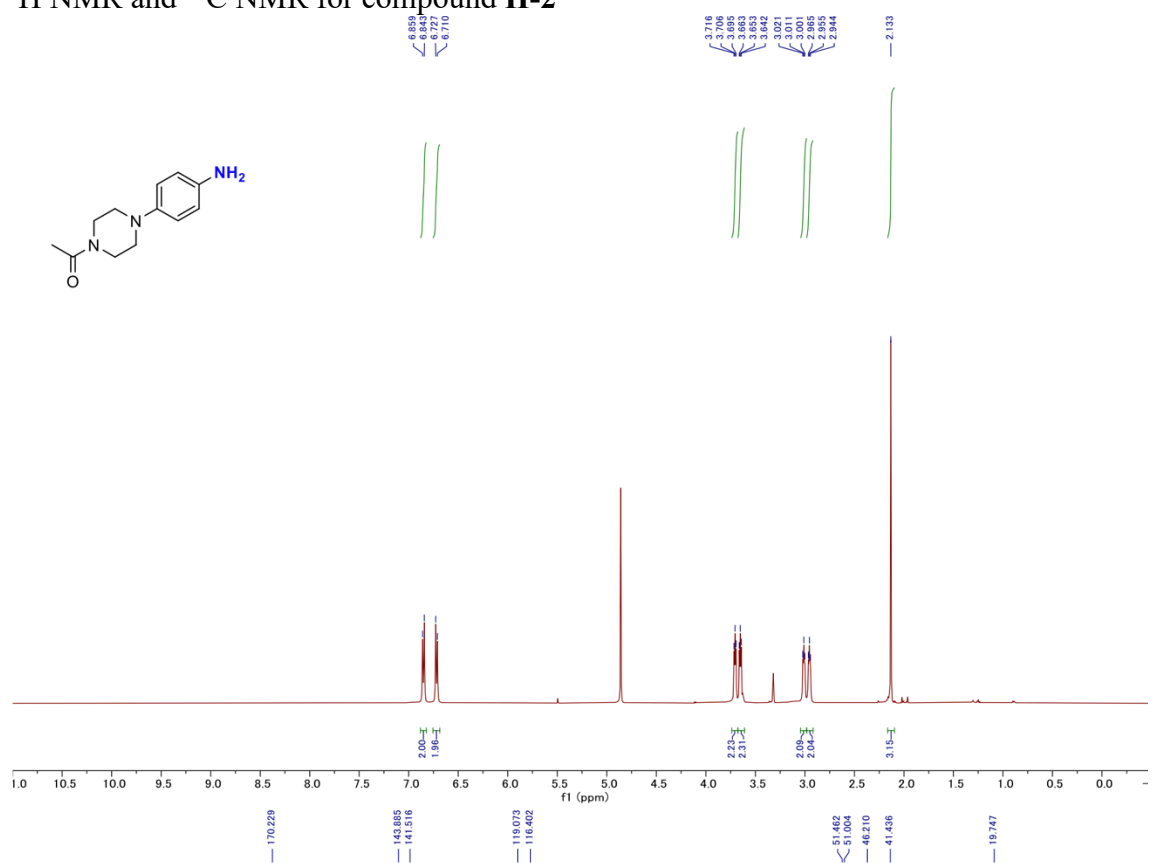
### 2.5.7. References

1. Mahajan, P. S.; Humne, V. T.; Tanpure, S. D.; Mhaske, S. B. Radical Beckmann Rearrangement and Its Application in the Formal Total Synthesis of Antimalarial Natural Product Isocryptolepine via C–H Activation. *Org. Lett.* **2016**, *18*, 3450–3453.
2. Lu, X.; Zhang, Z.; Ren, X.; Pan, X.; Wang, D.; Zhuang, X.; Luo, J.; Yu, R.; Ding, K. Hybrid Pyrimidine Alkynyls Inhibit the Clinically Resistance Related Bcr-AblT315I Mutant. *Bioorg. Med. Chem. Lett.* **2015**, *25*, 3458–3463.
3. Street, L. J.; Baker, R.; Davey, W. B.; Guiblin, A. R.; Jelley, R. A.; Reeve, A. J.; Routledge, H.; Sternfeld, F.; Watt, A. P. Synthesis and Serotonergic Activity of N,N-Dimethyl-2-[5-(1,2,4-Triazol-1-ylmethyl)-1H-Indol-3-yl]Ethylamine and Analogs: Potent Agonists for 5-HT<sub>1D</sub> Receptors. *J. Med. Chem.* **1995**, *38*, 1799–1810.
4. Dimitriou, E.; Jones, R. H.; Pritchard, R. G.; Miller, G. J.; O'Brien, M. Gas-Liquid Flow Hydrogenation of Nitroarenes: Efficient Access to a Pharmaceutically Relevant Pyrrolbenzo[1,4]Diazepine Scaffold. *Tetrahedron* **2018**, *74*, 6795–6803.
5. Hulme, C.; Foley, C.; Small Molecule Inhibitors of Dyrk/Clk and Uses Thereof. U.S. Patent No. US 2020039989 A1, 2020
6. Lee, N. R.; Bikovtseva, A. A.; Cortes-Clerget, M.; Gallou, F.; Lipshutz, B. H. Carbonyl Iron Powder: A Reagent for Nitro Group Reductions under Aqueous Micellar Catalysis Conditions. *Org. Lett.* **2017**, *19*, 6518–6521.
7. Dalu, F.; Scorciapino, M. A.; Cara, C.; Luridiana, A.; Musinu, A.; Casu, M.; Secci, F.; Cannas, C. A Catalyst-Free, Waste-Less Ethanol-Based Solvothermal Synthesis of Amides. *Green Chem.* **2018**, *20*, 375–381.
8. Cheng, H.-G.; Pu, M.; Kundu, G.; Schoenebeck, F. Selective Methylation of Amides, N - Heterocycles, Thiols, and Alcohols with Tetramethylammonium Fluoride. *Org. Lett.* **2020**, *22*, 331–334.
9. William, A. D.; Lee, A. C.-H.; Blanchard, S.; Poulsen, A.; Teo, E. L.; Nagaraj, H.; Tan, E.; Chen, D.; Williams, M.; Sun, E. T.; Goh, K. C.; Ong, W. C.; Goh, S. K.; Hart, S.; Jayaraman, R.; Pasha, M. K.; Ethirajulu, K.; Wood, J. M.; Dymock, B. W. Discovery of the Macrocycle 11-(2-Pyrrolidin-1-yl-ethoxy)-14,19-dioxo-5,7,26-triazatetracyclo[19.3.1.1(2,6).1(8,12)]heptacos-1(25),2(26),3,5,8,10,12(27),16,21,23-decaene (SB1518), a Potent Janus Kinase 2/Fms-Like Tyrosine Kinase-3 (JAK2/FLT3) Inhibitor for the Treatment of Myelofibrosis and Lymphoma. *J. Med. Chem.* **2011**, *54*, 4638–4658.

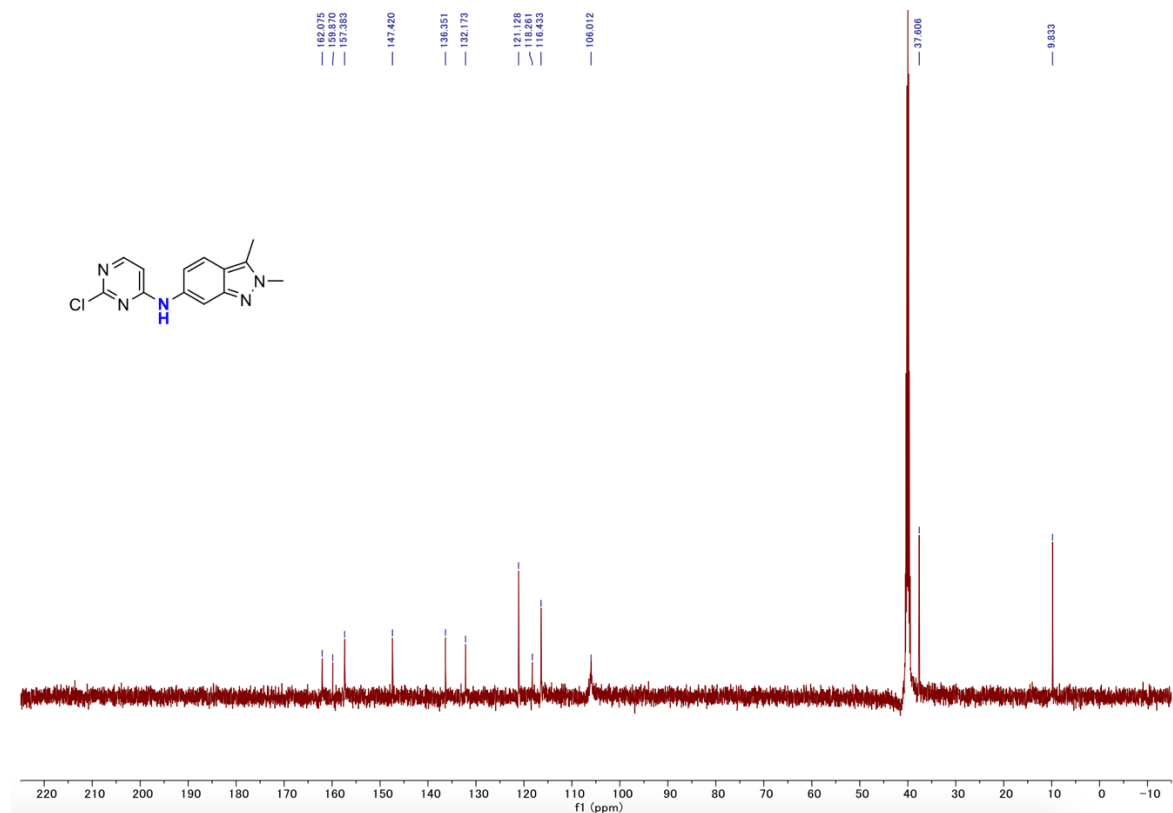
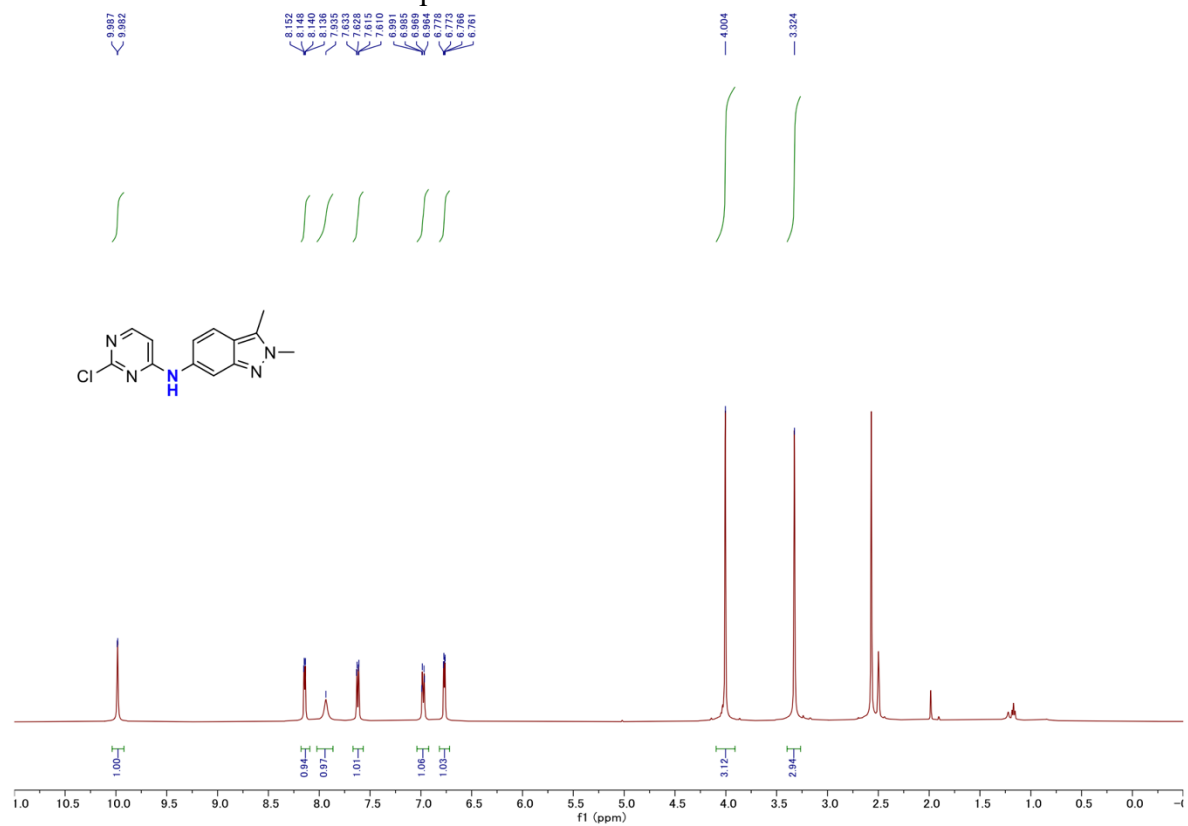
10. Elancheran, R.; Saravanan, K.; Choudhury, B.; Divakar, S.; Kabilan, S.; Ramanathan, M.; Das, B.; Devi, R.; Kotoky, J. Design and Development of Oxobenzimidazoles as Novel Androgen Receptor Antagonists. *Med. Chem. Res.* **2016**, *25*, 539–552.
11. Pawar, G. G.; Brahmanandan, A.; Kapur, M. Palladium(II)-Catalyzed, Heteroatom-Directed, Regioselective C–H Nitration of Anilines Using Pyrimidine as a Removable Directing Group. *Org. Lett.* **2016**, *18*, 448–451.
12. Chakraborty, B.; Paine, T. K. Aromatic Ring Cleavage of 2-Amino-4-Tert-Butylphenol by a Nonheme Iron(II) Complex: Functional Model of 2-Aminophenol Dioxygenases. *Angew. Chem., Int. Ed.* **2013**, *52*, 920–924.
13. Goossen, L. J.; Knauber, T. Concise Synthesis of Telmisartan via Decarboxylative Cross-Coupling. *J. Org. Chem.* **2008**, *73*, 8631–8634.
14. Lee, N. R.; Cortes-Clerget, M.; Wood, A. B.; Lippincott, D. J.; Pang, H.; Moghadam, F. A.; Gallou, F.; Lipshutz, B. H. Coolade. A Low-Foaming Surfactant for Organic Synthesis in Water. *ChemSusChem* **2019**, *12*, 3159–3165.
15. Li, Z.; Zhang, X.; Qin, J.; Tan, Z.; Han, M.; Jin, G. Efficient and Practical Synthesis of 3',4',5'-Trifluoro-[1,1'-Biphenyl]-2-Amine: A Key Intermediate of Fluxapyroxad. *Org. Process Res. Dev.* **2019**, *23*, 1881–1886.
16. Long, Y.; Yu, M.; Ochnik, A. M.; Karanjia, J. D.; Basnet, S. KC.; Kebede, A. A.; Kou, L.; Wang, S. Discovery of Novel 4-Azaaryl-N-Phenylpyrimidin-2-Amine Derivatives as Potent and Selective FLT<sub>3</sub> Inhibitors for Acute Myeloid Leukaemia with FLT3 Mutations. *Eur. J. Med. Chem.* **2021**, *213*, 113215.
17. Zhu, W.; Bao, X.; Ren, H.; Da, Y.; Wu, D.; Li, F.; Yan, Y.; Wang, L.; Chen, Z. N-Phenyl Indole Derivatives as AT1 Antagonists with Anti-Hypertension Activities: Design, Synthesis and Biological Evaluation. *Eur. J. Med. Chem.* **2016**, *115*, 161–178.
18. Przypis, L.; Walczak, K. Z. Copper(II)-Catalyzed Iodinations of Carbazoles: Access to Functionalized Carbazoles. *J. Org. Chem.* **2019**, *84*, 2287–2296.

## 2.5.8. NMR spectra

$^1\text{H}$  NMR and  $^{13}\text{C}$  NMR for compound **II-2**

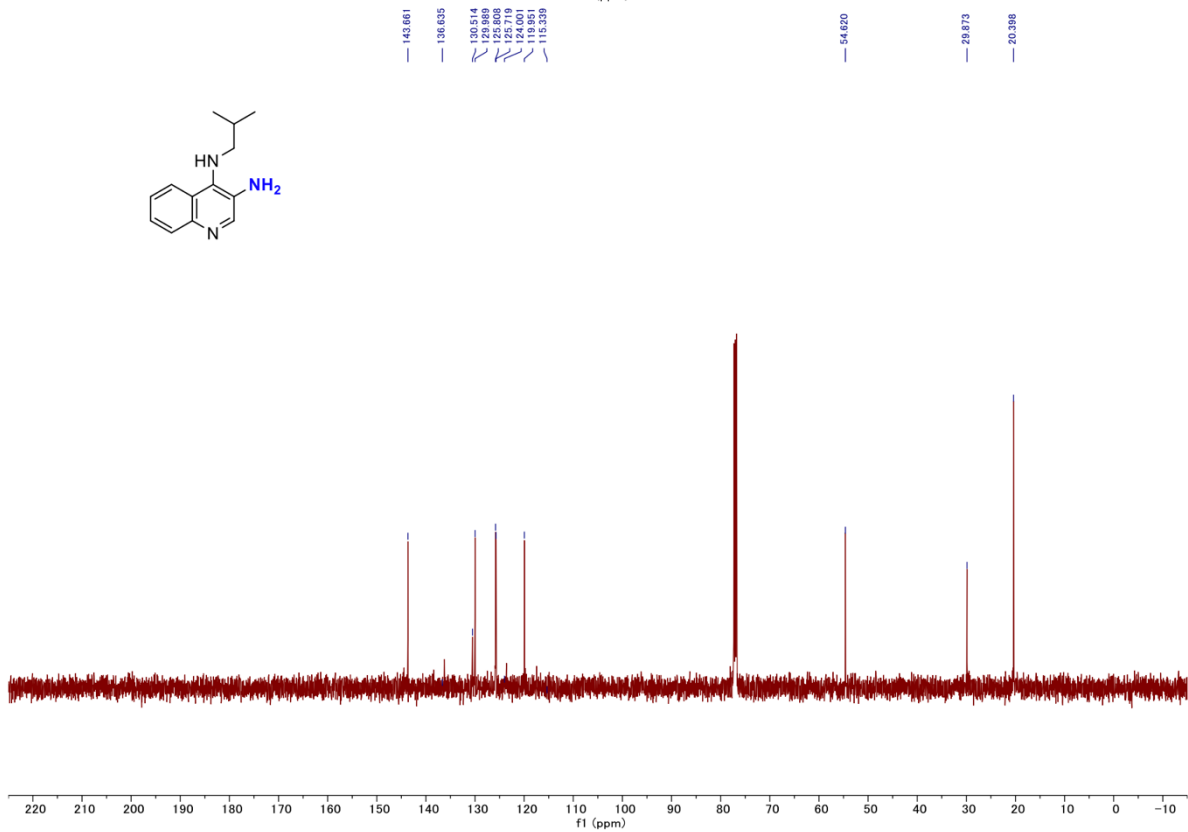
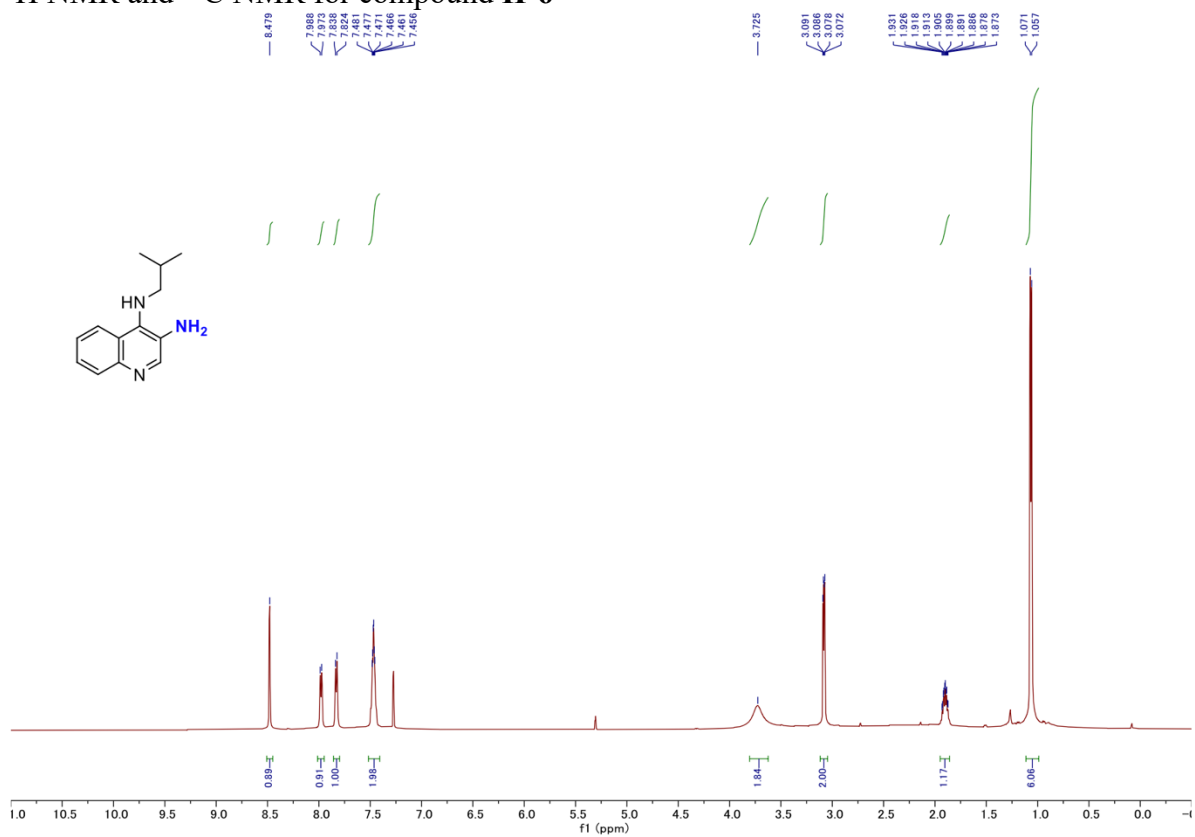


# $^1\text{H}$ NMR and $^{13}\text{C}$ NMR for compound II-4

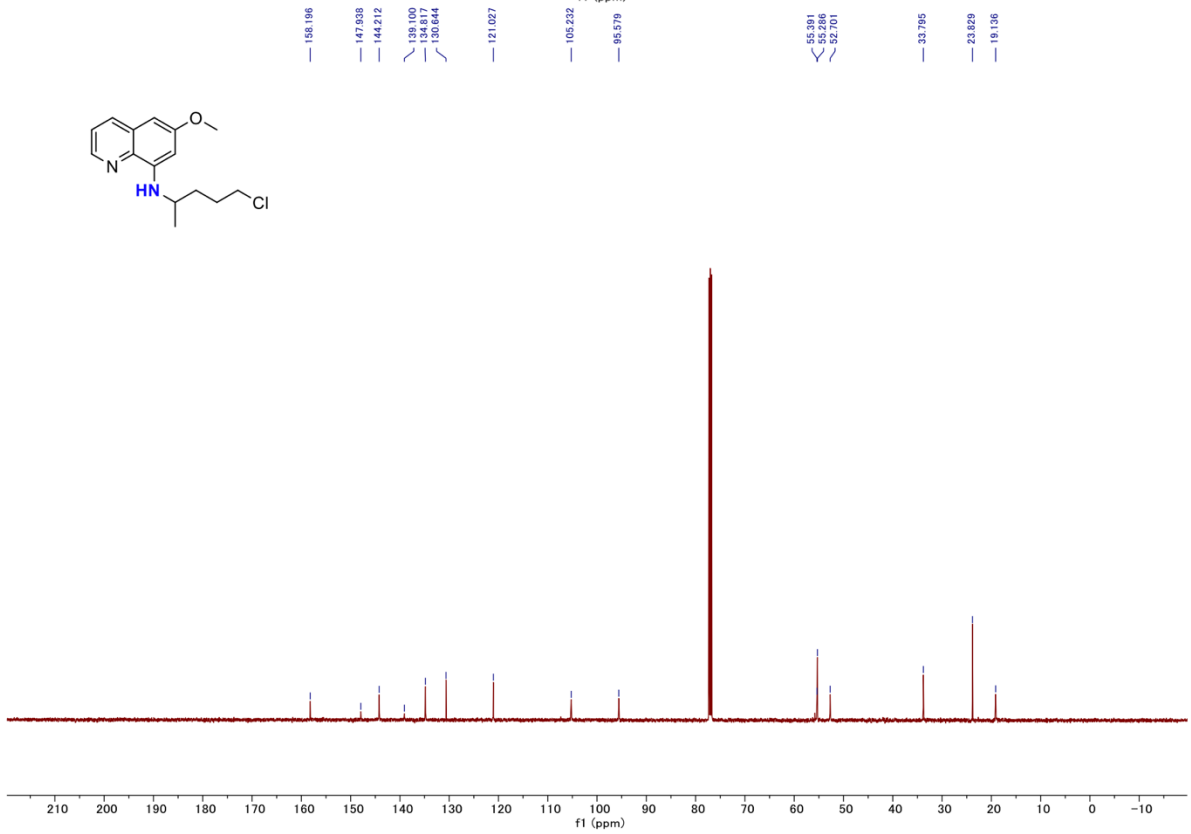
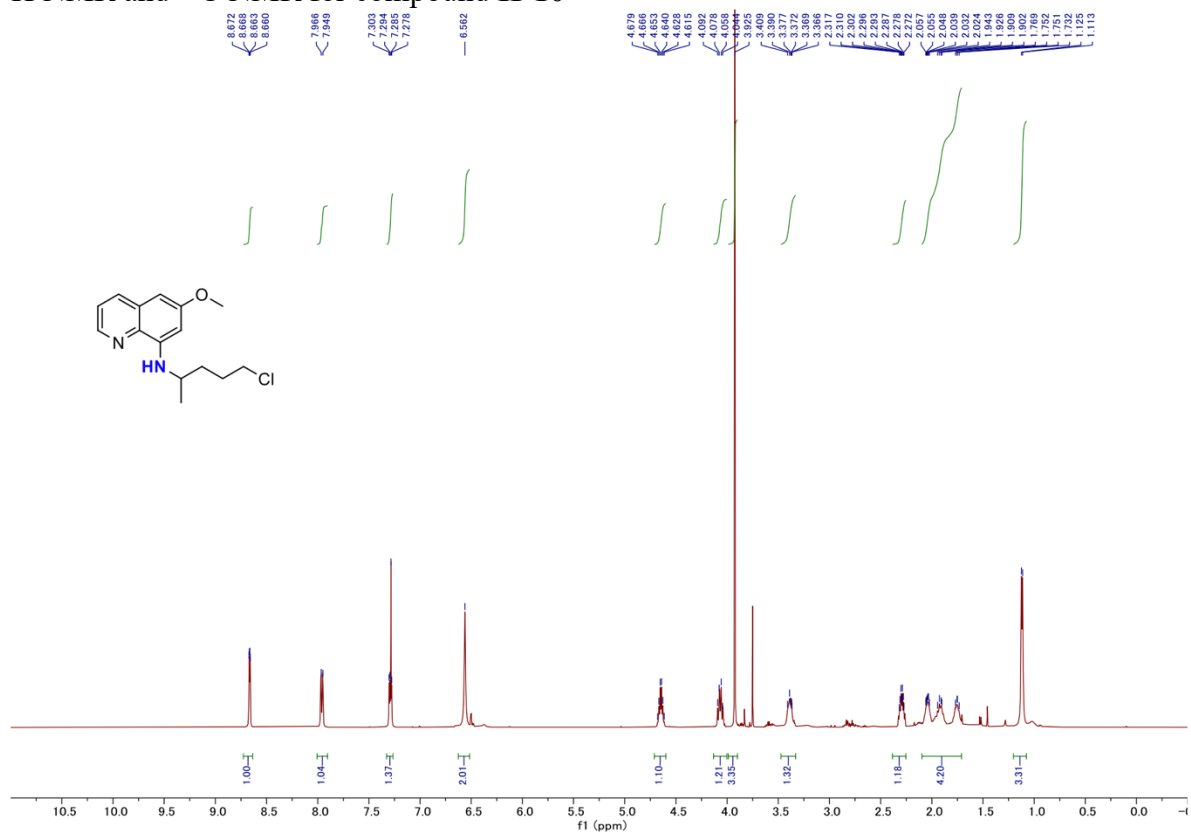




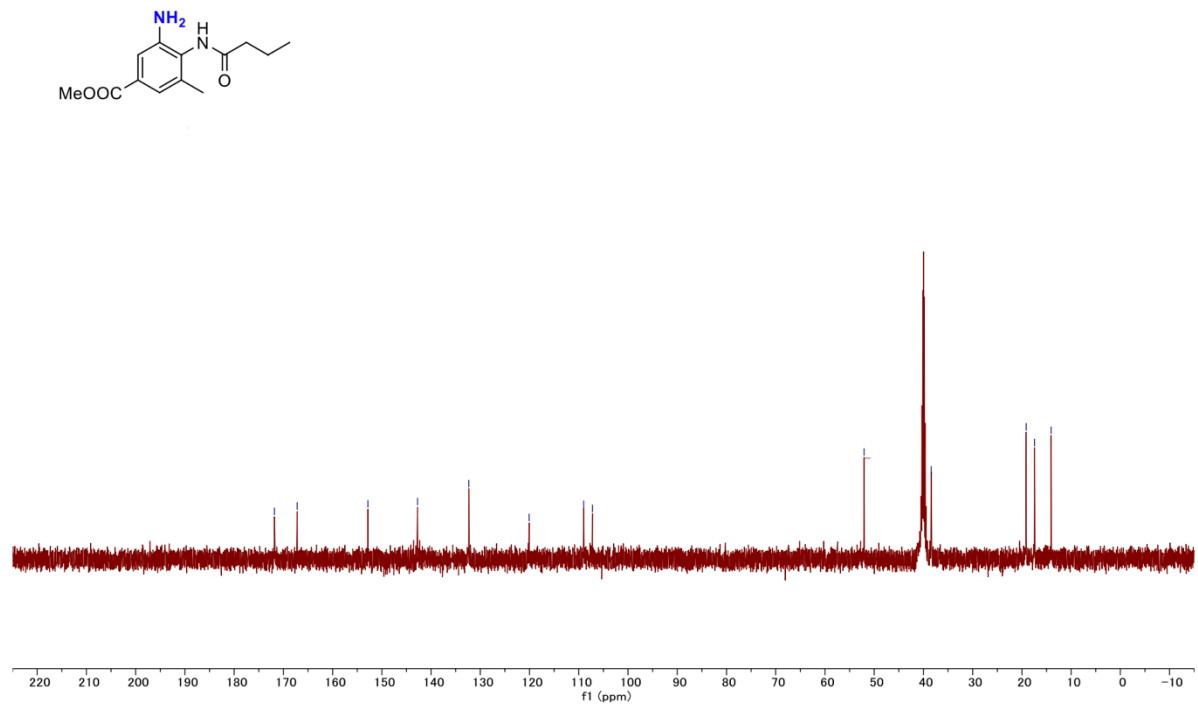
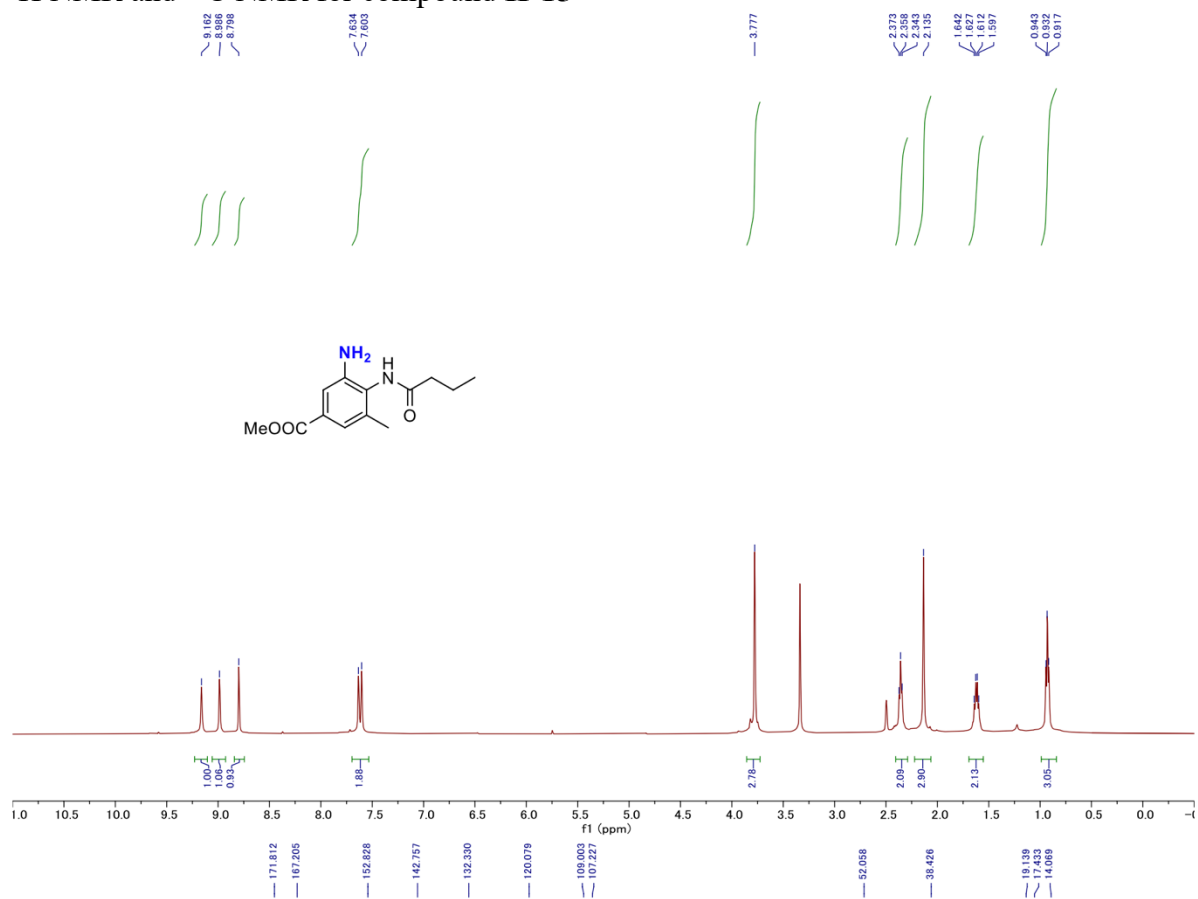
# $^1\text{H}$ NMR and $^{13}\text{C}$ NMR for compound II-6



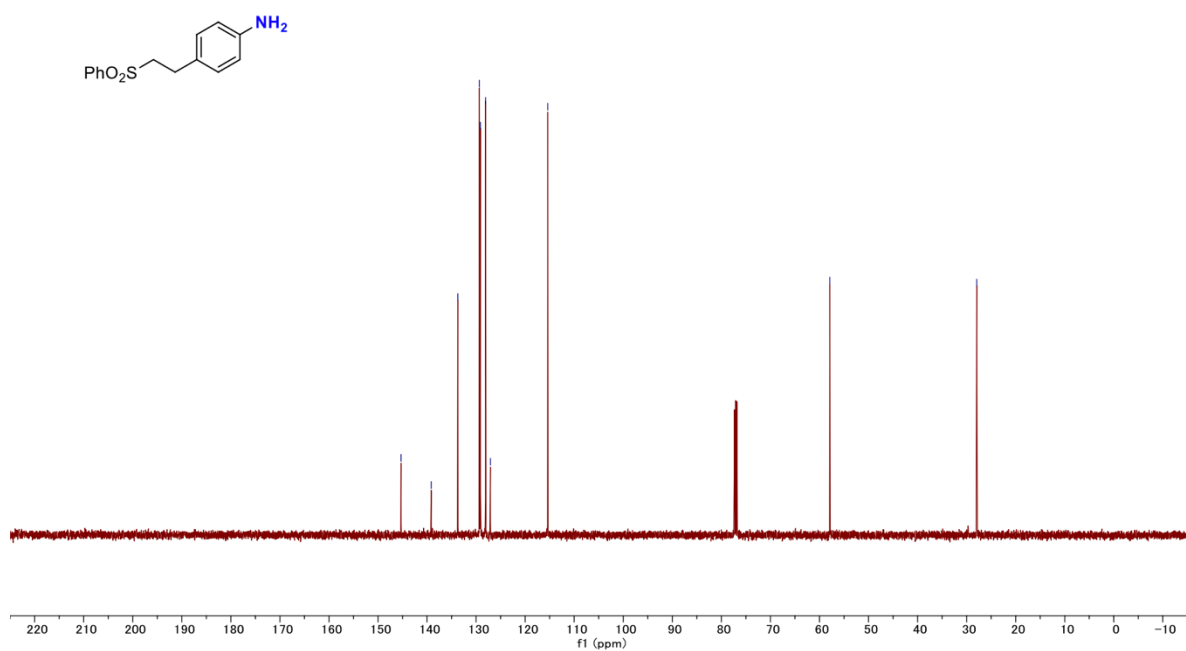
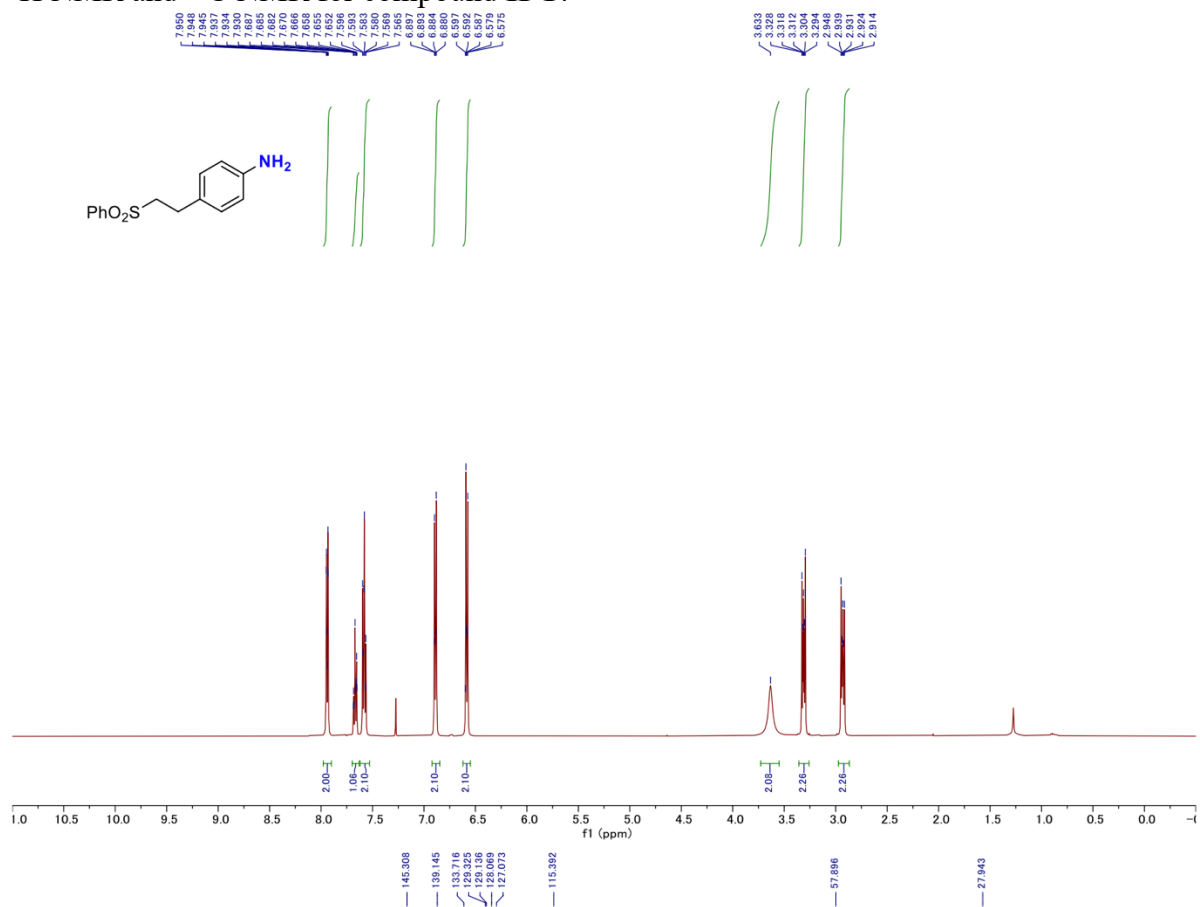
<sup>1</sup>H NMR and <sup>13</sup>C NMR for compound II-10



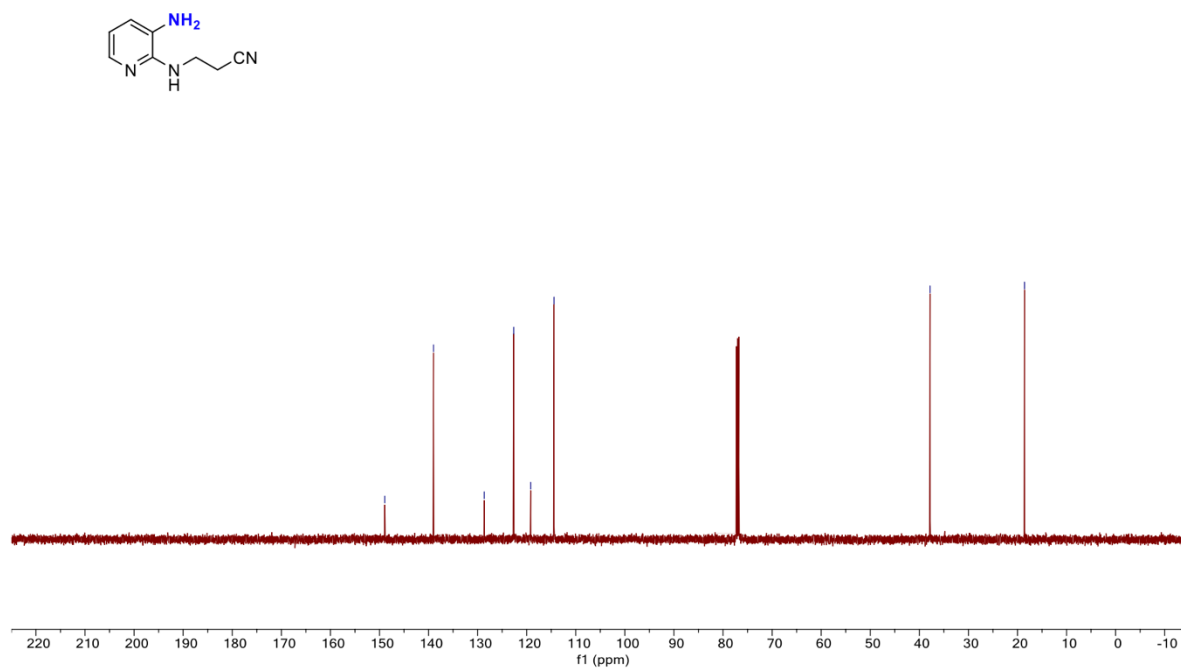
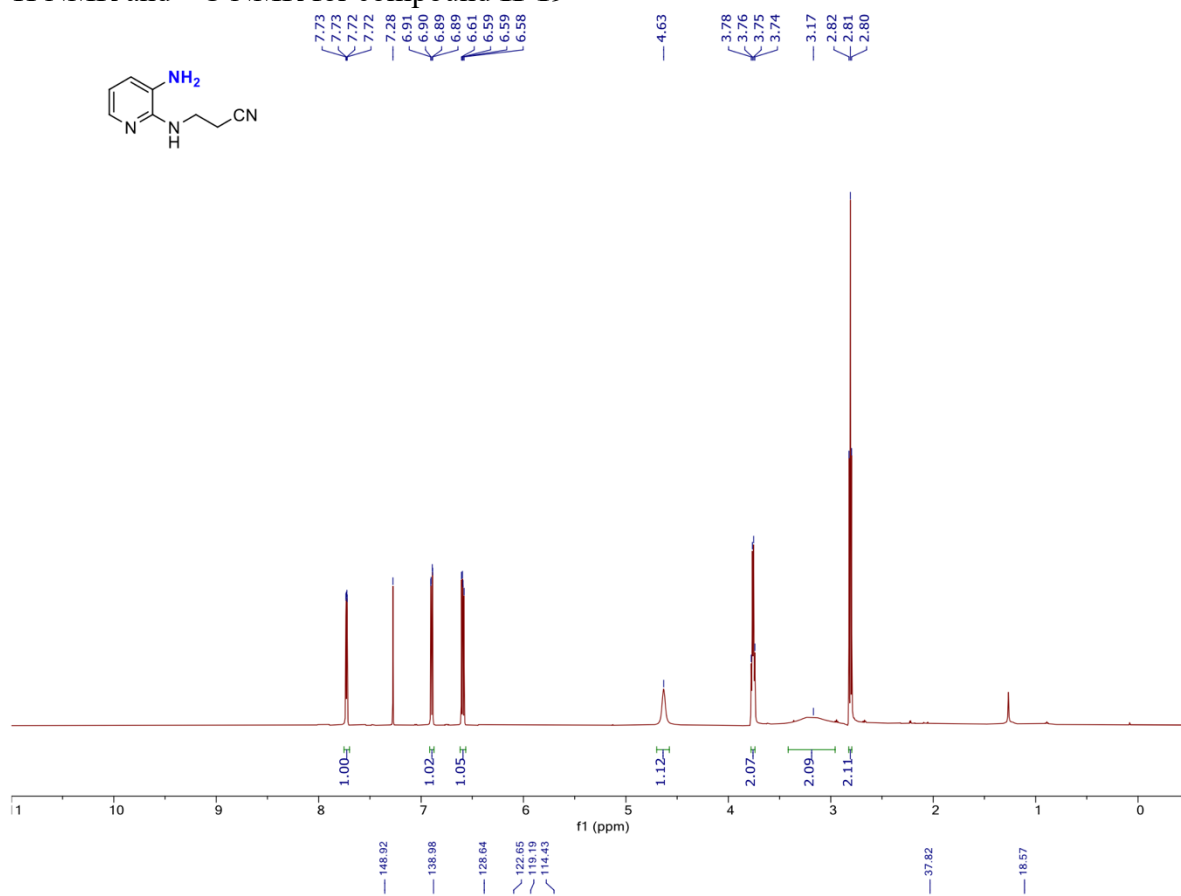
# $^1\text{H}$ NMR and $^{13}\text{C}$ NMR for compound II-15



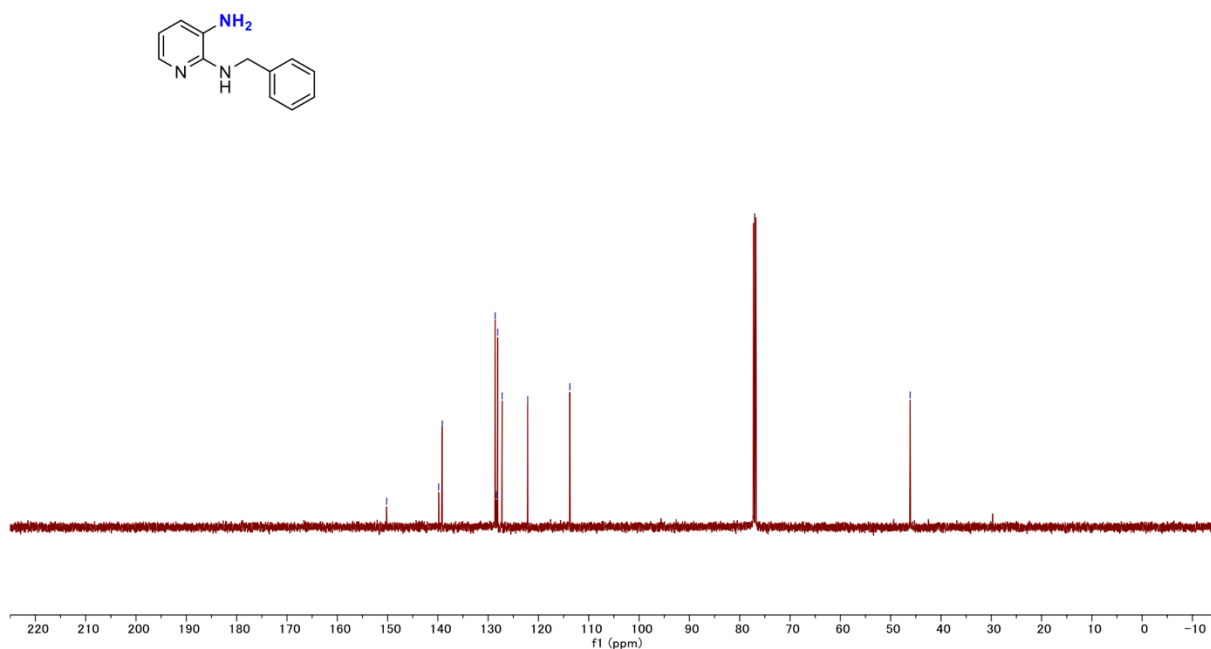
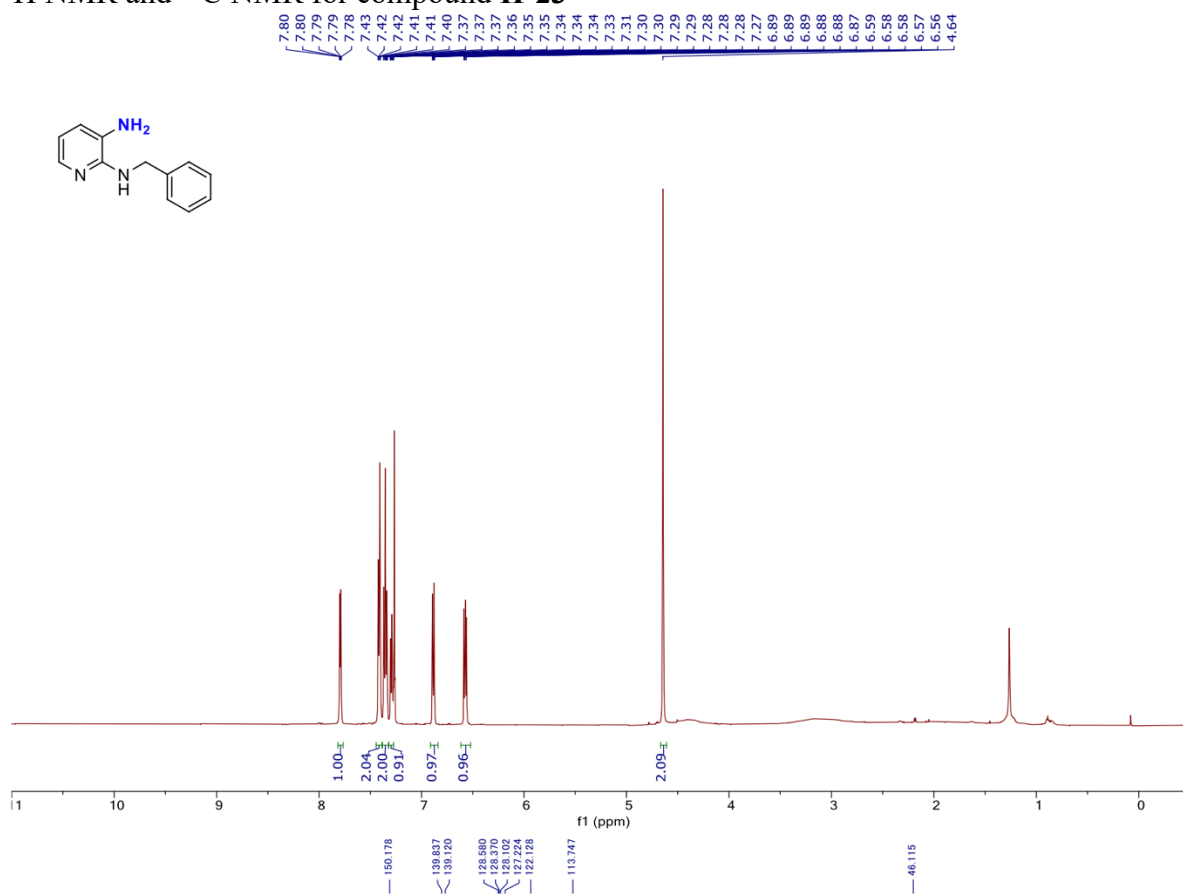
<sup>1</sup>H NMR and <sup>13</sup>C NMR for compound II-17



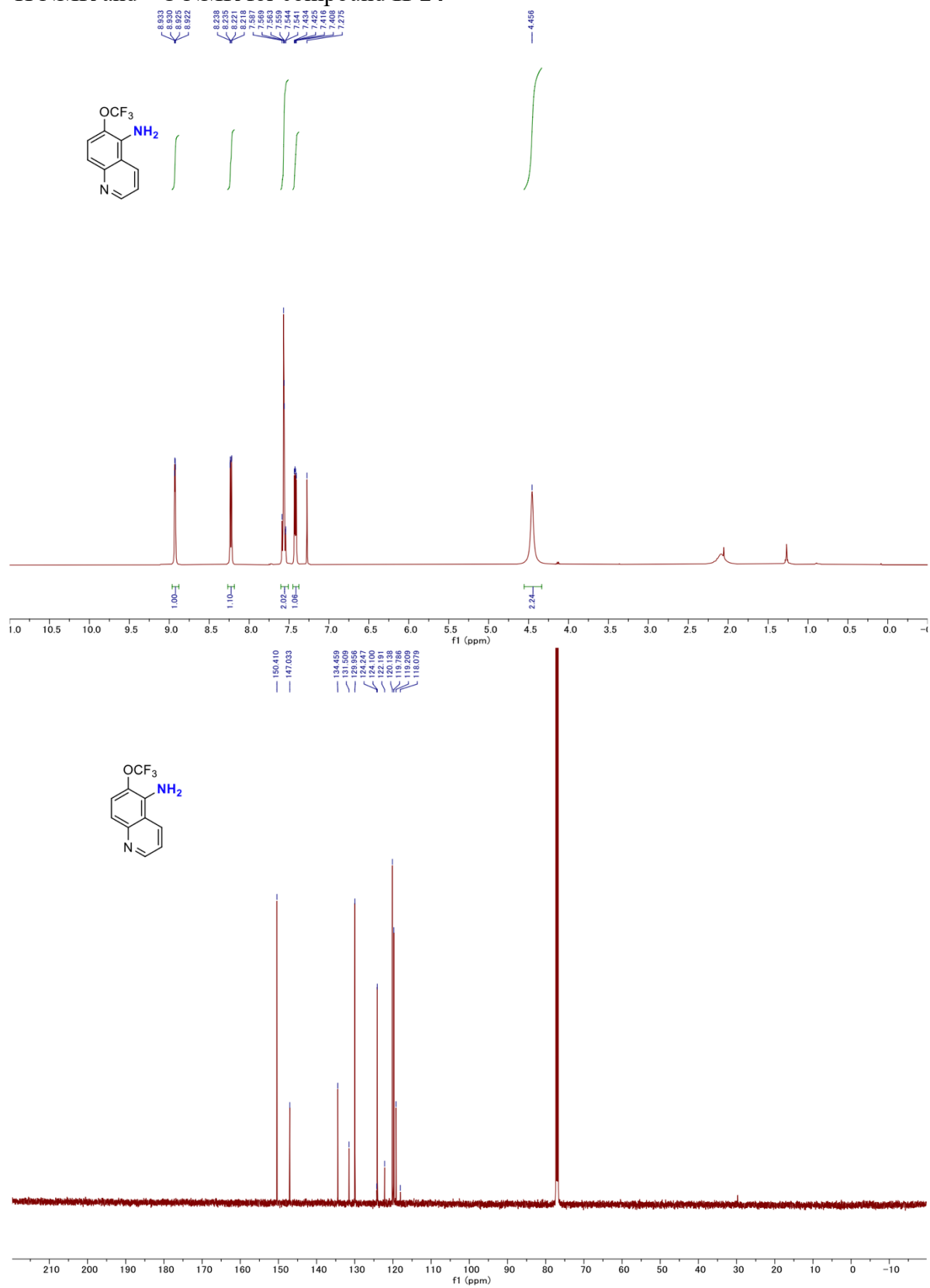
$^1\text{H}$  NMR and  $^{13}\text{C}$  NMR for compound **II-19**



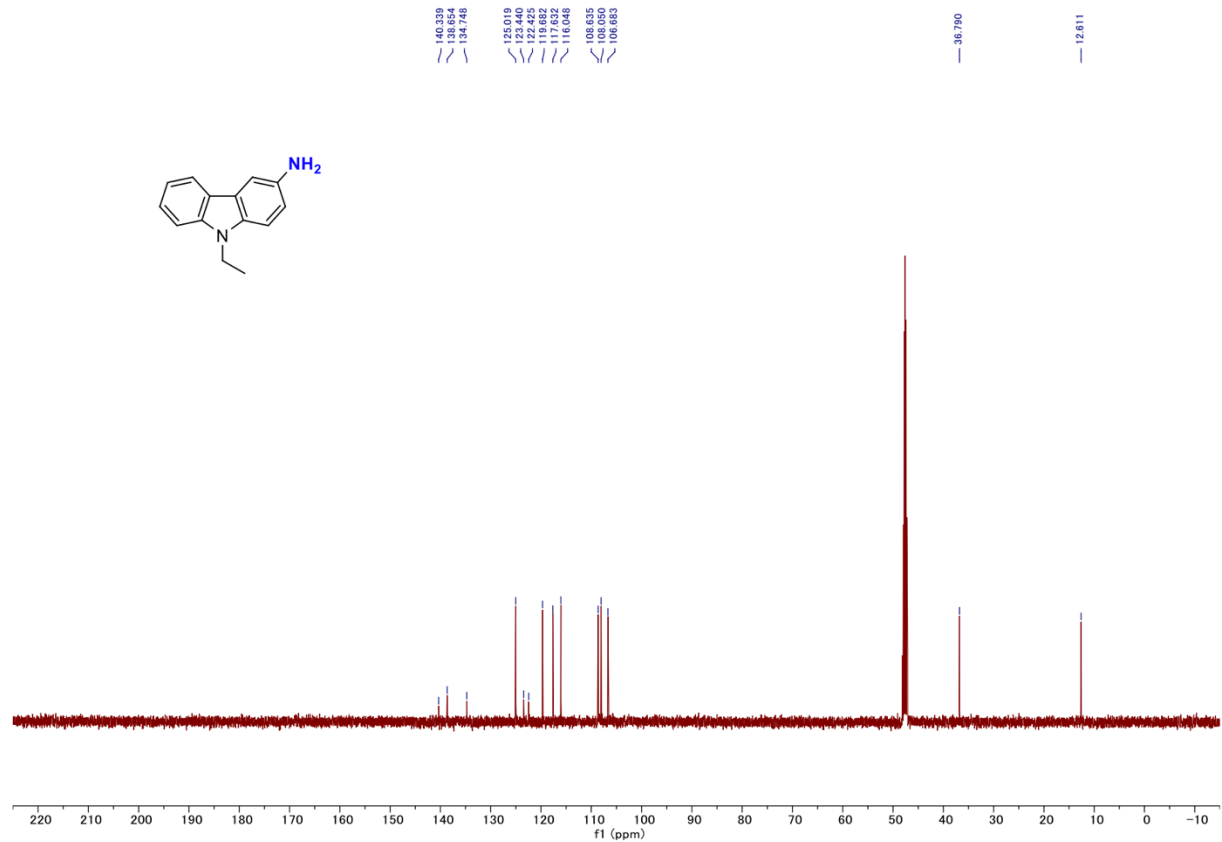
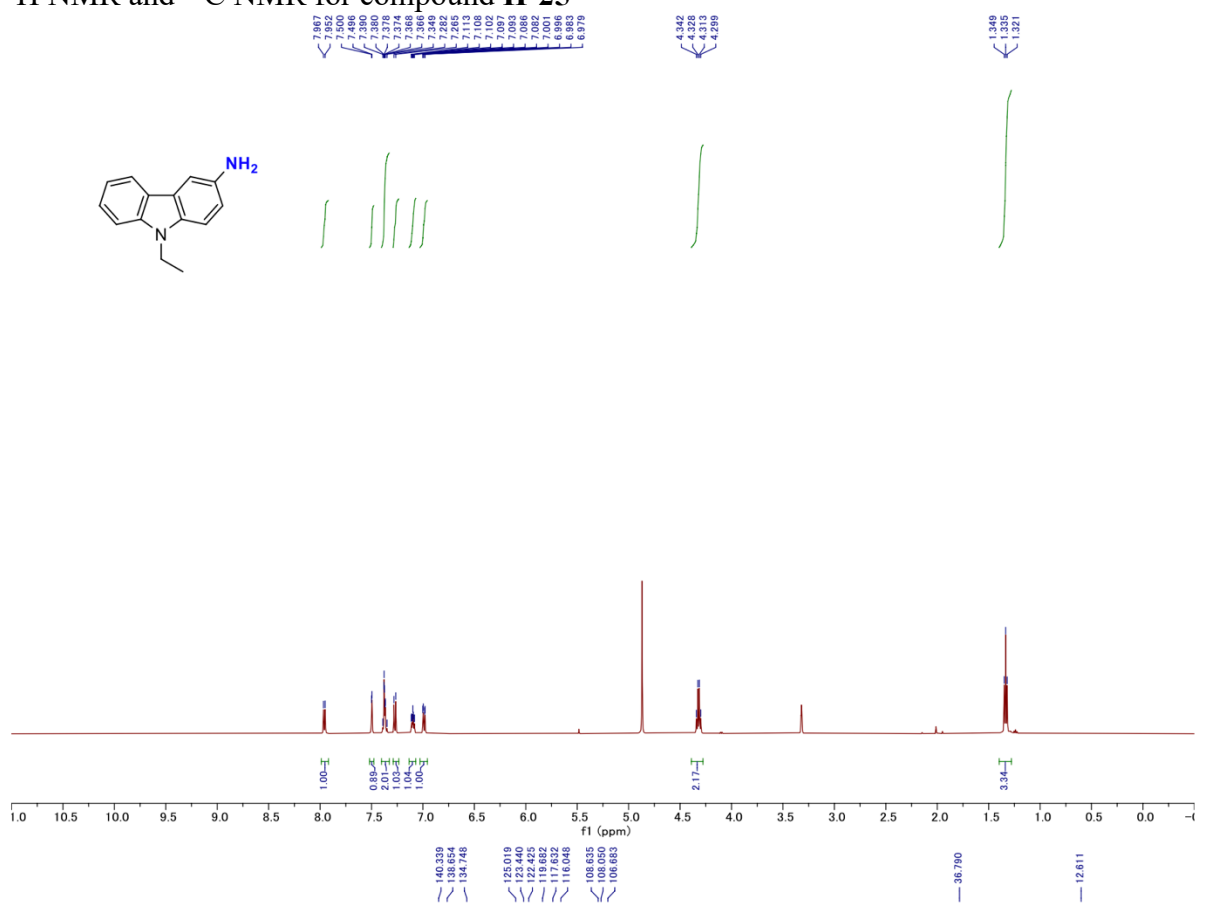
# $^1\text{H}$ NMR and $^{13}\text{C}$ NMR for compound II-23



# $^1\text{H}$ NMR and $^{13}\text{C}$ NMR for compound II-24

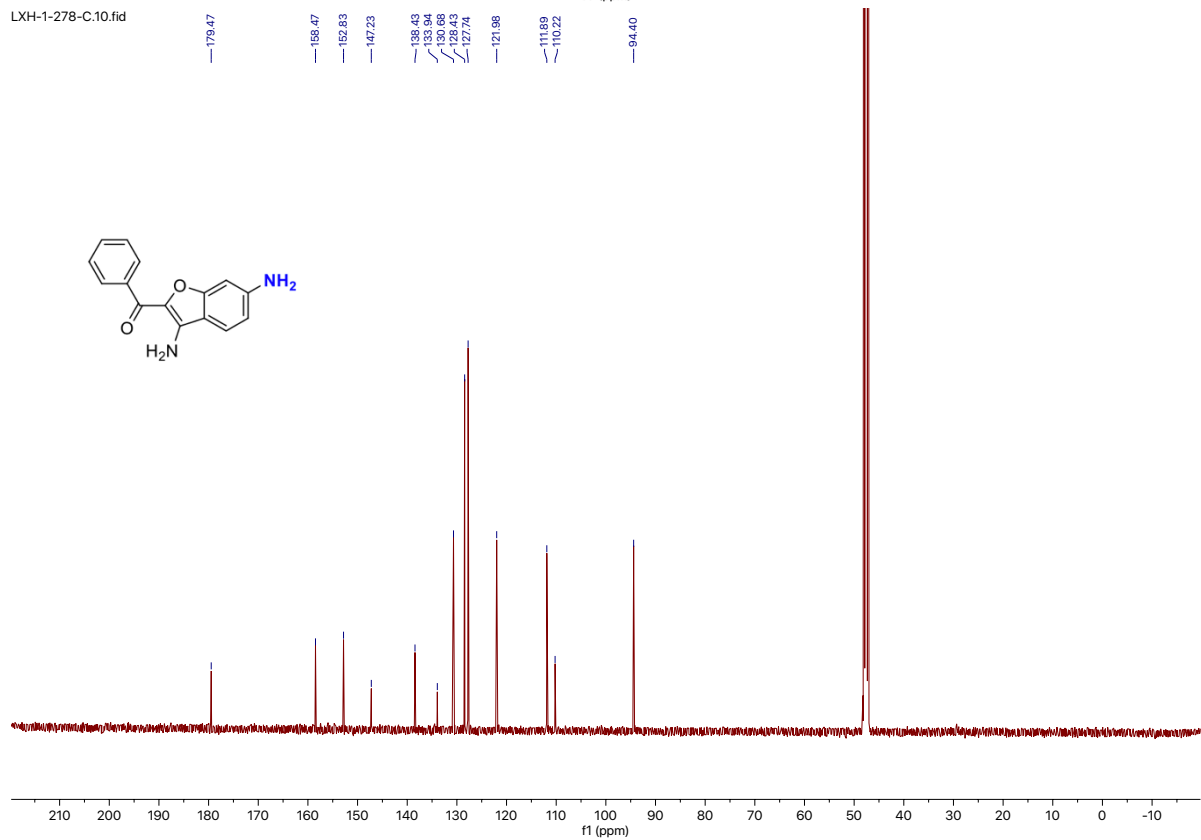
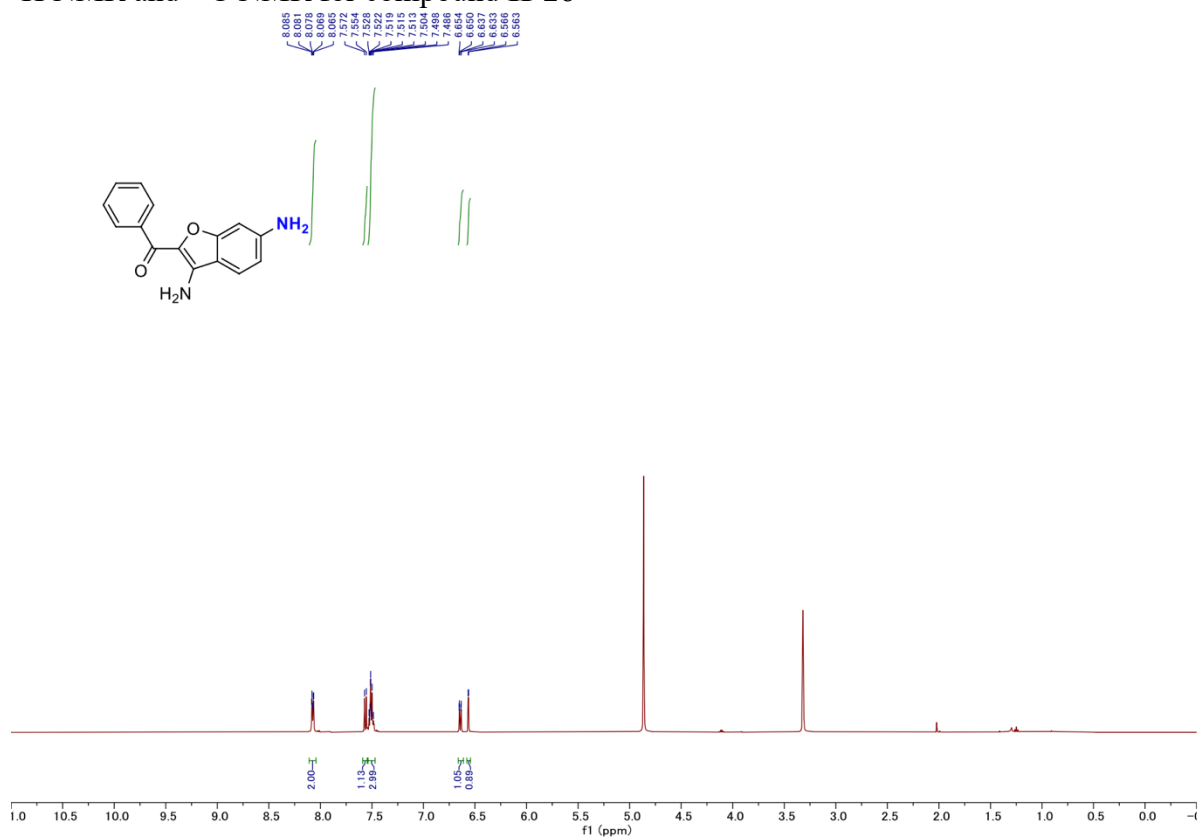


$^1\text{H}$  NMR and  $^{13}\text{C}$  NMR for compound **II-25**



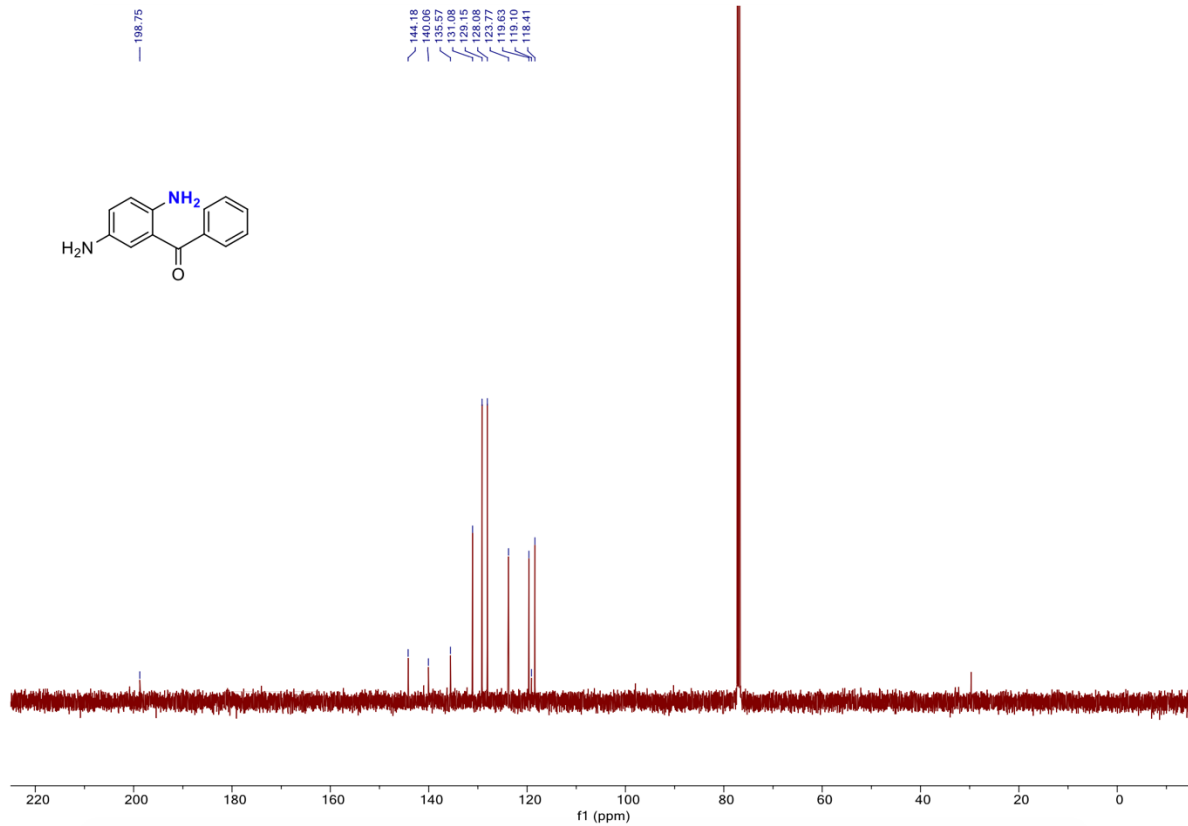
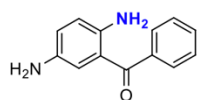
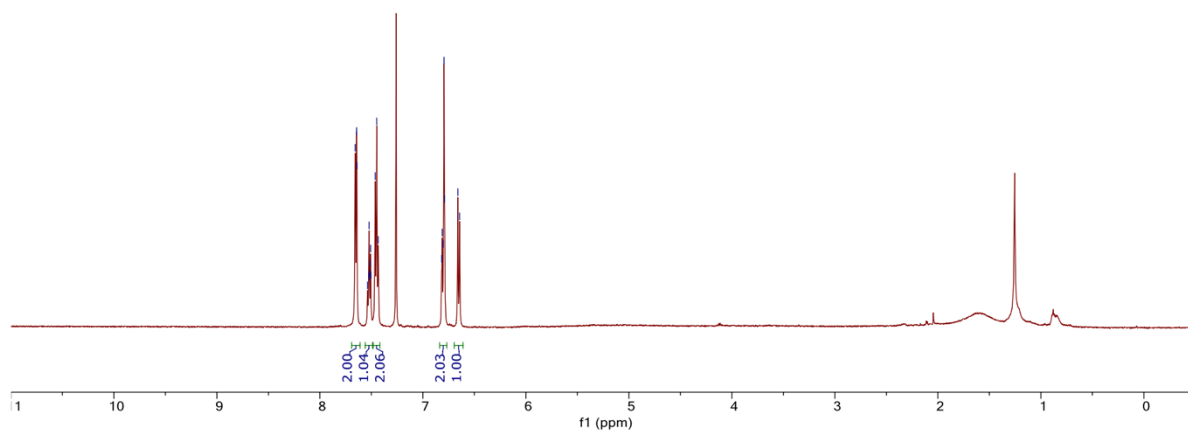
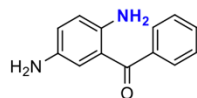


# $^1\text{H}$ NMR and $^{13}\text{C}$ NMR for compound II-26

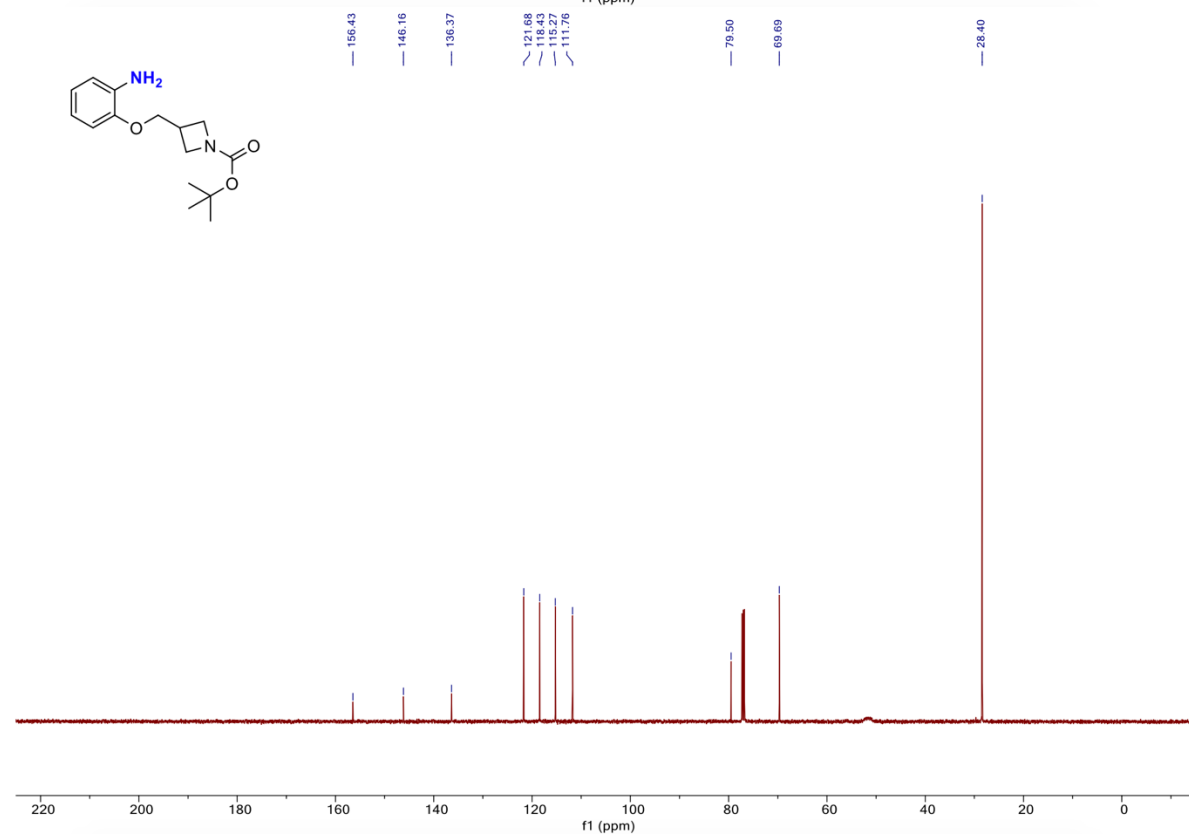
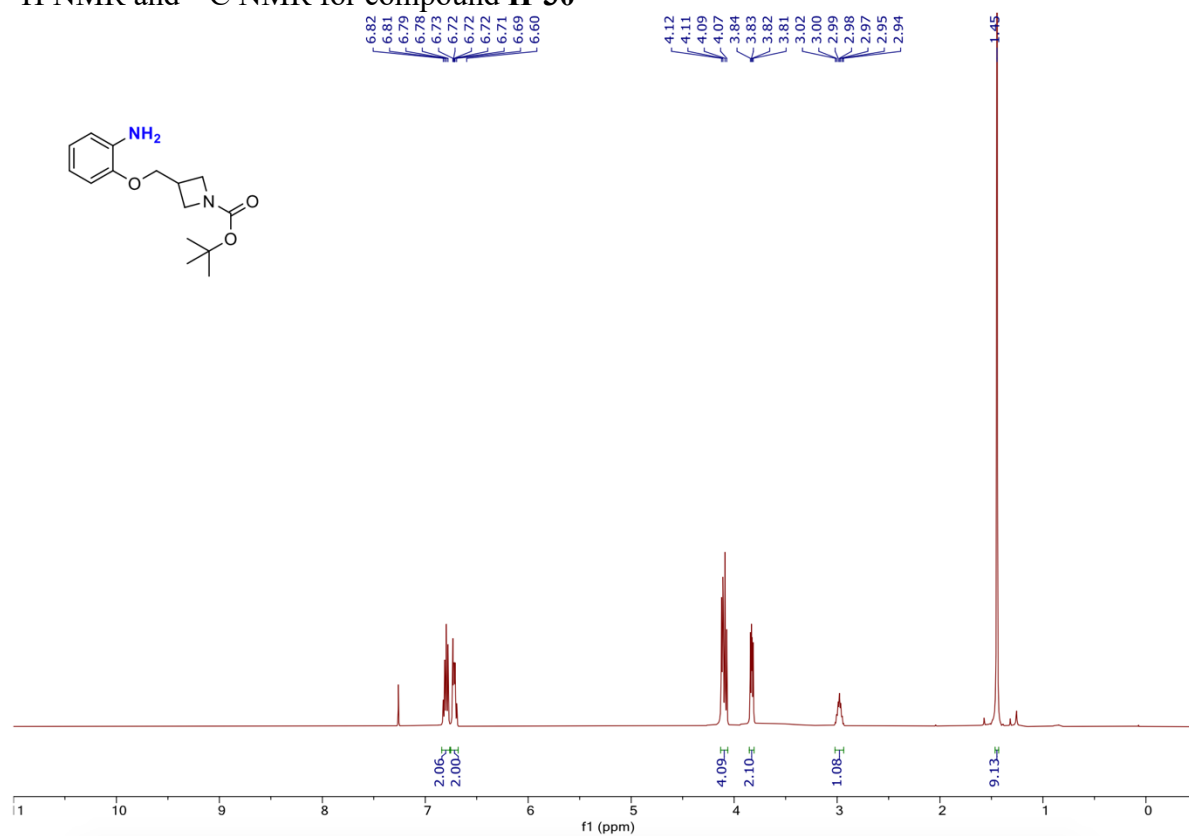


$^1\text{H}$  NMR and  $^{13}\text{C}$  NMR for compound **II-27**

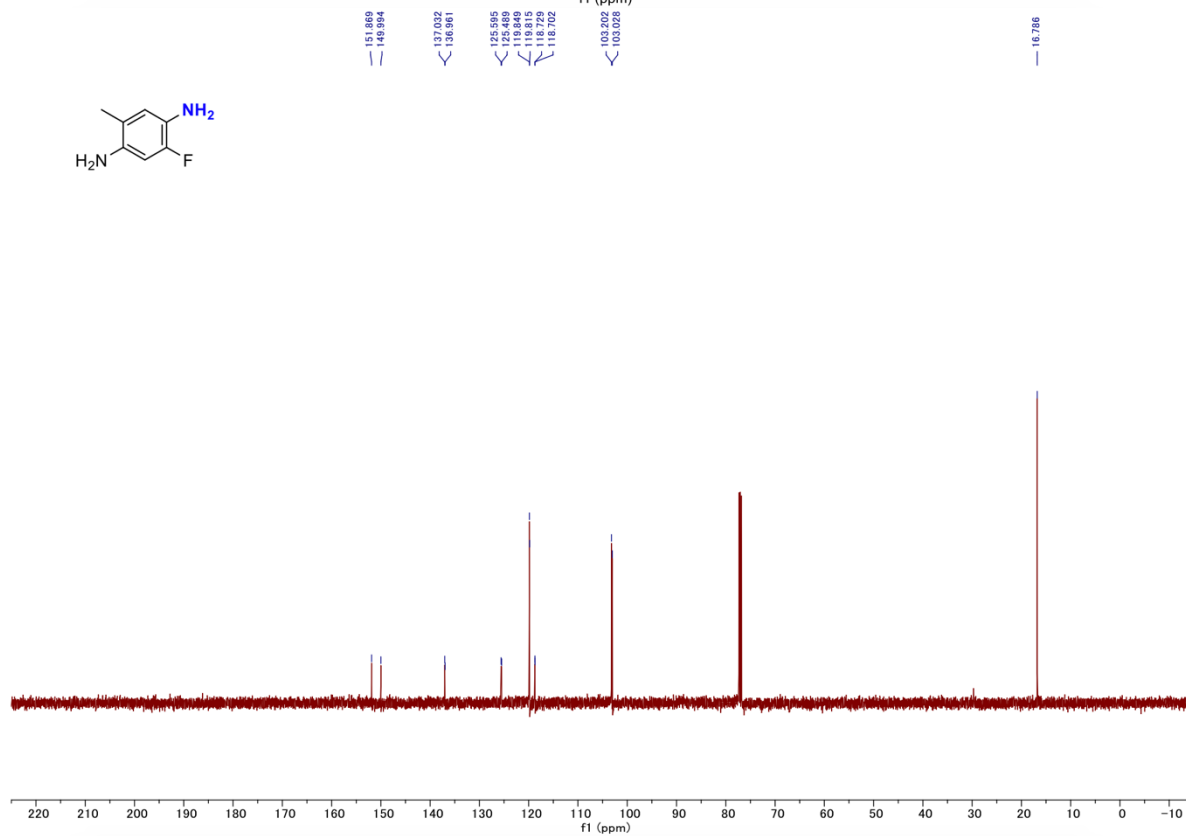
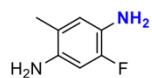
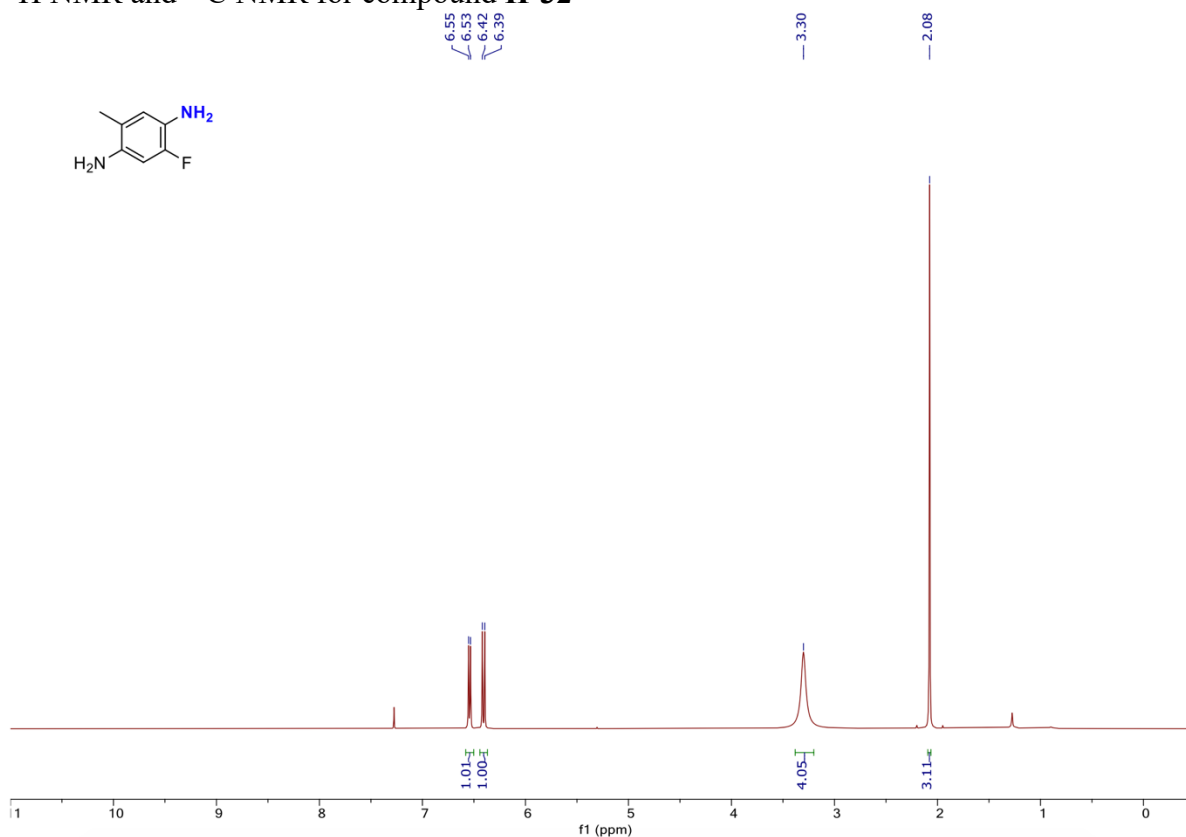
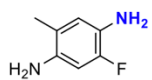
7.66  
7.64  
7.64  
7.54  
7.53  
7.53  
7.52  
7.52  
7.51  
7.51  
7.50  
7.46  
7.45  
7.43  
6.82  
6.81  
6.80  
6.79  
6.79  
6.66  
6.64



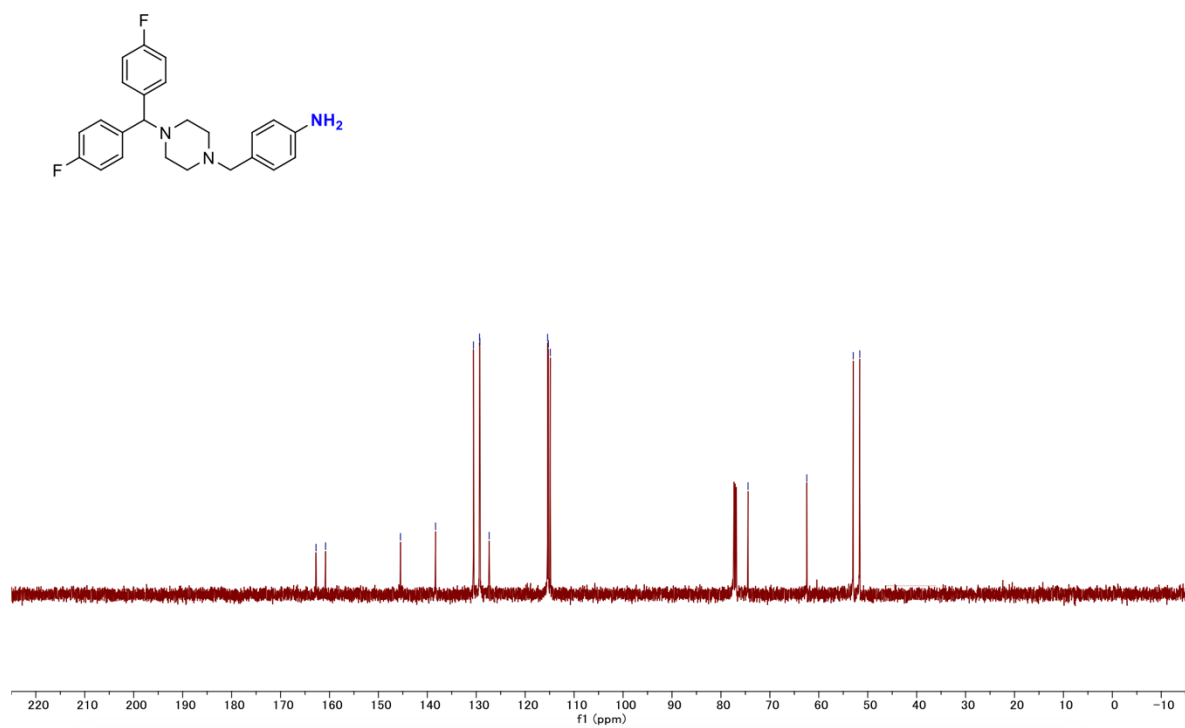
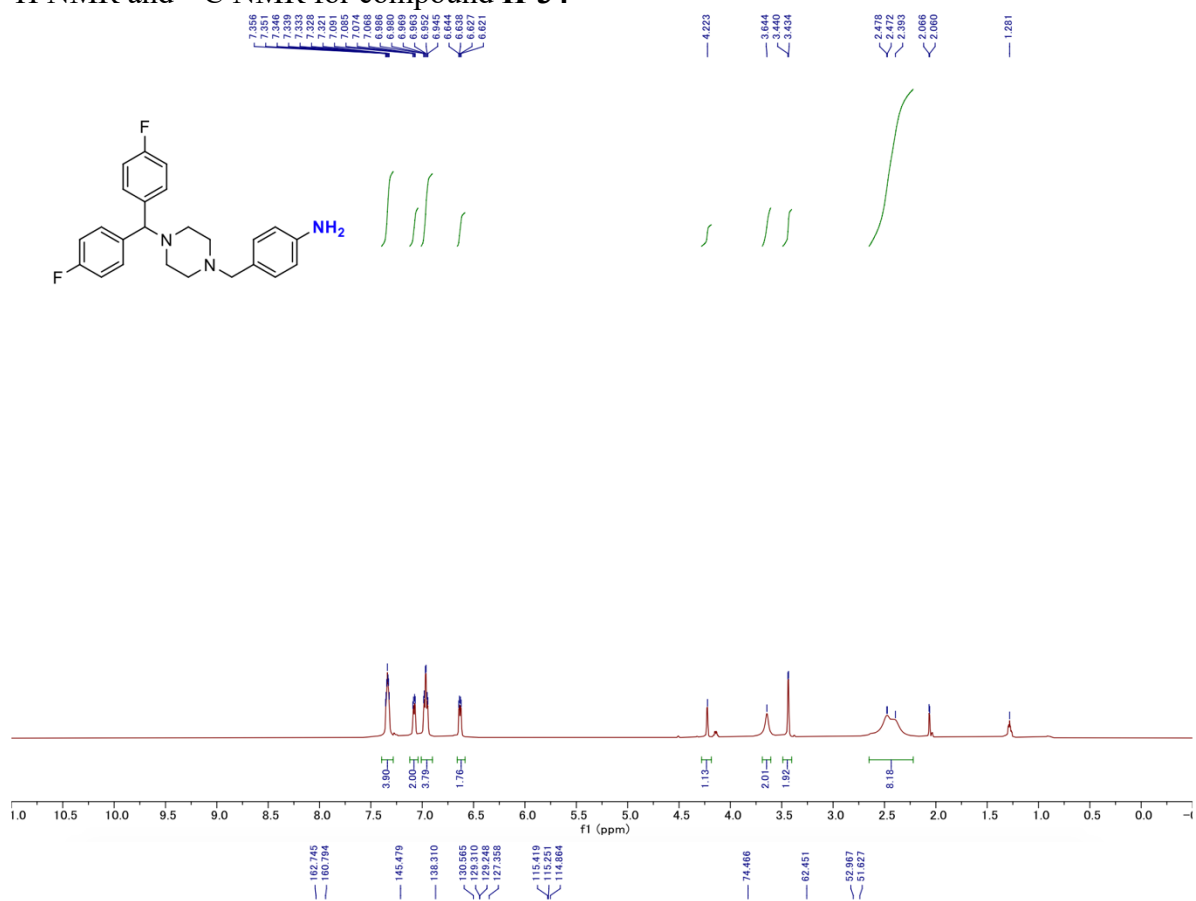
$^1\text{H}$  NMR and  $^{13}\text{C}$  NMR for compound **II-30**



# $^1\text{H}$ NMR and $^{13}\text{C}$ NMR for compound **II-32**



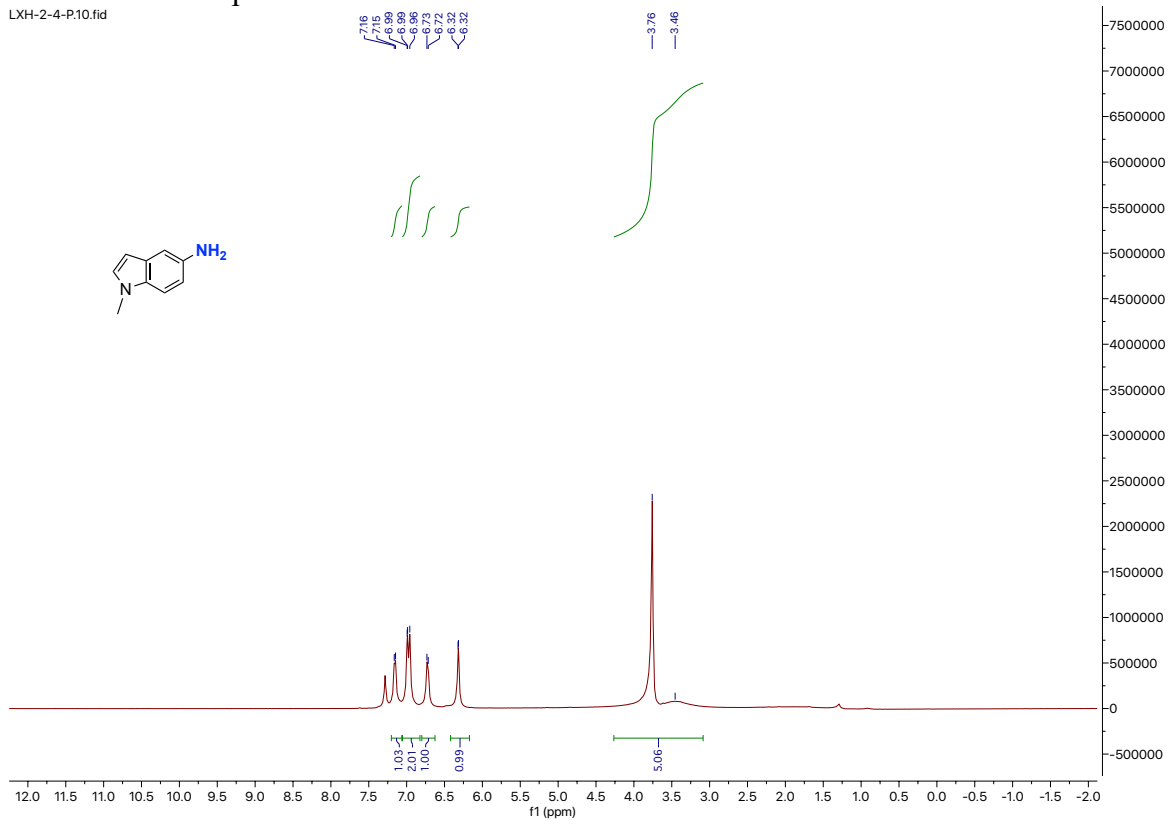
$^1\text{H}$  NMR and  $^{13}\text{C}$  NMR for compound II-34





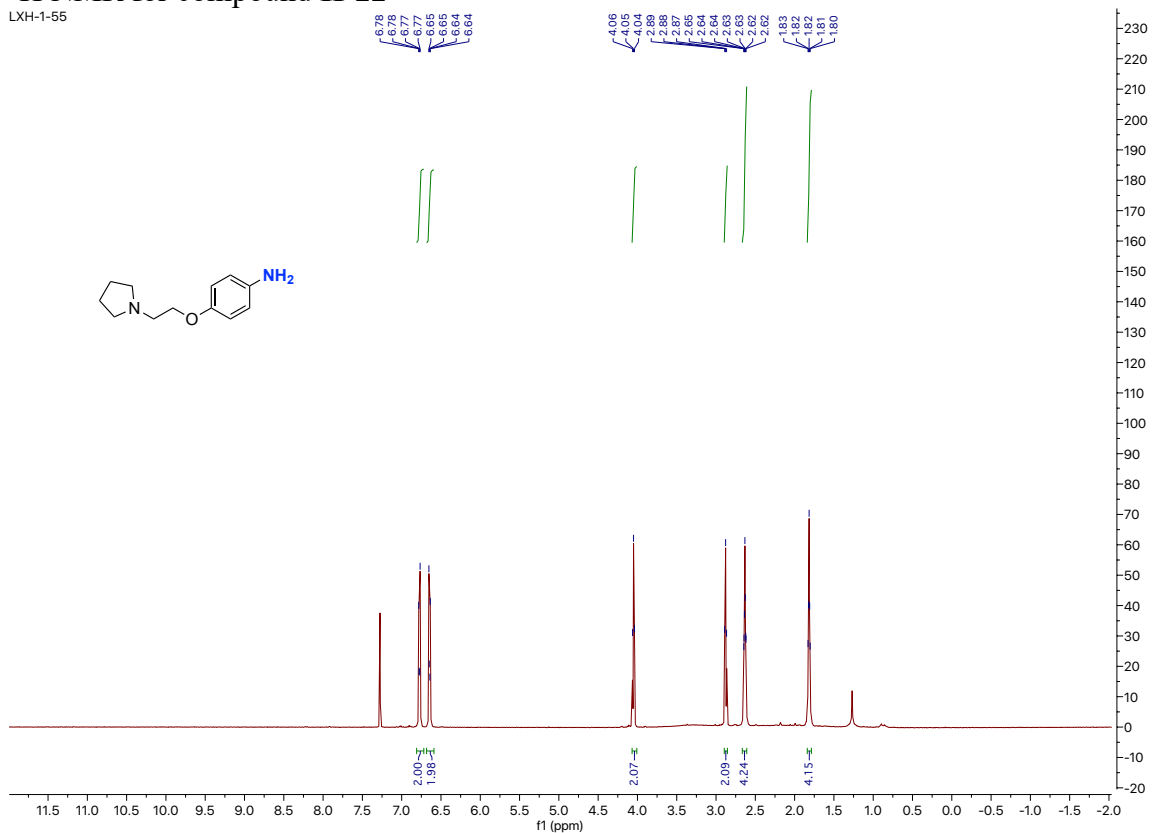
# <sup>1</sup>H NMR for compound II-21

LXH-2-4-P.10.fid



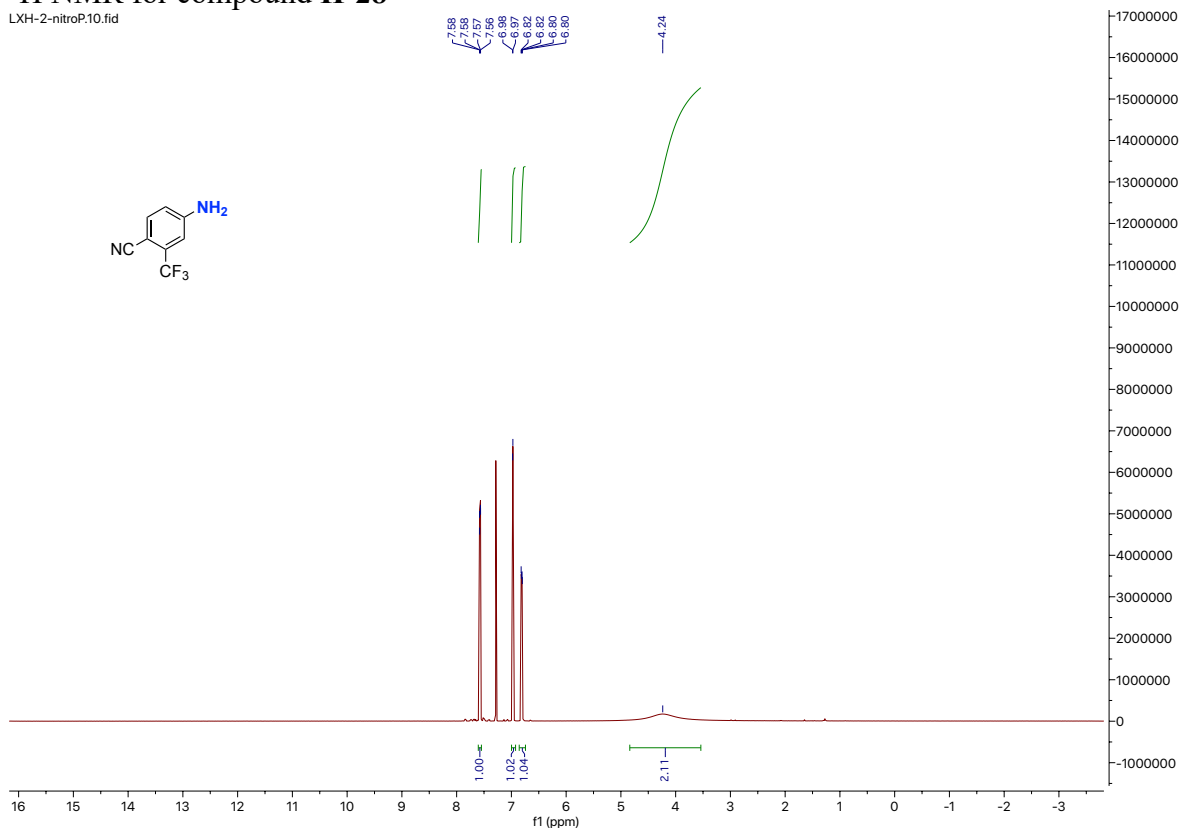
# <sup>1</sup>H NMR for compound II-22

LXH-1-55



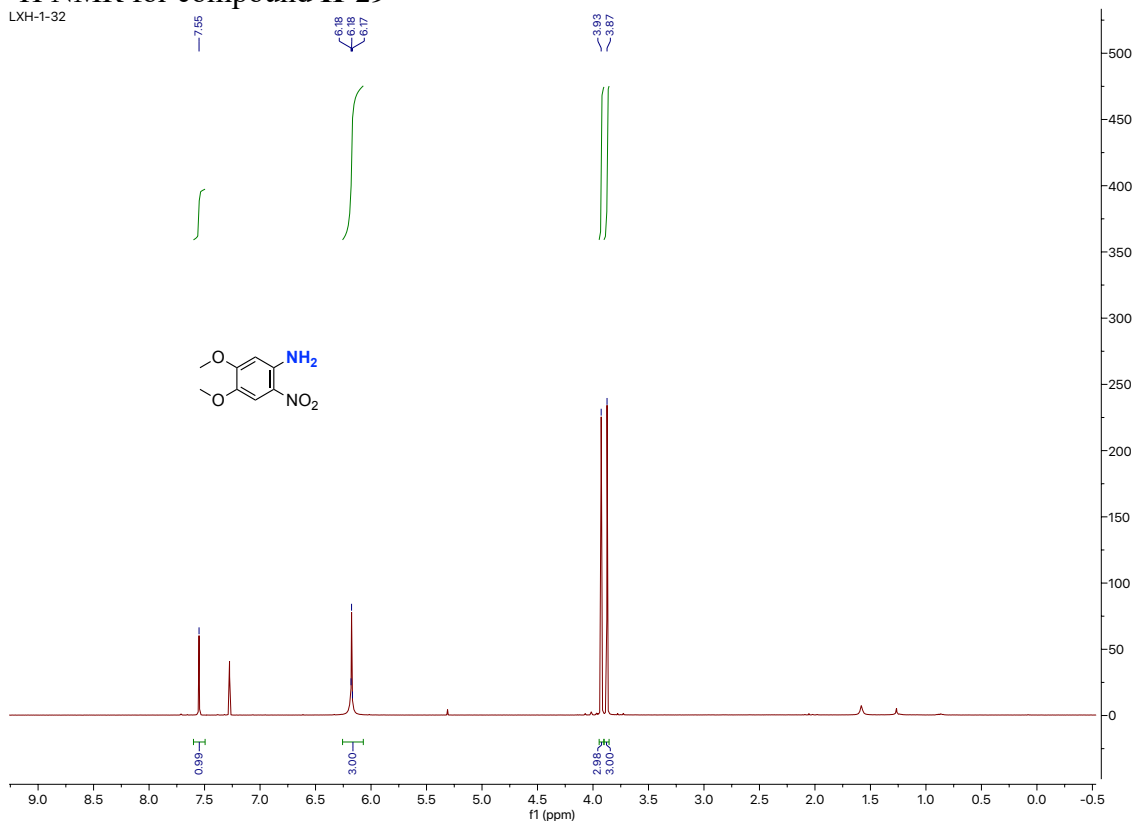
# <sup>1</sup>H NMR for compound II-28

LXH-2-nitroP.10.fid



# <sup>1</sup>H NMR for compound II-29

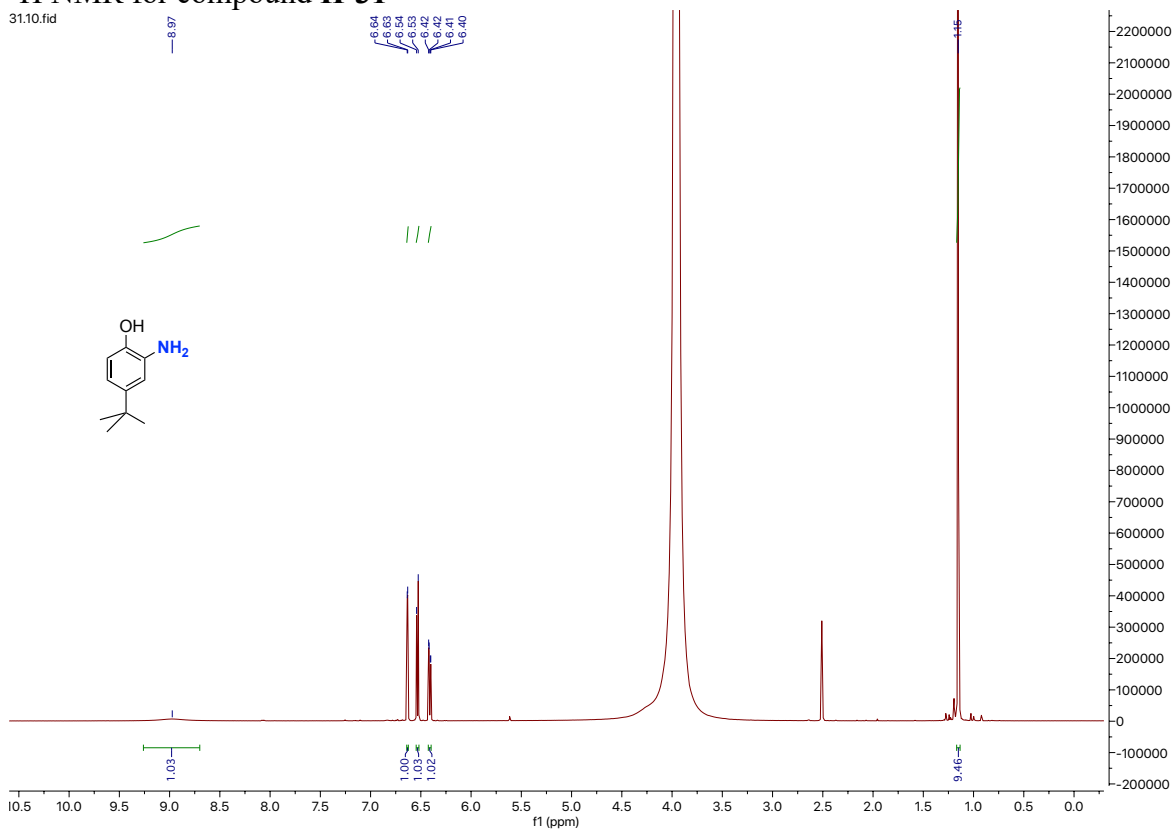
LXH-1-32





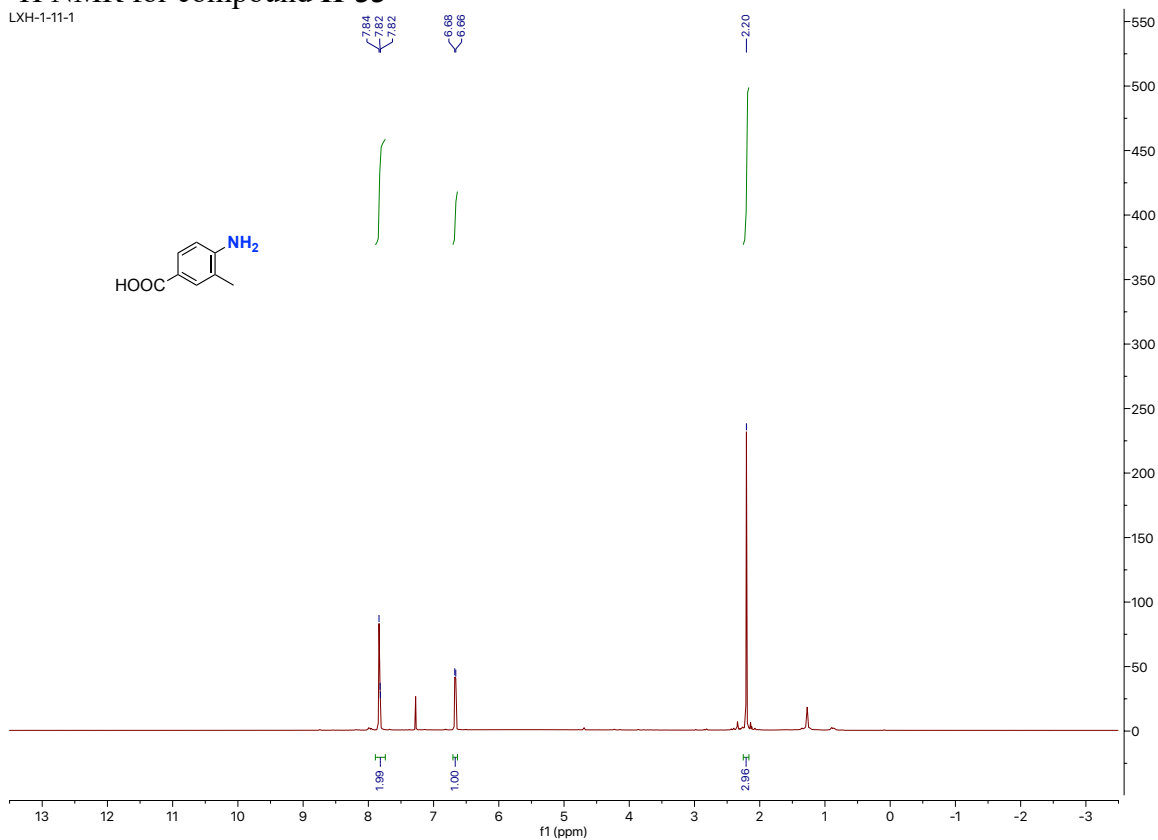
# <sup>1</sup>H NMR for compound II-31

31.10.fid

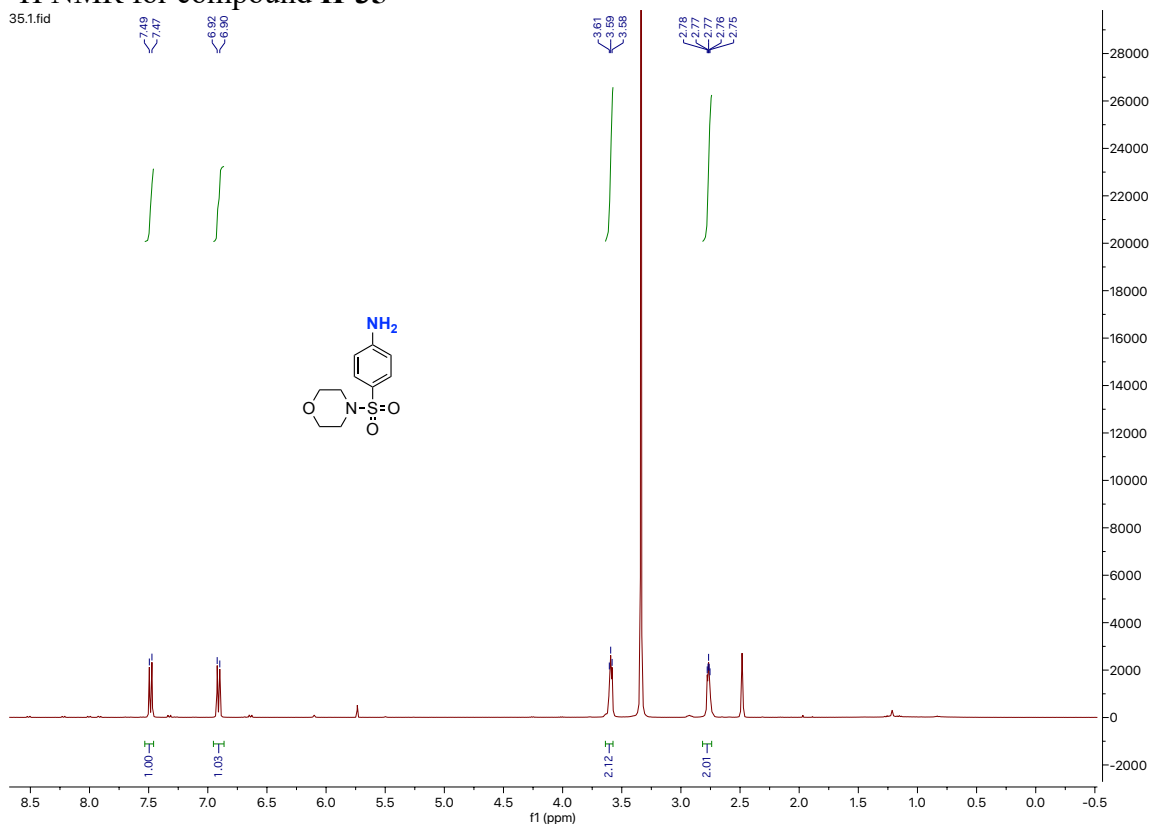


# <sup>1</sup>H NMR for compound II-33

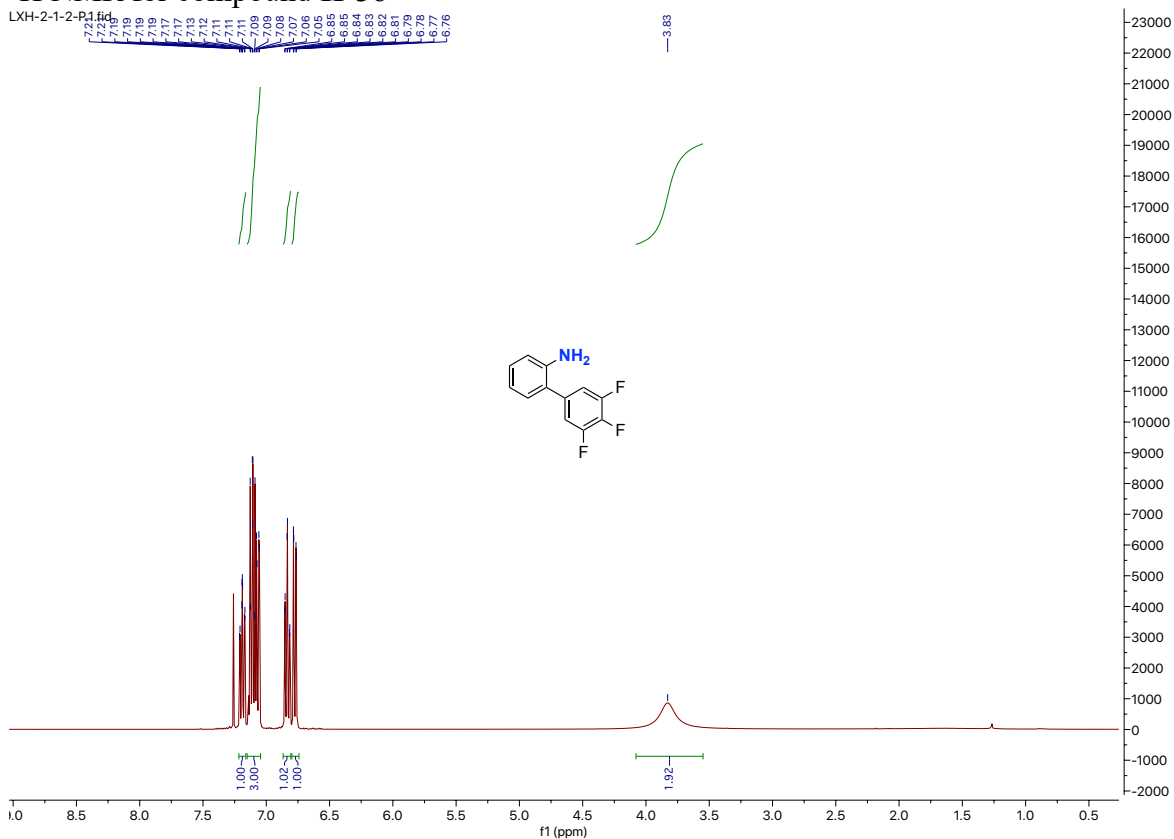
LXH-1-11-1



# <sup>1</sup>H NMR for compound II-35



# <sup>1</sup>H NMR for compound II-36



### **III. Impact of Nonionic Surfactants on Reactions of IREDs. Applications to Tandem Chemoenzymatic Sequences in Water**

Reproduced with permission from:

Li, X.; Hu, Y.; Bailey, J. D.; Lipshutz, B. H. Impact of Nonionic Surfactants on Reactions of IREDs. Applications to Tandem Chemoenzymatic Sequences in Water. *Org. Lett.* **2023**, acs.orglett.3c02790.

Copyright © 2023 American Chemical Society.

### 3.1. Background and introduction

#### 3.1.1. Project background

The pursuit of efficient, selective, and environmentally sustainable synthetic methods is a pivotal aspect of organic chemistry, especially within the pharmaceutical industry where the continuous need for nonracemic compounds is fundamental.<sup>1</sup> Central to this endeavor, the synthesis of chiral amines is critical due to their ability to interact specifically with chiral biological targets such as enzymes and receptors, a specificity that is essential for the creation of targeted and effective pharmacological treatments.<sup>2</sup> According to statistics, chiral amine moieties are present in about 40% of active pharmaceutical ingredients; examples are shown in Figure III-1. Therefore, advancing methodologies for the synthesis of chiral amines is of paramount importance, having significant implications in the development of pharmaceuticals and influencing the course of medicinal chemistry.

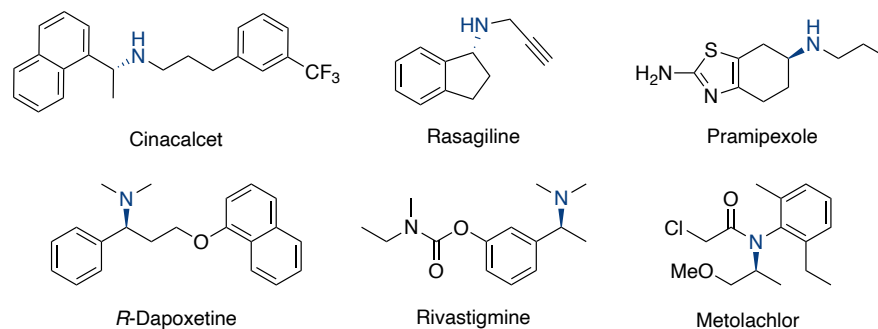


**Figure III-1.** representative pharmaceuticals containing nonracemic amines

In recent decades, the field of asymmetric catalysis has significantly advanced, the synthesis of chiral amines becoming a pivotal area of research in modern synthetic chemistry.<sup>3-8</sup> This field encompasses various methodologies, including asymmetric hydrogenation,<sup>4</sup> reductive amination,<sup>5</sup> hydroamination,<sup>6,7</sup> and allylic amination,<sup>8</sup> etc. While these techniques have achieved considerable success, yielding good-to-excellent enantioselectivities, they frequently rely on the use of costly precious metals such as iridium

(Ir), rhodium (Rh), and ruthenium (Ru), along with nonracemic ligands. Additionally, these methods often involve the use of organic solvents which contribute to waste generation. Despite their effectiveness, the reliance on such resources renders these approaches inherently unsustainable. This highlights an ongoing need for novel, environmentally friendly methods that can be more readily and sustainably applied to the synthesis of chiral amines.

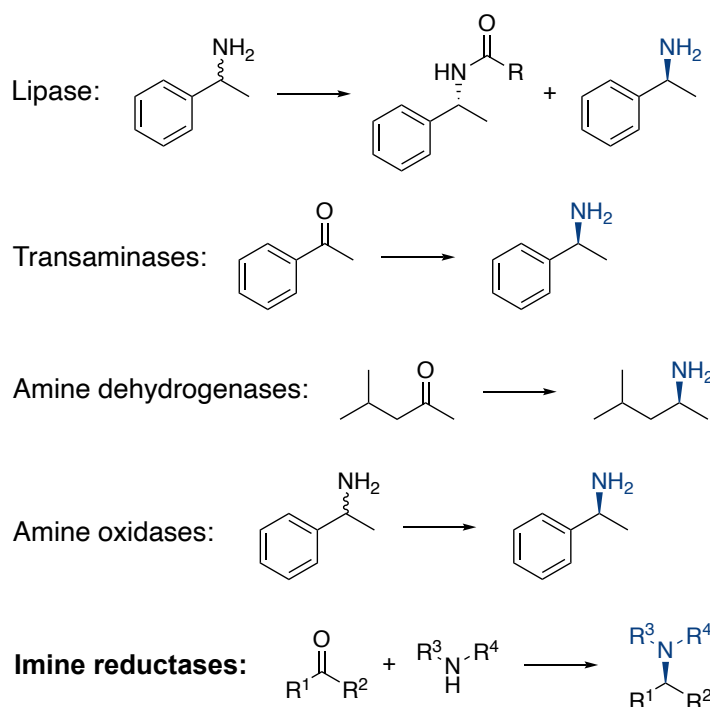
**Table III-1.** Comparison of reaction conditions and outcome between organometallic catalysis and biocatalysis.

Organometallic catalysis	Bio-catalysis
<ul style="list-style-type: none"> <li>• Expensive precious metals (Ir, Rh, Ru, etc.)</li> <li>• Complex chiral ligands</li> <li>• Waste-generating organic solvents</li> <li>• High temperature</li> </ul>	<ul style="list-style-type: none"> <li>• Aqueous media</li> <li>• Mild conditions (near-ambient temperature and pH)</li> <li>• Unparalleled stereo- and chemo-selectivity</li> </ul>

The advent of biocatalysis, highlighted by the awarding of the 2018 Nobel Prize in chemistry for the development of enzyme-driven biocatalysis, presents a compelling alternative to traditional strategies.<sup>10,11</sup> This approach brings a suite of benefits that frequently surpass those of traditional methods. The level of stereoselectivity and chemoselectivity obtained through enzymatic processes is often unparalleled, reliably producing the desired enantiomer. Moreover, the capacity of these methods to operate in aqueous environments, coupled with their inherently milder reaction conditions, provides a way for more environmentally friendly synthetic pathways. Consequently, enzymatic catalysis, now backed by Nobel Prize-winning research, stands out as an appealing choice for synthesis.

Among the variety of biocatalysts studied (Scheme III-1),<sup>12,13</sup> imine reductases (IREDs)<sup>14-16</sup> have emerged as extremely useful for the stereoselective reduction of imines to their corresponding amines, thereby playing a crucial role in the synthesis of chiral amines. A primary challenge in utilizing IREDs is the equilibrium of imine formation, which tends to be

unfavorable in aqueous environments, often resulting in lower conversion levels in IRED-catalyzed reductions. Additionally, there are limitations regarding the compatibility of specific ketone and amine combinations. For instance, substrates such as aryl ketones pose particular difficulties, as they tend to be unstable when transformed into imines in aqueous conditions, making them generally unsuitable for IRED applications.<sup>15</sup> Hence, while IREDs represent a powerful tool in the enzymatic synthesis of chiral amines, the limitations related to substrate scope and conversion efficiency necessitate thorough exploration and, ultimately, the development of innovative approaches to overcome these challenges.



**Scheme III-1.** Common enzymes used in the synthesis of chiral amines.

Surfactants, though long established by nature, have recently been recognized as potentially impacting enzymatic reactions. Their ability to self-assemble into micelles creates nanostructured environments, acting as alternative reservoirs for both water-insoluble reactants and, notably, the newly formed products generated by various enzymes. These micelles offer a suitable hydrophobic environment which can significantly enhance the extent

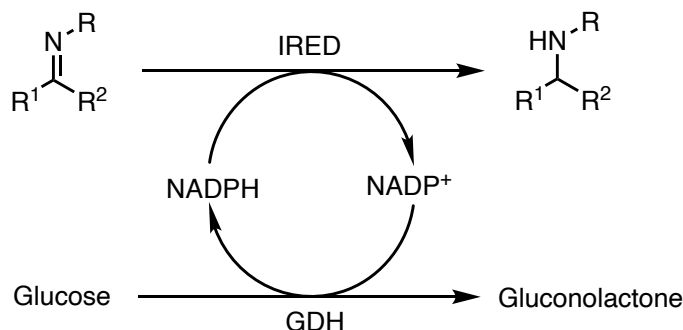
of conversion associated with enzymatic reactions by mitigating the inherent instability of certain substrates or products in aqueous conditions, thereby improving their efficiency in forming the desired product. This advantageous role of surfactants has already been effectively demonstrated with a range of enzymes, including ketoreductases (KREDs),<sup>17</sup> ene reductases (EREDs),<sup>18</sup> amine transaminases (ATAs),<sup>19</sup> and lipases.<sup>20</sup> These successful applications suggest a bright future for the use of tailored surfactants in reactions catalyzed by IREDs. Consequently, the current study investigates this promising approach, aiming to document the effects of introducing a surfactant into the aqueous medium on the enzymatic conversion to secondary amines using IRED.

### ***3.1.2. Reaction mechanism of IRED***

Imine reductases (IREDs) are identified as NADPH-dependent oxidoreductases, where NADPH, widely recognized as a reductant in enzymatic reduction cycles, is integral as a cofactor in these enzymes. Its crucial role involves the facilitation of hydride transfer to the imine, generating the amine product. The catalytic cycle's continuity relies on the regeneration of the oxidized cofactor (NADP<sup>+</sup>) back to its reduced state (NADPH), typically facilitated by an external enzymatic system such as formate dehydrogenase (FDH) or glucose dehydrogenase (GDH).

The configuration of the IRED's active site is pivotal in determining the stereoselectivity of the hydride transfer. While the precise mechanism remains elusive, emerging studies offer insights and hypotheses.<sup>14</sup> Mitsukura's solution studies<sup>21</sup> on enzyme Q1EQE0 from *Streptomyces kanamyceticus* reveal that IRED monomers feature a typical N-terminal Rossmann domain and a C-terminal bundle, linked by an interdomain helix of approximately 20 amino acids. It's observed that two monomers form a dimer through significant domain sharing, with the active site positioned at the interface of one subunit's N-terminal domain and

the C-terminal bundle of another. Here, NADPH binds, creating a cleft across the enzyme's breadth. Additional research<sup>22-25</sup> indicates that an aspartate or tyrosine residue may act as the proton donor in the reduction of C=N bonds, noting a decrease in IRED activity when Asp or Tys is mutated to Ala, though their exact role in the mechanism or stereospecificity remains unclear.



**Scheme III-2.** Reaction mechanism of IRED

### 3.2. Result and Discussion

#### 3.2.1. Surfactant screening

A preliminary investigation explored the effects of various nonionic surfactants (including TPGS-750-M, PTS-600, Tween 60, Brij 30, Savie, Mulsifan 4000 MS, and lauryl glucose) on the enzymatic conversion of seven different substrates (**III-1- III-7**) to their corresponding secondary amines (Table III-2). For each substrate, the specific IRED that had previously been identified as optimal in surfactant-free screenings was utilized. In line with earlier research,<sup>17-20</sup> it was observed that the surfactants' presence in the buffered aqueous medium can substantially affect the levels of conversion to the targeted secondary amines.

For substrate **III-1**, surfactants like TPGS-750-M, PTS-600, and Brij 30 demonstrated comparable effectiveness, leading to an approximate 40% enhancement in conversion compared to buffer-only conditions. In the case of substrate **III-2**, which involves the same



cyclohexanone component but is paired with an aromatic amine, a similar trend was observed with TPGS-750-M and PTS-600. However, Tween 60, relatively ineffective on substrate **III-1**, yielded the highest conversion rate (97%) for substrate **III-2**, while Brij 30 actually decreased the conversion to 18%, which was lower than the 66% achieved using only buffer. The conversion of an unsymmetrical ketone to nonracemic secondary amine **III-3** also resulted in about a 30% improvement in the presence of TPGS-750-M or PTS-600.

Notably, when applied to aryl ketones **III-4- III-7**, which are typically challenging for IRED-catalyzed conversions due to the instability of their intermediate imines in water, the addition of surfactants still yielded some improvement, albeit of a more modest nature (10-20%, occasionally under 10%). This outcome carries significant implications, particularly considering the role of aryl ketone derivatives in the synthesis of various active pharmaceutical ingredients (APIs), such as *R*-dapoxetine, cinacalcet, rivastigmine, and rasagiline (see Figure III-1). The potential impact of this improvement, therefore, should not be overlooked, given its relevance to pharmaceutical manufacturing.

In summary, these findings indicate that the addition of a surfactant can notably enhance IRED performance over a non-amphiphilic buffered medium. This improvement is likely attributed to a "reservoir effect" from the nanomicelles, which provide alternative environments for both substrates and predominantly the products, thereby diminishing enzymatic inhibition.<sup>17</sup>

**Table III-2.** Screening of the aqueous reaction medium involving various surfactants.<sup>a</sup>

substrate	III-1 <sup>b</sup>	III-2 <sup>b</sup>	III-3 <sup>b</sup>	III-4 <sup>c</sup>	III-5 <sup>c</sup>	III-6 <sup>c</sup>	III-7 <sup>c</sup>
enzyme	IRED-33	IRED-18	IRED-69	IRED-18	IRED-72	IRED-17	IRED-69
buffer	54	66	40	45	45	14	15
2 wt % TPGS-750-M	95	95	72	60	48	29	22
2 wt % PTS-600	98	87	70	60	43	35	27
2 wt % Tween 60	56	97	11	43	36	31	6
2 wt % Brij 30	94	18	38	64	44	27	24
2 wt % Savie	-	-	-	53	45	31	5
2 wt % Mulsifan 4000 MS	-	-	trace	49	39	14	5
2 wt % lauryl glucose	-	-	trace	28	9	0	0

<sup>a</sup> Conversions were determined by <sup>1</sup>H NMR. Color reflects the extent of conversions compared with pure buffer. ■ >30%, ■ 20-30%, ■ 10-20%, ■ 0-10%, ■ no improvement, “-”: not tested.

<sup>b</sup> Reaction conditions (Method A): ketone substrate (0.01 mmol), amine substrate (2 equiv), IRED (2 mg/mL), NADP<sup>+</sup> (1 mM), GDH-101 (1 mg/mL), D-glucose (25 mM), aqueous buffer pH = 8.0, 35 °C, 20 h. <sup>c</sup> (Method B): imine formation: ketone substrate (0.15 mmol), amine substrate (2 equiv), C<sub>4</sub>F<sub>9</sub>SO<sub>3</sub>H (0.5 equiv), DMSO (1 M). IRED reduction: crude imine mixture (contains 0.01 mmol imine), IRED (2 mg/mL), NADP<sup>+</sup> (1 mM), GDH-101 (1 mg/mL), D-glucose (25 mM), aqueous buffer pH = 8.0, 35 °C, 20 h. Conversions represent overall conversions for two steps.

### 3.2.2. Kinetic studies

Further investigations into the effects of various nonionic surfactants on the kinetics of these biocatalytic processes revealed distinct outcomes for four different substrates, as presented in Figure III-2. Notably, for amine product **III-2** from cyclohexanone **III-8** and an

electron-rich aniline **III-9** (Figure III-2A), introducing a mere 2 wt % surfactant not only enhanced the final conversion by around 30% but also significantly accelerated the reaction rate. In aqueous buffer, the conversion peaked at 66% after seven hours. However, incorporation of three varied amphiphiles led to nearly complete conversion in a shorter time frame of 4-5 hours. When the amine component was switched to benzylamine **III-10** (Figure III-2B), the surfactant's influence became even more dramatic, enhancing the conversion by approximately 40%-45%: 95% conversion with 2 wt % TPGS-750-M and 98% with 2 wt % PTS-600, in contrast to the 54% conversion achieved using buffer only.

In the case of a slightly more lipophilic ketone, substrate **III-11** (Figure III-2C), the impact of surfactant concentration on its conversion to the amine product **III-13** was also examined. Similar to previous observations with EREDs<sup>18</sup> and ATAs,<sup>19</sup> lipophilic substrates and particularly their products tend to be more responsive to surfactants, largely due to improved solubilization by nanomicelles in water. Contrary to initial expectations, however, the conversion of substrate **III-11** to product **III-13** did not exhibit a significant variance compared to simpler substrates. The difference in conversion rates between the buffer-only medium and the medium with 2 wt % TPGS-750-M was only about 15-20%. Surprisingly, higher surfactant concentrations (4 and 8 wt %) led to a reduction in conversion, though it still remained above the buffer-only level. This outcome is different from the trends observed in our previous studies.<sup>17-20</sup> Nevertheless, the process involved in IRED reductions is primarily an intermolecular one, beginning with the *in situ* formation of an imine. Without surfactant, this imine is captured by the enzyme for subsequent reduction. While in the presence of nanomicelles there is a possibility for the imine to either stay within the enzyme or move into the water and then into a micelle, engaging in dynamic exchange within the aqueous environment. This increases the chances of the imine reverting to the ketone via hydrolysis.

While the "reservoir effect"<sup>17</sup> still exists, it varies depending on the binding constants of the substrate/product with the micellar interior, rendering it unpredictable. Therefore, selecting a surfactant that achieves an optimal balance becomes crucial, rather than simply increasing the concentration of any given surfactant.

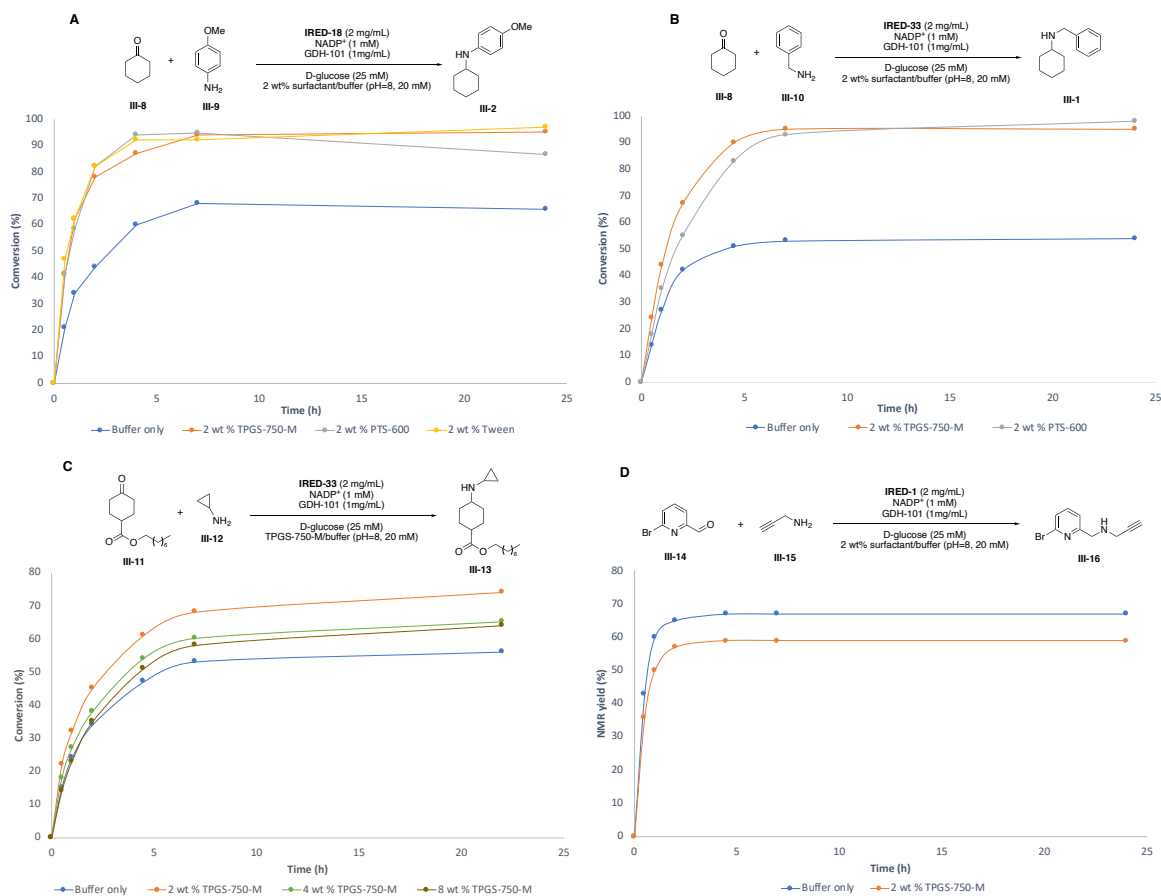


**Figure III-2.** Kinetic study of reductive aminations using IREDs. Conversions were monitored by <sup>1</sup>H NMR. NMR yields were monitored by <sup>1</sup>H NMR using tetrachloroethane as internal standard.

The behavior of aldehyde substrate **III-14** also presented an unexpected result. The addition of 2 wt % TPGS-750-M in the buffered medium surprisingly led to a decrease in the conversion to amine **III-16**, compared to using the buffer alone, as shown in Figure III-2D. This outcome might be attributed to the instability of the aldehyde substrate. Observations

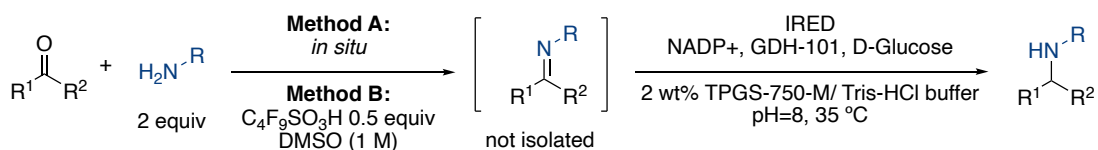
indicated that only trace amounts of the aldehyde remained after a mere 30 minutes of reaction time, suggesting the occurrence of undesired side reactions or decomposition pathways. Alternatively, the extent of hydration may have played a role. Given that micellar media tend to concentrate substrates within their core to high levels (exceeding 2 M),<sup>26</sup> it's possible that such environments could also enhance these undesired reactions, especially when compared to the more dilute conditions present in buffer-only setups. This phenomenon highlights the complexity of surfactant-mediated reactions and the need to consider the stability of substrates under these concentrated conditions.

### 3.2.3. *Substrate scope*

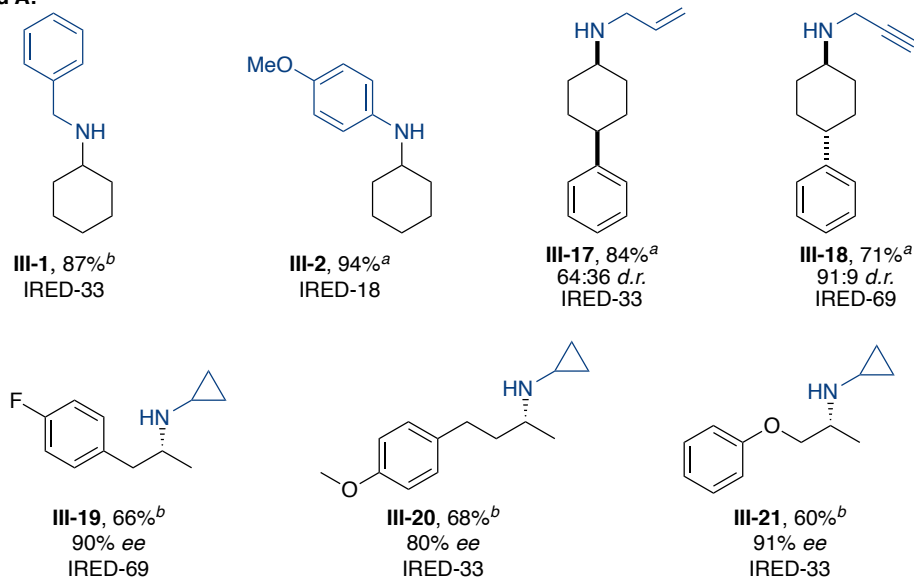
Following a comprehensive surfactant screening, TPGS-750-M was identified as the most effective for IRED-catalyzed reductions in terms of generality. Thus, it was chosen for subsequent detailed investigations concerning diastereoselectivity and asymmetric induction under optimized conditions. Figure III-3 illustrates the development of two distinct methodologies tailored for aliphatic and aromatic ketones, respectively.

Method A entails simultaneous addition of the ketone, amine, IREDs, and cofactors, facilitating *in situ* imine formation, which is then reduced by IREDs to yield the target amine. Cyclohexanone, when reacted with benzylamine and *p*-anisidine, demonstrates high reactivity, resulting in excellent yields of amines **III-1** and **III-2**. The reaction involving 4-phenylcyclohexanone and allylamine produces two conformers with a diastereomeric ratio of 64:36 (*cis:trans*). Interestingly, replacing allylamine with propargylamine reverses this selectivity, leading to a 91:9 (*trans:cis*) ratio. Furthermore, asymmetric ketones like 4-fluorophenylacetone (producing product **III-19**), anisylacetone (producing product **III-20**), and phenoxyacetone (producing product **III-21**) were evaluated, generating nonracemic amines with moderate-to-high yields and excellent enantiomeric excesses.

In the case of aromatic ketones, Method A proved to be less effective, likely due to their reduced electrophilicity. As a result, a separate imine formation step was necessitated (Method B). A representative procedure involves mixing the amine and ketone with a Brønsted acid, such as C<sub>4</sub>F<sub>9</sub>SO<sub>3</sub>H (0.5 equiv), in concentrated DMSO (1 M), a co-solvent compatible with IRED. Subsequent research indicated that HOAc (0.5 equiv) could effectively replace C<sub>4</sub>F<sub>9</sub>SO<sub>3</sub>H, addressing health concerns associated with the perfluorinated acid (as detailed in section 3.5.2, Table III-4). Following formation of the imine, a buffer containing IREDs, cofactors, and surfactant is added to the same vial leading to imine reduction. This two-step, one-pot process efficiently yields nonracemic amines, including benzylic amines **III-22** and **III-23**, as well as substituted pyridine **III-24**, with remarkable enantioselectivity and yields. Altering the amine component from cyclopropylamine to benzylamine led to a reduction in the isolated yield. However, synthesizing the same compound (**III-19**) through traditional organic methods would require expensive metal catalysts like iridium or ruthenium, carefully designed chiral ligands, organic solvents, elevated temperatures, and high H<sub>2</sub> pressure.<sup>27-30</sup>



**Method A:**



**Method B:**

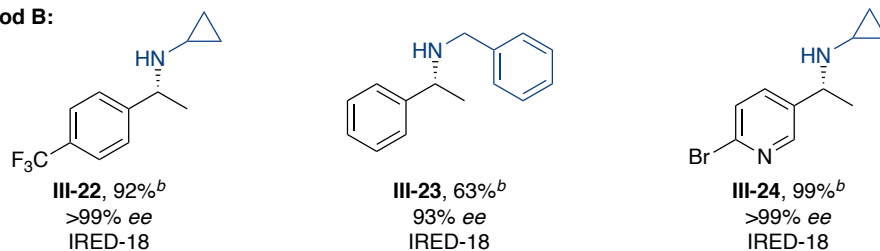


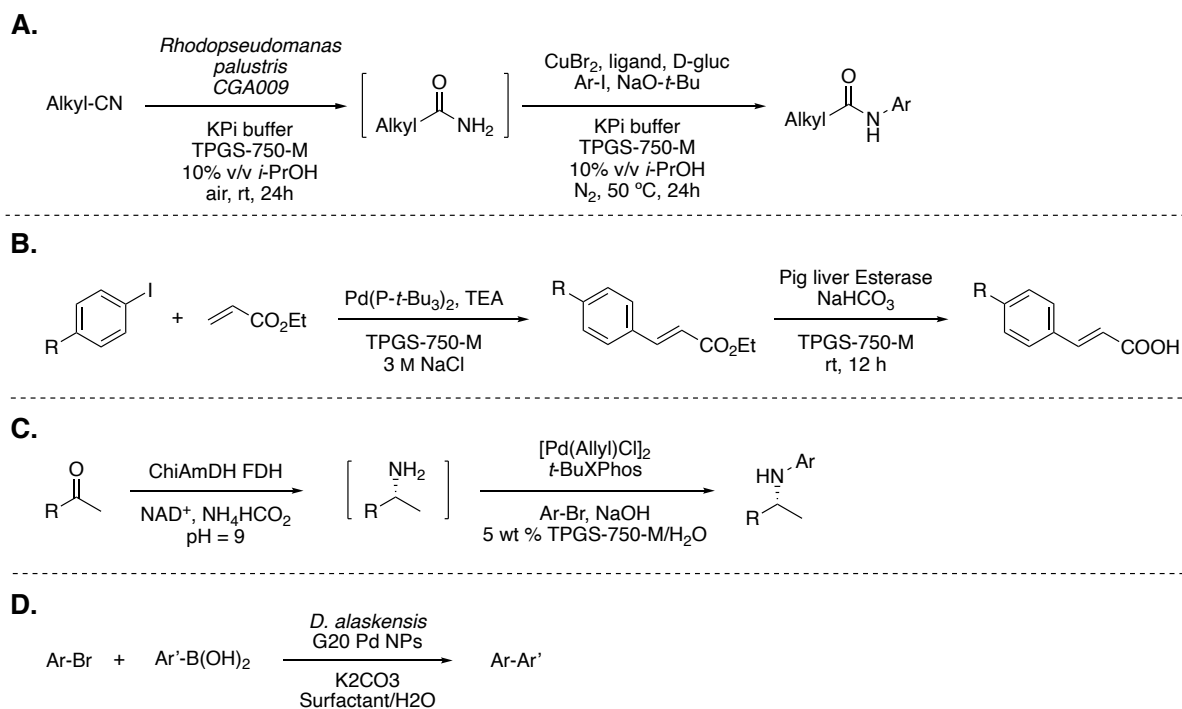
**Figure III-3.** Substrate scope; Method A conditions: ketone substrate (0.1 mmol), amine substrate (2 equiv), IRED (2 mg/mL), NADP<sup>+</sup>(1 mM), GDH-101 (1 mg/mL), D-glucose (25 mM), aqueous buffer pH = 8.0, 35 °C, 20 h. Method B conditions: imine formation: ketone substrate (0.2 mmol), amine substrate (2 equiv), C<sub>4</sub>F<sub>9</sub>SO<sub>3</sub>H (0.5 equiv), DMSO (1 M). IRED reduction: crude imine mixture (contains 0.1 mmol imine), IRED (2 mg/mL), NADP<sup>+</sup>(1 mM), GDH-101 (1 mg/mL), D-glucose (25 mM), aqueous buffer pH = 8.0, 35 °C, 20 h. Isolated yields are shown. % ee was determined by chiral HPLC. <sup>a</sup> Product was isolated as Cbz-protected amine. <sup>b</sup> Product was isolated as trifluoroacetyl derivative.

### 3.2.4 Tandem Chemoenzymatic Sequences

The integration of surfactants into aqueous enzymatic reactions extends beyond just facilitating the reservoir effect; it also enables the execution of tandem chemoenzymatic sequences in one pot. This methodology enhances both time<sup>31</sup> and pot<sup>32</sup> economies, while simultaneously diminishing waste streams, particularly those typically generated during the work-up and purification of intermediates.

Scheme III-3 shown several representative literature examples illustrating the successful implementation of telescoped chemoenzymatic sequences in aqueous environments using TPGS-750-M. The Micklefield group's research on amide synthesis from aliphatic nitriles demonstrates that 2 wt % TPGS-750-M enhances conversion levels in the N-arylation step and significantly increases the overall reaction concentration. (Scheme III-3A)<sup>33</sup> The Hastings group reported that TPGS-750-M facilitates organometallic-catalyzed reactions, including Mizoroki-Heck (MH), ring-closing metathesis (RCM), and cross metathesis (CM) reactions, to be combined with lipase-catalyzed ester hydrolysis in one-pot. (Scheme III-3B)<sup>34</sup> Additionally, Turner, Parmeggiani, and collaborators outlined a methodology for synthesizing non-racemic N-arylamines by merging asymmetric reductive aminations, catalyzed by an amine dehydrogenase (AmDH), with Buchwald-Hartwig aminations. (Scheme III-3C)<sup>35</sup> Beyond conventional multi-step chemoenzymatic sequences, a novel approach by Horsfall and colleagues suggests an alternative integration of chemical and biological processes. They developed biogenic Pd nanoparticles to catalyze Suzuki-Miyaura couplings, indicating that the catalyst itself incorporates both chemical and biological components. Here again, TPGS-750-M provides the necessary aqueous micellar conditions for the cross-coupling reactions. (Scheme III-3D)<sup>36</sup> The increasing volume of literature in this field highlights the rising prominence of this methodology.



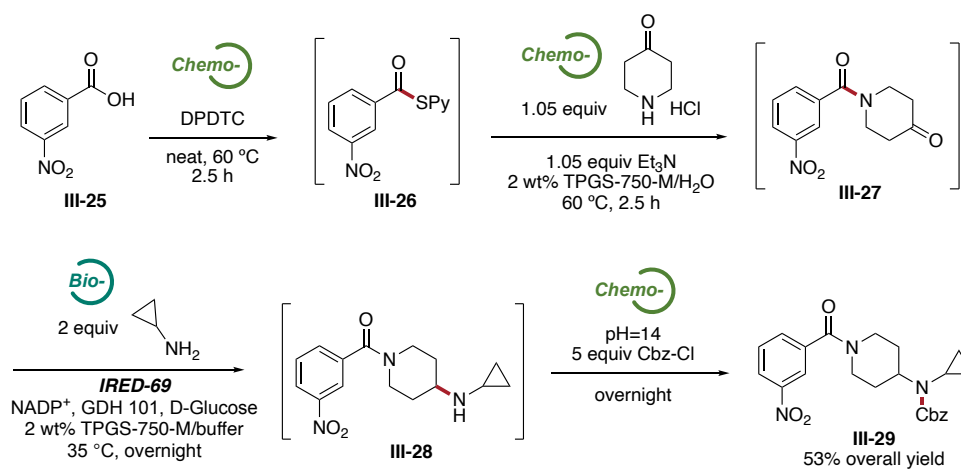


**Scheme III-3.** Selected literature examples of chemoenzymatic reactions in TPGS-750-M aqueous solution

Here, we demonstrate that imine reductases (IREDs) can be employed in tandem chemoenzymatic sequences to enhance molecular complexity. Schemes III-4- III-6 showcase distinct, yet representative, tandem sequences where IREDs are integrated at various stages of the process, illustrating the versatility and utility of IREDs in advancing synthetic complexity.

In the first sequence (Scheme III-4), our newly developed methodology for amide formation<sup>37</sup> was utilized to prepare ketoamide **III-27**. The process began with the transformation of carboxylic acid **III-25** into its corresponding thioester **III-26**. This conversion was efficiently carried out by stirring the acid under neat conditions with DPDTC (DiPyridylDiThioCarbonate), a reagent readily synthesized on a multi-gram scale using 2-mercaptopyridine and triphosgene, both of which are commercially available. Following this,

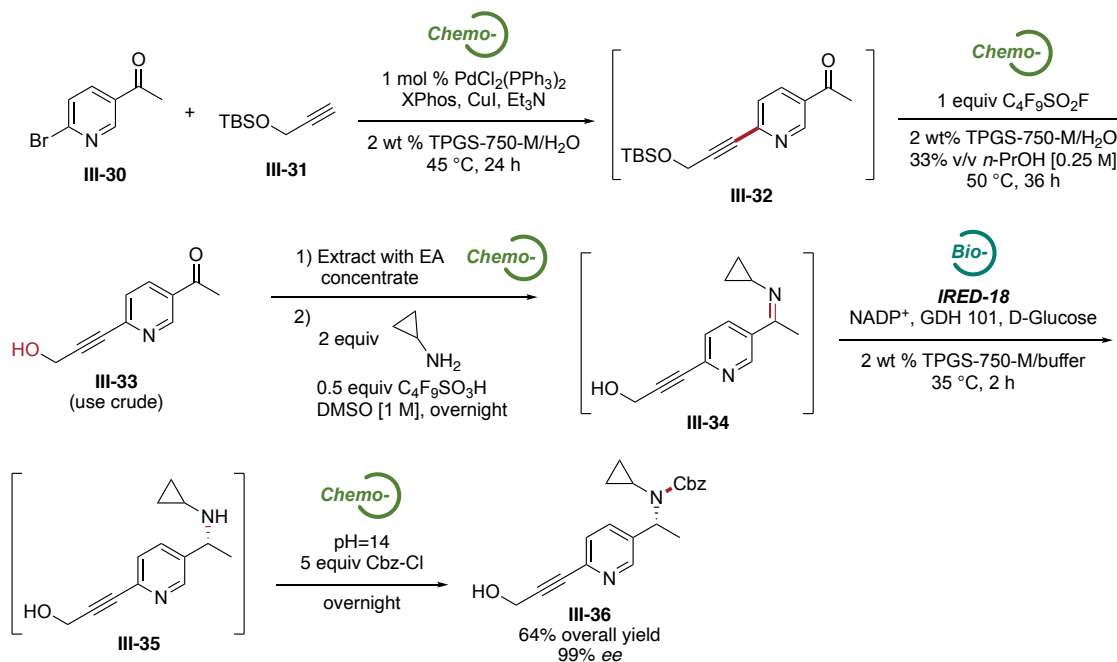
4-piperidone in its hydrochloride salt form was added, leading to the successful formation of ketoamide **27** in 0.5 M 2 wt % TPGS-750-M/H<sub>2</sub>O solution. Subsequently, a TPGS-750-M/buffer solution containing cyclopropylamine and the necessary co-factors was introduced, resulting in the imine reduction product **III-28**. The reaction media was then basified, to which Cbz-Cl was added to protect the secondary amine, yielding the final product in 53% yield over four steps.



**Scheme III-4.** Tandem 4-step, chemo-chemo-bio-chemo sequence

The second sequence demonstrates the feasibility of a 5-step tandem chemoenzymatic catalysis process that incorporates a one-pot imine formation-IREd reduction (Scheme III-5). In this case, 3-acetyl-6-bromopyridine (**III-30**) and TBS-protected propargyl alcohol (**III-31**) underwent a Sonogashira reaction facilitated by 1 mol % PdCl<sub>2</sub>(PPh<sub>3</sub>)<sub>2</sub> and XPhos in a 2 wt % TPGS-750-M aqueous solution,<sup>38</sup> resulting in the formation of internal alkyne **III-32**. Subsequently, one equivalent of a lipophilic SuFEx reagent was added directly to the reaction mixture to deprotect the TBS group,<sup>39</sup> yielding propargyl alcohol **III-33**. The crude reaction product was then extracted using EtOAc (with the EtOAc being recoverable) and reacted with cyclopropylamine in concentrated DMSO, forming imine **III-34**. This imine solution in DMSO was subsequently transferred into a 2 wt % TPGS-750-M/buffer solution, and upon

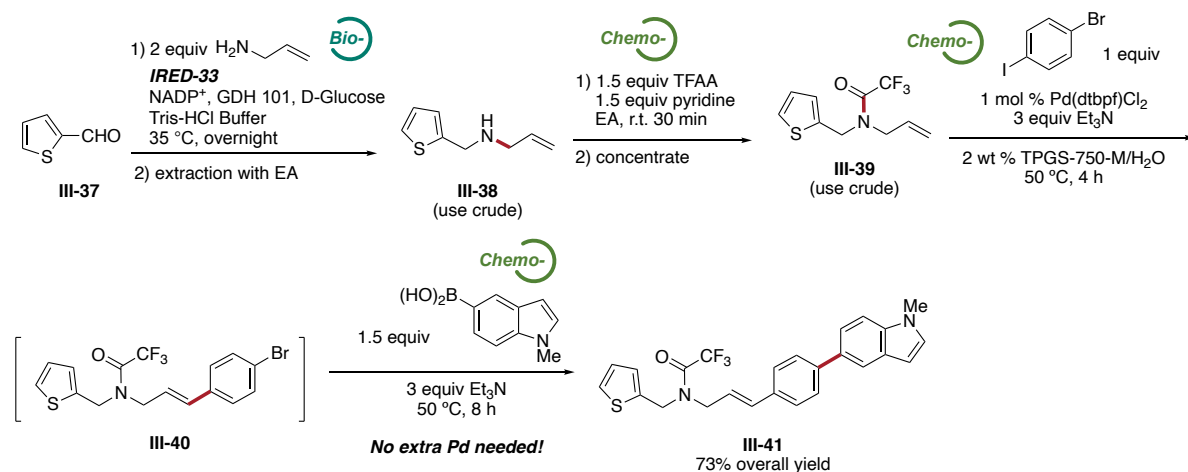
the addition of IRED and co-factors, the imine was enantioselectively reduced to the chiral amine **III-35**. In the final step, the reaction mixture's pH was adjusted to 14, followed by the introduction of an excess of Cbz-Cl, which resulted in the formation of the protected amine **III-36**. This sequence achieved an impressive 99% enantiomeric excess and a 64% overall yield across the five steps.



**Scheme III-5.** Tandem 5-step, chemo-chemo-chemo-bio-chemo sequence

The potential for seamlessly combining chemo- and bio-catalytic processes was further demonstrated through a 4-step "Bio-Chemo-Chemo-Chemo" sequence conducted within a single pot (Scheme III-6). Initially, an IRED-catalyzed reaction was performed between 2-thiophenecarboxaldehyde (**III-37**) and allyl amine, which, after an extraction and protection step, yielded the tertiary allyl amine derivative (**III-39**). Following the removal of EtOAc, two successive cross-coupling reactions were executed within the aqueous micellar medium. The first reaction was a Heck reaction, selectively targeting the iodo group on 1-bromo-4-iodobenzene.<sup>40</sup> This step resulted in the formation of a disubstituted alkene (**III-40**) with a bromine residue on one side. Notably, additional palladium catalyst was not added for the

subsequent Suzuki coupling.<sup>41</sup> Instead, this step cleverly utilized the residual palladium from the Heck reaction, significantly optimizing "metal economy" by reducing the average palladium loading to just 5000 ppm (0.5 mol %) for each coupling reaction.<sup>42</sup> This strategic utilization of palladium not only exemplifies efficiency but also aligns with sustainable chemical practices. Consequently, this innovative 4-step process led to a high isolated yield of 73% for the final product (**III-41**), underscoring the efficacy and practicality of combining different catalytic techniques in a single-pot synthesis.



**Scheme III-6.** Tandem 4-step, bio-chemo-chemo-chemo sequence

### 3.3. Summary

In summary, this study evaluated the impact of surfactants on IRED-catalyzed imine reductions. It is shown that nonionic surfactants such as TPGS-750-M, substantially enhance conversion and accelerate reaction times just by their inclusion in the aqueous reaction medium. Additionally, the study successfully demonstrated efficient tandem sequences that integrate chemocatalysis and biocatalysis, both performed in water, demonstrating the efficiency and sustainability of integrating surfactants into enzymatic reactions for chemical synthesis.

### 3.4. References

1. Top 200 SMALL Molecule Drugs by Sales in 2022, a poster made by Jon T. Njardarson's group, <https://bpb-us-e2.wpmucdn.com/sites.arizona.edu/dist/9/130/files/2023/11/NjardarsonGroup2022SmallMoleculeTopPosterV3.pdf> (accessed 2023-12-6)
2. Nugent, T. C. *Chiral Amine Synthesis: Methods, Developments and Applications*; John Wiley & Sons, 2010.
3. Yin, Q.; Shi, Y.; Wang, J.; Zhang, X. Direct Catalytic Asymmetric Synthesis of  $\alpha$ -Chiral Primary Amines. *Chem. Soc. Rev.* **2020**, *49*, 6141–6153.
4. Cabré, A.; Verdaguer, X.; Riera, A. Recent Advances in the Enantioselective Synthesis of Chiral Amines via Transition Metal-Catalyzed Asymmetric Hydrogenation. *Chem. Rev.* **2022**, *122*, 269–339.
5. Reshi, N. U. D.; Saptal, V. B.; Beller, M.; Bera, J. K. Recent Progress in Transition-Metal-Catalyzed Asymmetric Reductive Amination. *ACS Catal.* **2021**, *11*, 13809–13837.
6. Yang, Y.; Shi, S.-L.; Niu, D.; Liu, P.; Buchwald, S. L. Catalytic Asymmetric Hydroamination of Unactivated Internal Olefins to Aliphatic Amines. *Science* **2015**, *349*, 62–66.
7. Pirnot, M. T.; Wang, Y.; Buchwald, S. L. Copper Hydride Catalyzed Hydroamination of Alkenes and Alkynes. *Angew. Chem., Int. Ed.* **2016**, *55*, 48–57.
8. Grange, R. L.; Clizbe, E. A.; Evans, P. A. Recent Developments in Asymmetric Allylic Amination Reactions. *New York* **2016**.
9. Grange, R. L.; Clizbe, E. A.; Evans, P. A. Recent Developments in Asymmetric Allylic Amination Reactions. *Synthesis* **2016**, *48*, 2911–2968.
10. Arnold, F. H. Directed Evolution: Bringing New Chemistry to Life. *Angew. Chem., Int. Ed.* **2018**, *57*, 4143–4148.
11. Lewis, R. D.; France, S. P.; Martinez, C. A. Emerging Technologies for Biocatalysis in the Pharmaceutical Industry. *ACS Catal.* **2023**, *13*, 5571–5577.
12. Ghislieri, D.; Turner, N. J. Biocatalytic Approaches to the Synthesis of Enantiomerically Pure Chiral Amines. *Top Catal* **2014**, *57*, 284–300.
13. Grogan, G. Synthesis of Chiral Amines Using Redox Biocatalysis. *Curr. Opin. Chem. Biol.* **2018**, *43*, 15–22.
14. Grogan, G.; Turner, N. J. InspiRED by Nature: NADPH-Dependent Imine Reductases (IREDs) as Catalysts for the Preparation of Chiral Amines. *Chem. Eur. J.* **2016**, *22*, 1900–1907.

15. Mangas-Sanchez, J.; France, S. P.; Montgomery, S. L.; Aleku, G. A.; Man, H.; Sharma, M.; Ramsden, J. I.; Grogan, G.; Turner, N. J. Imine Reductases (IREDS). *Curr. Opin. Chem. Biol.* **2017**, *37*, 19–25.
16. Gilio, A. K.; Thorpe, T. W.; Turner, N.; Grogan, G. Reductive Aminations by Imine Reductases: From Milligrams to Tons. *Chem. Sci.* **2022**, *13*, 4697–4713.
17. Cortes-Clerget, M.; Akporji, N.; Zhou, J.; Gao, F.; Guo, P.; Parmentier, M.; Gallou, F.; Berthon, J.-Y.; Lipshutz, B. H. Bridging the Gap between Transition Metal- and Bio-Catalysis via Aqueous Micellar Catalysis. *Nat Commun* **2019**, *10*, 2169.
18. Akporji, N.; Singhanian, V.; Dussart-Gautheret, J.; Gallou, F.; Lipshutz, B. H. Nanomicelle-Enhanced, Asymmetric ERED-Catalyzed Reductions of Activated Olefins. Applications to 1-Pot Chemo- and Bio-Catalysis Sequences in Water. *Chem. Commun.* **2021**, *57*, 11847–11850.
19. Dussart-Gautheret, J.; Yu, J.; Ganesh, K.; Rajendra, G.; Gallou, F.; Lipshutz, B. H. Impact of Aqueous Micellar Media on Biocatalytic Transformations Involving Transaminase (ATA); Applications to Chemoenzymatic Catalysis. *Green Chem.* **2022**, *24*, 6172–6178.
20. Singhanian, V.; Cortes-Clerget, M.; Dussart-Gautheret, J.; Akkachairin, B.; Yu, J.; Akporji, N.; Gallou, F.; Lipshutz, B. H. Lipase-Catalyzed Esterification in Water Enabled by Nanomicelles. Applications to 1-Pot Multi-Step Sequences. *Chem. Sci.* **2022**, *13*, 1440–1445.
21. Mitsukura, K.; Suzuki, M.; Shinoda, S.; Kuramoto, T.; Yoshida, T.; Nagasawa, T. Purification and Characterization of a Novel (*R*)-Imine Reductase from *Streptomyces* Sp. GF3587. *Biosci. Biotechnol. Biochem.* **2011**, *75*, 1778–1782.
22. Rodríguez-Mata, M.; Frank, A.; Wells, E.; Leipold, F.; Turner, N. J.; Hart, S.; Turkenburg, J. P.; Grogan, G. Structure and Activity of NADPH-Dependent Reductase Q1EQE0 from *Streptomyces Kanamyceticus*, Which Catalyses the *R*-Selective Reduction of an Imine Substrate. *ChemBioChem* **2013**, *14*, 1372–1379.
23. Gourley, D. G.; Schüttelkopf, A. W.; Leonard, G. A.; Luba, J.; Hardy, L. W.; Beverley, S. M.; Hunter, W. N. Pteridine Reductase Mechanism Correlates Pterin Metabolism with Drug Resistance in Trypanosomatid Parasites. *Nat. Struct. Biol.* **2001**, *8*, 521–525.
24. Scheller, P. N.; Fademrecht, S.; Hofelzer, S.; Pleiss, J.; Leipold, F.; Turner, N. J.; Nestl, B. M.; Hauer, B. Enzyme Toolbox: Novel Enantiocomplementary Imine Reductases. *ChemBioChem* **2014**, *15*, 2201–2204.
25. Man, H.; Wells, E.; Hussain, S.; Leipold, F.; Hart, S.; Turkenburg, J. P.; Turner, N. J.; Grogan, G. Structure, Activity and Stereoselectivity of NADPH-Dependent Oxidoreductases Catalysing the *S*-Selective Reduction of the Imine Substrate 2-Methylpyrroline. *ChemBioChem* **2015**, *16*, 1052–1059.
26. Lipshutz, B. H.; Ghorai, S.; Abela, A. R.; Moser, R.; Nishikata, T.; Duplais, C.; Krasovskiy, A.; Gaston, R. D.; Gadwood, R. C. TPGS-750-M: A Second-Generation

- Amphiphile for Metal-Catalyzed Cross-Couplings in Water at Room Temperature. *J. Org. Chem.* **2011**, *76*, 4379–4391.
27. Han, Z.; Wang, Z.; Zhang, X.; Ding, K. Spiro[4,4]-1,6-Nonadiene-Based Phosphine–Oxazoline Ligands for Iridium-Catalyzed Enantioselective Hydrogenation of Ketimines. *Angew. Chem., Int. Ed* **2009**, *48*, 5345–5349.
28. Chen, F.; Ding, Z.; He, Y.; Qin, J.; Wang, T.; Fan, Q.-H. Asymmetric Hydrogenation of N-Alkyl and N-Aryl Ketimines Using Chiral Cationic Ru(Diamine) Complexes as Catalysts: The Counteranion and Solvent Effects, and Substrate Scope. *Tetrahedron* **2012**, *68*, 5248–5257.
29. Pan, H.-J.; Zhang, Y.; Shan, C.; Yu, Z.; Lan, Y.; Zhao, Y. Asymmetric Transfer Hydrogenation of Imines Using Alcohol: Efficiency and Selectivity Are Influenced by the Hydrogen Donor. *Angew. Chem., Int. Ed.* **2016**, *55*, 9615–9619.
30. Reetz, M. T.; Bondarev, O. Mixtures of Chiral Phosphorous Acid Diesters and Achiral P Ligands in the Enantio- and Diastereoselective Hydrogenation of Ketimines. *Angew. Chem., Int. Ed.* **2007**, *46*, 4523–4526.
31. Hayashi, Y. Time Economy in Total Synthesis. *J. Org. Chem.* **2021**, *86*, 1–23.
32. Hayashi, Y. Pot Economy and One-Pot Synthesis. *Chem. Sci.* **2016**, *7*, 866–880.
33. Bering, L.; Craven, E. J.; Sowerby Thomas, S. A.; Shepherd, S. A.; Micklefield, J. Merging Enzymes with Chemocatalysis for Amide Bond Synthesis. *Nat. Commun.* **2022**, *13*, 380.
34. Hastings, C. J.; Adams, N. P.; Bushi, J.; Kolb, S. J. One-Pot Chemoenzymatic Reactions in Water Enabled by Micellar Encapsulation. *Green Chem.* **2020**, *22*, 6187–6193.
35. Cosgrove, S. C.; Thompson, M. P.; Ahmed, S. T.; Parmeggiani, F.; Turner, N. J. One-Pot Synthesis of Chiral *N*-Arylamines by Combining Biocatalytic Aminations with Buchwald–Hartwig *N*-Arylation. *Angew. Chem., Int. Ed.* **2020**, *59*, 18156–18160.
36. Era, Y.; Dennis, J. A.; Wallace, S.; Horsfall, L. E. Micellar Catalysis of the Suzuki Miyaura Reaction Using Biogenic Pd Nanoparticles from *Desulfovibrio Alaskensis*. *Green Chem.* **2021**, *23*, 8886–8890.
37. Freiberg, K. M.; Kavthe, R. D.; Thomas, R. M.; Fialho, D. M.; Dee, P.; Scurria, M.; Lipshutz, B. H. Direct Formation of Amide/Peptide Bonds from Carboxylic Acids: No Traditional Coupling Reagents, 1-Pot, and Green. *Chem. Sci.* **2023**, *14*, 3462–3469.
38. Jin, B.; Gallou, F.; Reilly, J.; Lipshutz, B. H. Ppm Pd-Catalyzed, Cu-Free Sonogashira Couplings in Water Using Commercially Available Catalyst Precursors. *Chem. Sci.* **2019**, *10*, 3481–3485.
39. Akporji, N.; Lieberman, J.; Maser, M.; Yoshimura, M.; Boskovic, Z.; Lipshutz, B. H. Selective Deprotection of the Diphenylmethylsilyl (DPMS) Hydroxyl Protecting Group

- under Environmentally Responsible, Aqueous Conditions. *ChemCatChem* **2019**, *11*, 5743–5747.
40. Lipshutz, B. H.; Taft, B. R. Heck Couplings at Room Temperature in Nanometer Aqueous Micelles. *Org. Lett.* **2008**, *10*, 1329–1332.
  41. Lipshutz, B. H.; Abela, A. R. Micellar Catalysis of Suzuki–Miyaura Cross-Couplings with Heteroaromatics in Water. *Org. Lett.* **2008**, *10*, 5329–5332.
  42. Hu, Y.; Li, X.; Jin, G.; Lipshutz, B. H. Simplified Preparation of ppm Pd-Containing Nanoparticles as Catalysts for Chemistry in Water. *ACS Catal.* **2023**, *13*, 3179–3186.



### 3.5. Experimental section

#### 3.5.1. General information

Reagents and chemicals were purchased from Sigma-Aldrich, Combi-Blocks, Alfa Aesar, or Acros Organics and used without further purification. Imine reductases (IREDs) Screening Kit containing 9 imine reductases enzymes and IRED-101, NADP<sup>+</sup> co-factors were purchased from Johnson Matthey® and were used as received. The enzyme and co-factors were stored at -18°C until use. Purchasing website: <https://matthey.com/en/products-and-markets/pgms-and-circularity/pgm-chemicals-and-catalysts/catalysts/chiral-amines-kit>. Deuterated solvents were purchased from Cambridge Isotopes Laboratories. TPGS-750-M is either prepared according to reported procedure<sup>1</sup> or supplied by PHT International (also available from Sigma-Aldrich, catalog #733857).

Thin-layer chromatography (TLC) was performed using Silica Gel 60 F254 plates (Silicycle, TLG-R10014B-323). Flash chromatography was performed manually using Silica Gel 60 (Silicycle, 40-63 nm). preparative TLC was performed using Silica Gel 60 F254 plates (Sigma-Aldrich, 1,000 µm thick, Z740216).

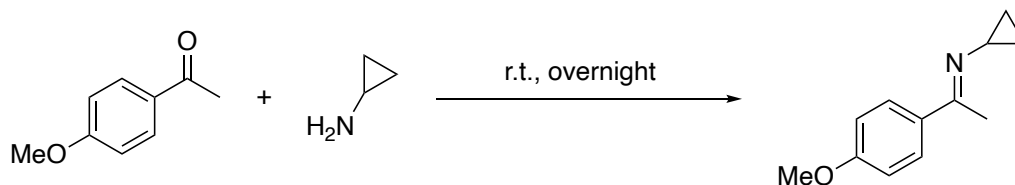
<sup>1</sup>H and <sup>13</sup>C NMR spectra were recorded on either a Bruker Avance III HD 400 MHz (400 MHz for <sup>1</sup>H, 100 MHz for <sup>13</sup>C), a Bruker Avance NEO 500 MHz (500 MHz for <sup>1</sup>H, 125 MHz for <sup>13</sup>C) or on a Varian Unity Inova 500 MHz (500 MHz for <sup>1</sup>H, 125 MHz for <sup>13</sup>C); CDCl<sub>3</sub> were used as solvents. Residual peaks for CHCl<sub>3</sub> in CDCl<sub>3</sub> (<sup>1</sup>H = 7.26 ppm, <sup>13</sup>C = 77.20 ppm) have been assigned. The chemical shifts are reported in part per million (ppm), the coupling constants *J* values are given in Hertz (Hz). The peak patterns are indicated as follows: bs, broad singlet; s, singlet; d, doublet; t, triplet; q, quartet; p, pentet; m, multiplet.

Chiral HPLC data were collected using an Agilent 1260 HPLC.

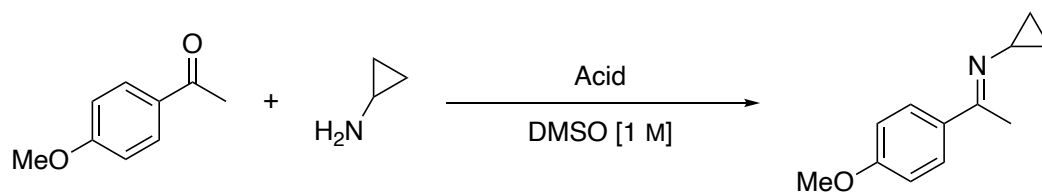
HRMS were recorded on a Waters GCT Premier GC or LC TOF mass spectrometer using ESI ionization

### 3.5.2. Optimization detail for imine formation

**Table III-3.** Initial screening for imine formation conditions



Entry	Solvent	Additive	Conversion
1	2 wt% TPGS-750-M/H <sub>2</sub> O [1 M]	C <sub>4</sub> F <sub>9</sub> SO <sub>3</sub> H (1 equiv)	12%
2	2 wt% TPGS-750-M/H <sub>2</sub> O [1 M]	none	28%
3	2 wt% TPGS-750-M/H <sub>2</sub> O [0.5 M]	none	20%
4	2 wt% SDS/H <sub>2</sub> O [1 M]	C <sub>4</sub> F <sub>9</sub> SO <sub>3</sub> H (1 equiv)	9%
5	2 wt% SDS/H <sub>2</sub> O [1 M]	none	37%
6	Heptane [0.5 M]	none	48%
7	Heptane [0.5 M]	4Å MS	48%
8	Heptane [0.5 M]	anhydrous MgSO <sub>4</sub>	7%
9	DMSO [0.5 M]	none	59%
10	DMSO [0.5 M]	4Å MS	N.R
11	DMSO [0.5 M]	anhydrous MgSO <sub>4</sub>	7%
12	DMSO [0.5 M]	C <sub>4</sub> F <sub>9</sub> SO <sub>3</sub> H (0.5 equiv)	75%
13	DMSO [0.5 M]	C <sub>4</sub> F <sub>9</sub> SO <sub>3</sub> H (0.2 equiv)	61%
14	<b>DMSO [1 M]</b>	<b>C<sub>4</sub>F<sub>9</sub>SO<sub>3</sub>H (0.5 equiv)</b>	<b>83%</b>
15	DMSO [2 M]	C <sub>4</sub> F <sub>9</sub> SO <sub>3</sub> H (0.5 equiv)	73%
16	DMSO [2 M]	C <sub>4</sub> F <sub>9</sub> SO <sub>3</sub> H (0.2 equiv)	53%

**Table III-4.** Further screening of acid catalyst

Acid	equivalent	conversion
C <sub>4</sub> F <sub>9</sub> SO <sub>3</sub> H	0.5	83%
Me-SO <sub>3</sub> H	0.5	63%
CSA	0.5	62%
<i>p</i> -TsOH·H <sub>2</sub> O	0.5	56%
TFA	1	N.R
HOAc	0.5	<b>89%</b>
HOAc	1	77%
HOAc	2	56%
HOAc	3	36%
HOAc	10	N.R

### 3.5.3. Procedure for preparation of tris-HCl buffer, and surfactant/buffer solutions

#### 100 mM tris-HCl buffer:

In a 500 mL beaker equipped with a magnetic stir bar, *tris*(hydroxymethyl)aminomethane (6.06 g) was dissolved in ~400 mL HPLC level water. Under gentle stirring at rt, concentrated HCl was added dropwise. After the pH reached 8 (indicated by a pH meter), the total volume was then adjusted to 500.0 mL by adding HPLC level water. The buffer solution was stored at rt.

#### surfactant/buffer solution:

To prepare the surfactant/buffer solution in certain concentration, simply dissolve the corresponding surfactant in *tris*-HCl buffer.

For example:

100 mL 2 wt % TPGS-750-M/buffer solution = 2 g TPGS-750-M + 98 mL *tris*-HCl buffer.

10 mL 2 wt % PTS-600/Buffer = 0.2 g PTS-600 + 9.8 mL *tris*-HCl buffer.

10 mL 4 wt % TPGS-750-M/buffer solution = 0.4 g TPGS-750-M + 9.6 mL *tris*-HCl buffer.

#### ***3.5.4. General procedure for IRED screening***

The screening of IREDs was conducted on 0.01mmol scale.

*Stock solution preparation:*

1. Starting material: In a 1-dram vial equipped with a magnetic stir bar, the ketone (0.15 mmol) and amine (0.3 mmol) were added and dissolved in DMSO (0.75 mL). The vial was then capped with a screw cap and stirred at rt for 5 min before use.

2. Co-factor: In a 2-dram vial equipped with a magnetic stir bar, NADP<sup>+</sup> (1 mM, 3.8 mg), GDH-101 (1 mg/mL, 5 mg), D-glucose (25 mM, 22.6 mg) were added. *tris*-HCl Buffer (5 mL) was then added to the vial and the solution was stirred at rt for 5 min before use.

*Reaction setup:*

To nine 1-dram vials, each equipped with a magnetic stir bar, IRED-1, IRED-3, IRED-17, IRED-18, IRED-33, IRED-44, IRED-49, IRED-69, IRED-72 (1 mg each) were added to one vial. The co-factor stock solution (0.5 mL) was then added via a 1 mL syringe followed by the starting material stock solution (0.05 mL) via a pipette gun. The reaction vial was capped with a screw cap and stirred vigorously (1000 rpm) in an aluminum block placed over an IKA hot plate at 35 °C for ~16 h.

*Work up:*

Each reaction mixture was basified with 5 M NaOH (~0.5 mL) to pH 13–14 (indicated by pH indicator paper). The resulting mixture was extracted with EtOAc (3 x 2 mL). The organic

layer was separated with the aid of a low-speed centrifuge for 5 min. The organic phases were combined, and volatiles were evaporated under reduced pressure. The crude residue was then dissolved in  $\text{CDCl}_3$  and analyzed by NMR. In terms of cases needing an internal standard, a fresh solution of  $\text{C}_2\text{H}_2\text{Cl}_4$  in  $\text{CDCl}_3$  is added as NMR solvent.

### ***3.5.5. General procedure for surfactant screening***

The screening of surfactant was conducted on 0.01 mmol scale.

#### *Stock solution preparation:*

1. Starting material: In a 1-dram vial equipped with a magnetic stir bar, the ketone (0.15 mmol) and amine (0.3 mmol) were added and dissolved in DMSO (0.75 mL). The vial was then capped with a screw cap and stirred at rt for 5 min before use.

2. Co-factor: In a 2-dram vial equipped with a magnetic stir bar, the chosen IRED (2 mg/mL, 10 mg),  $\text{NADP}^+$  (1 mM, 3.8 mg), GDH-101 (1 mg/mL, 5 mg), D-glucose (25 mM, 22.6 mg) was added. *tris*-HCl buffer (0.5 mL\*) was then added to the vial and the solution was then stirred at rt for 5 min before use.

\* In contrast to IRED screening and time course studies, which utilize the same surfactant in all reactions using a co-factor stock solution, in this experiment, the concentration of the stock solution was maximized by using only 0.5 mL of buffer. This approach minimizes fluctuations in surfactant concentration.

#### *Reaction setup:*

To the same nine 1-dram-vials each equipped with a magnetic stir bar, a different surfactant/buffer solution (0.5 mL) was added to each corresponding vial. The co-factor stock solution (0.05 mL) was then added via a pipette gun followed by the starting material stock solution, also (0.05 mL) via a pipette gun. The reaction vial was capped with a screw cap and

stirred vigorously (1000 rpm) in an aluminum block placed over an IKA hot plate at 35 °C for ~16 h.

*Work up:*

The work up and method of analysis are the same as for the IRED screening, described in section 3.5.4.

**3.5.6. General procedure for obtaining kinetic data**

The time-course study was conducted on reactions run on a 0.01 mmol scale.

*Stock solution preparation:*

1. Starting material: In a 1-dram vial equipped with a magnetic stir bar, the ketone (0.3 mmol) and amine (0.6 mmol) were added and dissolved in DMSO (1.5 mL). The vial was then capped with a screw cap and stirred at rt for 5 min before use.

2. Cofactor: In a 20 mL vial equipped with a magnetic stir bar, the chosen IRED (2 mg/mL, 22 mg), NADP<sup>+</sup> (1 mM, 8.4 mg), GDH-101 (1 mg/mL, 11 mg), D-glucose (25 mM, 49.7 mg) were added. *tris*-HCl buffer (11 mL) was then added to the vial and the solution was then stirred at rt for 5 min before use.

*Reaction setup:*

To seven 1-dram-vials equipped with a magnetic stir bar, the cofactor stock solution (0.5 mL) was added via a 1 mL syringe followed by the starting material stock solution (0.05 mL) via a pipette gun. The reaction vial was capped with a screw cap and stirred vigorously (1000 rpm) in an aluminum block placed over an IKA hot plate at 35 °C. The reactions were sequentially stopped at 0.5 h, 1 h, 2 h, 4 h, 7h, 20/24 h according to the work up procedure. Each reaction was repeated three times, and the average or the most reasonable data was chosen for inclusion in the kinetic curve.

*Work up:*

The work up and method of analysis are the same as used previously for IRED screening, described in section 3.5.4.

### ***3.5.7. General procedure for the synthesis of secondary amines by IRED***

#### ***Method A***

The ketone (0.10 mmol) and amine (0.20 mmol) reaction partners were added to a 20 mL vial equipped with a magnetic stir bar. A solution of 2 wt % TPGS-750-M in a *tris*-HCl buffer (5 mL, pH = 8) was then added and the mixture stirred at 35 °C for 2 min to afford an emulsified solution. IRED (2 mg/mL, 10 mg), NADP<sup>+</sup> (1 mM, 3.8 mg), GDH-101 (1 mg/mL, 5 mg), D-glucose (25 mM, 22.6 mg) were then added sequentially. The reaction vial was capped with a screw cap and stirred vigorously (1000 rpm) in an aluminum block placed over an IKA hot plate at 35 °C.

*Workup:* The reaction mixture was basified with 5 M NaOH (~3 mL) to pH 13–14 (indicated by pH indicator paper). The resulting mixture was extracted with EtOAc (5 x 5.0 mL). The organic layer was separated with the aid of a low-speed centrifuge for 5 min. The combined organic phases were collected and dried over anhydrous MgSO<sub>4</sub>. Volatiles were evaporated under reduced pressure. The residue was then derivatized to facilitate isolation and characterization.

*Cbz protection:* To a stirred solution of the crude product in DCM (0.5 mL) was added sodium carbonate (3 equiv, 0.30 mmol, 31.8 mg), and benzyl chloroformate (3.0 equiv, 0.30 mmol, 51.2 mg, 42.6  $\mu$ L). Upon completion of the reaction, the solvents were evaporated *in vacuo*. The Cbz-protected amines were purified *via* preparative TLC with 0-10% EtOAc/hexanes.

*N-Trifluoroacetyl derivatization:* To a stirred solution of the extracted crude product in DCM (0.5 mL) were added pyridine (1.5 equiv, 0.15 mmol, 11.9 mg, 12.1  $\mu$ L) and TFAA (1.5

equiv, 0.15 mmol, 31.5 mg, 20.9  $\mu$ L). Upon completion of the reaction, saturated NaHCO<sub>3</sub> solution (1 mL) was added, the mixture was then vortexed, and the organic layer separated. The trifluoroacetyl derivatized amines were purified *via* preparative TLC with 0-10% EtOAc/hexanes.

### ***Method B***

*Imine formation:* The ketone (0.20 mmol) and amine (2 equiv, 0.40 mmol) were added to a 1-dram vial containing C<sub>4</sub>F<sub>9</sub>SO<sub>3</sub>H (0.5 equiv, 0.1 mmol, 30 mg) and DMSO (0.2 mL), and the resulting mixture was capped with a screw cap and stirred vigorously (1000 rpm) at rt. overnight giving crude imine. The formation of the expected crude imine was confirmed by NMR, the sample being prepared by dissolving ~10  $\mu$ L reaction mixture in ~0.8 mL CDCl<sub>3</sub>.

*IRED reduction:* IRED (2 mg/mL, 10 mg), NADP<sup>+</sup> (1 mM, 3.8 mg), GDH-101 (1 mg/mL, 5 mg), and D-glucose (25 mM, 22.6 mg) were added to a 20 mL vial equipped with a magnetic stir bar. A solution of 2 wt % TPGS-750-M in a *tris*-HCl buffer (5 mL, pH = 8) was then added. The crude imine-containing reaction (0.1 mL) was then added to this mixture via a syringe. The reaction vial was then capped with a screw cap and stirred vigorously (1000 rpm) in an aluminum block placed over an IKA hot plate at 35 °C. Workup and derivatization methods are same as used above.

### ***3.5.8. General procedure for the synthesis of standard racemic secondary amines***

*For amines III-19- III-21:*

To a 2-dram vial equipped with a magnetic stir bar, ketone (0.5 mmol) was added dissolved in THF (0.2 M, 2.5 mL). Amine (1.1 equiv, 0.55 mmol) and HOAc (1 equiv, 0.03 mL) were sequentially added. The mixture was stirred for 1 min before adding NaBH(OAc)<sub>3</sub> (1.5 equiv, 0.75 mmol, 159 mg). The resulting mixture was then stirred at rt overnight. Upon



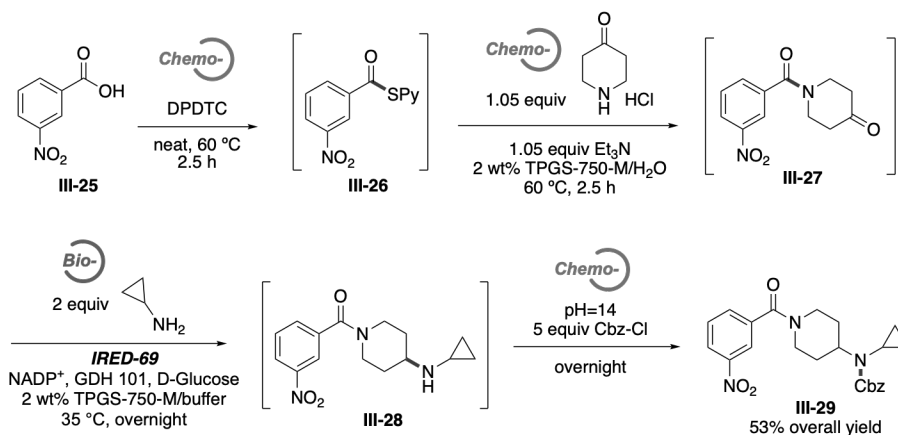
completion, 5 M NaOH (~2 mL) was added to quench the reaction. Then EtOAc (1 mL) was added and the phases were separated. The aqueous phase was further extracted with EtOAc (2 x 2 mL). The organic phases were combined, dried over anhydrous MgSO<sub>4</sub>, and then filtered. The solvent was then removed under reduced pressure to obtain the crude racemic amine. The crude product was directly subjected to trifluoroacetyl derivatization using TFAA following the same procedure as described in section 2.5.

*For amines III-22- III-24:*

The ketone (0.5 mmol) and amine (2 equiv, 1 mmol) were added to a 2-dram vial containing C<sub>4</sub>F<sub>9</sub>SO<sub>3</sub>H (0.5 equiv, 0.25 mmol, 75 mg) and DMSO (0.5 mL), and the resulting mixture was capped with a screw cap and stirred vigorously (1000 rpm) at rt. overnight. Then, sodium borohydride (2 equiv, 1 mmol, 37.8 mg) and THF (1 mL) were added. The resulting reaction mixture was stirred for another 2 h at rt. Upon completion, the reaction was quenched by the addition of water (2 mL). The crude product was extracted using EtOAc (3 x 2 mL). The organic phases were combined, dried over anhydrous MgSO<sub>4</sub>, and filtered. The solvent was then removed under reduced pressure to obtain crude racemic amine. The crude material was directly subjected to trifluoroacetyl derivatization using the same procedure described in section 2.5.

### 3.5.9. 1-Pot sequence

Sequence A:



#### Step 1: Thioester formation

To a 1-dram vial, a magnetic stir bar, 3-nitrobenzoic acid (0.1 mmol, 16.7 mg) and DPDTC (1.05 equiv, 0.105 mmol, 26.1 mg) were added. The content was stirred (~400 rpm) in an aluminum block placed over an IKA hot plate at 60 °C until full consumption of the acid, as determined by TLC (~2.5 h).

#### Step 2: Amide formation

Upon completion, piperidin-4-one hydrochloride (1.05 equiv, 0.105 mmol, 14.3 mg), triethylamine (1.05 equiv, 0.105 mmol, 10.6 mg, 14.6  $\mu\text{L}$ ) and 2 wt % TPGS-750-M/H<sub>2</sub>O solution (0.5 M, 0.2 mL) were directly added and stirred in an aluminum block placed over an IKA hot plate at 60 °C until complete consumption of the thioester (~2.5 h).

#### Step 3: IRED reduction

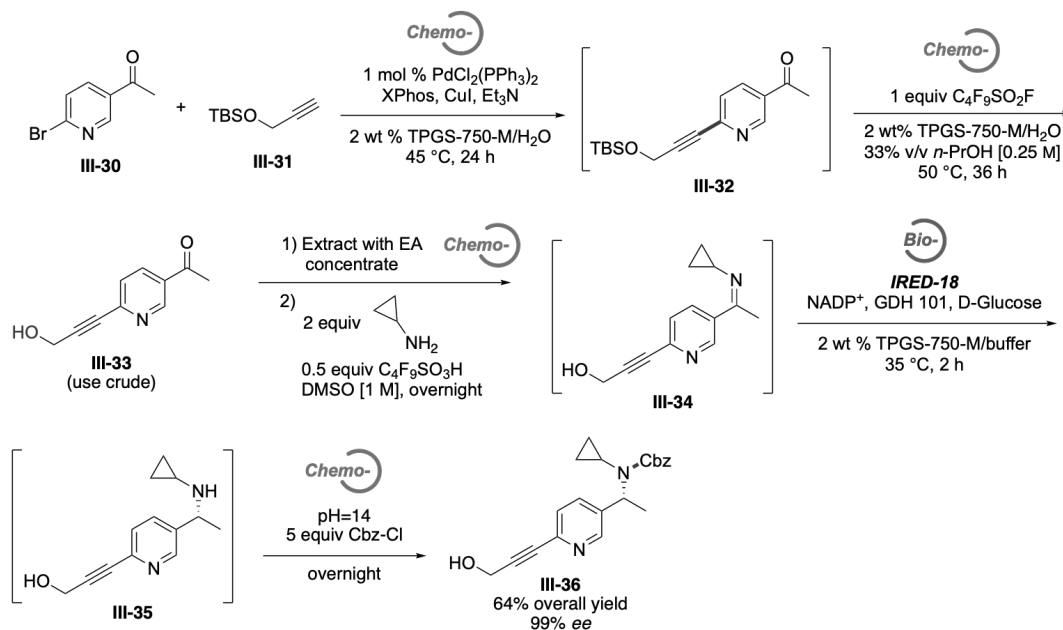
IRED-69 (2 mg/mL, 10 mg), NADP<sup>+</sup> (1 mM, 3.8 mg), GDH-101 (1 mg/mL, 5 mg), and D-glucose (25 mM, 22.6 mg) were added to a 10-dram vial containing a magnetic stir bar. The first portion of 2 wt % TPGS-750-M in *tris*-HCl buffer solution (3 mL, pH = 8) was added into the 10-dram vial and the resulting mixture stirred for 1 min to dissolve the IRED and cofactors. Then, the amide formed in the previous reaction mixture (in a 1-dram vial) was

transferred into the 10-dram vial using a pipette. The second portion of 2 wt % TPGS-750-M in *tris*-HCl buffer solution (2 mL, pH = 8) was used to help by washing the 1-dram vial, done three times. Then, cyclopropanamine (2 equiv, 0.2 mmol, 14  $\mu$ L) was added. The reaction vial was capped with a screw cap and stirred vigorously (1000 rpm) in an aluminum block placed over an IKA hot plate at 35  $^{\circ}$ C for 12 h.

*Step 4: Cbz protection*

The reaction mixture was basified by adding NaOH (~100 mg) to pH = 14 (indicated by pH indicator paper). Benzyl chloroformate (5.0 equiv, 0.50 mmol, 85.3 mg, 71.1  $\mu$ L) was then added in one portion. The reaction was then stirred for another 8 h until fully complete. The resulting mixture was extracted with EtOAc (5 x 5.0 mL). The organic layer was separated with the aid of a low-speed centrifuge for 5 min. The combined organic phases were collected and dried over anhydrous MgSO<sub>4</sub>. Volatiles were evaporated under reduced pressure. The product **III-29** was purified *via* preparative TLC with 50% EtOAc/hexanes as a white solid (22.3 mg, 53% yield).

*Sequence B:*



### *Step 1: Sonogashira coupling*

To a flame-dried 1-dram vial equipped with an oven-dried stir bar was added 1-(6-bromopyridin-3-yl)ethan-1-one (0.2 mmol, 40 mg) and *t*-butyldimethyl(prop-2-yn-1-yloxy)silane (2 equiv, 0.4 mmol, 68 mg). The vial was then transferred into an argon-purged glove box to which was added PdCl<sub>2</sub>(PPh<sub>3</sub>)<sub>2</sub> (0.01 equiv, 0.002 mmol, 1.4 mg), XPhos (0.01 equiv, 0.01 equiv, 1 mg), and CuI (0.02 equiv, 0.004 mmol, 0.76 mg). The vial was sealed with a rubber septum and removed from the glove box. Then, triethylamine (2 equiv, 0.4 mmol, 40.5 mg, 55  $\mu$ L) and 2 wt % TPGS-750-M/H<sub>2</sub>O (0.4 mL) were added to the vial via syringe and the vial was then stirred vigorously under constant argon pressure at 45 °C in an aluminum block placed over an IKA hot plate for 24 h.

### *Step 2: Deprotection*

After complete consumption of starting material, the septum was removed. Nonafluorobutane-1-sulfonyl fluoride (1 equiv, 0.2 mmol, 60.4 mg) was added to the vial under an argon flow. 2 wt % TPGS-750-M/H<sub>2</sub>O (0.13 mL) and *n*-PrOH (0.27 mL) were added via syringe. The vial was sealed with a rubber septum and stirred vigorously under constant argon pressure at 50 °C in an aluminum block placed over an IKA hot plate for 36 h. The progress of the reaction was monitored by TLC.

### *Step 3: Imine formation*

After 36 h, the septum was removed. The aqueous reaction mixture was extracted with EtOAc (5 x 1 mL). The organic layer was combined and the solvent was removed *in vacuo*. To the vial containing the crude intermediate, nonafluorobutane-1-sulfonic acid (30 mg, 0.1 mmol, 0.5 equiv) was added. Then DMSO (0.2 mL) and cyclopropanamine (2 equiv, 0.4 mmol, 22.8 mg, 28  $\mu$ L) were added to the vial. The vial was capped and stirred vigorously at rt overnight. The progress of the reaction was monitored by crude <sup>1</sup>H NMR.

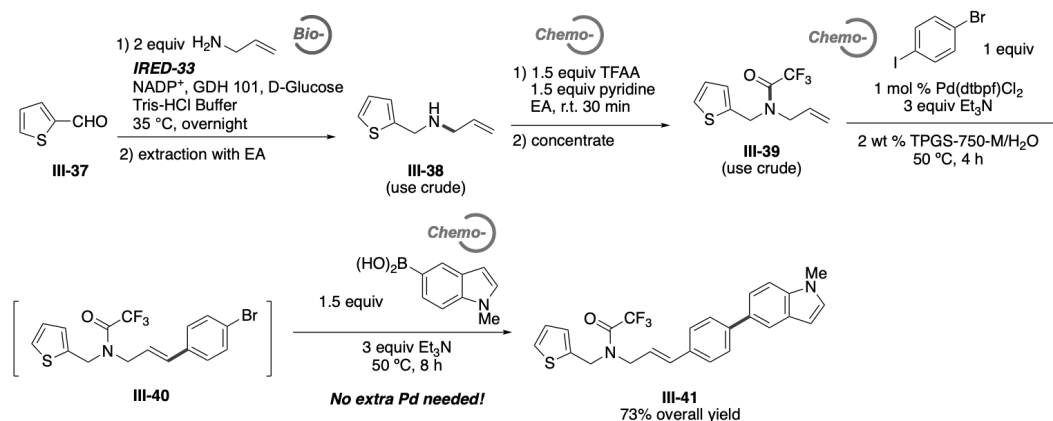
#### Step 4: IRED reduction

After complete consumption of starting material, the cap was removed. In a 10-dram vial, IRED-18 (2 mg/mL, 20 mg), NADP<sup>+</sup> (1 mM, 7.6 mg), GDH-101 (1 mg/mL, 10 mg), and D-glucose (25 mM, 45.2 mg) were added and dissolved in 10 mL 2 wt % TPGS-750-M/buffer to make a solution. Then the imine solution in DMSO was added to the aqueous solution with washed in using minimal amounts of DMSO. The vial was capped and stirred vigorously at 35 °C in an aluminum block placed over an IKA hot plate for 2 h. The progress of the reaction was monitored by crude <sup>1</sup>H NMR.

#### Step 5: Cbz protection

After complete consumption of starting material, the reaction mixture was basified by adding NaOH (~100 mg) to pH = 14 (indicated by pH indicator paper). Then, benzyl chloroformate (170.6 mg, 1 mmol, 0.14 mL) was added via syringe and the contents of the vial were stirred vigorously for 24 h. The resulting mixture was extracted with EtOAc (5 x 10 mL). The organic layer was separated with the aid of a low-speed centrifuge for 5 min. The combined organic phases were collected and dried over anhydrous MgSO<sub>4</sub>. The volatiles were evaporated under reduced pressure and the product **III-36** was purified *via* preparative TLC using 70% EtOAc/hexanes as a yellow oil (44.5 mg, 64% overall yield, 99% ee).

#### Sequence C:



*Step 1: IRED reduction:*

Thiophene-2-carbaldehyde (0.10 mmol) and allylamine (0.20 mmol) were added to a 20 mL vial equipped with a magnetic stir bar. *tris*-HCl Buffer (5 mL, pH = 8) was then added and the mixture stirred at 35 °C for 2 min to afford an emulsified solution. IRED (2 mg/mL, 10 mg), NADP<sup>+</sup> (1 mM, 3.8 mg), GDH-101 (1 mg/mL, 5 mg), and D-glucose (25 mM, 22.6 mg) were then added sequentially. The reaction vial was capped with a screw cap and stirred vigorously (1000 rpm) at 35 °C in an aluminum block placed over an IKA hot plate for 12 h. Upon completion, the reaction mixture was basified with 5 M NaOH (~3 mL) to pH 13–14 (indicated by pH indicator paper). The resulting mixture was extracted with EtOAc (5 x 5.0 mL). The organic layer was separated with the aid of a low-speed centrifuge for 5 min. The combined organic phases were collected and dried over anhydrous MgSO<sub>4</sub>. The volatiles were evaporated under reduced pressure and the residue was then transferred to a 1-dram vial using minimal EtOAc.

*Step 2: Trifluoroacetyl derivatization:*

The 1-dram vial containing the crude reaction mixture was equipped with a magnetic stir bar. Pyridine (1.5 equiv, 0.15 mmol, 11.9 mg, 12.1 μL) and TFAA (1.5 equiv, 0.15 mmol, 31.5 mg, 20.9 μL) were added sequentially. The resulting mixture was then stirred at rt for 4 h. Upon completion of the reaction, solvent was removed under reduced pressure.

*Step 3: Mizoroki-Heck coupling:*

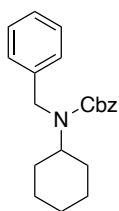
Pd(dtbpf)Cl<sub>2</sub> (1 mol %, 0.001 mmol, 0.7 mg) and 1-bromo-4-iodobenzene (1 equiv, 0.1 mmol, 28.1 mg) were then added to the vial. The vial was capped with a rubber septum then evacuated and backfilled with argon three times. Next, Et<sub>3</sub>N (3 equiv, 0.3 mmol, 42 μL), then 2 wt % TPGS-750-M aqueous solution (0.5 M, 0.2 mL) were added via syringe through the

septum. The vial was stirred vigorously at 45 °C in an aluminum block placed over an IKA hot plate for 4 h.

*Step 4: Suzuki-Miyaura coupling:*

After cooling to rt, the septum was removed and (1-methyl-1*H*-indol-5-yl)boronic acid (1.5 equiv, 0.15 mmol, 26.3 mg) was added. The vial was then sealed with a new rubber septum and the headspace was purged using argon and a vent needle for 5 min, and Et<sub>3</sub>N (3 equiv, 0.3 mmol, 42 μL) was added via syringe through the septum. The resulting mixture was then stirred vigorously at 45 °C in an aluminum block placed over an IKA hot plate for 8 h. Upon completion, the mixture was extracted with EtOAc (3 x 1 mL), the organic phases were combined, dried over anhydrous MgSO<sub>4</sub>, and filtered. The solvent was then removed under reduced pressure to obtain the crude racemic amine, which was further purified *via* preparative TLC with 15% EtOAc/hexanes ( $R_f = 0.30$ ) to give product **III-41** as a pale brown oil (32.9 mg, 73% yield).

**3.5.10. Analytical data**



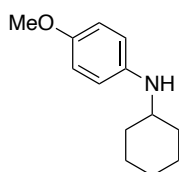
**benzyl benzyl(cyclohexyl)carbamate (III-1)**

Following method A and using enzyme IRED-33, the product was isolated *via* preparative TLC with 5% EtOAc/hexanes ( $R_f = 0.45$ ) as a colorless oil; 28.1 mg from a 0.1 mmol batch, 87% yield.

**<sup>1</sup>H NMR** (400 MHz, chloroform-*d*)  $\delta$  7.46 – 7.09 (m, 10H), 5.17 (d,  $J = 38.3$  Hz, 2H), 4.46 (s, 2H), 3.94 (d,  $J = 70.1$  Hz, 1H), 1.78 – 1.56 (m, 5H), 1.45 – 1.21 (m, 4H), 1.09 – 0.94 (m, 1H).

**<sup>13</sup>C NMR** (126 MHz, chloroform-*d*)  $\delta$  156.9, 156.3, 139.8, 136.8, 128.4, 128.3, 127.8, 127.1, 126.7, 126.6, 67.0, 56.5, 47.3, 46.5, 31.6, 31.0, 25.9, 25.5.

**HRMS** (ESI-TOF)  $m/z$ :  $[M]^+$  calcd for C<sub>21</sub>H<sub>25</sub>NO<sub>2</sub> 323.1885; found 323.1887.



### ***N*-cyclohexyl-4-methoxyaniline (III-2)**

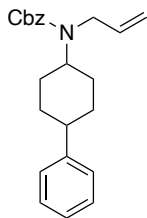
Following method A and using enzyme IRED-18, the product was isolated *via* flash column chromatography using 7% EtOAc/hexanes ( $R_f = 0.30$ ) as a yellow-brown oil, 19.4 mg from a 0.1 mmol batch, 94% yield.

**<sup>1</sup>H NMR** (400 MHz, chloroform-*d*)  $\delta$  6.80 – 6.72 (m, 2H), 6.61 – 6.54 (m, 2H), 3.74 (s, 3H), 3.16 (tt,  $J = 10.2, 3.7$  Hz, 1H), 2.64 (s, 1H), 2.05 (dp,  $J = 9.9, 3.6, 2.9$  Hz, 2H), 1.75 (dq,  $J = 11.1, 3.8$  Hz, 2H), 1.69 – 1.60 (m, 1H), 1.34 (ddt,  $J = 13.0, 11.7, 3.3$  Hz, 2H), 1.25 – 1.18 (m, 1H), 1.17 – 1.07 (m, 2H).

**<sup>13</sup>C NMR** (101 MHz, chloroform-*d*)  $\delta$  151.9, 141.5, 114.9, 55.9, 52.9, 33.6, 26.0, 25.1.

Spectral data matched those previously reported.<sup>2</sup>





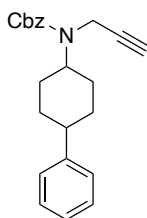
**benzyl allyl(4-phenylcyclohexyl)carbamate (III-17)**

Following method A and using enzyme IRED-69, the product was isolated *via* preparative TLC with 5% EtOAc/hexanes ( $R_f = 0.20$ ) as a white solid; 29.2 mg from a 0.1 mmol batch, 84% yield.

$^1\text{H NMR}$  (400 MHz, chloroform- $d$ )  $\delta$  7.37 – 7.28 (m, 9H), 7.19 (tq,  $J = 6.7, 1.8$  Hz, 1H), 5.74 (ddt,  $J = 18.0, 10.5, 5.5$  Hz, 1H), 5.13 (s, 2H), 5.00 (dt,  $J = 11.9, 1.8$  Hz, 2H), 3.71 (d,  $J = 5.5$  Hz, 2H), 3.03 (dq,  $J = 5.3, 2.6$  Hz, 1H), 2.33 – 2.24 (m, 2H), 1.87 (td,  $J = 16.1, 14.3, 5.4$  Hz, 2H), 1.63 – 1.57 (m, 5H).

$^{13}\text{C NMR}$  (126 MHz, chloroform- $d_3$ )  $\delta$  156.1, 143.9, 137.0, 135.8, 128.4, 128.3, 127.8, 127.8, 127.5, 125.5, 115.7, 66.9, 55.9, 35.5, 29.7, 29.4, 26.4.

**HRMS** (ESI-TOF)  $m/z$ :  $[\text{M}]^+$  calcd for  $\text{C}_{23}\text{H}_{27}\text{NO}_2$  349.2042; found 349.2040.



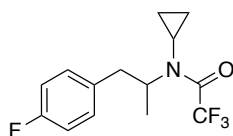
**benzyl (4-phenylcyclohexyl)(prop-2-yn-1-yl)carbamate (III-18)**

Following method A and using enzyme IRED-69, the product was isolated *via* preparative TLC with 5% EtOAc/hexanes ( $R_f = 0.20$ ) as a pale yellow oil; 24.7 mg from a 0.1 mmol batch, 71% yield.

**<sup>1</sup>H NMR** (400 MHz, chloroform-*d*)  $\delta$  7.43 – 7.27 (m, 9H), 7.20 (t,  $J = 7.0$  Hz, 1H), 5.18 (s, 2H), 4.09 (s, 1H), 3.99 – 3.81 (m, 2H), 3.04 (t,  $J = 4.1$  Hz, 1H), 2.31 (dt,  $J = 14.8, 3.2$  Hz, 2H), 2.16 – 2.05 (m, 1H), 1.88 (dq,  $J = 14.0, 5.2$  Hz, 2H), 1.72 (qd,  $J = 9.6, 8.2, 3.3$  Hz, 4H).

**<sup>13</sup>C NMR** (126 MHz, chloroform-*d*)  $\delta$  155.6, 143.9, 136.8, 128.5, 128.4, 127.9, 127.8, 127.5, 125.6, 81.2, 70.7, 67.3, 55.9, 35.7, 29.4, 26.3.

**HRMS** (ESI-TOF)  $m/z$ :  $[M]^+$  calcd for C<sub>23</sub>H<sub>25</sub>NO<sub>2</sub> 347.1885; found 347.1888.



***N*-cyclopropyl-2,2,2-trifluoro-*N*-(1-(4-fluorophenyl)propan-2-yl)acetamide (III-19)**

Following method A and using enzyme IRED-69, the product was isolated *via* preparative TLC with 5% EtOAc/hexanes ( $R_f = 0.30$ ) as a pale yellow solid, 19.2 mg from a 0.1 mmol batch, 66% yield, 90% *ee*.

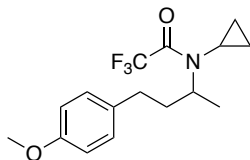
**<sup>1</sup>H NMR** (400 MHz, chloroform-*d*)  $\delta$  7.17 – 7.10 (m, 2H), 6.98 (td,  $J = 8.6, 1.6$  Hz, 2H), 3.95 (dt,  $J = 9.1, 6.5$  Hz, 1H), 3.31 (dd,  $J = 13.7, 9.2$  Hz, 1H), 2.77 (dd,  $J = 13.7, 6.4$  Hz, 1H), 2.48 (tt,  $J = 7.5, 4.2$  Hz, 1H), 1.43 (d,  $J = 6.9$  Hz, 3H), 0.82 – 0.56 (m, 4H).

**<sup>13</sup>C NMR** (101 MHz, chloroform-*d*)  $\delta$  162.97 (q,  $^1J_{CF} = 244.6$  Hz), 159.3 (q,  $^2J_{CF} = 36.0$  Hz), 134.6, 134.6, 130.4, 130.3, 116.3 (q,  $^1J_{CF} = 288.2$  Hz), 115.3 (q,  $^2J_{CF} = 21.3$  Hz), 61.9, 38.7, 31.1, 18.1, 8.9, 7.8.

**<sup>19</sup>F NMR** (376 MHz, chloroform-*d*)  $\delta$  -69.38, -116.39.

The enantioselectivity was determined by HPLC analysis: Chiralcel<sup>®</sup> 5  $\mu$ m OD-H column 150 x 4.6 mm, isopropanol : *n*-hexane = 1:99, flow rate 0.5 mL/min, I = 260 nm,  $t_1 = 4.86$  min,  $t_2 = 5.06$  (major).

**HRMS** (ESI-TOF)  $m/z$ :  $[M]^+$  calcd for C<sub>14</sub>H<sub>15</sub>F<sub>4</sub>NO 289.1090; found 289.1099.



***N*-cyclopropyl-2,2,2-trifluoro-*N*-(4-(4-methoxyphenyl)butan-2-yl)acetamide (III-20)**

Following method A and using enzyme IRED-33, the product was isolated *via* preparative TLC with 5% EtOAc/hexane ( $R_f = 0.25$ ) as a colorless oil, 21.4 mg from a 0.1 mmol batch, 68% yield, 80% *ee*.

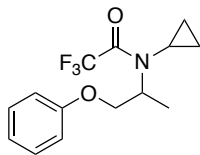
**$^1\text{H}$  NMR** (400 MHz, chloroform-*d*)  $\delta$  7.12 – 7.05 (m, 2H), 6.87 – 6.78 (m, 2H), 4.03 – 3.92 (m, 1H), 3.78 (s, 3H), 2.90 – 2.69 (m, 1H), 2.61 – 2.47 (m, 2H), 2.24 – 2.09 (m, 1H), 1.90 (ddt,  $J = 13.4, 9.7, 6.7$  Hz, 1H), 1.35 (d,  $J = 6.9$  Hz, 3H), 0.94 – 0.81 (m, 4H).

**$^{13}\text{C}$  NMR** (126 MHz, chloroform-*d*)  $\delta$  159.4 (q,  $^2J_{CF} = 35.8$  Hz), 158.0, 133.3, 129.2, 116.6 (q,  $^1J_{CF} = 288.54$  Hz) 113.9, 57.7, 55.3, 36.1, 32.3, 29.5, 18.7, 8.5, 7.7.

**$^{19}\text{F}$  NMR** (376 MHz, chloroform-*d*)  $\delta$  -68.90.

The enantioselectivity was determined by HPLC analysis: Chiralpak IG column (4.6 mm  $\times$  25 cm, 5 micron) isopropanol : *n*-hexane = 5:95, flow rate 1 mL/min,  $I = 230$  nm,  $t_1 = 6.87$  min (major),  $t_2 = 7.63$  min.

**HRMS** (ESI-TOF)  $m/z$ :  $[\text{M}]^+$  calcd for  $\text{C}_{16}\text{H}_{20}\text{F}_3\text{NO}_2$  315.1446; found 315.1460.



***N*-cyclopropyl-2,2,2-trifluoro-*N*-(1-phenoxypropan-2-yl)acetamide (III-21)**

Following method A and using enzyme IRED-33, the product was isolated *via* preparative TLC with 5% EtOAc/hexane ( $R_f = 0.30$ ) as a colorless oil, 17.3 mg from a 0.1 mmol batch, 60% yield, 91% *ee*.

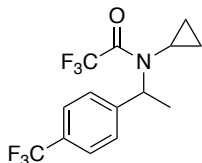
$^1\text{H NMR}$  (400 MHz, chloroform-*d*)  $\delta$  7.31 – 7.24 (m, 2H), 6.99 – 6.93 (m, 1H), 6.90 – 6.84 (m, 2H), 4.45 (t,  $J = 9.1$  Hz, 1H), 4.22 (q,  $J = 7.0$  Hz, 1H), 3.99 (dd,  $J = 9.7, 5.0$  Hz, 1H), 3.03 – 2.86 (m, 1H), 1.45 (d,  $J = 7.1$  Hz, 3H), 1.10 – 0.86 (m, 4H).

$^{13}\text{C NMR}$  (101 MHz, chloroform-*d*)  $\delta$  159.6 (q,  $^2J_{CF} = 36.1$  Hz), 158.3, 129.6, 121.2, 116.3 q, ( $^1J_{CF} = 288.9$  Hz), 114.5, 8.0, 58.6, 31.0, 15.1, 8.8, 8.6.

$^{19}\text{F NMR}$  (376 MHz, chloroform-*d*)  $\delta$  -69.25.

The enantioselectivity was determined by HPLC analysis: Chiralcel<sup>®</sup> 5  $\mu\text{m}$  OD-H column 150 x 4.6 mm, isopropanol : *n*-hexanes = 5:95, flow rate 1 mL/min, I = 230 nm,  $t_1 = 5.18$  min,  $t_2 = 5.81$  (major).

**HRMS** (ESI-TOF)  $m/z$ :  $[\text{M}]^+$  calcd for  $\text{C}_{14}\text{H}_{16}\text{F}_3\text{NO}_2$  287.1133; found 287.1143.



***N*-cyclopropyl-2,2,2-trifluoro-*N*-(1-(4-(trifluoromethyl)phenyl)ethyl)acetamide (III-22)**

Following method B and using enzyme IRED-18, the product was isolated *via* preparative TLC with 7% EtOAc/hexanes ( $R_f = 0.30$ ) as a colorless oil, 31.9 mg from a 0.1 mmol batch, 92% yield, >99% *ee*.

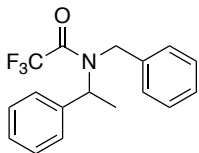
$^1\text{H NMR}$  (400 MHz, chloroform-*d*)  $\delta$  7.59 (d,  $J = 8.1$  Hz, 2H), 7.38 (d,  $J = 8.0$  Hz, 2H), 5.54 (d,  $J = 9.0$  Hz, 1H), 2.79 (s, 1H), 1.79 (d,  $J = 7.1$  Hz, 3H), 0.91 – 0.51 (m, 4H).

$^{13}\text{C}$  NMR (126 MHz, chloroform-*d*)  $\delta$  160.1 (q,  $^2J_{\text{CF}} = 36.7$  Hz), 144.9, 129.7 (q,  $^2J_{\text{CF}} = 32.6$  Hz), 126.9, 124.1 (q,  $^1J_{\text{CF}} = 172.16$  Hz), 125.5 (q,  $^3J_{\text{CF}} = 3.8$  Hz), 116.6 (q,  $^1J_{\text{CF}} = 287.8$  Hz), 56.4, 28.6, 16.8, 8.8, 6.6.

$^{19}\text{F}$  NMR (376 MHz, chloroform-*d*)  $\delta$  -62.59, -68.84.

The enantioselectivity was determined by HPLC analysis: Chiralcel<sup>®</sup> 5  $\mu\text{m}$  OD-H column 150 x 4.6 mm, isopropanol : *n*-hexane = 0.5:99.5, flow rate 1 mL/min, I = 254 nm,  $t_1 = 14.29$  min (major),  $t_2 = 16.65$  min

**HRMS** (ESI-TOF) *m/z*:  $[\text{M}]^+$  calcd for  $\text{C}_{14}\text{H}_{13}\text{F}_6\text{NO}$  325.0901; found 325.0895.



### ***N*-benzyl-2,2,2-trifluoro-*N*-(1-phenylethyl)acetamide (III-23)**

Following method B and using enzyme IRED-18, the product was isolated *via* preparative TLC with 20% EtOAc/hexanes ( $R_f = 0.35$ ) as a white solid, 33.6 mg from a 0.1 mmol batch, 99% yield, >99% *ee*.<sup>3</sup>

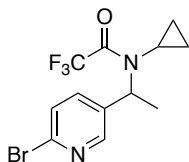
$^1\text{H}$  NMR (400 MHz, chloroform-*d*)  $\delta$  7.46 – 6.97 (m, 10H), 5.53 (dq,  $J = 59.0, 7.1$  Hz, 1H), 4.67 (dd,  $J = 16.2, 6.5$  Hz, 1H), 4.18 (dd,  $J = 118.7, 16.1$  Hz, 1H), 1.51 (dd,  $J = 53.8, 7.1$  Hz, 3H).

$^{13}\text{C}$  NMR (126 MHz, chloroform-*d*) rotomeric mixture  $\delta$  157.7 (q,  $^2J_{\text{CF}} = 35.3$  Hz), 157.5 (q,  $^2J_{\text{CF}} = 35.3$  Hz), 138.8, 138.1, 137.0, 136.3, 128.9, 128.6, 128.4, 128.1, 127.8, 127.4, 127.4, 127.2, 127.1, 117.1 (q,  $^1J_{\text{CF}} = 288.5$  Hz), 116.7 (q,  $^1J_{\text{CF}} = 288.5$  Hz), 56.0, 55.7 (q,  $^3J_{\text{CF}} = 3.5$  Hz), 48.7, 48.7, 46.9, 18.3, 17.2.

$^{19}\text{F}$  NMR (376 MHz, chloroform-*d*)  $\delta$  -67.56, -68.04.

The enantioselectivity was determined by HPLC analysis: Chiralcel® 5  $\mu\text{m}$  OD-H column 150 x 4.6 mm, isopropanol : *n*-hexanes = 10:90, flow rate 1 mL/min, I = 210 nm,  $t_1$  = 8.67 min (major),  $t_2$  = 9.35 min

**HRMS** (ESI-TOF)  $m/z$ :  $[\text{M}]^+$  calcd for  $\text{C}_{12}\text{H}_{12}\text{BrF}_3\text{N}_2\text{O}$  338.0066; found 338.0099.



***N*-(1-(6-bromopyridin-3-yl)ethyl)-*N*-cyclopropyl-2,2,2-trifluoroacetamide (III-24)**

Following method B and using enzyme IRED-18, the product was isolated *via* preparative TLC with 5% EtOAc/hexanes ( $R_f$  = 0.20) as a colorless oil, 19.4 mg from a 0.1 mmol batch, 63% yield, 93% *ee*.

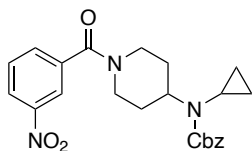
**$^1\text{H}$  NMR** (400 MHz, chloroform-*d*)  $\delta$  8.28 (s, 1H), 7.54 – 7.38 (m, 2H), 5.38 (q,  $J$  = 7.2 Hz, 1H), 2.79 (s, 1H), 1.76 (d,  $J$  = 7.2 Hz, 3H), 0.91 – 0.60 (m, 4H).

**$^{13}\text{C}$  NMR** (126 MHz, chloroform-*d*)  $\delta$  159.9 (q,  $^2J_{\text{CF}}$  = 36.3 Hz), 148.6, 141.2, 137.3, 135.7, 127.9, 116.4 (q,  $^1J_{\text{CF}}$  = 287.8 Hz), 55.3, 29.7, 29.0, 16.6, 9.0, 6.9.

**$^{19}\text{F}$  NMR** (376 MHz, chloroform-*d*)  $\delta$  -68.97.

The enantioselectivity was determined by HPLC analysis: Chiralcel® 5  $\mu\text{m}$  OD-H column 150 x 4.6 mm, isopropanol : *n*-hexanes = 10:90, flow rate 1 mL/min, I = 280 nm,  $t_1$  = 4.37 min,  $t_2$  = 4.58 min (major)

**HRMS** (ESI-TOF)  $m/z$ :  $[\text{M}]^+$  calcd for  $\text{C}_{17}\text{H}_{16}\text{F}_3\text{NO}$  307.1184; found 307.1190.



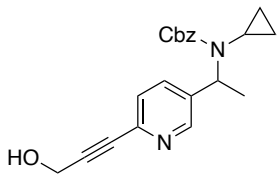
**benzyl cyclopropyl(1-(3-nitrobenzoyl)piperidin-4-yl)carbamate (III-29)**

Following one-pot sequence **A**, the product was purified *via* preparative TLC with 50% EtOAc/hexanes ( $R_f = 0.25$ ) as a white solid, 22.3 mg from a 0.1 mmol batch, 53% yield.

$^1\text{H NMR}$  (500 MHz, chloroform-*d*)  $\delta$  8.32 – 8.26 (m, 2H), 7.73 (d,  $J = 7.5$  Hz, 1H), 7.62 (t,  $J = 7.8$  Hz, 1H), 7.41 – 7.30 (m, 5H), 5.16 (s, 2H), 4.84 (s, 1H), 3.92 (tt,  $J = 12.2, 3.8$  Hz, 1H), 3.71 (s, 1H), 3.13 (s, 1H), 2.81 (s, 1H), 2.49 (tt,  $J = 7.1, 3.9$  Hz, 1H), 1.96 (dd,  $J = 130.6, 76.4$  Hz, 5H), 0.85 (td,  $J = 7.2, 5.2$  Hz, 2H), 0.77 – 0.69 (m, 2H).

$^{13}\text{C NMR}$  (126 MHz, chloroform-*d*)  $\delta$  167.6, 157.3, 148.1, 137.6, 136.6, 132.9, 129.8, 128.5, 128.0, 127.9, 124.5, 122.2, 67.2, 57.6, 47.7, 42.4, 31.0, 30.0, 27.6, 8.6.

**HRMS** (ESI-TOF)  $m/z$ :  $[\text{M}]^+$  calcd for  $\text{C}_{23}\text{H}_{25}\text{N}_3\text{O}_5$  423.1794; found 423.1792.



**benzyl cyclopropyl(1-(6-(3-hydroxyprop-1-yn-1-yl)pyridin-3-yl)ethyl)carbamate (III-36)**

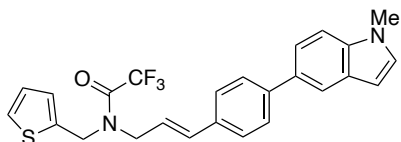
Following one-pot sequence **A**, the product was purified *via* preparative TLC with 70% EtOAc/hexanes ( $R_f = 0.20$ ) as a yellow oil, 44.5 mg from a 0.2 mmol batch, 64% yield, 99% *ee*.

$^1\text{H NMR}$  (400 MHz, chloroform-*d*)  $\delta$  8.52 (d,  $J = 2.2$  Hz, 1H), 7.63 (dd,  $J = 8.0, 2.2$  Hz, 1H), 7.44 – 7.32 (m, 6H), 5.21 (s, 2H), 4.99 (s, 2H), 3.91 (q,  $J = 6.7$  Hz, 1H), 1.93 (td,  $J = 6.3, 3.3$  Hz, 1H), 1.37 (d,  $J = 6.7$  Hz, 3H), 0.42 – 0.28 (m, 3H), 0.19 (ddt,  $J = 9.5, 6.9, 2.9$  Hz, 1H).

$^{13}\text{C NMR}$  (126 MHz, chloroform-*d*)  $\delta$  154.6, 149.3, 141.3, 140.8, 134.9, 134.4, 128.7, 128.6, 128.4, 127.1, 86.4, 81.7, 70.1, 56.1, 56.0, 29.1, 23.4, 6.9, 6.2.

The enantioselectivity was determined by HPLC analysis: Chiralcel® 5 µm OD-H column 150 x 4.6 mm, isopropanol : *n*-hexanes = 25:75, flow rate 1 mL/min, I = 230 nm,  $t_1 = 9.00$  min (major),  $t_2 = 9.54$  min

**HRMS** (ESI-TOF)  $m/z$ :  $[M+Na]^+$  calcd for  $C_{21}H_{22}N_2O_3Na$  373.1528; found 373.1527.



**(*E*)-2,2,2-trifluoro-*N*-(3-(4-(1-methyl-1*H*-indol-5-yl)phenyl)allyl)-*N*-(thiophen-2-ylmethyl)acetamide (III-41)**

Following one-pot sequence **C**, the product was purified *via* preparative TLC with 15% EtOAc/hexanes ( $R_f = 0.30$ ) as a pale brown oil, 32.9 mg from a 0.1 mmol batch, 73% yield.

**$^1H$  NMR** (500 MHz, chloroform-*d*)  $\delta$  7.92 – 7.87 (m, 1H), 7.68 (dd,  $J = 12.3, 8.0$  Hz, 2H), 7.50 (tt,  $J = 14.9, 7.4$  Hz, 3H), 7.42 (dd,  $J = 8.6, 3.9$  Hz, 1H), 7.35 (ddd,  $J = 20.9, 4.9, 1.4$  Hz, 1H), 7.15 – 7.00 (m, 3H), 6.70 – 6.55 (m, 2H), 6.15 (dtd,  $J = 15.4, 6.7, 1.9$  Hz, 1H), 4.84 (d,  $J = 2.8$  Hz, 2H), 4.22 (dd,  $J = 6.4, 4.2$  Hz, 2H), 3.86 (d,  $J = 2.1$  Hz, 3H).

**$^{13}C$  NMR** (126 MHz, chloroform-*d*) rotomeric mixture  $\delta$  156.9 (q,  $^2J_{CF} = 35.3$  Hz), 156.5 (q,  $^2J_{CF} = 35.3$  Hz), 142.8, 142.5, 137.34, 137.32, 136.43, 136.39, 135.0, 134.9, 133.9, 133.6, 132.09, 132.00, 129.67, 129.63, 129.03, 129.01, 128.0, 127.6, 127.5, 127.1, 127.0, 126.93, 126.89, 126.5, 126.4, 121.7, 121.15, 121.10, 119.31, 119.28, 116.6 (q,  $^2J_{CF} = 288.5$  Hz), 116.5 (q,  $^1J_{CF} = 288.5$  Hz), 109.57, 109.54, 101.43, 101.41, 48.7 (q,  $^3J_{CF} = 3.3$  Hz), 47.4, 44.8 (q,  $^2J_{CF} = 3.7$  Hz), 43.5, 33.0.

**$^{19}F$  NMR** (376 MHz,  $CDCl_3$ )  $\delta$  -67.84, -68.70.

**HRMS** (ESI-TOF)  $m/z$ :  $[M+Na]^+$  calcd for  $C_{25}H_{21}F_3N_2OSNa$  477.1224; found 477.1207.



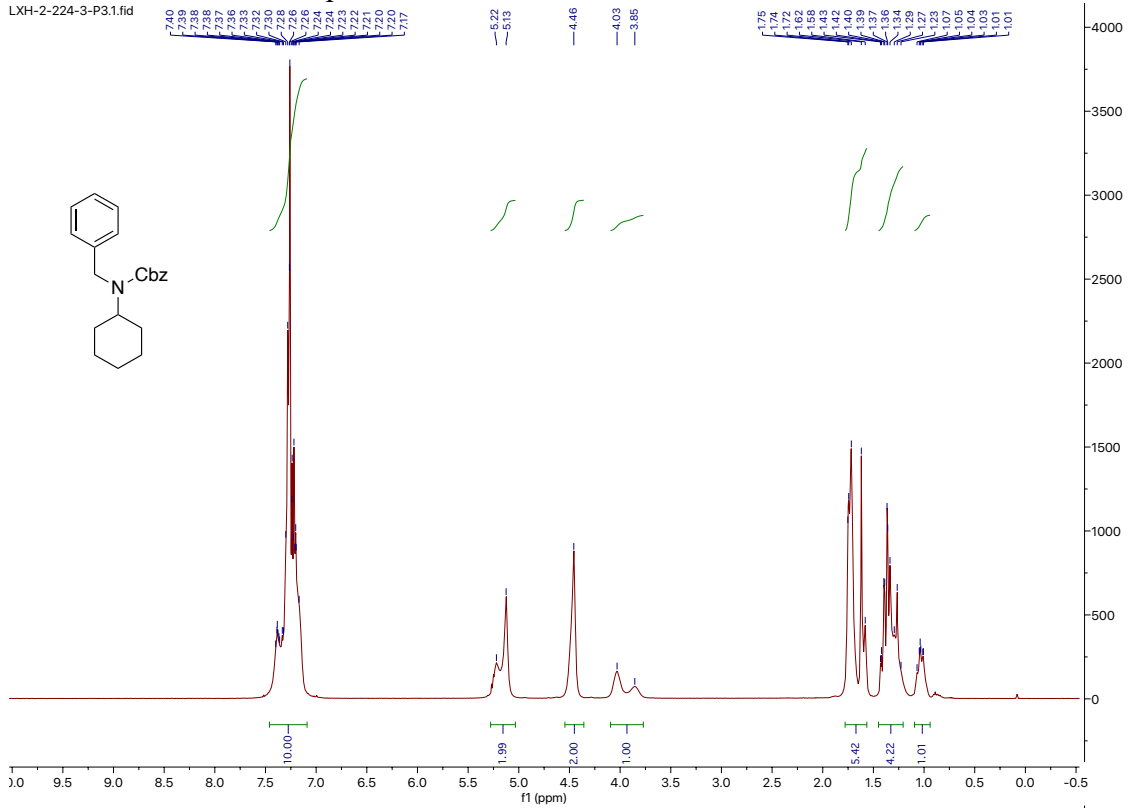
### 3.5.11. References

1. Lipshutz, B. H.; Ghorai, S.; Abela, A. R.; Moser, R.; Nishikata, T.; Duplais, C.; Krasovskiy, A.; Gaston, R. D.; Gadwood, R. C. TPGS-750-M: A Second-Generation Amphiphile for Metal-Catalyzed Cross-Couplings in Water at Room Temperature. *J. Org. Chem.* **2011**, *76*, 4379–4391.
2. Lei, Q.; Wei, Y.; Talwar, D.; Wang, C.; Xue, D.; Xiao, J. Fast Reductive Amination by Transfer Hydrogenation “on Water.” *Chem. Euro. J.* **2013**, *19*, 4021–4029.
3. Cheetham, C. A.; Massey, R. S.; Pira, S. L.; Pritchard, R. G.; Wallace, T. W. Atroposelective Formation of Dibenz[c,e]Azepines via Intramolecular Direct Arylation with Centre-Axis Chirality Transfer. *Org. Biomol. Chem.* **2011**, *9*, 1831.

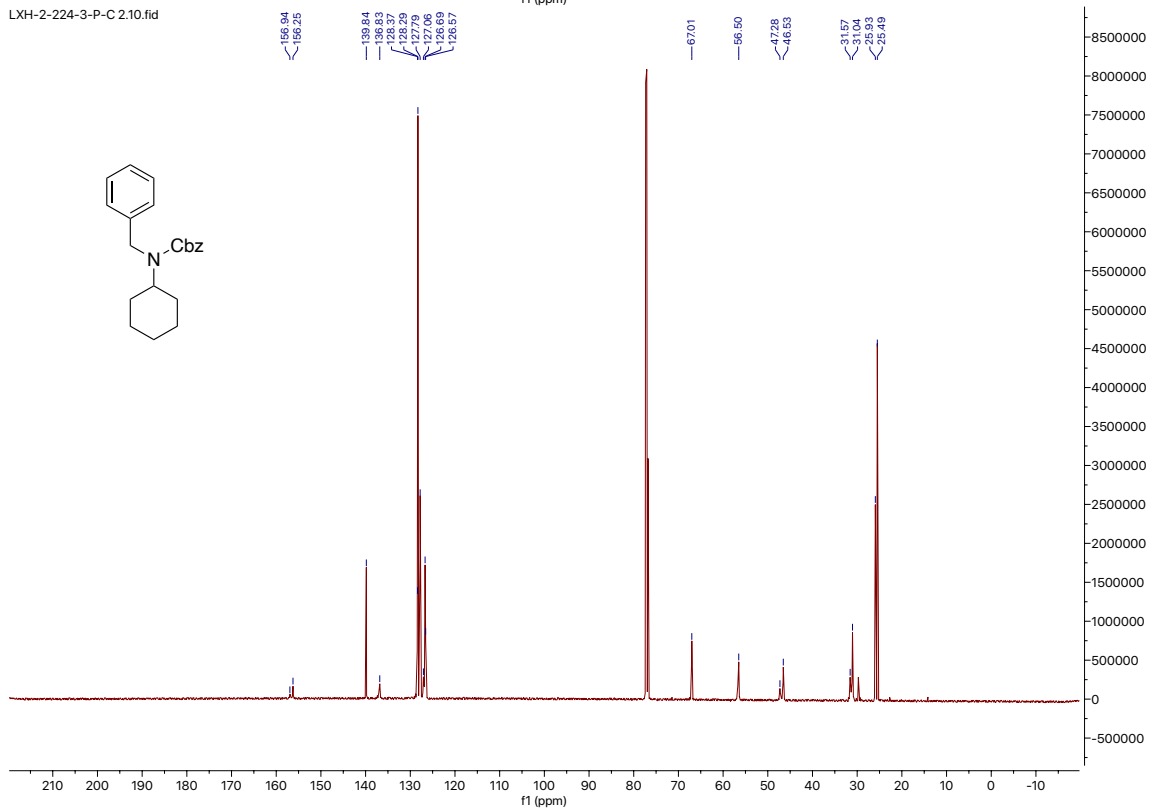
### 3.5.12. NMR Spectra

#### $^1\text{H}$ and $^{13}\text{C}$ NMR of compound III-1

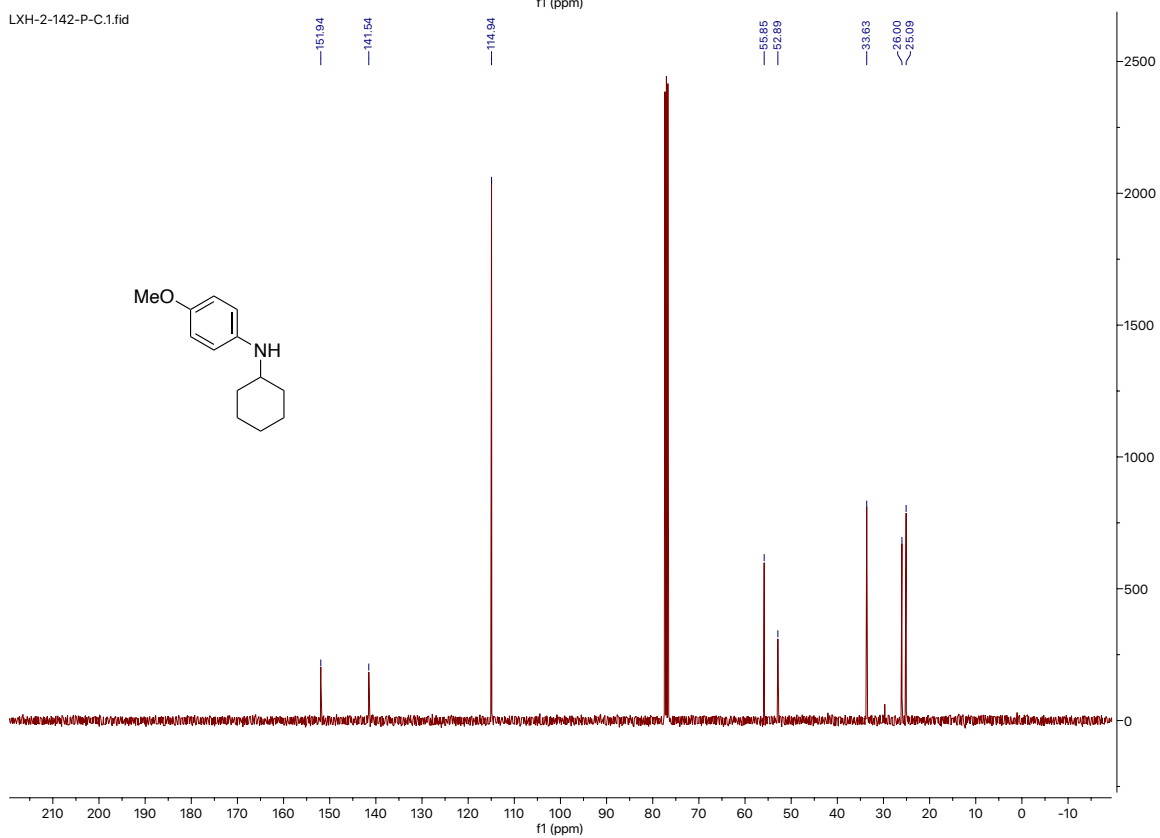
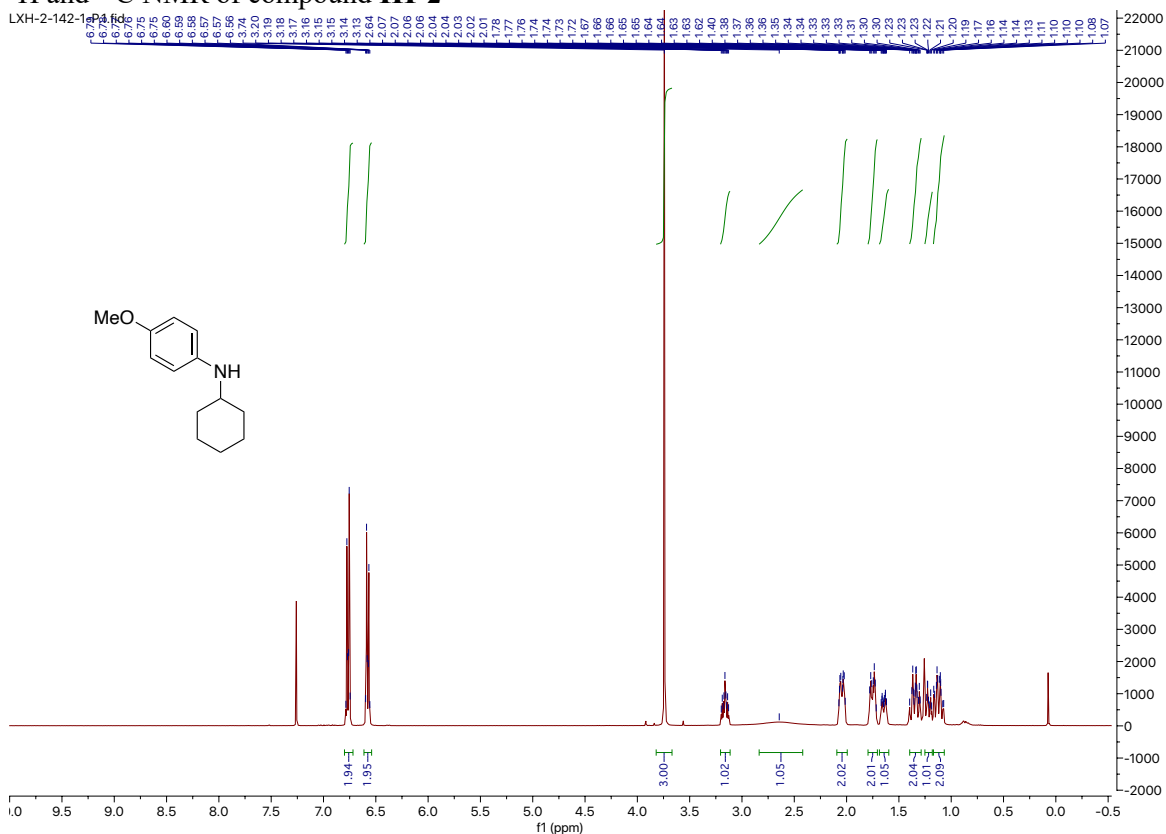
LXH-2-224-3-P3.1.fid



LXH-2-224-3-P-C 2.10.fid



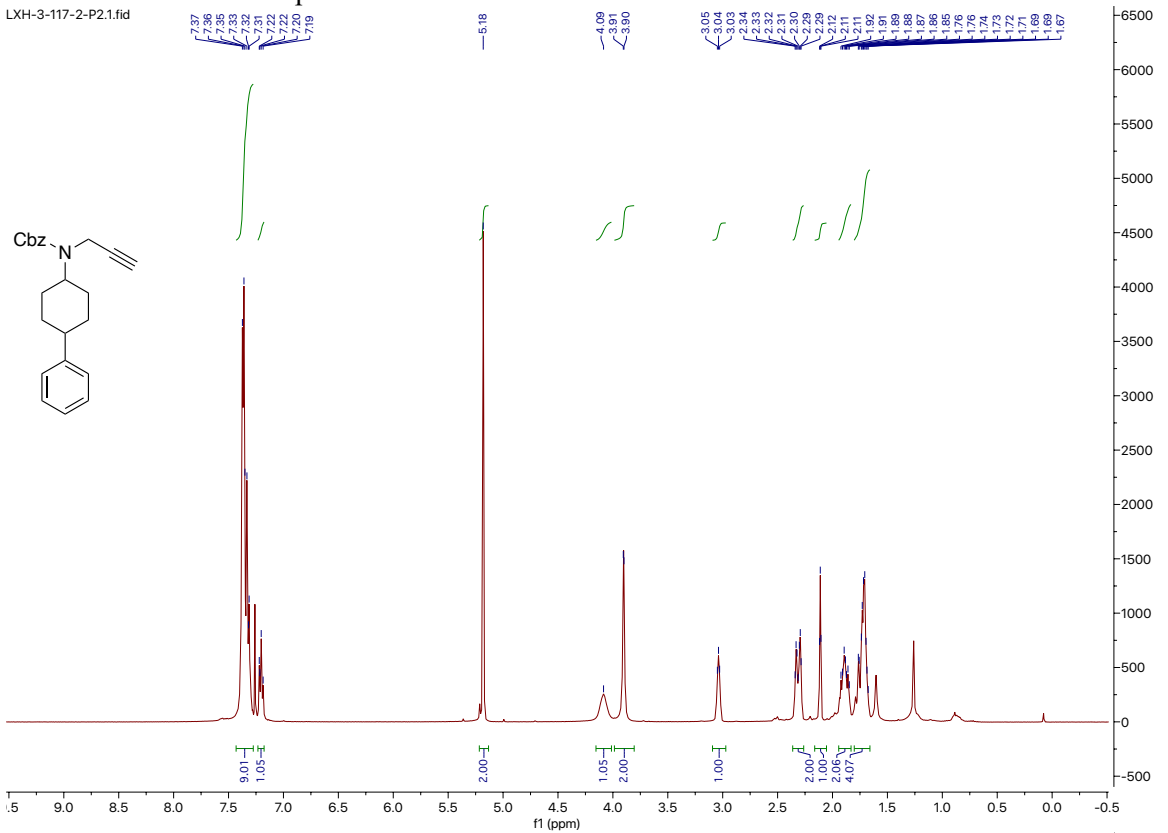
# <sup>1</sup>H and <sup>13</sup>C NMR of compound III-2



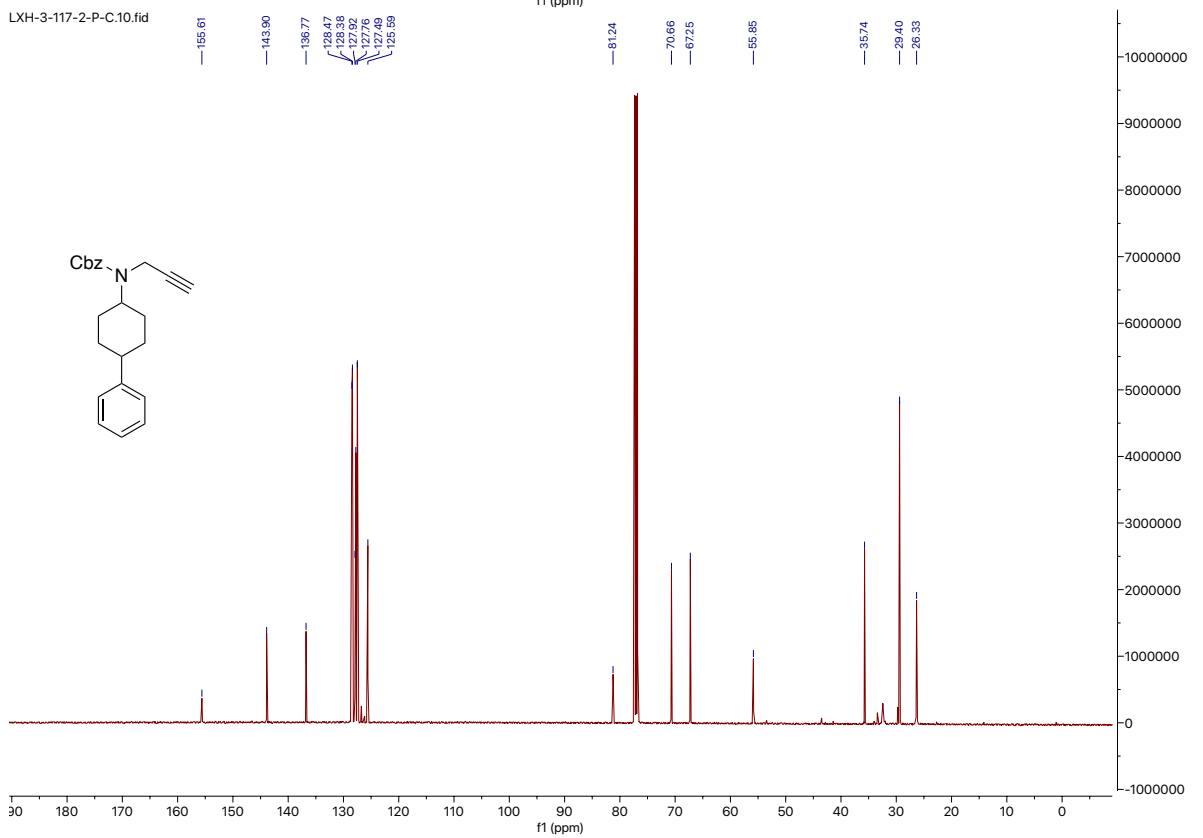


<sup>1</sup>H and <sup>13</sup>C NMR of compound III-18

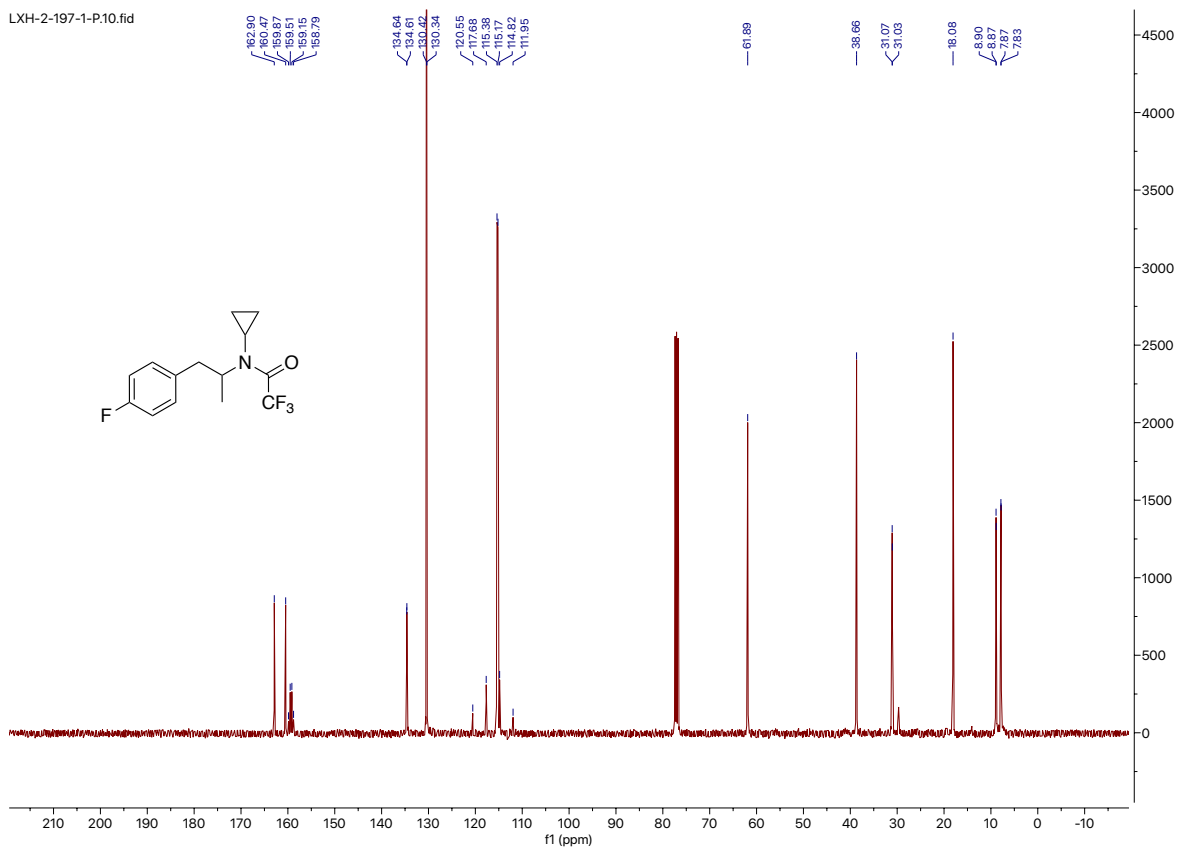
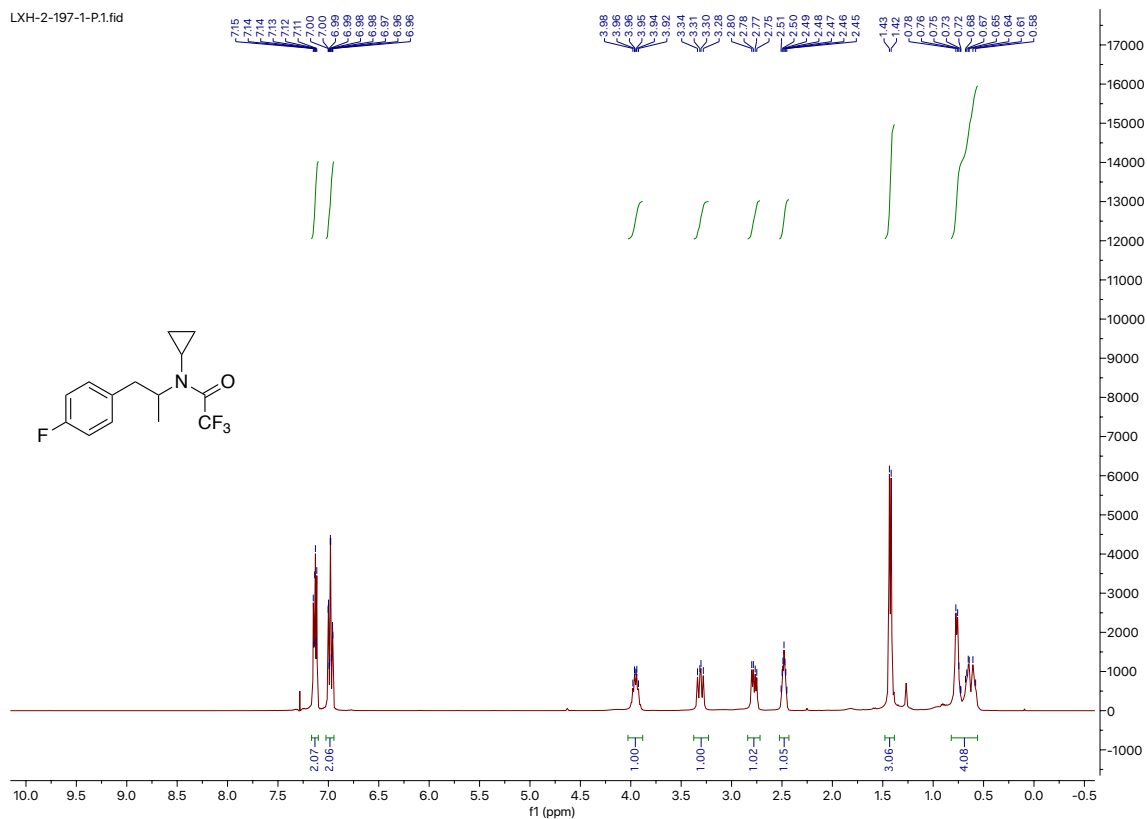
LXH-3-117-2-P2.1.fid



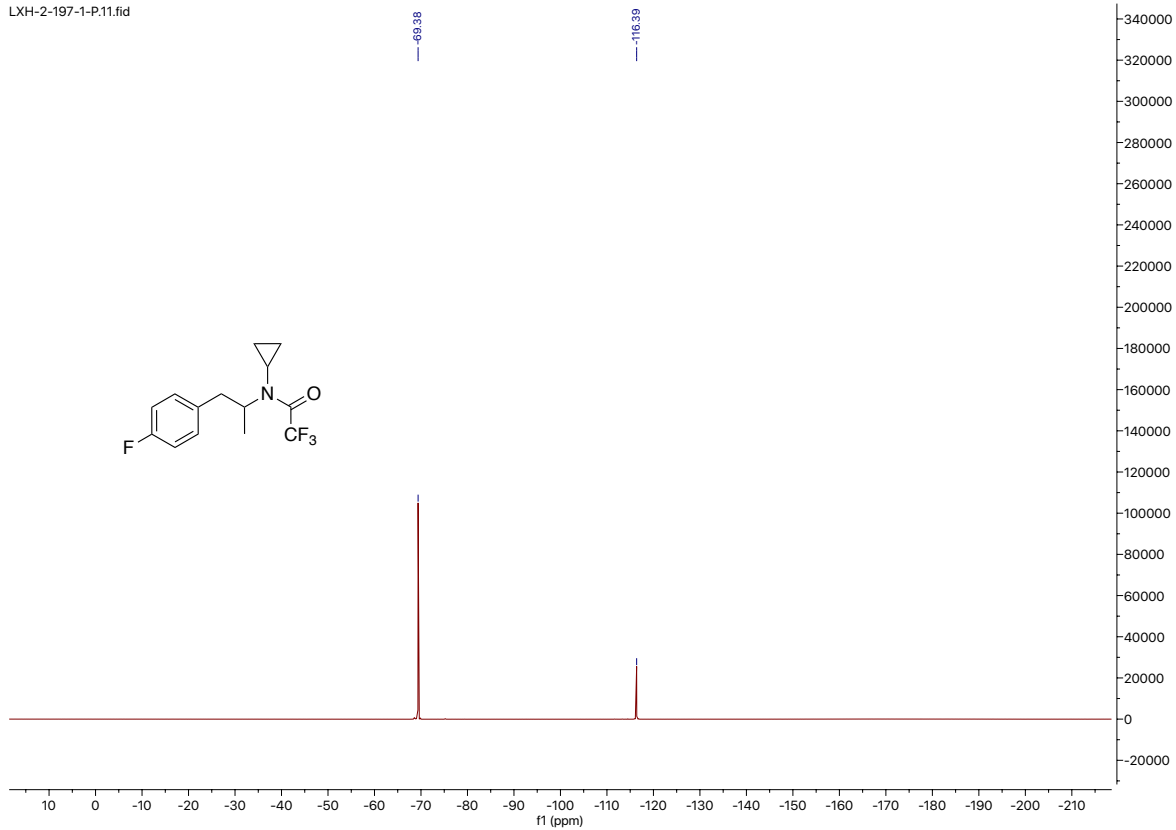
LXH-3-117-2-P-C.10.fid



# $^1\text{H}$ , $^{13}\text{C}$ , and $^{19}\text{F}$ NMR of compound III-19

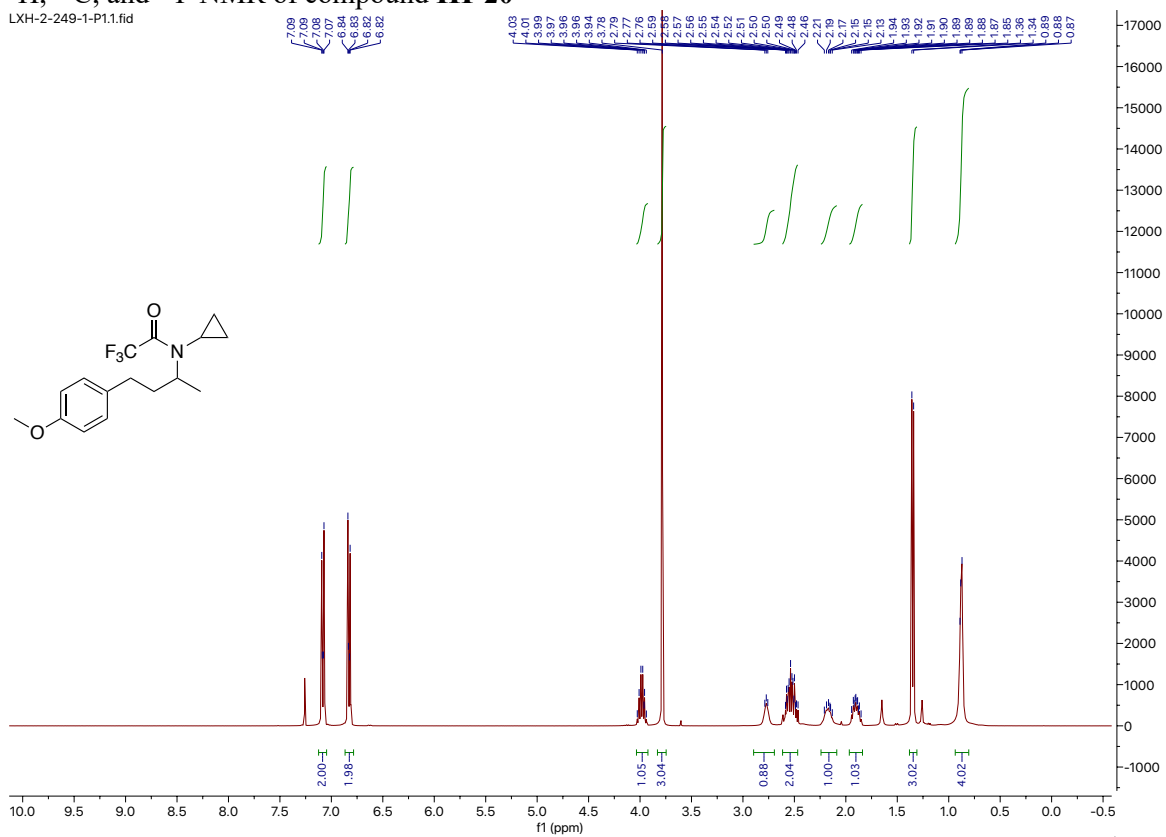


LXH-2-197-1-P,11.fid

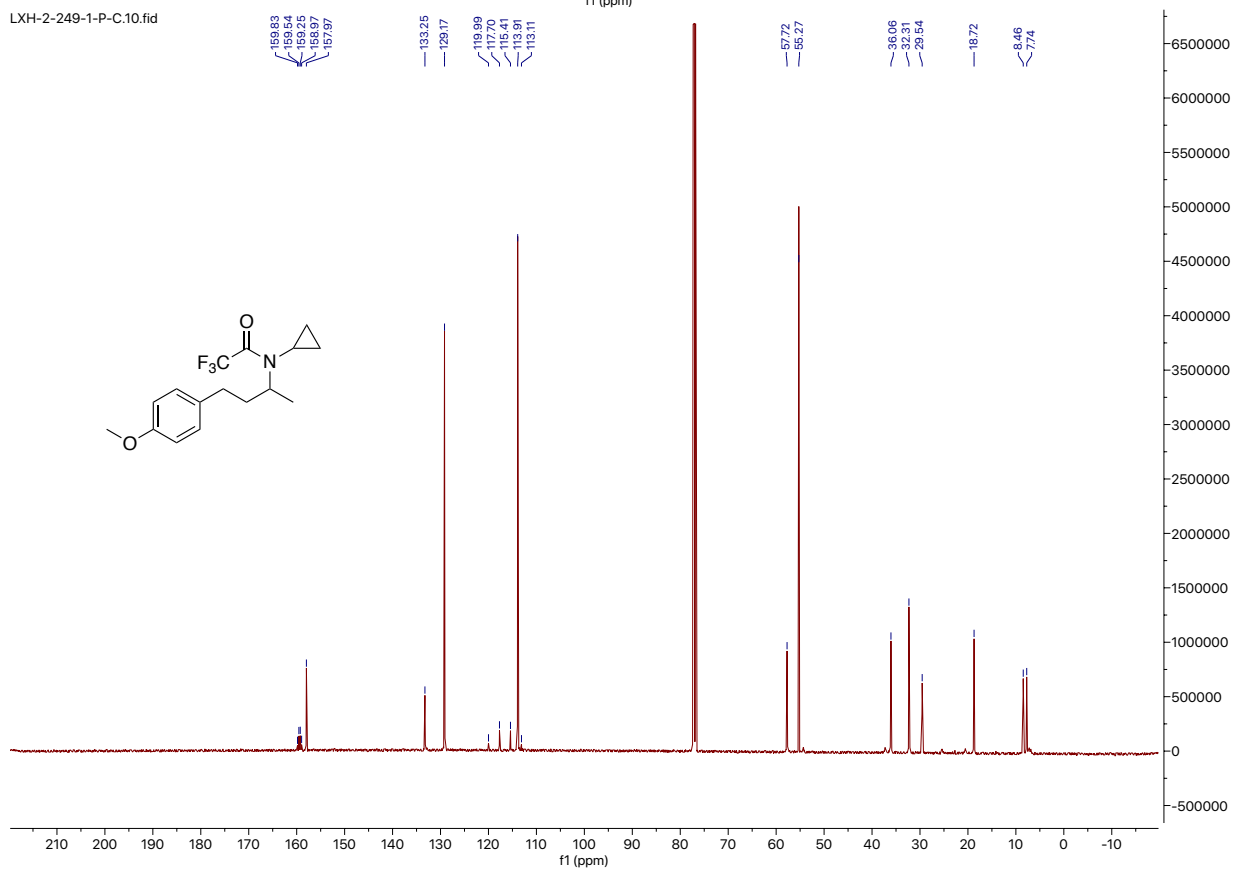


<sup>1</sup>H, <sup>13</sup>C, and <sup>19</sup>F NMR of compound III-20

LXH-2-249-1-P1.1.fid

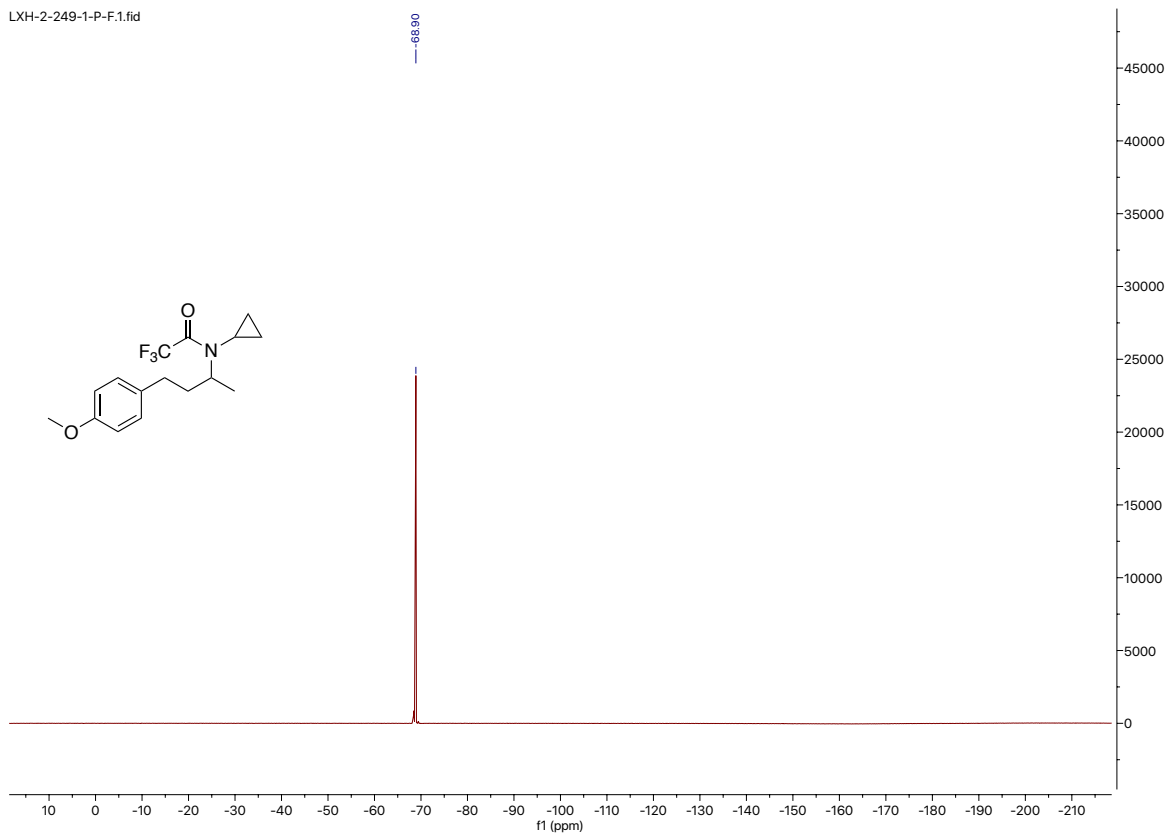


LXH-2-249-1-P-C.10.fid



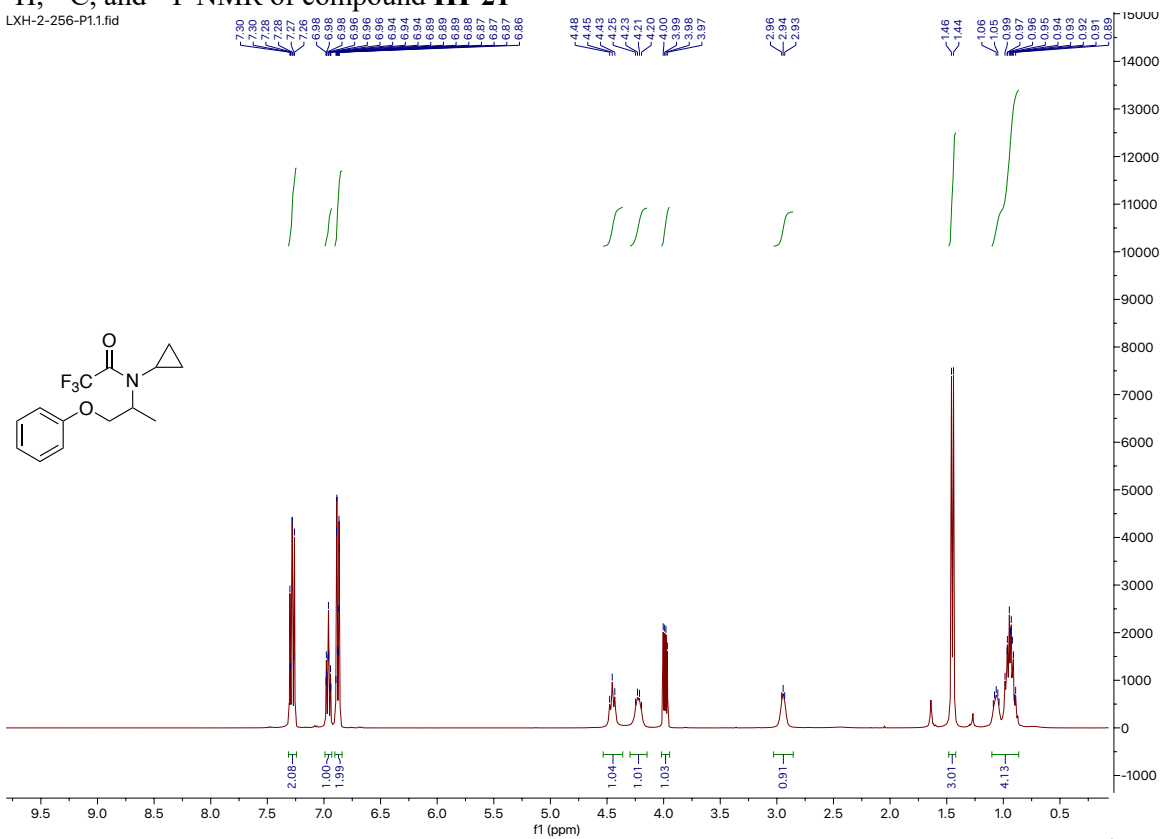


LXH-2-249-1-P-F.1.fid

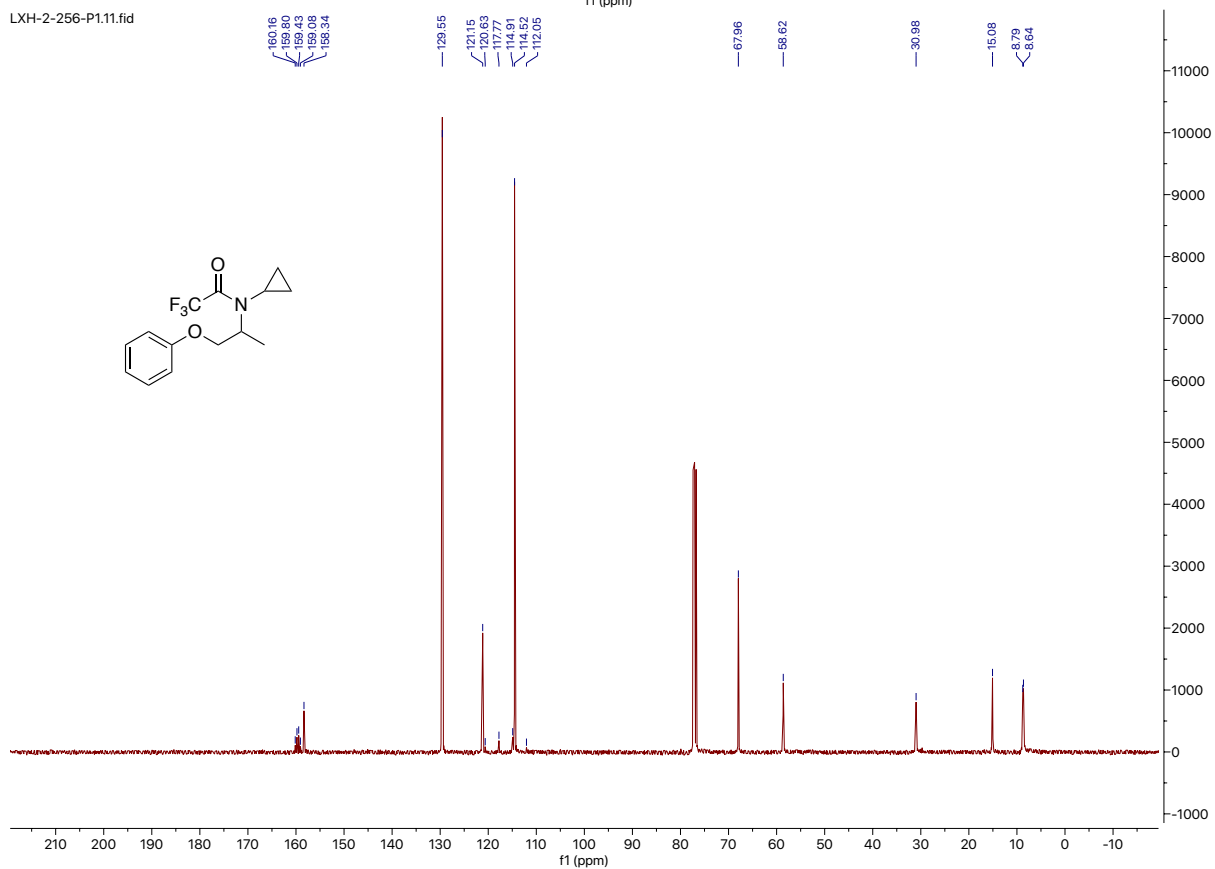


<sup>1</sup>H, <sup>13</sup>C, and <sup>19</sup>F NMR of compound III-21

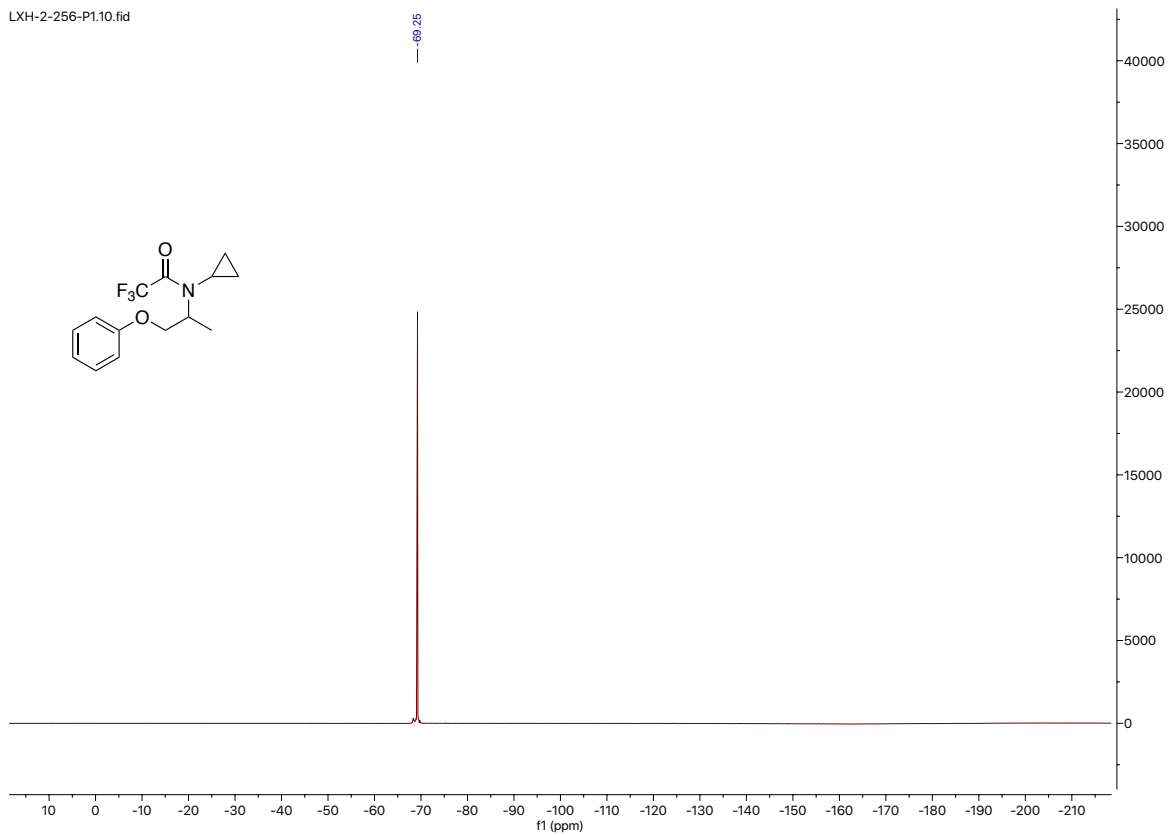
LXH-2-256-P1.1.fid



LXH-2-256-P1.11.fid

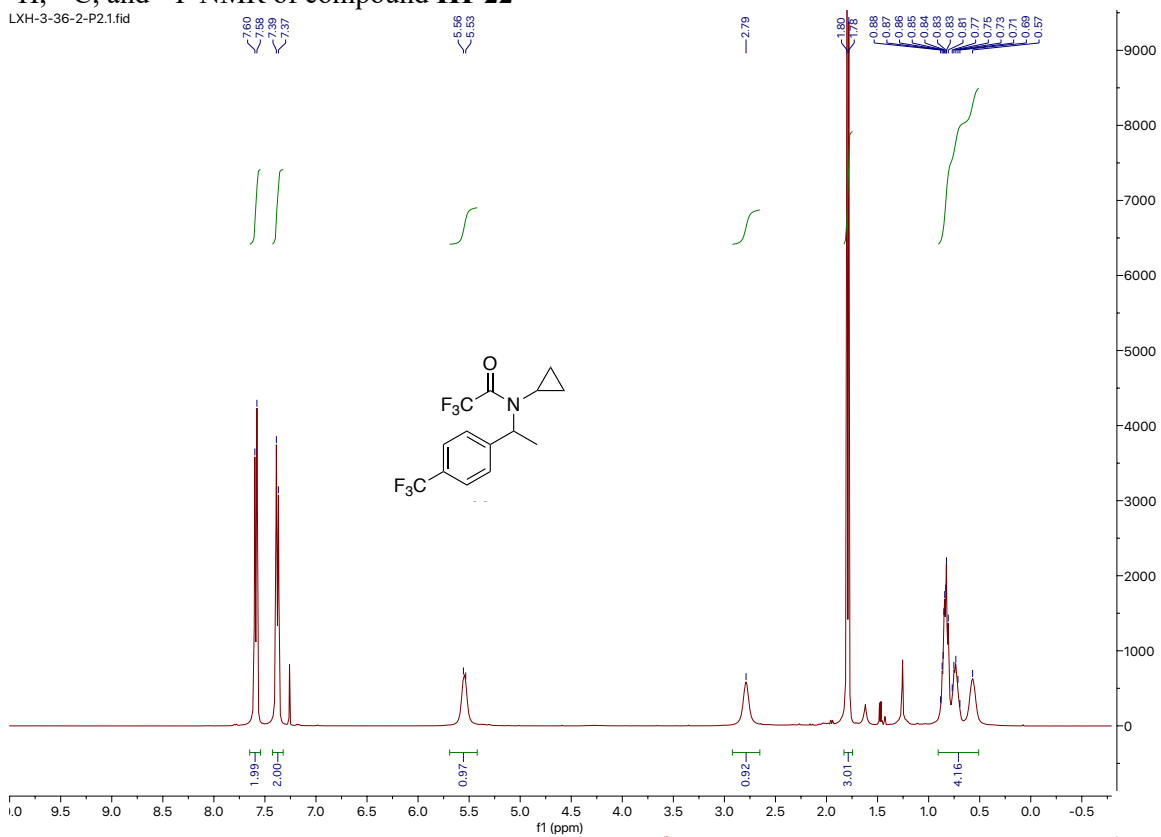


LXH-2-256-P1.10.fid

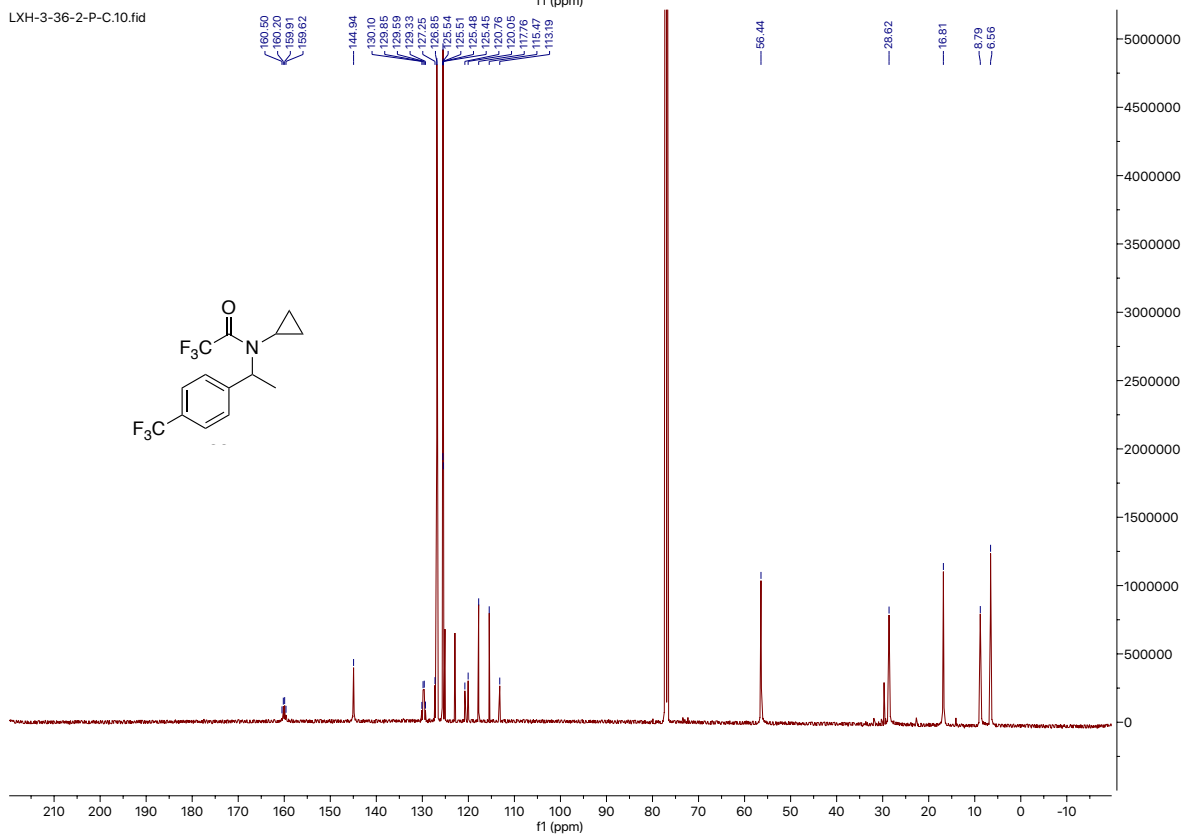


<sup>1</sup>H, <sup>13</sup>C, and <sup>19</sup>F NMR of compound III-22

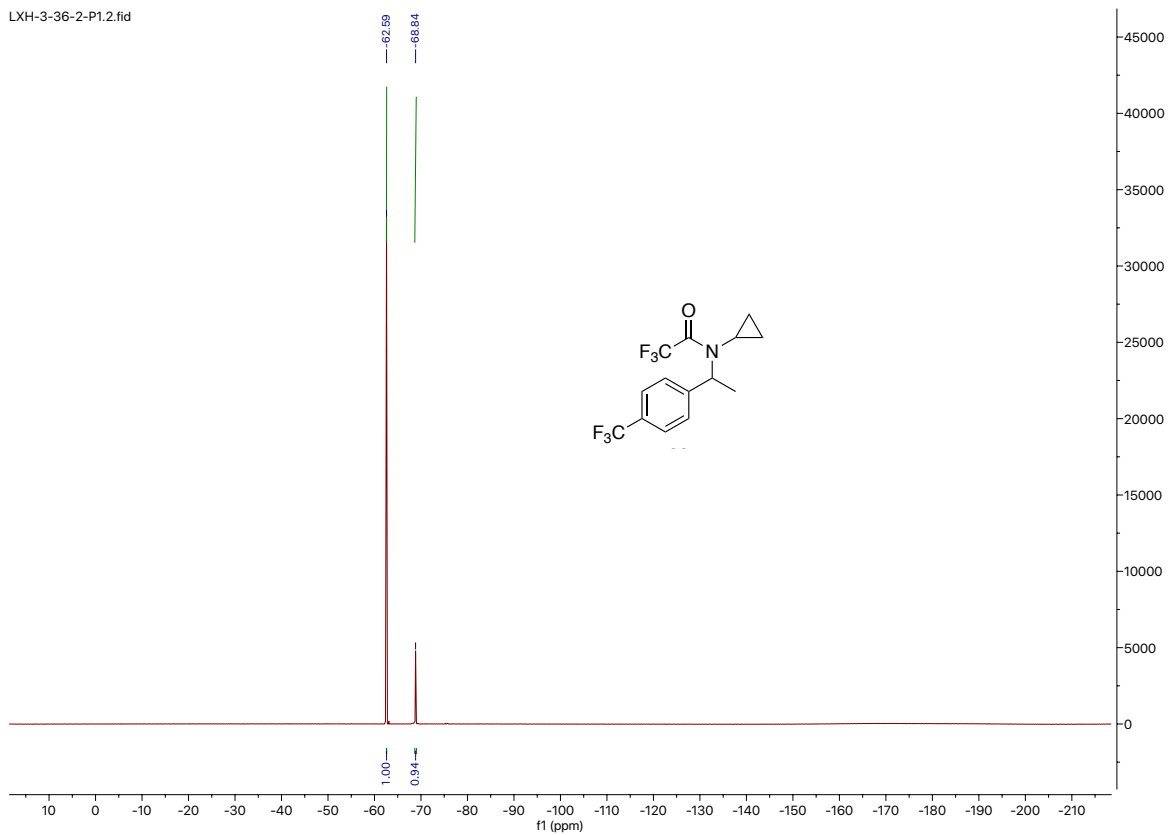
LXH-3-36-2-P21.fid



LXH-3-36-2-P-C.10.fid

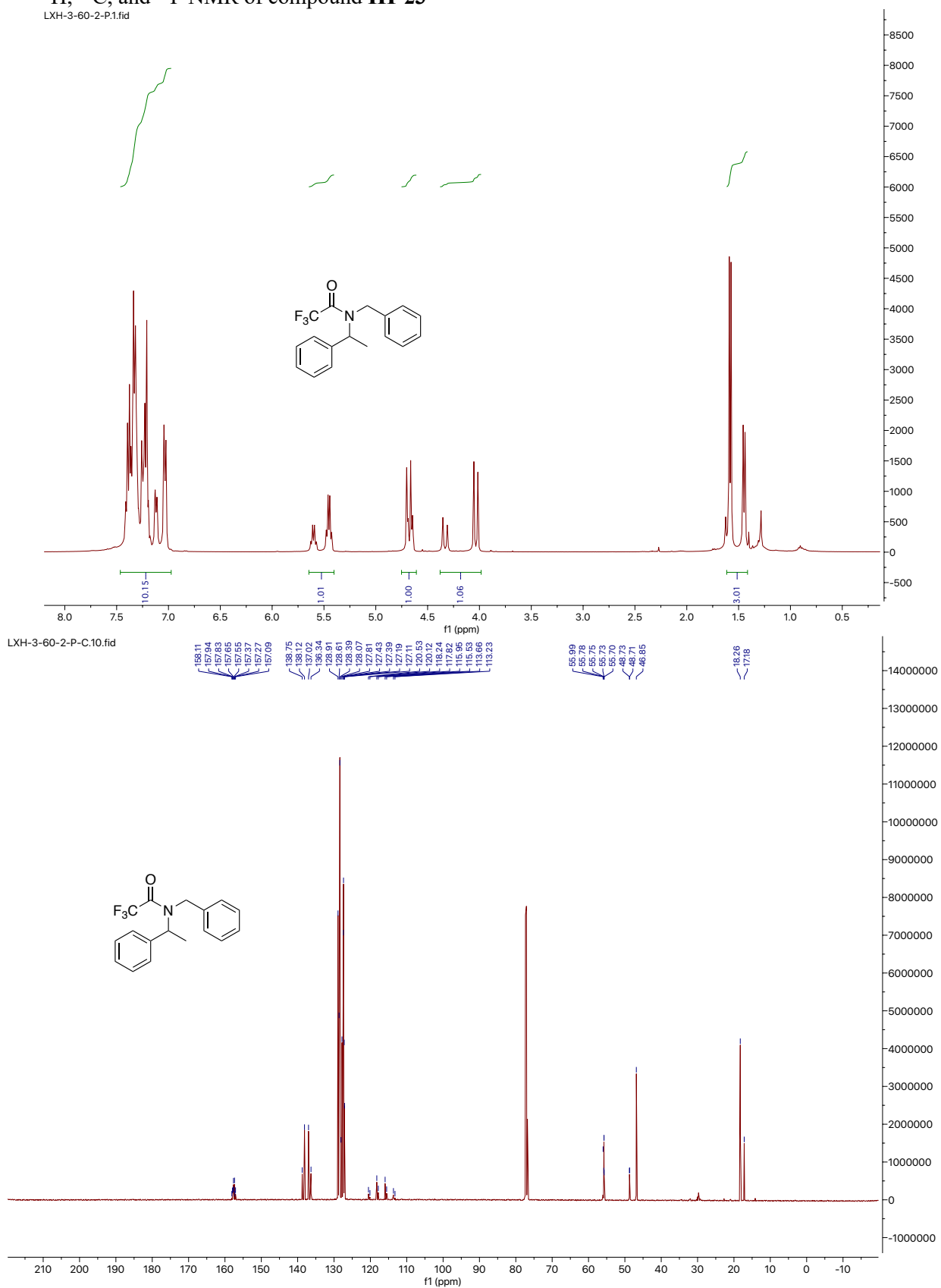


LXH-3-36-2-P1.2.fid

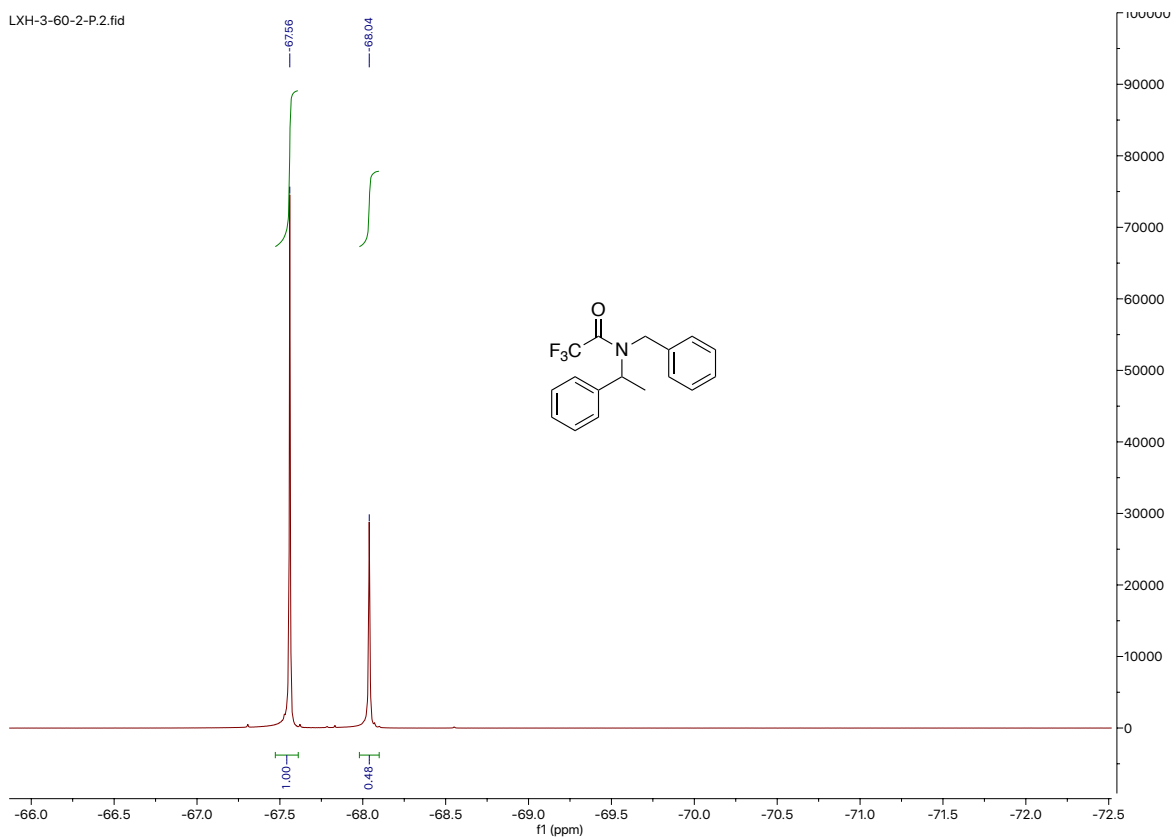


<sup>1</sup>H, <sup>13</sup>C, and <sup>19</sup>F NMR of compound III-23

LXH-3-60-2-P1.fid

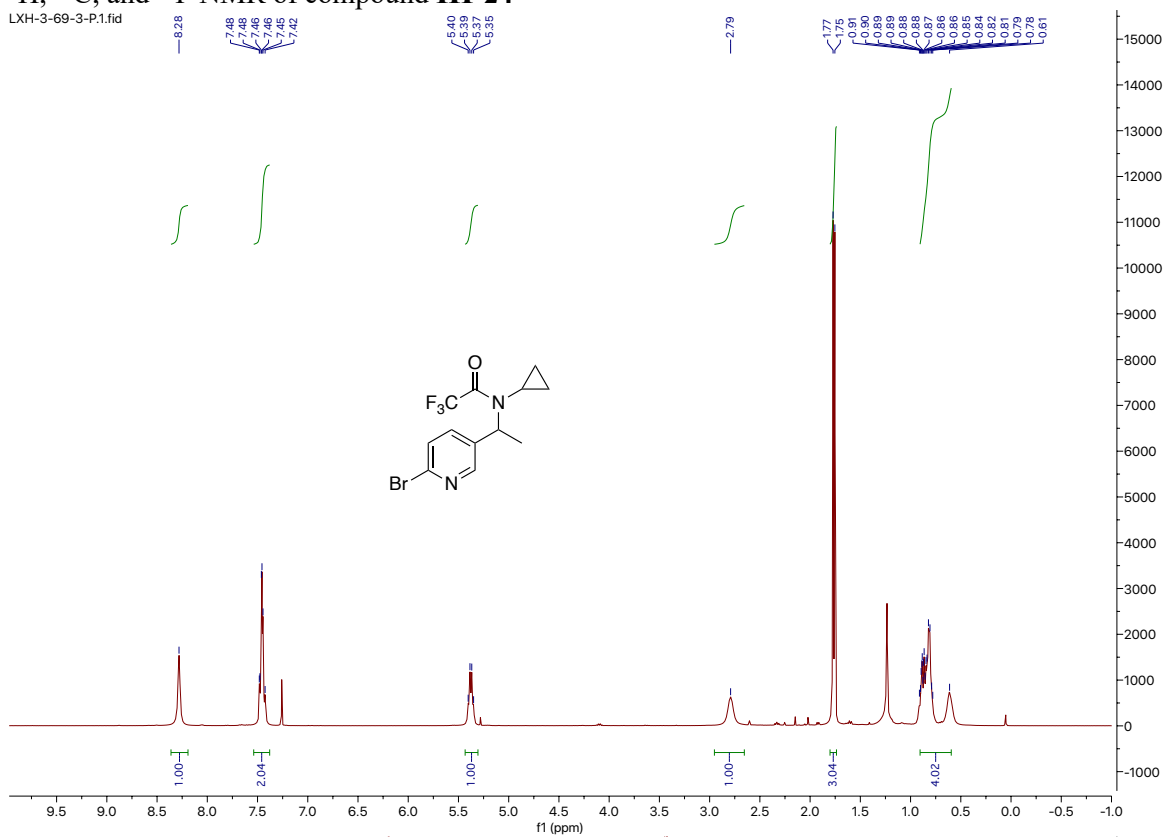


LXH-3-60-2-P.2.fid

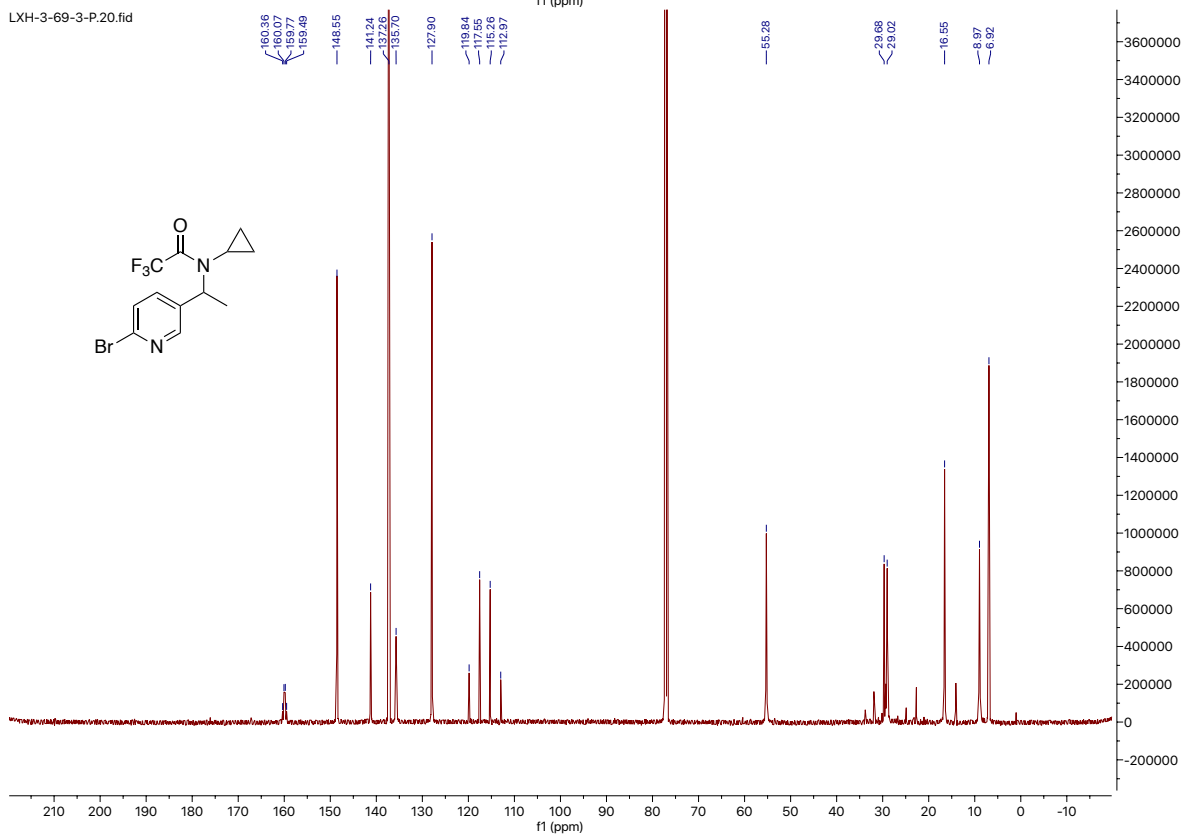


<sup>1</sup>H, <sup>13</sup>C, and <sup>19</sup>F NMR of compound III-24

LXH-3-69-3-P.1.fid

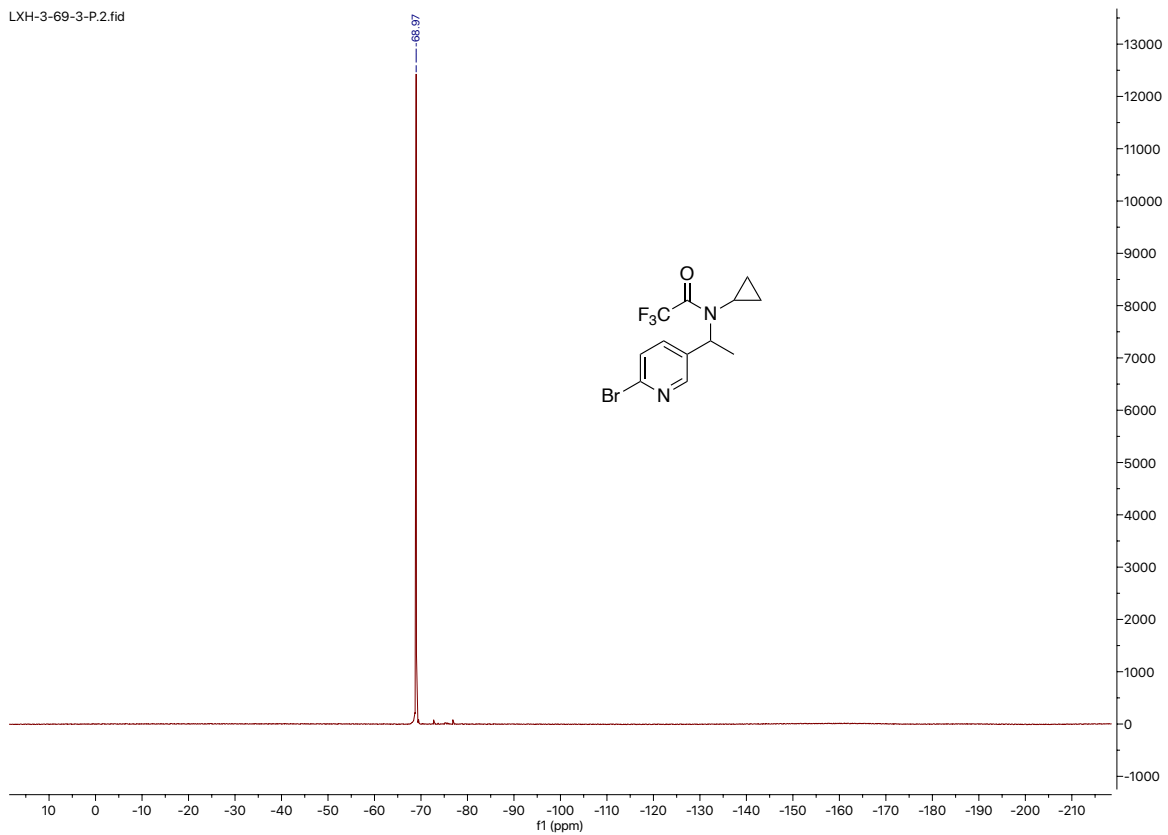


LXH-3-69-3-P.20.fid



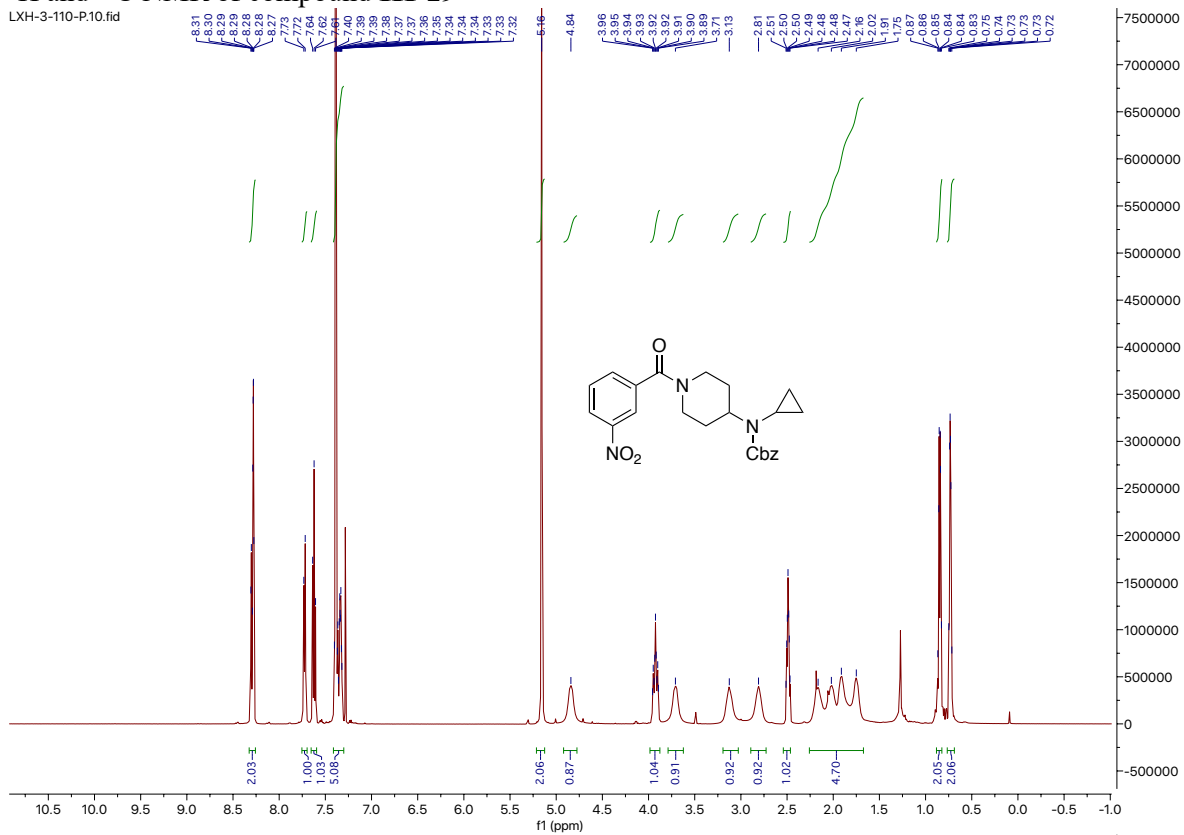


LXH-3-69-3-P.2.fid

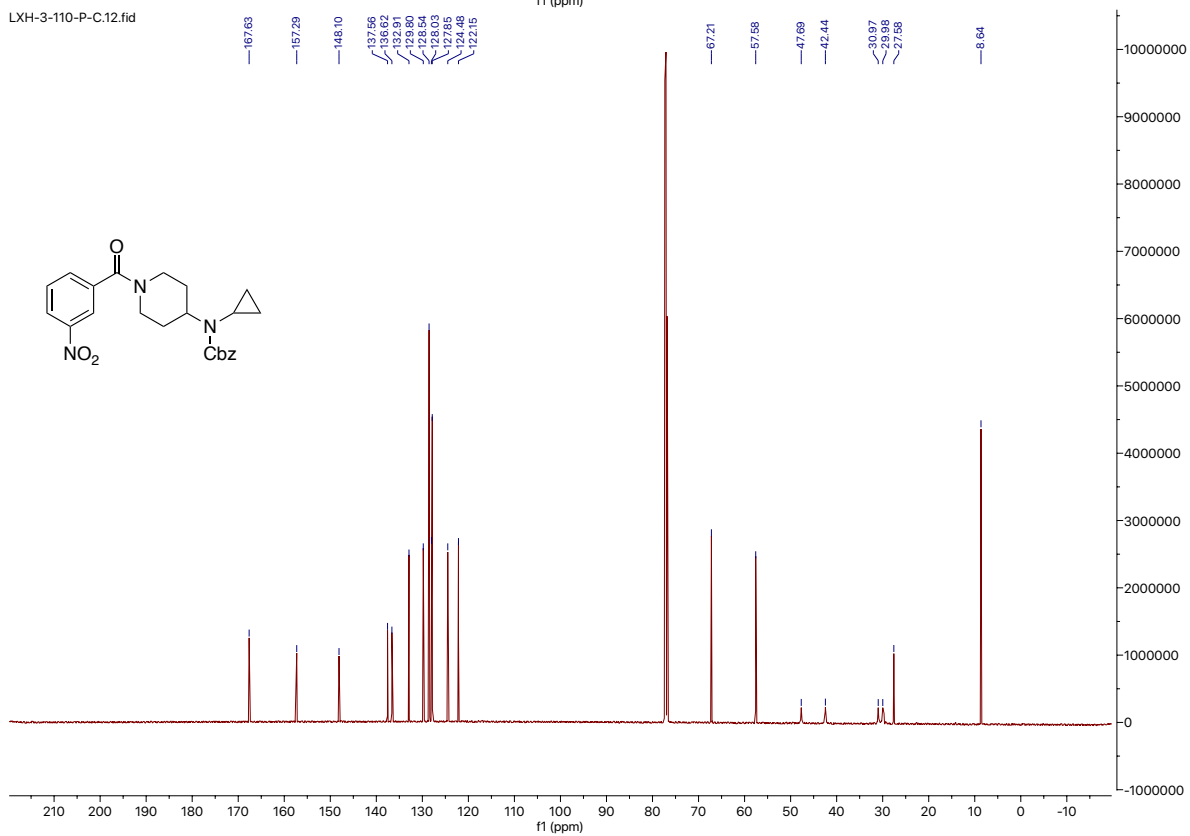


# <sup>1</sup>H and <sup>13</sup>C NMR of compound III-29

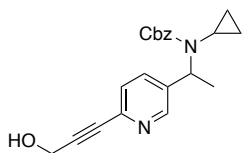
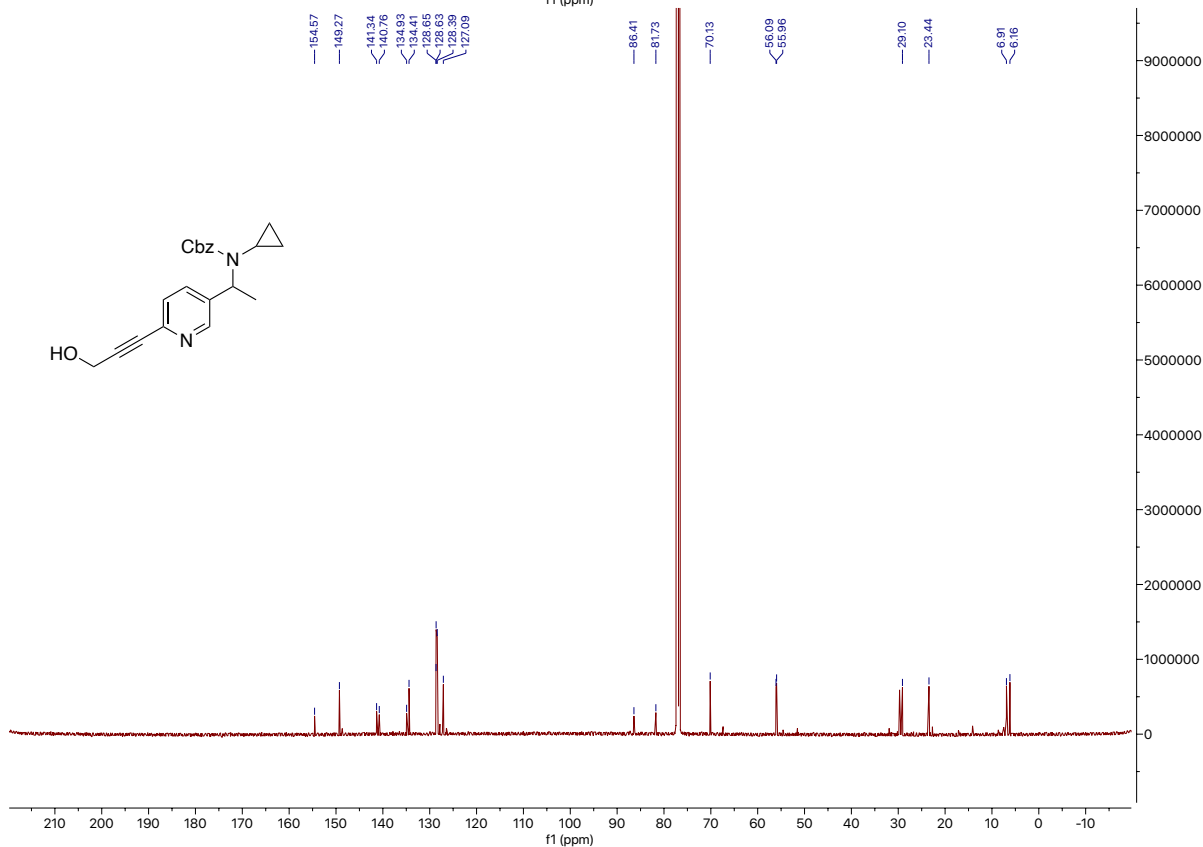
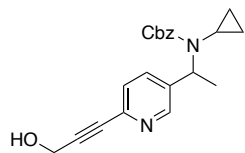
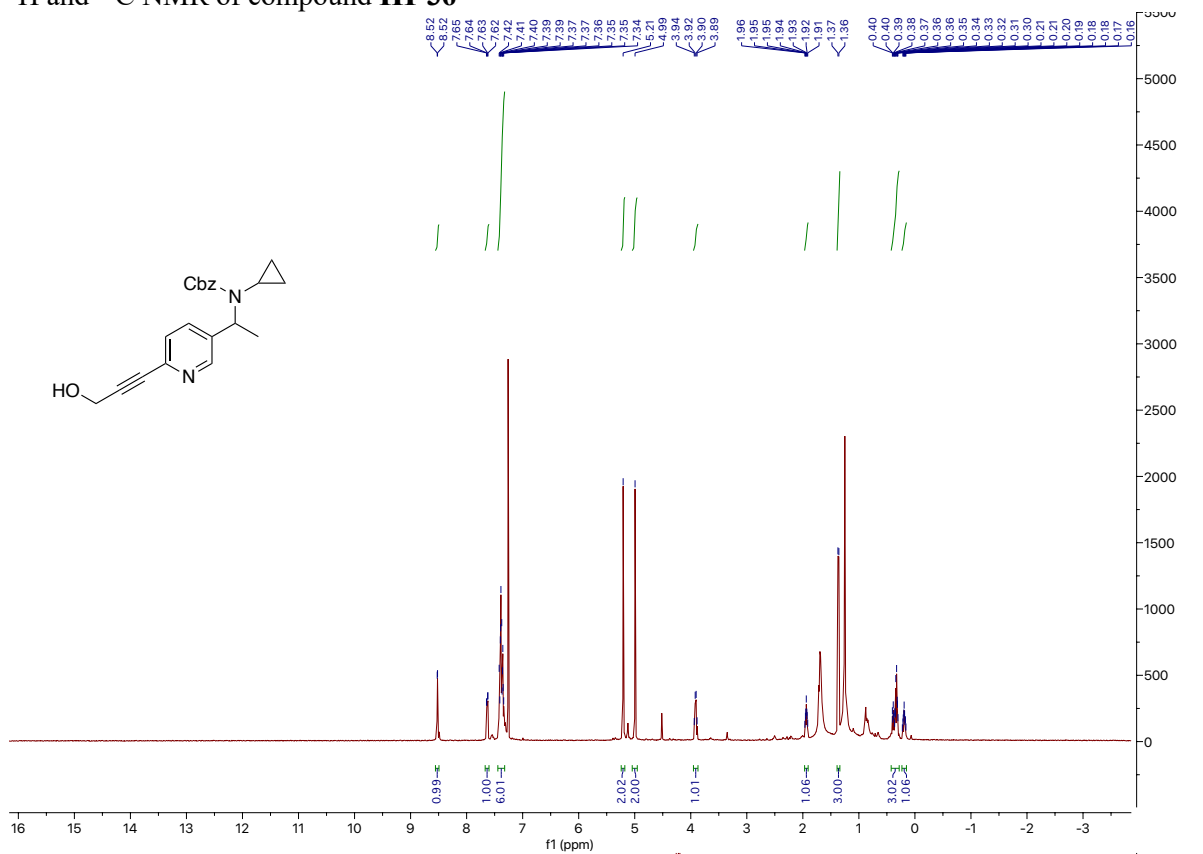
LXH-3-110-P.10.fid



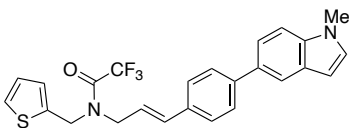
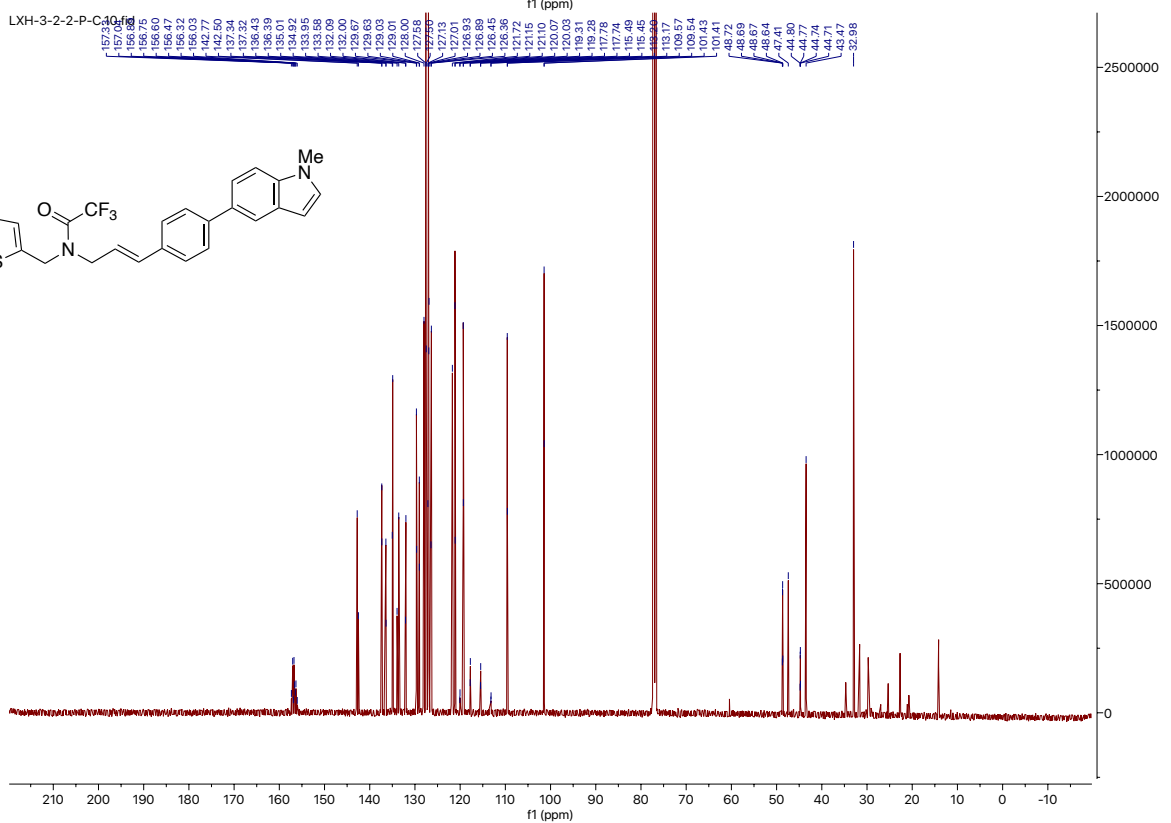
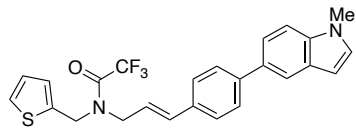
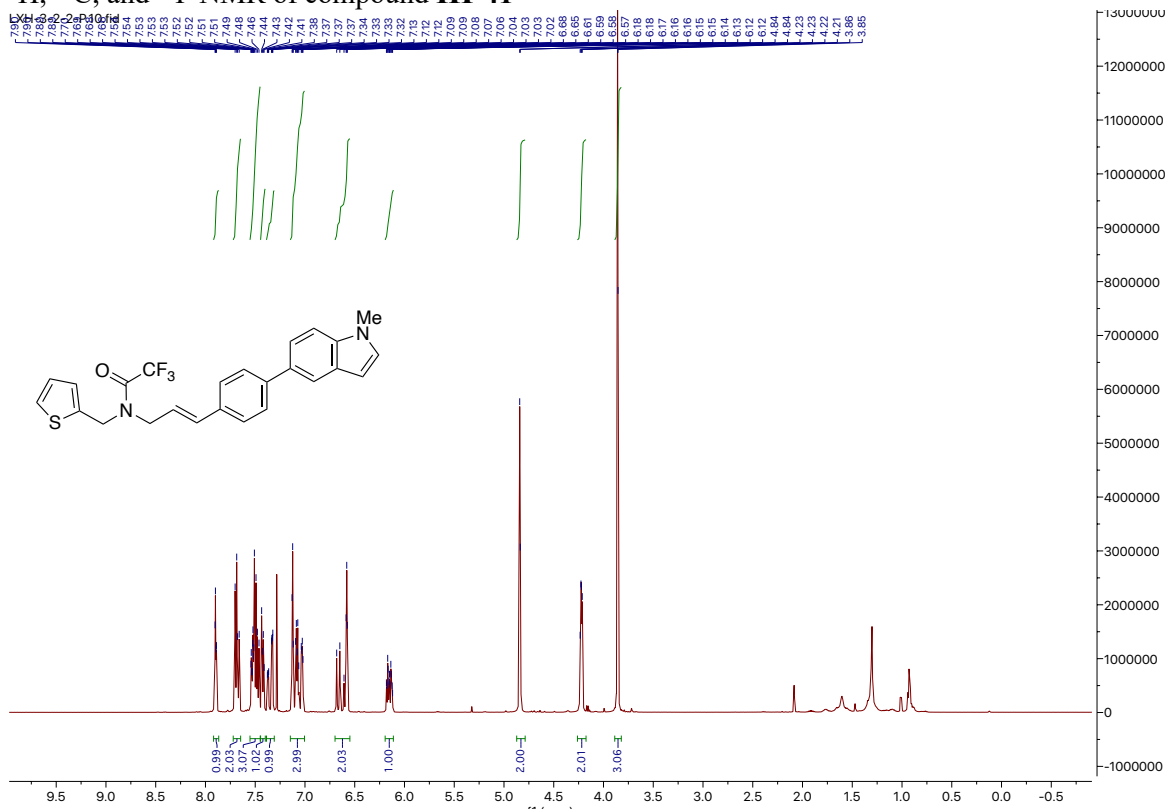
LXH-3-110-P-C.12.fid



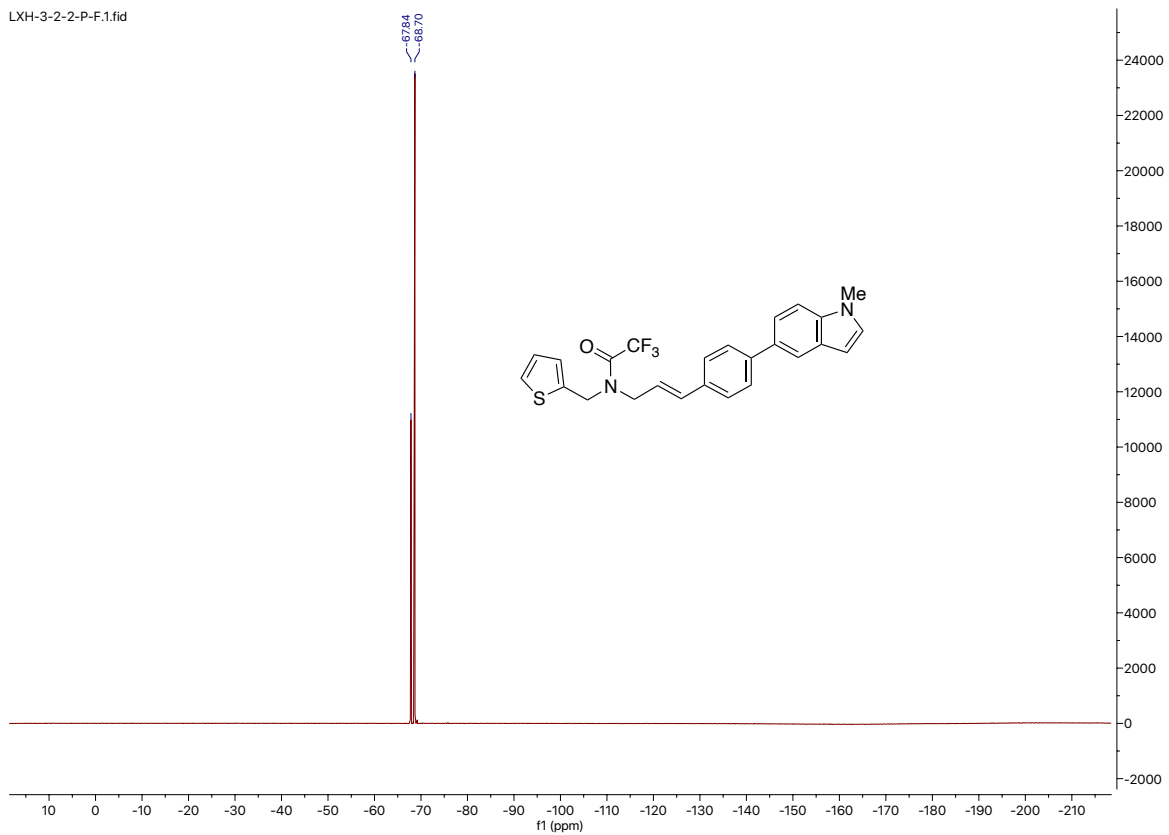
$^1\text{H}$  and  $^{13}\text{C}$  NMR of compound **III-36**



<sup>1</sup>H, <sup>13</sup>C, and <sup>19</sup>F NMR of compound III-41

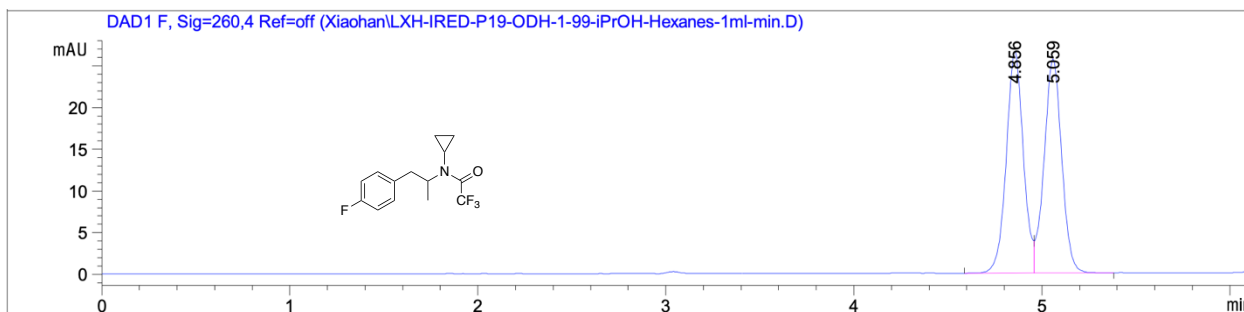


LXH-3-2-2-P-F.1.fid



### 3.5.13. HPLC traces

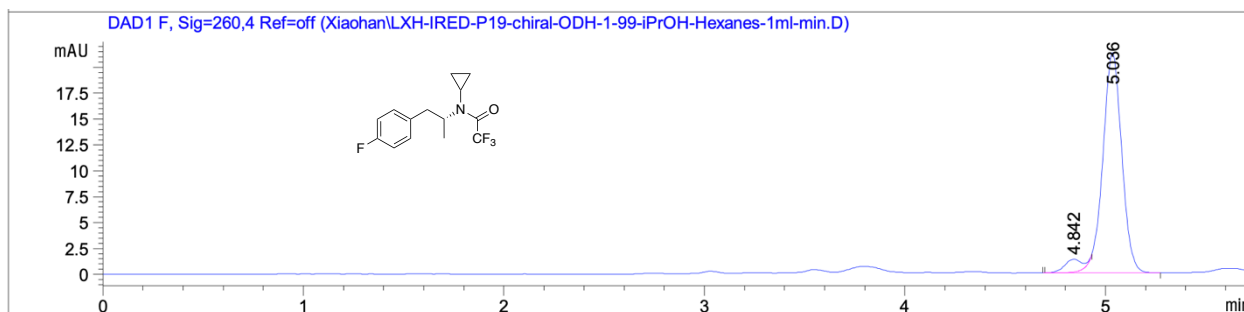
#### HPLC analysis of compound III-19



Signal 6: DAD1 F, Sig=260,4 Ref=off

Peak #	RetTime [min]	Type	Width [min]	Area [mAU*s]	Height [mAU]	Area %
1	4.856	BV	0.0975	167.58356	26.58898	50.1005
2	5.059	VB	0.0999	166.91100	25.64359	49.8995

Totals : 334.49455 52.23257

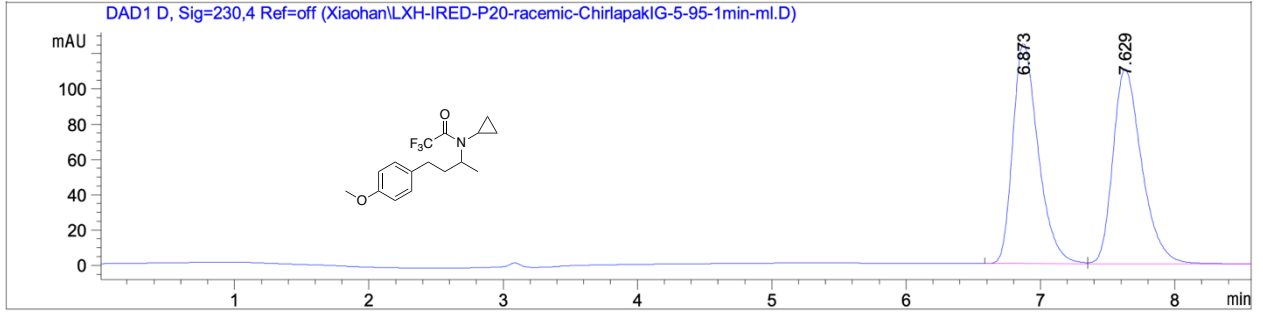


Signal 6: DAD1 F, Sig=260,4 Ref=off

Peak #	RetTime [min]	Type	Width [min]	Area [mAU*s]	Height [mAU]	Area %
1	4.842	BV E	0.0869	7.08221	1.23480	4.8056
2	5.036	VB R	0.1009	140.29204	21.27486	95.1944

Totals : 147.37425 22.50967

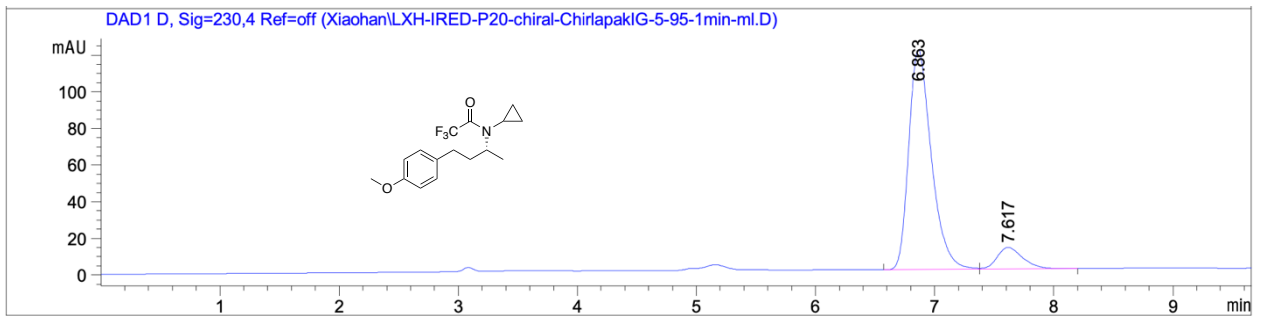
# HPLC analysis of compound III-20



Signal 4: DAD1 D, Sig=230,4 Ref=off

Peak #	RetTime [min]	Type	Width [min]	Area [mAU*s]	Height [mAU]	Area %
1	6.873	BV	0.1989	1636.75269	124.87010	49.9397
2	7.629	VBA	0.2255	1640.70251	110.34817	50.0603

Totals : 3277.45520 235.21827

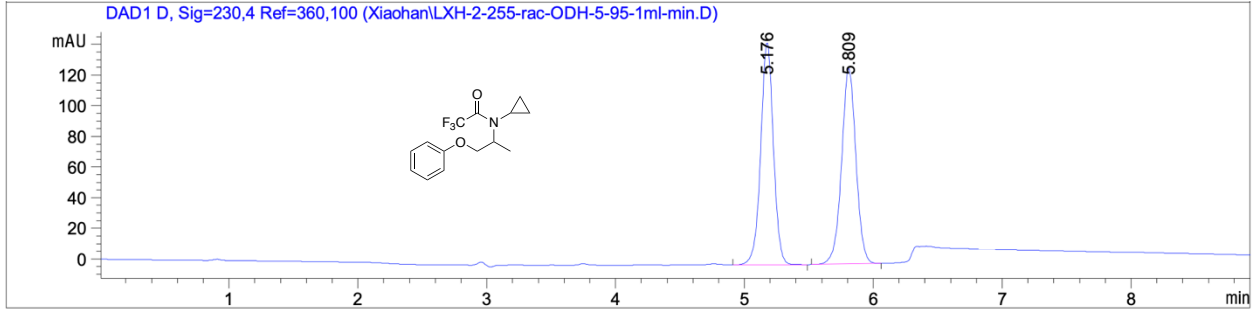


Signal 4: DAD1 D, Sig=230,4 Ref=off

Peak #	RetTime [min]	Type	Width [min]	Area [mAU*s]	Height [mAU]	Area %
1	6.863	BV	0.2016	1581.49500	120.14835	89.8606
2	7.617	VB	0.2270	178.44769	11.89378	10.1394

Totals : 1759.94269 132.04213

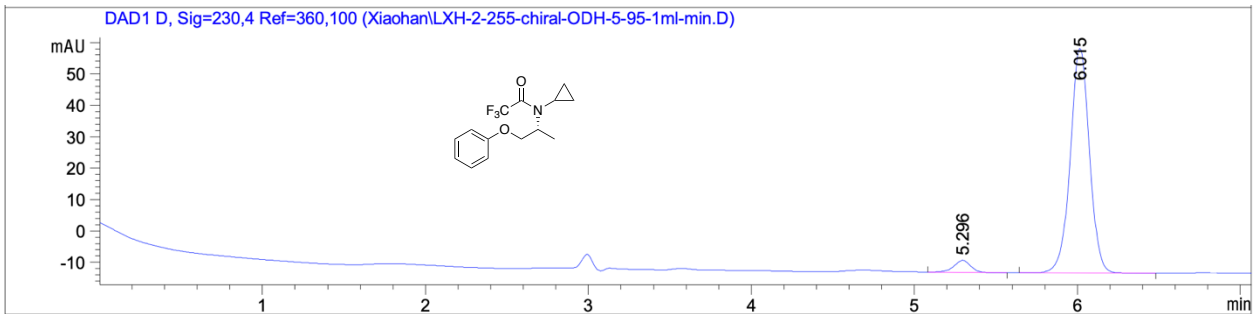
# HPLC analysis of compound III-21



Signal 4: DAD1 D, Sig=230,4 Ref=360,100

Peak #	RetTime [min]	Type	Width [min]	Area [mAU*s]	Height [mAU]	Area %
1	5.176	BB	0.1037	990.37103	144.92329	49.9990
2	5.809	BB	0.1187	990.41125	127.41290	50.0010

Totals : 1980.78229 272.33620



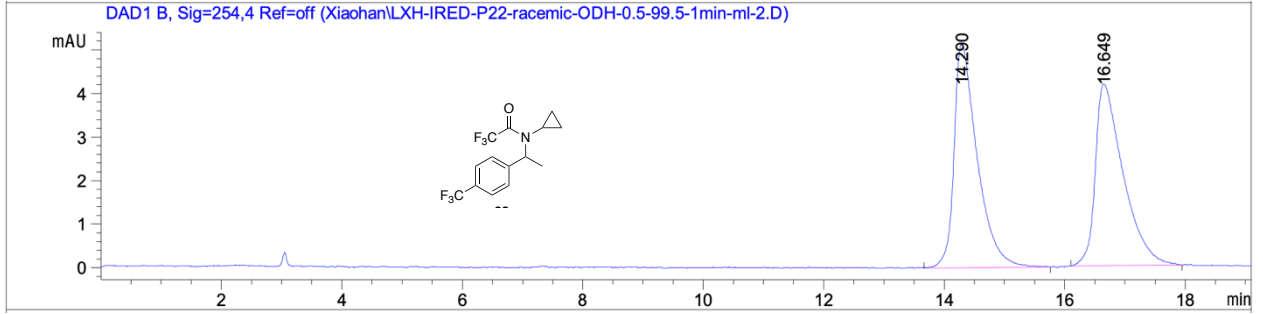
Signal 4: DAD1 D, Sig=230,4 Ref=360,100

Peak #	RetTime [min]	Type	Width [min]	Area [mAU*s]	Height [mAU]	Area %
1	5.296	BB	0.1099	27.71737	3.85501	4.5175
2	6.015	BB	0.1255	585.84119	71.54139	95.4825

Totals : 613.55856 75.39640



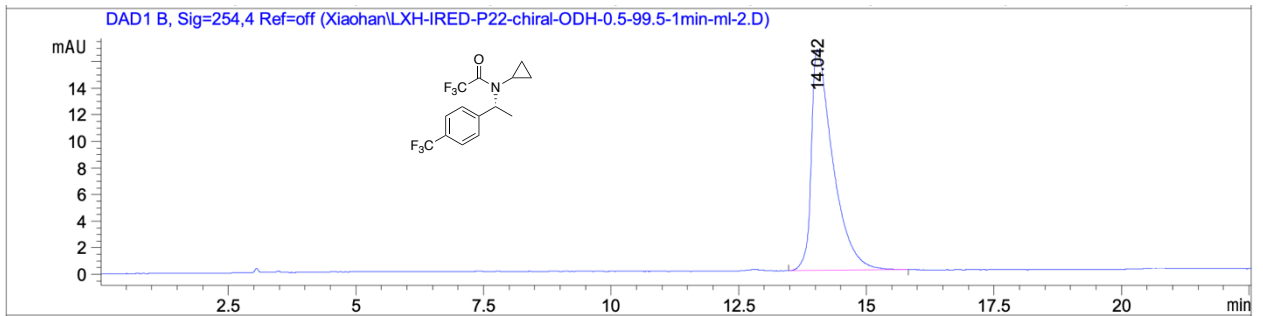
# HPLC analysis of compound III-22



Signal 2: DAD1 B, Sig=254,4 Ref=off

Peak #	RetTime [min]	Type	Width [min]	Area [mAU*s]	Height [mAU]	Area %
1	14.290	BB	0.3809	137.10574	5.14519	50.6276
2	16.649	BB	0.4461	133.70642	4.16980	49.3724

Totals : 270.81216 9.31499

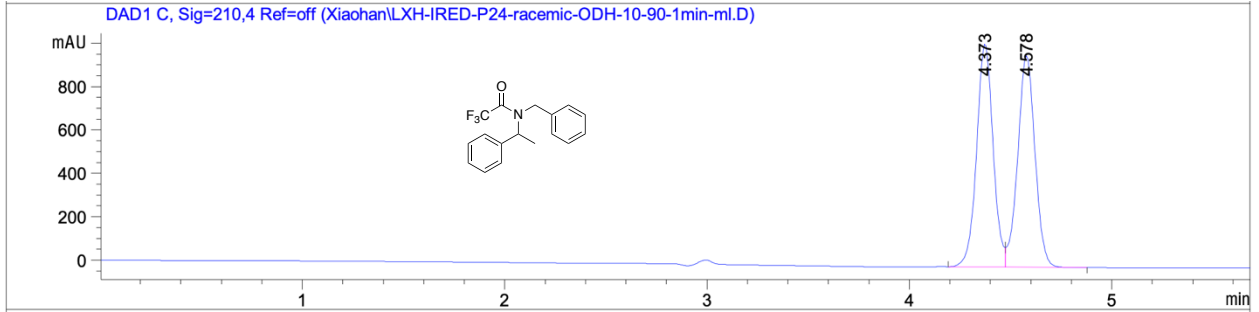


Signal 2: DAD1 B, Sig=254,4 Ref=off

Peak #	RetTime [min]	Type	Width [min]	Area [mAU*s]	Height [mAU]	Area %
1	14.042	BB	0.4252	489.58072	16.64042	100.0000

Totals : 489.58072 16.64042

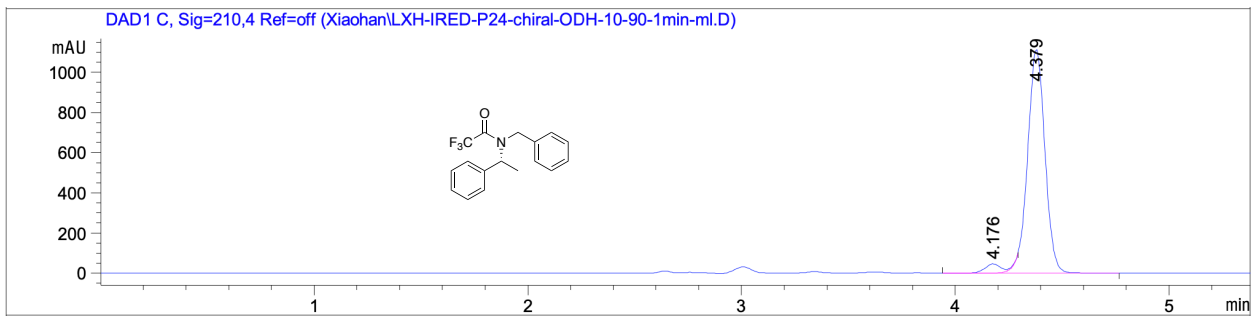
# HPLC analysis of compound III-23



Signal 3: DAD1 C, Sig=210,4 Ref=off

Peak #	RetTime [min]	Type	Width [min]	Area [mAU*s]	Height [mAU]	Area %
1	4.373	BV	0.0859	5804.85400	1028.19824	50.0946
2	4.578	VB	0.0912	5782.93896	974.46301	49.9054

Totals : 1.15878e4 2002.66125

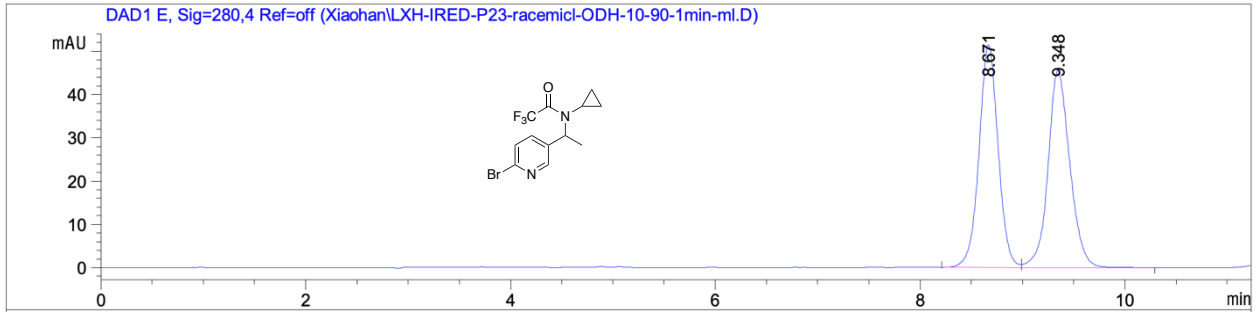


Signal 3: DAD1 C, Sig=210,4 Ref=off

Peak #	RetTime [min]	Type	Width [min]	Area [mAU*s]	Height [mAU]	Area %
1	4.176	BV E	0.0805	246.26407	45.97052	3.7383
2	4.379	VB R	0.0884	6341.37793	1114.71472	96.2617

Totals : 6587.64200 1160.68524

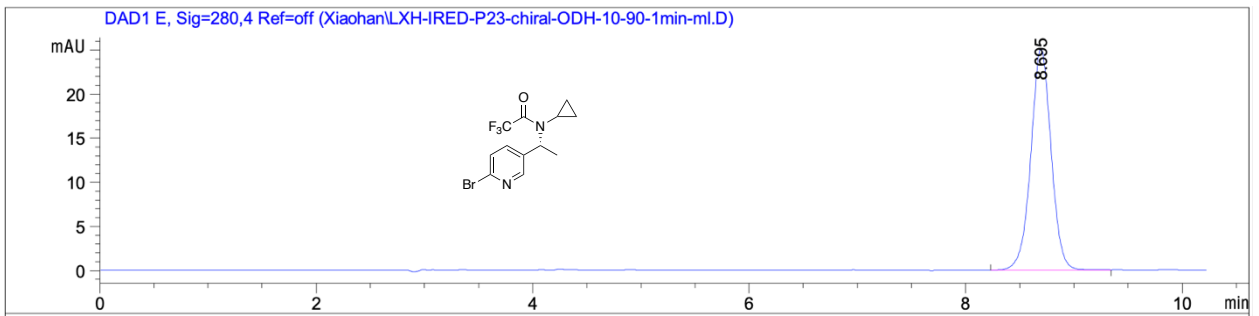
# HPLC analysis of compound III-24



Signal 5: DAD1 E, Sig=280,4 Ref=off

Peak #	RetTime [min]	Type	Width [min]	Area [mAU*s]	Height [mAU]	Area %
1	8.671	BV	0.1994	667.07153	51.41983	49.7054
2	9.348	VB	0.2253	674.97882	45.44992	50.2946

Totals : 1342.05035 96.86975

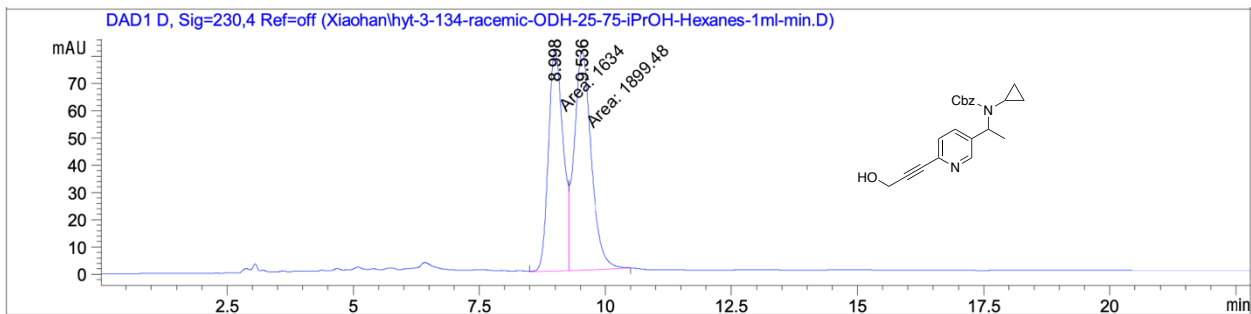


Signal 5: DAD1 E, Sig=280,4 Ref=off

Peak #	RetTime [min]	Type	Width [min]	Area [mAU*s]	Height [mAU]	Area %
1	8.695	BB	0.1995	326.37201	25.14106	100.0000

Totals : 326.37201 25.14106

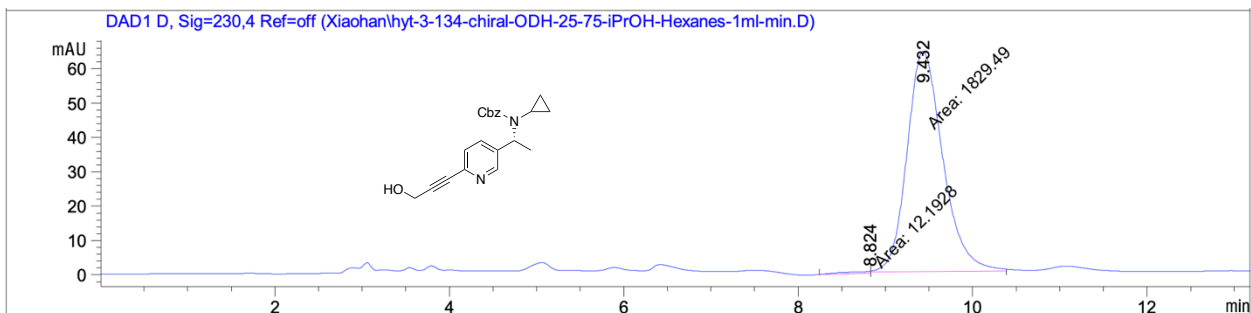
# HPLC analysis of compound III-36



Signal 4: DAD1 D, Sig=230,4 Ref=off

Peak #	RetTime [min]	Type	Width [min]	Area [mAU*s]	Height [mAU]	Area %
1	8.998	MF	0.3355	1633.99805	81.16051	46.2433
2	9.536	FM	0.3938	1899.48193	80.38520	53.7567

Totals : 3533.47998 161.54572



Signal 4: DAD1 D, Sig=230,4 Ref=off

Peak #	RetTime [min]	Type	Width [min]	Area [mAU*s]	Height [mAU]	Area %
1	8.824	MM	0.3434	12.19279	5.91770e-1	0.6620
2	9.432	MM	0.4753	1829.48706	64.14630	99.3380

Totals : 1841.67985 64.73807

## **IV. Allylations of Aryl/Heteroaryl Ketones: Neat, Clean, and Green. Applications to Targets in the Pharma- and Nutraceutical Industries**

Reproduced from:

Li, X.; Wood, A.; Lee, N.; Gallou, F.; Lipshutz, B. H. “Allylations of Aryl/Heteroaryl Ketones: Neat, Clean, and Green. Applications to Targets in the Pharma- and Nutraceutical Industries.” *Green Chem.*, **2022**, *24*, 4909-4914.

with permission from the Royal Society of Chemistry.

## ***4.1. Background and introduction***

### ***4.1.1. $\alpha$ -allylation of ketones***

The  $\alpha$ -allylation of ketones represents a fundamental and extensively studied process in the realm of organic synthesis, significantly advancing the field of C-C bond formation.<sup>1-9</sup> The profound impact of this reaction is attributed to the versatility of ketone-derived enolate chemistry and the prevalence of  $\alpha$ -substituted ketones and their derivatives in bioactive molecules, highlighting the reaction's applicability to medicinal chemistry and drug development. Additionally, the wide availability of over 10<sup>5</sup> commercially available ketone types exemplifies the reaction's extensive scope and its integral role in the synthesis of diverse organic compounds.<sup>10</sup>

The development of  $\alpha$ -allylation chemistry commenced in the early 20th century. Mechanistically, these reactions often begin with the deprotonation of ketones using strong bases like lithium hexamethyldisilazide (LHMDS), lithium diisopropylamide (LDA), or metal hydrides (e.g., NaH, KH). This process generates highly reactive alkali metal enolates, which can be transmetalated to more stable intermediates like silyl<sup>11-14</sup> or tin<sup>15-17</sup> enolates. These intermediates are particularly suited for subsequent palladium-catalyzed allylic alkylations, a transformative approach known as the Tsuji-Trost reaction (Scheme IV-1A).<sup>16-22</sup> This reaction has undergone significant evolution, incorporating a variety of transition metals such as ruthenium,<sup>23</sup> rhodium,<sup>24,25</sup> and iridium,<sup>26-29</sup> each offering unique contributions in terms of regioselectivity and stereoselectivity, thereby broadening the reaction's utility in complex molecule synthesis.

In recent years, the focus has shifted towards enantioselective  $\alpha$ -allylation, with the design of chiral catalysts, predominantly chiral phosphine ligands paired with palladium, achieving high enantiomeric excess, crucial for the synthesis of chiral drugs and natural products. A

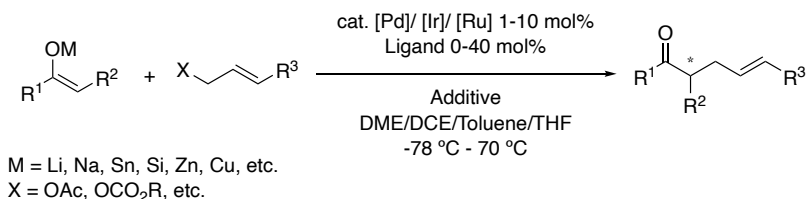
notable advancement in this realm is the decarboxylative strategy developed by Stoltz, which utilizes allyl  $\beta$ -ketoesters or allyl enol carbonates to yield  $\alpha$ -allylated ketones with high efficiency and stereoselectivity (Scheme IV-1B).<sup>30-36</sup> However, the scope of these enantioselective transformations is largely confined to cyclic ketones, with linear ketones posing a significant challenge. Further explorations have extended to decarboxylative allylations using other transition metals such as Ru<sup>37-39</sup> or Ir,<sup>40</sup> although these, too, are met with limitations in substrate scope.

Recent trends in  $\alpha$ -allylation have also seen the emergence of methods that include decarboxylative allylic alkylations (Scheme IV-1C)<sup>41-43</sup> and the allylation of ketone enamines (Scheme IV-1D).<sup>44-48</sup> These novel methodologies not only offer fresh approaches to achieving  $\alpha$ -allylation but also provide enhanced regio- and enantio-selectivity. Nevertheless, from an environmental standpoint, many of these techniques are less than ideal. They often necessitate high concentrations of expensive metal catalysts, complex ligands, and the use of potentially harmful organic solvents like dichloroethane (DCE) and toluene, often under extreme temperature conditions. Moreover, their applicability tends to be limited to a narrow range of specific substrates, diminishing their practicality in broader synthetic applications.

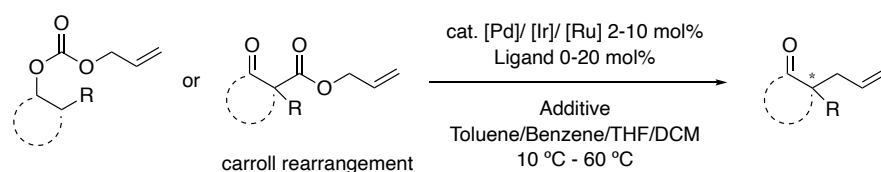
A more straightforward approach involves pre-activating allyl electrophiles, such as allyl halides, a fundamental reaction commonly taught at the undergraduate level. This avoids the need for expensive metal catalysts and accommodates a broader substrate range. Despite the traditional nature of this method, it remains popular for synthesizing achiral molecules. Nonetheless, it presents its own set of challenges, as it typically requires strong bases like sodium hydride, LDA, or LHMDS. This is particularly problematic for ketones with tertiary  $\alpha$ -carbons, where limited availability of  $\alpha$ -protons and increased steric hindrance are issues. Consequently, there is a growing demand for novel methodologies that adhere to green

chemistry principles, focusing on the use of less hazardous reagents and solvents, while operating under more environmentally benign conditions.

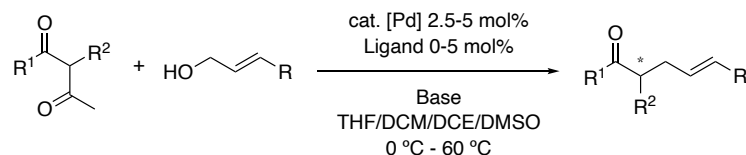
**A** Allylation of Ketone Enolates:



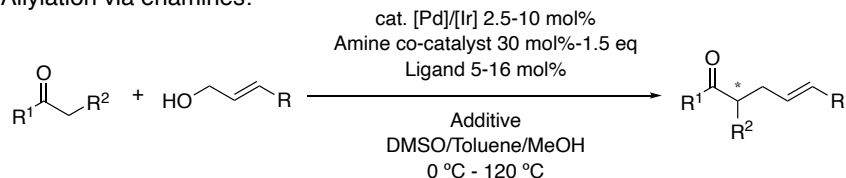
**B** Decarboxylative Allylation:



**C** Decarboxylative Allylation:



**D** Allylation via enamines:



**Scheme IV-1.** Prior art for  $\alpha$ -allylation of ketones

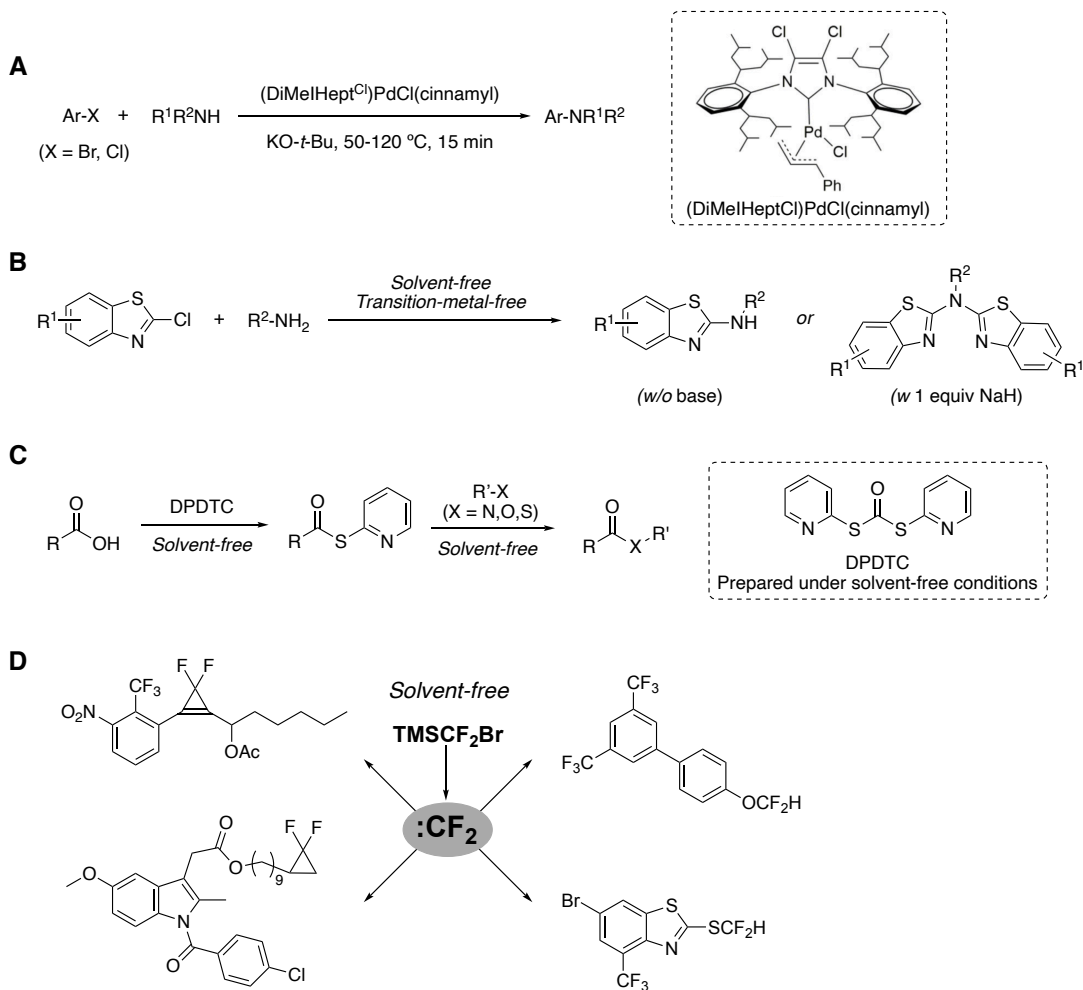
**4.1.2. Solvent-free reactions**

The principle of green chemistry, which is predicated on the design of chemical products and processes to minimize or eliminate the production and use of hazardous substances, has emerged as a pivotal guiding force in contemporary chemical research.<sup>49</sup> A critical challenge in actualizing the principles of green chemistry is the conventional reliance on organic solvents. As per the American Chemical Society's Green Chemistry Institute, organic solvents



account for a significant proportion of the total organic waste produced by the chemical industry, notably in pharmaceutical manufacturing.<sup>50,51</sup> These solvents, predominantly volatile organic compounds (VOCs), present substantial environmental and health hazards, characterized by their toxicity, emission potential, and contribution to hazardous waste.

Efforts to mitigate solvent pollution have led to the adoption of aqueous-phase reactions, utilizing recyclable water containing small amounts of designer surfactants.<sup>52</sup> Such approaches have made commendable strides towards reducing solvent-related environmental impact. However, the seminal analysis by Sheldon and colleagues emphatically posits that “The best solvent is no solvent...”<sup>53</sup> highlighting the ultimate goal of green chemistry. This ethos has catalyzed the shift towards solvent-free reactions,<sup>54-58</sup> which resonate profoundly with the 12 principles of green chemistry, particularly those advocating for waste prevention and the use of safer solvents and auxiliaries. In 2021, the Organ group reported a solvent-free amination process using a hyper-branched Pd-NHC pre-catalyst, (DiMeIHept<sup>Cl</sup>)Pd(cinnamyl). (Scheme IV-2A)<sup>59</sup> This method is adaptable to various nucleophiles, including aniline, alkylamine, carbazole, and indole, and can be scaled to multi-gram levels for synthesizing a range of secondary and tertiary amine derivatives. The absence of a solvent in this process significantly increases reactant concentration, allowing for low Pd catalyst loading (0.1 mol%) and rapid reaction times (15 minutes). In the same year, the Chen group introduced a solvent-free, transition-metal-free amination reaction between 2-chlorobenzothiazoles and primary amine. (Scheme IV-2B)<sup>60</sup> This reaction is notable for its switchability, with both base-free and NaH-promoted conditions selectively yielding desired mono- and di-heteroarylation products.



#### Scheme IV-2. Recent advances in solvent-free reactions in organic synthesis

Recently, our team has reported on sustainable methods for amidation, esterification, and thioesterification, utilizing in situ-generated 2-thiopyridine esters derived from dipyridyldithiocarbamate (DPDTC) and carboxylic acids. (Scheme IV-2C)<sup>61,62</sup> This method allows all steps, including the synthesis of novel coupling reagent DPDTC, to be conducted under solvent-free conditions. Furthermore, ongoing solvent-free research in our group involves difluorocarbene (:CF<sub>2</sub>) insertion into various substrates, promising a spectrum of difluoromethylated compounds with wide-ranging applications in the chemical industry. (Scheme IV-2D) This forthcoming work, to be detailed in due time, signifies our commitment to developing and implementing greener and more efficient chemical processes. Overall, by

obviating the need for liquid solvents, solvent-free reactions directly confront and address the challenges of solvent waste, emissions, and toxicity, thereby offering a more sustainable and environmentally benign alternative to conventional chemical processes.

Besides, the adoption of solvent-free methodologies necessitates a paradigm shift in conventional synthesis and catalysis approaches. This transition is leading a novel direction in research and development, with the potential to fundamentally revolutionize chemical reaction processes. The advent of solvent-free techniques, such as mechanochemistry,<sup>63,64</sup> microwave-assisted synthesis,<sup>65,66</sup> and the utilization of solid catalysts,<sup>67,68</sup> represents a strategic and innovative counter to the limitations traditionally imposed by solvent usage. These methodologies not only align seamlessly with the principles of green chemistry but also typically result in enhanced reaction efficiency, reduced energy consumption, and streamlined process operations. The progression towards solvent-free reactions transcends a mere trend; it is an essential evolution in the quest for sustainable and responsible chemical research and manufacturing.

## ***4.2. Result and Discussion***

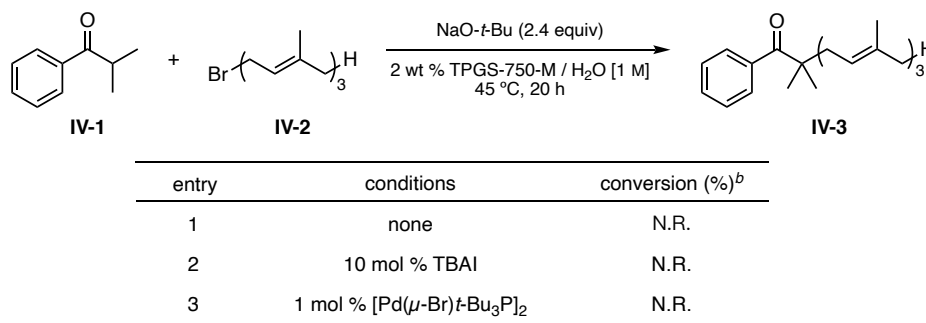
### ***4.2.1. Condition screening***

The initial hypothesis was that an enolization/allylation protocol could be successfully implemented under aqueous micellar conditions, drawing inspiration from our recently disclosed  $\alpha$ -arylations of ketones conducted under similar aqueous conditions.<sup>69</sup> Despite the apparent challenges posed by the relatively high pKa of the starting ketones, approximately 20, compared to the lower pKa of the predominantly water-based reaction medium, around 15, this approach might seem counterintuitive. However, the key to enabling this method lies in the use of the designer surfactant TPGS-750-M.<sup>70</sup> This surfactant forms nanomicelles with

hydrophobic inner cores, providing an environment conducive to enolization and  $\alpha$ -allylation.<sup>70,71</sup>

Contrary to expectations set by prior successes on  $\alpha$ -arylations in water,<sup>70</sup> a surprising outcome was encountered when an aryl bromide was replaced by an allylic bromide. Despite replicating the exact conditions of successful  $\alpha$ -arylations; i.e., using the same ketone, aqueous medium, and base, the anticipated  $\alpha$ -allylated ketone product was not formed. Attempts to alter various reaction parameters were unsuccessful in changing this outcome. These findings led to the conclusion that the "chemistry in water" approach, previously effective, was not suitable in this context, as evidenced by the experimental data (Table IV-1).

**Table IV-1.** Initial attempts at allylation in water<sup>a</sup>



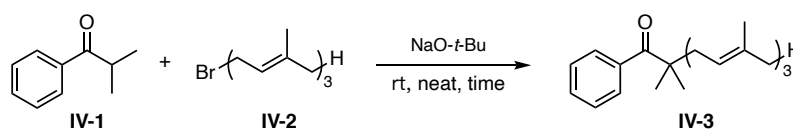
<sup>a</sup>Reaction conditions: isobutyrophenone (0.30 mmol), farnesyl bromide (0.90 mmol), NaO-*t*-Bu (0.72 mmol), 2 wt % TPGS-750-M (0.3 mL), 45 °C, 20 h. <sup>b</sup>Conversion determined by <sup>1</sup>H NMR; N.R. = no reaction.

The unexpected ineffectiveness of the 'chemistry in water' approach in  $\alpha$ -allylation highlights the need to investigate alternative methodologies in organic synthesis. Viewed through the glasses of green chemistry, the solvent-free approach emerges as a particularly attractive option. This method, when managed properly for safety, particularly during scale-up (as discussed later), not only adheres to the principles of waste reduction and minimization of hazardous substances but also opens up new possibilities for enhancing reaction efficiency

and selectivity. The absence of a solvent can lead to faster reaction rates, simplified purification processes, and potentially more straightforward reaction pathways.

Switching to solvent-free conditions for reactions that had previously been unsuccessful in an aqueous medium led to remarkable efficiency. The targeted  $\alpha$ -allylated ketones were synthesized in high yields, notably within minutes. A representative example on a small scale (0.40 mmol) involved the combination of farnesyl bromide with NaO-*t*-Bu, followed by the addition of isobutyrophenone. Conducting this procedure with 1.5 equivalents of the bromide and an equimolar amount of base at room temperature led to optimal results: complete conversion to the desired ketone (Table IV-2, entry 8). Efforts to reduce the quantity of allyl bromide or base were not successful, failing to achieve high conversion even with increased temperatures or the presence of an iodide source. Although the majority of these reactions were conducted over a 12-hour period (Table 2, entries 1-7), it was generally found that such prolonged reaction times were unnecessary for the successful completion of these reactions.

**Table IV-2.** Optimization under solvent-free conditions<sup>a</sup>

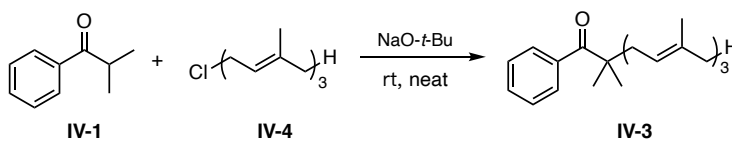


entry	bromide	NaO- <i>t</i> -Bu	additive/change	conversion (%) <sup>b</sup>
1	1.2 equiv	1.5 equiv	-	68
2	1.2 equiv	1.5 equiv	10 mol % TBAI	65
3	1.2 equiv	1.5 equiv	45 °C	68
4	1.2 equiv	2.4 equiv	45 °C	83
5	1.5 equiv	1 equiv	-	70
6	1.5 equiv	1.2 equiv	-	80
7	1.5 equiv	1.5 equiv	-	99
8	<b>1.5 equiv</b>	<b>1.5 equiv</b>	<b>20 min</b>	<b>98</b>

<sup>a</sup>Reaction conditions: isobutyrophenone (0.40 mmol), rt, each reaction was run for 12 h unless noted otherwise. <sup>b</sup>Conversion determined by <sup>1</sup>H NMR.

In consideration of the higher cost associated with allyl bromide relative to allyl chloride, the possibility of replacing allyl bromide with allyl chloride was evaluated. The results of these experiments, conducted with farnesyl chloride under diverse conditions, are detailed in Table IV-3. Employing the optimal conditions previously determined for allyl bromide, the reaction yielded a high conversion to the desired product, albeit with an extended reaction time (Table IV-3, entry 1). Notably, incorporation of an iodide salt to facilitate an *in-situ* Finkelstein reaction proved to significantly accelerate the reaction rate. For instance, complete conversion was achieved within three hours using just 2 mol % of KI or NaI (entries 4 and 5). Furthermore, the use of NaI, an especially cost-effective iodide salt, even at a minimal concentration of 0.5 mol %, resulted in full conversion over a period of five hours (entry 6). This clearly demonstrates a direct relationship between the quantity of iodide present and the time required to reach full reaction completion.

**Table IV-3.** Optimization using an allylic chloride



entry	additive	conversion (%) <sup>b</sup>
1	none	93 (20 h)
2	10 mol % TBAI	93 (1 h), 100 (3 h)
3	10 mol % KI	93 (1 h), 100 (3 h)
4	2 mol % KI	100 (3 h)
5	2 mol % NaI	100 (3 h)
6	0.5 mol % NaI	89 (3 h), 100 (5 h)

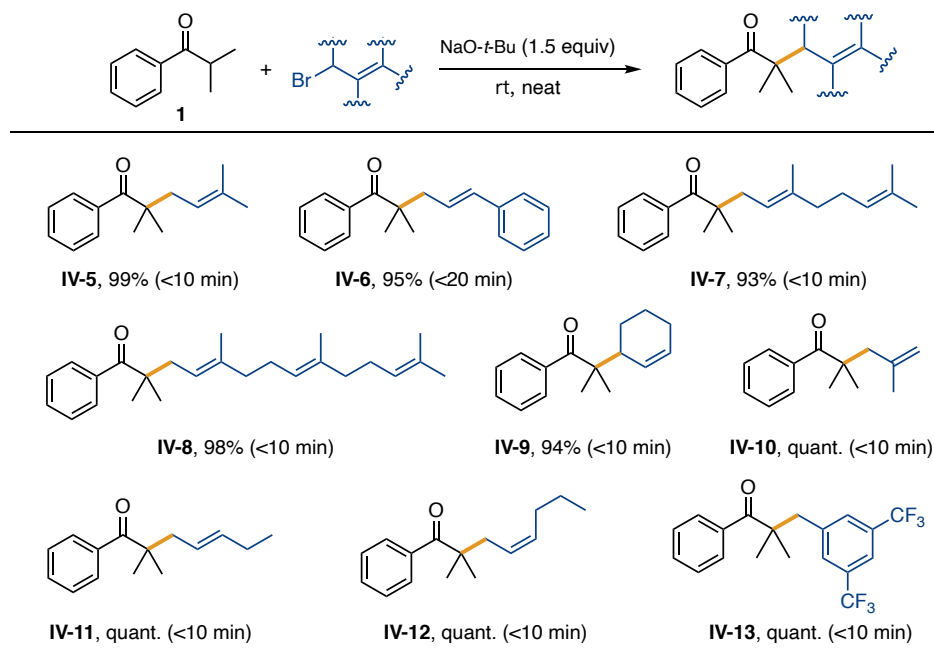
<sup>a</sup>Reaction conditions: isobutyrophenone (0.40 mmol), farnesyl chloride (0.60 mmol), NaO-*t*-Bu (0.60 mmol), rt. <sup>b</sup>Conversion determined by <sup>1</sup>H NMR.

#### 4.2.2. Substrate scope

Under optimized conditions, the scope of this solvent-free  $\alpha$ -allylation reaction was thoroughly investigated. Initially, we examined variations in the allylic bromide using isobutyrophenone, with results presented in Table IV-4. Allylic bromides such as prenyl (**IV-5**), geranyl (**IV-7**), and farnesyl (**IV-8**) proved to be highly effective, completing the reaction in under 10 minutes and consistently delivering excellent isolated yields. Cinnamyl bromide (**IV-6**), despite being a solid (albeit with a low melting point), did not pose any issues, yielding the desired product in high yield. The successful use of cyclic 3-bromocyclohex-1-ene (**IV-9**) and methallyl bromide (**IV-10**) indicated that branched allylic bromides were also compatible with this method. Interestingly, employment of a more reactive benzylic bromide also yielded a favorable outcome, producing product **IV-13** in quantitative yield. Notably, the reaction exhibited regioselectivity; for instance, using *E*-cinnamyl bromide led to product **IV-6**, and *E*-2-pentenyl bromide resulted in product **IV-11**, with only products from attack at the  $\alpha$ -site being observed. The stereochemical outcome was assessed using *Z*-2-hexenyl bromide, which produced product **IV-12**, indicating the preservation of stereochemical integrity. This is in contrast to the outcomes typically seen in traditional  $\alpha$ -allylation of ketones in organic solvents.<sup>21</sup>

In direct comparison with prior art, product **IV-5**, previously synthesized in THF or *t*-BuOH over a span of 4-8 hours,<sup>72,73</sup> was prepared using our solvent-free method in just 10 minutes. Similarly, the production of product **IV-7**, traditionally achieved through enolate formation (with LDA at low temperatures) followed by the addition of allylic bromide, required a reaction time of 16 hours with a yield of only 71%.<sup>74</sup> In stark contrast, our approach significantly reduces the reaction time while enhancing yield and efficiency, showcasing the advantages of the solvent-free  $\alpha$ -allylation methodology.

**Table IV-4.** Variations in the allylic bromide<sup>a</sup>



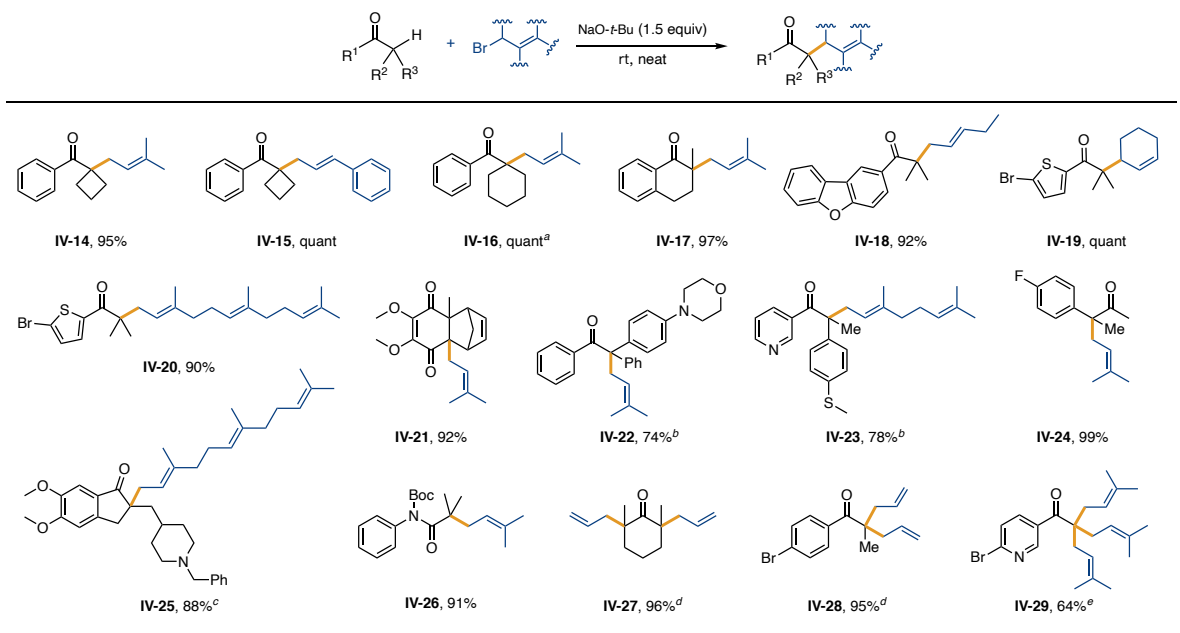
<sup>a</sup>Reaction conditions unless otherwise noted: ketone (0.40 mmol), allyl bromide (0.60 mmol), NaO-*t*-Bu (0.60 mmol), neat, rt. Yields are for isolated, purified products.

The versatility of the solvent-free  $\alpha$ -allylation reaction was further demonstrated by examining the nature of different participating ketones, as detailed in Table IV-5. Ketones with cyclic substitution at the  $\alpha$ -position, such as cyclobutyl or cyclohexyl moieties, were compatible, forming adducts **IV-14**, **IV-15**, and **IV-16** with various bromides. The reaction proceeded smoothly with cyclic ketones, including  $\alpha$ -methylated tetralone, yielding the corresponding products **IV-17**. Heteroaromatic ketones, exemplified by 1-(dibenzo[*b,d*]furan-2-yl)-2-methylpropan-1-one (**IV-18**) and 1-(5-bromothiophen-2-yl)-2-methylpropan-1-one (**IV-19**, **IV-20**), also readily underwent  $\alpha$ -allylation in high isolated yields. The formation of products **IV-22** and **IV-23** from ketones with sterically hindered substituents at the  $\alpha$ -site resulted in somewhat diminished yields and extended reaction times. Notably, these ketones



were solids as starting materials, posing challenges to the onset of reaction. However, as the reaction progressed, the *in-situ* generation of *t*-BuOH acted as a “lubricating fluid”, facilitating stirring. The synthesis of product **IV-24** is particularly noteworthy, suggesting thermodynamically controlled enolization in such unsymmetrical ketones. A more complex example involves  $\alpha$ -functionalized indanone **IV-25**, known as donepezil, showcasing the potential for late-stage functionalization under these solvent-free conditions. Reactions with  $\alpha$ -methylene-containing ketones, such as product **IV-28**, led to double allylation, indicating a propensity for poly-allylation. Thus, incorporating a hydrogen surrogate (e.g., silicon, sulfur) is necessary to achieve mono-allylation. For a methyl ketone, tri-allylated product **IV-29** was obtained under identical conditions. Utilizing 2,6-dimethylcyclohexanone as the educt led to symmetrical cyclohexanone **IV-27**, with allylation occurring on both sides of the carbonyl group. The successful application of this technology to other carbonyl derivatives, including the synthesis of prenylated amide **IV-26**, further support the prospects for further application of this solvent-free allylation methodology.

**Table IV-5.** Variations in the ketone partners<sup>a</sup>



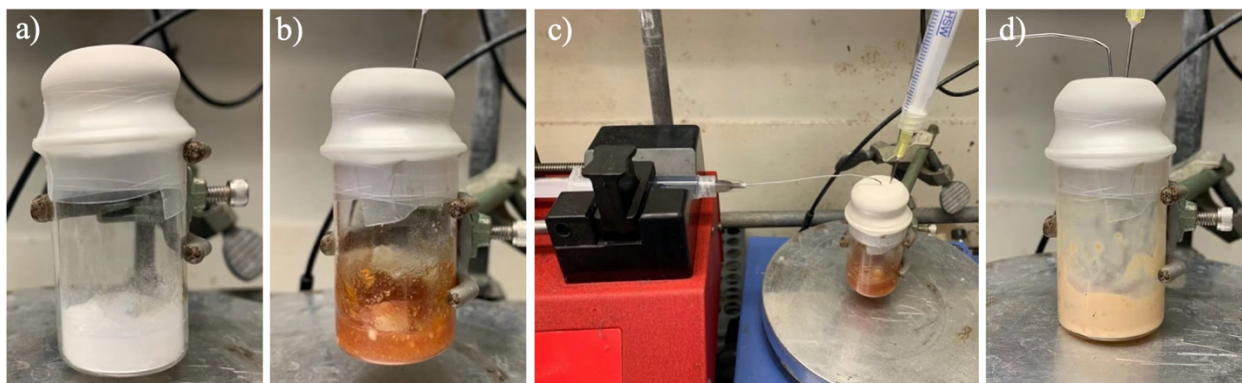
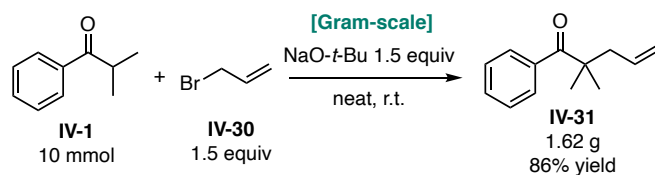
<sup>a</sup>Reaction conditions unless otherwise noted: ketone (0.40 mmol), allyl bromide (0.60 mmol), NaO-*t*-Bu (0.60 mmol), neat, rt, 1 h. Yields are for isolated purified, products. <sup>b</sup>overnight. <sup>c</sup>3 h. <sup>d</sup>5 h. <sup>e</sup>Using 1.20 mmol of allyl bromide and 1.20 mmol of NaO-*t*-Bu. <sup>f</sup>Using 1.80 mmol of allyl bromide and 1.80 mmol of NaO-*t*-Bu.

#### 4.2.3. Calorimetry study and gram-scale reaction

Despite the numerous advantages of solvent-free reactions, there often exists a concern regarding their safety, particularly in terms of thermal stability and control. This is particularly pertinent when scaling up reactions for industrial applications, where the potential for exothermic behavior and consequent risks can be significant. To address these safety considerations and provide a deeper understanding of the thermal properties of our solvent-free  $\alpha$ -allylation process, a comprehensive calorimetric study was conducted by our collaborators at Novartis.

Utilizing the model reaction between isobutyrophenone (**IV-1**) and prenyl bromide, calorimetric data indicated a substantial heat release of approximately 525 kJ/kg at room temperature (refer to section 4.5.9). However, it is important to note that due to instrumental limitations, all reagents were mixed in a single portion, thereby representing a maximal heat release scenario. Under more controlled conditions, such as dropwise addition of reagents or the use of an ice bath, the reaction's exothermic nature can be significantly moderated. Further safety assessment through differential scanning calorimetry (DSC), which can indicate the magnitude of exothermic decomposition reactions as well as the approximate onset temperature of where such exotherms occur, showed only two minor exothermic reactions commencing above 40 °C and 70 °C, suggesting no immediate risk of decomposition or explosion as temperature increases. Consequently, while scaling up this reaction is certainly feasible, it necessitates careful planning and mitigation.

As a practical example of safely conducting these reactions on a larger scale with appropriate mitigation measures, a gram-scale reaction was carried out using isobutyrophenone (**IV-1**) and simple allyl bromide (**IV-30**) (Scheme IV-3). A syringe pump setup facilitated the controlled, dropwise addition of isobutyrophenone to the mixture of base and allyl bromide. This approach yielded the corresponding ketone **IV-31** in 86% yield after a 15-minute addition period followed by an additional 30 minutes of stirring. The success of this gram-scale reaction not only exemplifies the practicality and scalability of our solvent-free  $\alpha$ -allylation methodology but also signifies a substantial step towards the broader adoption of such environmentally sustainable and efficient practices in industrial settings.



a) Adding NaO<sup>t</sup>Bu. b) Adding the allylic bromide in one portion. c) Adding isobutyrophenone dropwise via syringe pump. d) After adding isobutyrophenone and stirring for 30 min.

**Scheme IV-3.** Gram-scale reaction

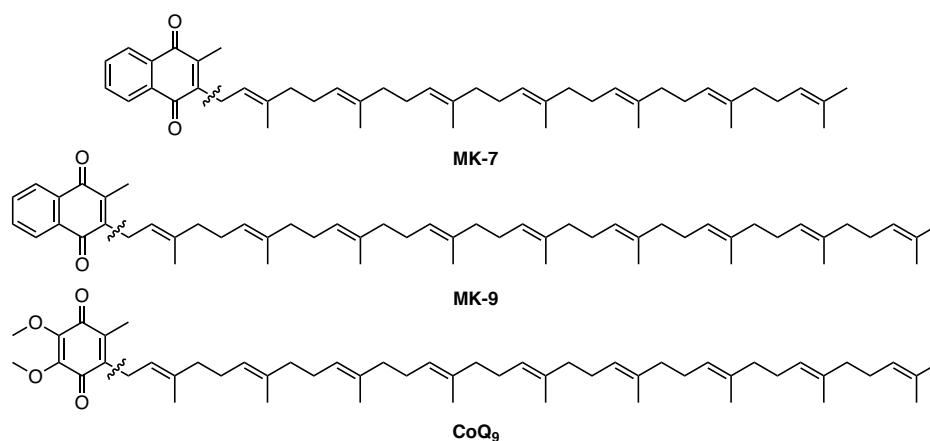
#### 4.2.4. Application: synthesis of MK-7, MK-9, CoQ<sub>9</sub>

Building upon the proven scalability and efficiency of our solvent-free  $\alpha$ -allylation technique, its application was extended to the synthesis of biologically significant compounds. This report highlights representative cases, including two compounds from the vitamin K<sub>2</sub> series,<sup>75</sup> MK-7 and MK-9, and delves into an application within the nutraceutical field, focusing on the synthesis of the notably expensive CoQ<sub>9</sub><sup>76</sup> (Figure IV-1).

MK-7 and MK-9, as crucial members of the vitamin K<sub>2</sub> family, are chemically known as menaquinones and are characterized by the length of their isoprenoid chains: MK-7 comprises seven isoprenoid units, while MK-9 contains nine. These forms of vitamin K<sub>2</sub> are integral to several physiological processes, especially blood coagulation and bone health.<sup>75</sup> MK-7, or menaquinone-7, is renowned for its high bioavailability and extended half-life in the human body relative to other vitamin K forms, enhancing its efficacy in bone mineralization and osteoporosis prevention. Additionally, its role in calcium metabolism extends to potential

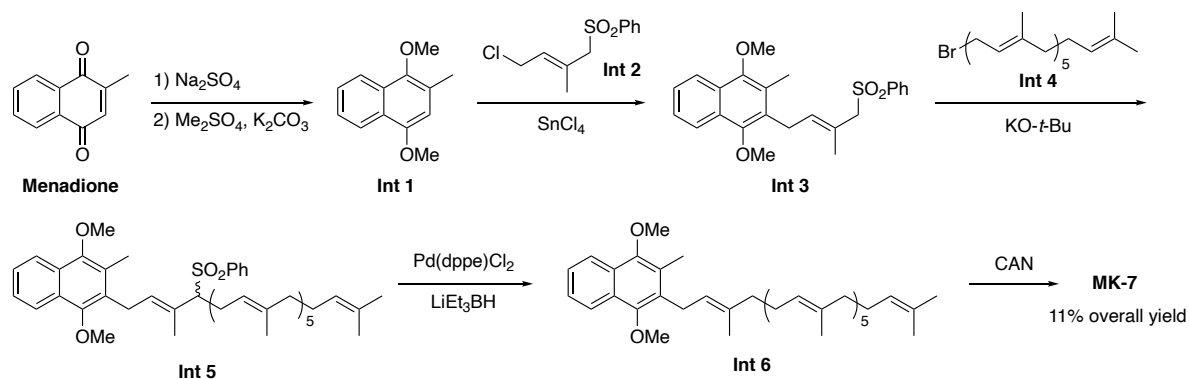
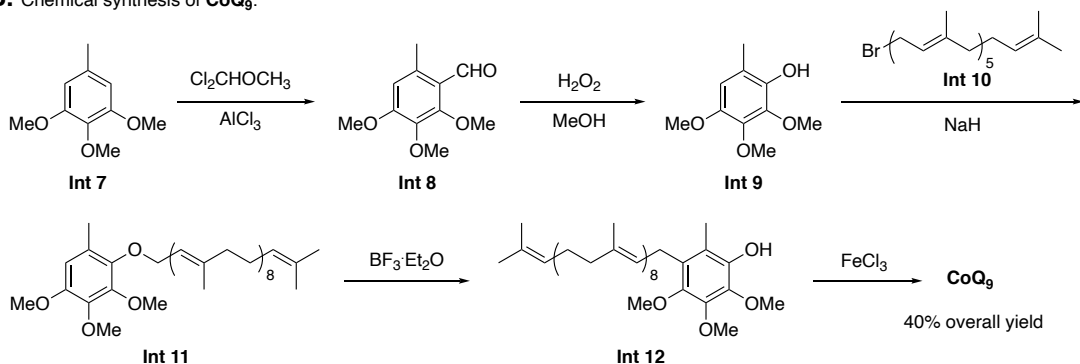
cardiovascular benefits by preventing arterial calcification. Notably, MK-7 has been identified as a potent pharmaceutical agent in the treatment of calciphylaxis, a condition characterized by calcium accumulation in fat and skin tissues.<sup>77</sup> MK-9, or menaquinone-9, though less researched than MK-7, is believed to confer similar health benefits due to its structural resemblance. It is naturally present in certain fermented foods and dairy products, enriching the dietary intake of vitamin K2.<sup>78</sup>

CoQ<sub>9</sub>, akin to the well-known nutritional supplement CoQ<sub>10</sub>, possesses nine isoprenoid units in its tail. Despite being less prevalent in dietary supplements and research than CoQ<sub>10</sub>, CoQ<sub>9</sub> shares similar biological functions and health benefits.<sup>79</sup> It is crucial in the mitochondrial electron transport chain for energy production at the cellular level and exhibits antioxidant properties, countering free radicals and oxidative stress. While CoQ<sub>10</sub> is commonly available commercially,<sup>80</sup> primarily produced through fermentation processes,<sup>81</sup> analogous production methods for lower homologs like CoQ<sub>9</sub> are not established, resulting in its high price (currently listed by Sigma-Aldrich at \$1260 for 5 mg, catalog number 27597),<sup>82</sup> which consequently restricts research into its biological activity. Developing efficient synthetic methodologies for CoQ<sub>9</sub> is imperative, not only to deepen our understanding of its biological roles but also to explore its potential in health and disease management.



**Figure IV-1.** Structures of MK-7, MK-9 and CoQ<sub>9</sub>

Scheme IV-4 outlines representative synthetic pathways for MK-7 and CoQ<sub>9</sub>. For MK-7,<sup>83</sup> the synthesis starts with the reduction of menadione, followed by methylation to yield **Int 1**. Next, Chlorosulfone (**Int 2**), derived from isopropene, is introduced through Friedel-Crafts alkylation to produce **Int 3**. The subsequent coupling of **Int 3** with hexaprenyl bromide (**Int 4**) constructs the required carbon skeleton for menaquinone MK-7. The synthesis concludes with desulfonation and subsequent oxidation, giving the target MK-7 with an 11% overall yield. Despite its capacity for high-purity products and scalability, the route's low yield constrains its extensive application. In the synthesis of CoQ<sub>9</sub>,<sup>84</sup> 3,4,5-trimethoxytoluene (**Int 7**) is employed as the starting material. A formylation reaction and subsequent Dakin oxidation give a phenol derivative (**Int 9**). This phenol then undergoes reaction with solanesyl bromide (**Int 10**) to produce the corresponding ether (**Int 11**). Further treatment with BF<sub>3</sub> etherate induces a rearrangement of the allyl side chain onto the vacant meta position, leading to **Int 12**. The final oxidation step was performed by treating **Int 12** with a simple oxidant FeCl<sub>3</sub> to give the final product CoQ<sub>9</sub> in an overall yield of 40%. This methodology constitutes one of the limited chemical synthesis routes for CoQ<sub>9</sub> and is adaptable to other ubiquinones such as CoQ<sub>1</sub>, CoQ<sub>2</sub>, and CoQ<sub>3</sub>, by simply modifying the allyl bromide used in the etherification step. However, enhancing the yield continues to be a critical challenge in these syntheses.

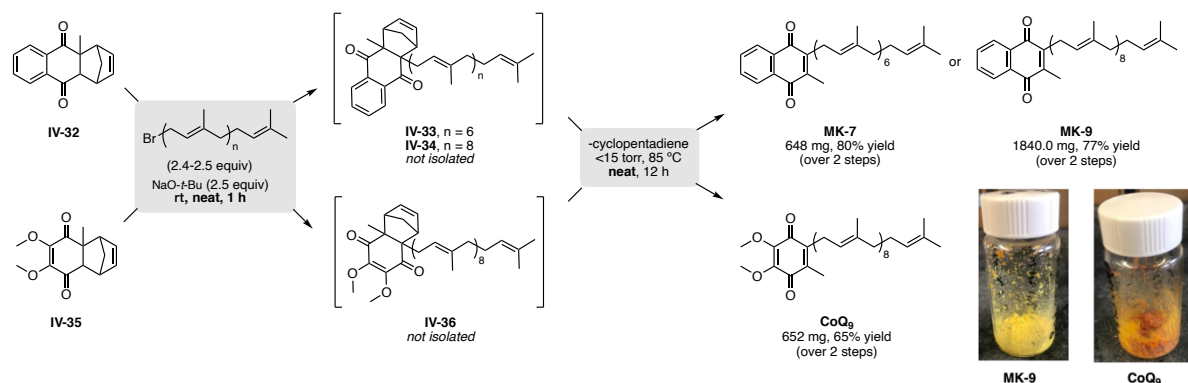
**A. Chemical synthesis of MK-7:****B. Chemical synthesis of CoQ<sub>9</sub>:****Scheme IV-4.** representative synthetic routes for MK-7 and CoQ<sub>9</sub>

Our first synthesis focused on MK-7 and MK-9. The route was building upon Ruttiman's ingenious Diels-Alder (DA)/retro-Diels-Alder strategy.<sup>85,86</sup> Starting with 2-methylnaphthoquinone, obtained via the oxidation of 2-methylnaphthalene,<sup>87</sup> the DA reaction with cyclopentadiene (Cp) yielded adduct **IV-32**. This adduct was ideally positioned for subsequent monoallylation (Scheme IV-5). Ruttiman's original method treated diketone adduct **IV-32** with base and phytol bromide to synthesize Vitamin K<sub>1</sub>.<sup>85,86</sup> By contrast, our approach to MK-7 involved neat  $\alpha$ -allylation of the same precursor resulting in compound **IV-33** within a 60-minute reaction time. Subsequently, MK-7 was obtained as a yellow solid (80% yield) by applying a retro-DA reaction at 85°C under vacuum, without any isolation

steps. The environmental efficiency of this process, with an E Factor of only 1.95, underscores its 'green' nature, a result of forgoing solvent use (detailed in section 4.5.8).<sup>88</sup>

For MK-9, the process started similarly with DA adduct **IV-32**. Here, the base (NaO-*t*-Bu; 2.52 equiv) was combined with nonprenoidal bromide, derived from the economically viable and readily available solanesol (a waste product from tobacco).<sup>89</sup> This allylation reaction, occurring at room temperature, took less than an hour to complete, leading to MK-9 precursor **IV-34** (Scheme IV-5). MK-9 was then yielded as a yellow solid (77% yield) following the same procedure as used for **IV-33**.

Regarding CoQ<sub>9</sub> synthesis, the only difference from vitamin K<sub>2</sub> is the DA adduct required, with CoQ<sub>9</sub> needing diketone **IV-35** as the coupling agent. By applying Ruttiman's retrosynthetic logic and utilizing the same base and solanesyl bromide,  $\alpha$ -allylation of **IV-35** was accomplished under conditions identical to those used previously, obtaining CoQ<sub>9</sub> precursor **IV-36**. A subsequent heat treatment under vacuum facilitated the desired retro-DA reaction, producing CoQ<sub>9</sub> as a yellow-red powder with a yield of 65%.



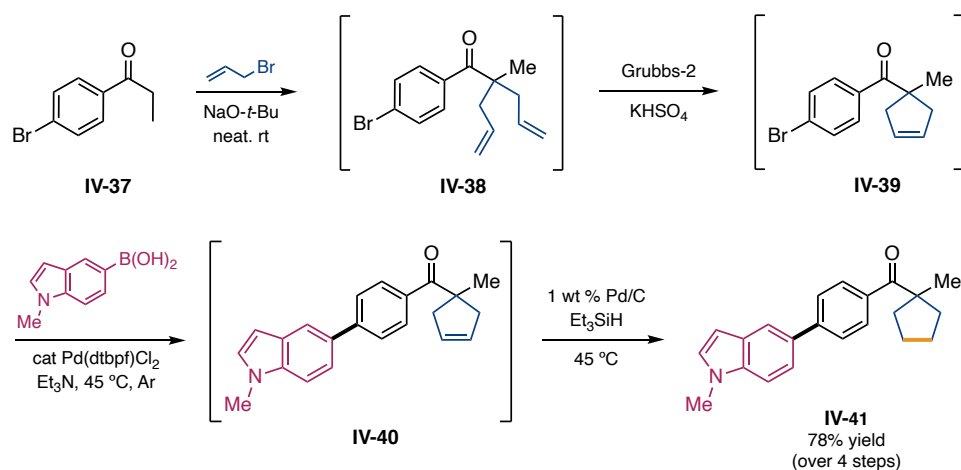
**Scheme IV-5.** Syntheses of MK-7, MK-9, and CoQ<sub>9</sub>

#### 4.2.5. One-pot sequence

The solvent-free  $\alpha$ -allylation reaction's utility is further exemplified via integration with other aqueous chemistries previously developed in our group.<sup>52</sup> As a representative example



of such 'telescoping' (Scheme IV-6), a solvent-free  $\alpha$ -allylation was seamlessly succeeded by three additional steps, all conducted under the same aqueous micellar conditions. This sequential process began with the double  $\alpha$ -allylation of ketone **IV-37**, forming product **IV-38**. This intermediate was then subjected to a ring-closing olefin metathesis reaction,<sup>90</sup> resulting in the formation of cyclopentene **IV-39**. Subsequently, without isolation, a Suzuki-Miyaura coupling was employed to transform the intermediate into biaryl compound **IV-40**.<sup>91</sup> The final step involved the reduction of this intermediate using our novel, low palladium concentration-catalyzed olefin hydrogenation method.<sup>92</sup> This four-step, one-pot sequence successfully yielded the final product **IV-41** with an overall efficiency of 78%, showcasing the methodology's potential in constructing complex molecular structures entirely under aqueous conditions.



**Scheme IV-6.** Representative 1-pot, 4-step sequence

### 4.3. Summary

In conclusion, our studies demonstrate that ketone  $\alpha$ -allylations can be conducted efficiently and simply in a neat state, by adding the ketone directly into a mixture of an allylic halide and an inexpensive base, NaO-*t*-Bu. These reactions are not only remarkably 'green,' avoiding the primary source of organic waste in chemical processes - solvents, but they also

featured fast reaction rates, typically reaching completion within minutes. While executing these reactions at smaller scale poses no significant concerns regarding exothermicity, larger-scale operations reveal considerable heat release, as evidenced by calorimetric analyses. Consequently, to ensure safety in these scenarios, procedural modifications, such as employing a cooling bath and/or slow addition of the ketone are recommended. Furthermore, the application of this solvent-free  $\alpha$ -allylation technique to synthesize compounds of interest, including those in the pharmaceutical and nutraceutical domains, has been successfully demonstrated, showcasing its versatility and potential use in various fields.

#### 4.4. References

1. Consiglio, G.; Waymouth, R. M. Enantioselective Homogeneous Catalysis Involving Transition-Metal-Allyl Intermediates. *Chem. Rev.* **1989**, *89*, 257–276.
2. Trost, B. M.; Van Vranken, D. L. Asymmetric Transition Metal-Catalyzed Allylic Alkylations. *Chem. Rev.* **1996**, *96*, 395–422.
3. Trost, B. M. Designing a Receptor for Molecular Recognition in a Catalytic Synthetic Reaction: Allylic Alkylation. *Acc. Chem. Res.* **1996**, *29*, 355–364.
4. Trost, B. M. Pd Asymmetric Allylic Alkylation (AAA). A Powerful Synthetic Tool. *Chem. Pharm. Bull.* **2002**, *50*, 1–14.
5. Hong, A. Y.; Stoltz, B. M. The Construction of All-Carbon Quaternary Stereocenters by Use of Pd-Catalyzed Asymmetric Allylic Alkylation Reactions in Total Synthesis. *Eur. JOC* **2013**, *2013*, 2745–2759.
6. Junk, L.; Kazmaier, U. The Allylic Alkylation of Ketone Enolates. *ChemistryOpen* **2020**, *9*, 929–952
7. Braun, M.; Meier, T. Tsuji–Trost Allylic Alkylation with Ketone Enolates. *Angew. Chem., Int. Ed.* **2006**, *45*, 6952–6955.
8. Trost, B. M.; Machacek, M. R.; Aponick, A. Predicting the Stereochemistry of Diphenylphosphino Benzoic Acid (DPPBA)-Based Palladium-Catalyzed Asymmetric Allylic Alkylation Reactions: A Working Model. *Acc. Chem. Res.* **2006**, *39*, 747–760.
9. Lu, Z.; Ma, S. Metal-Catalyzed Enantioselective Allylation in Asymmetric Synthesis. *Angew. Chem., Int. Ed.* **2008**, *47*, 258–297.

10. Donohoe, T. J.; Pilgrim, B. S.; Jones, G. R.; Bassuto, J. A. Synthesis of Substituted Isoquinolines Utilizing Palladium-Catalyzed  $\alpha$ -Arylation of Ketones. *Proc. Natl. Acad. Sci. U.S.A.* **2012**, *109*, 11605–11608.
11. Tsuji, J.; Minami, I.; Shimizu, I. Palladium-Catalyzed Allylation of Ketones and Aldehydes with Allylic Carbonates via Silyl Enol Ethers under Neutral Conditions. *Chem. Lett.* **1983**, *12*, 1325–1326.
12. Seto, M.; Roizen, J. L.; Stoltz, B. M. Catalytic Enantioselective Alkylation of Substituted Dioxanone Enol Ethers: Ready Access to C( $\alpha$ )-Tetrasubstituted Hydroxyketones, Acids, and Esters. *Angew. Chem., Int. Ed.* **2008**, *47*, 6873–6876.
13. Bélanger, É.; Cantin, K.; Messe, O.; Tremblay, M.; Paquin, J.-F. Enantioselective Pd-Catalyzed Allylation Reaction of Fluorinated Silyl Enol Ethers. *J. Am. Chem. Soc.* **2007**, *129*, 1034–1035.
14. Muraoka, T.; Matsuda, I.; Itoh, K. Rhodium-Catalyzed Substitution of Allylic Carbonates with Enoxysilanes. *Tetrahedron Lett.* **2000**, *41*, 8807–8811.
15. Shi, G.; Huang, X.; Zhang, F.-J. Regioselectivity in the Addition of Carbon Nucleophiles to 1-Fluoro and 1, 1-Difluoro  $\pi$ -Allylpalladium Complexes. *Tetrahedron Lett.* **1995**, *36*, 6305–6308.
16. Trost, B. M.; Schroeder, G. M. Palladium-Catalyzed Asymmetric Alkylation of Ketone Enolates. *J. Am. Chem. Soc.* **1999**, *121*, 6759–6760.
17. Trost, B. M.; Schroeder, G. M. Palladium-Catalyzed Asymmetric Allylic Alkylation of Ketone Enolates. *Chem. Eur. J.* **2005**, *11*, 174–184.
18. Noreen, S.; Zahoor, A. F.; Ahmad, S.; Shahzadi, I.; Irfan, A.; Faiz, S. Novel Chiral Ligands for Palladium-Catalyzed Asymmetric Allylic Alkylation/ Asymmetric Tsuji-Trost Reaction: A Review. *Curr. Org. Chem.* **2019**, *23*, 1168–1213.
19. Ferraccioli, R.; Pignataro, L. Tsuji-Trost Type Functionalization of Allylic Substrates with Challenging Leaving Groups: Recent Developments. *COC* **2015**, *19*, 106–120.
20. Tsuji, J. The Tsuji–Trost Reaction and Related Carbon–Carbon Bond Formation Reactions: Overview of the Palladium–Catalyzed Carbon–Carbon Bond Formation via  $\pi$ -Allylpalladium and Propargylpalladium Intermediates. In *Handbook of Organopalladium Chemistry for Organic Synthesis*; John Wiley & Sons, Ltd, 2002; pp 1669–1687.
21. Usui, I.; Schmidt, S.; Breit, B. Dual Palladium- and Proline-Catalyzed Allylic Alkylation of Enolizable Ketones and Aldehydes with Allylic Alcohols. *Org. Lett.* **2009**, *11*, 1453–1456.
22. Trost, B. M.; Schroeder, G. M.; Kristensen, J. Palladium-Catalyzed Asymmetric Allylic Alkylation of  $\alpha$ -Aryl Ketones. *Angew. Chem., Int. Ed.* **2002**, *41*, 3492–3495.

23. Kanbayashi, N.; Yamazawa, A.; Takii, K.; Okamura, T.; Onitsuka, K. Planar-Chiral Cyclopentadienyl-Ruthenium-Catalyzed Regio- and Enantioselective Asymmetric Allylic Alkylation of Silyl Enolates under Unusually Mild Conditions. *Adv. Synth. Catal.* **2016**, *358*, 555–560.
24. Evans, P. A.; Lawler, M. J. Regio- and Diastereoselective Rhodium-Catalyzed Allylic Substitution with Acyclic  $\alpha$ -Alkoxy-Substituted Copper(I) Enolates: Stereodivergent Approach to 2,3,6-Trisubstituted Dihydropyrans. *J. Am. Chem. Soc.* **2004**, *126*, 8642–8643.
25. Evans, P. A.; Clizbe, E. A.; Lawler, M. J.; Oliver, S. Enantioselective Rhodium-Catalyzed Allylic Alkylation of Acyclic  $\alpha$ -Alkoxy Substituted Ketones Using a Chiral Monodentate Phosphite Ligand. *Chem. Sci.* **2012**, *3*, 1835.
26. Graening, T.; Hartwig, J. F. Iridium-Catalyzed Regio- and Enantioselective Allylation of Ketone Enolates. *J. Am. Chem. Soc.* **2005**, *127*, 17192–17193.
27. Chen, W.; Chen, M.; Hartwig, J. F. Diastereo- and Enantioselective Iridium-Catalyzed Allylation of Cyclic Ketone Enolates: Synergetic Effect of Ligands and Barium Enolates. *J. Am. Chem. Soc.* **2014**, *136*, 15825–15828.
28. Chen, M.; Hartwig, J. F. Iridium-Catalyzed Enantioselective Allylic Substitution of Unstabilized Enolates Derived from  $\alpha,\beta$ -Unsaturated Ketones. *Angew. Chem., Int. Ed.* **2014**, *53*, 8691–8695.
29. Chen, M.; Hartwig, J. F. Iridium-Catalyzed Enantioselective Allylic Substitution of Enol Silanes from Vinylogous Esters and Amides. *J. Am. Chem. Soc.* **2015**, *137*, 13972–13979.
30. Reeves, C. M.; Eidamshaus, C.; Kim, J.; Stoltz, B. M. Enantioselective Construction of  $\alpha$ -Quaternary Cyclobutanones by Catalytic Asymmetric Allylic Alkylation. *Angew. Chem., Int. Ed.* **2013**, *52*, 6718–6721.
31. Numajiri, Y.; Pritchett, B. P.; Chiyoda, K.; Stoltz, B. M. Enantioselective Synthesis of  $\alpha$ -Quaternary Mannich Adducts by Palladium-Catalyzed Allylic Alkylation: Total Synthesis of (+)-Sibirinine. *J. Am. Chem. Soc.* **2015**, *137*, 1040–1043.
32. Alexy, E. J.; Zhang, H.; Stoltz, B. M. Catalytic Enantioselective Synthesis of Acyclic Quaternary Centers: Palladium-Catalyzed Decarboxylative Allylic Alkylation of Fully Substituted Acyclic Enol Carbonates. *J. Am. Chem. Soc.* **2018**, *140*, 10109–10112.
33. Trost, B. M.; Xu, J.; Schmidt, T. Ligand Controlled Highly Regio- and Enantioselective Synthesis of  $\alpha$ -Acyloxyketones by Palladium-Catalyzed Allylic Alkylation of 1,2-Enediol Carbonates. *J. Am. Chem. Soc.* **2008**, *130*, 11852–11853.
34. Trost, B. M.; Xu, J.; Schmidt, T. Palladium-Catalyzed Decarboxylative Asymmetric Allylic Alkylation of Enol Carbonates. *J. Am. Chem. Soc.* **2009**, *131*, 18343–18357.

35. Trost, B. M.; Xu, J. Palladium-Catalyzed Asymmetric Allylic  $\alpha$ -Alkylation of Acyclic Ketones. *J. Am. Chem. Soc.* **2005**, *127*, 17180–17181.
36. Trost, B. M.; Xu, J. Regio- and Enantioselective Pd-Catalyzed Allylic Alkylation of Ketones through Allyl Enol Carbonates. *J. Am. Chem. Soc.* **2005**, *127*, 2846–2847.
37. Ogawa, S.; Miyata, K.; Kawakami, S.; Tanaka, S.; Kitamura, M. CpRuII-Chiral Bisamidine Complex Catalyzed Asymmetric Carroll-Type Decarboxylative Allylation of  $\beta$ -Keto Allyl Esters. *Tetrahedron* **2020**, *76*, 130888.
38. Constant, S.; Tortoioli, S.; Müller, J.; Lacour, J. An Enantioselective CpRu-Catalyzed Carroll Rearrangement. *Angew. Chem., Int. Ed.* **2007**, *46*, 2082–2085.
39. Burger, E. C.; Tunge, J. A. Ruthenium-Catalyzed Decarboxylative Allylation of Nonstabilized Ketone Enolates. *Org. Lett.* **2004**, *6*, 2603–2605.
40. He, H.; Zheng, X.-J.; Li, Y.; Dai, L.-X.; You, S.-L. Ir-Catalyzed Regio- and Enantioselective Decarboxylative Allylic Alkylations. *Org. Lett.* **2007**, *9*, 4339–4341.
41. Zhou, X.-L.; Ren, L.; Wang, P.-S. Palladium(II)-Catalyzed Deacylative Allylic C–H Alkylation. *J. Org. Chem.* **2017**, *82*, 9794–9800.
42. Grenning, A. J.; Van Allen, C. K.; Maji, T.; Lang, S. B.; Tunge, J. A. Development of Asymmetric Deacylative Allylation. *J. Org. Chem.* **2013**, *78*, 7281–7287.
43. Grenning, A. J.; Tunge, J. A. Deacylative Allylation: Allylic Alkylation via Retro-Claisen Activation. *J. Am. Chem. Soc.* **2011**, *133*, 14785–14794.
44. Huo, X.; Yang, G.; Liu, D.; Liu, Y.; Gridnev, I. D.; Zhang, W. Palladium-Catalyzed Allylic Alkylation of Simple Ketones with Allylic Alcohols and Its Mechanistic Study. *Angew. Chem., Int. Ed.* **2014**, *53*, 6776–6780.
45. Ibrahim, I.; Córdova, A. Direct Catalytic Intermolecular  $\alpha$ -Allylic Alkylation of Aldehydes by Combination of Transition-Metal and Organocatalysis. *Angew. Chem., Int. Ed.* **2006**, *45*, 1952–1956.
46. Zhao, X.; Liu, D.; Guo, H.; Liu, Y.; Zhang, W. C–N Bond Cleavage of Allylic Amines via Hydrogen Bond Activation with Alcohol Solvents in Pd-Catalyzed Allylic Alkylation of Carbonyl Compounds. *J. Am. Chem. Soc.* **2011**, *133*, 19354–19357.
47. Weix, D. J.; Hartwig, J. F. Regioselective and Enantioselective Iridium-Catalyzed Allylation of Enamines. *J. Am. Chem. Soc.* **2007**, *129*, 7720–7721.
48. Chen, J.-P.; Peng, Q.; Lei, B.-L.; Hou, X.-L.; Wu, Y.-D. Chemo- and Regioselectivity-Tunable Pd-Catalyzed Allylic Alkylation of Imines. *J. Am. Chem. Soc.* **2011**, *133*, 14180–14183.

49. Anastas, P.; Eghbali, N. Green Chemistry: Principles and Practice. *Chem. Soc. Rev.* **2010**, *39*, 301–312.
50. Jimenez-Gonzalez, C.; Ponder, C. S.; Broxterman, Q. B.; Manley, J. B. Using the Right Green Yardstick: Why Process Mass Intensity Is Used in the Pharmaceutical Industry To Drive More Sustainable Processes. *Org. Process Res. Dev.* **2011**, *15*, 912–917.
51. Sharma, S.; Das, J.; Braje, W. M.; Dash, A. K.; Handa, S. A Glimpse into Green Chemistry Practices in the Pharmaceutical Industry. *ChemSusChem* **2020**, *13*, 2859–2875.
52. Cortes-Clerget, M.; Yu, J.; A. Kincaid, J. R.; Walde, P.; Gallou, F.; H. Lipshutz, B. Water as the Reaction Medium in Organic Chemistry: From Our Worst Enemy to Our Best Friend. *Chem. Sci.* **2021**, *12*, 4237–4266.
53. Sheldon, R. A. Green Solvents for Sustainable Organic Synthesis: State of the Art. *Green Chem.* **2005**, *7*, 267–278.
54. Tanaka, K.; Toda, F. Solvent-Free Organic Synthesis. *Chem. Rev.* **2000**, *100*, 1025–1074.
55. Garay, A. L.; Pichon, A.; James, S. L. Solvent-Free Synthesis of Metal Complexes. *Chem. Soc. Rev.* **2007**, *36*, 846.
56. Martins, M. A. P.; Frizzo, C. P.; Moreira, D. N.; Buriol, L.; Machado, P. Solvent-Free Heterocyclic Synthesis. *Chem. Rev.* **2009**, *109*, 4140–4182.
57. Walsh, P. J.; Li, H.; de Parrodi, C. A. A Green Chemistry Approach to Asymmetric Catalysis: Solvent-Free and Highly Concentrated Reactions. *Chem. Rev.* **2007**, *107*, 2503–2545.
58. Tanaka, K. *Solvent-Free Organic Synthesis*; John Wiley & Sons, 2009.
59. Semeniuchenko, V.; Sharif, S.; Day, J.; Chandrasoma, N.; Pietro, W. J.; Manthorpe, J.; Braje, W. M.; Organ, M. G. (DiMeIHept<sup>Cl</sup>)Pd: A Low-Load Catalyst for Solvent-Free (Melt) Amination. *J. Org. Chem.* **2021**, *86*, 10343–10359.
60. Cheng, H.; Zhu, Y.-Q.; Liu, P.-F.; Yang, K.-Q.; Yan, J.; Sang, W.; Tang, X.-S.; Zhang, R.; Chen, C. Switchable and Scalable Heteroarylation of Primary Amines with 2-Chlorobenzothiazoles under Transition-Metal-Free and Solvent-Free Conditions. *J. Org. Chem.* **2021**, *86*, 10288–10302.
61. Freiberg, K. M.; Ghiglietti, E.; Scurria, M.; Lipshutz, B. H. Use of Dipyridyldithiocarbonate (DPDTC) as an Environmentally Responsible Reagent Leading to Esters and Thioesters under Green Chemistry Conditions. *Green Chem.* **2023**, *25*, 9941–9947.
62. Freiberg, K. M.; Kavthe, R. D.; Thomas, R. M.; Fialho, D. M.; Dee, P.; Scurria, M.; Lipshutz, B. H. Direct Formation of Amide/Peptide Bonds from Carboxylic Acids: No Traditional Coupling Reagents, 1-Pot, and Green. *Chem. Sci.* **2023**, *14*, 3462–3469.

63. Friščić, T.; Mottillo, C.; Titi, H. M. Mechanochemistry for Synthesis. *Angew. Chem., Int. Ed.* **2020**, *59*, 1018–1029.
64. Howard, J. L.; Cao, Q.; Browne, D. L. Mechanochemistry as an Emerging Tool for Molecular Synthesis: What Can It Offer? *Chem. Sci.* **2018**, *9*, 3080–3094.
65. S. Varma, R. Solvent-Free Organic Syntheses. Using Supported Reagents and Microwave Irradiation. *Green Chem.* **1999**, *1*, 43–55.
66. Bougrin, K.; Loupy, A.; Soufiaoui, M. Microwave-Assisted Solvent-Free Heterocyclic Synthesis. *J. Photochem. Photobiol. C* **2005**, *6*, 139–167.
67. Dhakshinamoorthy, A.; Asiri, A. M.; Alvaro, M.; Garcia, H. Metal Organic Frameworks as Catalysts in Solvent-Free or Ionic Liquid Assisted Conditions. *Green Chem.* **2018**, *20*, 86–107.
68. Jambhulkar, D.K.; Ugwekar, R. P.; Barai, D. P. A Review on Solid Base Heterogeneous Catalysts: Preparation, Characterization and Applications. *Chem. Eng. Commun.* **2022**, *209*, 433–484.
69. Wood, A. B.; Roa, D. E.; Gallou, F.; Lipshutz, B. H.  $\alpha$ -Arylation of (Hetero)Aryl Ketones in Aqueous Surfactant Media. *Green Chem.* **2021**, *23*, 4858–4865.
70. Lipshutz, B. H.; Ghorai, S.; Abela, A. R.; Moser, R.; Nishikata, T.; Duplais, C.; Krasovskiy, A.; Gaston, R. D.; Gadwood, R. C. TPGS-750-M: A Second-Generation Amphiphile for Metal-Catalyzed Cross-Couplings in Water at Room Temperature. *J. Org. Chem.* **2011**, *76*, 4379–4391.
71. Bihani, M.; Ansari, T. N.; Finck, L.; Bora, P. P.; Jasinski, J. B.; Pavuluri, B.; Leahy, D. K.; Handa, S. Scalable  $\alpha$ -Arylation of Nitriles in Aqueous Micelles Using Ultrasmall Pd Nanoparticles: Surprising Formation of Carbanions in Water. *ACS Catal.* **2020**, *10*, 6816–6821.
72. Su, H.; Li, W.; Xuan, Z.; Yu, W. Copper-Catalyzed Cyclization and Azidation of  $\gamma,\delta$ -Unsaturated Ketone O-Benzoyl Oximes. *Adv. Synth. Catal.* **2015**, *357*, 64–70.
73. Du, W.; Zhao, M.-N.; Ren, Z.-H.; Wang, Y.-Y.; Guan, Z.-H. Copper-Catalyzed 5-Endo-Trig Cyclization of Ketoxime Carboxylates: A Facile Synthesis of 2-Arylpyrroles. *Chem. Commun.* **2014**, *50*, 7437.
74. Snyder, S. A.; Treitler, D. S.; Schall, A. A Two-Step Mimic for Direct, Asymmetric Bromonium- and Chloronium-Induced Polyene Cyclizations. *Tetrahedron* **2010**, *66*, 4796–4804.
75. Schwalfenberg, G. K. Vitamins K1 and K2: The Emerging Group of Vitamins Required for Human Health. *J. Nutr. Metab.* **2017**, *2017*, 1–6.

76. Molyneux, S.; Lever, M.; Florkowski, C.; George, P. Plasma Total Coenzyme Q9 (CoQ9) in the New Zealand Population: Reference Interval and Biological Variation. *Clin. Chem.* **2007**, *53*, 802–803.
77. Tumlin, J. A.; Darke, P. L.; and Rudey, J. M. Methods and compositions for preventing or treating calciphylaxis. U.S. Patent US10736858B2, August 11, 2020.
78. Tarvainen, M.; Fabritius, M.; Yang, B. Determination of Vitamin K Composition of Fermented Food. *Food Chem.* **2019**, *275*, 515–522.
79. Lekli, I.; Das, S.; Das, S.; Mukherjee, S.; Bak, I.; Juhasz, B.; Bagchi, D.; Trimurtulu, G.; Krishnaraju, A. V.; Sengupta, K.; Tosaki, A.; Das, D. K. Coenzyme Q<sub>9</sub> Provides Cardioprotection after Converting into Coenzyme Q<sub>10</sub>. *J. Agric. Food Chem.* **2008**, *56*, 5331–5337.
80. For selected CoQ<sub>10</sub> supplier, see: Puritan's Pride, <https://www.puritan.com/co-q-10-055>, (accessed Dec 2023)
81. Page, A. C.; Gale, P.; Wallick, H.; Walton, R. B.; McDaniel, L. E.; Woodruff, H. B.; Folkers, K. Coenzyme Q. XVII. Isolation of Coenzyme Q<sub>10</sub> from Bacterial Fermentation. *Arch. Biochem. Biophys.* **1960**, *89*, 318–321.
82. For selected CoQ<sub>9</sub> supplier, see: <https://www.sigmaldrich.com/US/en/product/sigma/27597>, (accessed Dec 2023)
83. Baj, A.; Wałejko, P.; Kutner, A.; Kaczmarek, Ł.; Morzycki, J. W.; Witkowski, S. Convergent Synthesis of Menaquinone-7 (MK-7). *Org. Process Res. Dev.* **2016**, *20*, 1026–1033.
84. Bovicelli, P.; Borioni, G.; Fabbrini, D.; Barontini, M. New Efficient Synthesis of Ubiquinones. *Synth. Commun.* **2008**, *38*, 391–400.
85. Netscher, T.; Bonrath, W.; Bendik, I.; Zimmermann, P.-J.; Weber, F.; Rüttimann, A. Vitamins, 5. Vitamin K. In *Ullmann's Encyclopedia of Industrial Chemistry*; John Wiley & Sons, Ltd, 2020; pp 1–25.
86. Rüttimann, A.; Lorenz, P. Ein neuer synthetischer Zugang zu Ubichinonen. *HCA* **1990**, *73*, 790–796.
87. Pancrazzi, F.; Maestri, G.; Maggi, R.; Viscardi, R. Oxidative Dearomatization of Phenols and Polycyclic Aromatics with Hydrogen Peroxide Triggered by Heterogeneous Sulfonic Acids. *Eur. J. Org. Chem.* **2021**, *2021*, 5407–5414.
88. Sheldon, R. A. E Factors, Green Chemistry and Catalysis: An Odyssey. *Chem. Commun.* **2008**, *29*, 3352–3365.



89. Machado, P. A.; Fu, H.; Kratochvil, R. J.; Yuan, Y.; Hahm, T.-S.; Sabliov, C. M.; Wei, C.; Lo, Y. M. Recovery of Solanesol from Tobacco as a Value-Added Byproduct for Alternative Applications. *Bioresour. Technol.* **2010**, *101*, 1091–1096.
90. Lipshutz, B. H.; Ghorai, S.; Aguinaldo, G. T. Ring-Closing Metathesis at Room Temperature within Nanometer Micelles Using Water as the Only Solvent. *Adv. Synth. Catal.* **2008**, *350*, 953–956.
91. Lipshutz, B. H.; Abela, A. R. Micellar Catalysis of Suzuki–Miyaura Cross-Couplings with Heteroaromatics in Water. *Org. Lett.* **2008**, *10*, 5329–5332.
92. Takale, B. S.; Thakore, R. R.; Gao, E. S.; Gallou, F.; Lipshutz, B. H. Environmentally Responsible, Safe, and Chemoselective Catalytic Hydrogenation of Olefins: ppm Level Pd Catalysis in Recyclable Water at Room Temperature. *Green Chem.* **2020**, *22*, 6055–6061.

## 4.5. Experimental section

### 4.5.1. General information

Reagents and chemicals were purchased from Sigma-Aldrich, Combi-Blocks, Alfa Aesar, or Acros Organics and used without further purification. NaO<sup>t</sup>Bu was purchased from Sigma-Aldrich. Heptaprenyl alcohol and 4a-methyl-1,4,4a,9a-tetrahydro-1,4-methanoanthracene-9,10-dione (**32**) was obtained from Anthem Biosciences and used as received. Solanesol and 2,3-dimethoxy-5-methyl-1,4-benzoquinone was purchased from Combi-Blocks (catalog No. QA-3041, QB-8707). Deuterated solvents were purchased from Cambridge Isotope Laboratories.

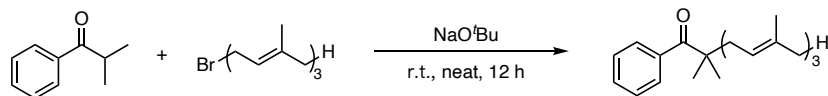
Thin-layer chromatography (TLC) was performed using Silica Gel 60 F254 plates (Merck, 0.25 mm thick). Flash chromatography was performed in an automated Biotage system using Silica Gel 60 (Silicycle, 40-63 nm).

<sup>1</sup>H and <sup>13</sup>C NMR spectra were recorded on either a Bruker Avance III HD 400 MHz (400 MHz for <sup>1</sup>H, 100 MHz for <sup>13</sup>C), a Bruker Avance NEO 500 MHz (500 MHz for <sup>1</sup>H, 125 MHz for <sup>13</sup>C) or on a Varian Unity Inova 500 MHz (500 MHz for <sup>1</sup>H, 125 MHz for <sup>13</sup>C); CDCl<sub>3</sub> were used as solvents. Residual peaks for CHCl<sub>3</sub> in CDCl<sub>3</sub> (<sup>1</sup>H = 7.26 ppm, <sup>13</sup>C = 77.20 ppm) have been assigned. The chemical shifts are reported in part per million (ppm), the coupling constants *J* values are given in Hertz (Hz). The peak patterns are indicated as follows: bs, broad singlet; s, singlet; d, doublet; t, triplet; q, quartet; p, pentet; m, multiplet.

HRMS were recorded on a Waters Micromass LCT TOF ES+ Premier mass spectrometer using ESI ionization.

#### 4.5.2. Optimization details

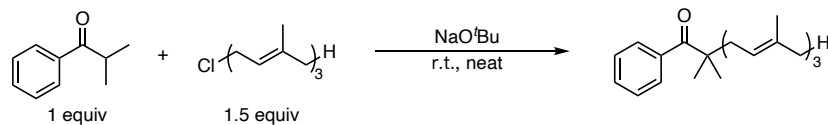
Screening conditions for neat reactions:



Bromide	NaO <sup>t</sup> Bu	Other	NMR yield <sup>a</sup>
3 equiv	2.4 equiv	2 wt % TPGS-750-M [1 M]	N.R.
3 equiv	2.4 equiv	1 mol % [Pd( $\mu$ -Br) <sup>t</sup> Bu <sub>3</sub> P] <sub>2</sub> <sup>b</sup>	N.R.
1.2 equiv	1.5 equiv	-	68% (30% SM)
1.5 equiv	1 equiv	-	70% (27% SM)
1.5 equiv	1.2 equiv	-	80% (15% SM)
1.5 equiv	1.5 equiv	-	99% (no SM)
1.2 equiv	1.5 equiv	10 mol % TBAI	65% (32% SM)
1.2 equiv	1.5 equiv	45 °C	68% (22% SM)
1.2 equiv	2.4 equiv	45 °C	83% (3% SM)
1.5 equiv	1.5 equiv	H <sub>2</sub> O [0.2 M]	N.R.
1.5 equiv	1.5 equiv	20 min	98% (no SM)

<sup>a</sup>With C<sub>2</sub>H<sub>2</sub>Cl<sub>4</sub> as internal standard. <sup>b</sup>In 2 wt % TPGS-750-M [1 M]

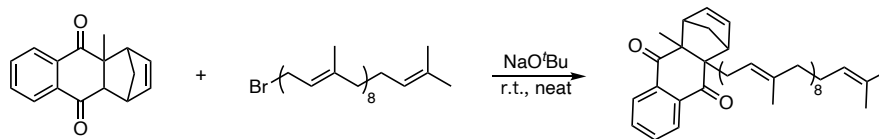
Screening of conditions using an allylic chloride:



Additive	conversion <sup>a</sup>
None	93% (overnight)
10 mol % TBAI	93% (1 h), Full conv. (3 h)
10 mol % KI	84% (1 h), Full conv. (3 h)
5 mol % TBAI	Full conv. (2h)
5 mol % KI	85% (2 h), Full conv. (4 h)
5 mol % NaI	90% (2 h), Full conv. (4 h)
2 mol % KI	Full conv. (3 h)
2 mol % NaI	Full conv. (3 h)
0.5 mol % NaI	89% (3 h), Full conv. (5 h)

<sup>a</sup> By crude NMR

Screening of conditions using solanesyl bromide:

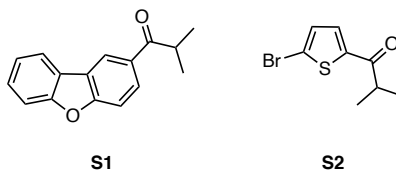


Bromide	NaO <sup>t</sup> Bu	conversion <sup>a</sup>
1.5 eq	1.5 eq	70%
2 eq	2 eq	79%
1.5 eq	3 eq	34%
3 eq	1.5 eq	85%
3 eq	3 eq	100%

<sup>a</sup> By crude NMR

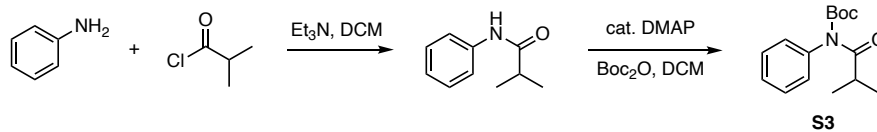
#### 4.5.3. Synthesis and characterization of substrates

Ketone substrates **S1** and **S2** were synthesized by Friedel-Crafts acylation using literature procedures<sup>1</sup>:



To a solution of anhydrous AlCl<sub>3</sub> (5.5 mmol, 1.1 equiv) in DCM (5 mL, 1 M), the acid chloride (5.5 mmol, 1.1 equiv) was added dropwise. The reaction mixture was stirred at rt for 10 min, followed by dropwise addition of a solution of arene (5 mmol, 1 equiv). The reaction was slowly heated to 50 °C and stirred until completion (monitored by TLC, ~3 h). The reaction mixture was cooled to rt and quenched with water, extracted with DCM (3 x 10 mL). The combined organic layer was then washed with sat. NaHCO<sub>3</sub> aq (10 mL) and water (10 mL), dried over anhydrous MgSO<sub>4</sub> and concentrated under reduced pressure. The crude product was purified by flash column chromatography on silica gel using a mixture of EtOAc and hexanes as elute giving ketones **S1** or **S2** in moderate yields (~70%).

Amide substrate **S3** was prepared via a literature procedure<sup>2,3</sup>:



Isobutyryl chloride (5 mmol, 0.53 mL, 1 equiv) was slowly added to a stirred solution of aniline (6 mmol, 0.55 mL, 1.2 equiv) and triethylamine (6 mmol, 0.8 mL, 1.2 equiv) in DCM (0.5 M, 20 mL) at rt. The reaction was stirred at rt for 24 h and then quenched with 1 M HCl (10 mL), then washed with 1 M HCl (2 x10 mL), followed by sat. NaHCO<sub>3</sub> aq (2 x10 mL). The organic layer was dried over anhydrous MgSO<sub>4</sub> and concentrated under reduced pressure to afford *N*-phenylisobutyramide as an off-white solid in 90% yield.

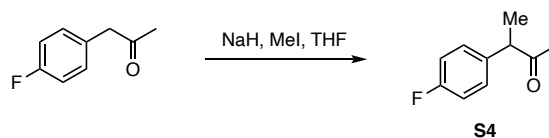
To an oven-dried 50 mL flask, *N*-phenylisobutyramide (3 mmol, 489.7 mg, 1 equiv), DMAP (0.3 mmol, 36.7 mg, 10 mol %) and DCM (15 mL, 0.2 M) was added. Boc<sub>2</sub>O (3.9 mmol, 0.9 mL, 1.3 equiv) was added in one portion and the reaction mixture was allowed to stir at rt overnight. The reaction was quenched by adding sat. NaHCO<sub>3</sub> aq (10 mL), extracted with EtOAc (3 x 10 mL), and washed with brine (10 mL). The combined organic layer was dried over anhydrous MgSO<sub>4</sub> and concentrated under reduced pressure. Purification by column chromatography using a mixture of EtOAc and hexanes as elute to give *N*-Boc-protected amide **S3** in 75% yield.

<sup>1</sup>H NMR (500 MHz, CDCl<sub>3</sub>) δ 7.43 – 7.32 (m, 3H), 7.11 – 7.05 (m, 2H), 3.64 (heptd, *J* = 6.7, 1.9 Hz, 1H), 1.41 (d, *J* = 1.9 Hz, 9H), 1.25 (dd, *J* = 6.8, 1.9 Hz, 6H).

<sup>13</sup>C NMR (126 MHz, CDCl<sub>3</sub>) δ 180.48, 152.76, 139.43, 128.92, 128.12, 127.62, 83.00, 34.73, 27.83, 19.59.

HRMS (ESI-TOF) *m/z*: [M]<sup>+</sup> calcd for C<sub>15</sub>H<sub>21</sub>NO<sub>3</sub>: 263.1521; found 263.1519.

*Preparation ketone S4.*<sup>4</sup>



An oven-dried 100 mL round bottom flask was charged with 60% dispersion of NaH in mineral oil (5.5 mmol, 220 mg, 1.1 equiv), THF (10 mL, 0.5 M), 1-(4-fluorophenyl)propan-2-one (5 mmol, 0.69 mL, 1 equiv), and the resulting mixture was warmed to rt and stirred for 30 min. After 30 min, the mixture was cooled to 0 °C and methyl iodide (0.5 mL, 8 mmol) was added dropwise. The reaction was stirred at 0 °C for 1 h, then warmed to rt and stirred for another 4 h. The reaction was quenched by adding sat. NH<sub>4</sub>Cl aq (10 mL), and extracted with Et<sub>2</sub>O (3 × 10 mL). The combined organic layer was then washed with brine (10 mL), dried over anhydrous MgSO<sub>4</sub>, filtered, and concentrated *in vacuo*. Purification by column chromatography using a mixture of EtOAc and hexanes as elute provided **S5** as a yellow oil in 88% yield.

**4.5.4. General procedure for solvent-free  $\alpha$ -allylation reactions**

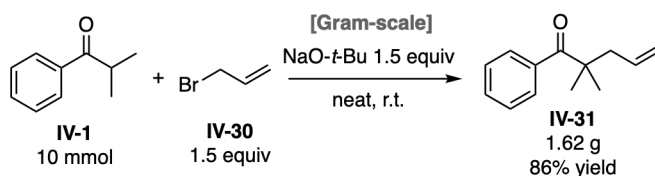
*For liquid ketone substrates:*

NaO<sup>t</sup>Bu (0.6 mmol, 57.7 mg, 1.5 equiv) was added to a 1-dram vial in a glovebox. The vial was then capped and removed from the glovebox. Allyl bromide (0.6 mmol, 1.5 equiv) and the ketone (0.4 mmol, 1 equiv) were then added sequentially to the vial. The vial was then capped and stirred vigorously (~1000 RPM). The reaction was monitored by thin-layer chromatography until deemed complete. The reaction mixture was then applied directly to a silica gel column and purified via column chromatography.

*For solid ketone substrates:*

The ketone (0.4 mmol, 1 equiv) was added to a 1-dram vial, then the vial was placed in a glovebox and NaO<sup>t</sup>Bu (0.6 mmol, 57.7 mg, 1.5 equiv) was added. The vial was then capped and removed from the glovebox. Allyl bromide (0.6 mmol, 1.5 equiv) was then added via syringe and the vial was capped and stirred vigorously (~1000 RPM). The reaction was monitored by thin-layer chromatography until deemed complete. The reaction mixture was then applied directly to a silica gel column and purified via column chromatography.

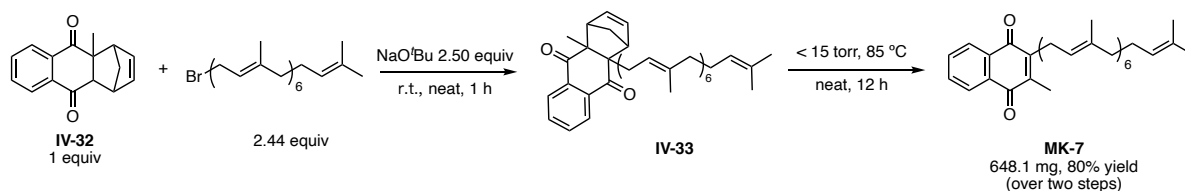
#### 4.5.5. Large-scale reaction



NaO<sup>t</sup>Bu (1.5 equiv, 15 mmol, 1.442 g) was added to a 20 mL vial in a glovebox. The vial was then capped and removed from the glovebox. Allyl bromide **IV-30** (1.5 equiv, 15 mmol, 1.3 mL) was then added to this vial in one portion. Isobutyrophenone **IV-1** (1 equiv, 10 mmol, 1.5 mL) was then added dropwise to the vial over 15 min via a syringe pump (adding rate 0.1 mL/min). The vial was stirred vigorously (~1000 RPM) during the whole process. After addition, the reaction mixture was allowed to stir for another 30 min. The reaction mixture was then passed through a silica gel pad (eluted with EtOAc) and concentrated under reduced pressure to afford 2,2-dimethyl-1-phenylpent-4-en-1-one (**IV-31**) as a light-yellow oil. (1.62 g, 86% yield).

#### 4.5.6. Procedures for gram scale syntheses of MK-7, MK-9, and CoQ<sub>9</sub>

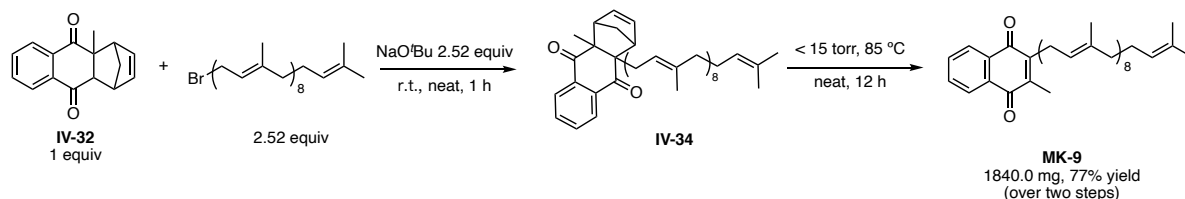
##### Gram synthesis of MK-7:



**$\alpha$ -Allylation:** To a 20 mL oven-dried scintillation vial was added freshly prepared heptaprenyl bromide (1.7 g, 3.05 mmol, 2.44 equiv) and a stir bar. 4a-Methyl-1,4,4a,9a-tetrahydro-1,4-methanoanthracene-9,10-dione (IV-32, 297.5 mg, 1.25 mmol, 1.00 equiv) was then added and allowed to disperse with gentle stirring. NaO'Bu (300 mg, 3.125 mmol, 2.50 equiv) was removed from a glove box in a 1-dram vial and added in one addition to the stirring reaction mixture at rt resulting in a red reaction mixture. The vial was then sealed and stirred rapidly (900 RPM) at rt. After 1 h, the reaction was complete by TLC.

**retro-Diels-Alder reaction:** The entire reaction mixture was then placed under high vacuum (<15 torr pressure) and heated in a 20 mL scintillation aluminum heating block to 85 °C internal temperature neat with no stirring. The reaction was allowed to heat until constant mass was observed from loss of cyclopentadiene, as well as completion by TLC. The resulting golden oil was then purified by flash chromatography (4% Et<sub>2</sub>O/hexanes) and dried under high vacuum resulting in a yellow solid (648.1 mg, 80% yield over two steps). R<sub>f</sub> = 0.60 (1:9 Et<sub>2</sub>O/hexanes).

##### Gram synthesis of MK-9:

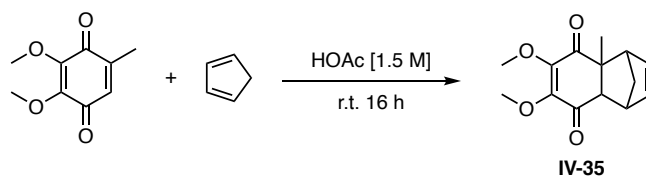




**$\alpha$ -Allylation:** To a 20 mL oven-dried scintillation vial was added freshly prepared solanesyl bromide (5.3 g, 7.65 mmol, 2.52 equiv) and a stir bar. 4a-Methyl-1,4,4a,9a-tetrahydro-1,4-methanoanthracene-9,10-dione (**IV-32**, 722 mg, 3.03 mmol, 1.00 equiv) was then added and allowed to disperse with gentle stirring. NaO<sup>t</sup>Bu (735 mg, 7.65 mmol, 2.52 equiv) was removed from a glove box in a 1-dram vial and added in one addition to the stirring reaction mixture at rt resulting in a red reaction mixture which warms slightly. The vial was then sealed and stirred rapidly (900 RPM) at rt. After 1 h, the reaction was deemed complete by TLC.

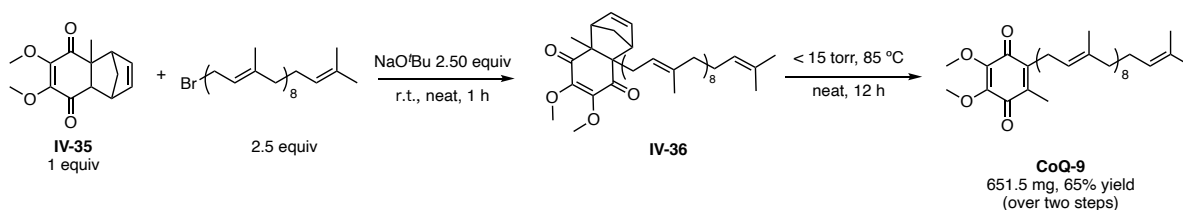
**retro-Diels-Alder reaction:** The entire reaction mixture was then placed under high vacuum (<15 torr pressure) and heated in a 20 mL scintillation vial aluminum heating block to 85 °C internal temperature neat with no stirring. The reaction was allowed to heat until constant mass was observed from loss of cyclopentadiene as well as completion by TLC. The resulting golden oil was then purified by flash chromatography (eluent: 4% Et<sub>2</sub>O/96% hexanes) and dried under hi-vacuum resulting in a yellow solid (1840.0 mg, 77 % yield). R<sub>f</sub> = 0.50 (1:9 Et<sub>2</sub>O/hexanes).

*Gram scale synthesis of CoQ<sub>9</sub>:*



Cyclopentadiene was freshly distilled from dicyclopentadiene.<sup>5</sup> The dimer was heated in an oven dried round bottom flask with a stir bar in an oil bath at 180 °C. The resulting vapors were collected in a water cooled short-path distillation head at 38-40 °C, and the condensed liquid was maintained at below freezing temperature (sodium chloride / ice bath).

To a 50 mL round bottomed flask was added the quinone (CoQ<sub>0</sub>; 5 g, 27.45 mmol, 1 equiv) and acetic acid (18 mL, 1.5 M). Freshly distilled cyclopentadiene (2.95 g, 3.8 mL, 1.62 equiv) was then added to the reaction mixture through a septum at rt. The reaction was then allowed to stir overnight at rt and was deemed complete by thin-layer chromatography. The pH of the reaction mixture was then adjusted to 9 (satd. bicarbonate solution, 150 mL) and extracted with diethyl ether (3 x 100 mL). The combined organics were treated with brine, dried over sodium sulfate, filtered, and dried under reduced pressure followed by high vacuum resulting in an opaque oil **IV-35** that yellowed over time (5.39 g, 80% yield).

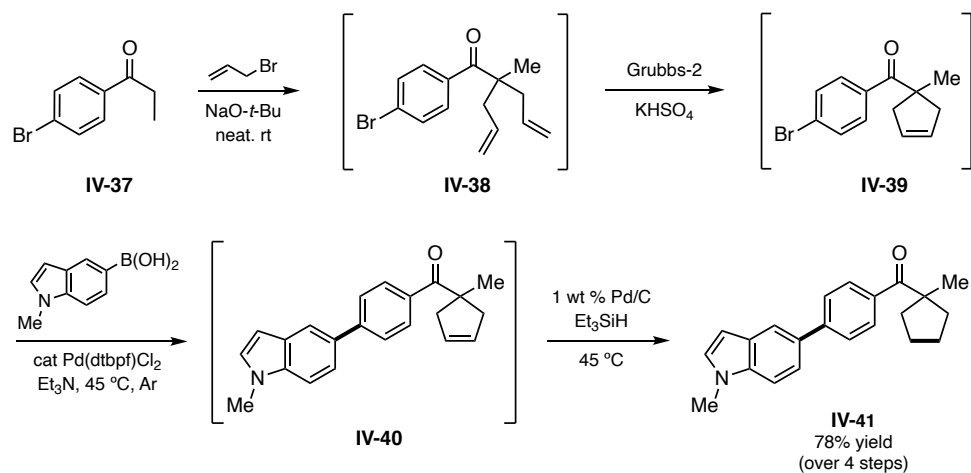


**$\alpha$ -Allylation:** To a 20 mL scintillation vial was added the Diels-Alder adduct **IV-35** (310 mg, 1.25 mmol, 1 equiv) and freshly prepared solanesyl bromide (2.17 g, 3.125 mmol, 2.5 equiv) along with a stir bar and the slurry was combined at rt with gentle stirring. NaO'Bu (300 mg, 3.125 mmol, 2.5 equiv) was then added in one portion and the stirring speed was increased to 900 RPM, resulting in a bright red slurry. The reaction was allowed to stir at rt for 1 h. The product mixture was then taken up in DCM, dried onto Celite, and purified via a 6-inch silica gel chromatographic column using two column volumes of hexanes, one of 10% Et<sub>2</sub>O/hexanes, and four 20% Et<sub>2</sub>O/hexanes, giving the product **IV-36** as a yellowish oil (757.4 mg, 70%).

**retro-Diels-Alder reaction:** The oil **IV-36** from the allylation reaction was transferred into a 20 mL scintillation vial, which was then evacuated to <15 torr and heated in an 85 °C aluminum block. After 16 h, the reaction had turned into a dark red oil and the reaction was complete by thin-layer chromatography. The oil was applied to Celite and purified using 20%

Et<sub>2</sub>O/hexanes on a silica gel column. The combined organics were then dried to a red oil which solidified under high vacuum to give CoQ<sub>9</sub> (651.5 mg, 93% yield).

#### 4.5.7. 1-Pot sequence



##### Step 1: $\alpha$ -allylation.

1-(4-Bromophenyl)propan-1-one **IV-37** (1 equiv, 0.4 mmol, 85.2 mg) was added to a 1-dram vial, after which the vial was moved to a glovebox and NaO<sup>t</sup>Bu (1.5 equiv, 1.0 mmol, 96.2 mg) was added. The vial was then capped and removed from the glovebox. Allyl bromide (2.0 equiv, 0.8 mmol, 69.1  $\mu$ L) was then added and the vial was capped and stirred vigorously (~1000 RPM). The reaction was monitored by thin-layer chromatography until complete.

##### Step 2: ring-closing metathesis.

To the reaction mixture was added Grubbs 2<sup>nd</sup> catalyst generation (2 mol %, 0.008 mmol, 6.8 mg) and KHSO<sub>4</sub> (0.6 equiv, 0.24 mmol, 32.7 mg). The vial was capped with a rubber septum and then evacuated and backfilled with argon three times. Next, 2 wt % TPGS-750-M solution in water (0.5 M, 0.8 mL) was added via syringe through the septum, then stirred vigorously at rt in an aluminum block placed over an IKA hot plate overnight.

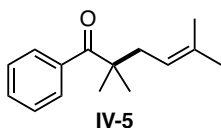
##### Step 3: Suzuki-Miyaura coupling.

Pd(dtbpf)Cl<sub>2</sub> (1 mol %, 0.004 mmol, 2.7 mg) and (1-methyl-1*H*-indol-5-yl)boronic acid (1.5 equiv, 0.60 mmol, 105 mg) were added sequentially to the vial. The vial was then sealed with a fresh rubber septum, and the headspace was purged using argon and a vent needle for 5 min. Next, Et<sub>3</sub>N (3 equiv, 1.2 mmol, 0.17 mL) was added via syringe through the septum. The vial was then stirred vigorously at 45 °C in an aluminum block placed over IKA hot plate for 4 h.

*Step 4: olefin hydrogenation.*

Pd/C (1 wt % from the supplier; 2000 ppm, 0.2 mol %, 8.5 mg) was added to the reaction mixture. The vial was capped with a rubber septum and Et<sub>3</sub>SiH (1.5 equiv, 0.6 mmol, 96 μL) was then added via microsyringe. The vial was stirred vigorously at 45 °C in an aluminum block placed over IKA hot plate overnight. Upon completion, the mixture was diluted with EtOAc and then combined directly with silica gel. The volatiles were evaporated under reduced pressure and semi-pure product was purified by flash chromatography over silica gel using 5% EtOAc in hexanes to afford **IV-25** as a light-yellow solid (97.8 mg, 78% overall yield).

**4.5.8. E Factor calculation**



Mass of product: 86.2 mg (0.4 mmol scale)

Mass of waste: (consider excess reagents)

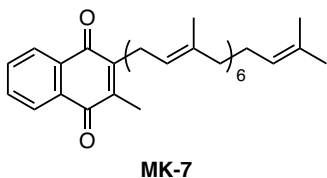
0.5 equiv 3,3-dimethylallylbromide + 0.5 equiv NaOtBu

= 0.4 mmol \* 0.5 \* 149.0 g/mol + 0.4 mmol \* 0.5 \* 96.1 g/mol

= 29.8 mg + 19.22 mg

= 49.02 mg

- E Factor = mass of waste / mass of product = 49.02 mg / 86.2 mg = **0.57**



Mass of product: 648.1 mg (1.25 mmol scale)

Mass of waste: (consider excess reagents)

1.44 equiv heptaprenyl bromide + 1.5 equiv NaOtBu + 1 equiv cyclopentadiene

$$= 1.44 * 1.25 \text{ mmol} * 696.7 \text{ g/mol} + 1.25 \text{ mmol} * 1.5 * 96.1 \text{ g/mol} + 1.25 \text{ mmol} * 66.1$$

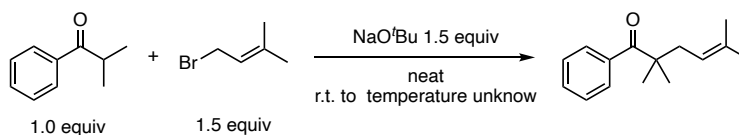
g/mol

$$= 1003 \text{ mg} + 180 \text{ mg} + 80.6 \text{ mg}$$

$$= 1265.6 \text{ mg}$$

- E Factor = mass of waste / mass of product = 1265.6 mg / 648.1 mg = **1.95**

#### 4.5.9. Calorimetry data



Procedure: Mixing cell was prepared as follows: 51.5 mg sodium *t*-butoxide (Aldrich, 359270, white solid) in the main tube and 133 mg brownish solution (53 mg isobutyrophenone in 80 mg 3,3-dimethylallylbromide mixed at rt) in the breakable tube, prepared under argon, after equilibration at 30 °C (in the furnace) with mixing.

Prefix of Enthalpy:

-: Exothermic

+: Endothermic

**SETARAM isotherm setup:**

	Atm	Temperature	Duration	Vessel
1.	Argon	30 °C	5 hr	Steel tube glass mixing cell

**SETARAM isotherm results:**

	Exo. Reaction	Enthalpy	Remarks
1.	Yes	-525 kJ/kg	-

**Comment:**

A significant exothermal signal (about -525 kJ/kg) is observed after the addition of alpha-Methylpropiophenon / Isobutyrophenon in 3,3 Dimethylallylbromid to NaOtBu. The measured energy corresponds to an adiabatic temperature increase of about 329°C [estimated heat capacity of the investigated samples:  $C_p = 1.6 \text{ kJ}/(\text{kg}\cdot\text{K})$ ].

 BT 2.15 (No option)	Experiment : SL-SAFLAB-296 Procedure : mixing cell Cell : HC Glas - Mixing cell	30.07.2021 Atmosphere : 1:Argon Mass : 184.5 (mg)
----------------------------------------------------------------------------------------------------------	---------------------------------------------------------------------------------------	---------------------------------------------------------

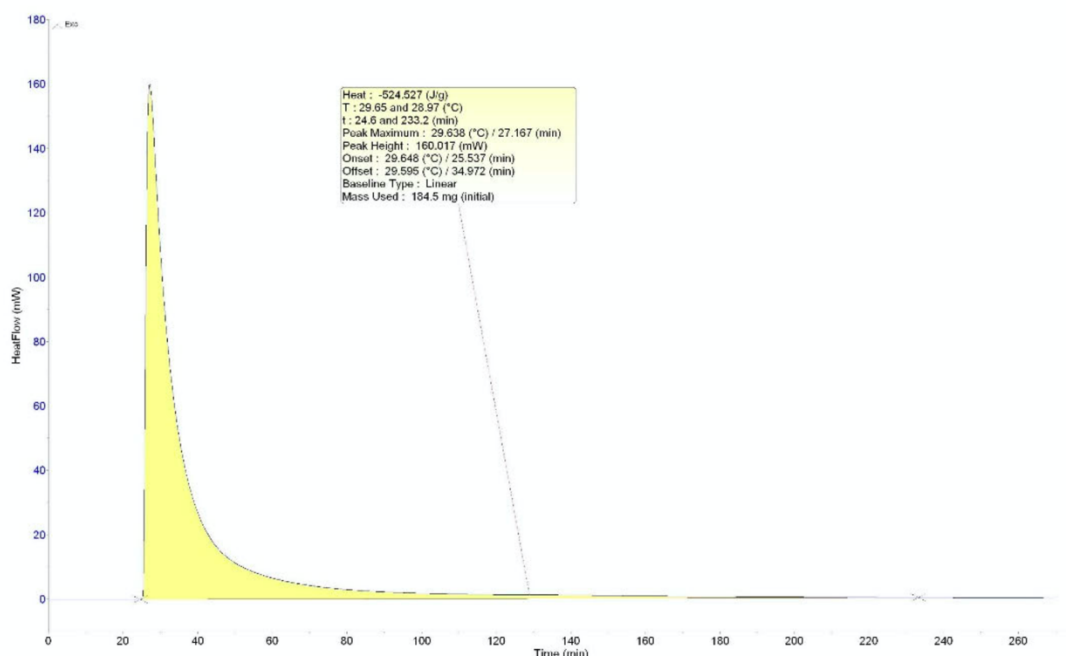


**Figure IV-2** Heatflow vs. reaction progress

**Prefix of Enthalpy:**

**-: Exothermic**

**+: Endothermic**

**SETARAM dynamic setup:**

	Atm	Range	Heating Rate	Vessel
2.	Argon	30 °C to 150 °C	6 K/h (0.1 K/min)	Steel tube glass mixing cell
3.	Argon	30 °C to 150 °C	6 K/h (0.1 K/min)	Steel tube glass mixing cell

**SETARAM dynamic results:**

	Exo. Reaction	Spont. Reac.	Enthalpy	Remarks
1.	Above ca. 40°C	No	-3 kJ/kg	-
2.	Above ca. 70°C	No	-2 kJ/kg	-

**Comment:**

The dynamic SETARAM thermostability test of the reaction mixture after the isothermal addition shows the onset of a first very weak exothermic reaction starting above ca. 40 °C (approx. -3 kJ/kg) and of a second one starting above ca. 70°C (approx. -2 kJ/kg).

 BT 2.15 (No option)	Experiment : SL-SAFLAB-296	30.07.2021
	Procedure : mixing cell	Atmosphere : 1:Argon
	Cell : HC Glas - Mixing cell	Mass : 184.5 (mg)

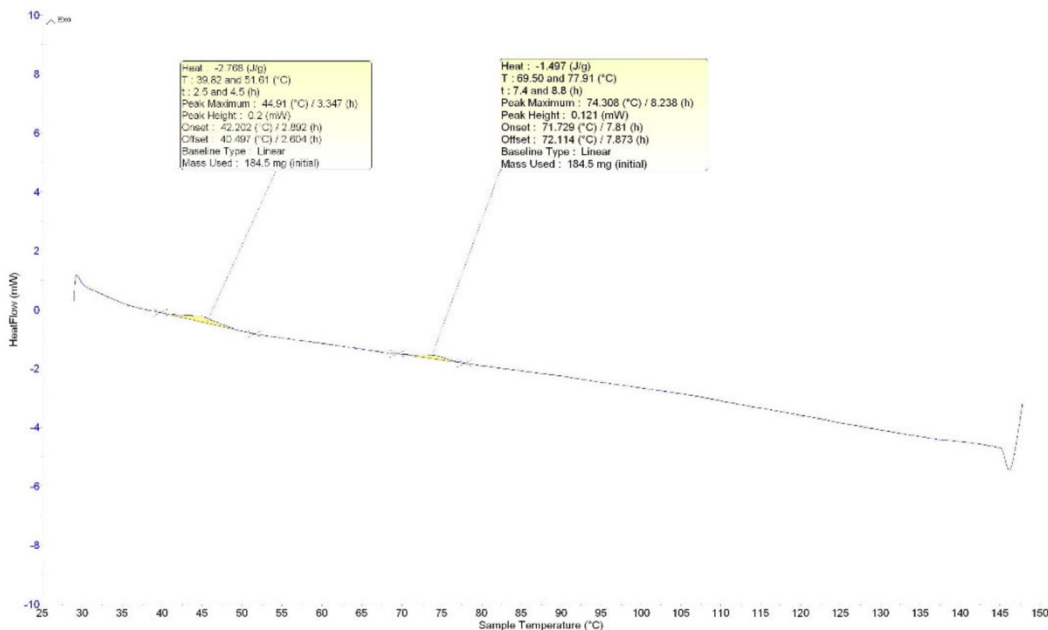
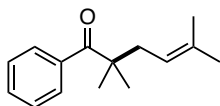


**Figure IV-3** Differential scanning calorimetry (DSC) of the reaction mixture

#### 4.5.10. Analytical data

HRMS for compound **MK-7**<sup>6</sup>, **MK-9**<sup>6</sup> are reported. All other compounds were characterized by <sup>1</sup>H and <sup>13</sup>C NMR, and HRMS.



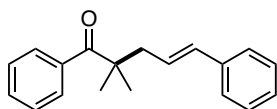
#### **2,2,5-trimethyl-1-phenylhex-4-en-1-one (IV-5)**

Colorless oil, flash chromatography using 2% EtOAc/hexanes; 86.2 mg; 99% yield.

<sup>1</sup>H NMR (500 MHz, CDCl<sub>3</sub>) δ 7.66 (dq, *J* = 6.9, 1.5 Hz, 2H), 7.48 – 7.44 (m, 1H), 7.41 (ddd, *J* = 8.5, 6.6, 1.5 Hz, 2H), 5.08 (ddq, *J* = 8.9, 6.0, 1.4 Hz, 1H), 2.45 (d, *J* = 7.4 Hz, 2H), 1.70 (t, *J* = 1.5 Hz, 3H), 1.57 (s, 3H), 1.32 (d, *J* = 1.5 Hz, 6H).

<sup>13</sup>C NMR (126 MHz, CDCl<sub>3</sub>) δ 209.42, 139.36, 134.32, 130.62, 128.03, 127.55, 119.77, 48.38, 38.99, 25.97, 25.77, 17.94.

HRMS (ESI-TOF) *m/z*: [M]<sup>+</sup> calcd for C<sub>15</sub>H<sub>20</sub>O: 216.1514; found 216.1513.



#### **(E)-2,2-dimethyl-1,5-diphenylpent-4-en-1-one (IV-6)**

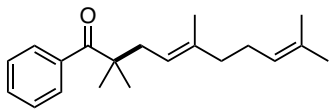
Colorless oil, flash chromatography using 2% EtOAc/hexanes; 100.2 mg; 95% yield.

<sup>1</sup>H NMR (500 MHz, CDCl<sub>3</sub>) δ 7.74 – 7.66 (m, 2H), 7.53 – 7.47 (m, 1H), 7.46 – 7.42 (m, 2H), 7.32 (dd, *J* = 7.2, 1.4 Hz, 4H), 7.23 (ddt, *J* = 6.6, 5.2, 1.9 Hz, 1H), 6.38 (dt, *J* = 15.9, 1.4 Hz, 1H), 6.17 (dt, *J* = 15.7, 7.5 Hz, 1H), 2.67 (dd, *J* = 7.5, 1.4 Hz, 2H), 1.42 (s, 6H).

<sup>13</sup>C NMR (126 MHz, CDCl<sub>3</sub>) δ 208.88, 139.17, 137.39, 133.29, 130.85, 128.51, 128.15, 127.65, 127.20, 126.15, 125.90, 48.17, 44.18, 25.94.

HRMS (ESI-TOF) *m/z*: [M]<sup>+</sup> calcd for C<sub>19</sub>H<sub>20</sub>O: 264.1514; found 264.1508.





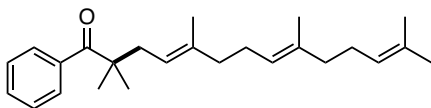
**(E)-2,2,5,9-tetramethyl-1-phenyldeca-4,8-dien-1-one (IV-7)**

Colorless oil, flash chromatography using 3% EtOAc/hexanes; 105.7 mg; 93% yield.

$^1\text{H NMR}$  (500 MHz,  $\text{CDCl}_3$ )  $\delta$  7.70 – 7.61 (m, 2H), 7.49 – 7.44 (m, 1H), 7.44 – 7.38 (m, 2H), 5.14 – 5.03 (m, 2H), 2.46 (d,  $J = 7.4$  Hz, 2H), 2.07 – 1.98 (m, 4H), 1.68 (d,  $J = 1.4$  Hz, 3H), 1.60 (d,  $J = 1.3$  Hz, 3H), 1.56 (d,  $J = 1.3$  Hz, 3H), 1.33 (s, 6H).

$^{13}\text{C NMR}$  (126 MHz,  $\text{CDCl}_3$ )  $\delta$  209.52, 139.42, 137.88, 131.41, 130.58, 128.04, 128.02, 127.53, 124.22, 119.80, 48.40, 39.95, 38.79, 26.56, 25.71, 17.70, 16.22.

**HRMS** (ESI-TOF)  $m/z$ :  $[\text{M}]^+$  calcd for  $\text{C}_{20}\text{H}_{28}\text{O}$ : 284.2140; found 284.2151.



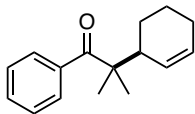
**(4E,8E)-2,2,5,9,13-pentamethyl-1-phenyltetradeca-4,8,12-trien-1-one (IV-8)**

Colorless oil, flash chromatography using 3% EtOAc/hexanes; 138.2 mg; 98% yield.

$^1\text{H NMR}$  (400 MHz,  $\text{CDCl}_3$ )  $\delta$  7.63 (d,  $J = 7.5$  Hz, 2H), 7.49 – 7.35 (m, 3H), 5.08 (t,  $J = 7.7$  Hz, 3H), 2.43 (d,  $J = 7.4$  Hz, 2H), 2.00 (dq,  $J = 21.5, 8.0$  Hz, 8H), 1.68 – 1.52 (m, 12H), 1.30 (s, 6H).

$^{13}\text{C NMR}$  (101 MHz,  $\text{CDCl}_3$ )  $\delta$  209.52, 139.41, 137.99, 137.89, 135.21, 135.08, 131.53, 131.28, 130.58, 128.02, 127.56, 127.53, 124.88, 124.40, 124.36, 124.04, 119.81, 119.72, 48.39, 40.25, 39.96, 39.73, 38.77, 32.00, 26.76, 26.61, 26.55, 26.35, 25.74, 25.71, 23.39, 17.69, 17.64, 16.27, 16.21, 16.03.

**HRMS** (ESI-TOF)  $m/z$ :  $[\text{M}]^+$  calcd for  $\text{C}_{25}\text{H}_{36}\text{O}$ : 352.2766; found 352.2749.



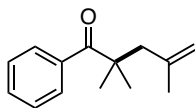
**(S)-2-(cyclohex-2-en-1-yl)-2-methyl-1-phenylpropan-1-one (IV-9)**

Colorless oil, flash chromatography using 3% EtOAc/hexanes; 85.8 mg; 94% yield.

**<sup>1</sup>H NMR** (400 MHz, CDCl<sub>3</sub>) δ 7.70 – 7.59 (m, 2H), 7.49 – 7.32 (m, 3H), 5.80 – 5.72 (m, 1H), 5.50 (dt, *J* = 10.3, 1.9 Hz, 1H), 2.87 (ddt, *J* = 11.3, 6.0, 2.8 Hz, 1H), 1.95 (ddt, *J* = 9.8, 5.3, 1.4 Hz, 2H), 1.77 (dt, *J* = 12.1, 3.6 Hz, 1H), 1.67 (ddt, *J* = 9.6, 5.2, 2.3 Hz, 1H), 1.53 – 1.43 (m, 1H), 1.36 – 1.25 (m, 4H), 1.22 (s, 3H).

**<sup>13</sup>C NMR** (126 MHz, CDCl<sub>3</sub>) δ 209.58, 139.49, 130.66, 129.30, 128.09, 127.60, 127.59, 50.78, 42.39, 25.13, 24.30, 22.66, 22.48, 22.45.

**HRMS** (ESI-TOF) *m/z*: [M]<sup>+</sup> calcd for C<sub>16</sub>H<sub>20</sub>O: 228.1514; found 228.1517.



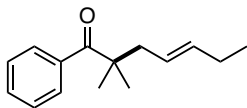
**2,2,4-trimethyl-1-phenylpent-4-en-1-one (IV-10)**

Colorless oil, flash chromatography using 2% EtOAc/hexanes; 80.9 mg; quantitative yield.

**<sup>1</sup>H NMR** (400 MHz, CDCl<sub>3</sub>) δ 7.72 – 7.63 (m, 2H), 7.49 – 7.33 (m, 3H), 4.83 – 4.79 (m, 1H), 4.65 (dd, *J* = 2.2, 1.1 Hz, 1H), 2.56 (d, *J* = 1.1 Hz, 2H), 1.64 (t, *J* = 1.1 Hz, 3H), 1.33 (s, 6H).

**<sup>13</sup>C NMR** (126 MHz, CDCl<sub>3</sub>) δ 209.00, 142.44, 139.04, 130.85, 128.07, 127.90, 114.56, 48.39, 47.56, 26.79, 24.39.

**HRMS** (ESI-TOF) *m/z*: [M]<sup>+</sup> calcd for C<sub>14</sub>H<sub>18</sub>O: 202.1358; found 202.1353.



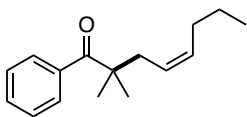
**(E)-2,2-dimethyl-1-phenylhept-4-en-1-one (IV-11)**

Colorless oil, flash chromatography using 3% EtOAc/hexanes; 86.5 mg; quantitative yield.

<sup>1</sup>H NMR (400 MHz, CDCl<sub>3</sub>) δ 7.69 – 7.58 (m, 2H), 7.49 – 7.33 (m, 3H), 5.42 (dtt, *J* = 14.8, 6.1, 1.1 Hz, 1H), 5.30 (dtt, *J* = 15.3, 7.2, 1.3 Hz, 1H), 2.41 (dd, *J* = 7.2, 1.1 Hz, 2H), 2.02 – 1.89 (m, 2H), 1.30 (s, 6H), 0.92 (t, *J* = 7.5 Hz, 3H).

<sup>13</sup>C NMR (126 MHz, CDCl<sub>3</sub>) δ 209.14, 139.32, 136.04, 130.68, 128.03, 127.61, 124.09, 47.95, 43.72, 25.77, 25.67, 13.85.

HRMS (ESI-TOF) *m/z*: [M]<sup>+</sup> calcd for C<sub>15</sub>H<sub>20</sub>O: 216.1514; found 216.1509.



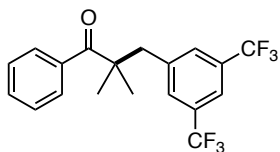
**(Z)-2,2-dimethyl-1-phenyloct-4-en-1-one (IV-12)**

Colorless oil, flash chromatography using 3% EtOAc/hexanes; 92.1 mg; quantitative yield.

<sup>1</sup>H NMR (400 MHz, CDCl<sub>3</sub>) δ 7.75 – 7.57 (m, 2H), 7.48 – 7.33 (m, 3H), 5.52 – 5.41 (m, 1H), 5.30 (dddt, *J* = 10.9, 9.2, 7.5, 1.7 Hz, 1H), 2.52 – 2.45 (m, 2H), 1.95 (qd, *J* = 7.3, 1.6 Hz, 2H), 1.32 (s, 8H), 0.87 (t, *J* = 7.4 Hz, 3H).

<sup>13</sup>C NMR (126 MHz, CDCl<sub>3</sub>) δ 209.11, 139.14, 132.74, 130.72, 128.06, 127.61, 124.69, 48.00, 38.03, 29.45, 25.78, 22.69, 13.83.

HRMS (ESI-TOF) *m/z*: [M]<sup>+</sup> calcd for C<sub>16</sub>H<sub>22</sub>O: 230.1671; found 230.1681.



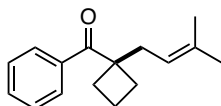
**3-(3,5-bis(trifluoromethyl)phenyl)-2,2-dimethyl-1-phenylpropan-1-one (IV-13)**

Colorless oil, flash chromatography using 3% EtOAc/hexanes; 149.6 mg; quantitative yield.

$^1\text{H NMR}$  (400 MHz,  $\text{CDCl}_3$ )  $\delta$  7.72 (s, 1H), 7.59 – 7.52 (m, 4H), 7.51 – 7.45 (m, 1H), 7.41 (dd,  $J = 8.2, 6.7$  Hz, 2H), 3.19 (s, 2H), 1.36 (s, 6H).

$^{13}\text{C NMR}$  (126 MHz,  $\text{CDCl}_3$ )  $\delta$  208.12, 140.59, 138.82, 131.61, 131.35, 131.20, 131.09, 130.82, 130.58, 130.55, 128.32, 127.47, 126.58, 124.41, 122.24, 120.56, 120.53, 120.50, 120.47, 120.44, 120.07, 48.71, 45.64, 26.09.

**HRMS** (ESI-TOF)  $m/z$ :  $[\text{M}]^+$  calcd for  $\text{C}_{19}\text{H}_{16}\text{F}_6\text{O}$ : 374.1105; found 274.1194.



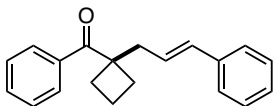
**(1-(3-methylbut-2-en-1-yl)cyclobutyl)(phenyl)methanone (IV-14)**

Colorless oil, flash chromatography using 3% EtOAc/hexanes; 86.7 mg; 95% yield.

$^1\text{H NMR}$  (500 MHz,  $\text{CDCl}_3$ )  $\delta$  7.87 – 7.81 (m, 2H), 7.55 – 7.49 (m, 1H), 7.46 – 7.40 (m, 2H), 5.01 (ddq,  $J = 8.8, 5.8, 1.4$  Hz, 1H), 2.75 – 2.65 (m, 4H), 2.18 – 2.05 (m, 3H), 1.89 – 1.80 (m, 1H), 1.64 (d,  $J = 1.4$  Hz, 3H), 1.41 (d,  $J = 1.4$  Hz, 3H).

$^{13}\text{C NMR}$  (126 MHz,  $\text{CDCl}_3$ )  $\delta$  204.50, 134.98, 134.40, 132.27, 129.03, 128.25, 118.97, 77.30, 77.05, 76.79, 53.20, 36.94, 30.37, 25.84, 17.73, 15.67.

**HRMS** (ESI-TOF)  $m/z$ :  $[\text{M}]^+$  calcd for  $\text{C}_{16}\text{H}_{20}\text{O}$ : 228.1514; found 228.1525.



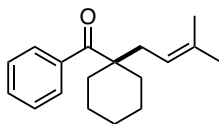
**(1-cinnamylcyclobutyl)(phenyl)methanone (IV-15)**

Light yellow oil, flash chromatography using 3% EtOAc/hexanes; 110.5 mg; quantitative yield.

**<sup>1</sup>H NMR** (400 MHz, CDCl<sub>3</sub>) δ 7.87 – 7.81 (m, 2H), 7.53 (td, *J* = 7.3, 1.5 Hz, 1H), 7.47 – 7.40 (m, 2H), 7.26 (dd, *J* = 4.2, 1.4 Hz, 4H), 7.19 (q, *J* = 4.0 Hz, 1H), 6.31 (dd, *J* = 15.7, 1.6 Hz, 1H), 6.04 (ddd, *J* = 15.8, 8.0, 6.6 Hz, 1H), 2.89 (d, *J* = 7.3 Hz, 2H), 2.77 – 2.66 (m, 2H), 2.22 (ddd, *J* = 12.6, 8.2, 3.4 Hz, 2H), 2.16 – 1.99 (m, 1H), 1.92 – 1.78 (m, 1H).

**<sup>13</sup>C NMR** (126 MHz, CDCl<sub>3</sub>) δ 204.23, 137.21, 134.90, 133.02, 132.48, 129.11, 128.45, 128.39, 127.23, 126.20, 124.98, 52.92, 41.98, 30.35, 15.55.

**HRMS** (ESI-TOF) *m/z*: [M]<sup>+</sup> calcd for C<sub>20</sub>H<sub>20</sub>O: 276.1514; found 276.1523.



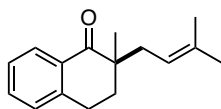
**(1-(3-methylbut-2-en-1-yl)cyclohexyl)(phenyl)methanone (IV-16)**

Colorless oil, flash chromatography using 3% EtOAc/hexanes; 102.5 mg; quantitative yield.

**<sup>1</sup>H NMR** (500 MHz, CDCl<sub>3</sub>) δ 7.65 – 7.59 (m, 2H), 7.49 – 7.36 (m, 3H), 5.10 (ddt, *J* = 8.8, 7.3, 1.5 Hz, 1H), 2.49 (d, *J* = 7.4 Hz, 2H), 2.24 – 2.17 (m, 2H), 1.70 (d, *J* = 1.4 Hz, 3H), 1.59 (s, 4H), 1.55 (tt, *J* = 11.2, 3.8 Hz, 3H), 1.44 (ddd, *J* = 13.5, 10.2, 3.5 Hz, 2H), 1.32 (tt, *J* = 7.7, 2.8 Hz, 3H).

**<sup>13</sup>C NMR** (126 MHz, CDCl<sub>3</sub>) δ 209.59, 140.32, 134.28, 130.37, 127.98, 127.23, 119.15, 52.96, 37.64, 34.38, 25.97, 23.04, 18.05.

**HRMS** (ESI-TOF)  $m/z$ :  $[M]^+$  calcd for  $C_{18}H_{24}O$ : 256.1827; found 256.1828.



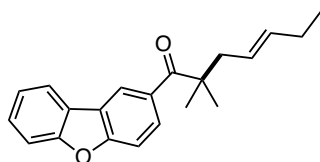
**(R)-2-methyl-2-(3-methylbut-2-en-1-yl)-3,4-dihydronaphthalen-1(2H)-one (IV-17)**

Light yellow oil, flash chromatography using 2% EtOAc/hexanes; 88.6 mg; 97% yield.

**$^1H$  NMR** (500 MHz,  $CDCl_3$ )  $\delta$  8.07 (dd,  $J = 7.8, 1.5$  Hz, 1H), 7.47 (td,  $J = 7.4, 1.5$  Hz, 1H), 7.35 – 7.30 (m, 1H), 7.24 (d,  $J = 7.7$  Hz, 1H), 5.15 (ddt,  $J = 8.4, 7.1, 1.4$  Hz, 1H), 2.99 (td,  $J = 6.4, 5.9, 2.1$  Hz, 2H), 2.37 (d,  $J = 7.3$  Hz, 1H), 2.28 (dd,  $J = 14.4, 7.9$  Hz, 1H), 2.10 (ddd,  $J = 13.2, 7.1, 5.8$  Hz, 1H), 1.91 (ddd,  $J = 13.6, 6.9, 5.6$  Hz, 1H), 1.73 (d,  $J = 1.6$  Hz, 3H), 1.62 (d,  $J = 1.4$  Hz, 3H), 1.19 (s, 3H).

**$^{13}C$  NMR** (126 MHz,  $CDCl_3$ )  $\delta$  202.58, 143.40, 134.44, 132.97, 131.74, 128.65, 127.99, 126.58, 119.42, 45.46, 34.97, 33.32, 26.07, 25.50, 21.93, 17.99.

**HRMS** (ESI-TOF)  $m/z$ :  $[M]^+$  calcd for  $C_{16}H_{20}O$ : 228.1514; found 228.1522.



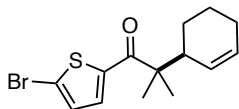
**(E)-1-(dibenzo[*b,d*]furan-2-yl)-2,2-dimethylhept-4-en-1-one (IV-18)**

Light yellow oil, flash chromatography using 2% EtOAc/hexanes; 112.8 mg; 92% yield.

**$^1H$  NMR** (400 MHz,  $CDCl_3$ )  $\delta$  8.35 (d,  $J = 1.8$  Hz, 1H), 7.98 (dt,  $J = 7.7, 1.1$  Hz, 1H), 7.88 (dd,  $J = 8.6, 1.9$  Hz, 1H), 7.61 – 7.55 (m, 2H), 7.50 (ddd,  $J = 8.3, 7.2, 1.4$  Hz, 1H), 7.38 (td,  $J = 7.5, 1.0$  Hz, 1H), 5.47 – 5.40 (m, 1H), 5.39 – 5.31 (m, 1H), 2.51 (dd,  $J = 7.1, 1.2$  Hz, 2H), 2.00 – 1.93 (m, 2H), 1.39 (s, 6H), 0.92 (t,  $J = 7.5$  Hz, 3H).

$^{13}\text{C}$  NMR (126 MHz,  $\text{CDCl}_3$ )  $\delta$  207.77, 157.45, 156.75, 136.11, 133.89, 127.78, 127.57, 124.15, 124.08, 123.91, 123.20, 121.23, 120.87, 111.90, 111.07, 48.03, 44.17, 26.21, 25.68, 13.87.

**HRMS** (ESI-TOF)  $m/z$ :  $[\text{M}]^+$  calcd for  $\text{C}_{21}\text{H}_{22}\text{O}_2$ : 306.1620; found 306.1635.



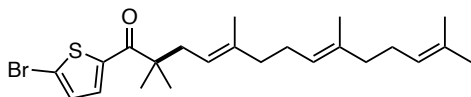
**(S)-1-(5-bromothiophen-2-yl)-2-(cyclohex-2-en-1-yl)-2-methylpropan-1-one (IV-19)**

Light yellow oil, flash chromatography using 3% EtOAc/hexanes; 125.3 mg; quantitative yield.

$^1\text{H}$  NMR (400 MHz,  $\text{CDCl}_3$ )  $\delta$  7.52 (d,  $J = 4.1$  Hz, 1H), 7.06 (d,  $J = 4.0$  Hz, 1H), 5.77 (ddd,  $J = 7.2, 5.3, 2.1$  Hz, 1H), 5.49 (dt,  $J = 10.4, 1.9$  Hz, 1H), 2.87 (ddt,  $J = 10.8, 5.4, 2.6$  Hz, 1H), 1.99 – 1.92 (m, 2H), 1.76 (dt,  $J = 12.6, 3.8$  Hz, 1H), 1.63 (ddt,  $J = 8.0, 4.7, 2.5$  Hz, 1H), 1.47 (tdd,  $J = 13.3, 6.5, 4.3$  Hz, 1H), 1.31 (s, 4H), 1.21 (s, 3H).

$^{13}\text{C}$  NMR (126 MHz,  $\text{CDCl}_3$ )  $\delta$  197.73, 144.48, 131.95, 130.81, 129.61, 126.87, 121.35, 50.38, 43.44, 25.04, 24.28, 22.96, 22.40, 21.62.

**HRMS** (ESI-TOF)  $m/z$ :  $[\text{M}]^+$  calcd for  $\text{C}_{14}\text{H}_{17}\text{BrOS}$ : 312.0183; found 312.0172.



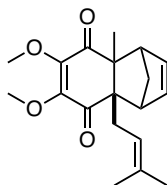
**(4E,8E)-1-(5-bromothiophen-2-yl)-2,2,5,9,13-pentamethyltetradeca-4,8,12-trien-1-one (IV-20)**

Light yellow oil, flash chromatography using 5% EtOAc/hexanes; 157.3 mg; 90% yield.

**<sup>1</sup>H NMR** (500 MHz, CDCl<sub>3</sub>) δ 7.54 (d, *J* = 4.1 Hz, 1H), 7.08 (dd, *J* = 4.1, 0.9 Hz, 1H), 5.17 – 5.01 (m, 3H), 2.49 (d, *J* = 7.5 Hz, 2H), 2.03 (dddd, *J* = 29.7, 14.2, 8.0, 3.8 Hz, 8H), 1.71 – 1.57 (m, 12H), 1.34 (s, 6H).

**<sup>13</sup>C NMR** (126 MHz, CDCl<sub>3</sub>) δ 197.55, 144.45, 138.35, 138.25, 135.24, 135.12, 131.96, 131.55, 131.28, 130.74, 124.79, 124.40, 124.36, 123.97, 121.20, 119.35, 119.27, 48.03, 40.20, 39.91, 39.72, 39.20, 32.00, 26.76, 26.61, 26.53, 26.32, 25.74, 25.72, 25.69, 25.61, 23.38, 17.70, 17.64, 16.30, 16.24, 16.03.

**HRMS** (ESI-TOF) *m/z*: [M]<sup>+</sup> calcd for C<sub>23</sub>H<sub>33</sub>BrOS: 436.1436; found 436.1422.



**(8a*S*)-6,7-dimethoxy-4a-methyl-8a-(3-methylbut-2-en-1-yl)-1,4,4a,8a-tetrahydro-1,4-methanonaphthalene-5,8-dione (IV-21)**

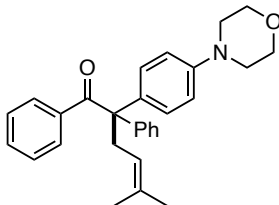
Bright yellow oil, flash chromatography using 8% EtOAc/hexanes; 116.3 mg; 92% yield.

**<sup>1</sup>H NMR** (400 MHz, CDCl<sub>3</sub>) δ 6.08 – 5.95 (m, 2H), 5.06 (ddp, *J* = 7.7, 5.9, 1.3 Hz, 1H), 3.86 (d, *J* = 15.3 Hz, 6H), 3.10 – 2.94 (m, 2H), 2.76 – 2.66 (m, 1H), 2.43 – 2.32 (m, 1H), 1.79 – 1.73 (m, 1H), 1.64 (t, *J* = 1.4 Hz, 3H), 1.56 (d, *J* = 1.4 Hz, 3H), 1.47 (s, 3H), 1.45 – 1.39 (m, 1H).

**<sup>13</sup>C NMR** (126 MHz, CDCl<sub>3</sub>) δ 198.85, 198.24, 150.79, 149.12, 137.96, 137.19, 134.45, 119.83, 60.30, 59.95, 59.28, 56.07, 54.41, 53.10, 43.44, 36.09, 26.03, 23.38, 17.91.

**HRMS** (ESI-TOF) *m/z*: [M]<sup>+</sup> calcd for C<sub>19</sub>H<sub>24</sub>O<sub>4</sub>: 316.1674; found 316.1658.





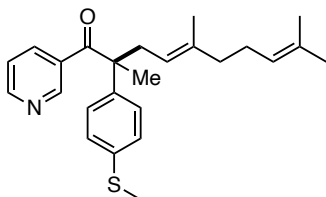
**5-methyl-2-(4-morpholinophenyl)-1,2-diphenylhex-4-en-1-one (IV-22)**

Dark yellow oil, flash chromatography using 10% EtOAc/hexanes; 125.8 mg; 74% yield.

$^1\text{H NMR}$  (400 MHz,  $\text{CDCl}_3$ )  $\delta$  7.53 – 7.45 (m, 2H), 7.35 – 7.16 (m, 10H), 7.01 – 6.80 (m, 2H), 4.89 (tt,  $J = 7.2, 1.6$  Hz, 1H), 3.98 – 3.79 (m, 4H), 3.19 (t,  $J = 4.8$  Hz, 4H), 3.10 (d,  $J = 7.1$  Hz, 2H), 1.51 (d,  $J = 1.6$  Hz, 3H), 1.12 (d,  $J = 1.4$  Hz, 3H).

$^{13}\text{C NMR}$  (126 MHz,  $\text{CDCl}_3$ )  $\delta$  202.21, 142.35, 138.27, 134.68, 131.20, 130.30, 129.54, 129.33, 127.96, 127.75, 126.64, 119.56, 115.25, 66.70, 64.10, 49.32, 38.76, 25.86, 17.53.

**HRMS** (ESI-TOF)  $m/z$ :  $[\text{M}]^+$  calcd for  $\text{C}_{29}\text{H}_{32}\text{NO}_2$ : 426.2428; found 426.2426.



**(E)-2,5,9-trimethyl-2-(4-(methylthio)phenyl)-1-(pyridin-3-yl)deca-4,8-dien-1-one**

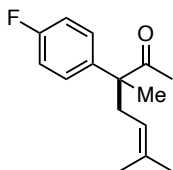
**(IV-23)**

Light yellow oil, flash chromatography using 10% EtOAc/hexanes; 122.8 mg; 78% yield.

$^1\text{H NMR}$  (400 MHz,  $\text{CDCl}_3$ )  $\delta$  8.66 – 8.59 (m, 1H), 8.57 (dd,  $J = 4.9, 1.7$  Hz, 1H), 7.72 (dt,  $J = 8.1, 2.0$  Hz, 1H), 7.26 – 7.15 (m, 5H), 5.01 (tq,  $J = 5.4, 1.5$  Hz, 1H), 4.88 (ddq,  $J = 8.2, 6.8, 1.5$  Hz, 1H), 2.79 (dd,  $J = 14.4, 8.2$  Hz, 1H), 2.66 (dd,  $J = 14.6, 6.5$  Hz, 1H), 2.48 (s, 3H), 2.02 – 1.88 (m, 4H), 1.67 (d,  $J = 1.4$  Hz, 3H), 1.57 (d,  $J = 1.3$  Hz, 3H), 1.53 (s, 3H), 1.37 (d,  $J = 1.4$  Hz, 3H).

$^{13}\text{C}$  NMR (126 MHz,  $\text{CDCl}_3$ )  $\delta$  202.13, 151.81, 150.60, 139.52, 138.86, 137.61, 136.79, 132.45, 131.44, 127.01, 126.87, 124.17, 123.01, 118.70, 54.91, 39.96, 37.53, 26.52, 25.73, 23.67, 17.70, 16.07, 15.62.

HRMS (ESI-TOF)  $m/z$ :  $[\text{M}]^+$  calcd for  $\text{C}_{25}\text{H}_{31}\text{NOS}$ : 393.2126; found 393.2135.



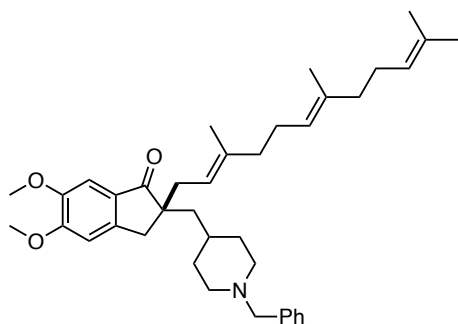
**3-(4-fluorophenyl)-3,6-dimethylhept-5-en-2-one (IV-24)**

Colorless oil, flash chromatography using 3% EtOAc/hexanes; 92.8 mg; 99% yield.

$^1\text{H}$  NMR (400 MHz,  $\text{CDCl}_3$ )  $\delta$  7.22 – 7.16 (m, 2H), 7.03 (t,  $J = 8.7$  Hz, 2H), 4.86 – 4.79 (m, 1H), 2.65 (dd,  $J = 14.7, 7.6$  Hz, 1H), 2.54 (dd,  $J = 14.8, 7.0$  Hz, 1H), 1.90 (s, 3H), 1.64 (d,  $J = 1.5$  Hz, 3H), 1.54 (s, 3H), 1.42 (s, 3H).

$^{13}\text{C}$  NMR (101 MHz,  $\text{CDCl}_3$ )  $\delta$  210.61, 162.96, 134.75, 128.12, 128.04, 119.22, 115.58, 115.37, 55.64, 36.10, 25.95, 25.84, 21.56, 17.97.

HRMS (ESI-TOF)  $m/z$ :  $[\text{M}]^+$  calcd for  $\text{C}_{15}\text{H}_{19}\text{FO}$ : 234.1420; found 234.2412.



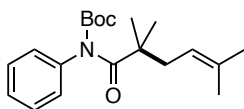
**(S)-2-((1-benzylpiperidin-4-yl)methyl)-5,6-dimethoxy-2-((2E,6E)-3,7,11-trimethyldodeca-2,6,10-trien-1-yl)-2,3-dihydro-1H-inden-1-one (IV-25)**

Yellow oil, flash chromatography using 5% MeOH/DCM; 205.5 mg; 88% yield.

**<sup>1</sup>H NMR** (400 MHz, CDCl<sub>3</sub>) δ 7.29 – 7.07 (m, 6H), 6.86 – 6.75 (m, 1H), 5.11 – 4.62 (m, 3H), 3.94 (d, *J* = 2.9 Hz, 3H), 3.89 (d, *J* = 2.5 Hz, 3H), 3.40 (s, 2H), 2.89 (s, 2H), 2.79 – 2.66 (m, 2H), 2.26 (d, *J* = 7.3 Hz, 2H), 2.07 – 1.71 (m, 10H), 1.71 – 1.52 (m, 12H), 1.52 – 1.36 (m, 4H), 1.32 – 1.19 (m, 3H).

**<sup>13</sup>C NMR** (101 MHz, CDCl<sub>3</sub>) δ 209.73, 155.45, 149.34, 148.36, 138.36, 138.16, 138.04, 135.04, 134.95, 131.47, 131.26, 129.74, 129.72, 129.21, 128.08, 126.87, 124.81, 124.35, 124.01, 119.37, 119.28, 109.73, 107.22, 104.32, 63.36, 56.13, 56.02, 53.74, 53.68, 53.21, 53.19, 43.79, 40.15, 39.88, 39.70, 36.96, 34.06, 33.53, 32.69, 31.89, 26.75, 26.64, 26.54, 26.36, 25.92, 25.74, 25.71, 23.37, 22.46, 17.70, 17.64, 16.36, 16.31, 15.89.

**HRMS** (ESI-TOF) *m/z*: [M+H]<sup>+</sup> calcd for C<sub>39</sub>H<sub>54</sub>NO<sub>3</sub>: 584.4098; found 584.4102.



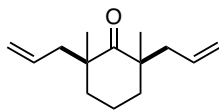
***tert*-butyl phenyl(2,2,5-trimethylhex-4-enoyl)carbamate (IV-26)**

Colorless oil, flash chromatography using 5% EtOAc/hexanes; 120.6 mg; 91% yield.

**<sup>1</sup>H NMR** (400 MHz, CDCl<sub>3</sub>) δ 7.35 (dd, *J* = 8.4, 6.9 Hz, 2H), 7.29 – 7.23 (m, 1H), 7.19 – 7.08 (m, 2H), 5.10 (ddt, *J* = 9.0, 7.5, 1.6 Hz, 1H), 2.30 (d, *J* = 7.5 Hz, 2H), 1.68 (d, *J* = 1.6 Hz, 3H), 1.55 (d, *J* = 1.4 Hz, 3H), 1.45 (s, 9H), 1.22 (s, 6H).

**<sup>13</sup>C NMR** (101 MHz, CDCl<sub>3</sub>) δ 184.53, 153.45, 138.89, 134.35, 128.90, 127.43, 127.19, 119.95, 82.37, 48.05, 40.04, 28.00, 26.01, 25.59, 17.96.

**HRMS** (ESI-TOF) *m/z*: [M]<sup>+</sup> calcd for C<sub>20</sub>H<sub>29</sub>NO<sub>3</sub>: 331.2148; found 331.2148.



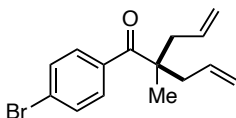
**2,6-diallyl-2,6-dimethylcyclohexan-1-one (IV-27)**

Mixture of *cis* and *trans* isomer. Colorless oil, flash chromatography using 5% EtOAc/hexanes. 79.1 mg, 96% yield.

$^1\text{H NMR}$  (400 MHz,  $\text{CDCl}_3$ )  $\delta$  5.74 – 5.53 (m, 2H), 5.10 – 4.95 (m, 4H), 2.46 – 2.28 (m, 2H), 2.22 – 2.05 (m, 2H), 1.85 – 1.62 (m, 4H), 1.59 – 1.52 (m, 2H), 1.08 (d,  $J = 16.2$  Hz, 6H).

$^{13}\text{C NMR}$  (101 MHz,  $\text{CDCl}_3$ )  $\delta$  219.44, 218.67, 134.60, 134.42, 117.99, 47.60, 47.56, 43.96, 43.93, 36.40, 35.92, 26.11, 25.06, 17.41, 17.37.

**HRMS** (ESI-TOF)  $m/z$ :  $[\text{M}]^+$  calcd for  $\text{C}_{14}\text{H}_{22}\text{O}$ : 206.1671; found 206.1681.



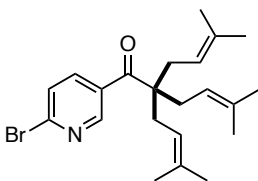
**2-allyl-1-(4-bromophenyl)-2-methylpent-4-en-1-one (IV-28)**

Colorless oil, flash chromatography using 2% EtOAc/hexanes; 111.4 mg; 95% yield.

$^1\text{H NMR}$  (400 MHz,  $\text{CDCl}_3$ )  $\delta$  7.52 (d,  $J = 1.3$  Hz, 4H), 5.68 (ddt,  $J = 17.4, 10.2, 7.3$  Hz, 2H), 5.08 – 4.96 (m, 4H), 2.64 – 2.54 (m, 2H), 2.41 – 2.32 (m, 2H), 1.27 (s, 3H).

$^{13}\text{C NMR}$  (126 MHz,  $\text{CDCl}_3$ )  $\delta$  206.83, 138.05, 133.42, 131.39, 129.24, 125.63, 118.67, 51.29, 43.17, 22.73.

**HRMS** (ESI-TOF)  $m/z$ :  $[\text{M}]^+$  calcd for  $\text{C}_{15}\text{H}_{17}\text{BrO}$ : 292.0463; found 292.0468.



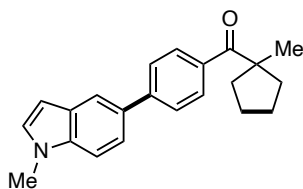
**1-(6-bromopyridin-3-yl)-5-methyl-2,2-bis(3-methylbut-2-en-1-yl)hex-4-en-1-one  
(IV-29)**

White solid, flash chromatography using 4% EtOAc/hexanes; 103.4 mg; 64% yield.

$^1\text{H NMR}$  (500 MHz,  $\text{CDCl}_3$ )  $\delta$  8.56 (d,  $J = 2.5$  Hz, 1H), 7.68 (dd,  $J = 8.2, 2.5$  Hz, 1H), 7.52 (d,  $J = 8.2$  Hz, 1H), 5.03 – 4.94 (m, 3H), 2.41 (d,  $J = 7.0$  Hz, 6H), 1.67 (d,  $J = 1.8$  Hz, 9H), 1.53 (s, 9H).

$^{13}\text{C NMR}$  (126 MHz,  $\text{CDCl}_3$ )  $\delta$  207.08, 148.60, 143.87, 137.33, 134.95, 134.92, 127.63, 118.68, 55.99, 33.05, 26.04, 17.99.

**HRMS** (ESI-TOF)  $m/z$ :  $[\text{M}+\text{H}]^+$  calcd for  $\text{C}_{22}\text{H}_{31}\text{BrNO}$ : 404.1589; found 404.1590.



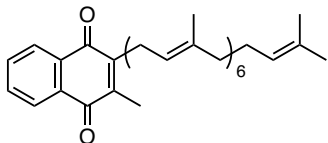
**(4-(1-methyl-1H-indol-5-yl)phenyl)(1-methylcyclopentyl)methanone (IV-41)**

Light yellow solid, flash chromatography using 5% EtOAc/hexanes; 99 mg; 78% yield.

$^1\text{H NMR}$  (400 MHz,  $\text{CDCl}_3$ )  $\delta$  7.98 (d,  $J = 8.5$  Hz, 2H), 7.89 (d,  $J = 1.7$  Hz, 1H), 7.71 (d,  $J = 8.5$  Hz, 2H), 7.51 (dd,  $J = 8.5, 1.8$  Hz, 1H), 7.40 (d,  $J = 8.5$  Hz, 1H), 7.10 (d,  $J = 3.1$  Hz, 1H), 6.56 (dd,  $J = 3.1, 0.9$  Hz, 1H), 3.84 (s, 3H), 2.51 – 2.25 (m, 2H), 1.72 (tdt,  $J = 10.4, 7.4, 5.0$  Hz, 6H), 1.48 (s, 3H).

$^{13}\text{C NMR}$  (101 MHz,  $\text{CDCl}_3$ )  $\delta$  205.95, 145.92, 136.65, 134.08, 131.54, 129.79, 129.76, 129.01, 126.78, 121.24, 119.70, 109.64, 101.56, 54.77, 38.09, 32.99, 27.46, 25.40.

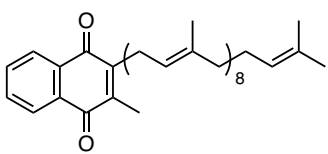
**HRMS** (ESI-TOF)  $m/z$ :  $[\text{M}]^+$  calcd for  $\text{C}_{22}\text{H}_{23}\text{NO}$ : 317.1780; found 317.1783.



**2-((2E,6E,10E,14E,18E,22E)-3,7,11,15,19,23,27-heptamethyloctacos-2,6,10,14,18,22,26-heptaen-1-yl)-3-methylnaphthalene-1,4-dione-ethane (1/1) (MK-7)**

**<sup>1</sup>H NMR** (400 MHz, CDCl<sub>3</sub>): δ 8.08 (ddt, *J* = 4.7, 3.1, 2.0 Hz, 2H), 7.68 (dd, *J* = 5.8, 3.3 Hz, 2H), 5.15 – 4.98 (m, 7H), 3.37 (d, *J* = 7.0 Hz, 2H), 2.19 (s, 3H), 2.11 – 1.89 (m, 24H), 1.79 (s, 3H), 1.68 (s, 3H), 1.59 (s, 12H), 1.56 (s, 6H).

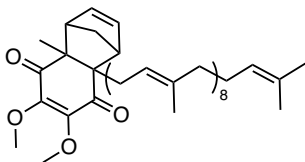
**<sup>13</sup>C NMR** (101 MHz, CDCl<sub>3</sub>): δ 185.4, 184.5, 146.1, 143.3, 137.5, 135.2, 134.9, 134.9, 134.9, 133.3, 133.3, 132.2, 132.1, 131.2, 126.3, 126.2, 124.4, 124.2, 124.1, 123.8, 119.0, 39.7, 39.7, 26.7, 26.7, 26.6, 26.5, 26.0, 25.7, 17.7, 16.4, 16.0, 16.0, 16.0, 12.7.



**2-methyl-3-((2E,6E,10E,14E,18E,22E,26E,30E)-3,7,11,15,19,23,27,31,35-nonamethylhexatriaconta-2,6,10,14,18,22,26,30,34-nonaen-1-yl)naphthalene-1,4-dione-ethane (1/1) (MK-9)**

**<sup>1</sup>H NMR** (400 MHz, CDCl<sub>3</sub>): δ 8.08 (ddt, *J* = 4.8, 3.2, 2.0 Hz, 2H), 7.73 – 7.63 (m, 2H), 5.17 – 4.98 (m, 9H), 3.37 (d, *J* = 6.9 Hz, 2H), 2.19 (s, 3H), 2.12 – 1.91 (m, 32H), 1.80 (d, *J* = 1.3 Hz, 3H), 1.68 (d, *J* = 1.4 Hz, 3H), 1.63 – 1.54 (m, 24H).

**<sup>13</sup>C NMR** (101 MHz, CDCl<sub>3</sub>): δ 185.4, 184.5, 146.1, 143.3, 137.5, 135.2, 134.9, 134.9, 134.9, 133.3, 133.2, 132.2, 132.1, 131.2, 126.3, 126.2, 124.4, 124.3, 124.2, 124.2, 124.1, 123.8, 119.1, 39.7, 39.7, 39.7, 29.7, 26.7, 26.7, 26.7, 26.6, 26.5, 26.0, 25.7, 17.7, 16.4, 16.0, 16.0, 16.0, 12.7.

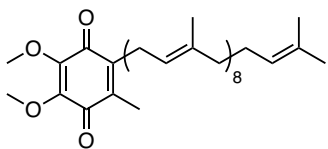


**6,7-dimethoxy-4a-methyl-8a-((2E,6E,10E,14E,18E,22E,26E,30E)-3,7,11,15,19,23,27,31,35-nonamethylhexatriaconta-2,6,10,14,18,22,26,30,34-nonaen-1-yl)-1,4,4a,8a-tetrahydro-1,4-methanonaphthalene-5,8-dione (IV-36)**

$^1\text{H NMR}$  (500 MHz,  $\text{CDCl}_3$ )  $\delta$  6.09 – 6.02 (m, 2H), 5.16 – 5.00 (m, 9H), 3.90 (s, 2H), 3.88 (s, 2H), 3.09 (q,  $J = 1.8, 1.3$  Hz, 1H), 3.01 (q,  $J = 2.3, 1.8$  Hz, 1H), 2.75 (dd,  $J = 15.2, 7.7$  Hz, 1H), 2.47 – 2.37 (m, 1H), 2.05 (q,  $J = 6.7, 5.7$  Hz, 16H), 2.01 – 1.91 (m, 18H), 1.81 – 1.71 (m, 2H), 1.68 (q,  $J = 1.4$  Hz, 3H), 1.59 (dd,  $J = 9.3, 1.2$  Hz, 26H), 1.51 – 1.44 (m, 4H).

$^{13}\text{C NMR}$  (126 MHz,  $\text{CDCl}_3$ )  $\delta$  198.84, 198.22, 150.82, 149.14, 138.05, 137.98, 137.19, 135.39, 135.03, 134.96, 134.94, 134.92, 134.90, 134.87, 131.22, 124.42, 124.28, 124.27, 124.26, 124.25, 124.23, 124.13, 123.76, 119.63, 60.27, 60.03, 59.33, 56.07, 54.46, 53.15, 43.47, 39.95, 39.75, 39.72, 36.06, 26.77, 26.73, 26.72, 26.69, 26.68, 26.53, 25.69, 23.38, 17.68, 16.39, 16.03, 16.00.

**HRMS** (ESI-TOF)  $m/z$ :  $[\text{M}+\text{Na}]^+$  calcd for  $\text{C}_{59}\text{H}_{88}\text{O}_4\text{Na}$ : 883.6590; found 883.6572.



**2,3-dimethoxy-5-methyl-6-((2E,6E,10E,14E,18E,22E,26E,30E)-3,7,11,15,19,23,27,31,35-nonamethylhexatriaconta-2,6,10,14,18,22,26,30,34-nonaen-1-yl)cyclohexa-2,5-diene-1,4-dione--ethane (1/1) (CoQ<sub>9</sub>)**

**<sup>1</sup>H NMR** (500 MHz, CDCl<sub>3</sub>) δ 5.15 – 5.03 (m, 9H), 4.93 (tq, *J* = 7.1, 1.4 Hz, 1H), 3.99 (s, 3H), 3.97 (s, 3H), 3.18 (d, *J* = 7.1 Hz, 2H), 2.05 (q, *J* = 6.2, 4.8 Hz, 16H), 2.01 (s, 3H), 2.00 – 1.91 (m, 16H), 1.73 (d, *J* = 1.3 Hz, 3H), 1.67 (d, *J* = 1.4 Hz, 3H), 1.62 – 1.55 (m, 24H).

**<sup>13</sup>C NMR** (126 MHz, CDCl<sub>3</sub>) δ 184.75, 183.90, 144.39, 144.25, 141.68, 138.85, 137.62, 135.24, 134.99, 134.94, 134.92, 134.91, 134.89, 134.87, 131.22, 124.42, 124.29, 124.28, 124.26, 124.25, 124.16, 123.86, 118.87, 61.12, 61.11, 39.75, 39.73, 39.71, 26.78, 26.72, 26.71, 26.70, 26.68, 26.63, 26.52, 25.69, 25.31, 17.67, 16.34, 16.04, 16.02, 16.00, 11.93.

**HRMS** (ESI-TOF) *m/z*: [M+Na]<sup>+</sup> calcd for C<sub>54</sub>H<sub>82</sub>O<sub>4</sub>Na: 817.6111; found 817.6114.

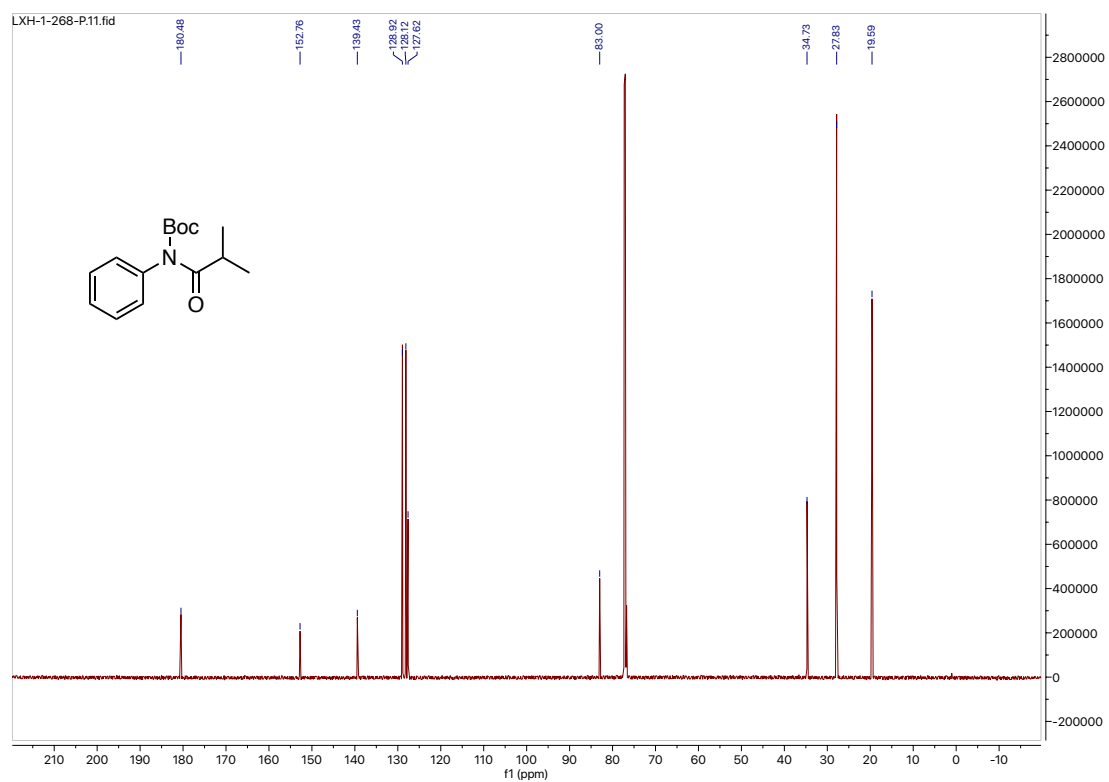
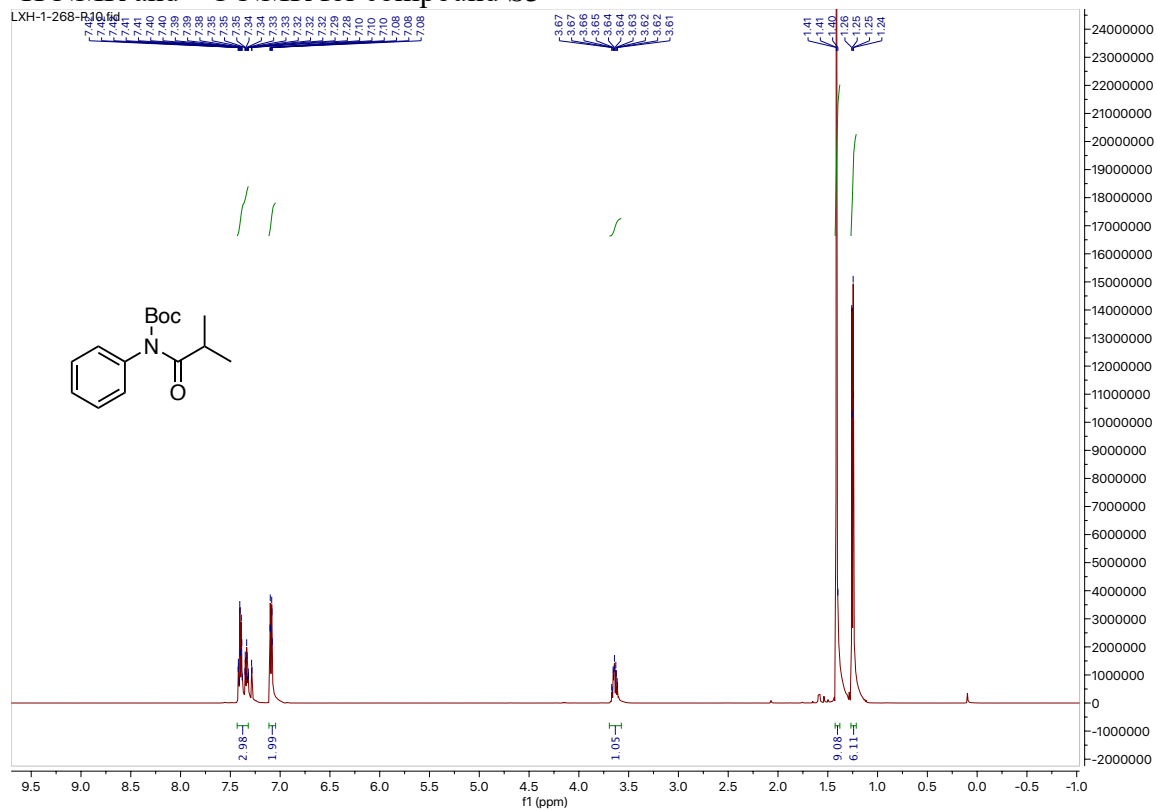
#### 4.5.11. References

1. Patpi, S. R.; Pulipati, L.; Yogeewari, P.; Sriram, D.; Jain, N.; Sridhar, B.; Murthy, R.; T, A. D.; Kalivendi, S. V.; Kantevari, S. Design, Synthesis, and Structure–Activity Correlations of Novel Dibenzo[*b,d*]Furan, Dibenzo[*b,d*]Thiophene, and *N*-Methylcarbazole Clubbed 1,2,3-Triazoles as Potent Inhibitors of *Mycobacterium Tuberculosis*. *J. Med. Chem.* **2012**, *55*, 3911–3922.
2. Tinnis, F.; Stridfeldt, E.; Lundberg, H.; Adolfsson, H.; Olofsson, B. Metal-Free *N*-Arylation of Secondary Amides at Room Temperature. *Org. Lett.* **2015**, *17*, 2688–2691.
3. Simas, A. B. C.; de Sales, D. L.; Pais, K. C. Acyclic Ketene Aminal Phosphates Derived from *N,N*-Diprotected Acetamides: Stability and Cross-Couplings. *Tetrahedron Lett.* **2009**, *50*, 6977–6980.
4. Majetich, G.; Liu, S.; Fang, J.; Siesel, D.; Zhang, Y. Use of Conjugated Dienones in Cyclialkylations: Total Syntheses of Arucadiol, 1,2-Didehydromiltirone, (±)-Hinokione, (±)-Nimbidiol, Sageone, and Miltirone. *J. Org. Chem.* **1997**, *62*, 6928–6951.
5. Cyclopentadiene and 3-chlorocyclopentene *Org. Synth.* **1952**, *32*, 41.
6. López, G.-D.; Suesca, E.; Álvarez-Rivera, G.; Rosato, A. E.; Ibáñez, E.; Cifuentes, A.; Leidy, C.; Carazzone, C. Carotenogenesis of *Staphylococcus Aureus*: New Insights and Impact on Membrane Biophysical Properties. *BBA - Mol. Cell. Biol. Lipids.* **2021**, *1866*, 158941.

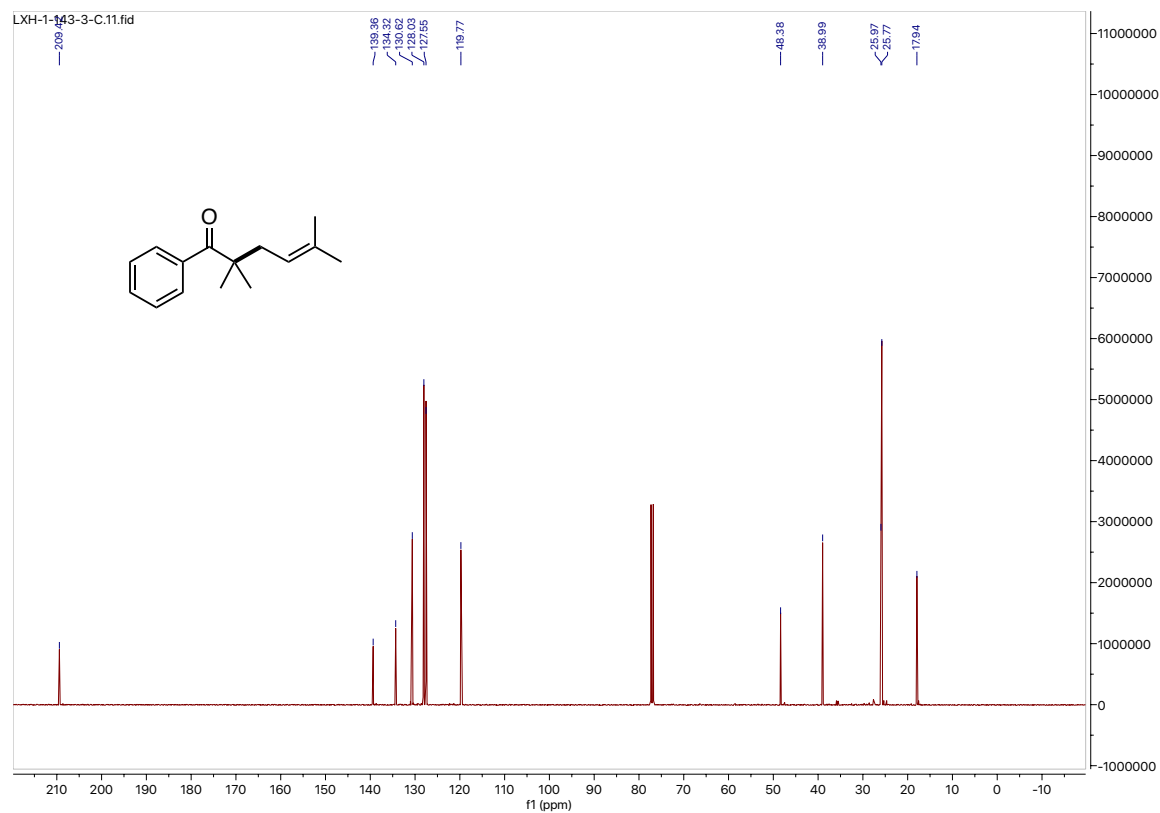
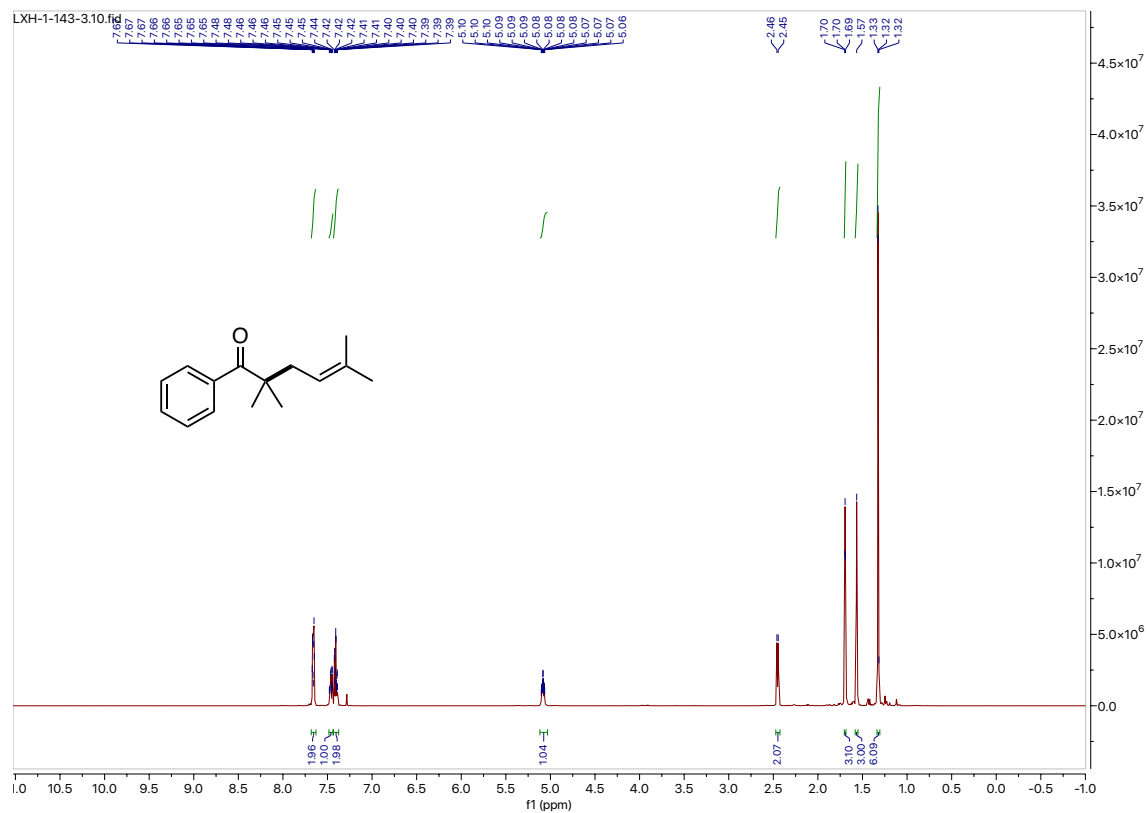


## 4.5.12. NMR spectra

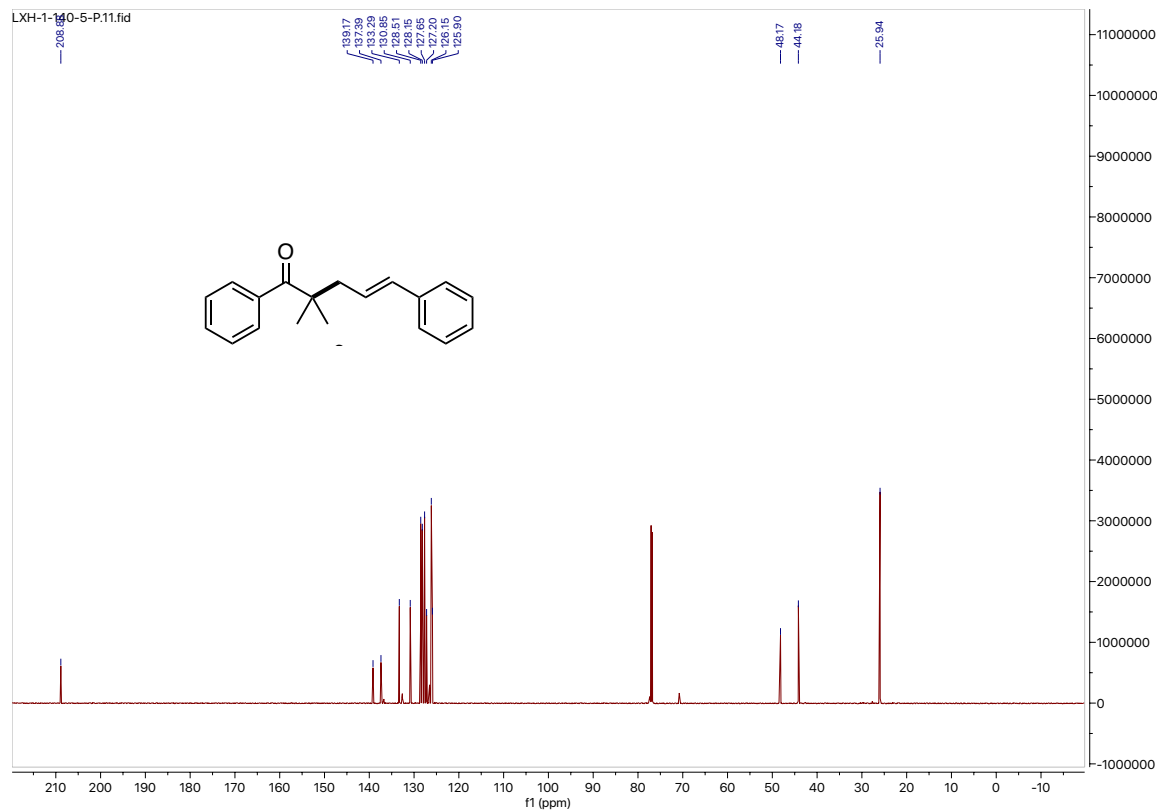
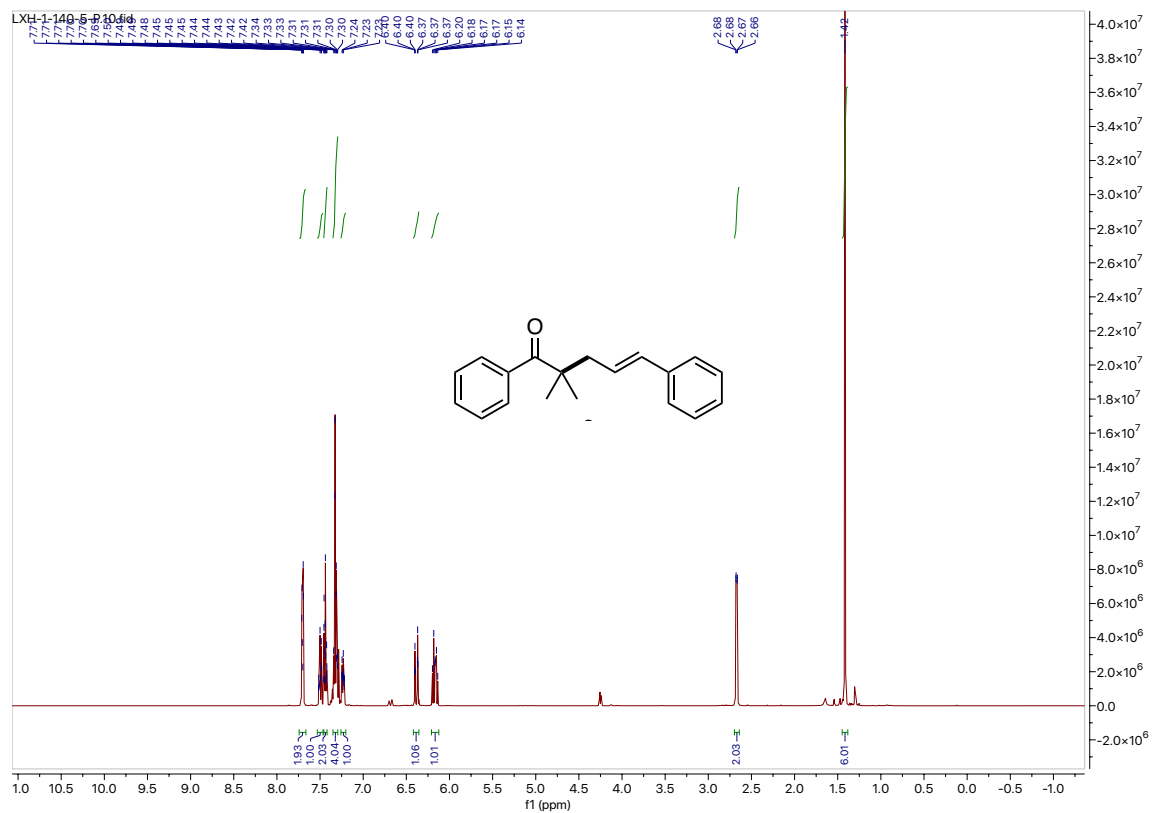
### $^1\text{H}$ NMR and $^{13}\text{C}$ NMR for compound S3



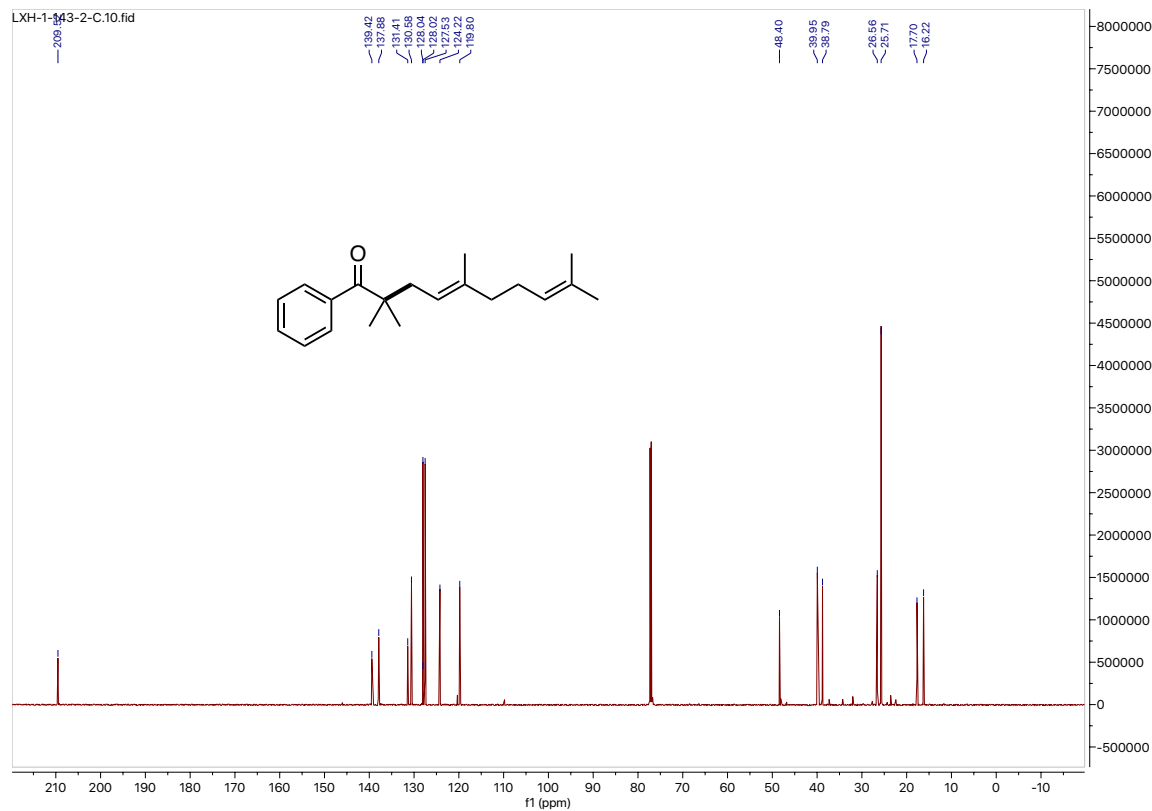
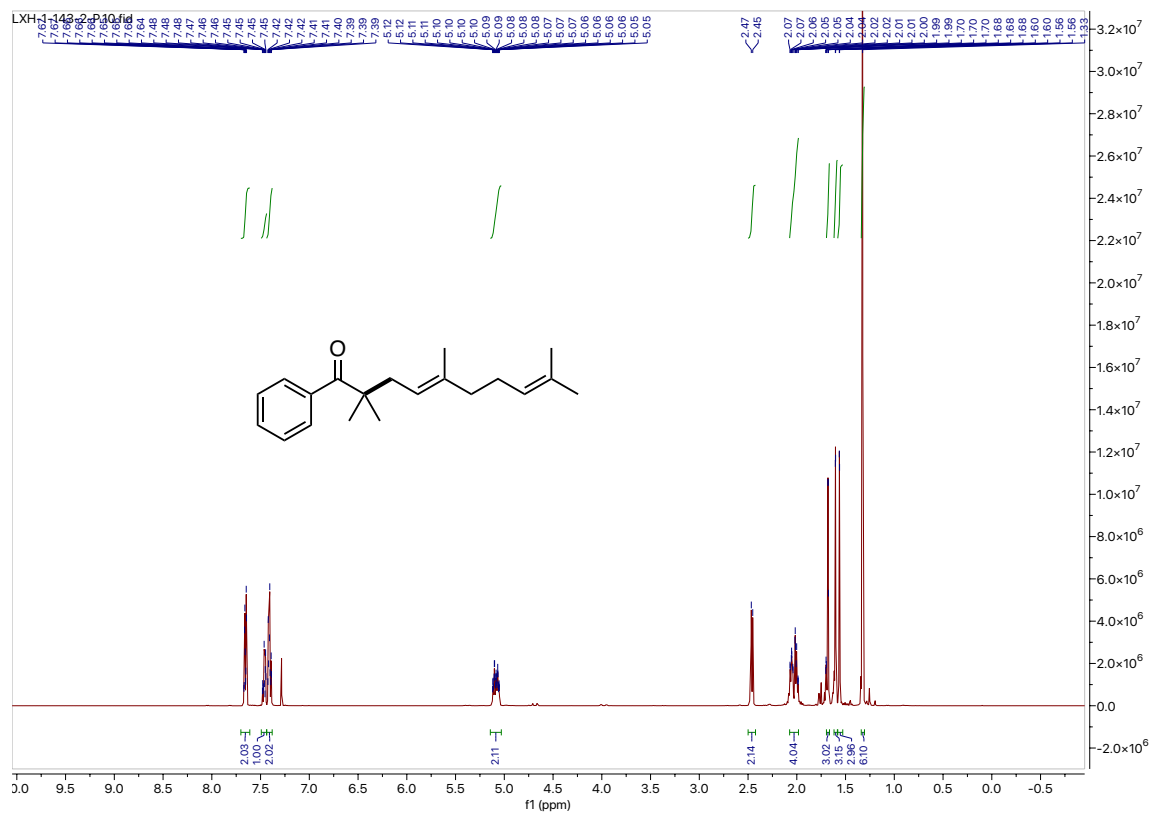
# <sup>1</sup>H NMR and <sup>13</sup>C NMR for compound IV-5



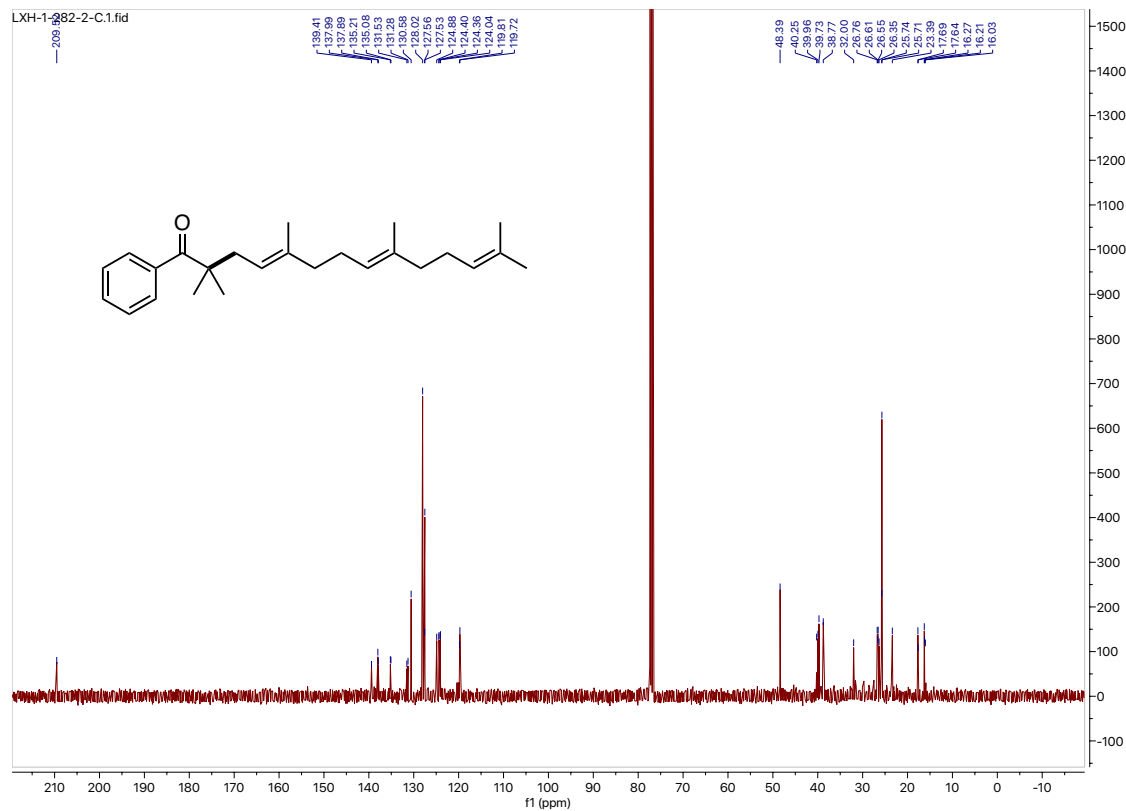
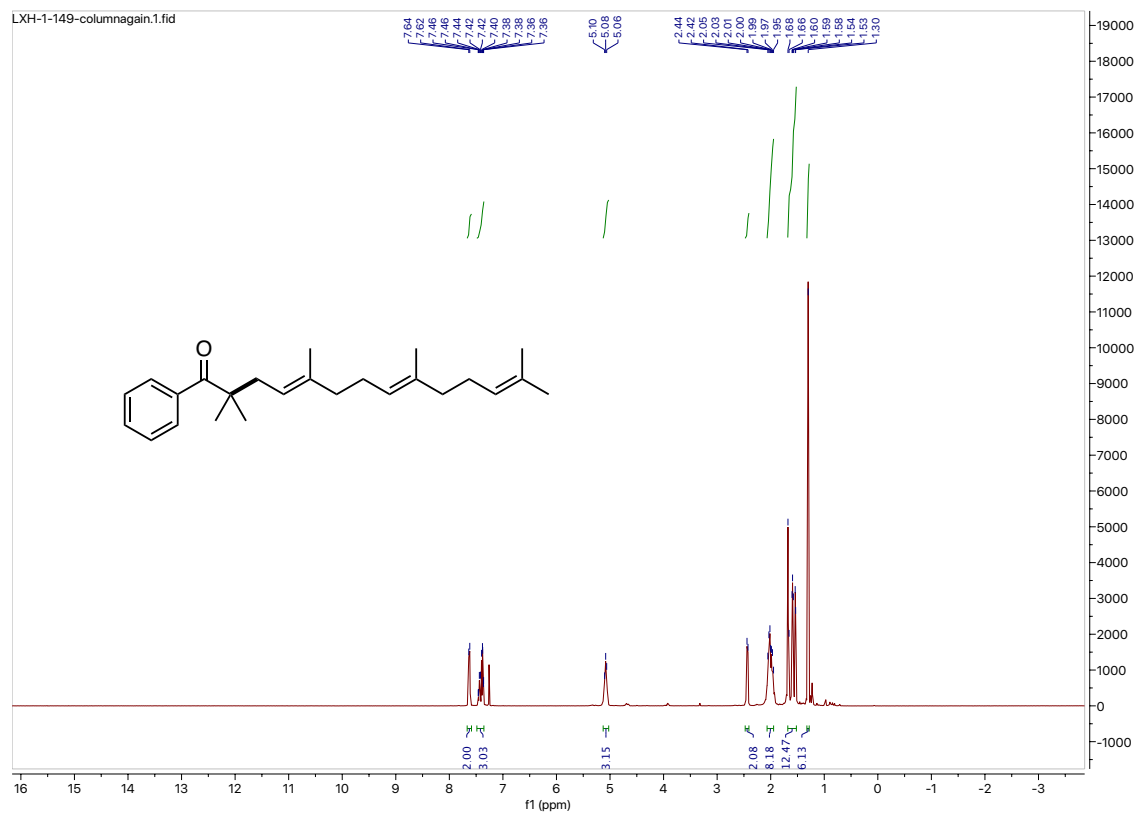
$^1\text{H}$  NMR and  $^{13}\text{C}$  NMR for compound IV-6



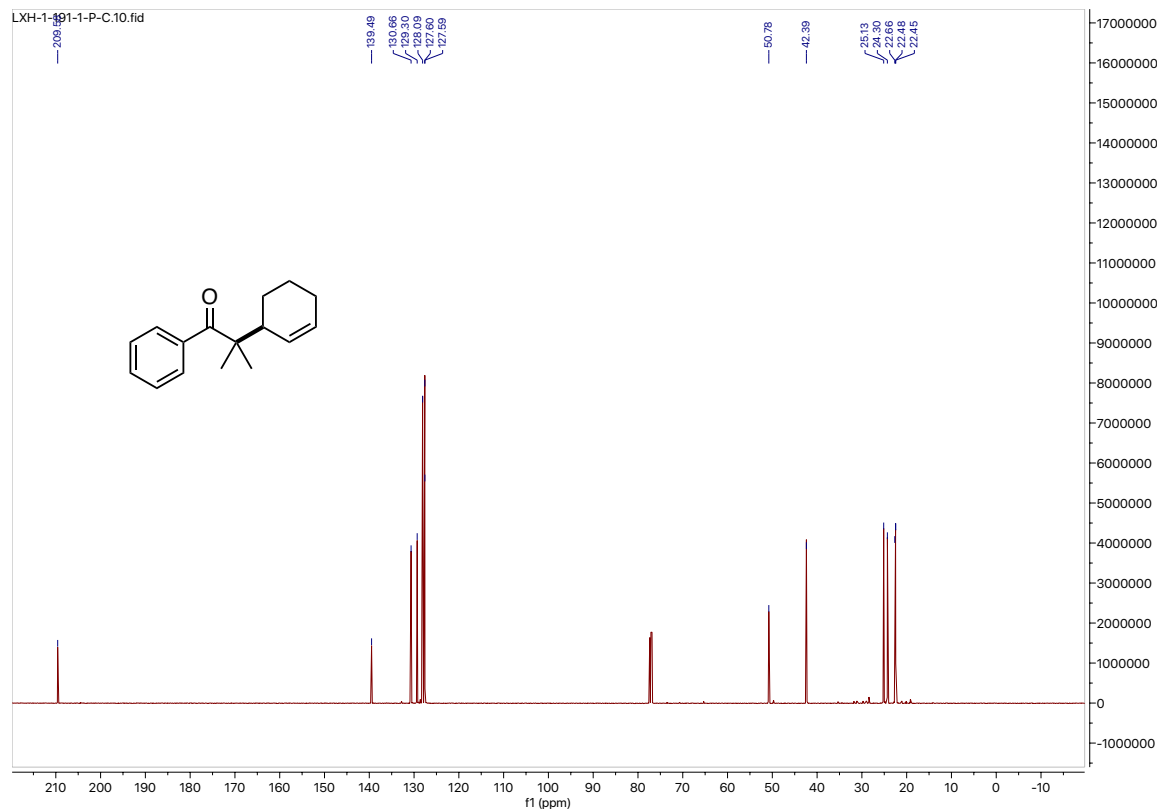
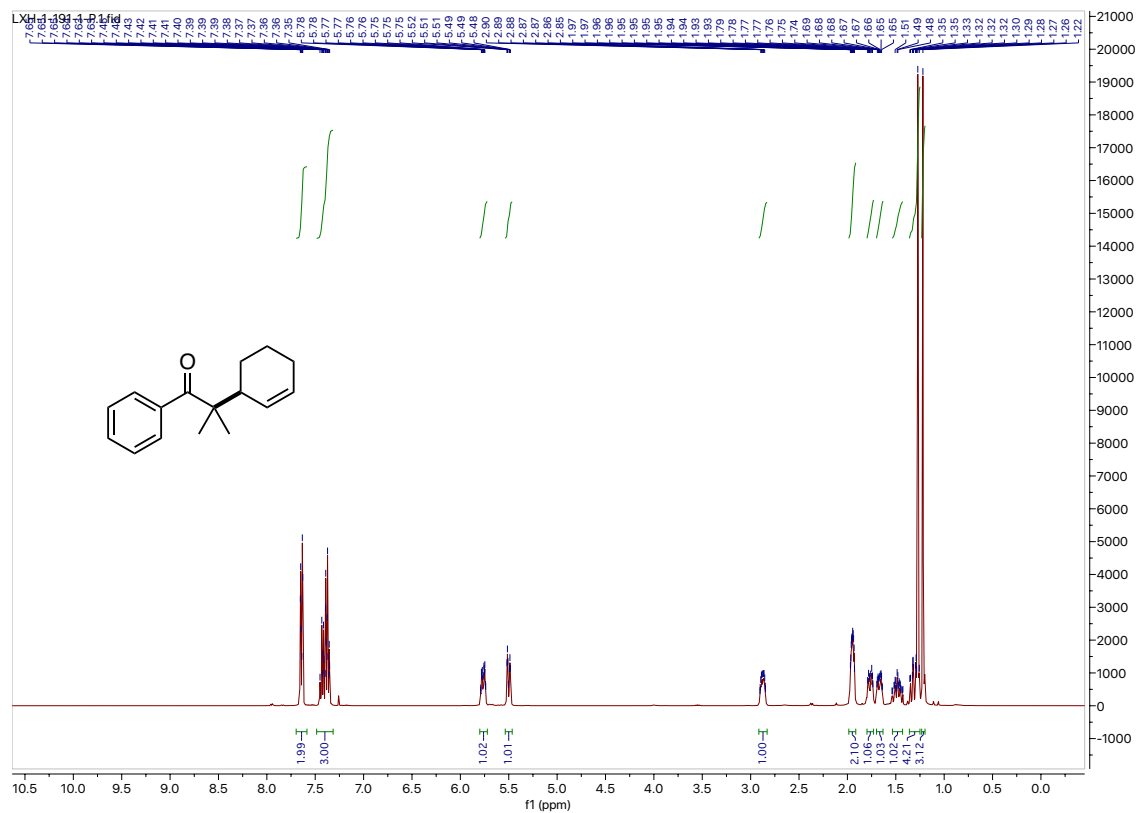
<sup>1</sup>H NMR and <sup>13</sup>C NMR for compound IV-7



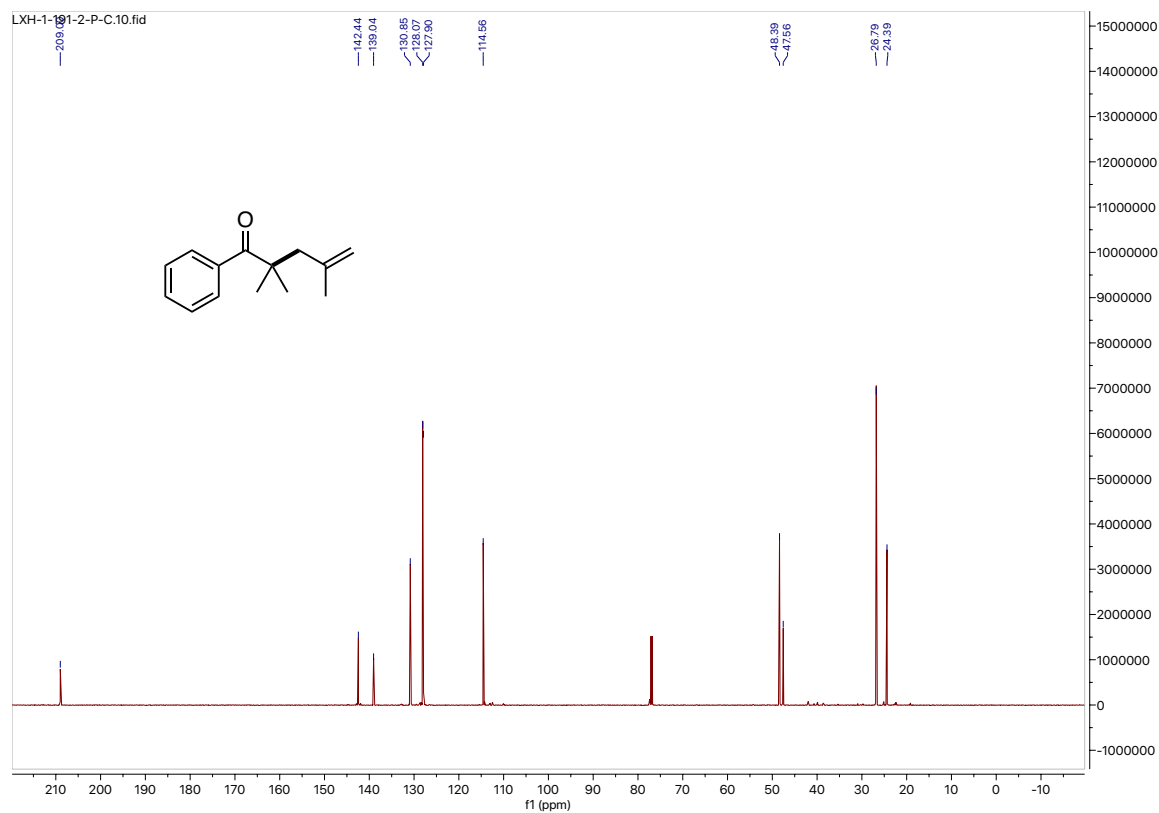
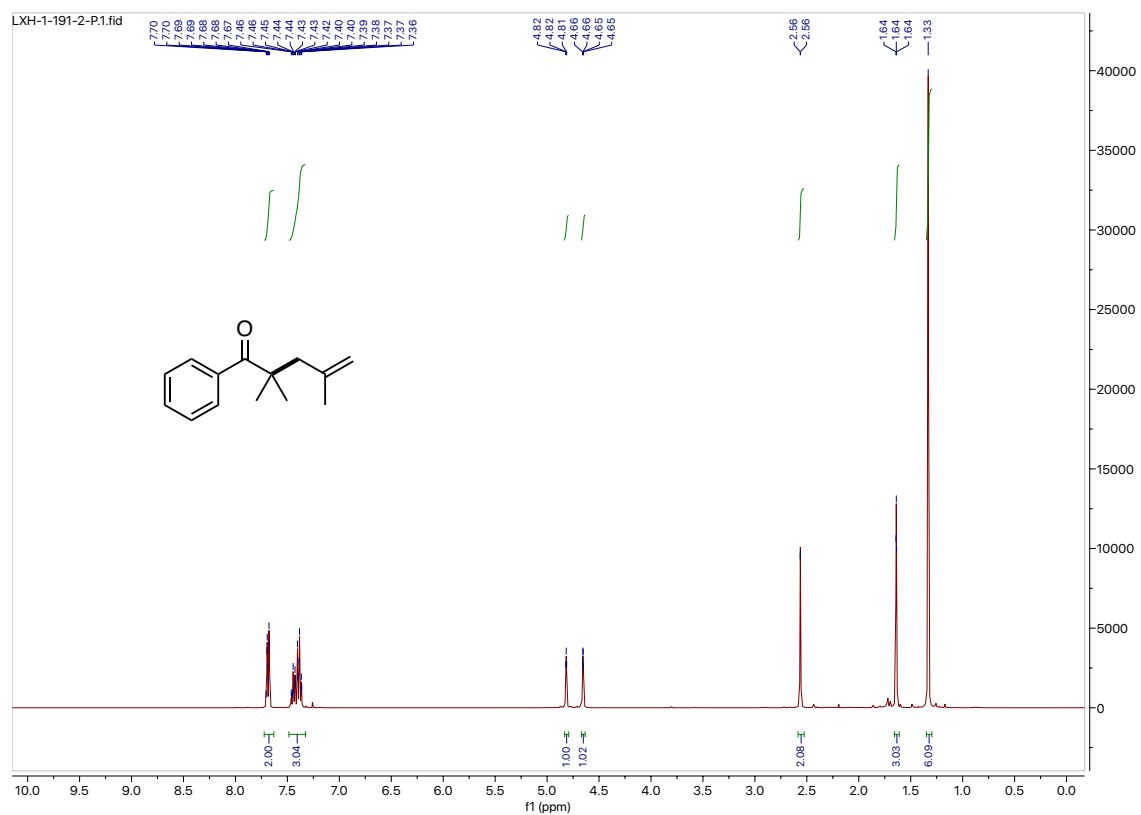
<sup>1</sup>H NMR and <sup>13</sup>C NMR for compound IV-8



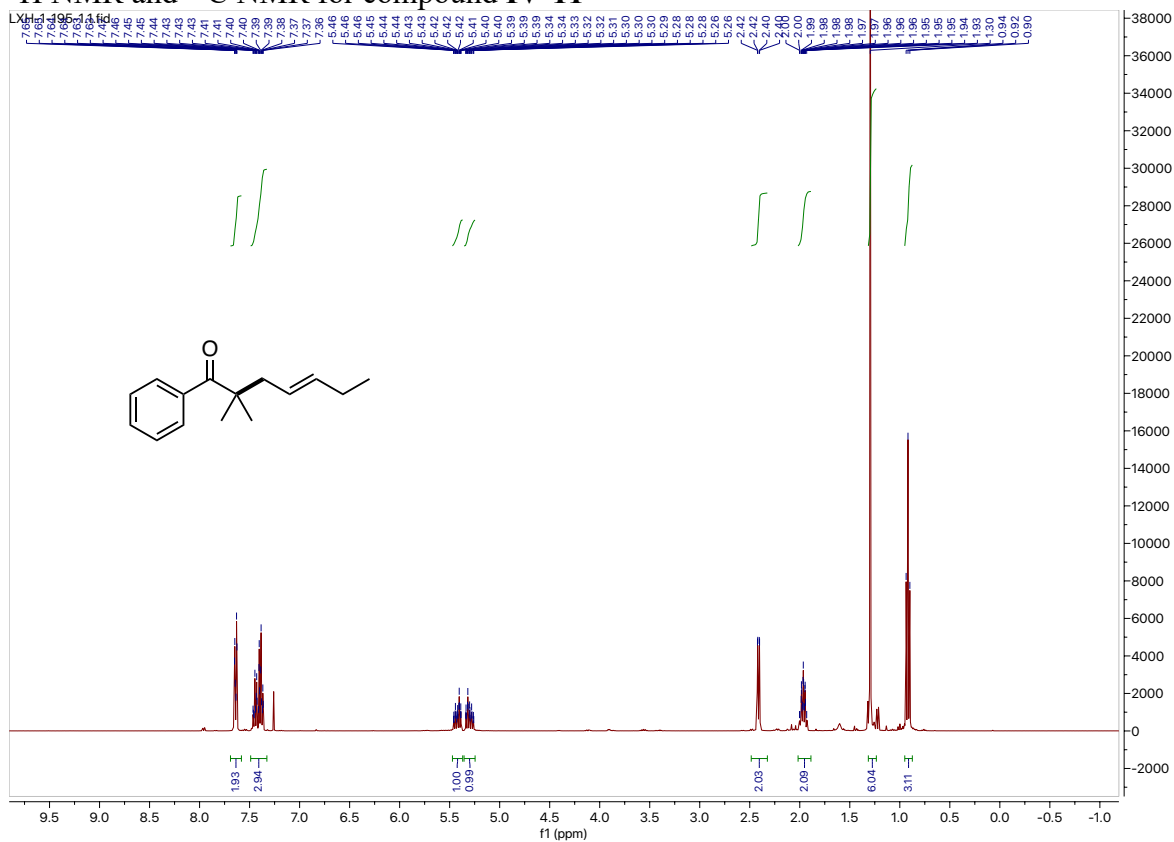
# $^1\text{H}$ NMR and $^{13}\text{C}$ NMR for compound IV-9



# $^1\text{H}$ NMR and $^{13}\text{C}$ NMR for compound IV-10

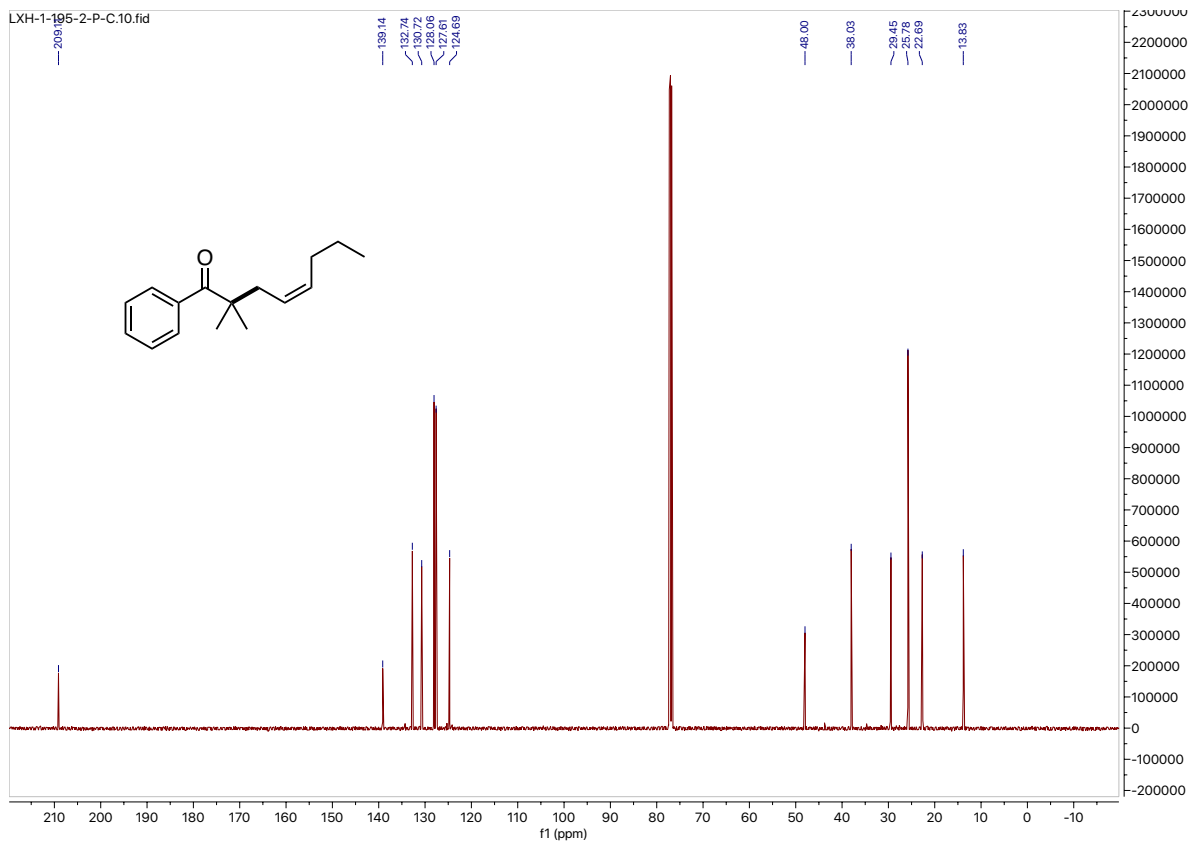
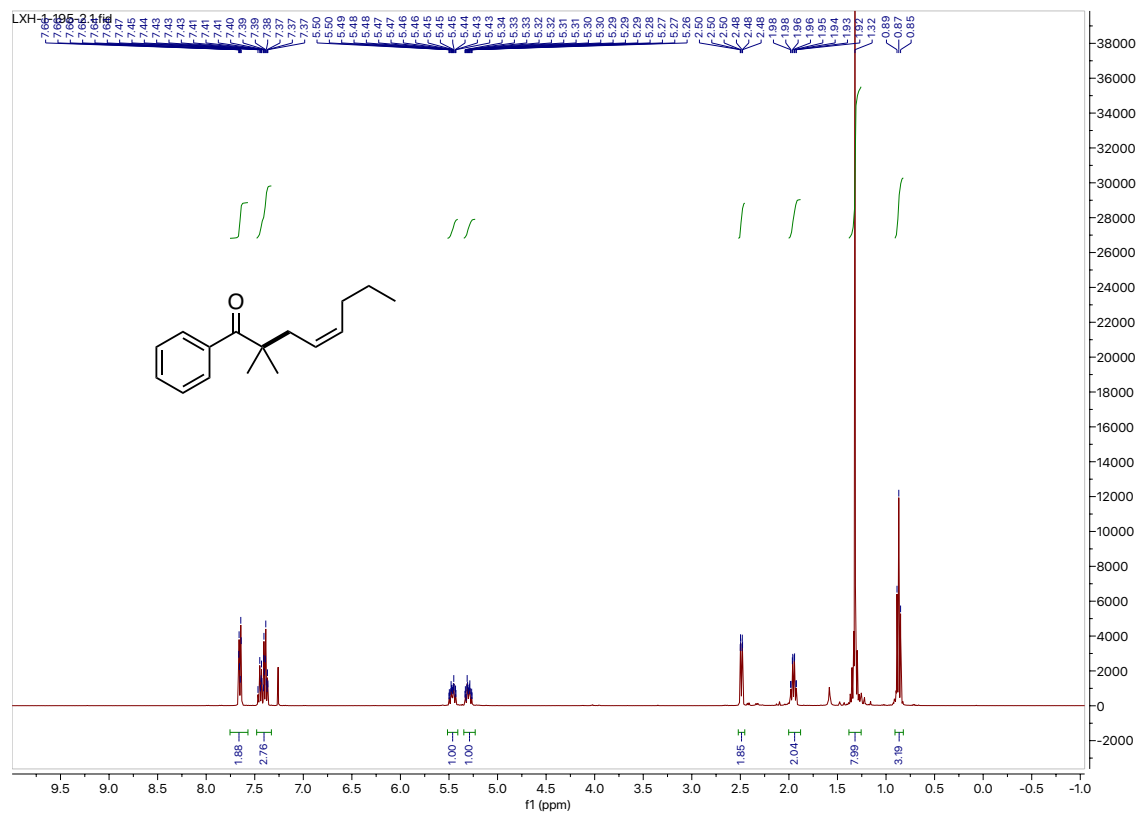


$^1\text{H}$  NMR and  $^{13}\text{C}$  NMR for compound IV-11

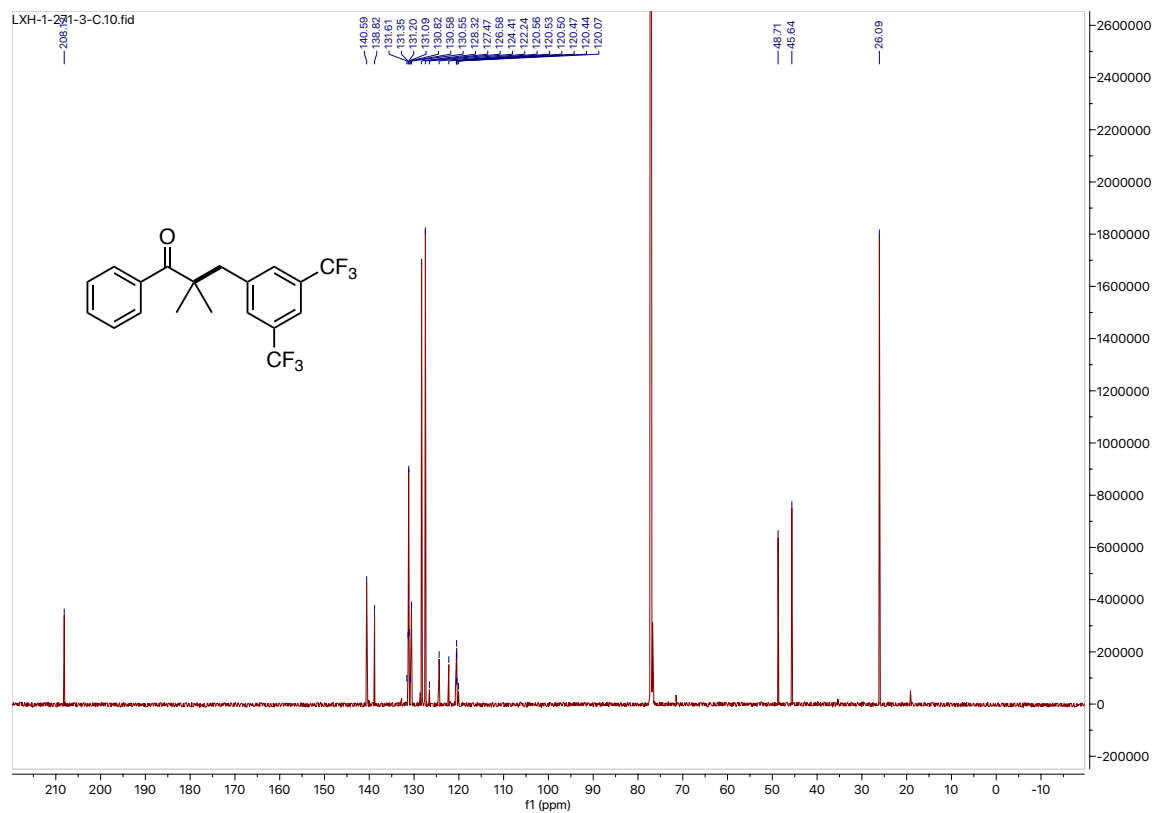
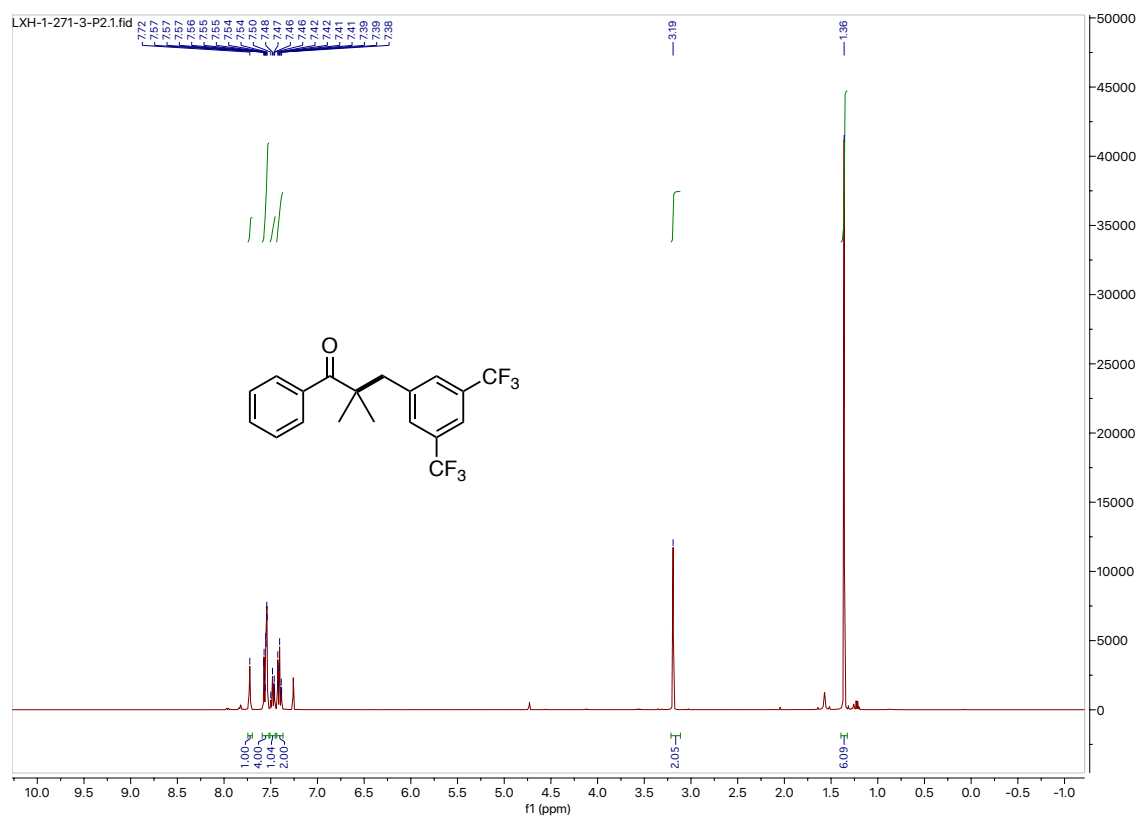




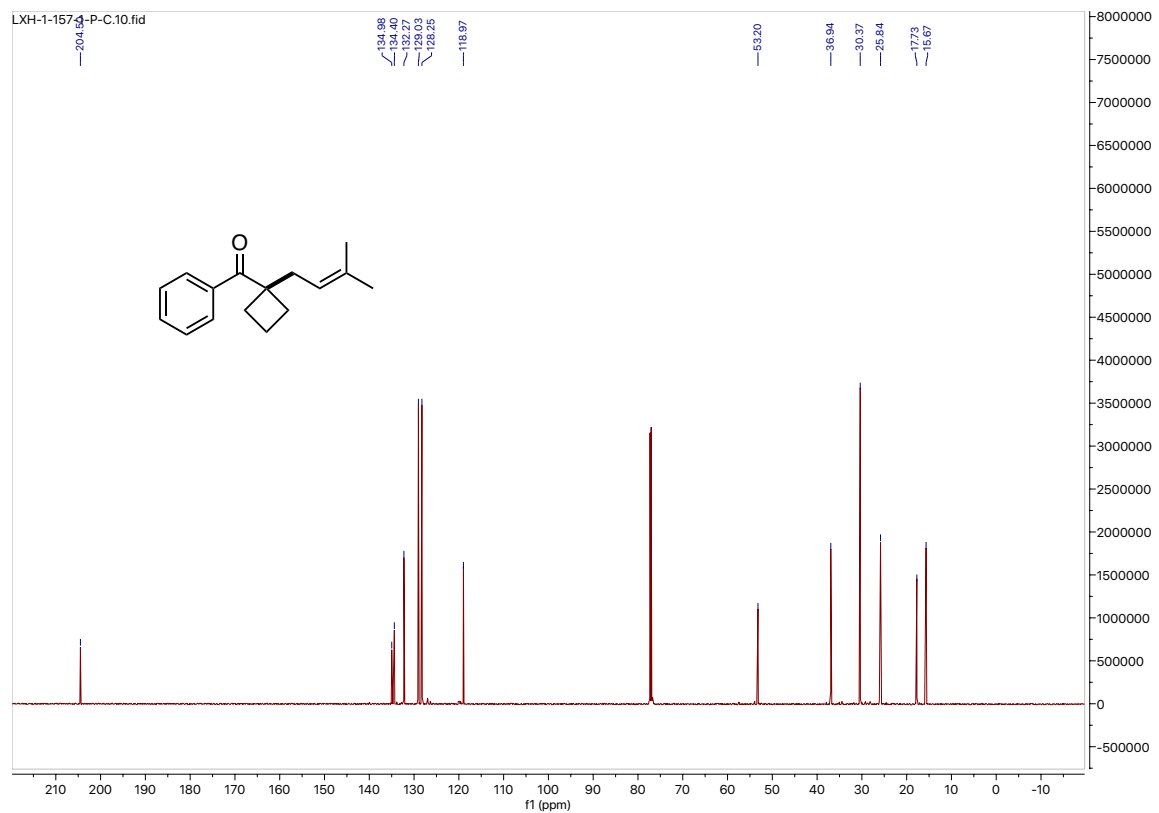
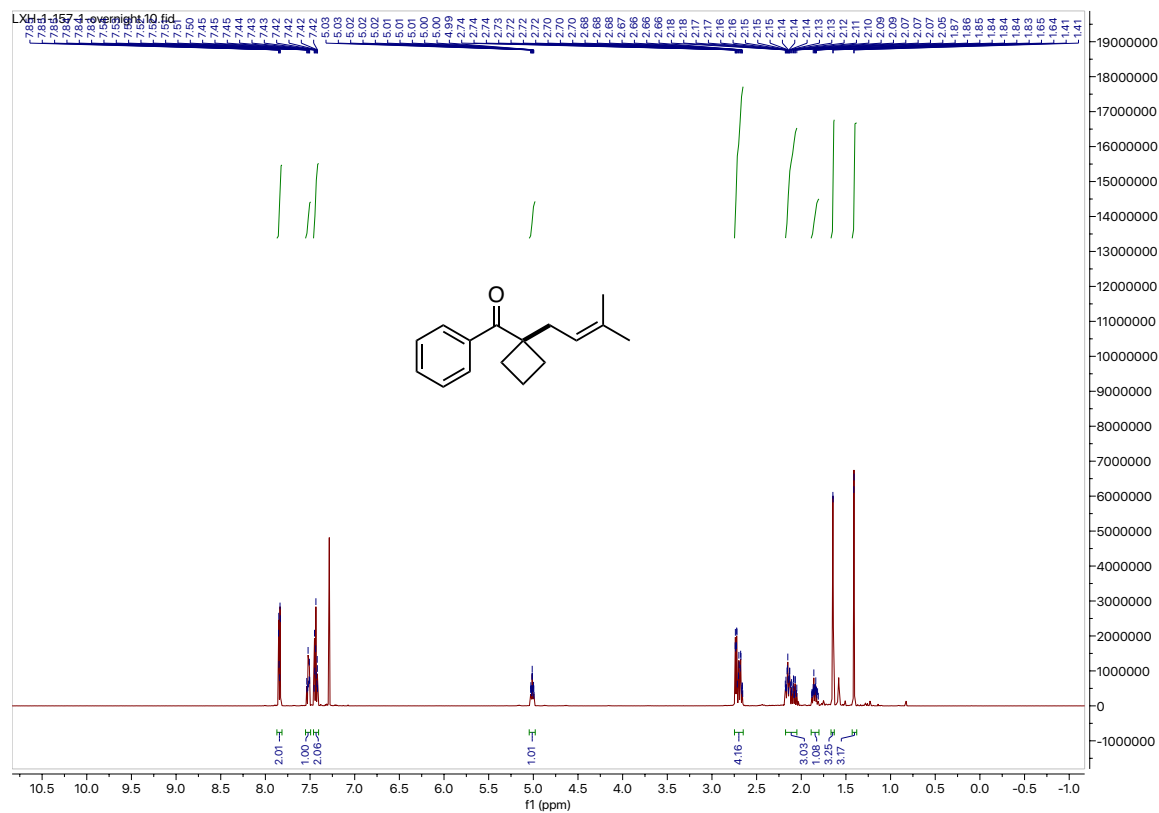
$^1\text{H}$  NMR and  $^{13}\text{C}$  NMR for compound IV-12



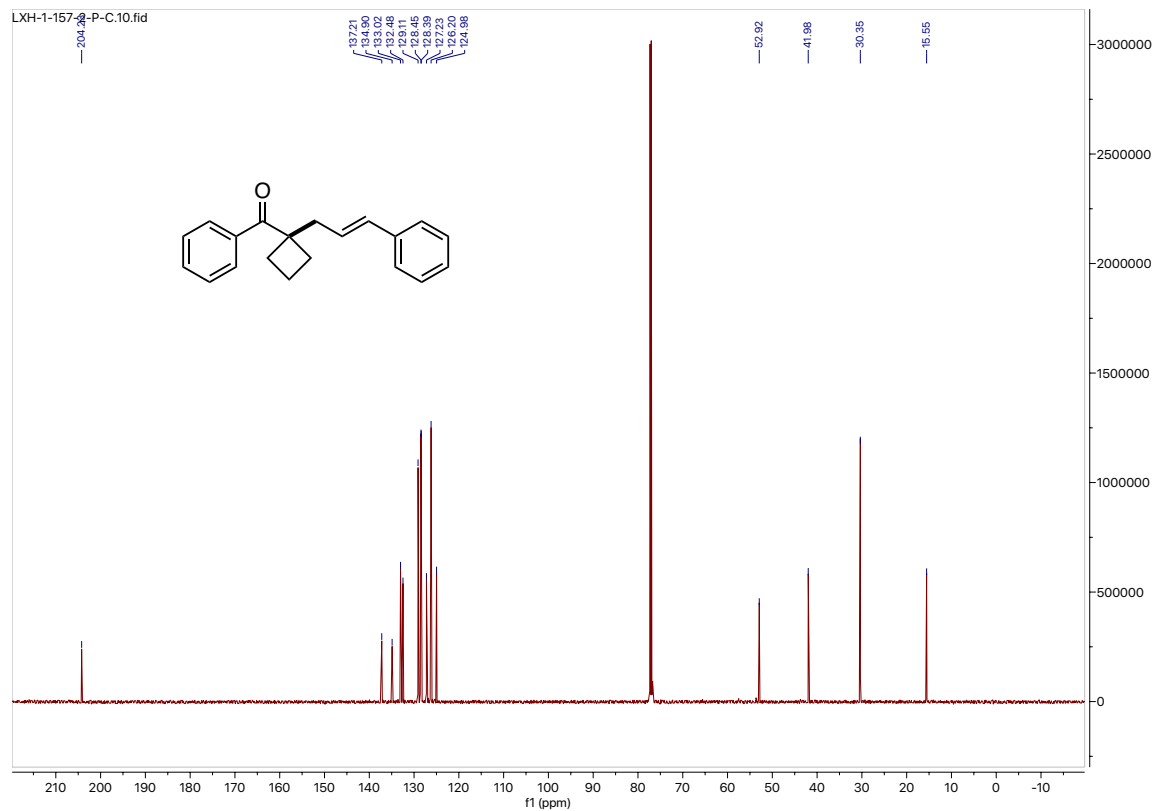
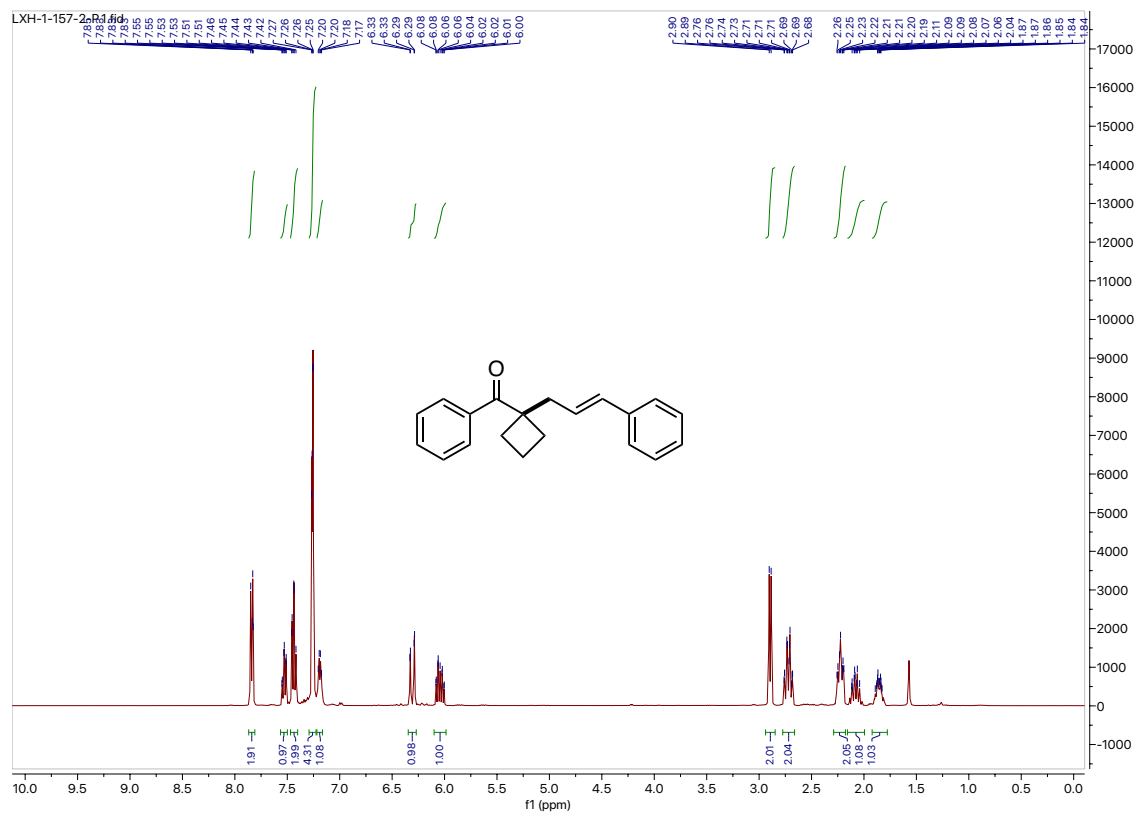
# $^1\text{H}$ NMR and $^{13}\text{C}$ NMR for compound IV-13



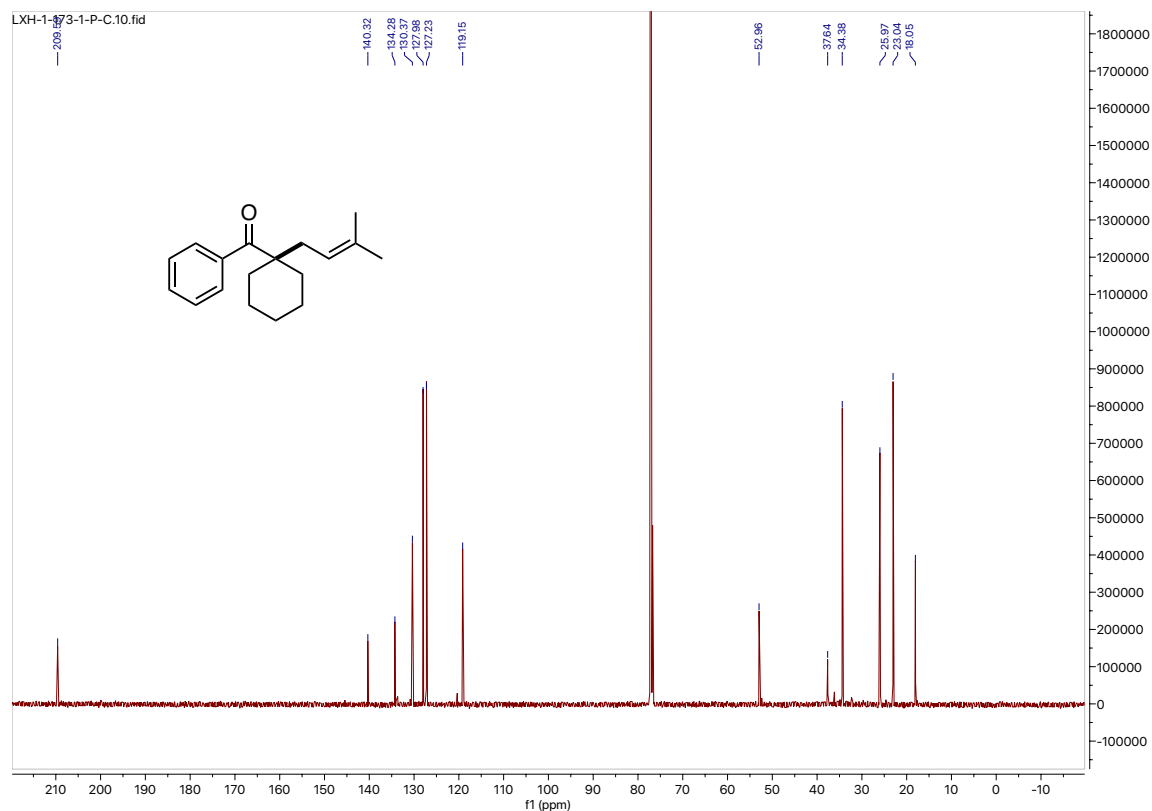
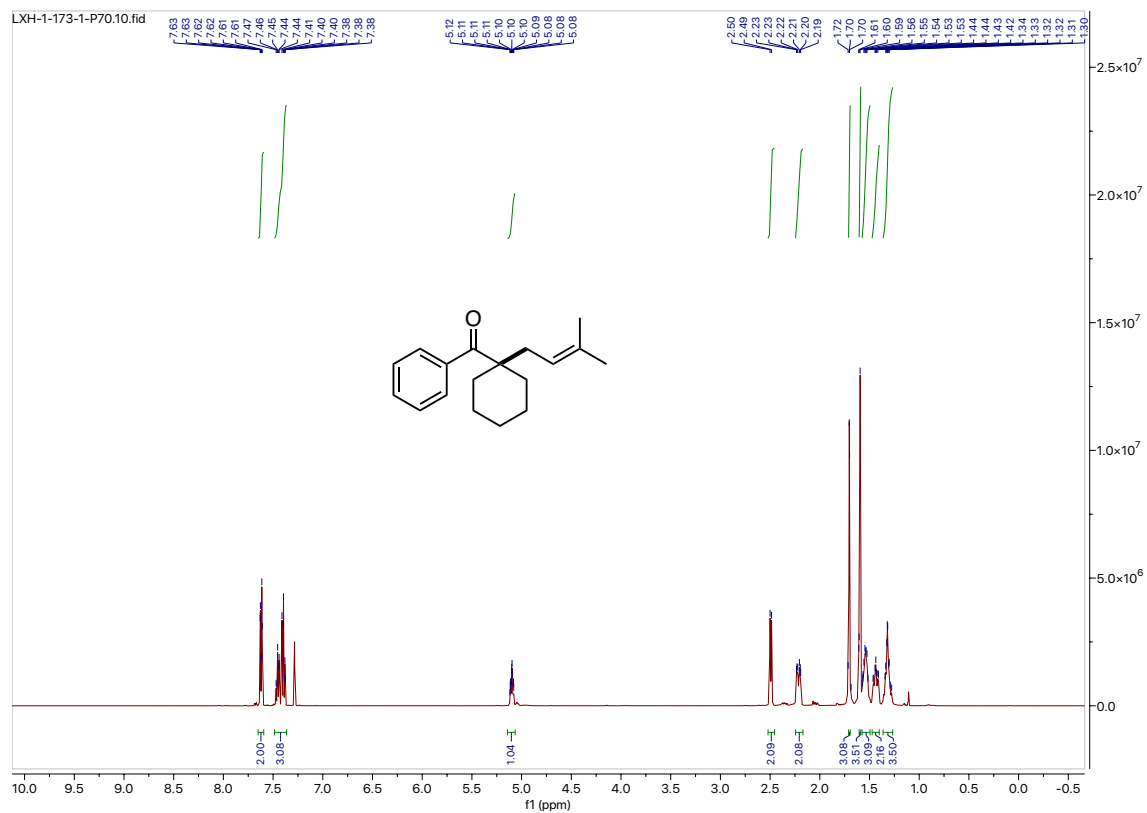
# $^1\text{H}$ NMR and $^{13}\text{C}$ NMR for compound IV-14



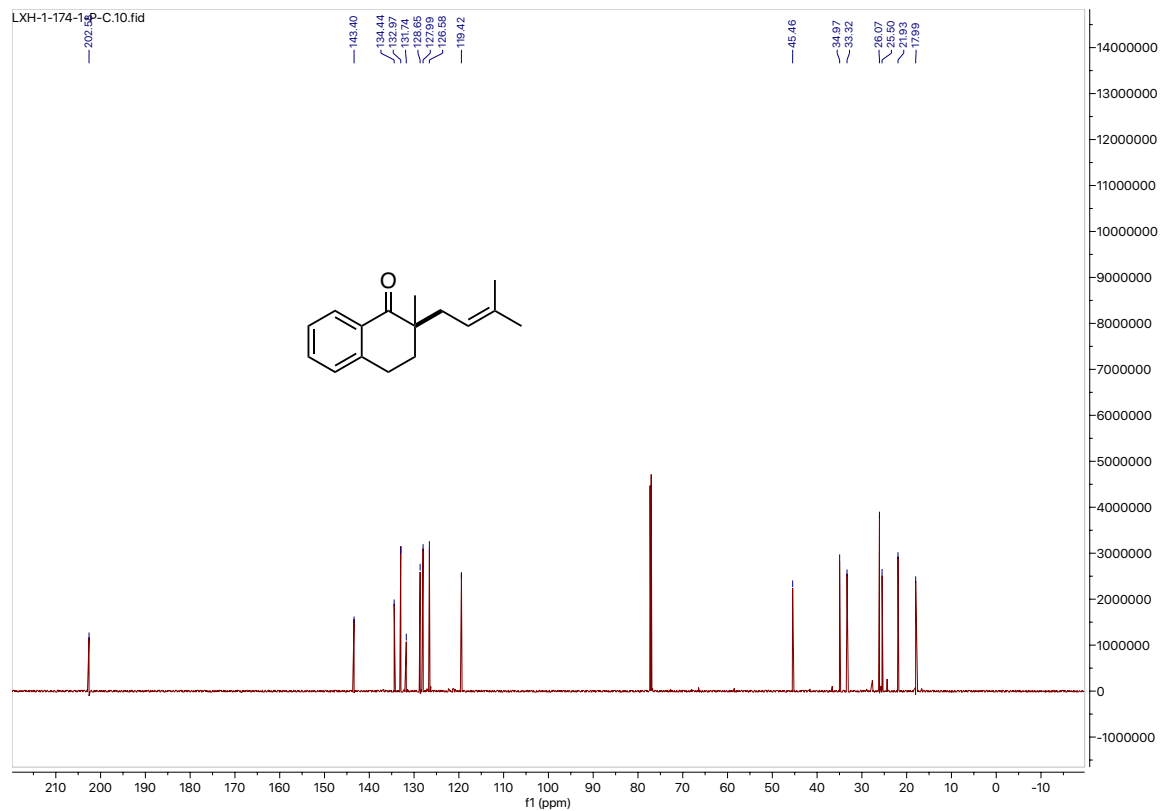
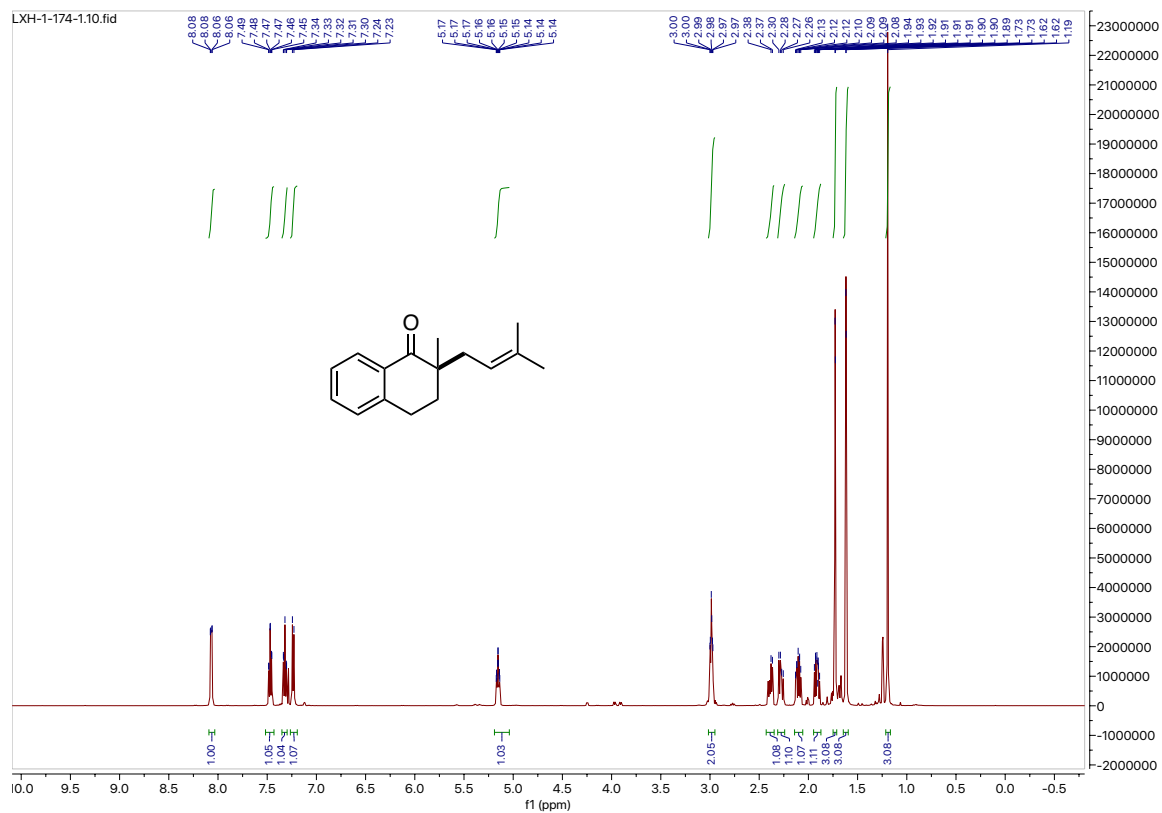
# $^1\text{H}$ NMR and $^{13}\text{C}$ NMR for compound IV-15



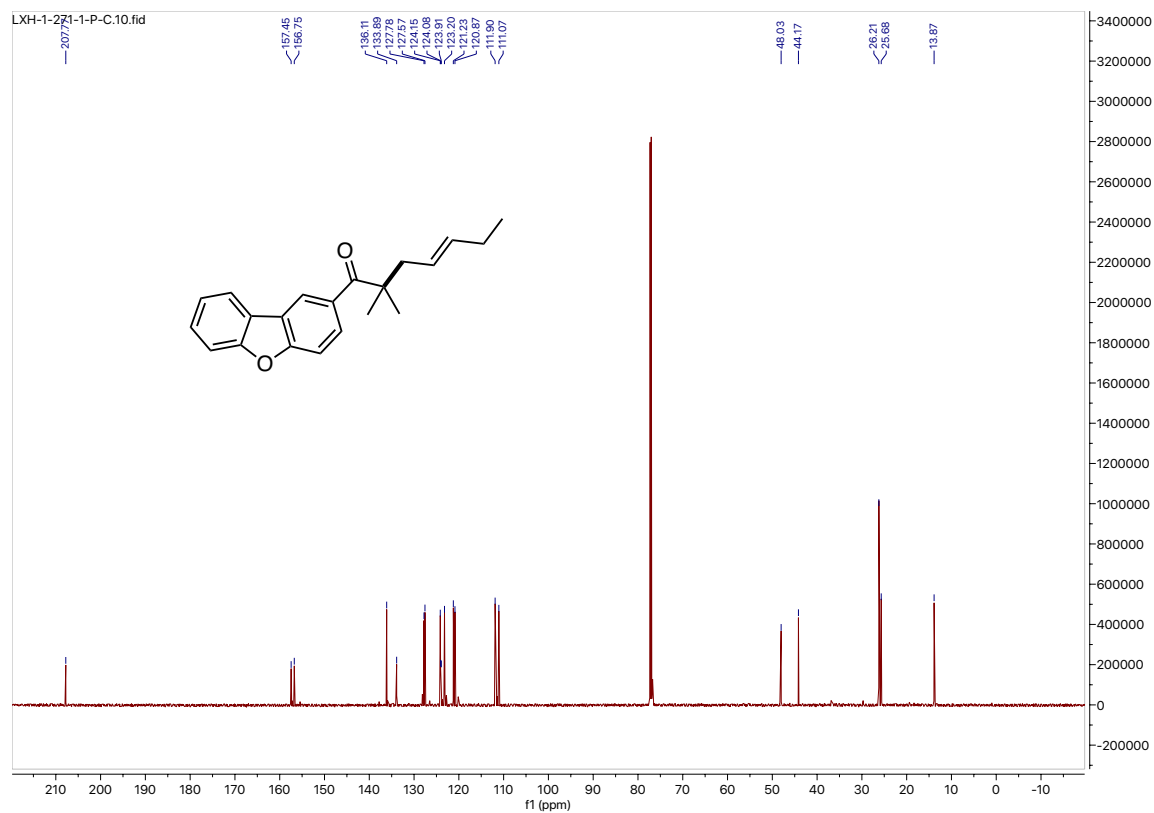
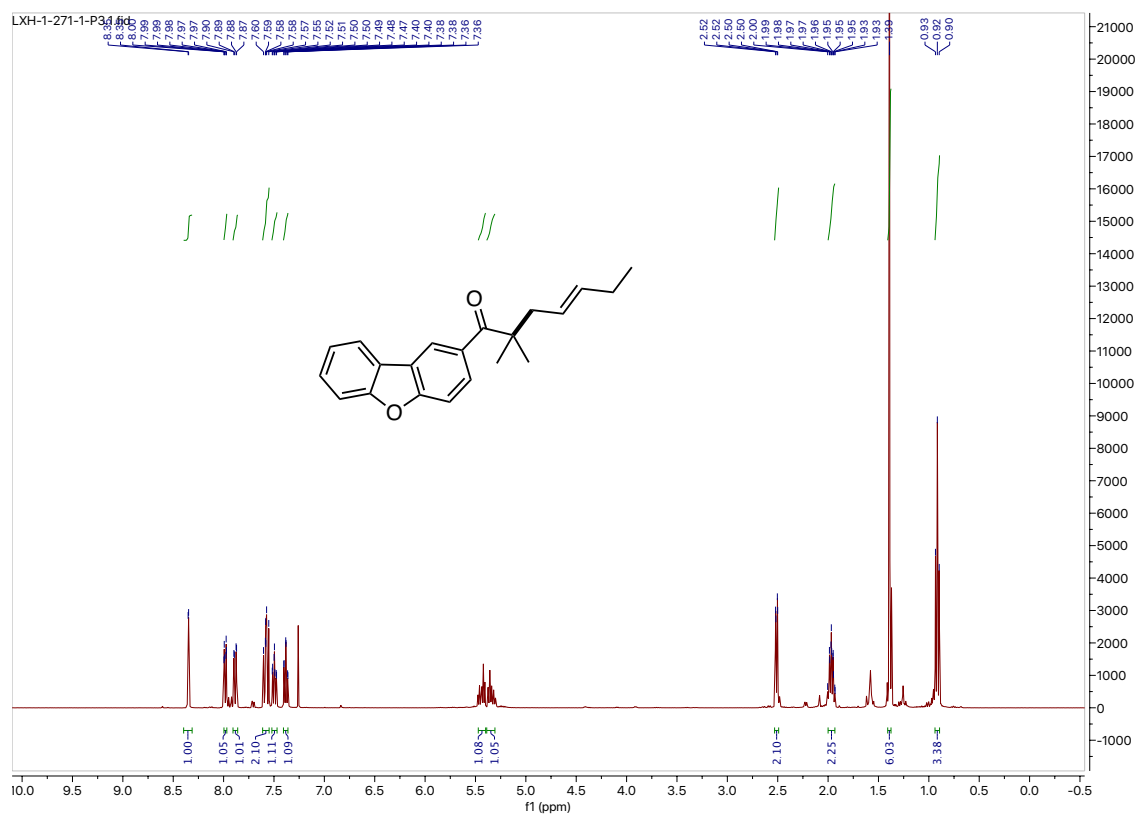
# $^1\text{H}$ NMR and $^{13}\text{C}$ NMR for compound IV-16



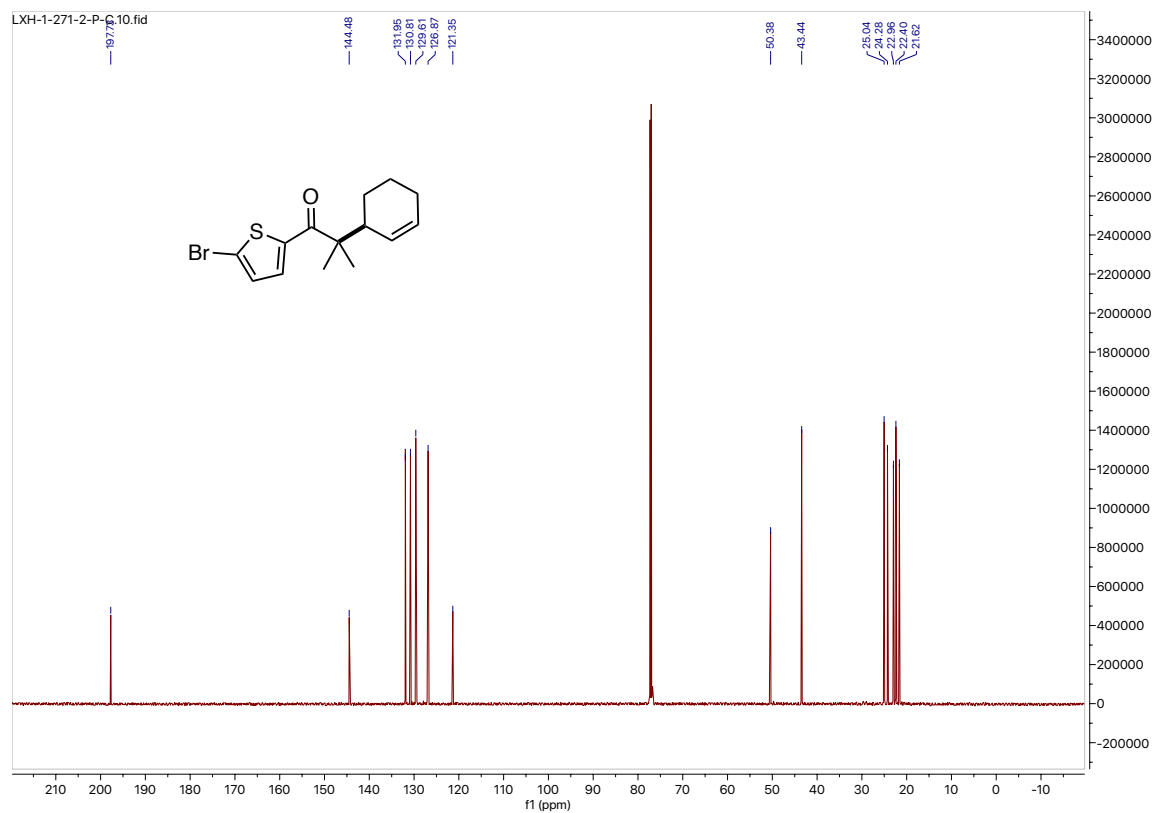
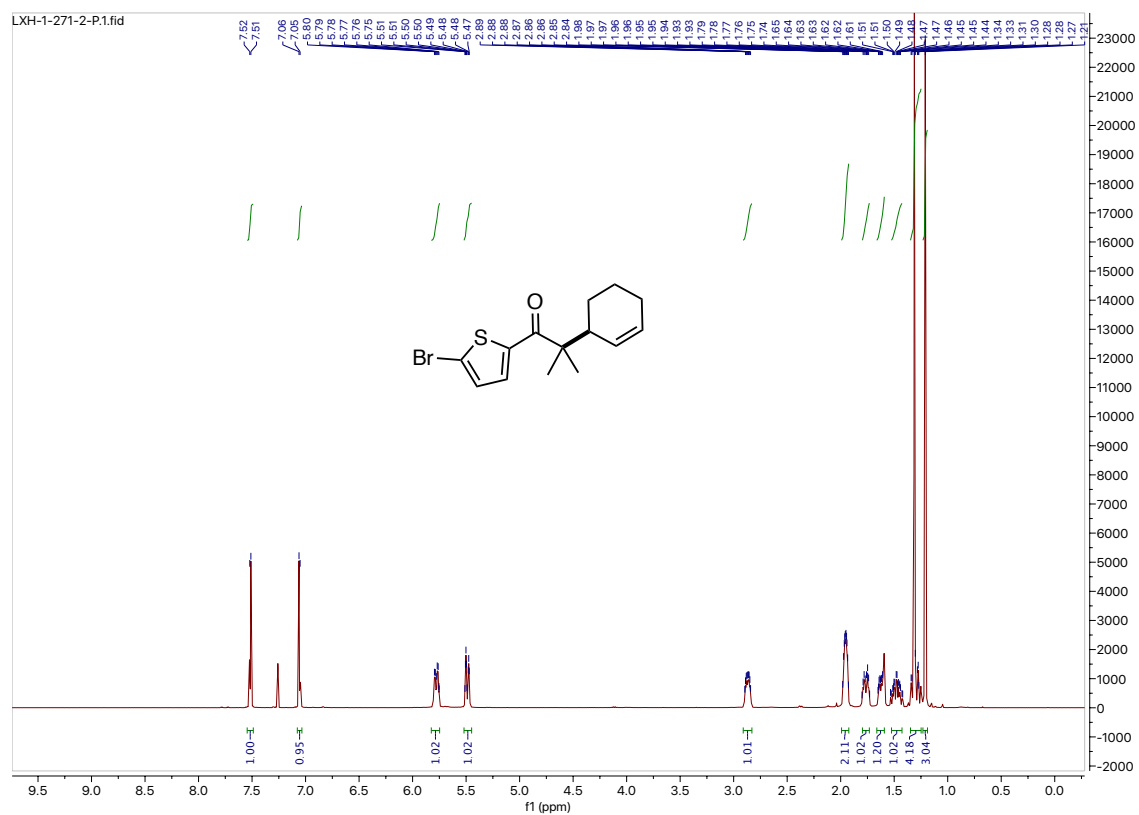
<sup>1</sup>H NMR and <sup>13</sup>C NMR for compound IV-17



# $^1\text{H}$ NMR and $^{13}\text{C}$ NMR for compound IV-18

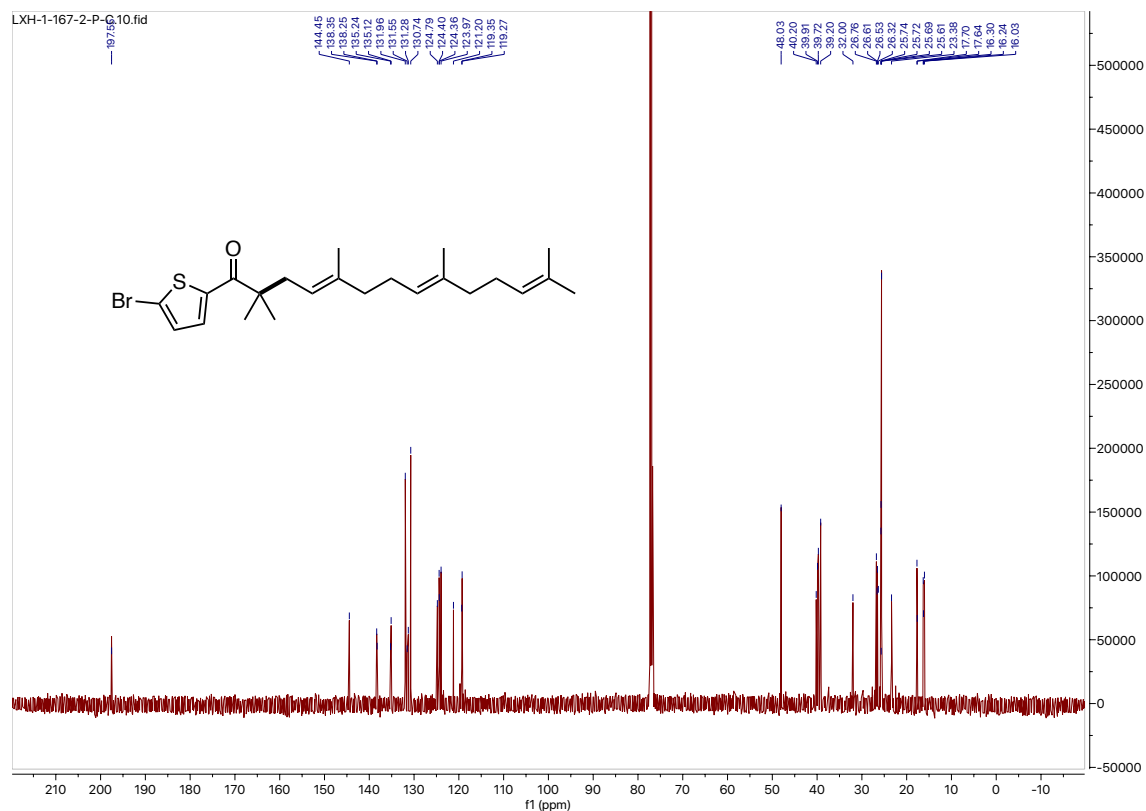
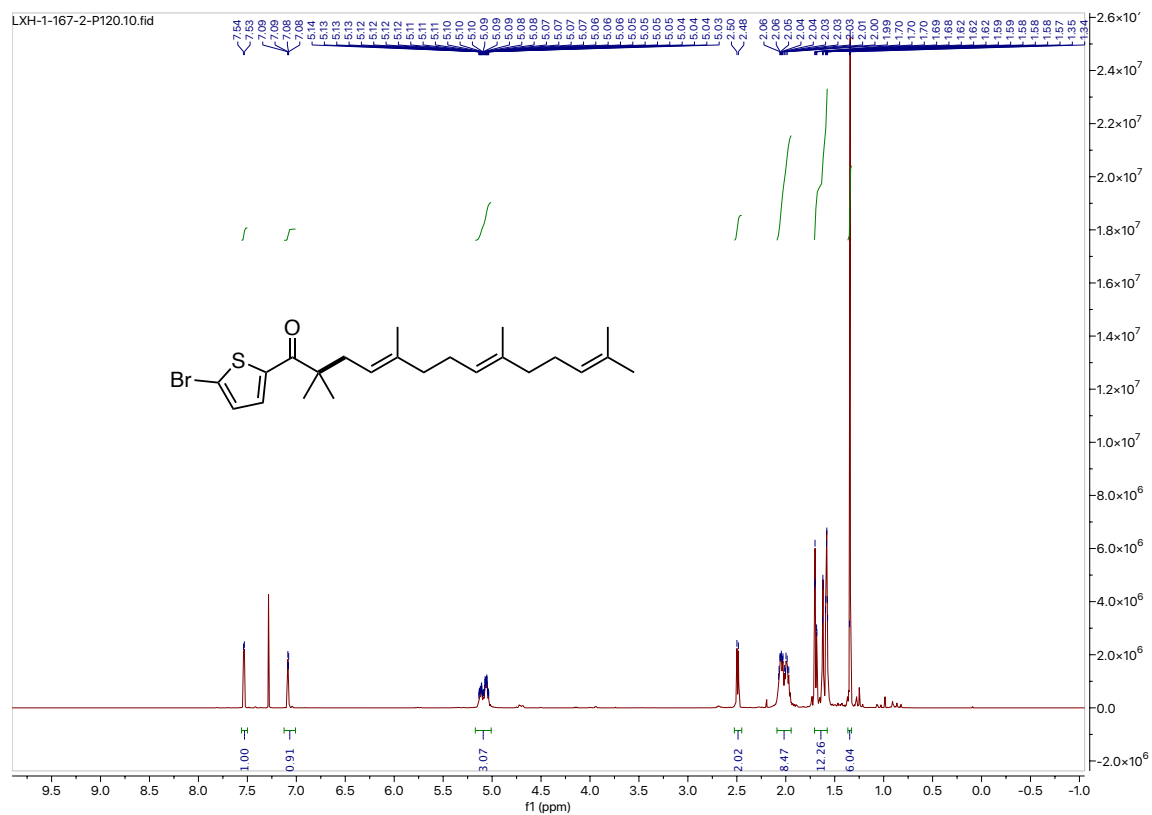


$^1\text{H}$  NMR and  $^{13}\text{C}$  NMR for compound IV-19

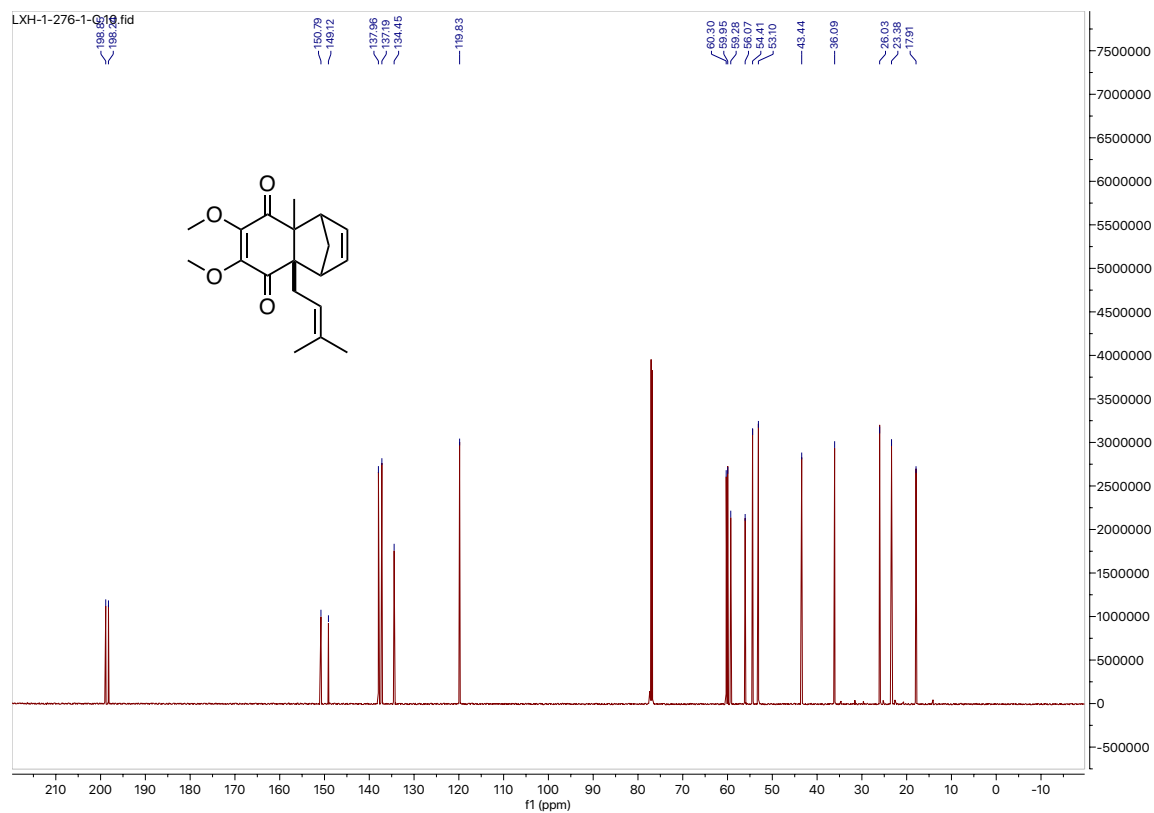
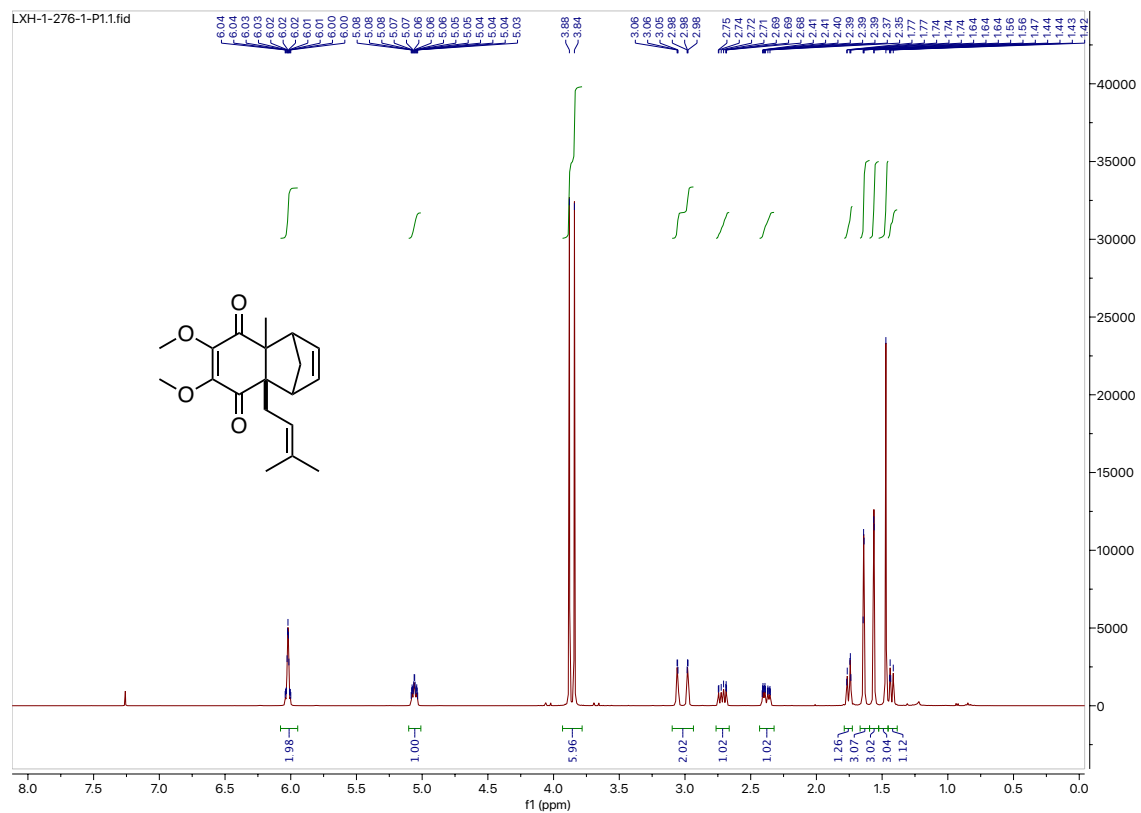




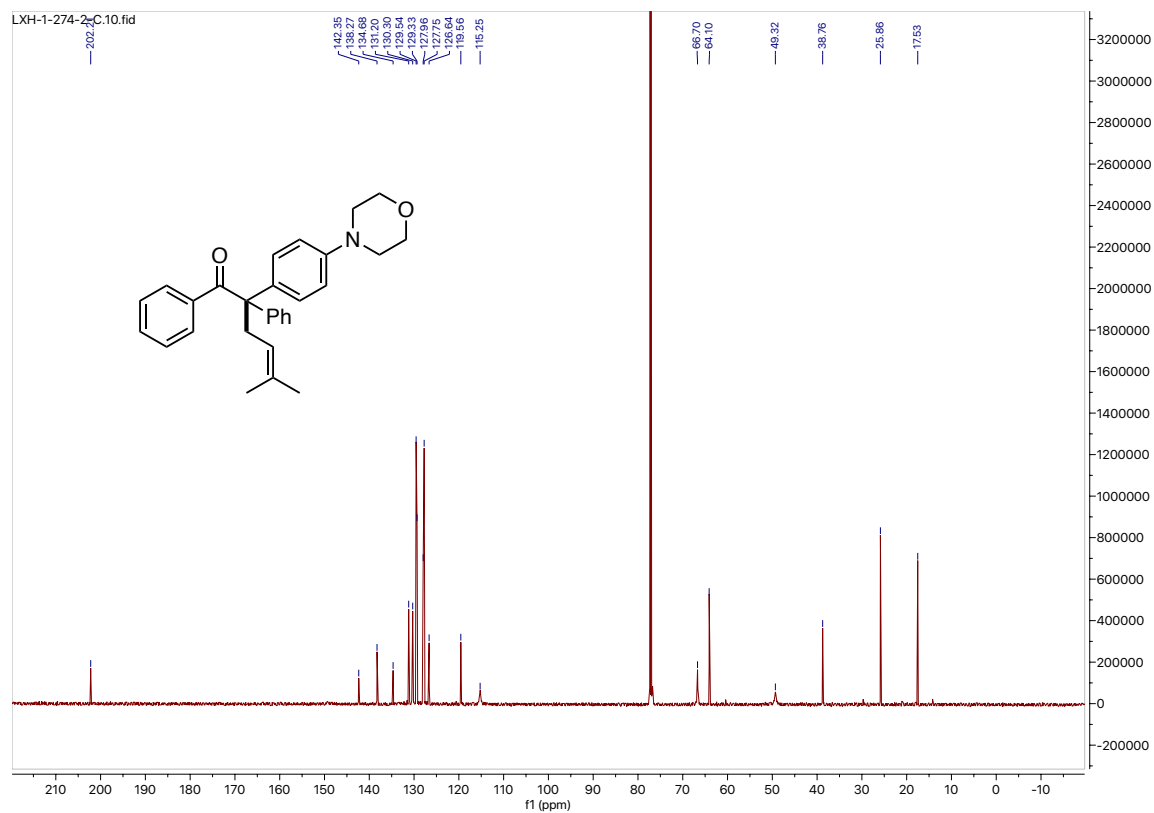
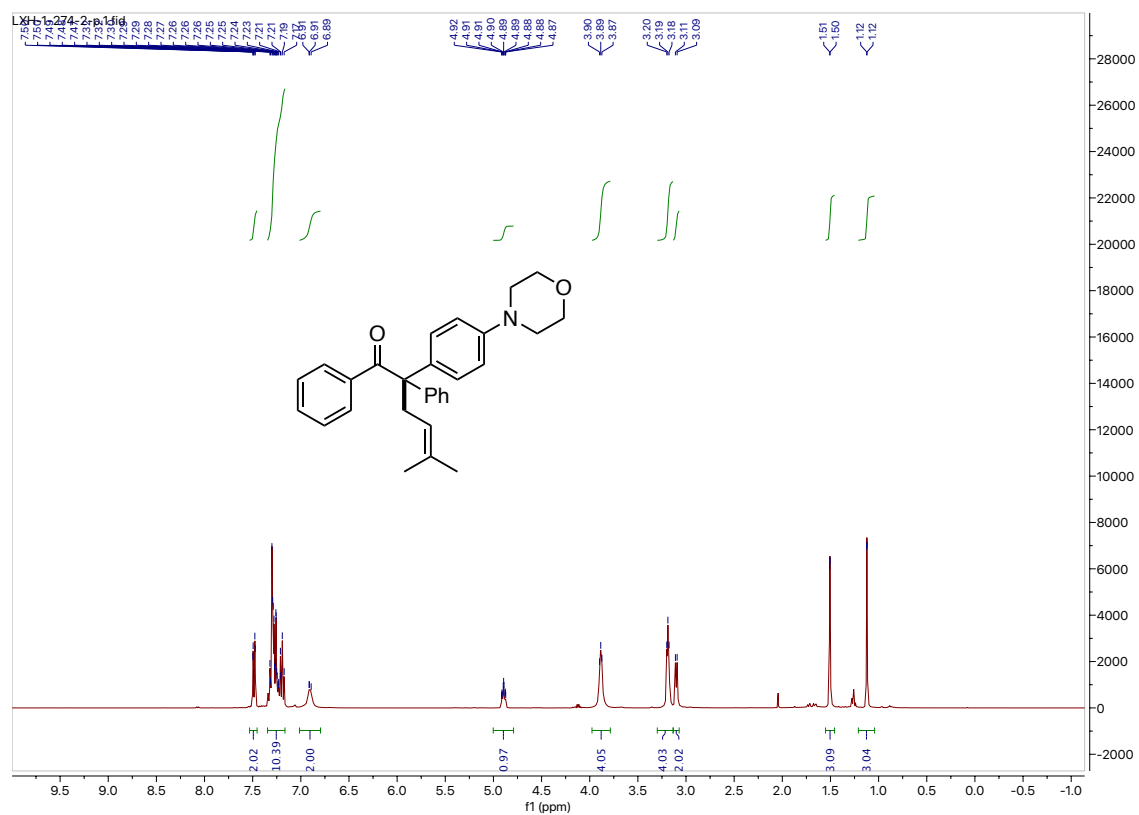
# $^1\text{H}$ NMR and $^{13}\text{C}$ NMR for compound IV-20



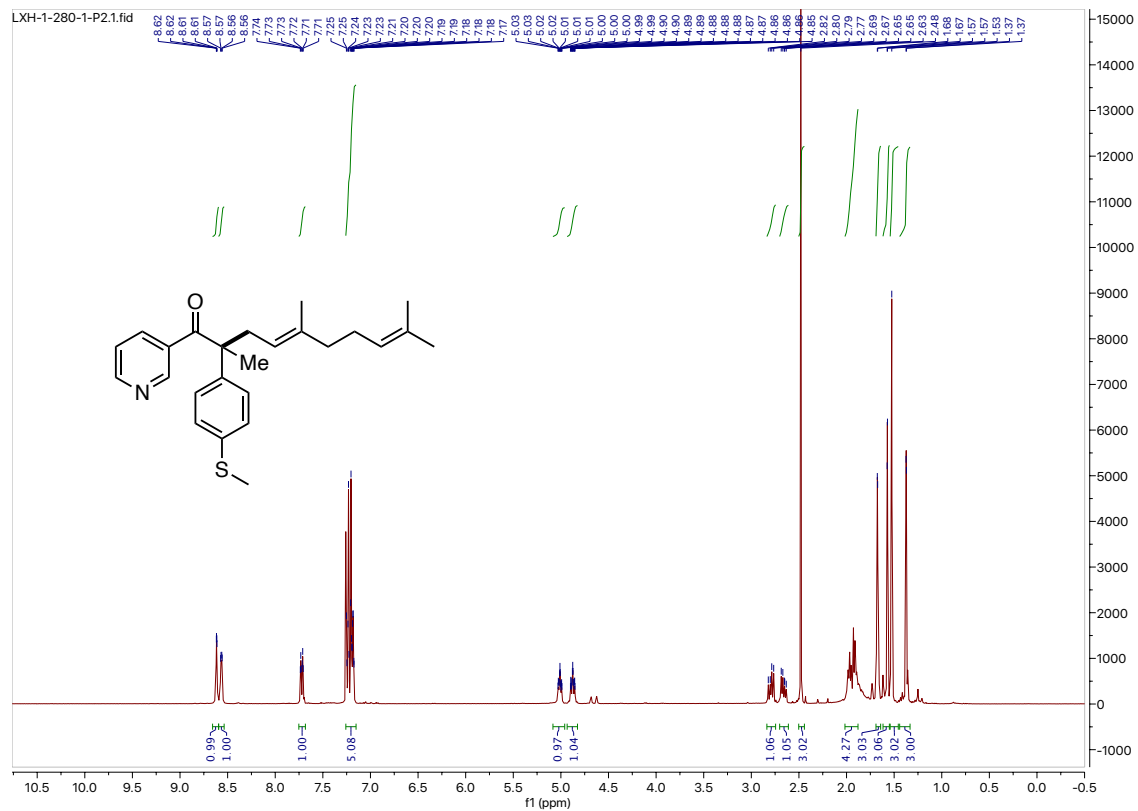
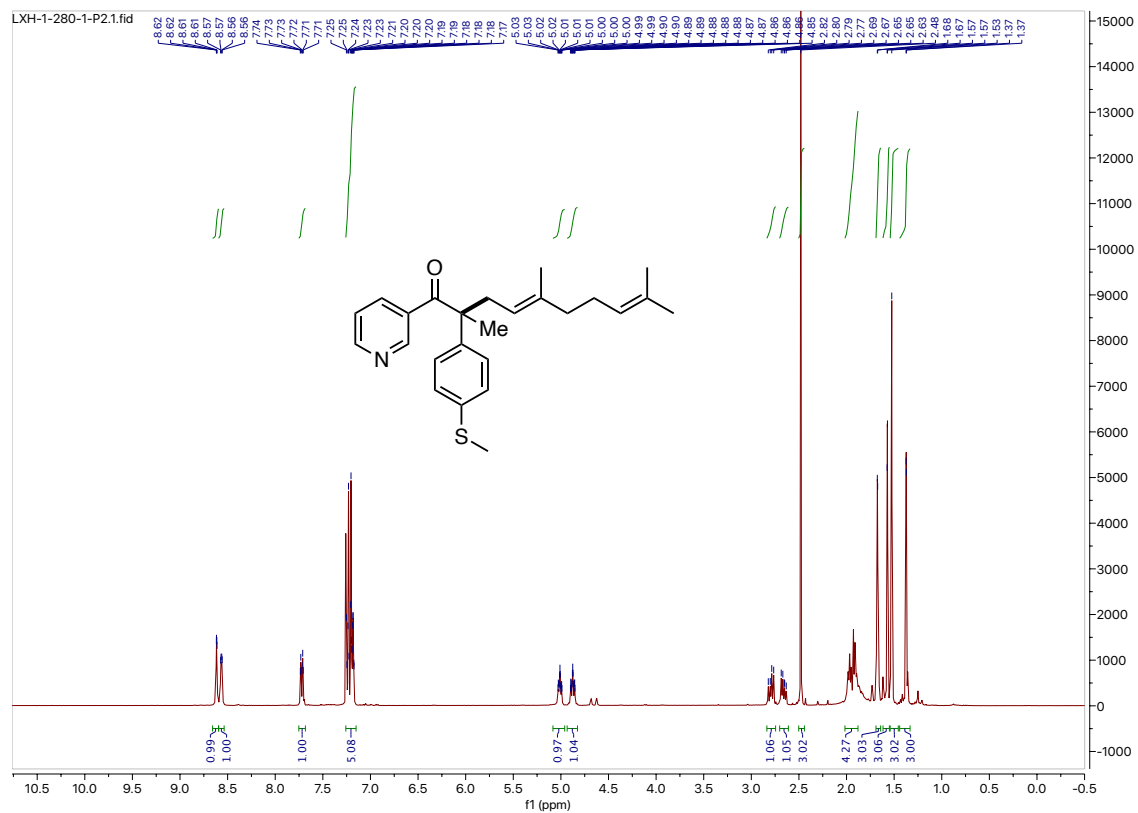
$^1\text{H}$  NMR and  $^{13}\text{C}$  NMR for compound IV-21



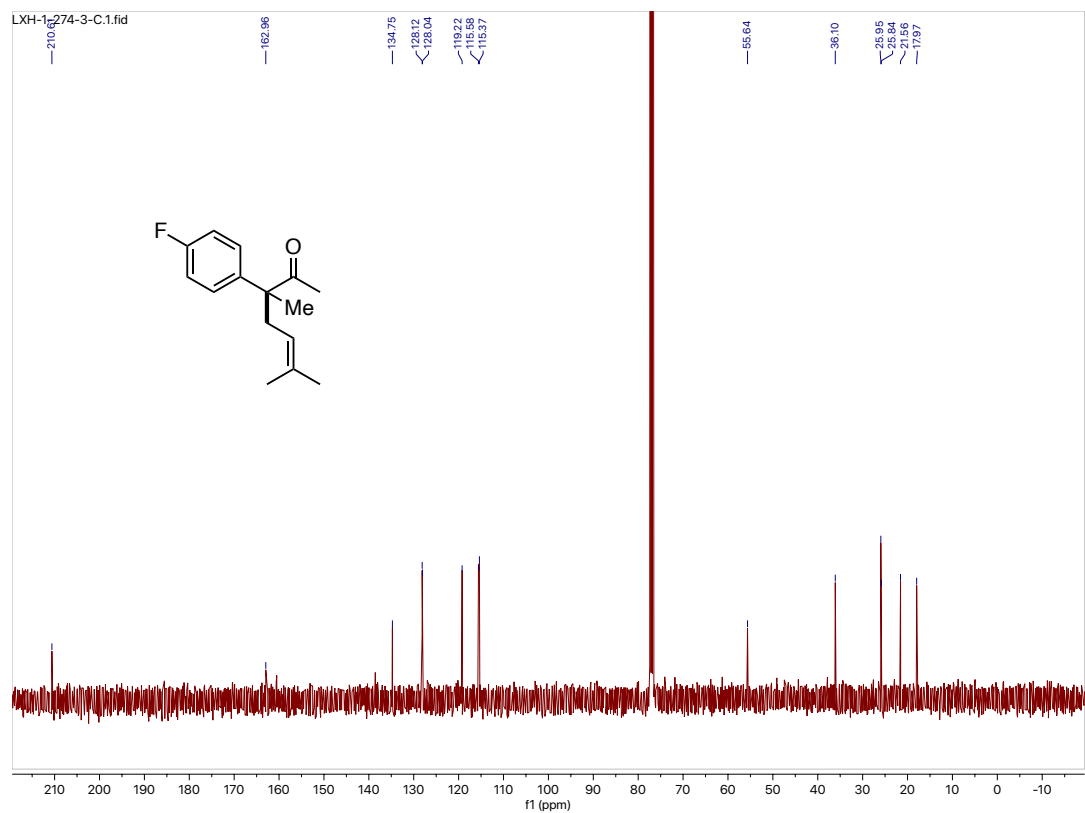
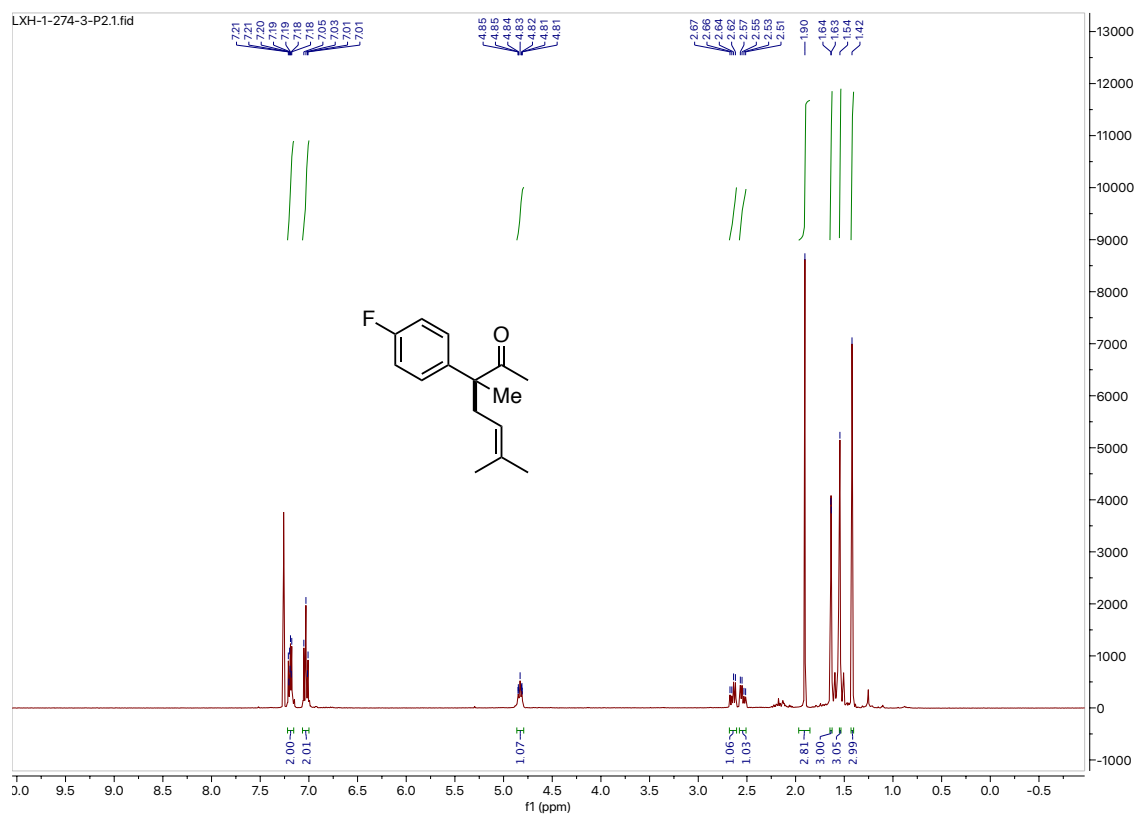
$^1\text{H}$  NMR and  $^{13}\text{C}$  NMR for compound IV-22



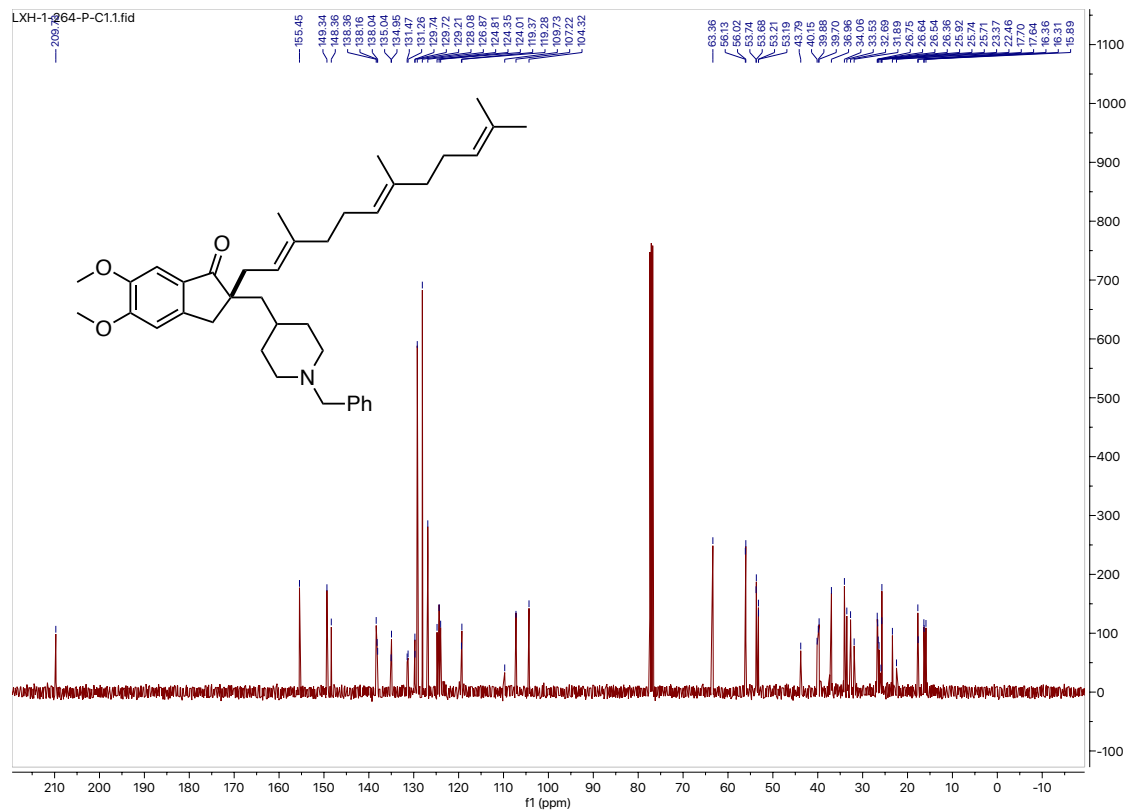
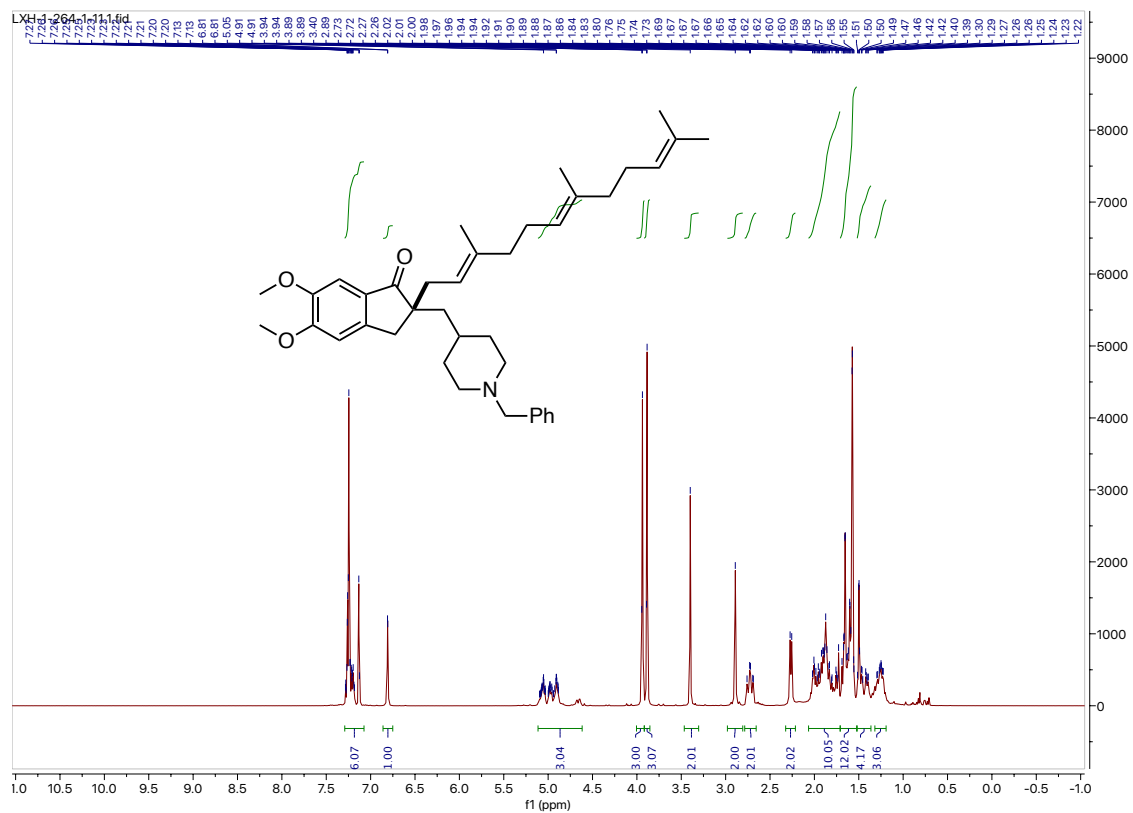
# $^1\text{H}$ NMR and $^{13}\text{C}$ NMR for compound IV-23



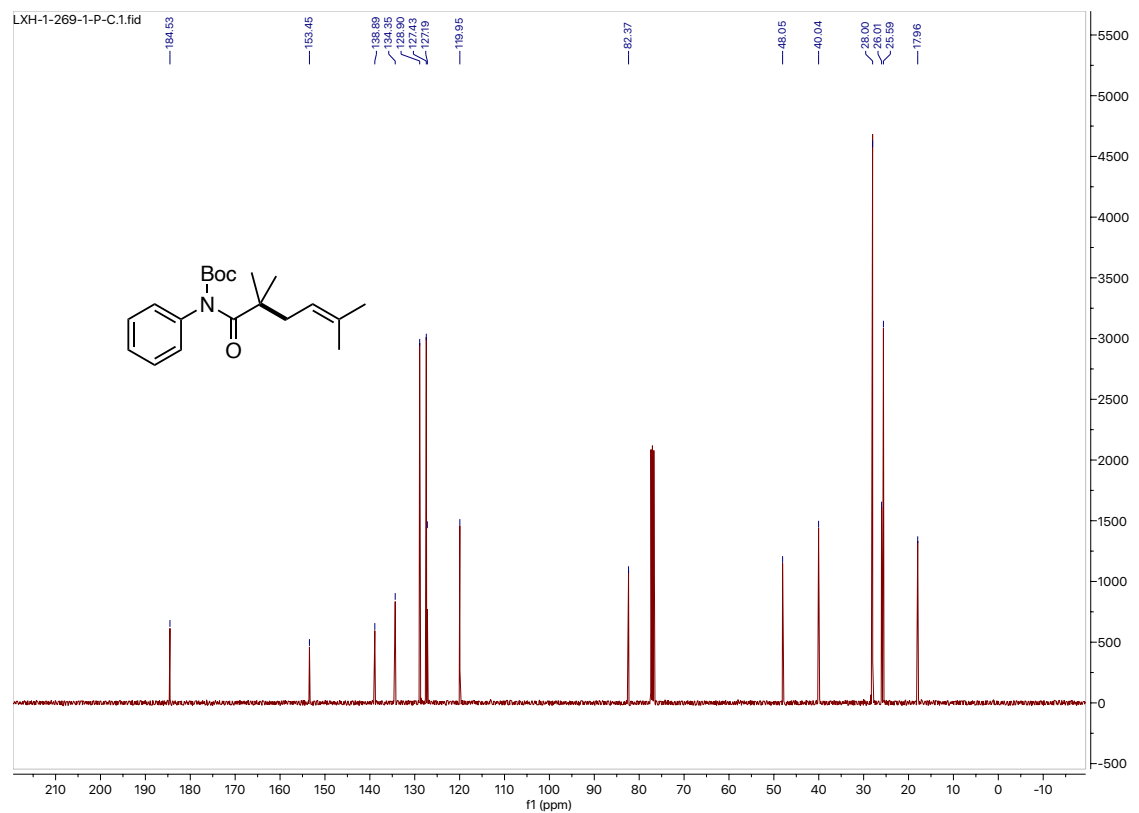
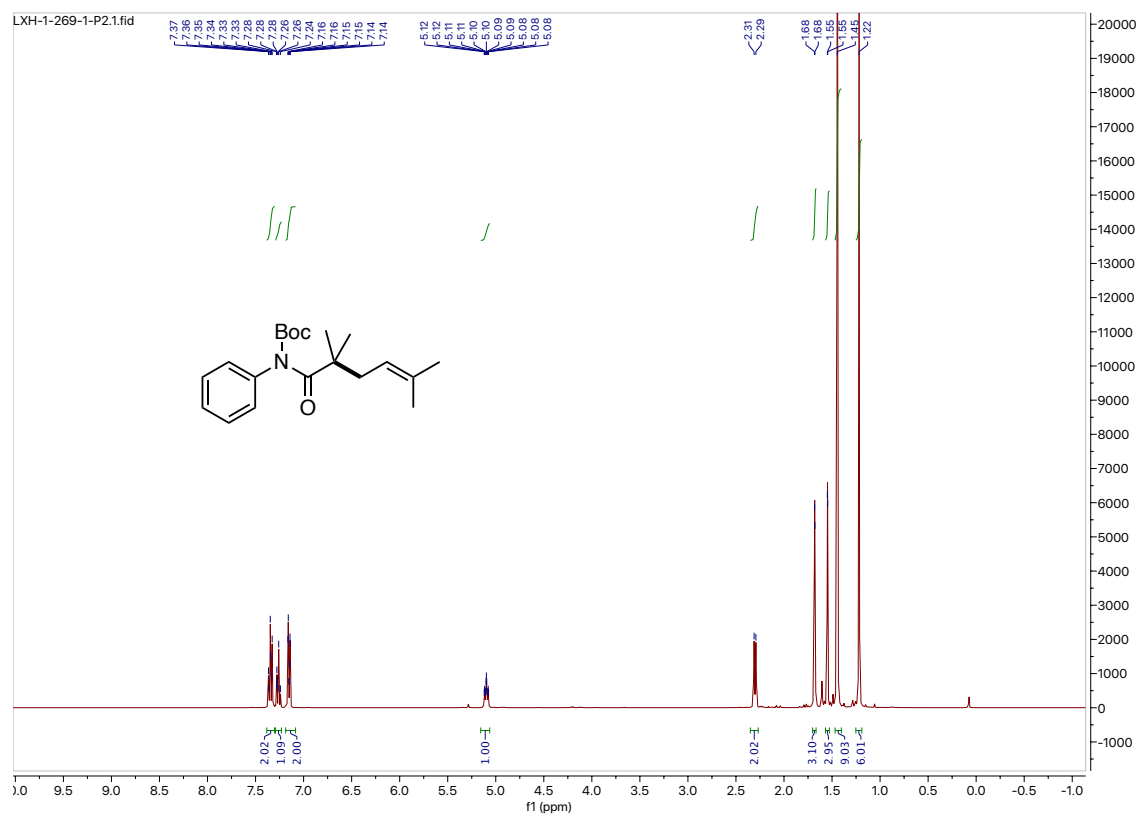
# $^1\text{H}$ NMR and $^{13}\text{C}$ NMR for compound IV-24



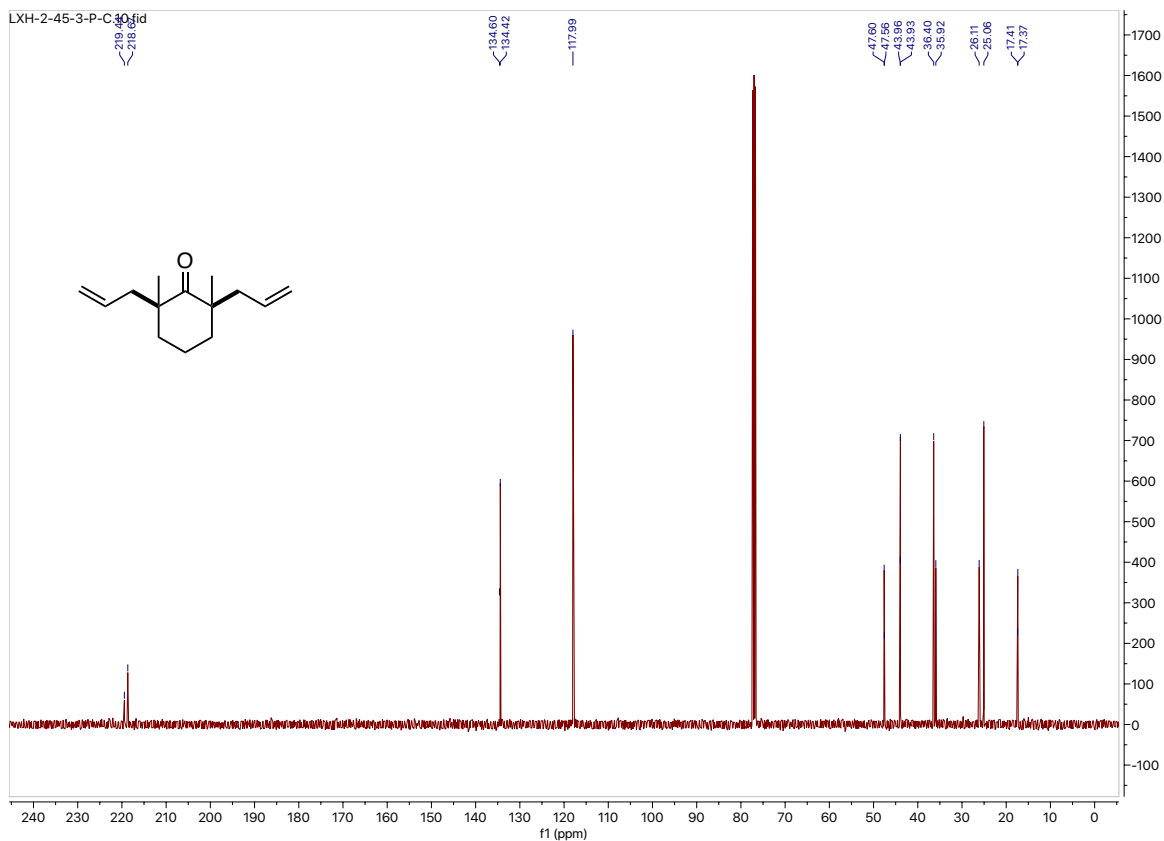
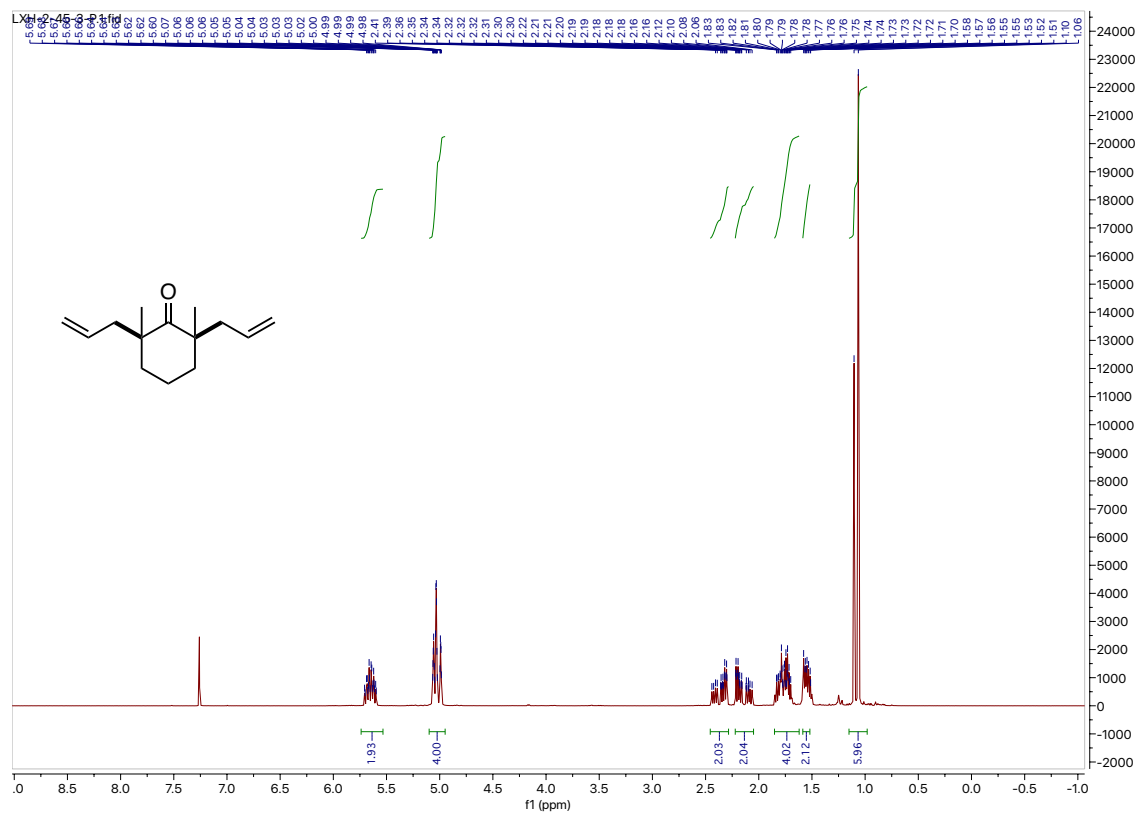
# $^1\text{H}$ NMR and $^{13}\text{C}$ NMR for compound IV-25



$^1\text{H}$  NMR and  $^{13}\text{C}$  NMR for compound IV-26

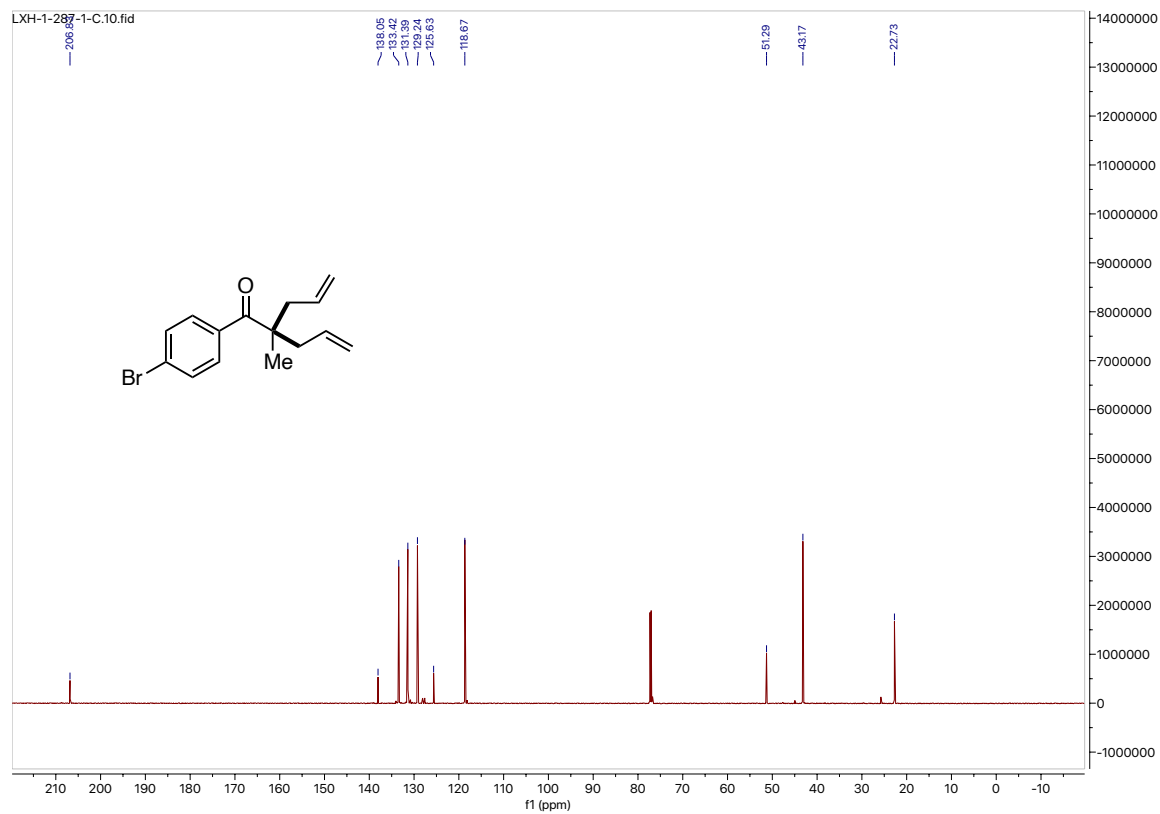
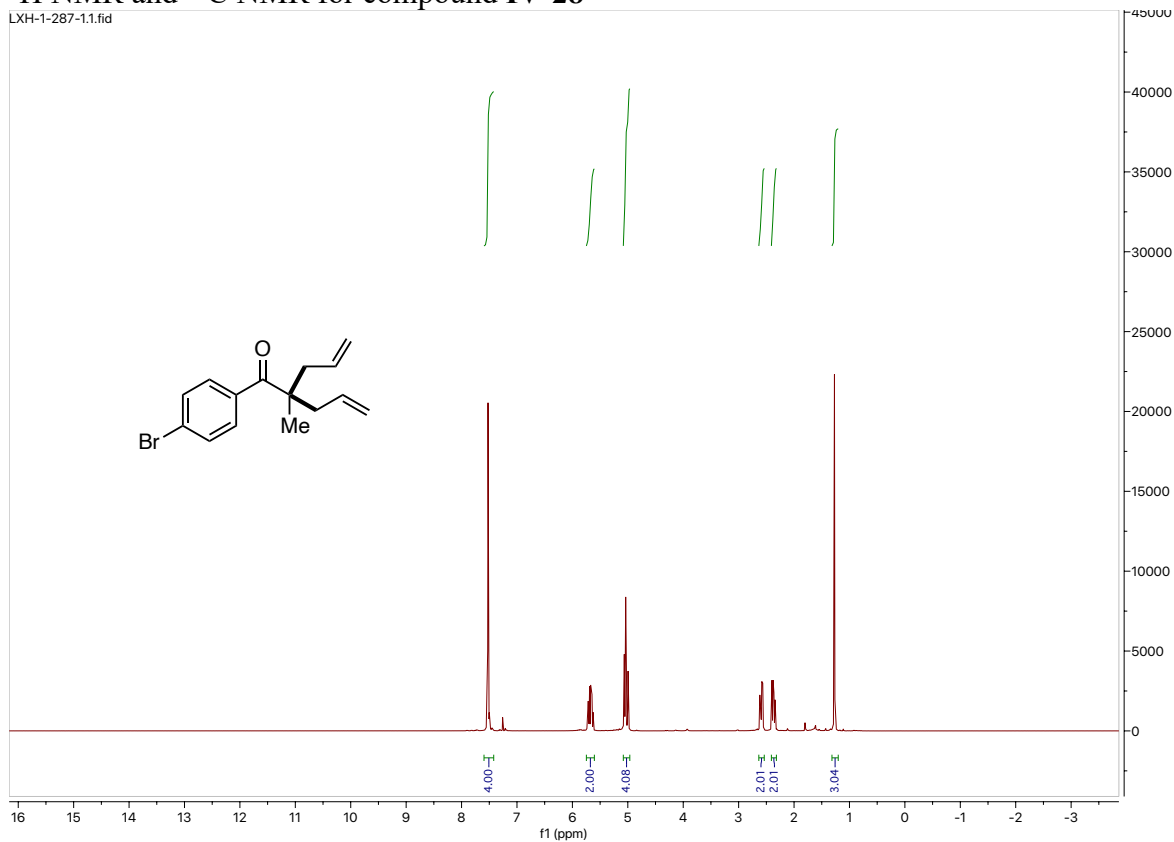


$^1\text{H}$  NMR and  $^{13}\text{C}$  NMR for compound IV-27

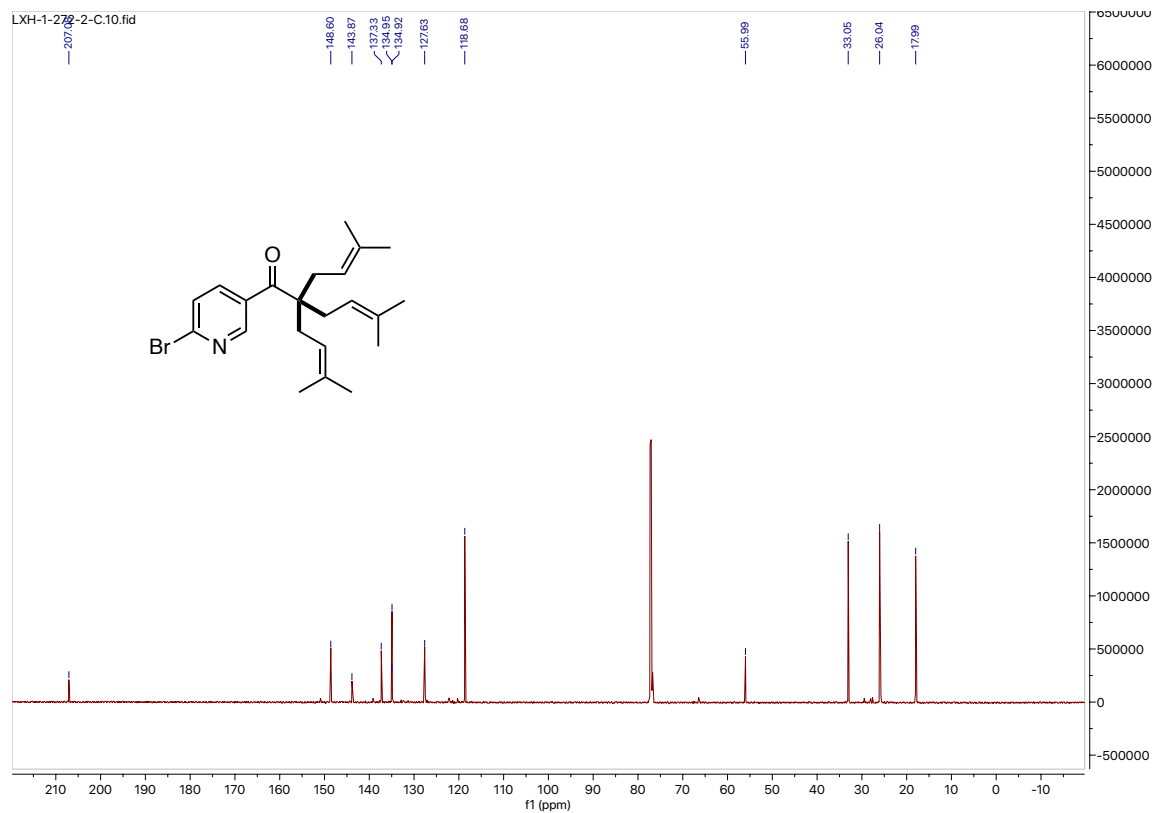
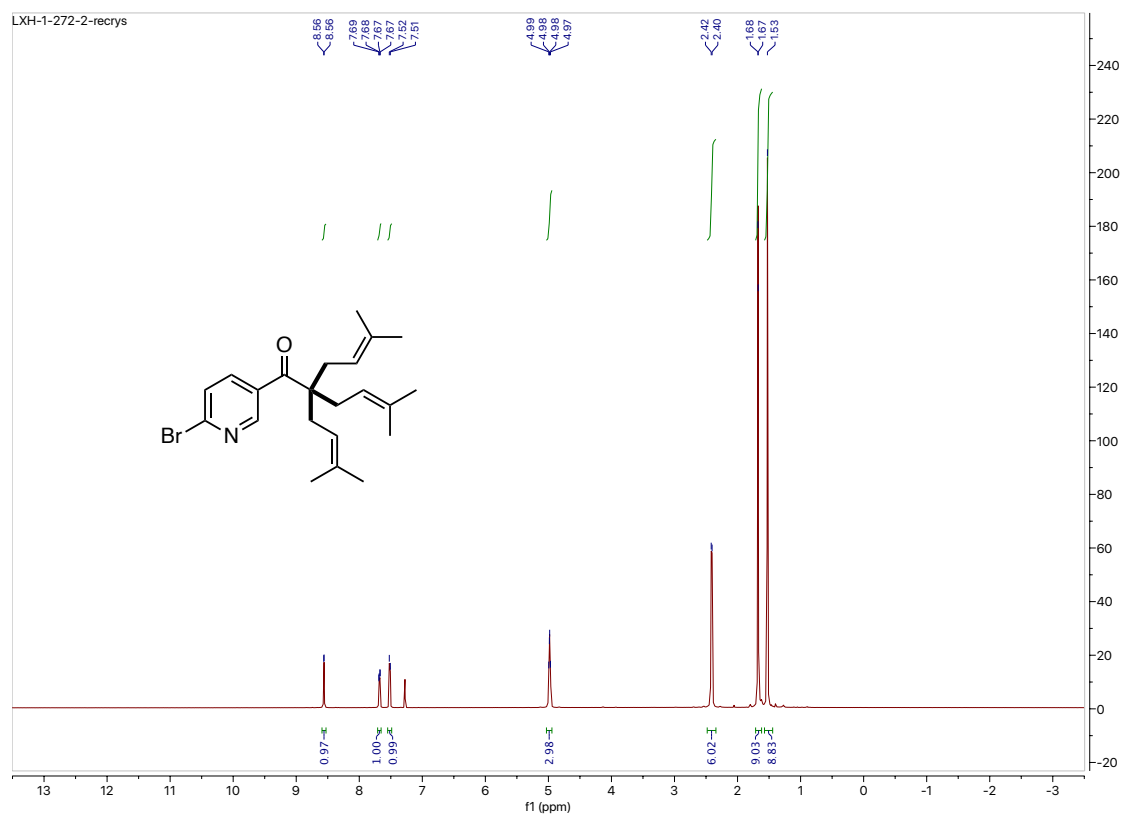




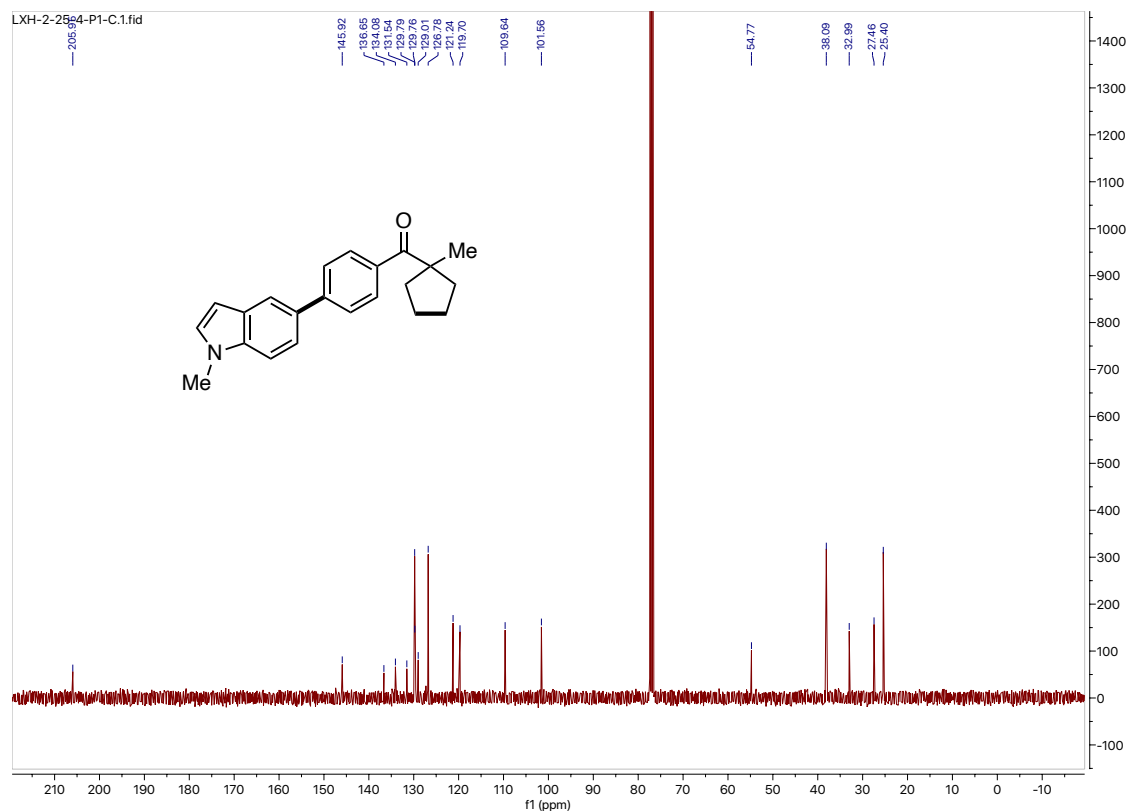
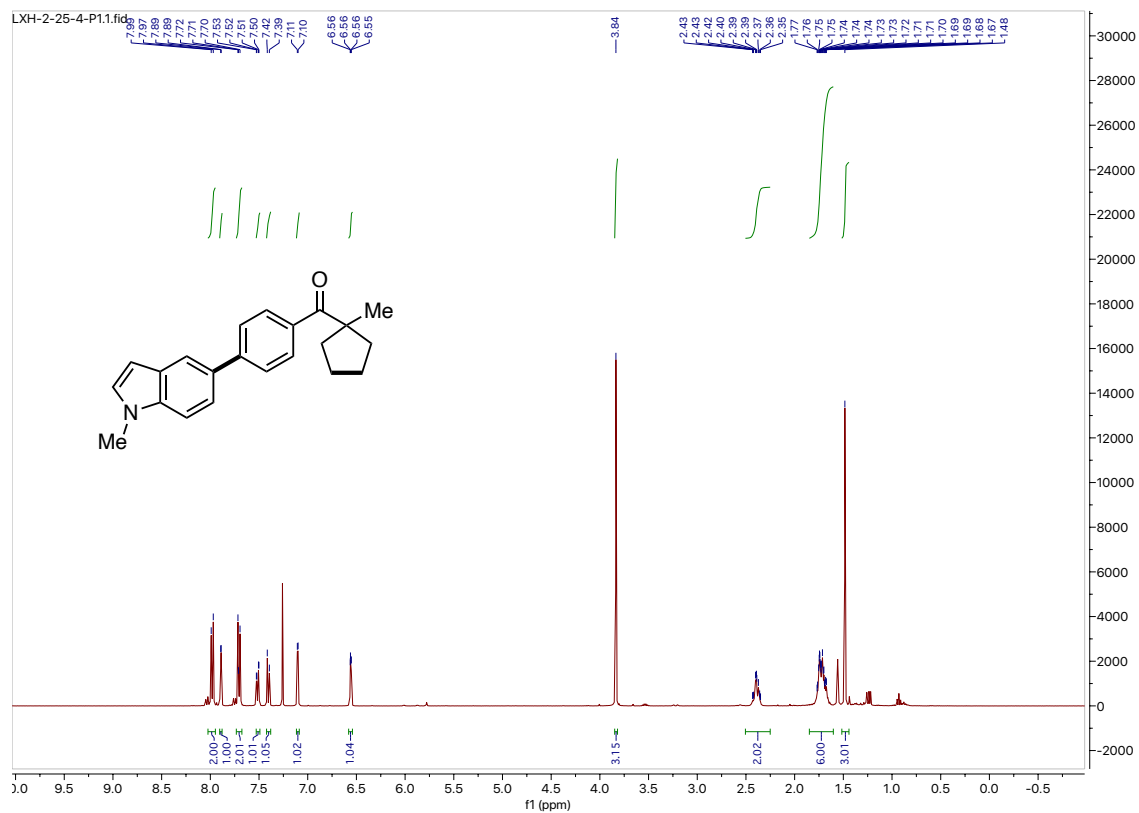
# $^1\text{H}$ NMR and $^{13}\text{C}$ NMR for compound IV-28



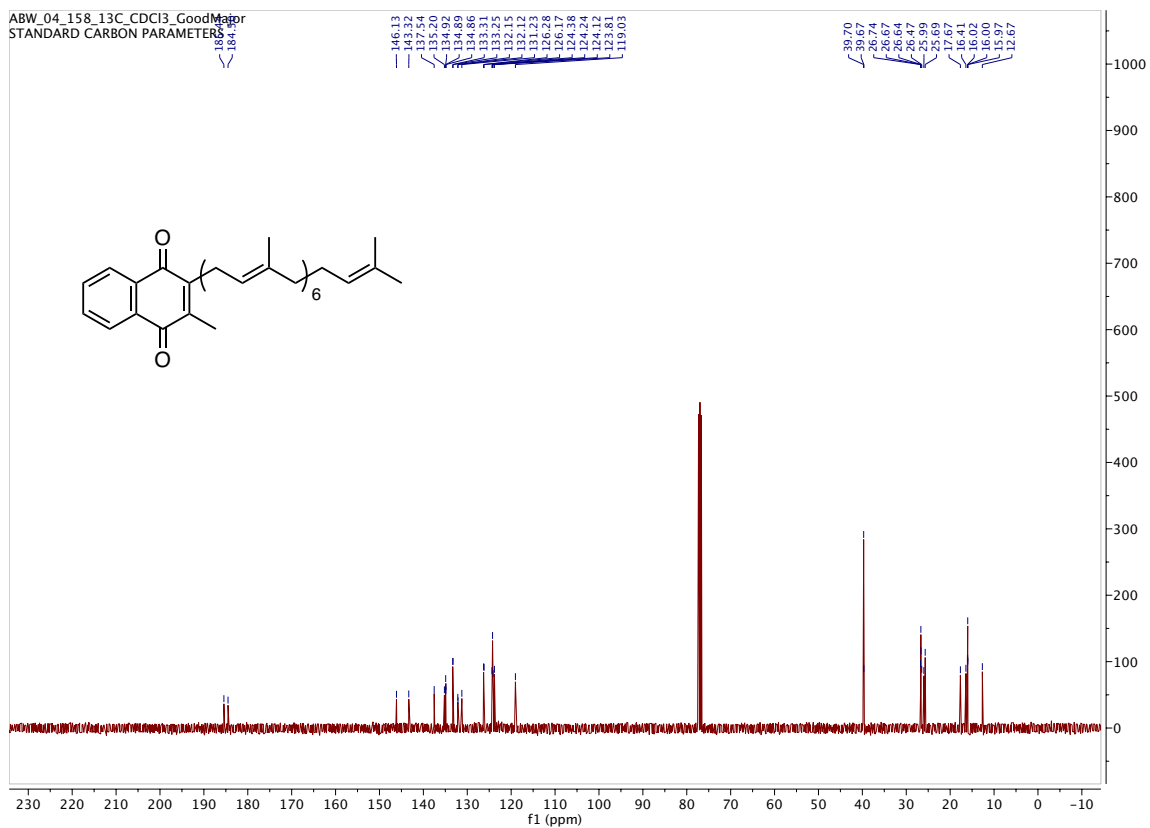
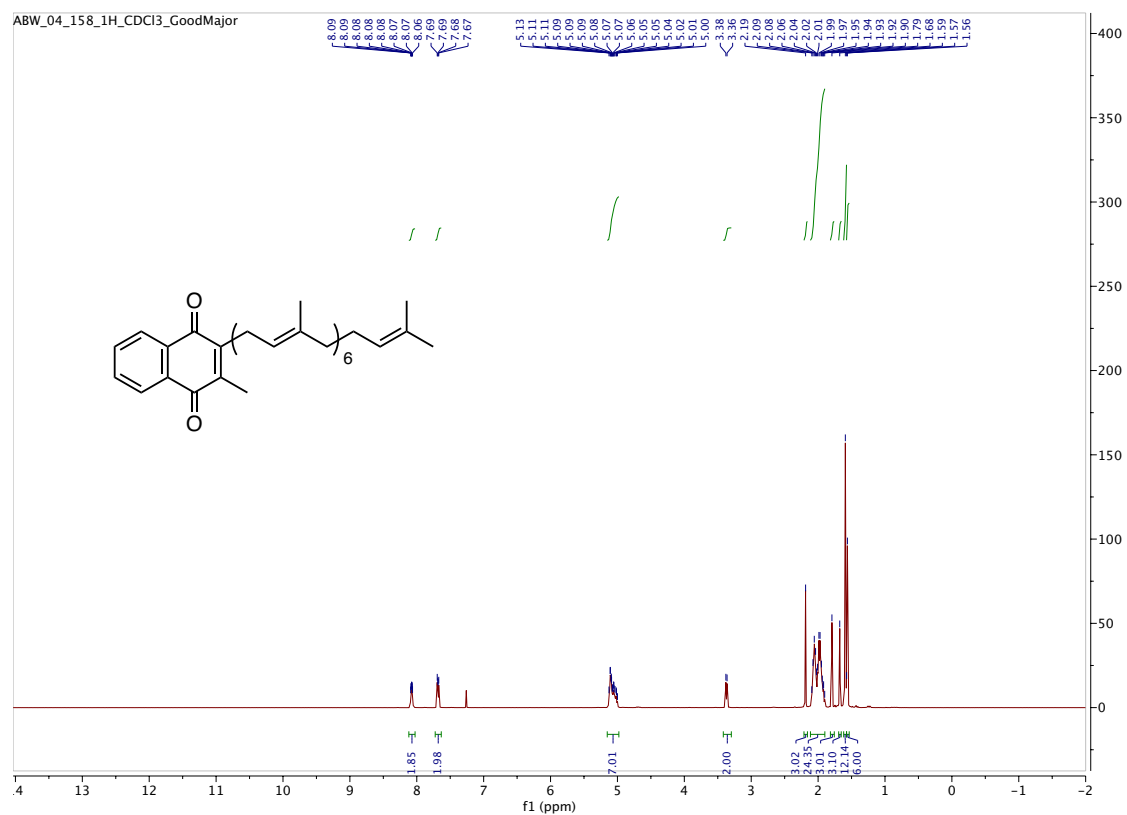
# $^1\text{H}$ NMR and $^{13}\text{C}$ NMR for compound IV-29



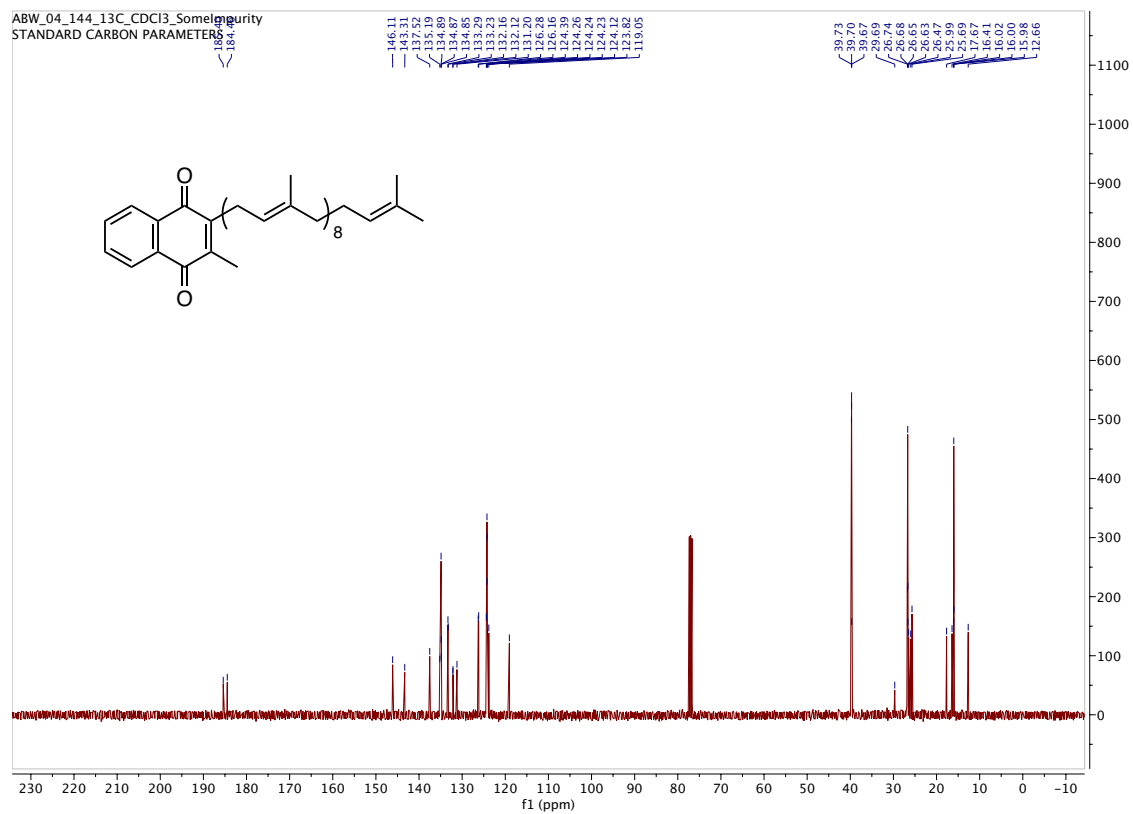
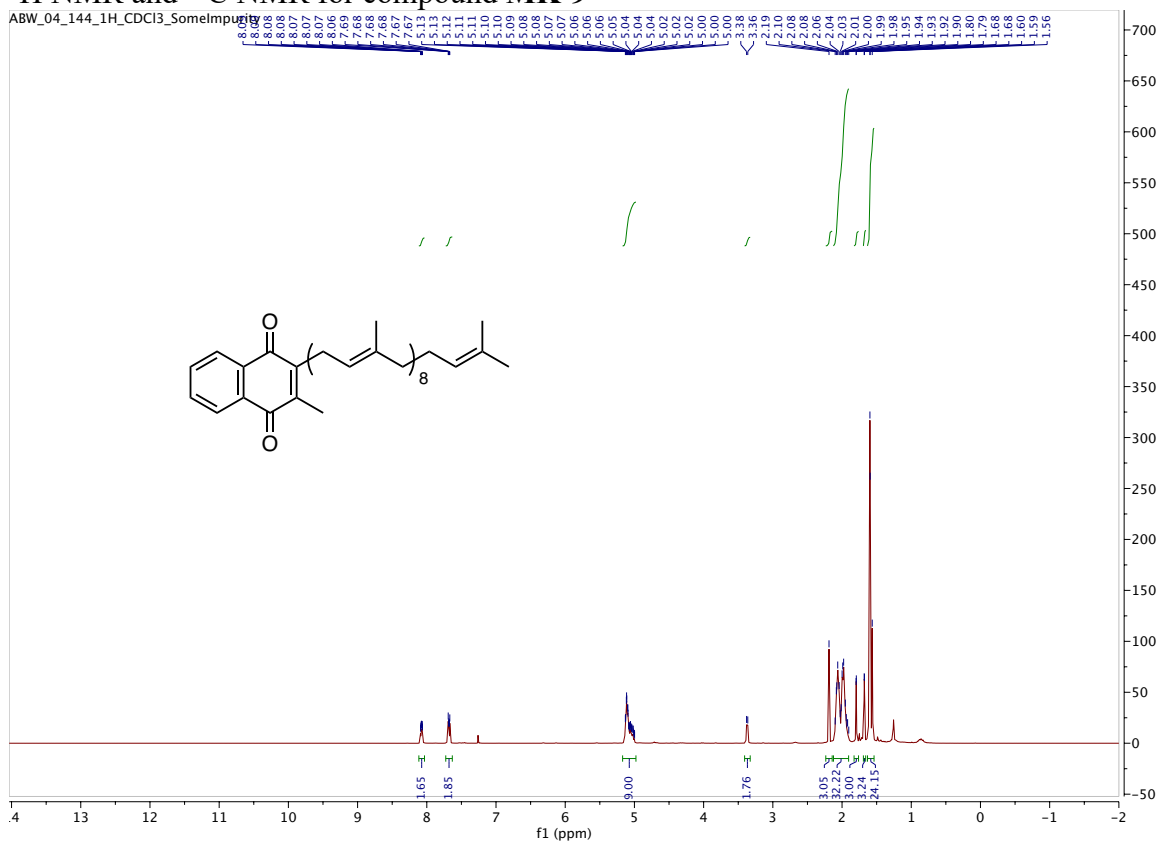
# $^1\text{H}$ NMR and $^{13}\text{C}$ NMR for compound IV-41



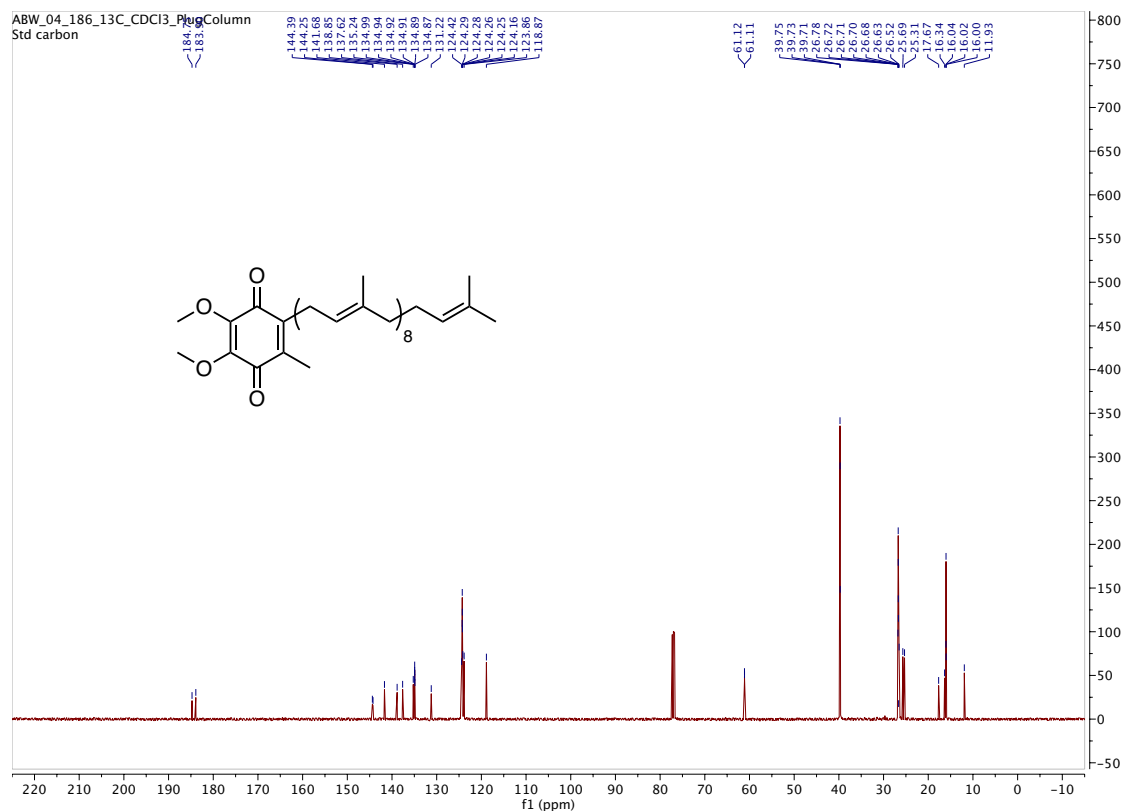
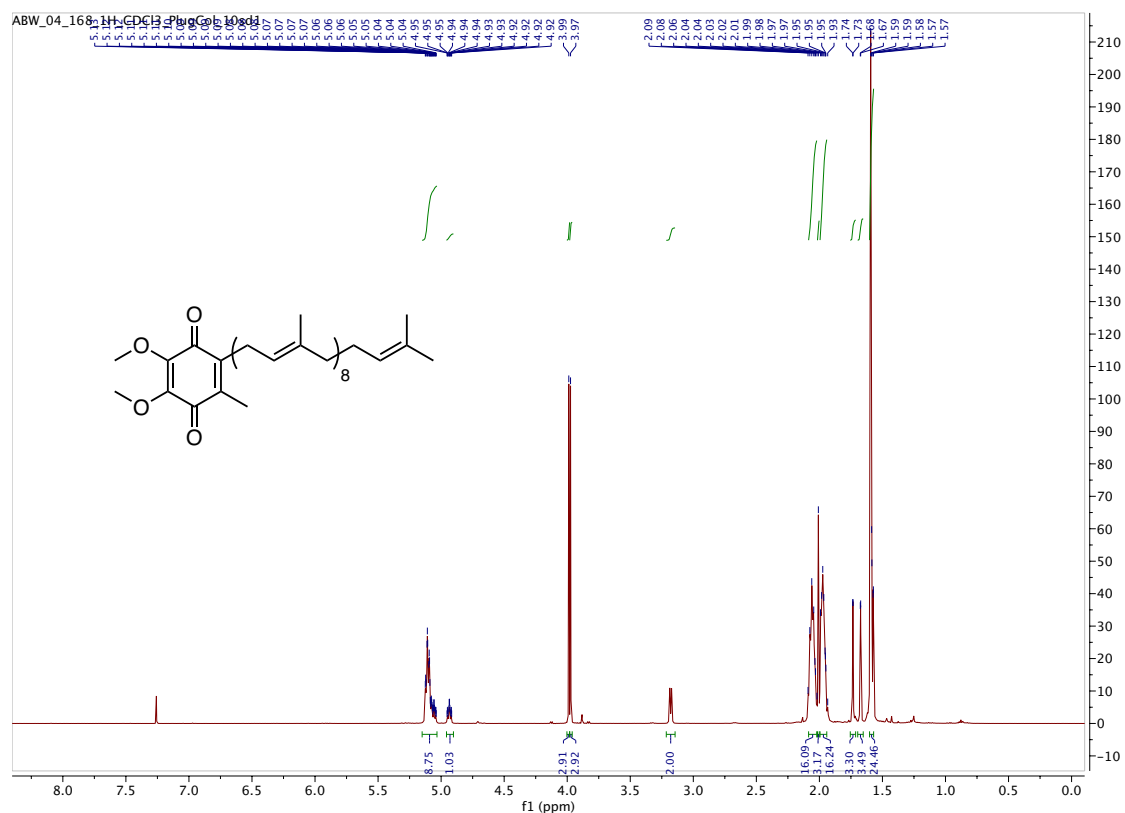
# <sup>1</sup>H NMR and <sup>13</sup>C NMR for compound MK-7



# <sup>1</sup>H NMR and <sup>13</sup>C NMR for compound MK-9



# <sup>1</sup>H NMR and <sup>13</sup>C NMR for compound CoQ<sub>9</sub>



<sup>1</sup>H NMR and <sup>13</sup>C NMR for compound IV-36

